ISWS/RI-81/75
REPORT OF INVESTIGATION 81
STATE OF ILLINOIS
DEPARTMENT OF REGISTRATION AND EDUCATION

Studies of Selected Precipitation Cases from METROMEX

STANLEY A. CHANGNON and RICHARD G. SEMONIN, Editors

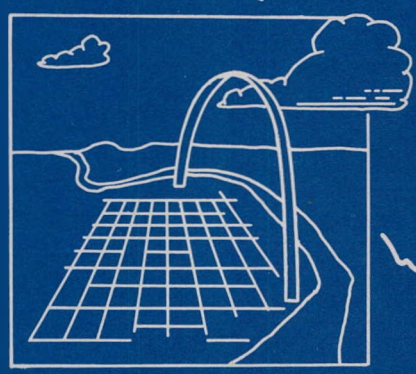

ILLINOIS STATE WATER SURVEY
URBANA
1975

REPORT OF INVESTIGATION 81

Studies of Selected Precipitation Cases from METROMEX

STANLEY A. CHANGNON and RICHARD G. SEMONIN, Editors

Title: Studies of Selected Precipitation Cases from METROMEX.

Abstract: In the analysis of METROMEX field data, nine rain periods (case days) in 1972 and 1973 were chosen for in-depth investigations aimed to better define the urban-related mechanisms that cause the summer rainfall in and east of St. Louis and Wood River to be greater than that in surrounding areas. The nine cases were selected to represent a variety of summer precipitation conditions in the St. Louis area. These investigations identified several urban-related conditions that contributed to the observed precipitation alterations. Principal findings were that the urban areas: 1) initiated and thus increased the number of raincells, 2) intensified rain and severe weather from the urban-initiated cells by their subsequent merger with each other or a later system, 3) intensified rain and severe weather from existing cells passing over the urban areas by the effect of their heat, moisture, and/or aerosol plumes, 4) produced these effects only when rain-conducive synoptic conditions existed, and 5) operated with a 'domino' effect in which urban cells beget more urban cells on the same day and tend to reinforce developments in a multi-day sequence in the same locale. The case studies also revealed missing or inadequate measurements critical for METROMEX or other field projects and provided guidance for direction of the research.

References: Changnon, Stanley A., and Richard G. Semonin, Editors. Studies of Selected Precipitation Cases from METROMEX. Illinois State Water Survey, Urbana, Report of Investigation 81, 1975.

Indexing Terms: Atmospheric chemistry, boundary layer, climatology, cloud physics, inadvertent weather and climate change, meteorology, pollution, rainfall, severe weather, urban climate, weather modification, weather radar.

STATE OF ILLINOIS
HON. DANIEL WALKER, Governor

DEPARTMENT OF REGISTRATION AND EDUCATION
RONALD E. STACKLER, J.D., Director

STATE WATER SURVEY DIVISION
WILLIAM C. ACKERMANN, D.Sc., Chief

URBANA
1975

Printed by authority of the State of Illinois—Ch. 127, IRS, Par. 58.29
(11-75-1500)

CONTENTS

Studies of Selected Precipitation Cases from METROMEX

Stanley A. Changnon and Richard G. Semonin,
Editors

A. INTRODUCTION

Evaluation of our progress in the analysis of METROMEX data collected during 1971–1973 led to a decision to pursue some descriptive case studies of nine precipitation periods in 1972 and 1973. These studies are each in-depth investigations, although they do not represent the most elaborate study that could be envisioned. They are, however, sufficiently extensive to describe the likely causes of the precipitation, or lack of precipitation, in each case. This report is the second in a series of Water Survey reports devoted to METROMEX (*Metro*politan *M*eteorological *Ex*periment).

The primary goal of these case studies was to focus the entire METROMEX field and research effort by attempting to define better the various urban factors leading to measurable changes in rainfall and severe weather in the St. Louis area. These studies will help to achieve the overall goal of METROMEX which is to define, understand, and evaluate urban-induced precipitation alteration due to man's activities. These extensive analyses also revealed several missing features of the field project, and this knowledge has been useful in redesigning the field effort in 1974–1975 and in directing the analytical procedures for concluding METROMEX. These procedures include: 1) identification of those variables essential for the description of a rain event; 2) evaluation of the quality of the available data with regard to describing a rain event; 3) establishment of a means for cataloging and storing essential data; and 4) establishment of a working data exchange between the various cooperating groups within METROMEX.

Approach

Nine cases (rain periods lasting usually 12 to 24 hours) were chosen to represent a variety of summer precipitation conditions in the St. Louis area. This report is organized to present the cases in their chronological order. Five of the cases are from a 7-day period in August 1973 and include a case with relatively small air mass showers and a very complex day with a relative severe squall line system followed by a cold frontal rain system. Other cases were chosen from August 1972 and July 1973. Since the majority of the summer precipitation in the St. Louis area is associated with squall lines, cold fronts, and squall areas, it is not surprising that the frequency of these synoptic events dominates the case studies. Two air mass situations are reported, one dealing with a post cold-frontal thunderstorm and the other with warm sector showers. Six squall lines are studied, two of which were associated with frontal systems and four in which no front impacted on the storm situation. Studies of a cold frontal passage and its associated precipitation and of a squall area with no front in the vicinity are also included.

This type of classification is from the general synoptic condition viewpoint and the individual case studies will describe the macroscale weather conditions in greater detail. Table A–1 lists the nine case days and briefly describes their precipitation events.

Different Survey scientists performed these nine case studies. In most instances, two scientists were assigned to each case and they are the authors of the case texts which follow. The scientists were asked to follow a certain organizational format in order to obtain some uniformity, but any special emphases in their analyses were left largely to their discretion.

Table A-1. Case Days Studied

Date	*Precipitation events*
11 August 1972	Local area showers developed forming a meso thunderstorm cluster just east of St. Louis with 2-inch rains
14 July 1973	Isolated thunderstorms developed over the urban area and merged with existing storm to form a cluster east of St. Louis with 1-inch rains
23 July 1973	Organized line of thunderstorms moved through the area, producing severe weather, but dissipating as it moved east
25-26 July 1973	Showers and storms developed in low-lands northwest of St. Louis and over the Alton urban area, and organized into a thunderstorm cluster with 3-inch rainfalls
7 August 1973	Small air mass showers developed west of St. Louis and over the Alton area, and only a few produced radar echoes that reached the ground
9 August 1973	Two rain systems occurred, one in the morning with showers throughout the area and one in the evening as a cold-front rain system dissipated while approaching the urban area
10 August 1973	Isolated air mass thunderstorms developed in the area, including two over the urban area, one of which developed into a cluster over the city with very heavy rainfall rates
12 August 1973	Large thunderstorm producing record rain rates and large hail developed over the urban area and became the start of a squall line that developed there and moved eastward
13 August 1973	Isolated storm developed over the urban area and then merged with a severe weather-producing squall line that passed; a cold front line of storms passed later

Other goals of this effort were to familiarize the senior METROMEX scientists with all types of data being collected and to encourage interaction between scientists who had been specializing in specific research areas (rain, synoptic weather, atmospheric chemistry, etc.).

Each case is presented in the following format:

1) *Synoptic weather conditions* including descriptions of the relevant macroscale and mesoscale conditions
2) *Precipitation morphology* including descriptions of the clouds and precipitation elements that made up the case
3) *Surface and atmospheric measurements* including relevant surface temperatures, humidity, winds, and aerosols plus any cloud physics data, low-level airflow information, soundings, and pollution (thermal and aerosol) conditions, as detected by aircraft and remote sensors
4) *Air and rainwater chemistry* involving surface and airborne measurements of pollutants and special tracers released to follow atmospheric motions

5) *Storm summary* presenting composites of all the case elements, deriving conclusions as to the urban role in affecting rainfall and severe weather, and identifying recommendations for future field activities and research

In most respects, each case is a separate, self-contained scientific paper. Each is complete in the format described above and includes an introduction describing the rationale for choosing the case for study as well as its own list of references.

Before proceeding into the texts of the nine cases, some background material is presented. First, the physical scene is set by a description of the study site geography. This includes the surface elevation and major physical features (hills, plains, and rivers). Also presented is information about the major land uses of the St. Louis area.

A section on data indicates their acquisition, types, and sites of collection. Because the case studies repeatedly refer to specific towns and instrument sites, directions, and measurements, abbreviations of these have been used extensively in the case study texts and are identified in the data section.

Site Geography

One of the major goals of the METROMEX field project is to delineate the causes for the observed precipitation anomaly east of the St. Louis metropolitan area. In the pursuit of determining these causes, the local terrain and land use must be recognized as potentially exerting an influence on the precipitation patterns. These features are shown in figure A-1.

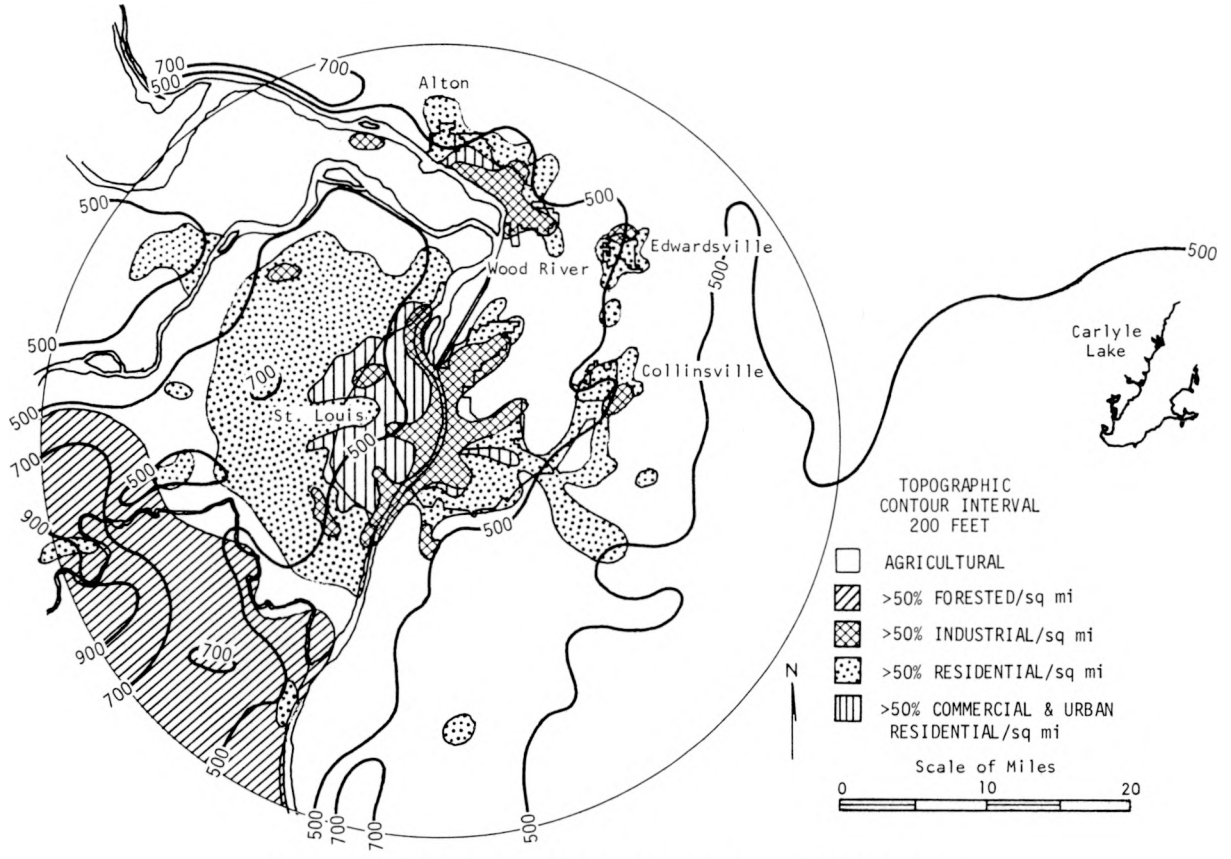

Figure A-1. Surface topography and land use types in METROMEX circle

The topography is shown in 200-foot intervals of altitude above mean sea level. With the exception of the extreme west-southwest edge of the research circle, very little change in the terrain occurs. There is a sharp bluff north and northwest of St. Louis along the Mississippi River. The slope of the land east of St. Louis is gradual and, in terms of contribution to the disturbance of airflow from the west or southwest, it would not be expected to contribute an effect as large as that from the urban structures. In general, storms moving into the area from the west-southwest move from the relatively low Ozark foothills onto a relatively flat plain with only a minor rise in elevation on the Illinois side due to the depression of the Mississippi floodplain extending north-south from Wood River. The preferred storm direction observed during METROMEX was from the west. Inspection of figure A-1, taking into account the orography and the position of St. Louis, shows that surface terrain has no significant variations along a west-east transect through the city. The change in elevation east of a line from Edwardsville to Collinsville is minor and reflects the flat agricultural plain which extends northeastward through central Illinois.

As can be noted in figure A-1, the largest percentage of land use in the METROMEX circle is devoted to agriculture. A moderate forested area exists in the Ozark foothills. The industrial and residential areas show that the large St. Louis metropolitan area is an entity separate from the Alton-Wood River industrial complex. The response of the atmosphere to the various types of land use will be referred to in the case studies. The highly industrialized areas produce copious quantities of aerosols, but the entire metropolitan area can also be considered to produce an urban plume of aerosols. Under appropriate wind conditions, the Alton-Wood River and the St. Louis areas can be readily distinguished as independent pollutant sources that possess individual characteristics of aerosol concentration.

B. DATA

Types and Acquisition

All of the data derived from the Water Survey's field measurements were utilized in each of the case studies. Some pertinent data were obtained from the other institutions involved in the METROMEX field program. In many cases, concurrent data were not available from the other research groups because the Survey field operations had extended for longer periods. Consequently, it was not possible to have a uniform data base for all nine cases.

The data compiled as input for these case studies were gathered from more than 650 instruments ranging in sophistication from simple hailpad passive sensors to instrumented aircraft. The data used were acquired from surface networks, remote sensors (lidars and radars), and aircraft.

The Survey's surface measurements included rainfall from 245 recording raingages; hail from 245 hailpads; temperature from 28 sites; surface wind from 7 sites; upper-air boundary layer wind from up to 12 sites with pibals and 3 with radiosondes; thunder occurrences from 10 sites, 6 of these with automatic recording devices; and air and rain chemistry data from 93 sites. In addition to these major surface installations, there were scattered numbers of other specialized equipment, such as cloud cameras, which were in the developmental stage and implemented for only brief excursions in the field.

The locations of these instruments are shown in figure B–1. The sensors all provided data which are useful to studies of the causes of precipitation modification. For example, data from the surface network of temperature and relative humidity recorders were used to derive additional variables such as dew point temperature, equivalent potential temperature, and the lifted condensation level for cloud formation. The recorded rainfall curves were processed to get 5-minute amounts and these were then analyzed to delineate *raincells*. The raincells were used as a principal means for the study of the modification of convective storms as they traversed the area. The hail sensor data with the raingages modified to record hailstorms were used to reconstruct individual hailstreaks and the volume and energy of the hailfalls. The thunder detectors were used to define which cells became thunderstorms and to indicate their intensity.

Data from the chemistry networks furnished quantities such as the deposition rate of specific elements. These were used to estimate the impact of low-level sources on the rainwater quality as well as to make inferences concerning their presence and effect on cloud processes. Through tracers intentionally placed in convective storms, the time required for the processing of materials in the precipitation mechanism was estimated.

The aircraft contracted by the Survey from Atmospherics Incorporated was used to release tracers into convective updrafts on five of the case days. The aircraft and its instruments were also used to obtain measurements of clouds plus data on condensation nuclei, temperature, moisture, and updraft speeds in convective clouds that were initiated or advected into the METROMEX circle. These data have been extremely valuable in discriminating between those clouds which were likely influenced by the urban–industrial area and those of a more rural character unaffected by man's industrial activities. As will be noted in the case studies, the urban aerosol, as measured by the aircraft condensation nuclei instrument, provided an invaluable tracer for material entering a cloud base. These observations left little doubt that the urban effluent was interacting within the cloud being measured.

The remote sensing of precipitation was by three weather radars. Two were located at Pere Marquette, northwest of St. Louis, and one at Greenville, 50 miles east of St. Louis. The FPS-18, 10-cm PPI radar at Pere Marquette was used to examine the morphology of precipitation

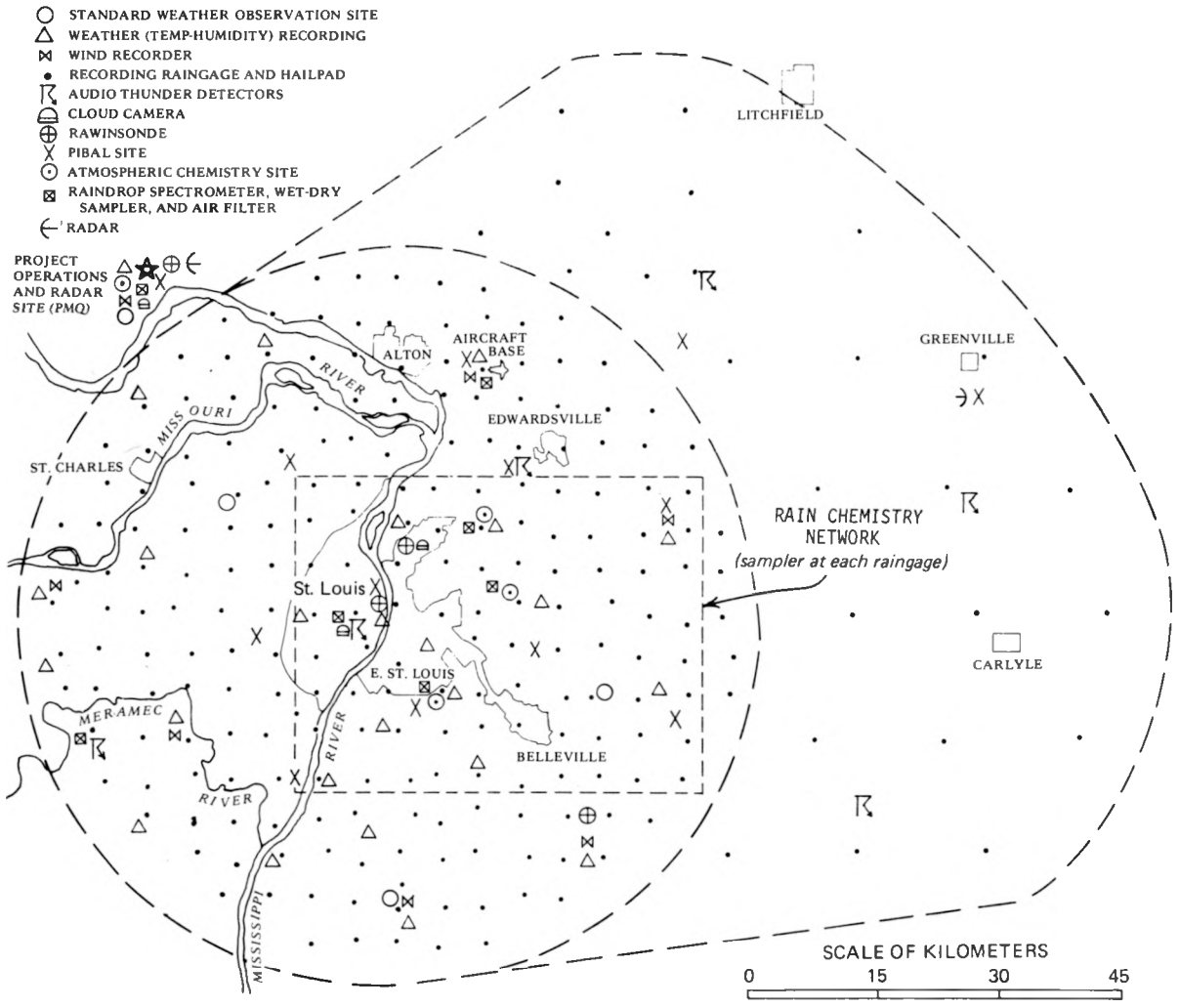

Figure B-1. Instrument sites for Water Survey equipment in 1972-1973

production and movement and to supplement the interpretation of raincell development as indicated by the surface raingage network. Data from the two TPS-10, 3-cm wavelength RHI radars were used to examine the 3-dimensional, time-varying structure of convective cells as they traversed the METROMEX circle. The RHI radars were extremely useful in determining the location in time and space of the formation of the first precipitation particles associated with a specific convective cloud. Both types of radars were also used to assess the merger of echoes, and the case studies indicated the importance of such mergers for the development of heavy rainfall.

The radiosonde and pibal data, which were available for six of the nine cases, were effectively used to define urban-related effects on the temperature and moisture structure of the low-level atmosphere. These data were also used to study the urban-related perturbations in the airflow. In two cases, lidar data were useful in defining the planetary boundary layer and the movement of surface effluents to cloud base levels.

Abbreviations for Data Types, Sites, and Measurements

In an effort to minimize text length, abbreviations are widely employed. These are used for the description of data (chemicals, clouds, project areas), for sites of all instruments and cultural features (towns), and for units of measurement (length, speed, degrees, etc.).

The instrument site abbreviations appear in table B-1. Their locations are shown on figure B-2. All other abbreviations appear in table B-2.

Throughout the case texts, the following units, unless specified otherwise, are used: all times are in Central Daylight Time; most surface temperatures are in degrees Fahrenheit; rainfall is in inches; radar reflectivity units are decibels; humidity is in percent; pressure is in millibars; and surface wind speeds are in miles per hour. The upper air wind data are in meters per second and upper air temperature in degrees centigrade.

Table B-1. Instrument Sites

Site	*Abbreviation*	*Site*	*Abbreviation*
Alton Civic Memorial Airport, IL	ALN	Leming Field Site, IL	LEM
St. Louis Memorial Arch, MO	ARC	Livingston, IL	LVT
Belleville Community College, IL	BCC	Machens Field Site, MO	MCH
Brighton, IL	BHN	Millstadt, IL	MDT
Scott Air Force Base, IL	BLV	Maryville, IL	MRV
Beavercreek Field Site, IL	BVK	Mascoutah, IL	MTA
Brentwood, MO	BWM	Mehlville, MO	MVM
Collinsville, IL	CLV	Nagel's Farm Field Site, IL	NGL
Cahokia Mounds, IL	CKM	O'Fallon, IL	OFN
Columbia, IL	CMB	Okawville, IL	OKV
Centreville, IL	CRV	Pere Marquette State Park, IL	PMQ
Doerr Field Site, IL	DRR	St. Charles, MO	SCH
Edwardsville, IL	EDW	Southern Illinois University–Edwardsville, IL	SIE
East St. Louis, IL	ESL	St. Jacobs, IL	SJB
Fernridge, MO	FNG	St. Louis University Field Site, MO	SLU
Freeburg, IL	FRB	South Roxana, IL	SRX
SIU Experimental Farm, IL	FRM	Lambert Field, MO	STL
Forest Park (in St. Louis)	FTP	Spirit of St. Louis Airport, MO	SUS
Granite City, IL	GRC	Tyson Valley, MO	TYV
Grover Field Site, MO	GVR	Weber Hill, MO	WBH
Imb's Station Field Site, IL	IMS	Waterloo, IL	WLO
Kimm's Farm Field Site, IL	KMM	Weiss Airport Field Site, MO	WSP
KMOX Field Site, IL	KMX	Wood River, IL	WDR

Acknowledgments

The research reported herein is the result of the support and efforts of a large variety of organizations and people.

Support for this research has come from the State of Illinois, the National Science Foundation (grants GI-38317, GK-38329, and GI-39213), and the Atomic Energy Commission now Energy Research and Development Administration (contract AEC-1199). The interest and scientific encouragement for METROMEX by the program managers of these federal agencies have helped make this report possible, and we therefore dedicate it to Edwin X. Berry of NSF and Robert Beadle of ERDA.

This research has been performed under the general direction of Dr. William C. Ackermann, Chief of the Illinois State Water Survey. The authors of the individual texts plus other senior staff members, particularly Bernice Ackerman, were the principal contributors to this report.

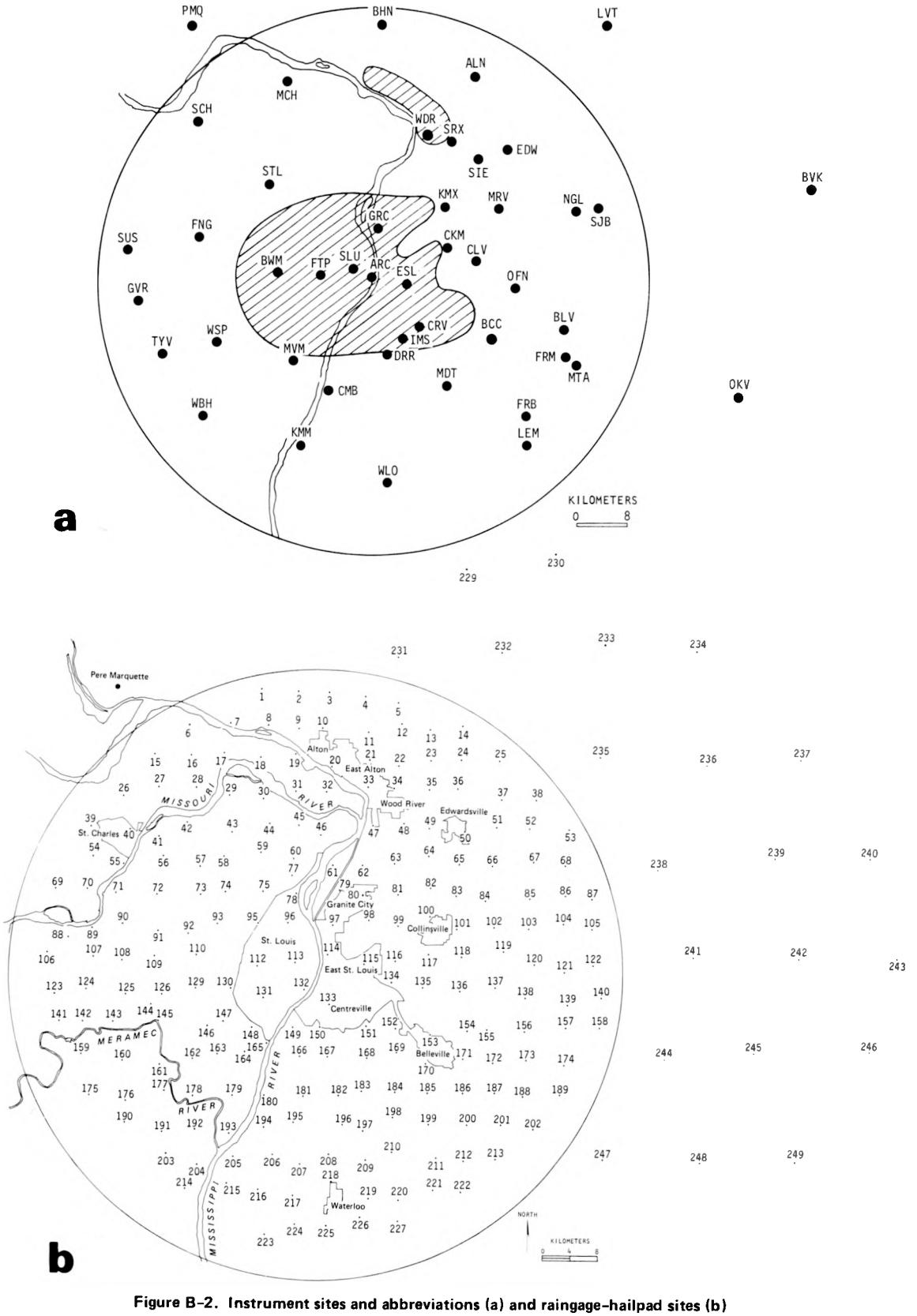

Figure B-2. Instrument sites and abbreviations (a) and raingage-hailpad sites (b)

Table B-2. Abbreviations

above ground level	AGL	minute(s)	min
acre-foot (feet)	ac-ft	mixing ratio	ω
Argonne National Laboratory	ANL	National Weather Service	NWS
Atmospherics Incorporated	AI	nautical mile(s)	n mi
centimeter(s)	cm	picograms per square centimeter	pg/cm^2
Central Daylight Time	CDT	plan position indicator radar	PPI
cloud condensation level	CCL	Precipitation Enhancement Program	PEP
cubic centimeter(s)	cc	radiosonde observations	Raob
condensation nuclei	CN	rainshowers	RW
constant altitude PPI	CAPPI	range-height indicator radar	RHI
decibel(s)	db, dbz	square centimeter(s)	cm^2
degree(s) Centigrade	C	square foot (feet)	ft^2
degree(s) Fahrenheit	F	square mile(s)	mi^2
degree(s) Kelvin	K	Stanford Research Institute	SRI
Design Experiment for Suppression of Hail	DESH	thunder	T
dew point	t_d	thundershowers	TRW
Eastern Illinois Network	EIN	wet bulb potential temperature	θ_w
echo frequency coverage	EFC		
equivalent potential temperature	θ_e	**Chemicals**	
Federal Aviation Agency	FAA		
feet per minute	ft/min	Calcium	Ca
foot (feet)	ft	Indium	In
gram(s)	g	Lithium	Li
gram(s) per cubic meter(s)	g/m^3	Magnesium	Mg
gram(s) per kilogram(s)	g/kg	Potassium	K
hour(s)	hr	Sodium	Na
inch(es)	in	Zinc	Zn
inch(es) per hour	in/hr		
inch(es) per mile	in/mi	**Clouds**	
knot(s)	kt		
level of free convection	LFC	altocumulus	Ac
liquid water content	LWC	altocumulus castellanus	AcCas
lifting condensation level	LCL	altostratus	As
maritime polar	mP	cumulonimbus	Cb
mean sea level	MSL	cirrus	Ci
meter(s)	m	cirrostratus	Ca
meter(s) per second	m/sec	cumulus	Cu
METROMEX	MMX	cumulus congestus	CuCong
mile(s)	mi	cumulus fractus	CuFra
mile(s) per hour	mi/hr	stratocumulus	Sc
millibar(s)	mb	stratus	St
		stratiformis	Str

Other Survey staff performed key roles in the field operations, including Donald Staggs, David Brunkow, Mark Gardner, Mark Edgington, Eberhard Brieschke, and Daniel Watson. Many university students, too numerous to mention, played important roles in the field operations. Another group of Survey staff members were instrumental in carrying out the data processing and various analyses, including Edna Anderson, Elmer Schlessman, Arthur Sims, Phyllis Stone, Marvin Clevenger, Ileah Trover, Robert Sinclair, Marion Busch, David Brunkow, Mark Gardner, Ronald Grosh, and Neil Towery. Again, many students assisted in the processing and analyses.

The Survey Graphic Arts staff under the direction of John Brother made a valuable input by preparing the large number of graphics required in the case study reports. The Editorial staff under the direction of J. Loreena Ivens also contributed significantly by carrying out the complex editing of texts from multiple authors; Suzi L. O'Connor prepared the camera-copy.

Many groups and individuals from other organizations contributed to the research. Thomas Henderson and Donald Duckering of Atmospherics Incorporated, who flew their aircraft in support of the Survey's METROMEX program, made many signal contributions to our data base by their skilled observations and efforts that continually extended beyond the conditions of their contract.

The loan of various data from the Cloud Physics Laboratory of the University of Chicago is gratefully acknowledged. Professor Roscoe Braham and his staff have willingly provided data and useful advice, and their data are identified in the specific case studies. Other forms of METROMEX data and/or results were obtained from Edward Uthe of Stanford Research Institute, Edward Miller of Argonne National Laboratory, and Richard Dirks and August Auer of the University of Wyoming. Their contributions are appreciated.

Supporting data, facilities, and the assistance of the National Weather Service, the Air Weather Service, and the Environmental Protection Agency were also important in the successful pursuance of the 1972–1973 field efforts and the research reported herein. Finally, many commercial firms, industries, and private citizens contributed by furnishing, at no cost, sites for our many instruments.

C. STORMS OF 11 AUGUST 1972

F. A. Huff and S. A. Changnon, Jr.

CONTENTS

C. STORMS OF 11 AUGUST 1972

INTRODUCTION

Thunderstorms and rainfall were recorded in portions of the MMX circle on 11 August 1972. The most outstanding event was a severe rainstorm accompanied by hail that occurred several miles E of St. Louis during the late afternoon and early evening. Two-hour rainfall amounts in the center of this storm were of an intensity that occurs at a given point in this region on an average of only once in 10 years. Operational observations and ensuing preliminary analysis of the severe rainstorm on 11 August 1972 revealed it to be a potentially urban-affected event because of 1) its position with respect to the city and 2) its development and sustainment from convective activity developing over and slightly downwind of the city. Other rainstorms on the circle were relatively light in total rainfall output. Also, data from the NWS climatic network (Climatological Data, August 1972, Illinois and Missouri) indicated no other heavy rainstorms in the St. Louis region during the period of the MMX storms. Consequently, a study was undertaken to identify the urban effect (if any), to determine its influence upon the rainfall and severe weather events, and to ascertain how the natural atmospheric precipitation processes were modified by the urban input.

In this case study, detailed analyses were made of all Water Survey data available from MMX operations on that day, and these analyses were supplemented by surface and upper air data from the NWS synoptic network and lidar data from SRI. Certain properties of clouds in the region were derived from cloud camera data, surface and aircraft observations, and cloud photographs taken by field personnel. Low-level AI aircraft flights provided pertinent information on the physical properties of the clouds, the means by which the convective storms were being maintained, and the fact that surface aerosols were reaching cloud base levels. Chemical tracers released by aircraft that day also provided useful information for defining the nature of the convective activity in the MMX circle.

Low-level Raob data provided by NWS from their St. Louis Arch soundings within the MMX circle and from their Salem soundings, a few miles E of the research area, were very helpful. No pibal data were available.

SYNOPTIC ANALYSES

The convective activity in the St. Louis region on 11 August was non-frontal. The mid-afternoon rainfall on the MMX circle resulted from individual storms (RW, TRW) generated in a squall zone of scattered convective activity that NWS radar summaries showed extending over all of Illinois and E Missouri at that time. However, the heavy rainstorm E of St. Louis that maximized in the 1700–1900 CDT period was associated with a definite squall line. The NWS radar summary at 1740, the time when the St. Louis storm was most intense on the MMX circle, indicated a squall line extending from E-central Illinois to just SW of St. Louis. This squall line showed little movement during the period of most intense rainfall, and radar reports indicated cloud tops of 40,000 to 50,000 ft in the St. Louis area. From analyses of radar and raingage data, it was quite clear that the heavy rainstorm developed over the MMX circle as part of the development of the squall line, and possibly was the initial area of development of this entire line.

Surface Weather Maps

Surface maps at 3-hr intervals throughout the day showed no frontal activity within several hundred miles. Airflow over Missouri and Illinois was from the SW around a high centered off the East Coast. Dew point temperatures gradually increased during the day and by 1600 CDT, shortly before the heavy storm and squall line were initiated, they exceeded 70F in SW and S-central Illinois, and a trough in the isobaric pattern was evident through W Illinois and the region of heavy storm development E of St. Louis. Features of the surface map at 1600 are shown in figure C-1. The presence of the trough and high dew points provided favorable surface conditions for the development of convective activity.

Upper Air Data

Figure C-2 shows the 850-mb height contours and dew point temperature patterns at 1900 CDT, near the end of the heavy storm period on the MMX circle. A slight trough in the contour pattern is indicated in a N-S direction through Illinois and the general region of the heavy rainstorm (SW Illinois). The highest dew points, however, were located well to the W of the storm area. On both the 0700 and 1900 charts, temperature and dew point differences were relatively large at 850 mb, ranging from 24C in the morning to 16C in the evening in the St. Louis area. In comparison, differences of only 1 to 2C existed in E Iowa throughout the day.

The contour patterns at 700-mb and 500-mb (figure C-3) showed the typical veering of winds with height. There was no evidence of the low-level trough detected on the surface and 850-mb level maps, but a shortwave was suggested over STL by a 5890 contour. The surface and upper air maps indicated that conditions for convective activity in the Illinois-Missouri region were generally favorable at the surface, but decreased with height. As a result, scattered convective activity might be expected with the destabilizing effect of diurnal heating, and moderate to heavy convective activity could occur on a localized basis.

Examination was made of the 0700 and 1900 soundings at Salem, approximately 60 mi E of the heavy rainstorm center. This sounding indicated relatively dry air aloft throughout the day and relatively stable conditions in the lower levels. Although the surface inversion of the early morning had been eliminated, there was still a shallow isothermal layer near 900-mb at 1900 (figure C-4b). Overall, the Salem sounding did not indicate conditions favorable for convective activity on 11 August. For example, a Showalter index of +7 was indicated at 1900.

Fortunately, low-level soundings were available also at ARC near the center of the MMX circle. These were taken at 0700 and 1400 CDT. The sounding for 1400 (figure C-4a), prior to start of rainfall in the circle, showed a wetter and less stable atmosphere than at Salem. A conditionally unstable lapse rate of 0.8C/100 m was present from 1000 mb to 800 mb. The mixing ratio varied from approximately 15 g/kg at the surface and 6 g/kg at 800 mb compared with 16 and 5 g/kg, respectively, for Salem at 1900. The Showalter index, as extrapolated from 700 mb to 500 mb with the Salem sounding, was a +1, which is favorable for strong convective activity.

Conclusions

From analyses of the upper air data, maps, and Raob, it is concluded that conditions were not generally favorable for the development of heavy rainstorms on 11 August in the Illinois-Missouri region except at scattered locations. One of these exceptions was the MMX circle, as shown by the ARC sounding at 1400 CDT and subsequent events. It is conceivable that the favorable

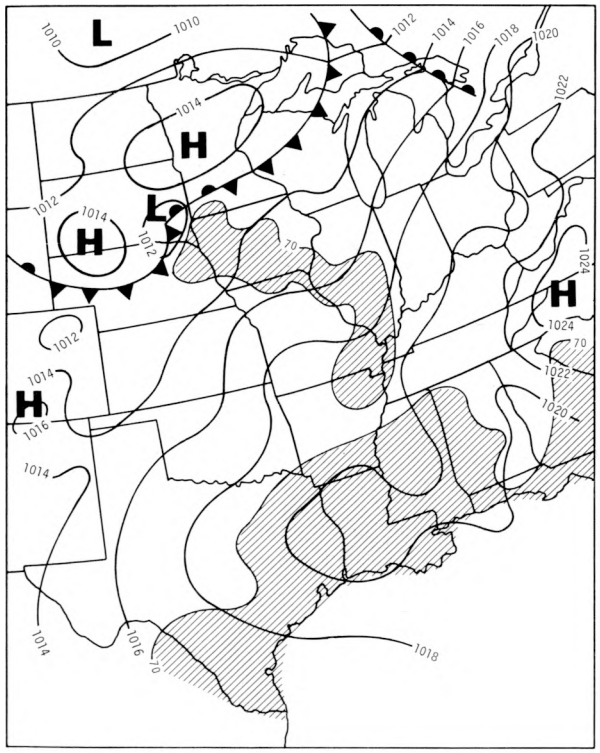

Figure C-1. Surface map at 1600 CDT

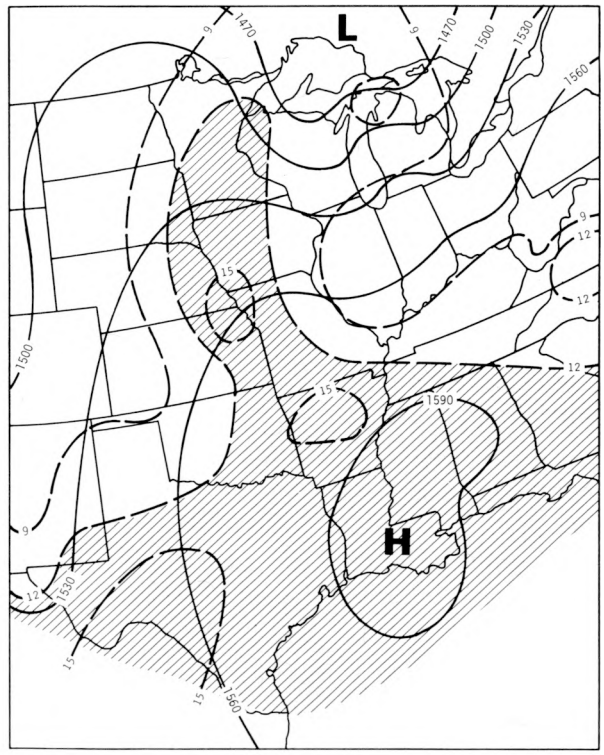

Figure C-2. 850-mb map at 1900 CDT

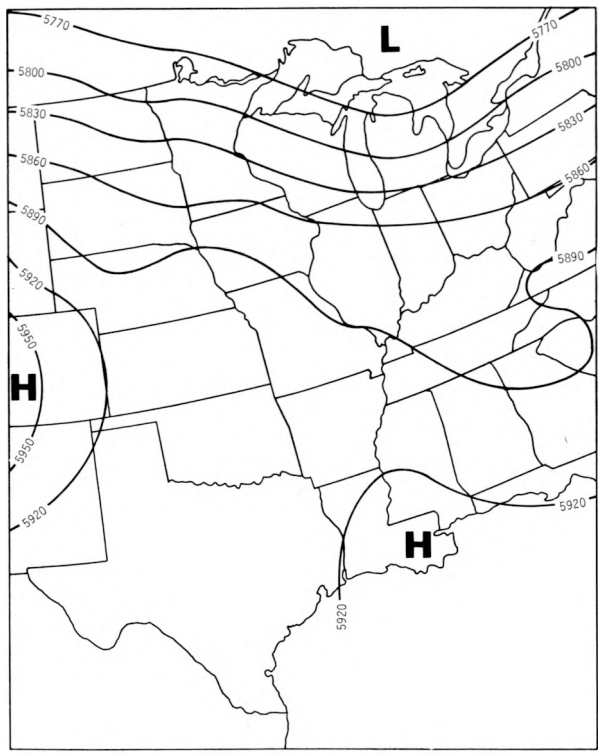

Figure C-3. 500-mb map at 1900 CDT

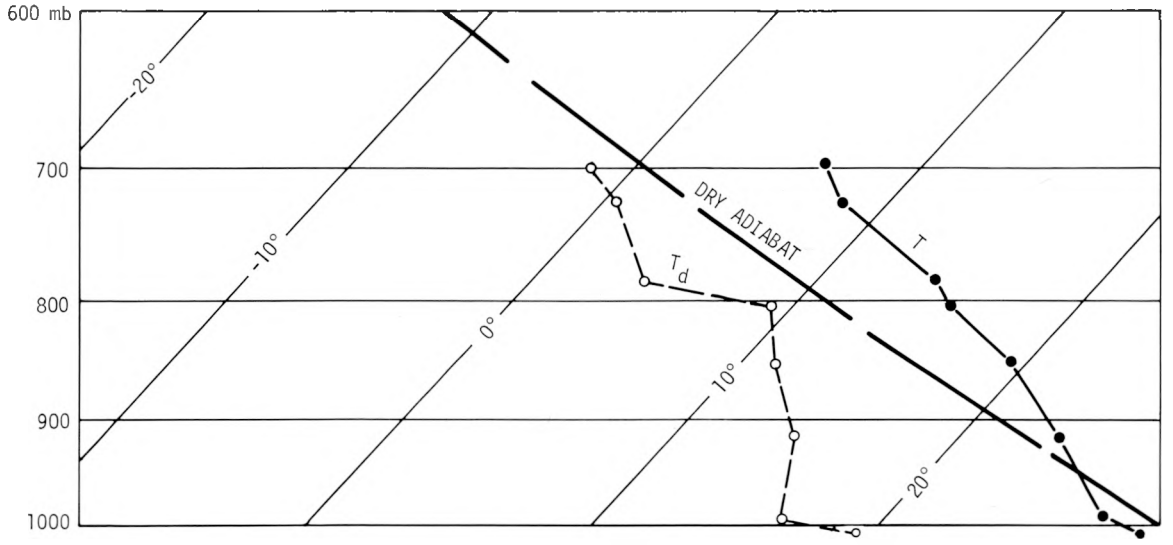

a. ARC, 1400 CDT

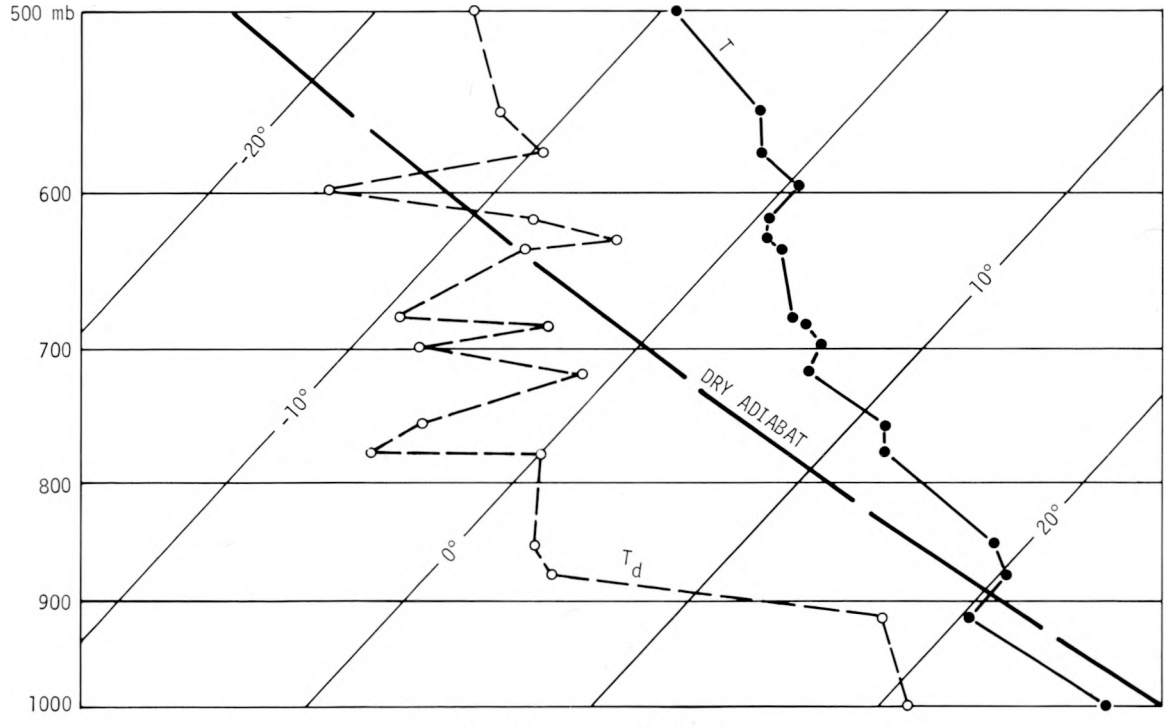

b. Salem, Illinois, 1900 CDT

Figure C–4. Radiosondes at St. Louis Arch and Salem

conditions in the MMX circle may have been related to the maximizing of temperature in the S part of the city and the peak in the dew point (moisture) distribution in and immediately downwind (E) of the city during the mid-afternoon.

REGIONAL RADAR AND RAINFALL ANALYSES

Radar Echo Distribution

Review of the NWS radar summaries was the initial step in the analyses of the rainfall history. These summaries provided an indication of the areal extent, duration, and intensity of the natural convective activity in and around the MMX circle.

At 0940 CDT, the radar summary map for the United States showed a region of scattered echoes producing light rainshowers with tops of 20,000 to 30,000 ft in S and central Iowa, N Illinois, S Wisconsin, and extending ENE into Michigan. Except in the extreme S and SE of the United States, no other convective activity was indicated at that time. Three hours later (1240) the light echo region persisted over N and N-central Illinois in approximately the same location as at 0940. However, a summary two hours later (1440) showed an increase in convective activity. Scattered TRW with tops of 30,000 to 47,000 ft were reported over SE Missouri. Scattered TRW and RW with tops in the vicinity of 30,000 ft were present in N and central Illinois, but no storms were observed in the St. Louis area.

By 1540 CDT, a large ill-defined squall zone oriented NNE–SSW encompassed all of Illinois, E Missouri, and extended into N Arkansas where it was near to merging with a large area of scattered convective activity extending W–E across the southern states from Texas to Florida (figure C–5). Widely scattered TRW and RW with tops in the range of 20,000 to 40,000 ft were

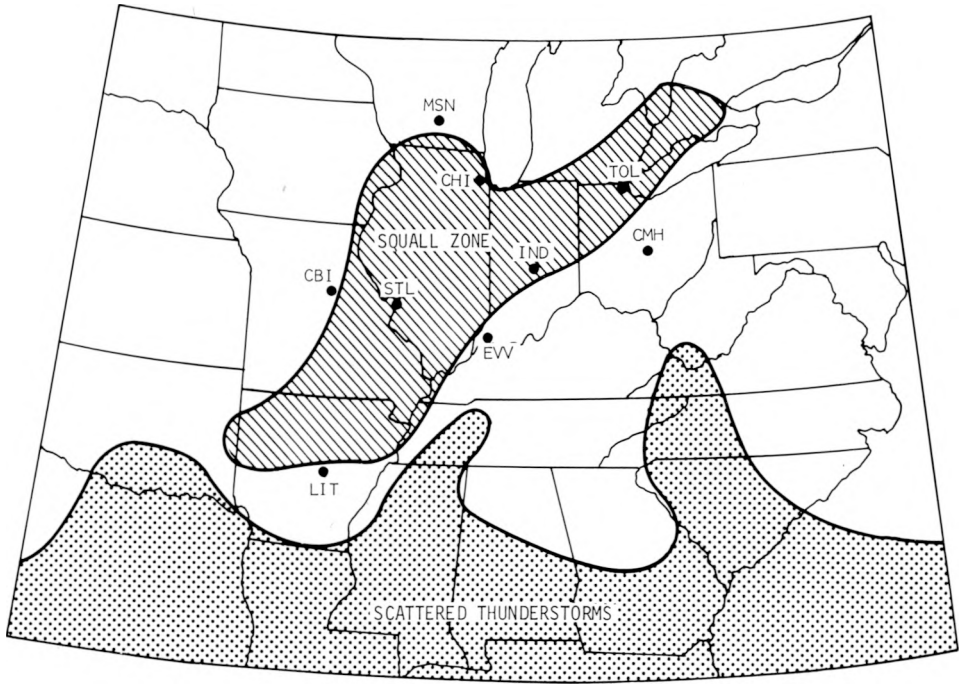

Figure C–5. Envelopes of radar echoes at 1540 CDT

observed in this squall zone. At 1640 CDT, the squall zone extended to the SW from N Indiana through the St. Louis area and on into Arkansas, where it joined the widespread southern convective activity. Echo tops of approximately 40,000 ft were most common in the Illinois–Missouri area of the squall zone.

At 1740 CDT, the squall zone of scattered echoes extended WSW from E Indiana to central Illinois, and then SSW through the St. Louis area and SE Missouri. Echo tops in the squall zone exceeded 40,000 ft in the St. Louis area. At this time, a squall line that extended from E-central Illinois to just SW of St. Louis was indicated within the squall zone. Some squall line storms exceeded 50,000 ft, including the storm in the St. Louis area.

By 2040 CDT, the radar map indicated a large decrease in convective activity throughout the Midwest and S United States. However, a portion of the squall zone still persisted on a ENE–WSW line from E-central Indiana to the St. Louis area. Echo tops were observed in the range from 29,000 to 49,000 ft, and the highest values were SE and ENE of St. Louis in S-central and SW Illinois. The map at 2130 CDT indicated persistence of the afternoon squall zone which was oriented ENE–WSW from S-central Indiana to the St. Louis area. By 2330 CDT, no activity was indicated in the St. Louis area, but the squall zone still persisted from S Indiana to SE Illinois.

The foregoing review of the national radar summary maps shows that convective activity was scattered but widespread over Illinois and E Missouri during the late afternoon and early evening when very heavy rainfall was recorded in some portions of the MMX circle. With scattered echoes building to 40,000 and 50,000 ft, the potential for naturally heavy rainfall was present in the Missouri–Illinois region. Furthermore, the natural convective activity had a relatively long duration, and radar observations indicated widely scattered RW and TRW in this region throughout the afternoon and evening.

Rainfall Distribution

Figure C–6 shows the regional rainfall pattern for Illinois and E Missouri during the 12-hr period beginning at 1300 CDT on 11 August. This incorporates the period from approximately 2 hr prior to the start of rainfall on the MMX circle until 3 hr after the rain ended. This map provides a generalized measure of the intensity and extent of the afternoon–evening rainfall resulting from the convective activity discussed in the radar summaries above. Figure C–6 was constructed from the NWS climatological network data only. With a density averaging approximately 1 raingage per 250 mi^2 in the Illinois–Missouri region, many small-area intense rainfalls were not recorded.

Figure C–6 indicates that most of the rainfall was confined to Illinois, and that relatively heavy amounts ($\geqslant$ 1 inch) fell in E-central and S-central Illinois. Only very scattered light rainfall was recorded in E Missouri, upwind of the MMX circle. *Thus, it appears that meteorological conditions favorable for development of strong convective storms were restricted mostly to Illinois, downwind of St. Louis and the MMX circle.* The nearest 1-inch amounts recorded in the climatic network were 60 to 80 mi to the E and NE of St. Louis. Figure C–6 also shows that the climatic network revealed no indication of heavy rainfall in the MMX circle. The heavy rainfall center near Urbana resulted from a storm in late afternoon. The center N of Mt. Vernon that resulted from a storm near midnight after rain had stopped on the MMX circle was the closest heavy rainfall to St. Louis. The light amounts in E Missouri were recorded in early to mid-afternoon.

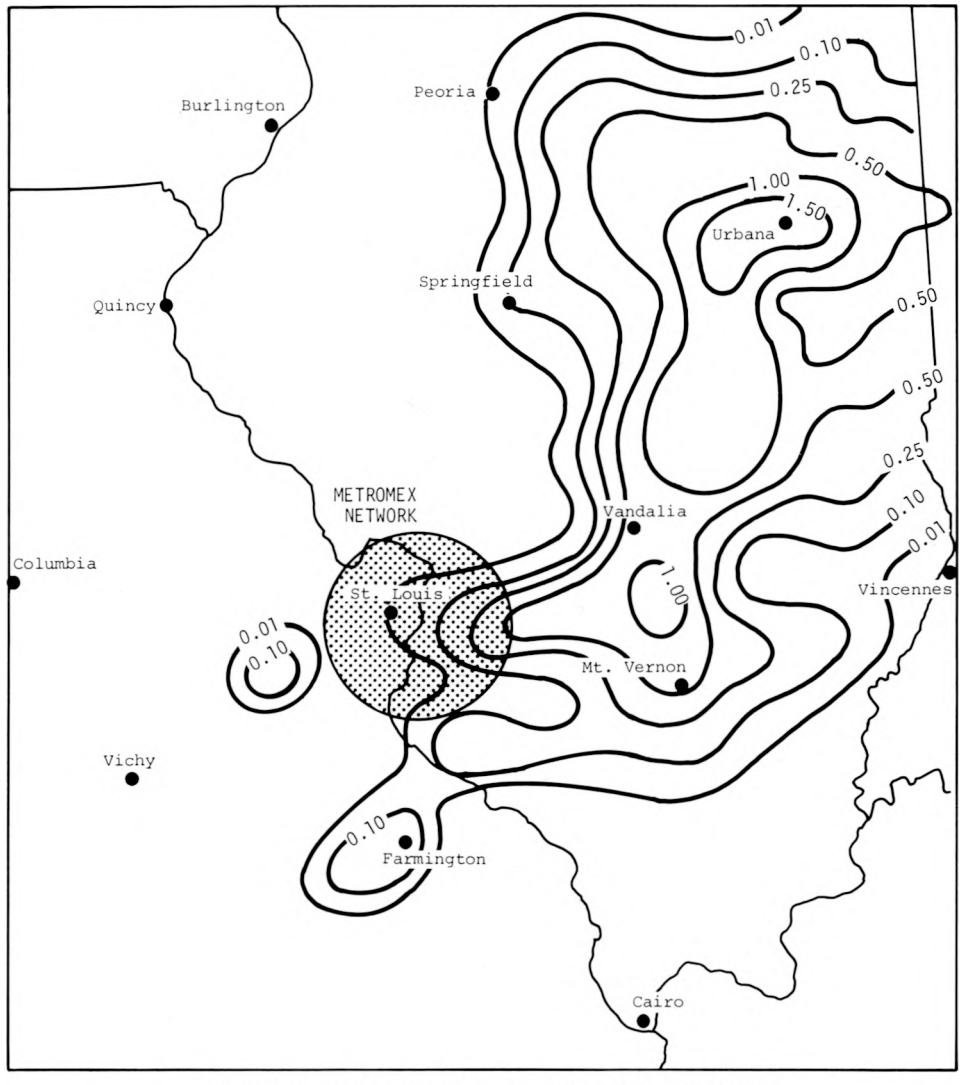

Figure C-6. Regional rainfall patterns for 1300 to 0100 CDT

TOTAL RAINFALL DISTRIBUTION

Figure C-7 shows the distribution of total storm rainfall on the MMX circle for the period 1510 to 2145 CDT. This incorporates the entire period of rainfall under study as a case event. The heaviest rainfall occurred 5-10 mi E of St. Louis where amounts exceeding 2.5 inches were recorded by two raingages. The general area of heavy rainfall ($\geq$ 1 inch) extended ESE from the E portion of the urban area for a distance of 14-15 mi and encompassed approximately 110 mi^2.

The rainfall in the major center E of the city occurred between 1615 and 1930 CDT. The rainfall within the 2.5-inch isohyet (figure C-7) occurred almost entirely in the 1700-1900 CDT period as shown by the mass curves for Sites 118 and 136 in figure C-8. The unusually heavy intensity of this storm center can be demonstrated by reference to point rainfall frequency relations for the region (Illinois State Water Survey, 1970), which show that 2-hr amounts exceeding 2.5 inches will occur on an average of only once in 10 years at any given point. Several rain bursts (periods of higher rates) are shown by the mass curves of figure C-8, and as discussed later, they were associated with the intensification of a quasi-stationary mesoscale system by mergers with other storms in the are

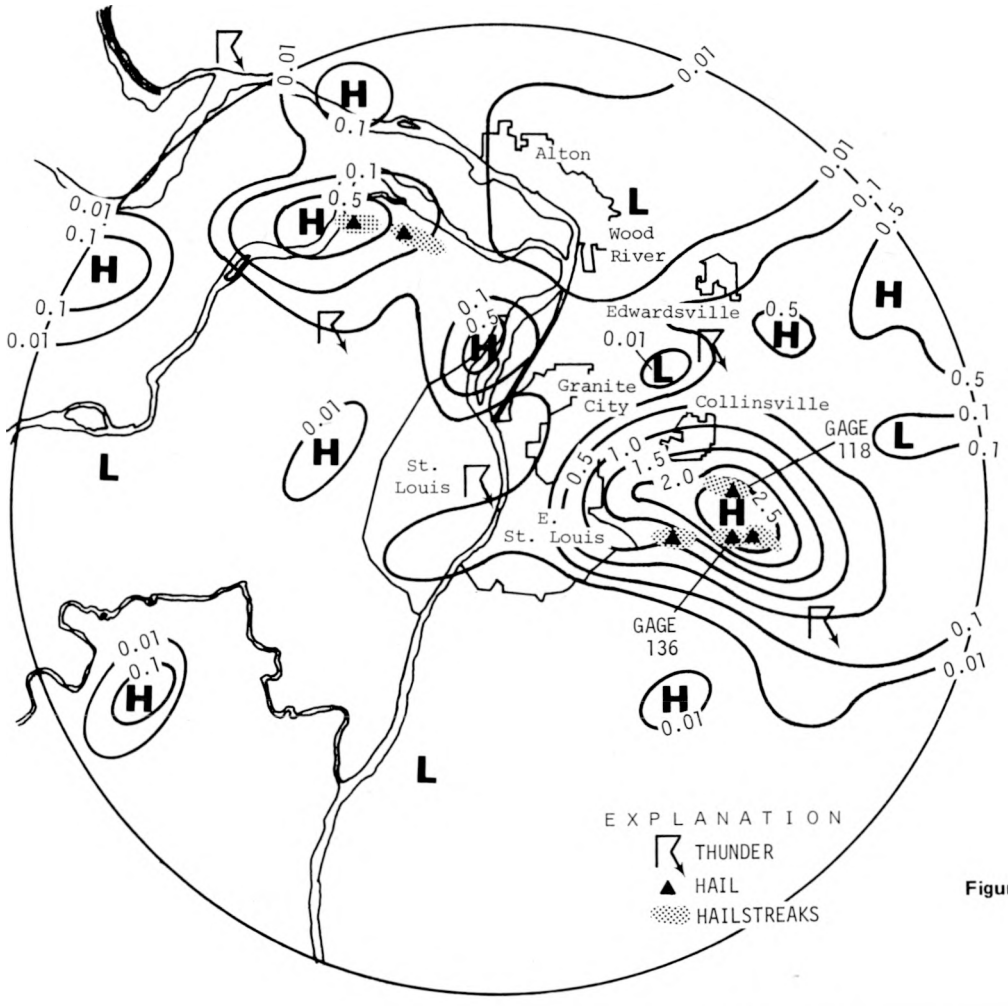

Figure C-7. Total storm rainfall on MMX circle

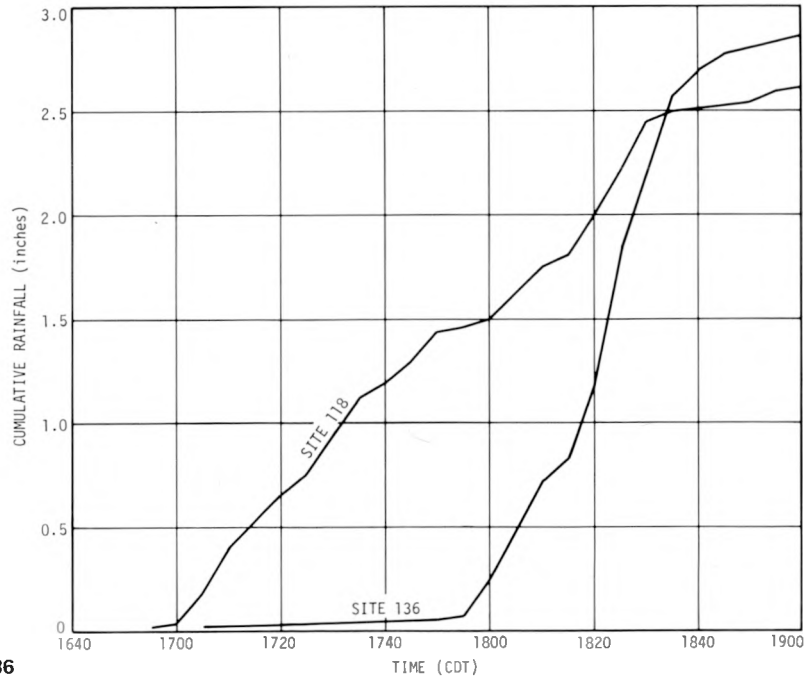

Figure C-8. Mass curves for Sites 118 and 136

Several minor rainfall centers are shown in figure C–7. The 0.5-inch center NW of St. Louis in the bottomlands of the Missouri River resulted from storms in mid-afternoon (1515–1630). The 0.5-inch center NW of Granite City was also a mid-afternoon occurrence. The minor highs SE and E of Edwardsville resulted from a combination of afternoon and evening storms.

RADAR ECHO AND RAINCELL ANALYSES

Analyses of the 10-cm PPI radar data and the raincell data from the MMX raingages revealed in considerable detail how and where individual convective storms developed, their interactions, their exposure to urban influences, and the potential urban effects on their development and/or intensification. In the following paragraphs, the radar and raincell data will be discussed together. They complement each other well and, when viewed simultaneously, provide considerable insight into the apparent urban role in producing the major rainfall center E of the city (figure C–7).

Mid-Afternoon Storms

Altogether, 35 separate surface raincells were identified within the MMX circle during the storm period (1515–2145). Basically, a surface raincell is defined as a closed isohyetal entity within an overall enveloping isohyet of a storm system and is derived from an analysis of 5-min rainfall amounts.

The first raincell (called 1a) was detected at 1515 CDT at Site 27 in the Missouri bottomlands NW of St. Louis, and was the initial contributor to the 0.5-inch high shown in that region on figure C–7. This raincell lasted approximately 30 min, moved in an ESE direction for approximately 8 mi, and produced a maximum 5-min rate of 0.8 in/hr. No radar observations of the raincell were available because it was within the 16-mi ground clutter cutoff of the 10-cm PPI.

The second raincell (1b) developed at 1545 CDT also in these bottomlands. It moved to the E for 10 mi and dissipated SW of Alton at 1635 CDT. These two cells accounted for the bottomlands rainfall high (figure C–7). Hail and thunder were associated with both of these air mass storms. The second storm was much more intense with a maximum rate of 3.32 in/hr from 1550 to 1555 CDT when hail was occurring. Interestingly, these raincells developed where the first Cu clouds within 40 mi of St. Louis began developing at 1300 CDT. This area of clouds was in the Missouri–Mississippi River floodplain NW of St. Louis. The raincell patterns clearly suggest that they were small storms and representative of typical summer afternoon air mass showers. Their formation above the relatively warm and moist bottomlands at the time of maximum heating and evaporation suggests that there may have been local destabilizing influences such as the heating and/or moisture from the bottomlands. The surface temperature (figure C–23b) and dew point patterns (figure C–24b) at 1500 reveal there was a pronounced warm moist anomaly in that area.

The third raincell (called cell 2) developed at 1545 just N of St. Louis and produced the minor high NW of Granite City shown in figure C–7. This storm moved slowly to the E and dissipated at about 1625. The maximum total rainfall of 0.48 inch occurred at Site 77 where the maximum 5-min rate of 3.24 in/hr was recorded from 1555 to 1600. There was no evidence of urban effects on this storm.

In summary, these three mid-afternoon showers had moderate durations (30-50 min) for air mass storms, produced heavy short-period rates in two cases ($>$ 3 in/hr), and each of the two bottomland thunderstorms produced a severe weather event (hail). All three storms moved relatively

slowly as is characteristic of summer air mass storms in this region. The bottomlands storms, which developed first, may have been stimulated in their development by excessive heat and moisture conditions in the river valley. This possibility is supported by subsequent analyses of surface air and dew point temperatures which show relatively high values in early afternoon along the Missouri River and in the bottomlands at the bend of the river, W of Alton. Furthermore, the mixing layer (discussed later) reached cloud base at 1500.

Late Afternoon and Early Evening Storms

The first radar observations with the 10-cm PPI became available at 1607 (figure C-9a) and showed the existence of two echoes. Echo 3 was located E of the river in the St. Louis urban area and echo 4 was situated just W of Granite City. Echo numbers were assigned to be in agreement with raincell numbers. Echo 3 was associated with a raincell (called 3) which was first detected in the surface rainfall at 1605–1610, just NE of the radar-indicated center and SE of Granite City. Echo 4 was apparently associated with raincell 2. The radar echo patterns in figure C-9 were made at a reduced receiver sensitivity (27 dbz) that was sufficient to eliminate very light rainfall on the PPI scope, and thereby to clearly outline the major convective elements.

Figure C-9b shows the radar presentation at 1625. Echoes 3 and 4 were still present and moving in an ENE direction. The development of echo 6 can be discerned on the SW edge of echo 3. Figure C-10a shows the raincell pattern for 1625–1630. A new cell (4) was located SW of Edwardsville, and raincell 3 associated with echo 3 was W of Collinsville. Raincell 2 had dissipated and was replaced by raincell 4.

Figure C-9c shows the radar presentation 15 min later at 1640, and figure C-10b shows the raincell pattern for 1640–1645. The radar presentation shows that echoes 3 and 4 had merged, and echo 6 had become disengaged from echo 3. The merger of 3 and 4 occurred at about 1630. A new echo (5) had developed over the S-central urban area of St. Louis. Figures C-9a and b indicate that echoes 3, 4, and 6 developed over the urban area just E of the river. Thus, it appears that by late afternoon the major source of generation of convective activity was over the urban area of St. Louis with a concentration over the S part of the city.

The raincell map for 1640–1645 (figure C-10b) is of major interest because it shows the development of raincell 6 on the S edge of Collinsville. Later analyses indicated that this raincell was the parent cell in the quasi-stationary mesoscale storm system that was primarily responsible for the extremely heavy rainfall center E of St. Louis (figure C-7). Figure C-9c shows a small echo intensity center near raincell 6, located near the S end of merged echo 3+4. A light raincell (5) that developed in the SW part of St. Louis was associated with echo 5.

Raincells 3 and 4 continued their ENE movement and by 1650 (figure C-10c) had merged E of Edwardsville. This was accompanied by an increase in rainfall rate. Similarly, figure C-10c shows a merger between raincells 5 and 6 as the result of the NE movement of raincell 5 and the quasi-stationary characteristic of 6. The associated radar map for 1652 (figure C-9d) shows the persistence of echo system 3+4 and the slow movements to the E of urban-generated echoes 5 and 6.

The raincell map 15 min later at 1705–1710 (figure C-10d) shows the merged cell 3+4 leaving the network. The merged cell 5+6 continued to show little movement but had intensified greatly to a 5-min mean rate of 2.80 in/hr at its center. By this time, three more raincells could be identified in the major storm region. These included 1) raincell 7, developing SE of the merged system, 2) raincell 8, located NW of the 5+6 center, and 3) raincell 9, in the E urban area, a cell first detected at 1645–1650 W of the river in the same area in which raincell 5 had developed earlier.

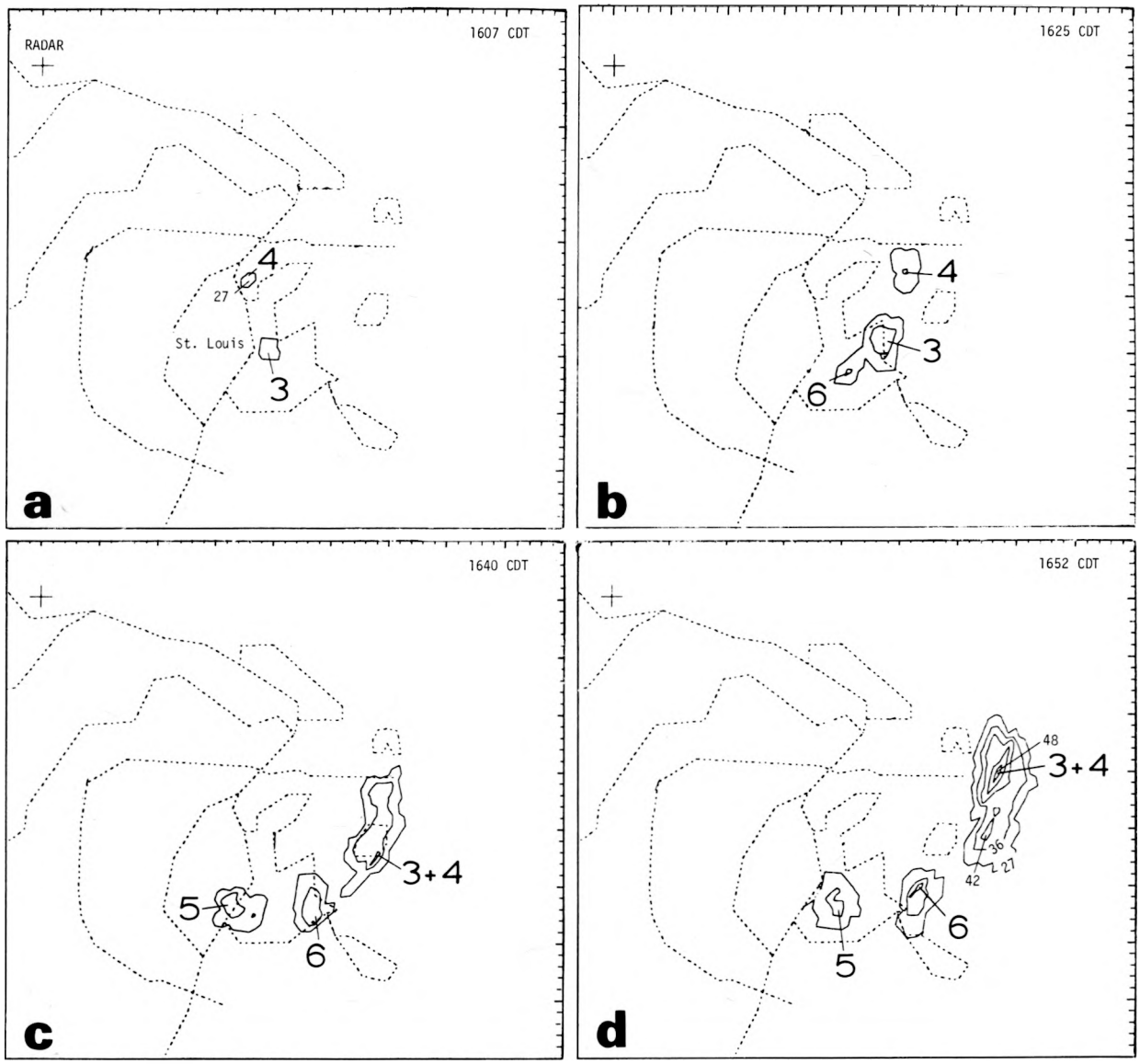

Figure C-9. Radar echo maps for 1607, 1625, 1640, and 1652 CDT (Reflectivity values for contours begin with outer contour at 27 dbz, then 34, 38, 42, and 49 dbz)

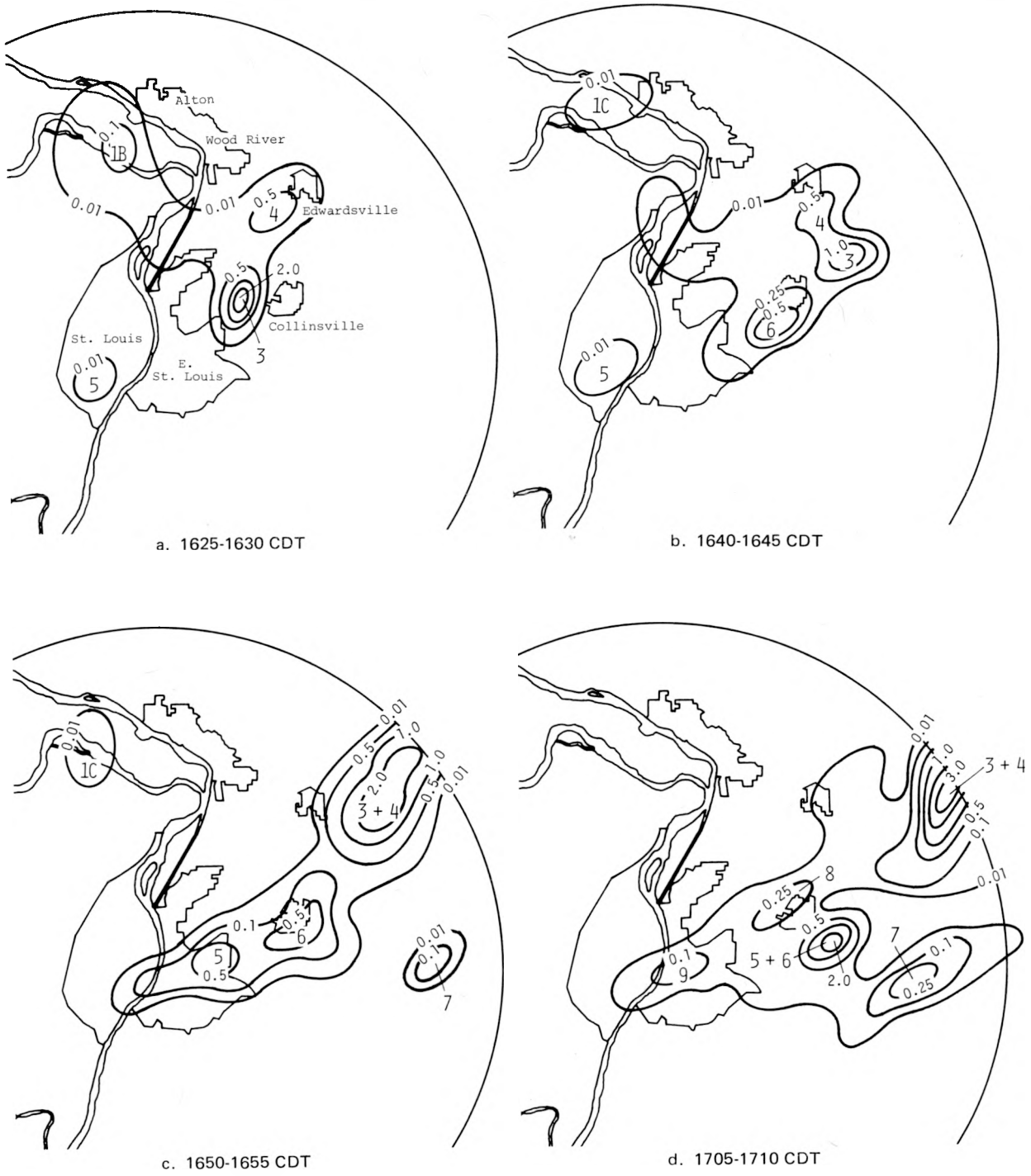

Figure C-10. Raincell maps for 1625, 1640, 1650, and 1705 CDT

The radar map for 1705 (figure C–11a) shows echo 5 overtaking echo 6 and near a merger state. Also, a new echo intensity center (8) appeared at the E edge of the urban area. Echo system 3+4 was still very much in evidence, although it could no longer be followed in the surface rainfall pattern because it had moved out of the MMX circle.

Progressing 10 min to 1715, figure C–12a shows the persistence of merged cell 5+6 near Site 118. Raincells 8 and 9 had merged by this time, and raincell 7, a relatively weak cell, was still identifiable. The radar map for 1720 (figure C–11b) shows the merged echo system (5+6+7+8) remaining quasi-stationary E of the urban area and 3+4 still in existence.

The raincell map at 1730–1735 (figure C–12b) indicates a large single cell in the storm area which resulted from the ingestion or merger of raincells 7, 8, and 9 into the parent circulation that originated with raincell 6. Heavy intensities with 5-min rates exceeding 2 in/hr were occurring at the center of the merged raincells. The equivalent radar map for 1730 (figure C–11c) also shows a single echo mass associated with echo system 5+6+7+8.

Examination of the raincell map 10 min later at 1740–1745 (figure C–12c) shows persistence of the quasi-stationary rain system. At this time, another raincell had developed at the E edge of the urban area. At 1742 two new echoes were present. Echo 11 had just developed over the SE urban area. Echo 12, which was first observed at the SW edge of Collinsville a few minutes earlier, was building to the S.

Figure C–13a shows the radar echo pattern at 1752 and the major changes that had taken place within the previous 10 min. This is also indicated on the raincell map in figure C–12d. The radar map indicates that the original merged echo system 5+6+7+8 was drifting very slowly to the E. Echoes 11 and 12 had merged by this time, grown substantially in areal extent, and intensified, as indicated by a maximum gain step of 42 dbz compared with a maximum of 33 dbz a few minutes earlier. Also, a new echo (13) had developed over the S urban area and was about to merge with echo 11+12.

The raincell pattern for 1750–1755 (figure C–12d) had expanded and intensified in the previous 10 min. The parent raincell (6) NE of Belleville showed a central intensity of 3.44 in/hr. New raincells 11, 12, and 13 had developed. Raincell 11, associated with the merged echo system 11 and 5+6, had a central rate of 3 in/hr. At this time, a division of the storm into two major systems was apparent in the surface rainfall pattern.

The radar map for 1802 (figure C–13b) indicates a complete merger of all echo systems into a single solid echo system. This represents the merger of 5 major echoes, two of which had been involved in earlier mergers. The raincell pattern (figure C–14a) also shows a single system with three centers corresponding to the earlier mergers of raincells 5 to 9, along with merged raincell 11+13 and raincell 12. The heaviest rate (2.89 in/hr) was still associated with the merged system established by the original parent cell (6), but a very heavy rate (2.52 in/hr) was recorded in the other merged system (11+13) in the region where the radar indicated a merger of 13 with 11+12. Hail was also recorded just after this merger.

The rainfall intensity increased in the next few minutes and reached a maximum in the 1825–1830 period (figure C–14b). At this time, the merged system had an exceptionally heavy 5-min rate of 7.77 in/hr at Site 136 where total storm rainfall maximized (figure C–7). This 5-min rate corresponds to an intensity expected only once in 25 years at any given point in this area (Illinois State Water Survey, 1970). Also, three new raincells (14, 15, and 16) occurred on the periphery of the major mesoscale system. Raincell 14 formed in the 1810–1815 period over the SE urban area, whereas 15 and 16 developed on the E side of the major system. The radar map for 1822 (figure C–13c) indicates a single major system extending to the E from the SE corner of the urban area with a split-off of a portion of this mass on the E side of the system.

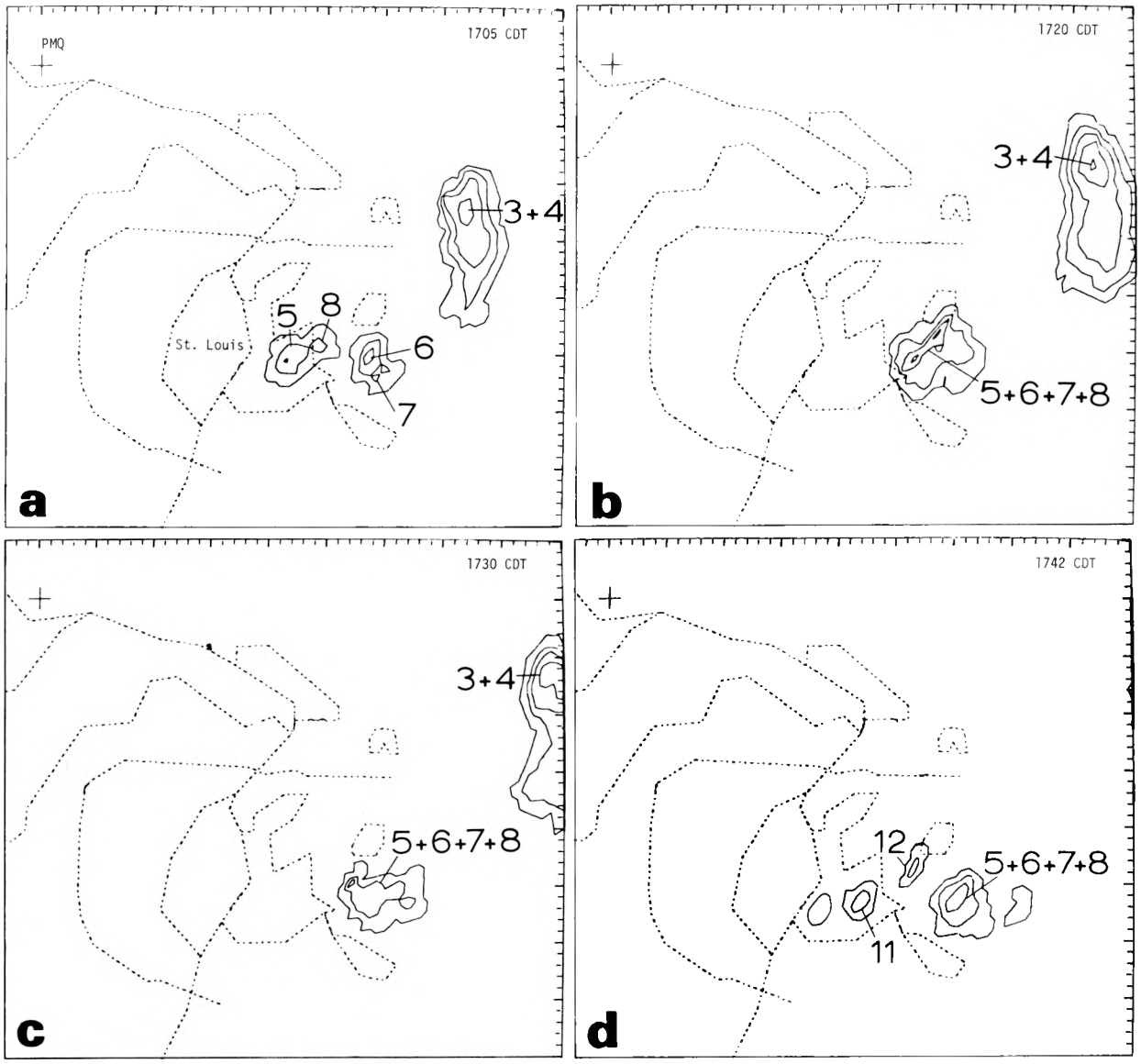

Figure C-11. Radar echo maps for 1705, 1720, 1730, and 1742 CDT (Reflectivity values for contours begin with 27 dbz, then 34, 38, 42, and 49 dbz)

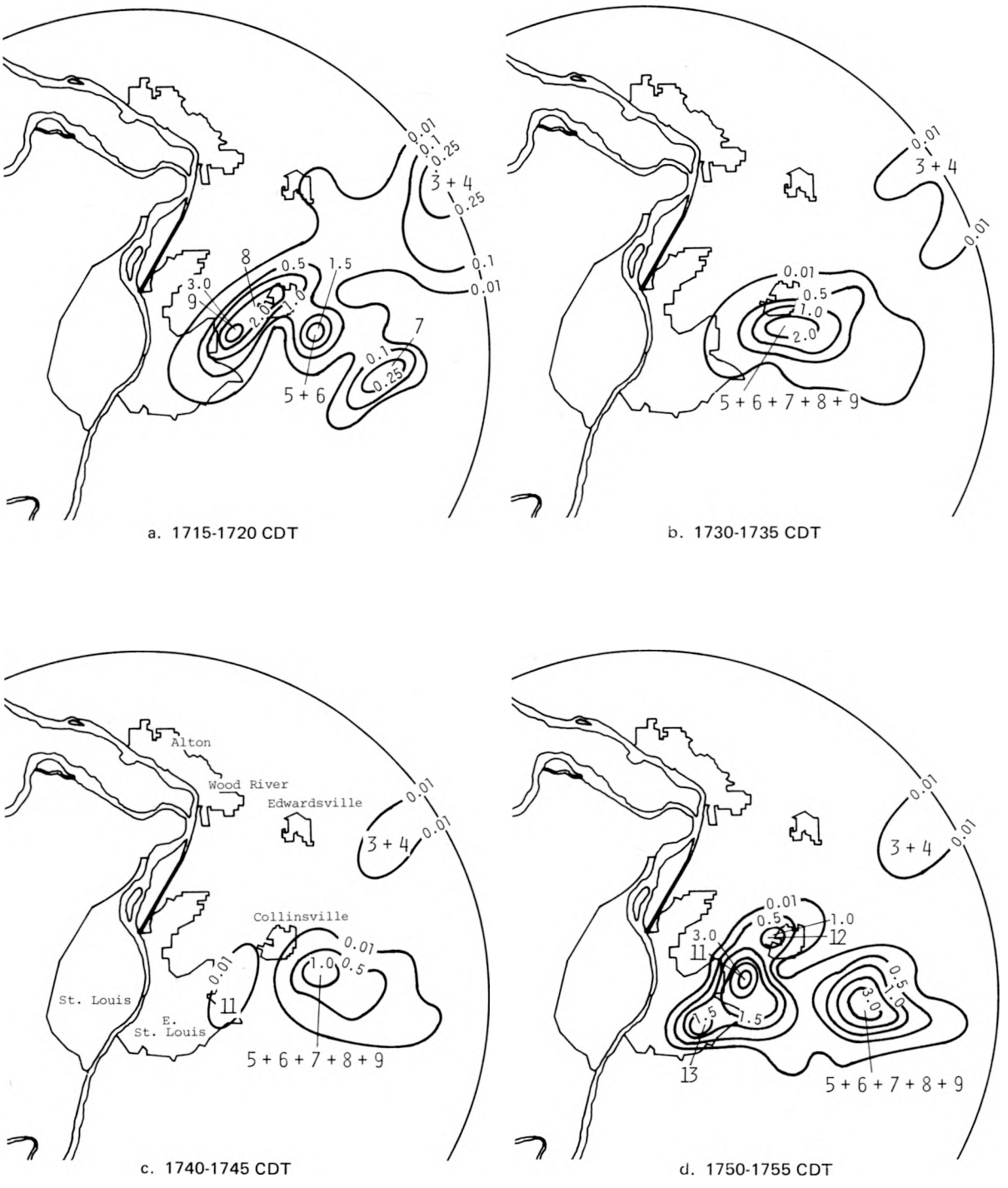

Figure C-12. Raincell maps for 1715, 1730, 1740, and 1750 CDT

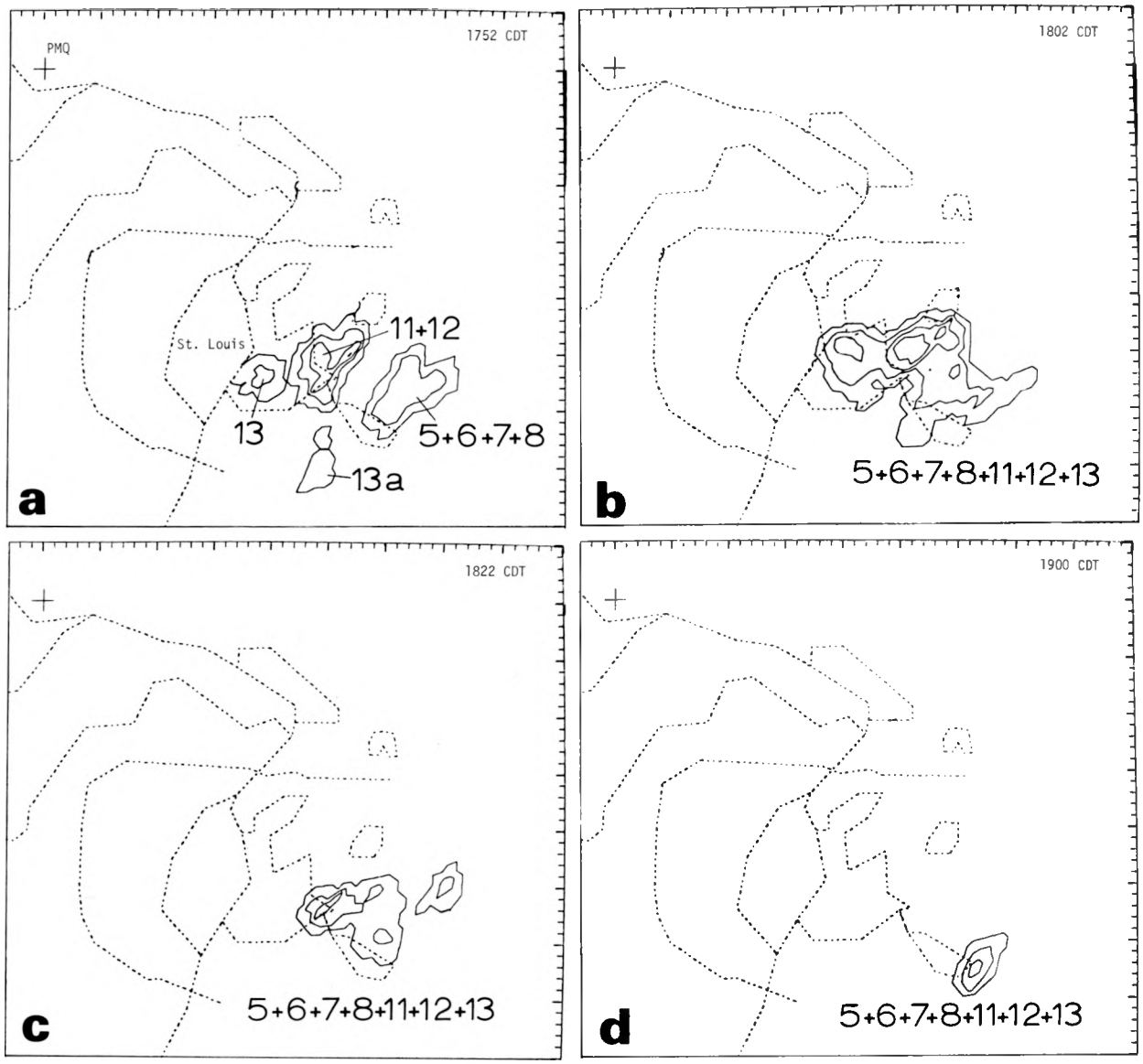

Figure C-13. Radar echo maps for 1752, 1802, 1822, and 1900 CDT (Reflectivity values for contours begin with 27 dbz, then 34, 38, 42, and 49 dbz)

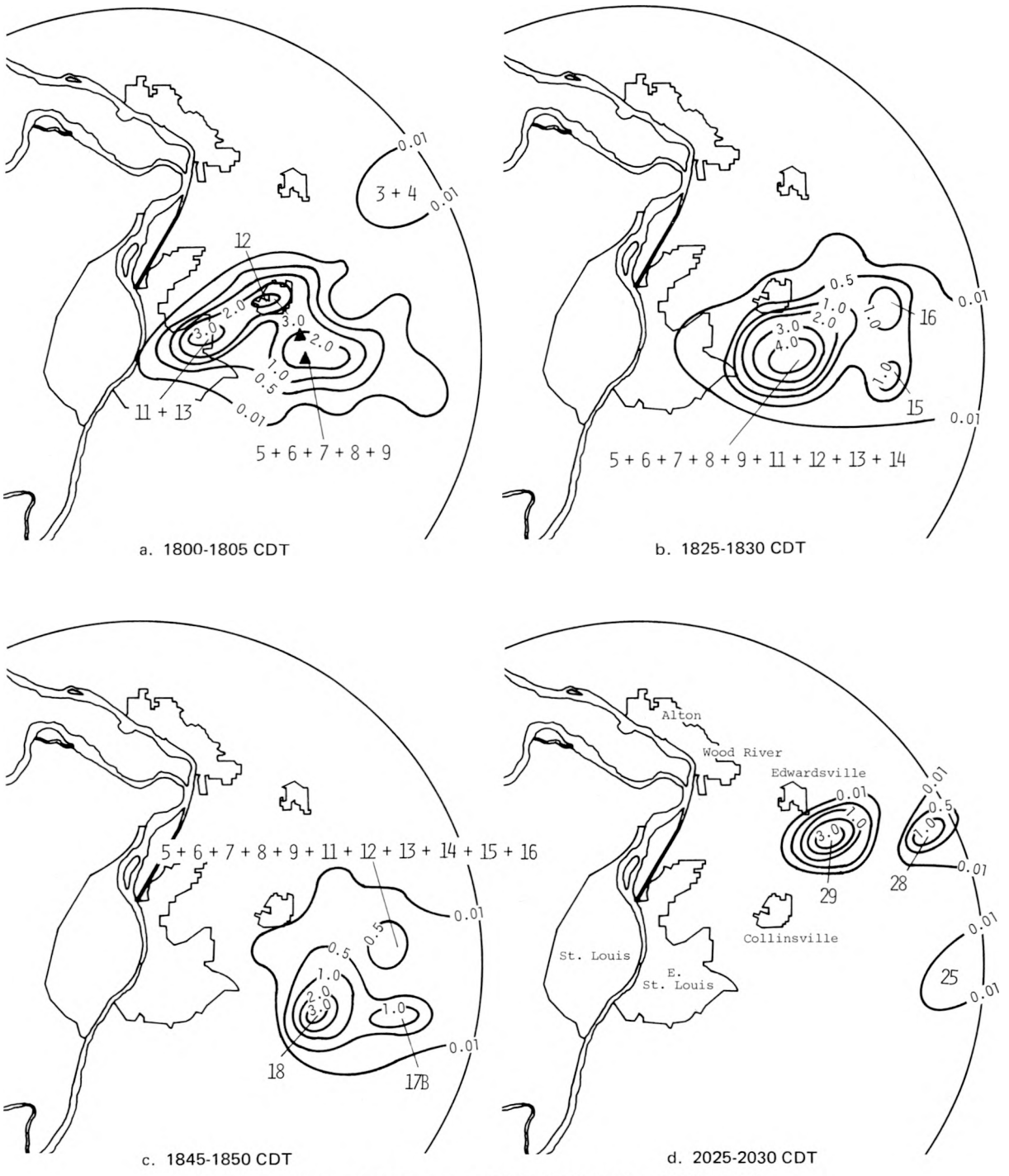

Figure C-14. Raincell maps for 1800, 1825, 1845, and 2025 CDT

The intensity of the major mesoscale system then gradually decreased as the system began slowly drifting to the NE. At 1845 (figure C–14c), the remainder of this system was centered near Site 120. Another raincell (18) which had developed on the eastern edge of Belleville at about 1835 was the major rain producer at this time with a central rate of 3.26 in/hr. Raincell 18 drifted slowly ENE at 10-12 mi/hr, decreased in intensity, and dissipated by 1935.

Figure C–13d shows the radar presentation at 1900. By this time, the rain system had largely dissipated except for the Belleville cell (18). By 1945, all rain had ended in the area encompassed by the major storm center E of the city.

Figure C–15a-c has been constructed to illustrate the magnitude of the rain generated from the mesoscale storm system E of the urban area on 11 August. Figure C–15a shows the total rainfall associated with 1) the parent raincell (6) and 2) that from all those cells (both before and after merger) that eventually merged to form the mesoscale system established by raincell 6. Figure C–15b shows the rainfall produced by raincell 6 plus that contributed by the other cells *after* they merged with the parent mesoscale system. Figure C–15c indicates the percent of total storm rainfall on 11 August that occurred with raincell 6 and the other cells after their merger with the parent system. At Site 136 where the storm (network) maximum of 2.86 inches was recorded, 97% of the rain was produced by the mesoscale system. At Site 118, where 2.62 inches fell, 94% of the total was associated with the parent system. Reference to the mass curves on figure C–8 shows that 2.51 inches of the 2.86 inches at Site 136 occurred in a 50-min period, 1755–1845. This intense rainfall started after the merger of the cells.

Evening Storms

Two areas of showers occurred on the MMX circle during the evening. Several light showers which contributed very little to the total rainfall occurred in the NW part of the circle. Another area of convective activity occurred in the E part of the circle in mid-evening. Figure C–14d shows the raincell pattern at 2025–2030 when the activity was at its peak. The radar indicated that all of the showers developed to the E from the Edwardsville and Collinsville area. None developed over the St. Louis urban area. All rain intensities in the evening storms were relatively light, except for a short time in the two raincells SE and ESE of Edwardsville in figure C–14d. The heaviest storm amount, 0.43 inch, was recorded in the storm just SE of Edwardsville (figure C–14d). There is no evidence indicating that the evening showers were urban-related.

Raincell Initiations and Mergers

The location of raincell initiations, as indicated by the 5-min rainfall maps, are shown in figure C–16a. They have been divided into several groups with dashed lines. Initiation times and maximum 5-min rainfall rates achieved sometime later in their life are shown for each. The locations of mergers between individual convective elements are indicated in figure C–16b. These convective elements consisted of one or more raincells that constituted distinct isohyetal systems separated in space at the surface.

Figure C–16a provides certain information relevant to the potential urban effects in the storm of 11 August (figure C–7). There was a total of 35 raincell initiations detected in the 2100 mi^2 network. Of these, 10 or 29% occurred in or within a short distance of the St. Louis urban area in a zone extending from SW St. Louis, ENE to the Collinsville area. Two cells formed just downwind (E) of Alton-Wood River, and two other cells formed just downwind of Belleville, which is considered part of the urban area of St. Louis. The vertical extent and location of urban effluents

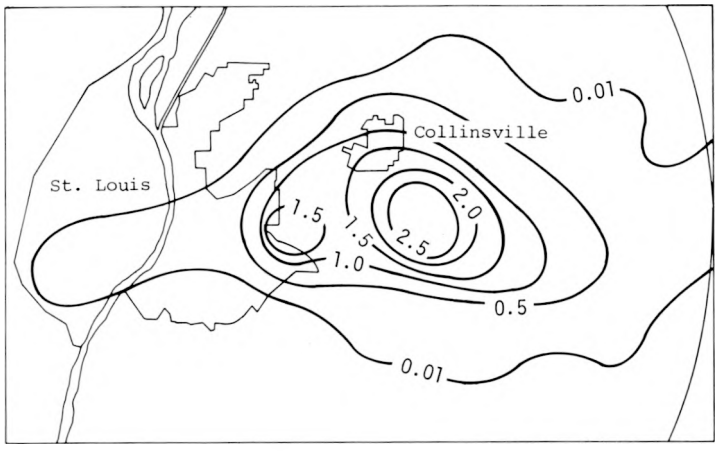

a. Total rainfall produced by all raincells associated with quasi-stationary mesosystem (before and after mergers)

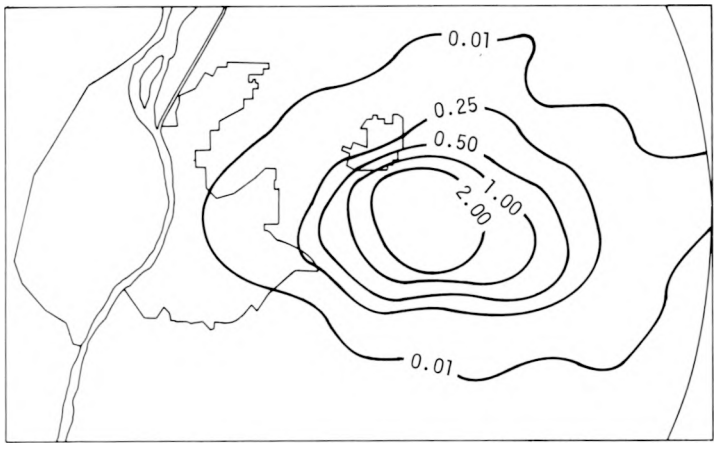

b. Total rainfall from parent raincell 6 and raincells after merger with mesosystem

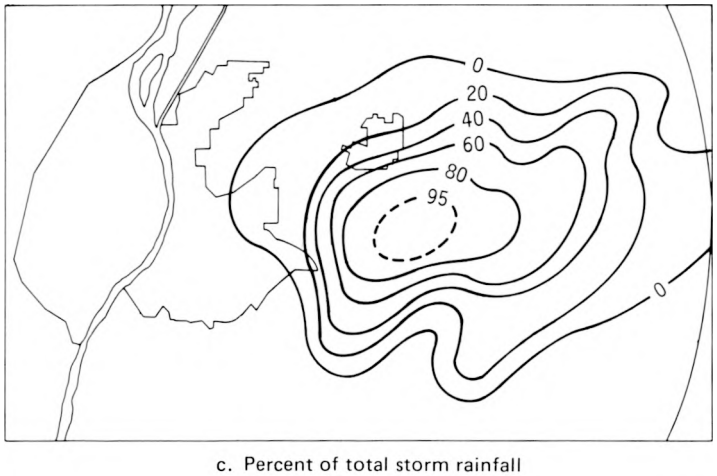

c. Percent of total storm rainfall produced in mesosystem

Figure C-15. Rainfall associated with mesoscale rain system

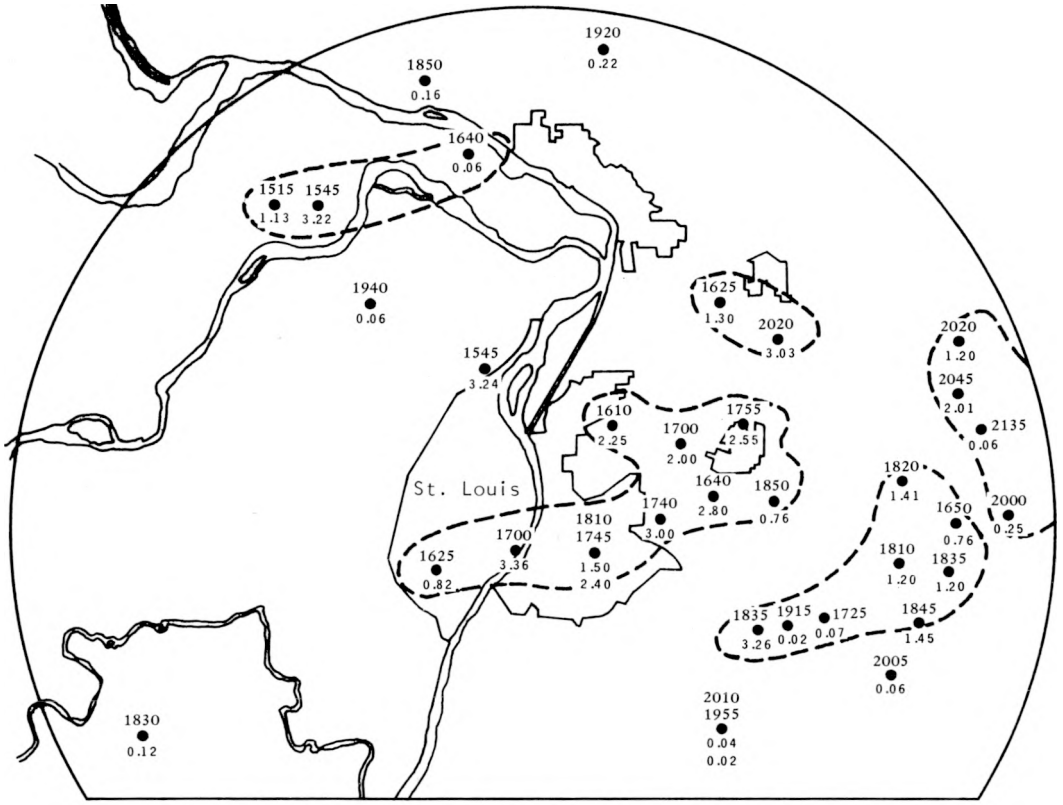

a. Raincell initiations with maximum 5-min rainfall rates

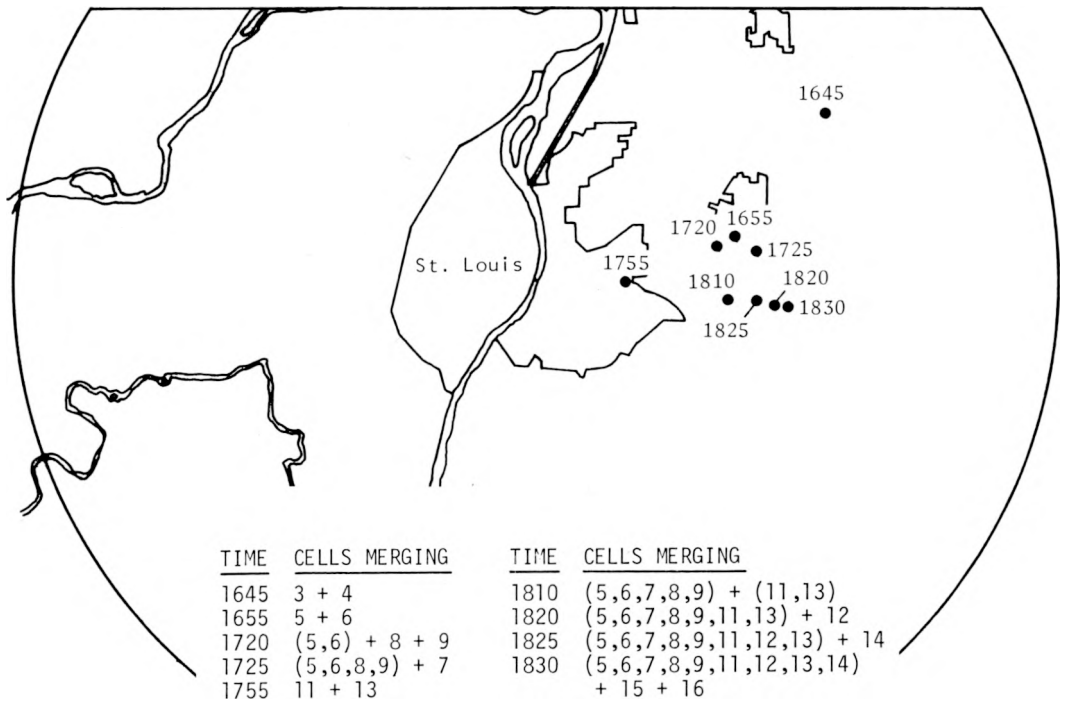

TIME	CELLS MERGING
1645	3 + 4
1655	5 + 6
1720	(5,6) + 8 + 9
1725	(5,6,8,9) + 7
1755	11 + 13

TIME	CELLS MERGING
1810	(5,6,7,8,9) + (11,13)
1820	(5,6,7,8,9,11,13) + 12
1825	(5,6,7,8,9,11,12,13) + 14
1830	(5,6,7,8,9,11,12,13,14) + 15 + 16

b. Raincell mergers

Figure C-16. Raincell initiations and mergers

during the 1300–1445 CDT period (see figures C–3, C–4, and C–26) help establish that thermal plumes, moisture plumes, and aerosols generated by the urban area extended more than 10 mi E of the Mississippi River at the 3000 ft AGL level. This finding establishes that 14, or 40%, of the raincell developments on 11 August were likely to have been urban-affected at their formation time.

Other raincell initiations farther downwind E of Collinsville and NE of Belleville cannot be eliminated as potentially urban-affected, but the probability is considerably less. However, this study suggests that the cells that formed downwind of Collinsville and Belleville in the 1700–1830 period were indirectly related to urban effects because of the large convergence zone likely to have been associated with the intense storm E of St. Louis. This mesoscale rain system was definitely supported by cells developing over the urban area, as pointed out in previous discussions of the raincell and radar data. The parent system evolving from raincell 6 ingested 11 separate raincells into its circulation during the life of the storm. All of the rainfall shown within the 1-inch isohyet in figure C–15a occurred with those raincells classified above as potentially urban-affected. Thus, they were the prime contributors to this heavy rainstorm (figures C–7, C–15).

The merger locations in figure C–16b all occurred within the major mesoscale system that produced the extremely heavy rainfall E of the city. As indicated earlier, mergers are frequently associated with intensification of convective rainfall and hail, and are a prime cause of severe rainstorms in Illinois.

Radar Echo Initiations and Mergers

Figure C–17 shows the location of radar echo system formations and mergers. A radar echo system was defined as an echo entity separated in space from other echoes and which may consist of one or several intensity centers within its enveloping isoecho. Of the 10 echo systems detected in the area of radar observations, 5 developed directly over the S-central to SE part of the urban area. Two others, one on the N side of the city and the other just SW of Collinsville, also have a high probability of urban effect. Thus, the radar observations show the urban area as the major region of development of convective activity that produced the heavy storm E of St. Louis. Furthermore, 3 of the 5 echo system mergers were associated with this heavy storm system. Thus, the radar echo initiations and mergers support the raincell analyses of similar events discussed above, and show that the major storm system was closely related to the development of convective activity in the urban area, and that sustainment and intensification of the mesoscale system was associated with the ingestion or merger of individual convective elements by the quasi-stationary mesoscale circulation E of the city.

Figure C–18 shows the inititation of radar echo intensity centers. As indicated above, an echo system or entity could have one or more intensity centers, depending upon whether it was a single-cell or multicellular storm. Figure C–18 shows that the urban area was the major source of intensity center developments. Of the 23 initiations detected, 14, or 61%, were in the urban or near-urban area extending from St. Louis to Collinsville and also including the Belleville region. The area of most frequent initiation (dashed line in figure C–18) extends ENE from S-central St. Louis for a distance of 25-30 mi, a distance which corresponds closely to the results of an earlier climatology study (Huff and Changnon, 1972) with respect to the urban area-of-effect.

The 3-cm RHI (TPS-10) radar was operated in a range-height mode to direct aircraft flights on 11 August. During portions of the storm period, its signal intensities were digitized and then recorded on tape by using the 10-cm PPI (FPS-18) signal processor. Data available for one interesting period, 1740–1805 CDT, were used to develop computer-drawn height-distance cross

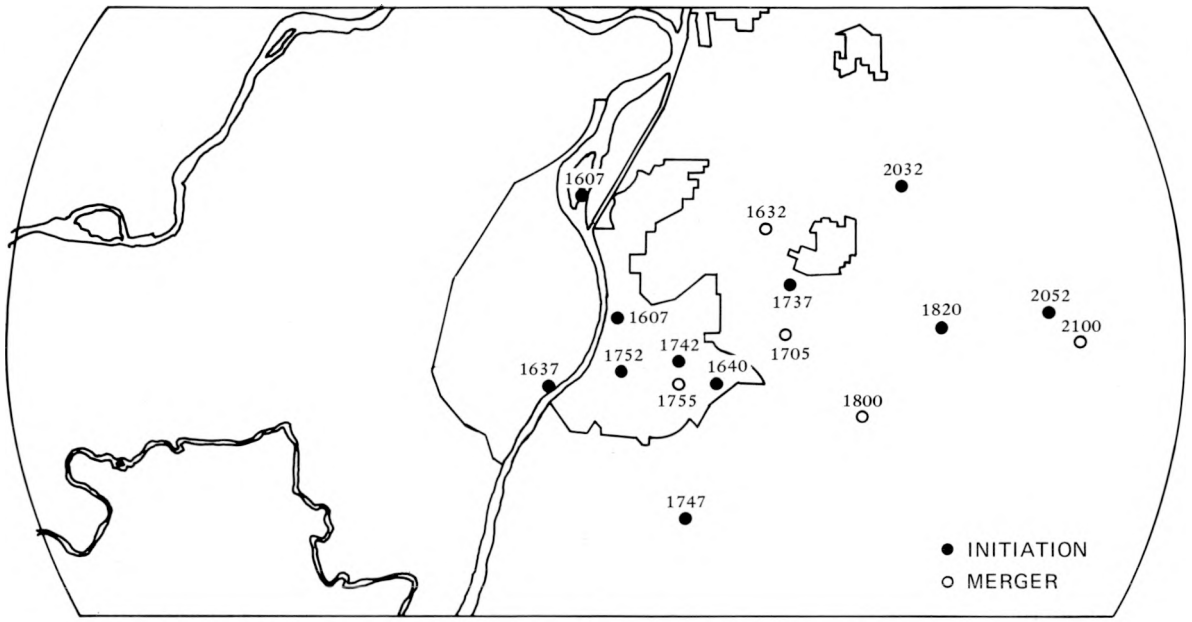

Figure C-17. Initiations and mergers of radar echo systems

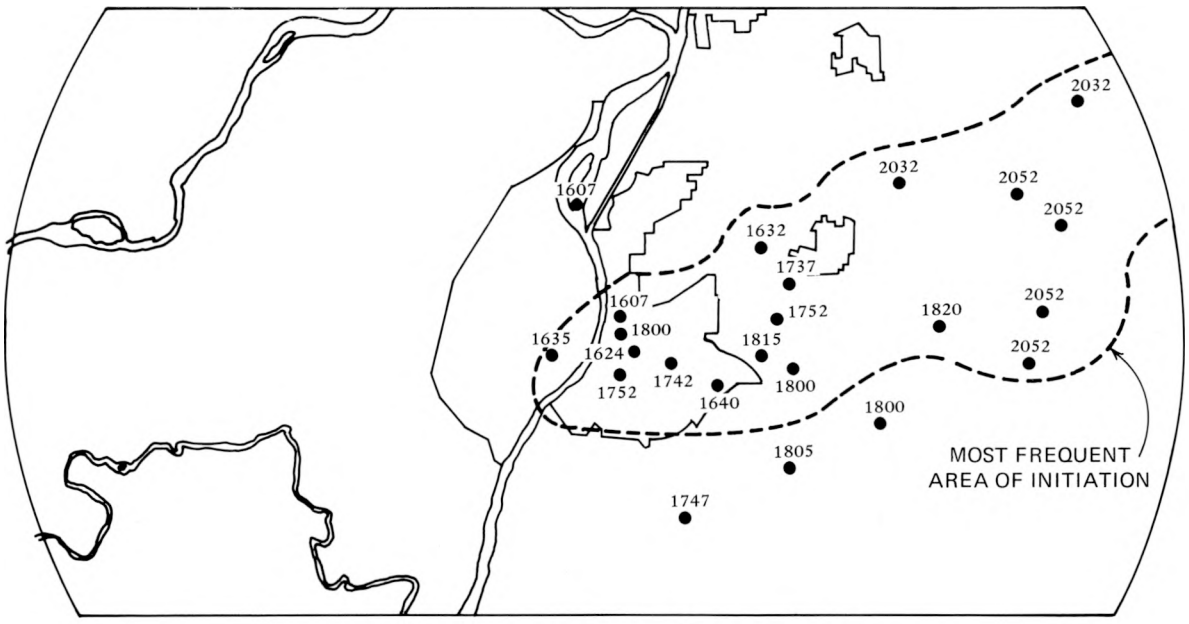

Figure C-18. Initiations of radar echo intensity centers

sections along vertical planes through two developing raincells (11 and 12) located on the rear edge of parent cell 6 shown on figure C-12a-d.

Figure C-19 shows a time sequence through the developing cores of cells 11 and 12. Echo intensity contours are for 34, 36, 38, and 42 dbz. These planes have WSW-ENE orientations through East St. Louis, Collinsville, and areas to the E. These show the 'first echoes,' based on these moderate reflectivities. Echo (raincell) 12 grew rapidly with rain (34 dbz) reaching the ground within 14 min after its initial appearance at 1740. New rear-side growth is suggested by the tilted shape of echo 12 at 1754, and a small front-side cell (12a) also appeared. Cell 11 also produced precipitation rapidly, reaching the ground at 1756, 10 min after its first appearance. Its shape at 1754, 1756, and 1800 also displayed a tendency to lean to the left (upshear) which is due to the new cell development on its rear (W) side. A double core of 36 dbz was present in cell 11 at 1754. Cells 11 and 12 both moved to the ENE at the same speeds, 30 km/hr. However, their horizontal growths led to a mid-level (4 to 8 km above ground) merger by 1800 which remained even as cell 11 began to dissipate at 1805. This merger was a part of the massive merger of most rain echoes at 1802 and detected by the 10-cm PPI radar (figure C-13b). The merger of cell 12b (located adjacent to and to the ENE of cell 12) with cell 12 also occurred by 1805, forming a major cell (maximum reflectivity > 42 dbz) with an apparent 'overhang' and weak echo area due entirely to the merger of the new cell.

The echo height history (figure C-19) illustrates four important facts about the 11 August storms: 1) more than half of the initial echoes of moderate intensity formed above 4.5-km level (above the freezing level) indicating that the ice phase was important in the rain process; 2) the precipitation and echoes grew rapidly after detection indicating that great instability was present; 3) echo shapes indicated the rear (W) side inflow and development area; and 4) the merger of echoes occurred first at mid-cloud levels of 4 to 8 km where precipitation development was most active. Hence, the tracer materials released at cloud base on 11 August could have been exchanged between the areas of active preciptation development.

Figure C-20 shows the height distribution of radar (3-cm RHI) detectable liquid water during four select times in a 1-hr period. The reflectivity Z has been converted to liquid water content M through the relation $M = 2.6 \times 10^{-3} Z^{0.6}$, and integrated in 0.5-km thick layers. The liquid water values given are for the entire echo mass (all cells) E of St. Louis (see figure C-13), including echoes 5, 6, 7, 8, 11, 12, and 13. Total mass values for these four 1-min periods also are listed in figure C-20.

At 1740, the curve of liquid water shows the profile for the then mature echo system 5+6 (as in the 1730 radar echo map on figure C-11c). The rapid development of new radar echoes 11, 12, and 13 by 1752 (as shown in figure C-13a) was accompanied by considerable vertical growth (figure C-20) and a large accumulation of water in the 3- to 6-km level. The merging of all echoes by 1802 (figure C-13b) relates to an even greater increase in liquid water (figure C-20), followed by a dumping process as reflected by a reduction in the profile and echo height at 1812 CDT. At the surface, this enormous dumping of water was accompanied by hailfalls and exceptionally heavy rain rates (figure C-14). Although these 3-cm radar data must be viewed with caution because of potential attenuation problems, they support and help explain how the new storms and their merger resulted in vertical growth, hail formation, an enormous intake of moisture, and a conversion to liquid water in a mid-level accumulation zone, followed rapidly by release of water and excessive rain rates. Mergers of individual storms are frequently associated with heavy rainstorms in Illinois (Huff, 1967; Huff and Changnon, 1964; Huff et al., 1958).

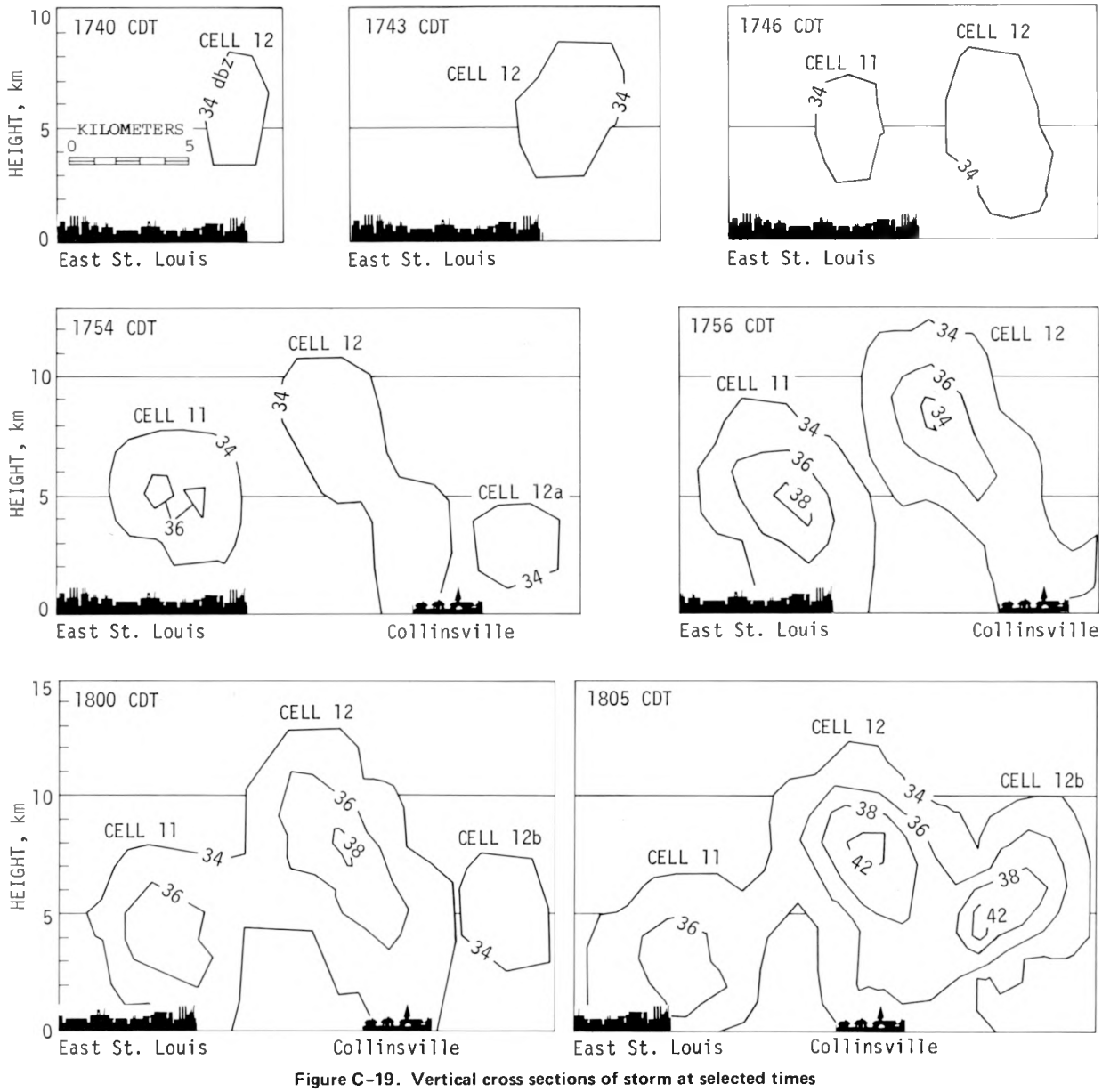

Figure C-19. Vertical cross sections of storm at selected times

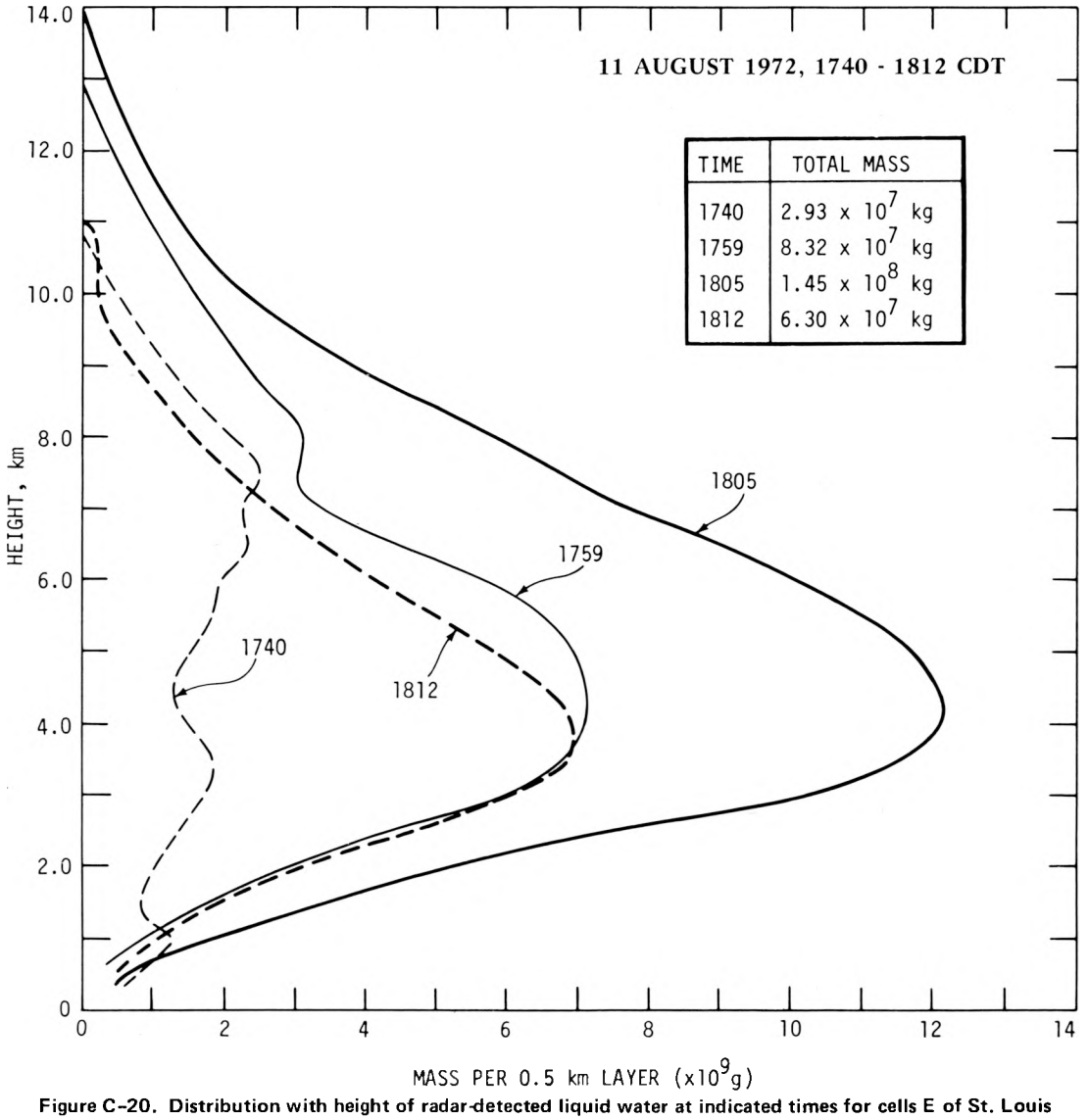

Figure C-20. Distribution with height of radar-detected liquid water at indicated times for cells E of St. Louis

Movement of Storms

Storm movements were determined from tracking radar echoes and raincells. Both types of movement analyses showed a general movement to the E of the convective storms with nearly all storms moving toward ESE, E, or ENE. A few selected raincell movements in various parts of the MMX circle are shown in figure C-21 to illustrate the type of movements and the distances involved.

Echo-Raincell Summary and Conclusions

Analyses of raincell and echo data (10-cm PPI) showed that the initial thunderstorms and rainshowers developed in mid-afternoon in the NW part of the MMX circle in the bottomlands of the Missouri River. It is quite likely that these air mass storms, which were accompanied by thun-

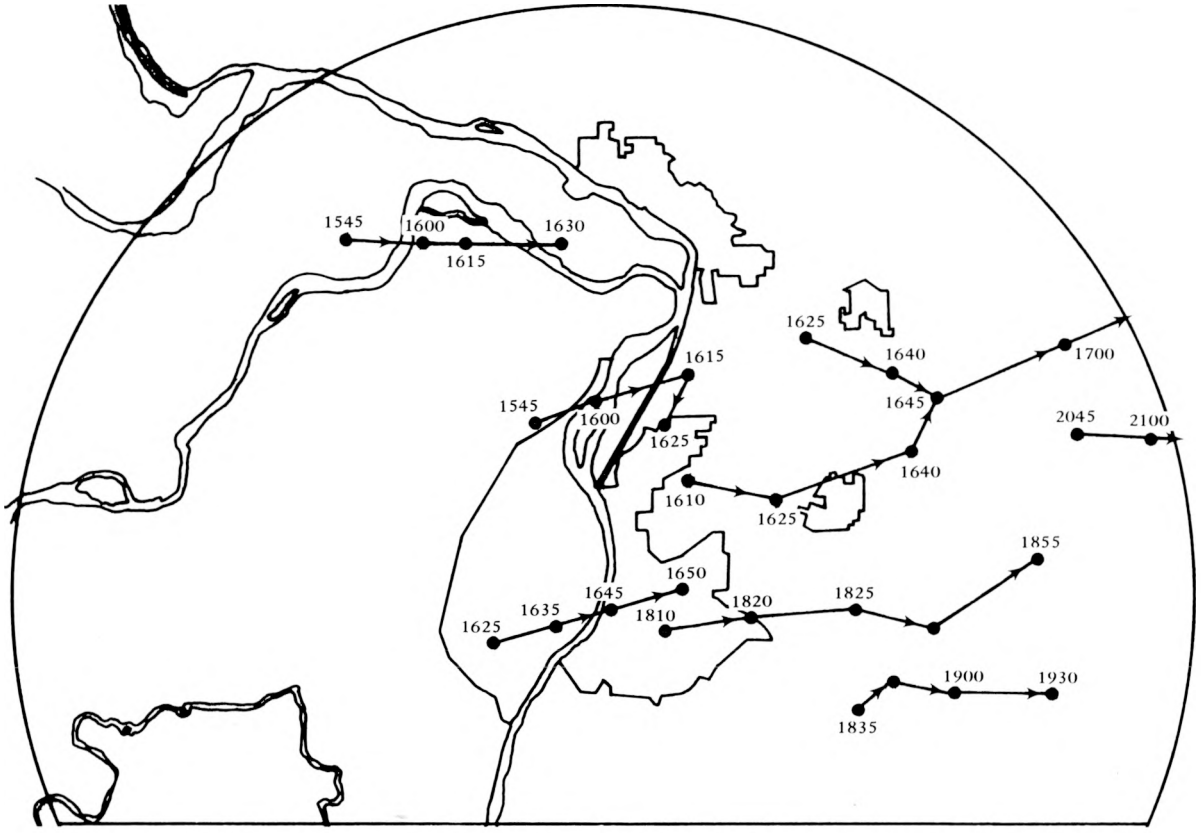

Figure C-21. Raincell movements

der and hail, were stimulated in their development and/or were intensified after formation by relatively hot moist pockets of air generated in the bottomlands. Surface air temperature and moisture patterns for the mid-afternoon (figure C-23b, C-24b) support this conclusion by indicating the bottomlands to be an extremely warm (93F) and moist (dew point of 73F) area in the circle.

The radar and raincell analyses provided strong evidence that the major storm system, centered approximately 7 mi E of the urban boundary, was related to urban effects. A quasi-stationary mesoscale system appeared to develop from a raincell first detected about 5 mi from the urban boundary, and this system maintained itself through the ingestion or merger of other cells with the parent system. Of the 35 raincells detected in the network on 11 August, 40% developed where surface conditions (temperature, moisture, aerosols) from the urban area reached cloud levels. The parent system merged with or ingested 11 separate convective storms of which several were intense multicellular storms. The most intense rainfall and hailfall in the storm center occurred following a major increase in storm heights, an enormous ingestion of liquid water, and a major merger about 1800. The echo analyses strongly supported the raincell analyses. They showed that the major storm was associated with a quasi-stationary echo system which maintained itself by merging with other echo systems, and that the most frequent region of echo development was within the urban area.

THUNDER ANALYSES

Thunder data from 3 recording sites (TYV, SLU, and EDW) and from 4 observer stations (PMQ, STL, BLV, and WLO) were investigated to describe thunderstorm activity in the MMX circle. All sites except TYV in the SW and WLO in the extreme S of the circle (see figure B-2) reported thunder sometime during the afternoon and/or evening of 11 August, and are plotted on figure C-7.

There were two periods of thunder activity in the area on 11 August. The first and most significant period occurred during the afternoon, beginning at 1525 CDT in the NW area of the circle and ending nearly 4 hr later (1915) in the SE part of the circle. The second period of thunder activity occurred from 2020 to 2035 and at only one station, EDW.

A principal analytical activity concerned efforts to identify which of the 35 raincells on this date were thunderstorms, and the time that they became thunderstorms. Table C-1 lists the 35 cells including the time of the first rain, the time that the rain rate first was > 0.25 in/hr, and the time when thunder began. Inspection of these data reveals that the raincells can be grouped into four categories based on space and time differences, as shown in table C-2. The data did not allow determination of the thunderstorm status of 4 raincells. Of the remaining 31 raincells, 55% were thunderstorms. Notably, 90% of the afternoon cells in and E of the city were thunderstorms.

Table C-1. Rain and Thunder Times (CDT) for Raincells on 11 August

Cell	*Rain start*	*Time rain rate >0.25 in/hr*	*Time when T or TRW began*	*Cell*	*Rain start*	*Time rain rate >0.25 in/hr*	*Time when T or TRW began*
1a	1515	1515	1525	17	1835	1835	1840
1b	1545	1545	1545	18	1835	1840	1850
1c	1640	never	never	19	1850	1850	unknown
2	1545	1550	1605	20	1850	never	never
3	1610	1610	1615	21	1915	never	never
4	1620	1625	1625	22	1920	never	never
5	1625	1645	1630	23	1940	never	never
6	1640	1640	1645	24	1955	never	never
7	1650	1705	never	25	2000	2005	never
8	1655	1700	1705	26	2005	never	never
9	1655	1710	1655	27	2010	never	never
10	1725	never	never	28	2020	never	unknown
11	1740	1745	1745	29	2020	2020	2020
12	1750	1750	1750	30	2045	2045	unknown
13	1750	1750	1750	31	2120	never	never
14	1810	1810	1810	32	2125	never	never
15	1815	1815	1820	33	2140	never	never
16	1820	1820	unknown				

Table C-2. Raincell-Thunderstorm Comparisons

	Number by location				
Thunderstorm class	*Cells in W, afternoon*	*Cells in and E of city, afternoon*	*Cells in N, evening*	*Cells in E, evening*	*Totals*
Unknown	0	2	0	1	3
No thunder	1	2	3	5	11
Thunder began					
⩽ 5 min after rain	1	10	0	1	12
5 to 10 min after rain	1	3	0	0	4
10 to 20 min after rain	0	1	0	0	1
Totals	3	18	3	7	31
Percent of number known that were thunderstorms	66	90	0	15	55

Twelve of the 17 thunder raincells became thunderstorms within 5 min after the start of rain at the ground. On the basis of past observations, this suggests relatively rapid electrification processes within the storms on 11 August.

The thunder frequency data from the two sites with such information, SLU and EDW, could not be used successfully to study frequencies because several cells were too close to these sites during much of the afternoon thunderstorm period. However, changes in frequency could be assessed on a general time scale. Both sites showed an increase in thunder frequency from the occasional class (defined as a rate of 6 to 18 strokes/hr) to the moderate class (19 to 30 strokes/hr) in the period from 1750 up through 1800, and this higher frequency lasted until about 1830. This increase in frequency occurred during the maximum rain production of the major storm when cells 11, 12, and 13 had matured and had begun to merge with core cells 5, 6, 7, 8, and 9. The increase in thunder activity also corresponds with the general period of hail initiation that first occurred at 1800. Apparently, the storms had reached an increased degree of severity in rain, hail, and thunder intensity at that time.

In summary, the thunderstorm data for 11 August show certain interesting facts. First, most of the afternoon raincells became thunderstorms. Further, most became thunderstorms quite rapidly after the first rain initiation at the ground showing that electrification was rapid and a potentially important process in the rain production. Second, only one of the 14 raincells in the evening became a thunderstorm. Thunder frequency information from around the major storm conglomerate E of the city in the afternoon showed an increase in the thunder (and thus electrical) activity as the storm reached maturity and began hail production.

HAIL ANALYSES

The study of the hailfalls (see figure C–7) and resulting hailstreaks on 11 August indicated there were two distinctly different types of hailfalls, both in time and space. They represent types of hailfalls different from those noted in previous Illinois hail studies (Changnon, 1970).

Initial Hailfalls NW of St. Louis

The first hail-producing storms on 11 August were from the first two raincells to occur, 1a and 1b, which fell in the floodplain NW of St. Louis. The hail from the first raincell (1a) was not notable in size, frequency, nor location of occurrence. It fell in the right flank of the storm, the most frequent location, and lasted less than 2 min. Interestingly, the hail began less than 10 min after the first rain started; thus, hail formation in the cell began rapidly, probably during the initial rain process.

The second hailfall, producing the second hailstreak of 11 August, occurred 35 min later. It was produced by the second air mass cell (1b) which had also formed in the floodplain (figure C–10a). Hail from cell 1b also fell less than 10 min after the cell's rain began, but in this case, the hail fell closer to the rain core. The hail ranged up to 1 inch in diameter, which is quite large for summer hail, but the fall lasted only 3 min, less than average (Changnon, 1970). The close geographical relationship of cell 1b to cell 1a and their potential dynamic interaction could explain why larger hail was produced in cell 1b after such a relatively short time of rain production. The third raincell (1c) that occurred in the bottomlands during the early afternoon did not produce hail. In summary, hail fell from the first storm of the day, not an uncommon occurrence for

hail in summer air mass storms (Changnon, 1970), but the hailstones were larger than normal. The rapid development of the hail after the first rain also suggests that strong initial updrafts were present, but the short point hailfall durations suggest a rapid weakening of the storms after the initial convective thrust of cell development.

Later Hailfalls E of St. Louis

The other four hailfalls, which formed four small hailstreaks, occurred more than 30 mi away and more than 2 hr later (figure C–7). These were 'E-side' hailfalls originating out of the raincells that had formed earlier in the St. Louis metropolitan area and merged.

The first of these hailfalls occurred at 1800, only 15 min after the merger of cells 6 and 9. The relationship of the hail and rain pattern for 1800–1805 CDT is shown in figure C–14a. The rainfall from cells 6 and 9 had been rapidly maximizing (> 2.5 in/hr) in the 5-min period just before the hailfall began. The second hailfall occurred 4 min later at 1804, and both hailfalls lasted 3 min. As shown in figure C–14a, the second hailfall occurred in an area where already merged raincells 6 and 9 had merged (on their rear or W sides) with raincells 11 and 13. All of these cells had formed originally over the urban complex. At the time of these two hailfalls, cells 6 and 9 were more than 60 min old and into their mature stages. Thus, this hail occurred late in the life of the parent cells, but it occurred as the cells reached a new precipitation maximum apparently from dynamic processes resulting from the merging of both mature and young cells.

The third hailfall E of the city occurred at 1837 CDT, and again occurred inside the rain core where the rate was > 2.5 in/hr. The hail occurred 20 min after the cells had merged and as they were merging with new raincell 18 (figure C–14b-c). The final hailfall of 6 min duration began at 1843 CDT and it occurred in the rain area between the core storm and cell 18 which was merging and rapidly intensifying.

In summary, the hail that occurred E of St. Louis fell either in heavy rain cores or just between cores that were in the process of merging. Point durations of hailfalls were near average, 3 to 4 min, and hailstone sizes were also average, 1/4 to 1/2 inch diameter. Hail in every case resulted within 5 to 20 min after major mature raincells merged with rapidly growing new flanking cells. These results, particularly in comparison with those for the earlier hail W of the city in the bottomlands, indicate that very different storm dynamic processes existed between the 'bottomland storms' and 'urban-related storms.' These results also give a clue as to how the apparent urban-related hail increases noted in previous climatic studies come about, that is, from the merger of thunderstorms generated in the urban area. Previous research (Changnon and Huff, 1961) showed that severe weather in Illinois often results after the merger of large convective cells. Dynamic processes are apparently enhanced, relating to more precipitation (Simpson et al., 1972) when mergers occur, either because of the growth of adjacent cells or because they have differential movements that result in an intercept course.

CLOUD ANALYSES

This section of the case study is divided into four parts: 1) a brief chronological review of the 11 August cloud conditions, 2) cloud dimensions, 3) cloud characteristics, and 4) a summary with recommendations relating to future field efforts.

The available data on clouds were successfully used to help understand the causes for the precipitation development and related weather conditions. In many ways, the cloud results proved invaluable in explaining 1) the impact of local factors on cloud and subsequent rain developments, 2) the major-storm development, and 3) the unique characteristics of certain storm structures. These data were also very helpful in developing conceptual models of local effects.

The data available consisted of: 1) hourly surface observations from PMQ (rural W), STL (urban), and BLV (rural E); 2) AI aircraft visual cloud observations (1300–1515 and 1600–1830 CDT) and 36 aerial oblique photographs (1610–1830); and 3) surface photographs of clouds, time lapse data for the entire day, and pointed camera shots (1700–1815 CDT). The best described cloud period on 11 August was from 1300 to 1830, and it was also the most critical to rain development and hence the most interesting period.

Chronology

The cloud period on 11 August can be interpreted as three distinct phases: morning (0800–1100 CDT), early afternoon (1200–1500 CDT), and late afternoon–evening (1600–2100 CDT). Each phase had distinctly different but interrelated cloud characteristics.

Morning period conditions were typical of many summer days. Ground fog and haze somewhat limited visibility to distances from 5 to 7 mi and from 0600 until about 1100 CDT, but there was no fog at STL, the urban station. The sky at sunrise was overcast with a thin Ci deck at 30,000 ft, but by 1100 the Ci coverage had become broken. STL and PMQ reported towering Cu to the NW from 0900 to 1000 CDT (well beyond St. Louis), and a few Cu (less than 0.1 sky coverage) with bases at 4000 ft appeared at STL and BLV between 1000 and 1100. In general, cloud coverage in the MMX circle began to decrease after 1000 and was least from 1000 to 1800 (0.4 to 0.3 sky coverage) allowing for good solar heating of much of the surface.

Early afternoon cloud conditions (1200–1500 CDT) represented a transition period. High thin scattered (0.3 to 0.4 sky coverage) Ci persisted everywhere throughout this period, but other cloud conditions were different on a regional basis. From W to E, PMQ had clear to scattered conditions through the period, STL skies were scattered to broken, and BLV had broken skies. Thus, the cloud coverage in general was greater to the E during this 3-hr period. Types of clouds also varied with PMQ reporting Ac and As to the W at 1300 and 1400. STL had no Ac or As but was the first to have Cu (0.4 at 1300), and total coverage at STL went from 0.3 at 1200 to 0.6 at 1300. BLV confirmed this by reporting Cu forming to the SW and WNW at 1300 CDT. Interestingly, rural visibility increased with time, going from 8 to 15 mi by 1500 at PMQ and from 8 to 14 mi at BLV, but visibility remained at 10 mi at STL (evidence of local pollution haze). The AI flight observations of clouds in the 1300–1500 period (made from N–S flights just E of St. Louis) indicated two areas of forming Cu, one extending from the center of St. Louis S for 25 mi along the Mississippi River Valley, and the other in the bottomlands NW of St. Louis.

The data from the time lapse all-sky camera at SLU were used to study the time and placement of the first 10 visible Cu on 11 August. The distance to a cloud is a function of its base height (usually visible up to 10 mi), and distances were analyzed for 11 August on the basis of locations within 3 mi of the site (Site 113, figure B–1) or up to 10 mi from it. The first six clouds all appeared at 1300 CDT (none was visible at 1255 CDT). Three were to the SSW at more than 3 mi (S of St. Louis), and three were to the W and WNW with two of these at 3 mi and one within 3 mi (W suburbs). The next four clouds appeared in the 1305–1310 period. Two of these were to the NE over the city, one to NNW, and one to the W. These data show the rapid initiation of small Cu over the urban area at 1300 CDT.

Late afternoon-evening period featured regional cloud complexities. In general, cloud coverage increased from 0.6 or 0.7 at 1500 CDT to 0.9 at 1600 and remained either 0.8 or 0.9 until after 2100. Multilayers were common with 1) scattered to broken Cu with bases at 4000 to 5000 ft; 2) scattered to broken Ac with bases at 12,000 (not at PMQ); and 3) scattered to broken Ci at 30,000 to 40,000 ft. In general, cloudiness continued to be greatest to the E and least to the W. Aircraft photographs revealed that the city was frequently in sunlight during the 1600–1800 period, whereas areas E of the urban complex were obscured by the heavy storm cloudiness.

Visibility remained remarkably good: 15 to 25 mi at PMQ; 10 to 14 mi at BLV; and 10 (constantly) at STL. Cb were reported E of STL at 1600, NW of BLV at 1700, and SE of PMQ by 1700. The large-cloud activity moved generally to the E during this period, and PMQ and STL continued to report towering Cu and Cb to the NE, E, and SE through 2100. The proximity of this activity to BLV resulted in overhead lightning and finally a report of Cb to the NNE at 2100 (cell 23).

Cloud Dimensions

No measurement of cloud tops or widths were made, although cloud boundaries were often visible because of 1) the extremely good visibility on 11 August (a general lack of haze), 2) absence of typical and numerous low clouds in and around the large CuCong and Cb, and 3) the relatively high cloud bases. These factors suggest a relatively clean and dry atmosphere. In general, the rural and urban cloud bases also were 500 to 1000 ft higher than those found on most other summer days in 1972.

Most cloud dimensional data available for 11 August relate to cloud bases. Ci heights varied between 25,000 and 40,000 ft with the higher values occurring at the end of the day. The Ac deck associated with the Cb activity was based at 12,000 ft. The Cu bases varied in height and were the most interesting and informative about urban effects. Surface observations of Cu bases for STL and BLV indicate a 1000 to 2000 ft difference (STL highest) between 1400 and 1700.

The SRI lidar data taken at Granite City (see figure C–29) show a cloud base at 5500 ft at 1500, with bases decreasing slightly to 5200 or 5300 ft by 1630. The aircraft data confirm this with an urban cloud base measured at 5400 ft AGL at 1610 CDT. Aircraft measurements of three rural clouds 20 mi S of St. Louis during 1450–1510 CDT revealed bases of 4400 to 4500 ft AGL (1000 ft lower than the 1500 urban value from the lidar). Later rural cloud bases, as measured by the aircraft at 1800 (W of STL), showed bases at 4200 ft compared with lidar urban values of 5100 ft at 1730 CDT. It is clear that a rural–urban difference in Cu bases existed in the afternoon of 11 August, the bases being about 1000 ft higher over the city.

The aircraft cloud base measurements made along the rear of the major storm cell (6) which had a base at 5400 ft over the city, showed it to decrease systematically as it moved E away from the city. The rear cloud feeder base was at 3800 ft by the time the storm was 10 mi E of St. Louis. Thus, the condensation level over the urban area was higher than over the rural area.

Cloud Characteristics

The cloud characteristics measured consisted of a few in-cloud liquid water measurements, updraft data (location with respect to the cloud or storm center, speed, and CN inflow), and cloud motions.

Motions of most Cu were slow, 5 to 10 mi/hr, and generally from W to E. The feeder Cu found in *every instance* on the rear (W) side of the parent clouds often moved more rapidly, 10 to 25 mi/hr. This is reflected in the photographs in figure C–22a and b, showing the rapid envelopment

a. The west side of the major storm with a new developing cell on its rear at 1818 CDT

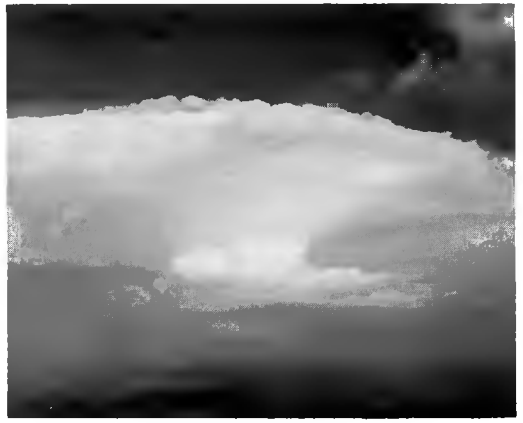

b. The envelopment of the new cell into the main storm 3 minutes later (1821 CDT)

c. Looking west under the cloud "shelf" where new raincells 11, 12, and 13 were developing at 1735 CDT. St. Louis and Mississippi River are in the background.

d. The development of raincell 13 at 1746 CDT

e. The development of the congestus that became raincell 11, taken at 1742 CDT

Figure C-22. Cloud photographs

of a feeder cloud (raincell 14) into the parent storm during a 3-min period between 1818 and 1821 CDT. These photographs reveal the exceptional visibility that allowed the entire major cloud system in the research area *plus* the feeder storms along its flanks and rear (W) side to be seen. Motions of the major clouds varied from WSW to ENE, W to E, and WNW to ESE.

Liquid water values were obtained from three CuCong located 20 mi (rural clouds) due S of St. Louis in the 1450–1510 CDT period. These values were taken 100 to 200 ft above cloud base and ranged between 0.2 and 0.4 g/m^3. These values were lower than any others measured in clouds of this type and height (above cloud base) in the summer of 1972. Values on three other days were from 0.3 to 0.8 g/m^3. This suggests relatively dry cloud air, a condition supported by the 'dry' atmosphere indicated by the higher than usual cloud bases, the excellent visibility, and the lack of many small Cu on 11 August.

The updraft data collected by AI aircraft are summarized in table C–3. These show that there was a distinct difference between urban and rural clouds. However, all of the urban values were from well-developed storms, whereas three of the five rural values were from showers. One very high value, 1500 ft/min, was found to the rear of raincell 3.

This day was characterized by *rear side (W) major indraft areas for all clouds,* including the CuCong in the rural areas. This prevailing tendency resulted in new cloud turret formation on the 'backside' or upwind of most clouds; those growing behind cell 6 during 1742–1746 CDT (raincells 11 and 13) appear in figure C–22d and e. However, the single major rain storm (raincell 6), which became the mesosystem, also had new cloud growth on its N and S flanks, as reflected in the surface photographs, and this observation is supported by the updraft measurements made in the 1710–1730 period. Individual updraft areas were found 'around the rain core' (of cell 6), but the primary indraft continued on the rear or W side. A view of this indraft area and the under-the-cloud shelf (new feeder cells 11, 12, and 13 were growing above) appears in figure C–22c (looking W toward St. Louis).

The cloud-base and updraft history of cell 6, which the aircraft remained with for about 1 hr during the Li tracer release (1640 to 1740 CDT), is of interest. The cloud base lowered and indraft speeds decreased as the storm moved away from the urban area. This may have been due to urban versus rural differences in condensation, or to storm age, but the storm's rain production did not decrease, but increased. The persistence of the updraft on cell 6 was also unusual in relation to most other updraft measurements for semi-isolated large clouds in the area during 1971–1973.

Table C-3. Cloud Updraft Speeds, Times, and Associated Raincells (if known)

Rural clouds		*Urban clouds*	
Speed (ft/min)	*Time and location*	*Speed (ft/min)*	*Time and location*
300	1450 S of STL	300	1606 cell 2
200	1730 E of cell 6	1500	1616 cell 3
300	1735 E of cell 6	500	1694 cells 5, 6
200	1803 WSW of STL	400	1700 cell 6
200	1808 WSW of STL	450	1705 cells 6, 9
		500	1715 cells 6, 9
Median		300	1720 cells 6, 9
200			
		Median	
		450	

Cloud Summary and Recommendations

The early cloud conditions on 11 August were typical of those found on many summer days, but the Cu later in the day had many features that were notably different from those found on most other summer days. The Cu, particularly the CuCong and larger types, differed by being higher based, lower in liquid water content near cloud base, more isolated with few smaller Cu, and by having long-lived updrafts in the rear (W) side of the cloud or storm center.

The sequence of the Cu development on 11 August clearly suggests local influences. The area's first Cu developed around 1300 after a relatively clear morning, and formed along the major river valleys and over the urban area. The first raincells in the area came from the CuCong that evolved from these 'valley Cu' and 'urban Cu.' However, the later and larger storms (raincells 2 through 13) all formed in clouds that originated over the St. Louis urban complex, and these subsequently 'drained' the area of any nearby rural clouds. This air mass self-generating type of storm concept is reinforced by the sequence of sky conditions (clearing and heating until 1300, and then cloud maximization by 1700).

Distinct rural–urban differences in clouds were found. The bases of afternoon Cu over the city averaged around 1000 ft higher than the rural ones. Furthermore, the median updraft speed of the urban clouds was 450 ft/min compared with 200 ft/min for the rural clouds.

Many cloud features reflect a relative dryness in the atmosphere. These included the exceptional visibility throughout the day, the high cloud bases, low liquid water contents, lack of small Cu, and general isolated nature of the larger Cb clouds.

Updraft characteristics were unique in that they were relatively persistent and always found on the rear (W) flank of the storm; but, those on 11 August were not different from seasonal averages of updraft speeds nor size of updraft area. The clouds of 11 August were classic 'rear side feeders,' but the largest core storm also had some updrafts and feeder clouds on all sides.

The results of these analyses clearly show the value of extensive cloud data for case studies. A large amount of photographic (aircraft and surface) documentation is invaluable, as is the aircraft rural–urban data on 1) cloud bases, 2) updraft characteristics, and 3) LWC. The useful mesoscale observations from the 1300–1500 aircraft (pre-storm) flight were helpful. Aircraft and surface photos taken at sufficient distances to encompass a storm mass are also very helpful.

TEMPERATURE, DEW POINT, AND SURFACE WIND ANALYSES

Air and Dew Point Temperatures

Data from the hygrothermograph network indicated the development of a peak in the air temperature pattern over SE St. Louis by mid-afternoon. This 'hot spot' corresponds closely with the region of frequent development of convective activity (figures C–9, C–11, C–13) that was the primary support for the quasi-stationary system producing the heavy rain E of St. Louis (figure C–7). Figure C–23 shows the air temperature pattern in early afternoon (1300) and mid-afternoon (1500), about 1 hr before development of the heavy storm. The pattern for 1300 is typical for early afternoon in summer with relatively high temperatures up the Mississippi River Valley and over the urban areas of St. Louis and Alton–Wood River. High values are also indicated in the Missouri River Valley. The map for 1500 shows a very strong air temperature gradient NE of St. Louis. This was caused by a sudden drop in temperature at the site E of Granite City and NW of Collinsville. The cause for this sudden drop is unknown, but it may have been caused by a strong downdraft

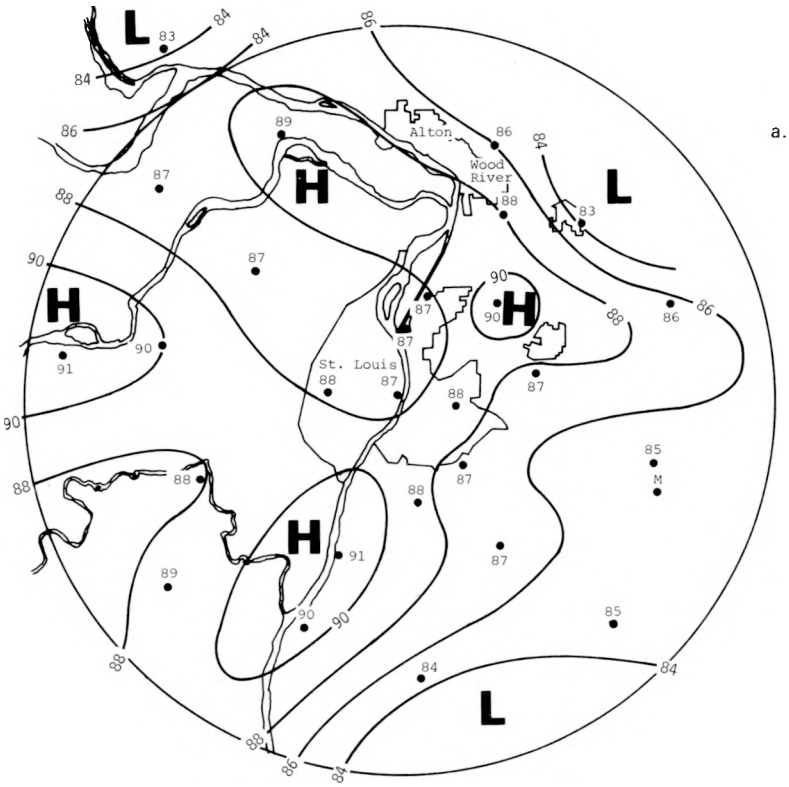

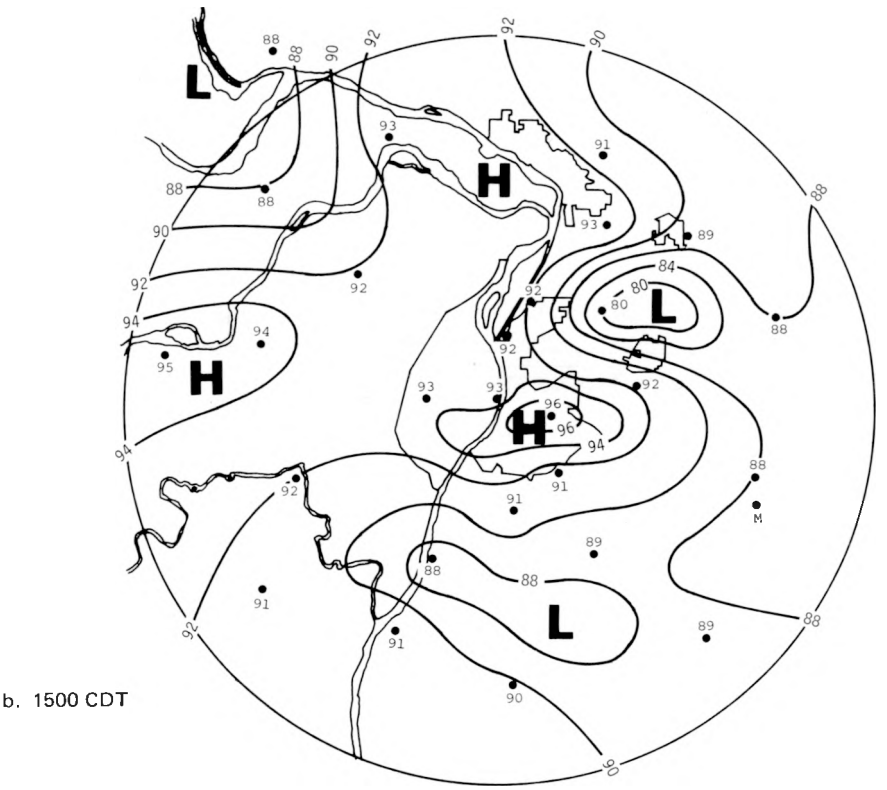

Figure C-23. Distribution of surface air temperatures

from a small but intense cell that was not detected by the raingage network or by the 10-cm PPI. The temperature peak is very evident over the E and SE urban area where, as indicated before, support for the major storm system was produced.

The dew point patterns from the hygrothermograph data are shown in figure C-24 for 1300 and 1500. At 1300 relatively high dew points extended S-N along the E side of the Mississippi River through East St. Louis. Much drier air was indicated over the hills SW of St. Louis. A relatively strong dew point gradient was indicated across the city. By 1500 the gradient in dew point temperature across the city had intensified still more, and dew points in the range from 72 to 74F were recorded over the E part of the urban area, a primary area of later convective development, and a few miles E of the city where the heavy storm was centered. Thus, a dew point of 75F was recorded at the site just S of Collinsville where the parent cell of the massive storm later developed. The hygrothermograph record indicates the dew point reached 77F and the air temperature was 92F just prior to the development of the parent cell on the S edge of Collinsville.

Overall, the surface temperature and dew point distributions in and E of St. Louis on the afternoon of 11 August were favorable for storm development, that is, they indicate very hot and humid conditions from the S part of St. Louis to the E through the area of maximum rainfall in figure C-7. The results in figure C-27 show that these surface anomalies were extending upward at least 3000 ft between 1300 and 1500. The area of peak temperatures corresponds closely with the most frequent area of convective development that reinforced the heavy rainstorm E of the city. Dew points also peaked in this region and in the area where the rainfall maximized.

The maximization of temperature in the S part of the city was most likely produced by the combination of urban and river valley effects. Preliminary results from a study of temperature distributions in 1972-1973 indicate that the region E of the river in East St. Louis is a frequent center of maximum temperatures. The dew point maximum exhibited in and E of St. Louis in the 11 August storm also appears to be a frequent occurrence from preliminary tabulations of the data for 1972-1973. There was no significant rainfall for 5 days prior to the storm of 11 August; therefore, the dew point maximum cannot be explained on the basis of excessive evapotranspiration from previous rains. A possible explanation is that the dew point maximum is the result of a high rate of evaporation and evapotranspiration that is induced by 1) the river itself, or, more likely, 2) the evapotranspiration from the sandy soil floodplain. This floodplain could induce evapotranspiration at a much higher than normal rate because the moisture is closer to the surface than in the claypan soils in the general region. If this is a cause of the anomaly, then this high-rate evapotranspiration may be further reinforced (see figure C-27) in the Alton-Wood River area by moisture discharges from the cooling towers of the four refineries there. In any case, if this apparent anomaly is proven to be persistent, it could be a significant factor in the production of the climatological rainfall maximum E of St. Louis (Huff and Changnon, 1972).

Surface Winds

The surface wind patterns indicated by the recording anemometer network are shown for three times in figure C-25. The early afternoon winds (1300 CDT) were mostly from the SW to WSW at 4-10 kt. No major changes were evident at mid-afternoon (1500) when winds ranged from SSW-WSW at 4-11 kt with no persistent changes from W-E or N-S. Figure C-25c shows the wind pattern at 1700 CDT shortly after development of the parent cell of the heavy rainstorm near Collinsville. At that time, the winds did show some indications of convergence into the area of the heavy rainstorm center S of Collinsville and E of St. Louis.

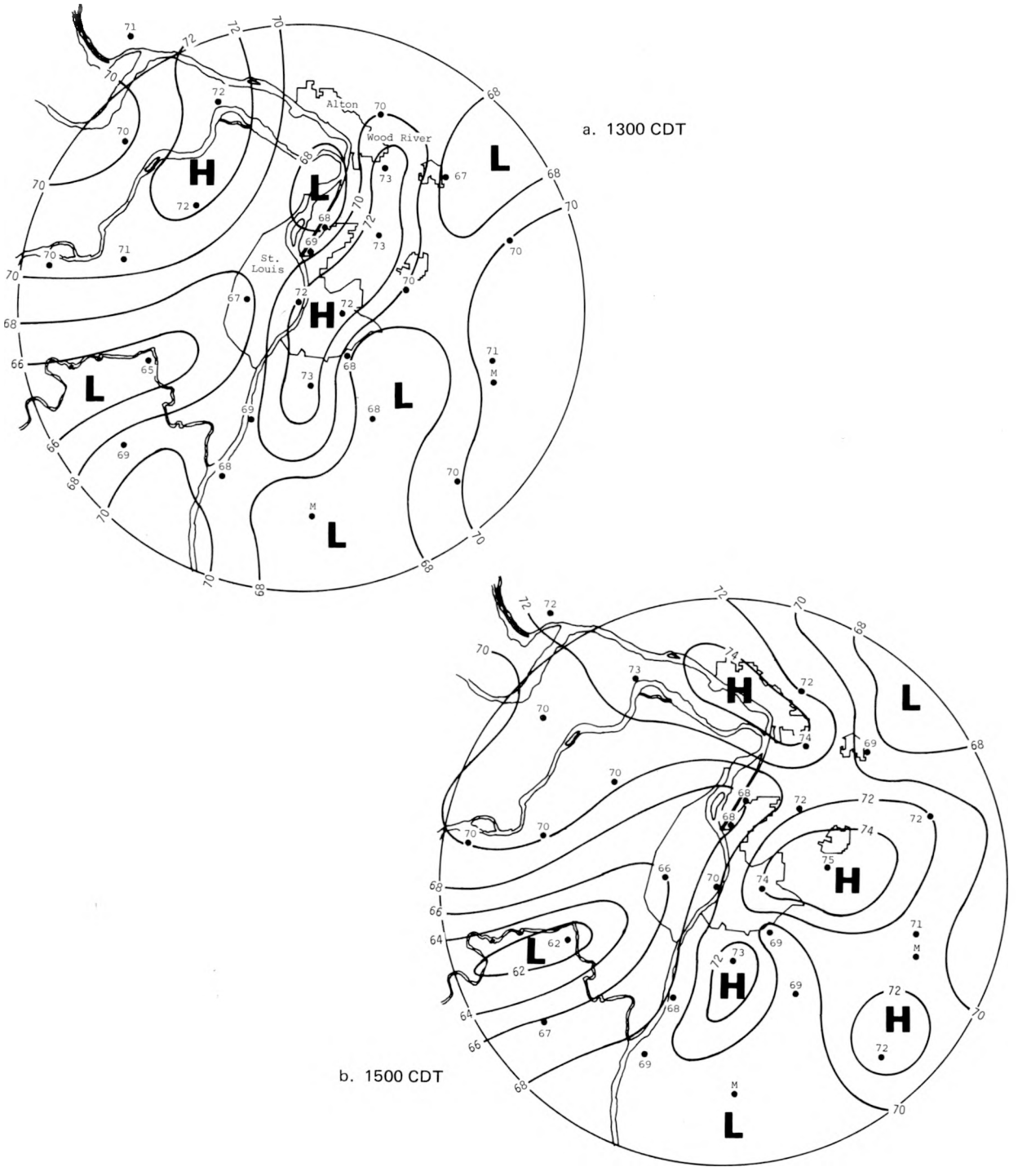

Figure C-24. Distribution of surface dew point temperatures

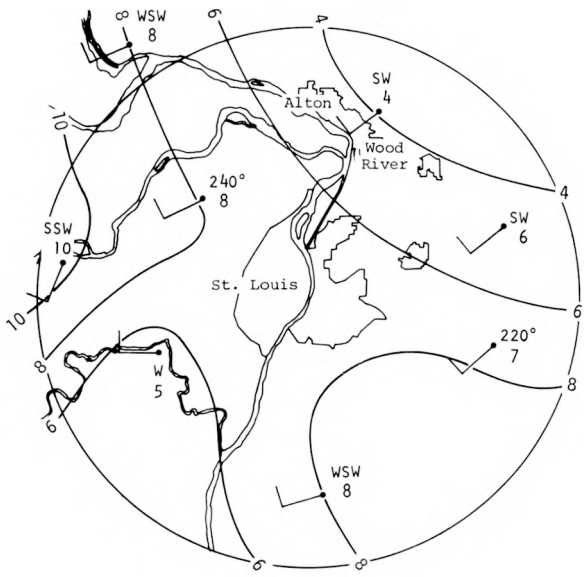

a. 1300 CDT

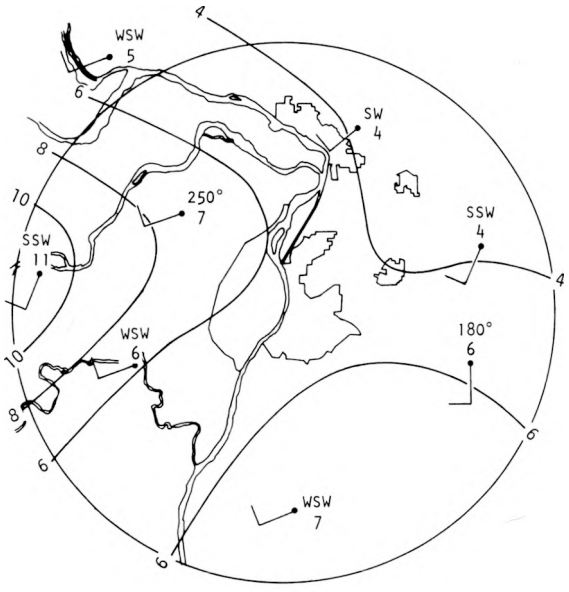

b. 1500 CDT

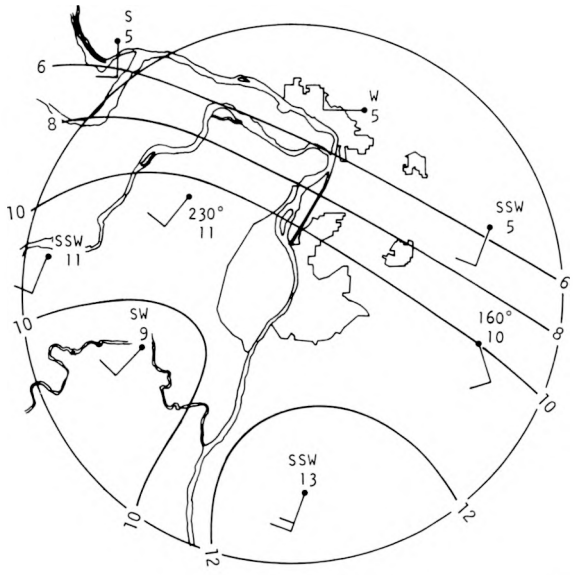

c. 1700 CDT

Figure C-25. Surface winds

POTENTIAL INTERACTIONS OF SURFACE CONDITIONS WITH CLOUD PROCESSES

Comparison of the time and space arrays of the cloud and rainfall developments on 11 August with the detailed surface temperature and moisture fields strongly suggests the presence of localized surface influences (bottomlands and urban) on the cloud and subsequent precipitation processes. Clear establishment of physical links between the surface characteristics and the cloud bases is of great importance in substantiating the apparent existence of surface effects on 11 August.

All possible sources of data that could substantiate or refute the surface–cloud base connections on 11 August were investigated. Unfortunately, the 10-site pibal and 3-site radiosonde project of the Water Survey had been terminated for 1972 on 10 August. Nevertheless a variety of useful data was found, including data from 1) a 3-level 'Metrodata Day' flight of the AI aircraft in the early afternoon, 2) the lidar of SRI operated at Granite City, 3) the mid-day radiosonde release from the NOAA radiosonde station in St. Louis, and 4) other cloud and inflow data from the second AI aircraft flight.

Aircraft Data

Fortunately, the early morning MMX forecast for 11 August was in error. A 'no-rain' day was forecast and hence a 'Metrodata Day' flight plan was instigated for all project aircraft. As part of this plan, the AI aircraft was assigned to fly 35-mi tracks at three levels (1500, 2500, and 3500 ft MSL) immediately (10 mi) downwind of St. Louis. The tracks of all MMX aircraft were designed to be 1) across the prevailing flow, and 2) of sufficient length and height to define the aerosol plume of the city.

The AI aircraft left ALN at 1257 CDT, flew NE to near Mt. Olive (figure C–26) to begin its first N to S flight (actually 010°–190° headings) to match the forecast prevailing low-level flow of 280° at 10 to 15 mi/hr. The flight from 1313 to 1342 CDT was at ~ 1000 ft AGL (1500 ft MSL) and the succeeding flights were S to N from 1346 to 1411 CDT at ~ 2000 ft AGL, and N to S from 1417 to 1444 CDT at about 3000 ft AGL. The 1-min readings of wet bulb and dry bulb temperatures (measured with a Mee electronic psychrometer) were determined from the continuous chart recordings of these values. The dry bulb and wet bulb temperature profiles (corrected for speed and elevation) have been plotted in figure C–27, and the condensation and freezing nuclei values for the three levels appear in figure C–28.

To examine for perturbations aloft of the surface-related anomalies (see figures C–23 and C–24) a 'regional gradient' was established for each curve (figures C–27 and C–28). It connected the regional 'background' values assumed to exist at the ends of each curve. Comparison of the aberrations around this gradient line with respect to the upwind locations of the urban areas, as labeled in figures C–27 and C–28, helped in searching for surface-related perturbations at the three flight levels.

The wet bulb temperature curves at all levels (figure C–27) show regional gradient curves indicating slightly higher values (0.5 to 1.5C) to the S than to the N. Clearly, the values anywhere along the flight track must be referenced to these gradients. Five perturbations around the lowest level flight (at 1000 ft AGL) were numbered for identification since they also appeared at the two higher levels. Positive anomalies (numbered 1, 2, 3, and 4) range from +0.5 to +1C at 1000 and 2000 ft, but only 3 and 4 are +0.5C at 3000 ft. Perturbation 1 appears to be related to Wood River, perturbation 2 to Granite City, 3 to the S St. Louis area, and 4 to a far S isolated source, a power plant (figure C–26). A consistent decrease in the wet bulb values, labeled perturbation 5, appears to be associated with the Alton–Wood River area, and this air extends to all flight levels.

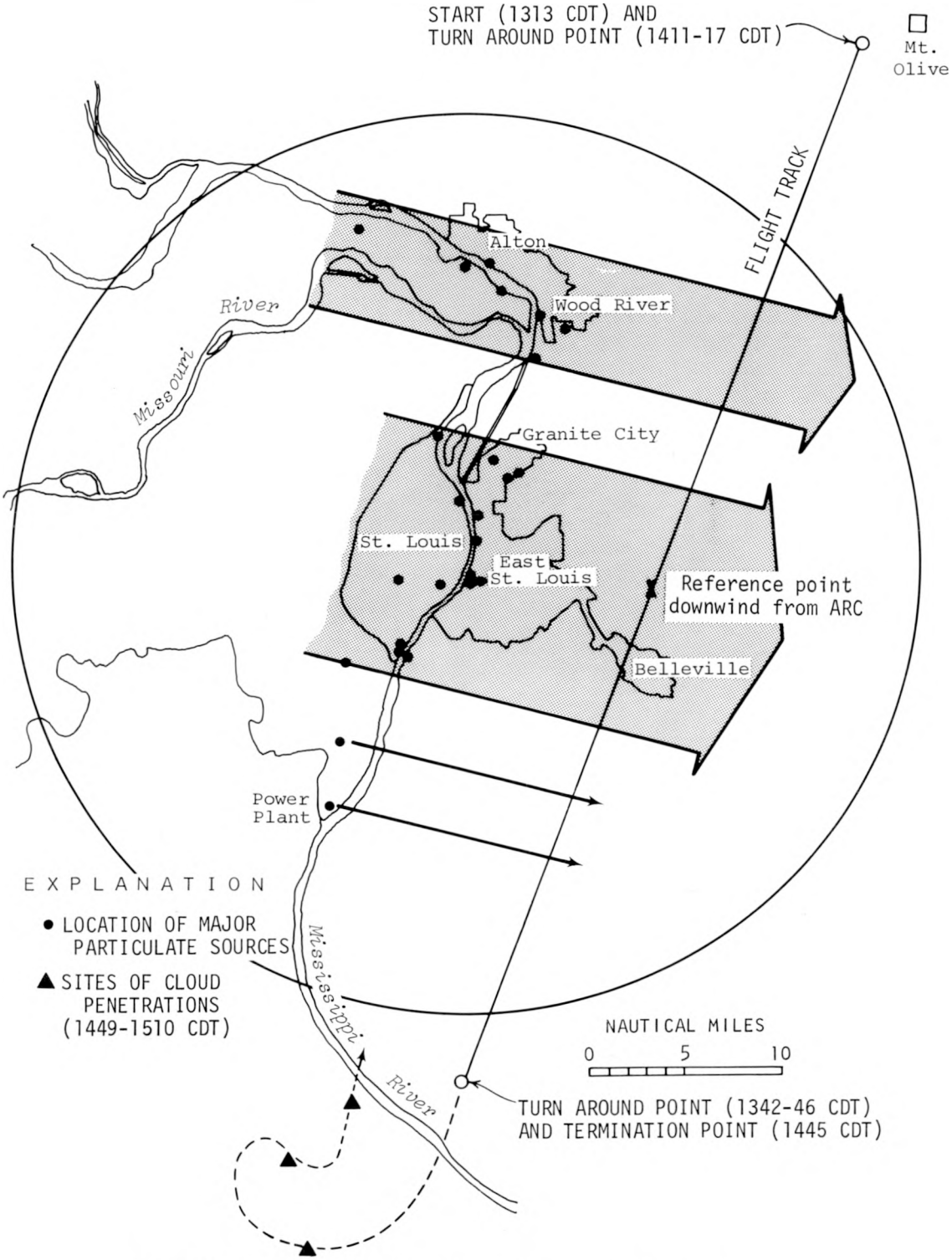

Figure C-26. Afternoon flight track and low-level flow from major particulate sources

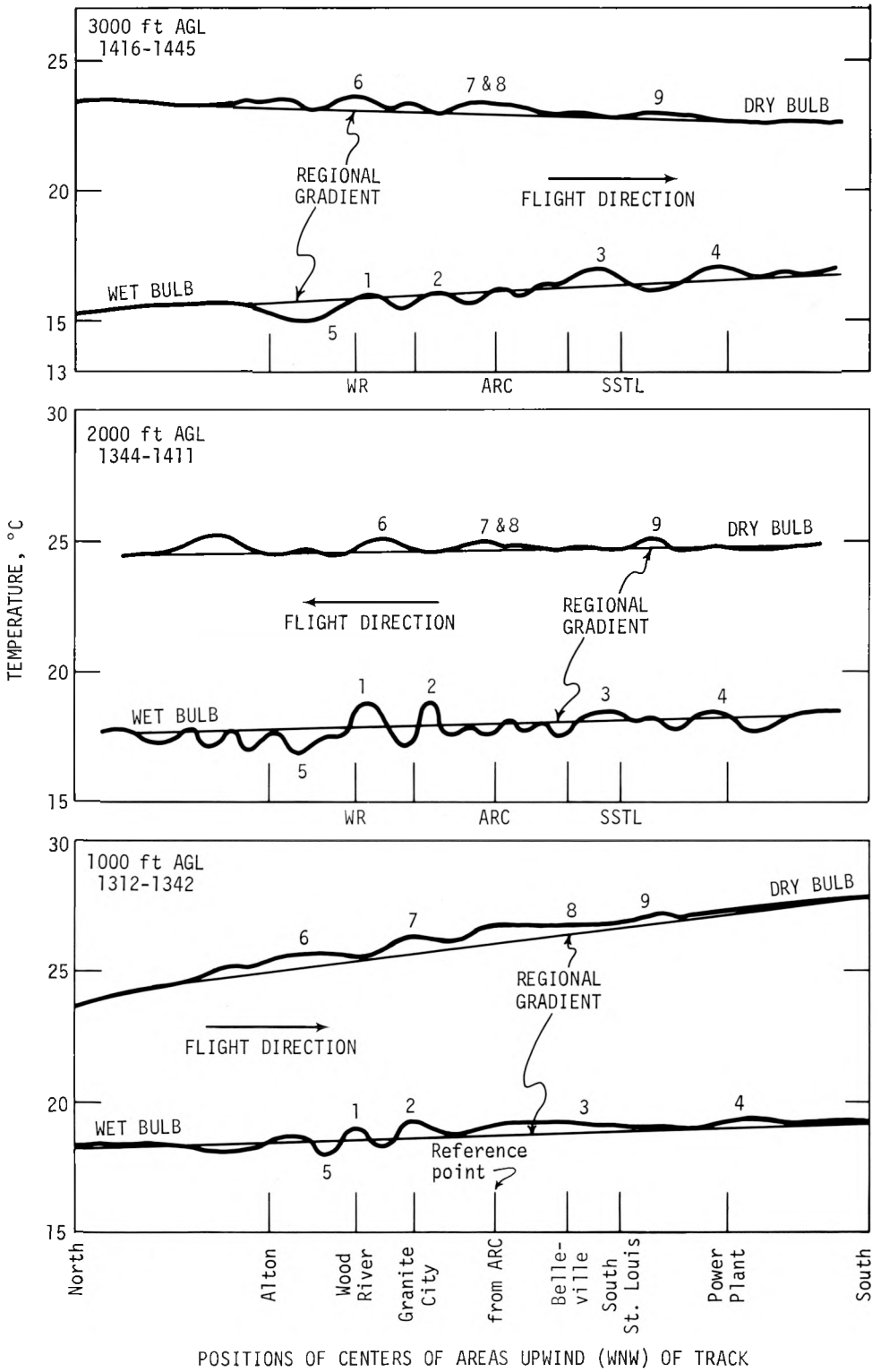

Figure C-27. Flight profiles of dry bulb and wet bulb temperatures above and E of urban-industrial area

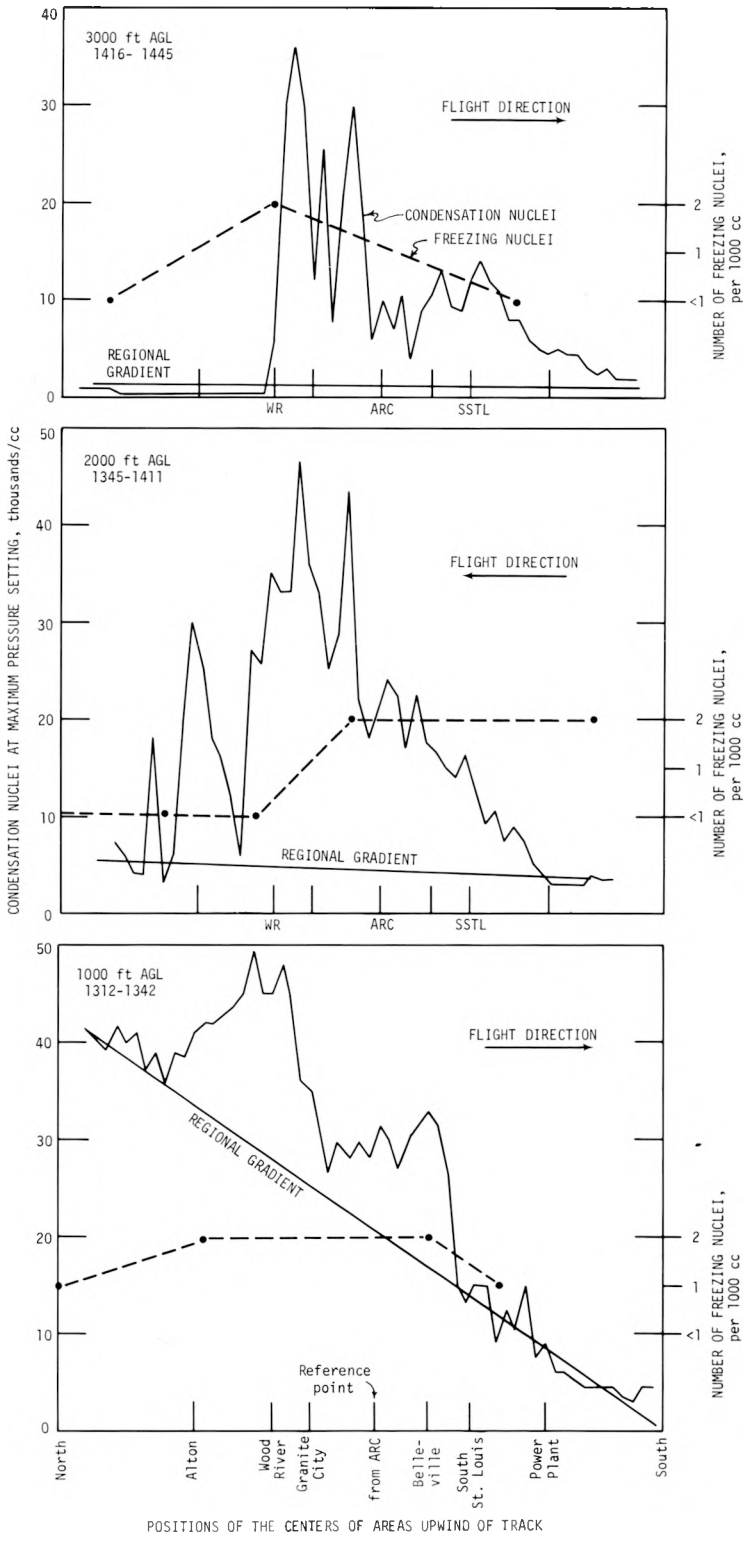

Figure C-28. CN and freezing nuclei values along flight track

Table C-4. Maximum Values of Surface-Related Perturbations
10 Miles from Source, 1300-1500 CDT

	Alton-Wood River			*Granite City-St. Louis*		
Height (ft AGL)	*Dry bulb (°C)*	*Wet bulb (°C)*	*CN (No/cc)*	*Dry bulb (°C)*	*Wet bulb (°C)*	*CN (No/cc)*
1000	+0.5	±0.5	22,000	+0.8	+0.5 to +1.0	16,000
2000	+0.5	±1.0	42,000	+0.5	+0.5 to +1.0	38,000
3000	+0.5	+0.25 to -0.75	34,000	+0.4	+0.6	29,000

The wet bulb data on figure C-27 have been summarized in table C-4. Surface effects existed in the low-level moisture field, seen at 3000 ft AGL which was still 1000 to 2000 ft below cloud bases on 11 August; but since the fluctuation is dependent on temperature, the moisture differences were slight.

The dry bulb temperature curves (figure C-27) showed distinctive regional gradients. The sizeable (3C) N to S increase at 1000 ft AGL was largely due to diurnal changes during the flight, as surface warming at this time and in the previous 2 hr had been at the rate of 3 to 4C per hour. Surface heating became constant around 1400 CDT, and the curves for 2000 and 3000 ft do not show evidence of continued dirunal heating at those heights. In fact, the gradient at 3000 ft suggests that the regional temperature field consisted of warmer air N of St. Louis than S of it during the early afternoon of 11 August. The perturbations in the dry bulb values that existed at all flight levels have been numbered on figure C-27. Perturbation 6 was obviously associated with the Alton and Wood River complex; perturbations 7 and 8 were associated with the Granite City and central St. Louis areas; and perturbation 9 was associated with S St. Louis. The perturbations are summarized in table C-4, showing positive departures of 0.5 to 0.8C at all flight levels.

Figure C-28 portrays the N to S profiles of the number of CN (at maximum pressure setting) and the freezing nuclei measured during the three flights. The CN data were 1-min values from a continuous recording from an Environment One CN detector. Regional gradients were drawn for the CN, but were not done for the freezing nuclei because too few measurements were made to establish such gradients. A N to S decrease appears in the regional CN gradients. A general downwind areal increase related to the entire St. Louis urban complex appears in the CN values at all levels, but certain maximums appear to be related to specific urban-industrial zones within the complex. One peak from Alton is found at 1000 and 2000 ft, but not at 3000 ft AGL. The greatest peak at all levels is related to the Wood River area, but its peak is displaced slightly to the S at the higher levels, as is the notable Granite City perturbation which also appears at all levels. The fourth perturbation is a broad one associated with East St. Louis and St. Louis. The CN data clearly show the penetration of surface effluents up to the 3000 ft level. Peak values were 49,000/cc at 1000 ft, 147,000/cc at 2000 ft, and 36,000/cc at 3000 ft. The differences between the peak values and the regional gradients are also shown in table C-4.

Occasional in-flight measurements of freezing nuclei (measured by a portable cold box ice nucleus detector) are also plotted in figure C-28 and are connected with a dashed line. Although sparse, these data suggest an urban-related increase of about 1 nucleus per 1000 cc at all levels.

Soundings and Remote Sensing Data

The continuous operation of the SRI lidar system and the ANL acoustic sounder gave valuable data on the height of the mixing layer. Both devices sense levels where temperature and aerosol concentrations differ drastically, and cloud base levels are detectable on the lidar (Uthe, 1972).

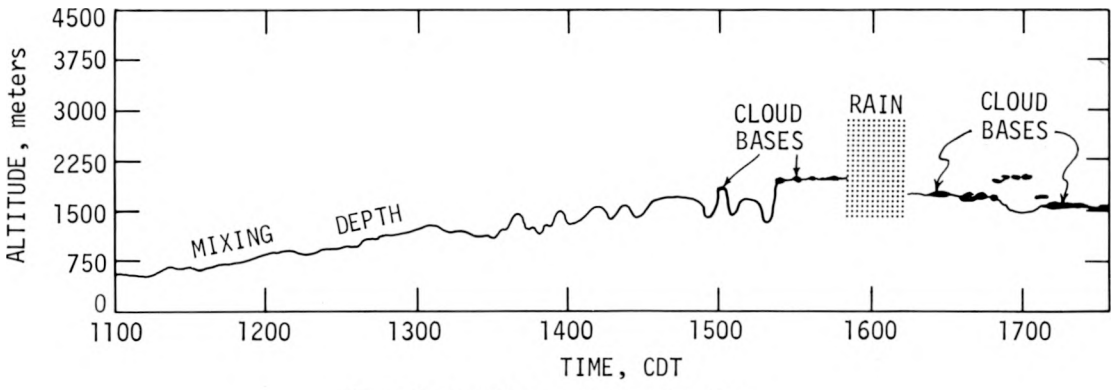

Figure C-29. Lidar-measured mixing depth

Figure C-29 portrays the top of the mixing depth from the lidar data. It began rising from the 500-m level shortly after 1100 CDT, reaching 1800 m by 1500 CDT when it first reached and/or interacted with a cloud base. Frequent excursions of thermals are seen after 1300. The acoustic sounder data for 1100 to 1300 agreed well with the lidar data, but the sounder data were useless after 1300 CDT because its vertical scale limit of 4000 ft had been reached. The NOAA-EPA radiosonde release at ARC occurred at 1400 (figure C-4a). It showed a minor inversion at 800 m, and a standard calculation of the mixing depth gave a value of 780 m. The lidar data at that time showed a slightly higher mixing depth of 900 to 1000 m.

The lidar data clearly established the fact that the surface effluents and atmospheric conditions (temperatures and moisture) could have reached cloud base levels by 1500 on 11 August. The inception or urban storms then occurred within 40 min. The initiation of the storms over the floodplains NW of St. Louis also occurred soon after (45 min) the mixing depth reached 4000 ft (1500 m) at around 1400 CDT (figure C-29). The cloud bases in that area were at about 4000 ft.

Other Data

The aircraft and lidar data for 11 August also provided two other indirect indications of surface-cloud interactions. First, as described in the cloud section, the Cu over the urban area had bases that were 1000 ft higher than those of rural clouds. This suggests that urban heating led to higher condensation levels.

The aircraft also measured several updrafts into Cu. In a few instances the CN values in the updraft were noted. The updraft air going into the base of a thunderstorm, and measured at 1700 CDT over Granite City at 5400 ft AGL, had a CN value of $4x10^4$. The CN in an updraft over Collinsville at a cloud base of 4000 ft AGL (1730 CDT) had a value of $3x10^4$. Both values are similar to those measured at the 2000 and 3000 ft levels during the flight 2 hr earlier. Updraft values of CN going into eight rural clouds were $2x10^3$ at 1500 CDT (S of the city) and $5x10^3$ at 1800 CDT (WSW of the city). Both values were measured around 4500 ft AGL, and were comparable to rural lower-level CN values. It seems clear 1) that the surface-related nuclei were reaching cloud base by mid-afternoon, 2) that these nuclei were being ingested in large quantities into updrafts of storms over and downwind of the city, and 3) that these storms could therefore be safely classed as 'urban-effect' storms.

Summary and Recommendations

The available flight and sounding data for 11 August clearly establish that surface effects reached levels where the bases of rural and urban clouds developed in early to mid-afternoon on 11 August. The development of showers and thunderstorms, first in the bottomlands and then over the urban area, occurred within 45 min after surface air was continuously available and interacting at cloud base levels.

The early afternoon aircraft profiles established that urban-industrial related heating, added moisture, and nuclei extended to and above the 3000-ft level. The CN data coupled with updraft measurements of CN showed that the urban-source CN were concentrated in large quantities in updrafts of storms over and near the city.

Insertion of the surface temperature and moisture data from the bottomlands, the urban areas, and the rural areas into cloud models should be of great benefit in ascertaining whether surface differentials in time and space (bottomland cells first, urban cells later, and none initiated over the rural areas) on 11 August were closely related to the observed conditions of cell occurrence, size, and timing.

The results of this analysis also show the great importance of two data sources for proving the surface–cloud interactions. First, aircraft downwind profiles at selected levels up to cloud base prior to the onset of precipitation are of immense value. Second, the lidar data taken at a point and along rural–urban profiles are invaluable in assessing the mixing depth in time and space. Finally, the concentrations of CN in updrafts should be measured in all cases and investigated more fully because they could offer a means of 'tagging' surface air and thus aiding in classifying urban-effect storms.

TRACER ANALYSES

One of the most informative meteorological experiments conducted on 11 August 1972 was the airborne release of two tracer materials into the updrafts of thunderstorms. The performance of the tracer mission, coupled with the nature of the storms, provides an exceptional amount of information about the convective characteristics of the storms on this day.

The aircraft was directed to perform a tracer mission with takeoff from ALN at 1600 CDT. By 1630, the aircraft was in a weak to moderate inflow area on the rear of a thunderstorm (rain-cell 3). The inflow area was located above the central part of St. Louis.

Two tracer burns were performed. The release of the first tracer material, lithium chloride generated from Lohse wing-tip burners (one on each wing), was initiated at 1632 directly above SLU. The Li release lasted slightly more than an hour and ended at 1739 just above Collinsville. During this 67-min release period, the aircraft flew a series of tight orbits below the inflow area that was believed by the aircraft crew to be on the W and rear side of the storms. The other tracer material was indium, which was released through the burning of 13 pyrotechnic flares containing In. The burning of the 13 flares began at 1646 CDT over NE St. Louis and continued until 1652 (6 min) over Granite City. The amount of Li Cl released in the 67-min period was 1.57 pounds, and the amount of In released in 6 min was 390 grams.

Updrafts and Clouds

The storm updrafts in which the tracers were released were defined by the aircraft crew as "good trailing edge inflow to major cloud development moving over the total network" (Henderson

and Duckering, 1972). The entire period of burning occurred over a rectangular area about 6 mi wide (N–S) and 12 mi long, extending from central St. Louis to the E edge of the Mississippi River floodplain in Illinois.

During the 67-min tracer flight with the releases constantly on the W side of the raincells, the airplane altitude gradually decreased. At the beginning of the burn at 1630 the aircraft was at 5300 ft MSL, and to stay in the main updraft area, its altitude gradually decreased to 3700 ft MSL at the end of the burn at 1739 CDT. Cloud bases decreased as they moved away from the urban area. The updraft speeds measured every 5 to 10 min by the tracer aircraft also varied during the burn period. In the early period (from 1630–1645), the speeds were measured at 300 ft/min, but from 1645 to 1720 the speeds measured were from 400 to 500 ft/min. During the last 20 min of the tracer mission, the updraft speed had diminished ranging from 200 to 300 ft/min. The coupling of this information with the raincell activity through 1740 CDT indicates that the storm was becoming mature by the end of the release. However, the storm was rejuvenated shortly after the Li tracer release terminated by the merger of feeder cells on its NW, W, and SW edges (cells 11, 12, and 13).

Chronology of Tracer Release and Rain Patterns

A good understanding of the tracer releases on 11 August can be obtained by comparing the flight track with the raincell patterns at different times during the release. For this reason, four 5-min rain patterns were chosen. The first of these, 1630–1635 CDT (figure C–30a) shows the flight track and raincells at the beginning of the Li burn. At this time, the aircraft pilot reported burning into a weak updraft (related to cell 3) on the rear (W) of the storm. The potential for burning into cell 5 also seemed apparent. The next pattern shown is for 1645–1650 (figure C–30b), and it represents the conditions during most of the 6-min In release. The tight orbiting of the aircraft is shown in the figure. By this time cell 5 had moved NE to merge with another new cell, 6. The light rain areas of these two cells were joined with the heavy rain core of merged cell 3+4. The inflow area reported at this stage had intensified to 500 ft/min and was located on the W side of the parent cell, apparently cell 6.

The next pattern shown is for 1710–1715 CDT (figure C–30c). At this time, two new cells had grown on the W flank of merged cells 5 and 6 and are labeled cells 8 and 9. The updraft area speed continued to be 500 ft/min and was clearly into the feeder cells on the W side of the parent storm. The final map shown is for 1725–1730 CDT (figure C–30d) which is near the end of the Li release. At this time, cells 5, 6, 8, and 9 had merged into one consolidated storm, and the tracer aircraft was releasing Li along the W edge of the rain shaft, close to the storm. Cells 3 and 4 had separated and were no longer in the MMX circle.

Figure C–31 is an isohyetal map based upon the combined rainfall production of cells 3, 4, 5, 6, 8, and 9, plus that from eight other cells (11–18) that occurred and merged with parent cells 5 and 6 during and after the Li and In releases. This figure includes all rainfall *potentially affected* by the tracer releases during 1630–1930 CDT. Basically, cells 3 and 4 exited from the MMX circle in a heavy rain stage and possibly could have deposited tracer materials beyond the tracer network. Cells 5 and 6 and the 10 feeder cells that merged with them (8, 9, 11–18) all largely initiated, rained, and terminated within the confines of the rain chemistry network delineated on figure C–31. Thus, it appears that a budget analysis of the Li and In for 11 August should show that much of the material released fell within the network. Inspection of figure C–31 shows that very heavy rainfall (> 2.5 inches at 2 raingages) did occur in the network from the 'treated storms.'

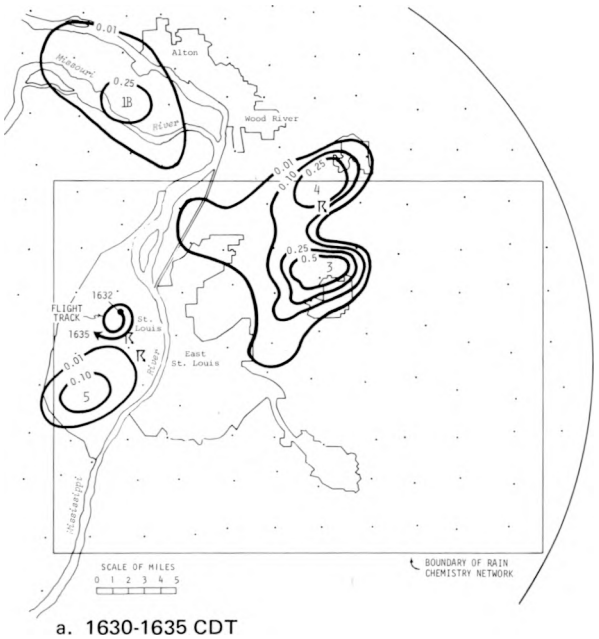

a. 1630-1635 CDT

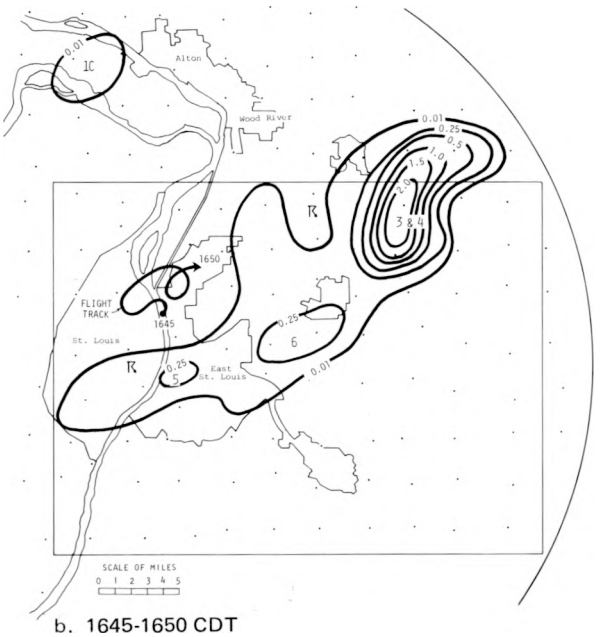

b. 1645-1650 CDT

c. 1710-1715 CDT

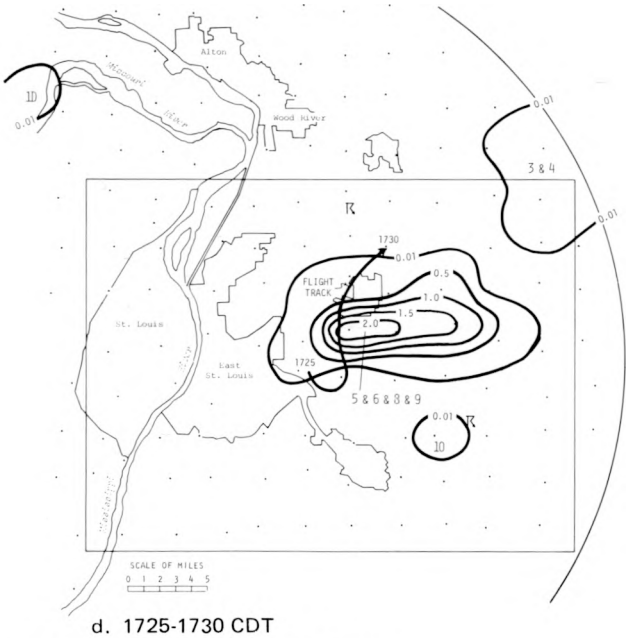

d. 1725-1730 CDT

Figure C-30. Flight tracks and rainfall during tracer releases for selected times

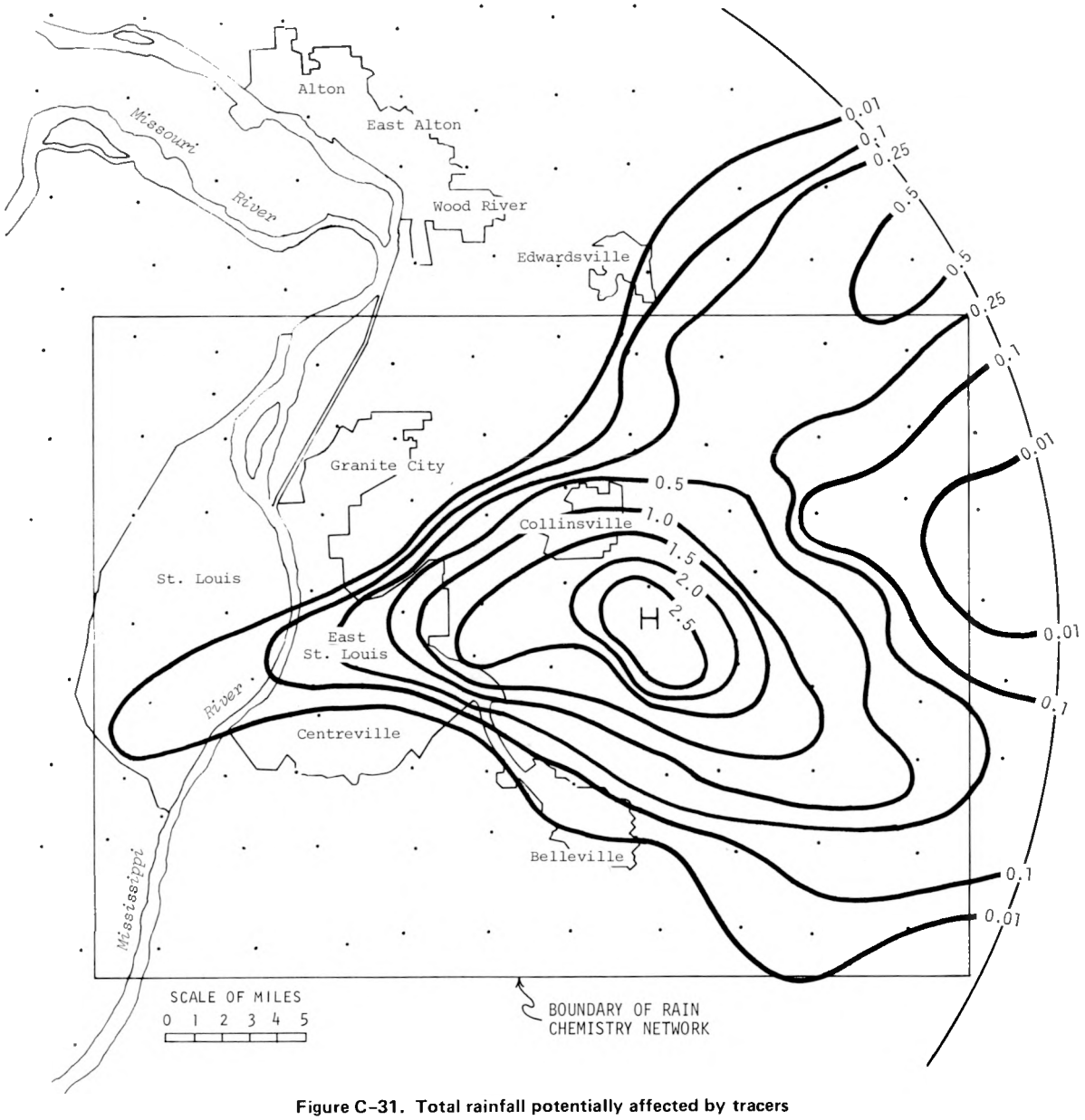

Figure C-31. Total rainfall potentially affected by tracers

Lithium Analyses

The Li deposition pattern for 11 August is shown on figure C-32. Iso-deposition lines are drawn for intervals of 500, 1000, and 2000 pg/cm^2. Also portrayed are select isohyetal lines and the hailfalls. A reasonably good relationship exists between the heaviest deposition and heavier rainfall values. The poorest relations are for the 500 to 1000 pg/cm^2 Li values in the NE area. These high values were associated with the early period of tracer release that went into cell 3+4. An envelope that includes the flight track during the 67-min Li release is also shown on figure C-32.

Figure C-33 is a graph that portrays the Li deposition values and their associated rainfall values containing potential Li. Several important facts are evident. First, background values appear to be $\leqslant$ 400 pg/cm^2. These occurred either with very light rains (< 0.1 inch) or no rain. The Li deposition begins to show a linear relationship to the potentially affected amount of rainfall for Li values above 400. The Li values associated with raincells 3 and 4 are denoted because they appeared to be relatively high; that is, greater deposition per rainfall quantity than in the later raincells of 11 August. Whether this is related to the initial tracer release or the nature of that storm is unknown. Five other relatively high deposition values are denoted on the graph. These are from

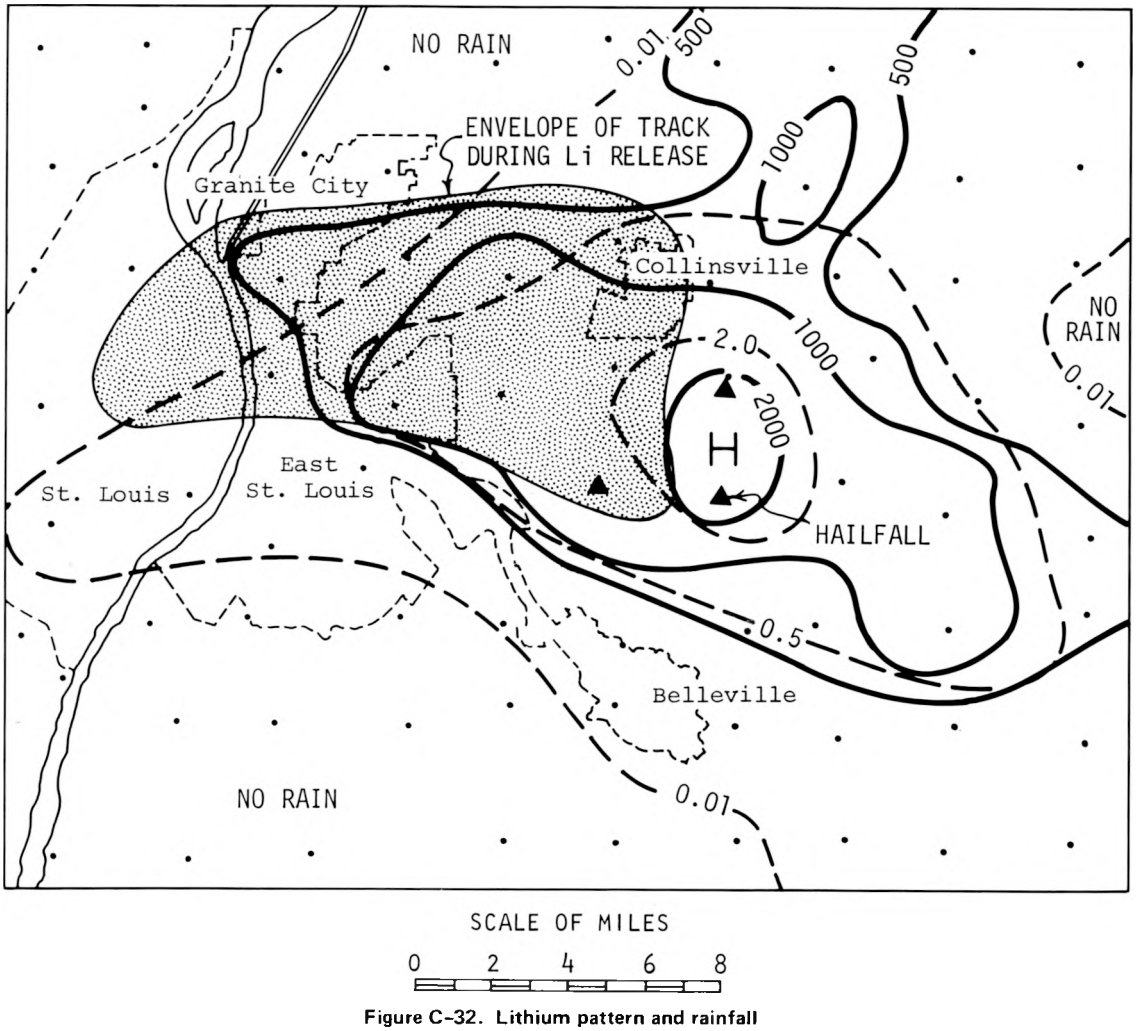

Figure C-32. Lithium pattern and rainfall

Page(s) Missing

from

Original Document

Pages 61 - 76 missing

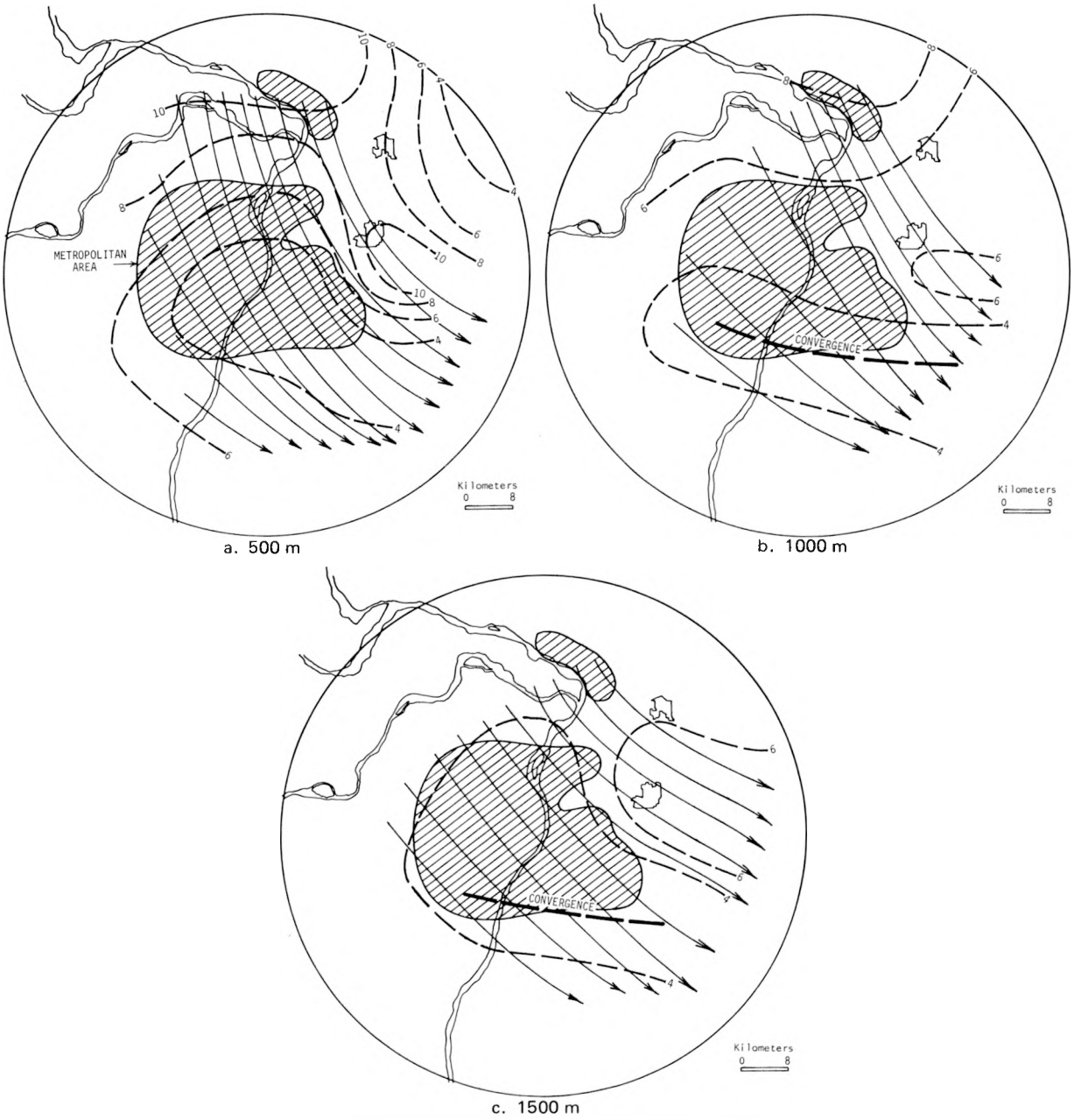

a. 500 m

b. 1000 m

c. 1500 m

Figure D-10. Low-level airflow 1530-1600 CDT

PRECIPITATION MORPHOLOGY

Clouds

Scattered high and middle clouds were observed at PMQ, STL, and BLV in the morning hours and in association with the frontal passage at 1000. A layer of middle clouds covered the NW quarter of the MMX circle during the afternoon and no obstructions to visibility were reported throughout the day. The middle cloudiness became overcast at PMQ and STL by 1800 (about 1 hr after the storms), while BLV experienced overcast conditions during the passage of the storm to the S of it at 1730.

At the time of the frontal passage, the surface observations at 1000 indicated only scattered clouds at all three stations. This absence of cloudiness permitted typical clear to partly cloudy sky and surface heating through early afternoon as reflected in the surface temperature distribution (figure D-6).

The middle level overcast straddled the freezing level at 14,500 ft MSL and this resulted in the abortion of a cloud penetration research flight because of aircraft icing. Such an icing condition is indicative of clouds with relatively high LWC composed of large droplets. The relationship between this antecedent, water-laden, middle cloudiness and the subsequent storm development is worthy of further investigation. The question of whether the cloudiness resulted from either earlier convective activity a short distance upwind of St. Louis or advection over the area as a result of macroscale air movement remains unanswered. A cursory examination of available satellite photos on 14 July suggests that advection is a reasonable explanation since stratiform cloudiness associated with the frontal system was observed. The satellite-observed clouds appeared to be due to over-running on the frontal surface and this resulted in a displacement of 100 to 200 mi between the surface frontal position and the middle clouds.

The continued SE advection of the extensive middle layer in the late afternoon was likely responsible for the nocturnal precipitation observed on the MMX circle on 14-15 July in association with the passage of a frontal wave through extreme S Illinois. A period of approximately 3 hr between the ending of the thunderstorm event and the initiation of the later stratiform rain indicates that these two events were independent occurrences.

Radar Echoes

The radar data from the University of Chicago 3-cm RHI at Greenville (figure B-1) was used to assist in the interpretation of the precipitation development. The radar observations were extremely instructive, but were also somewhat complex and the analysis was carried out only during the initial period of storm development. Also, since the 3-cm radar is subject to occasional precipitation attenuation, the data became suspect when intervening rainfall was present and for this reason no analysis was performed after 1700.

The storm's initiation could not be viewed since it was over 70 mi from the radar which has a range limitation of 65 mi. However, the ESE movement of the storm toward the radar allowed analysis of significant features of the echo morphology during much of the critical period of rapid precipitation development.

This first storm of 14 July was initially photographed by the radar at 1555 as it moved into the MMX circle at the extreme W edge. The movement of the echo (A) was to the ESE at an average speed of 26 kt. The top of the storm was observed at 13,000 ft and it underwent an oscillating growth, reaching 20,000 ft by 1620. Two echoes (B and C) independent of A developed at 1620 as shown on figure D-11.

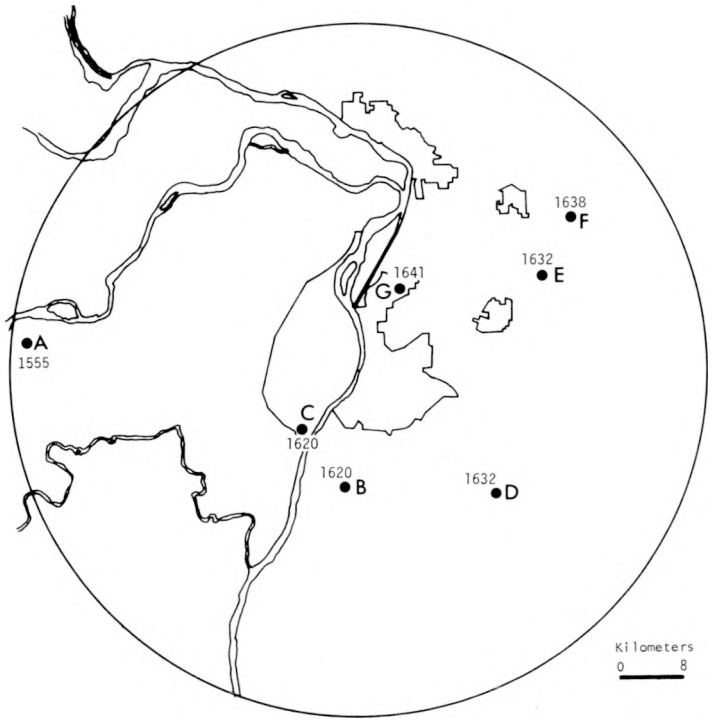

Figure D-11. Location and time of the first appearance of echoes between 1555 and 1700 CDT

The locations of all first echoes observed during the period between 1555 and 1700 (figure D-11) were determined by the azimuth and range of the maximum top observed at the stated times. None of these echoes had significant movements during their lifetimes, and only echoes B, C, and D were of importance to the 14 July thunderstorm.

The first echoes B and C were detected at altitudes of 11,000 and 17,000 ft, respectively. The precipitation from these echoes was not observed at surface raingages until 20 min later for echo B and only 10 min later for echo C. These echoes were separated by approximately 7 mi and while echo B showed occasional slight movement to the ESE, echo C remained stationary.

Echo C grew to a maximum top of 24,000 ft during the 15-min period between its initial detection and its merger with echo A at 1635. By contrast, echo B showed very little vertical growth until it was no longer distinguished from the well-developed primary cell at 1700. The maximum top of echo B oscillated between 14,000 and 16,000 ft during its 40-min lifetime as an isolated echo.

The growth of the echo tops for echoes A, B, C, D, and E is shown on figure D-12. There were two features of the development of echoes B, C, and D which are important for an interpretation of the possible urban effects on storm morphology. First, these echoes developed in advance of the major migratory system in proximity to the convergence zone (shown on figure D-10b and c). Second, the new echoes did not have significant movements until after the completion of their merger with the primary storm, echo A.

The apparent relationship between first echo development and the convergence zone is expected, and the link to the urban area is made through the creation of convergence by the urban canopy in the NW flow regime at the sub-cloud base. In this sense, the urban effect is a secondary one because convergence alone is not a sufficient condition for storm development. As has been shown, other conditions (instability, moisture, etc.) conducive to shower and storm development were present, but the urban-related convergence zone dictated where they occurred. The relatively

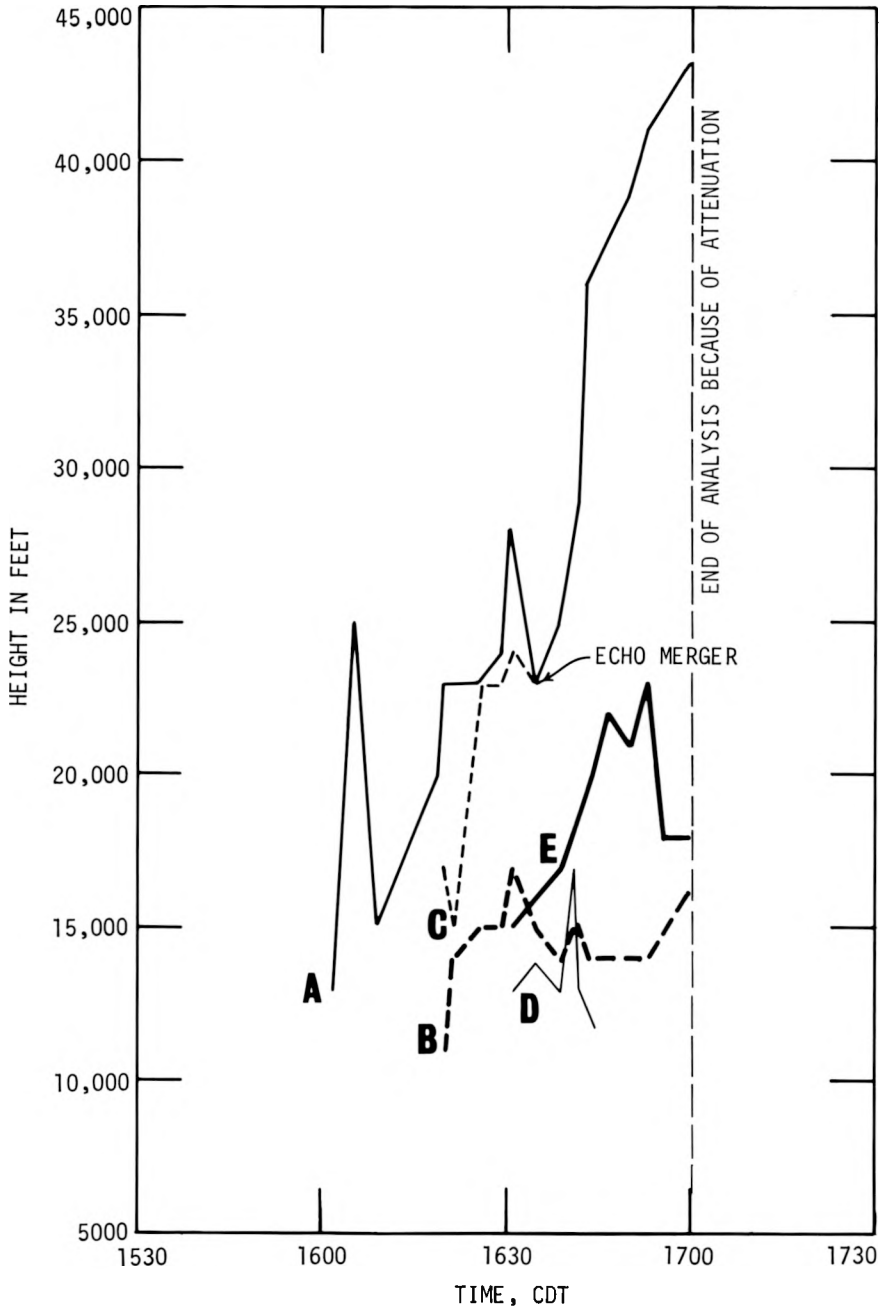

Figure D-12. Maximum top growth of primary echo A and first echoes

little movement of the first echoes during the 15 to 35 min that the major system was progressing toward them at a steady rate implies: 1) the clouds associated with the echoes had roots on the ground, and 2) the stationary echoes (and clouds) were exposed to the direct influence of the urban environment as they were directly downwind from strong surface sources of heat, moisture, and aerosols.

The rapid growth of echo A after merger with echo C parallels the precipitation production with a time lag of approximately 10 min. The physical mechanism responsible for increased precipitation efficiency of merging systems has not been fully explained, although considerable observational evidence is available.

The other first echoes (E, F, and G) NE of the main storm track did not show anomalous behavior, although all of them appeared in the area of the climatologically defined rainfall maximum (Huff and Changnon, 1972), and they were exposed to the same macroscale conditions. These showers existed for $<$ 60 min with growth and dissipation characteristics similar to that of echo E (figure D–12).

From the available data, it is difficult to categorize where the main storm development was most pronounced in relation to its motion. The first echo merger between echoes A and C occurred on the left flank (N side) of the storm relative to the motion of echo A. Later echo mergers occurred directly in front or slightly to the left of the main storm, suggesting that the growth took place not only along the convergence zone but also to the city-side of echo A.

The RHI radar profiles for 1644 and 1659 are shown on figure D–13. The merger of echoes A and C is estimated to have occurred at 1635 when the maximum top of A reached 23,000 ft. It is apparent from the figure that, generally, the merger of two echoes did not result in the complete envelopment of the two entities; instead, either one will develop at the expense of the other, or one will exhibit a rapid growth with respect to the lesser development of the other. In this case, echo A continued to grow at a very slow rate while echo C explosively grew to 45,000 ft during the 24 min after merger. The growth rate of echo C exceeded 2300 ft/min during this period with an average rate of 900 ft/min.

Unfortunately, the 3-cm RHI radar signal became attenuated during the subsequent continuation of this storm development and further interpretation was prohibited. The early storm growth was characterized by the movement of the primary storm to the ESE with scattered first echo development to the E and NE of it. The progression and intensification of the storm was in response to the merger of independent echoes in proximity to the downwind urban area. The first echoes that were not associated with the city nor with the primary system exhibited lesser shower growth rates and shorter durations.

Raincells

The first rain on 14 July was observed near the Portage des Sioux power plant at 1455 and lasted 40 min. During this interval no rain was recorded elsewhere in the MMX circle. The production of clouds from the twin stacks of this power installation is quite common, but measurable confirmation of precipitation directly attributable to such artificial clouds has been rare. Precipitation also occurred in the bottomlands where first echo frequency, raincell initiation, and rainfall are all increased, presumably by the moister and warmer air (Huff, 1974).

Shortly after the dissipation of raincell 1, a new cell migrated into the network at the extreme W boundary. This rain event (echo A) began on the network at 1555 and is labeled 2 on figure D–14. Raincell 9 was a large but nonconvective rain entity likely due to middle and high cloudiness that advected from the main convective system during its passage toward the ESE.

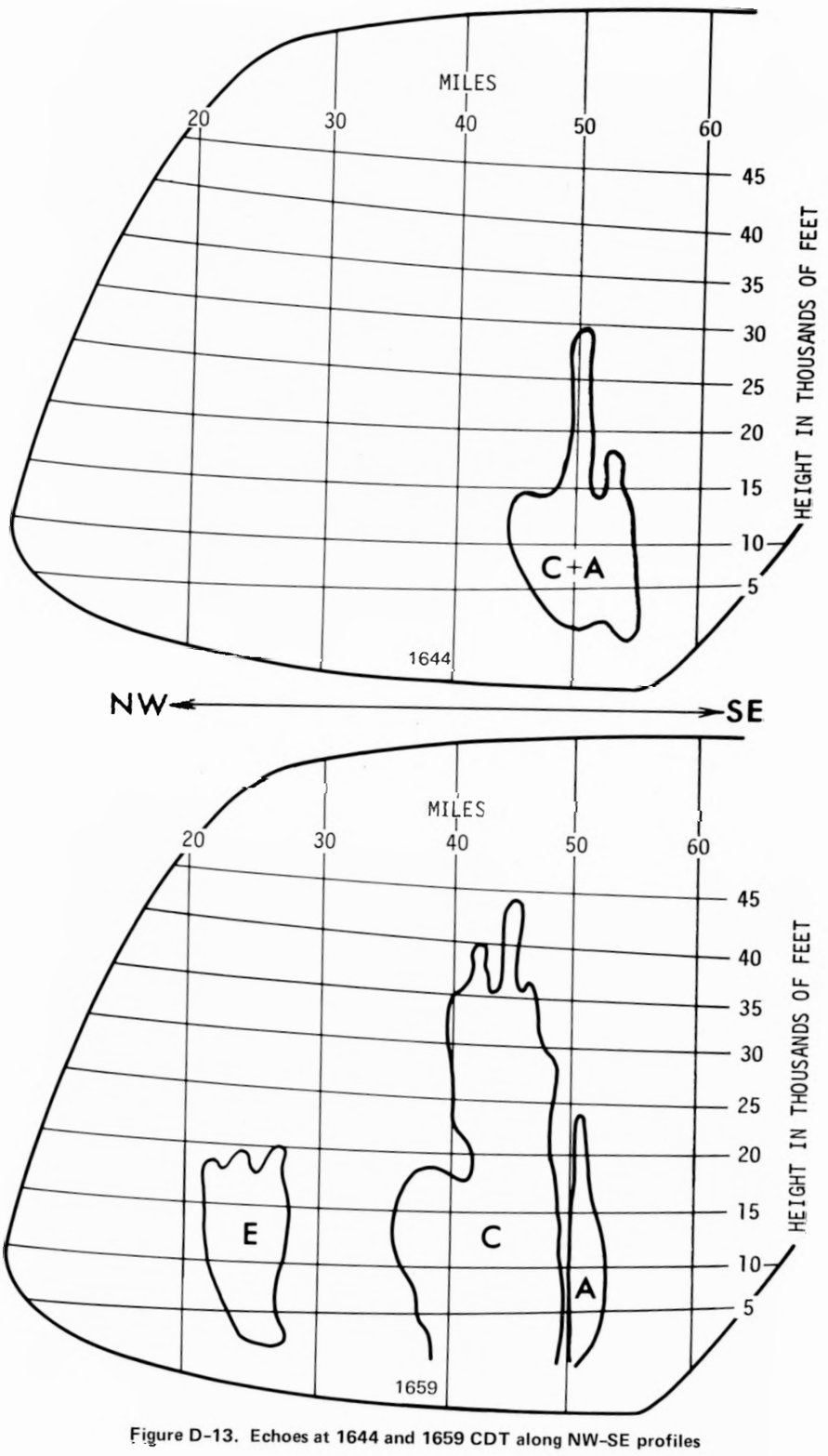

Figure D-13. Echoes at 1644 and 1659 CDT along NW-SE profiles

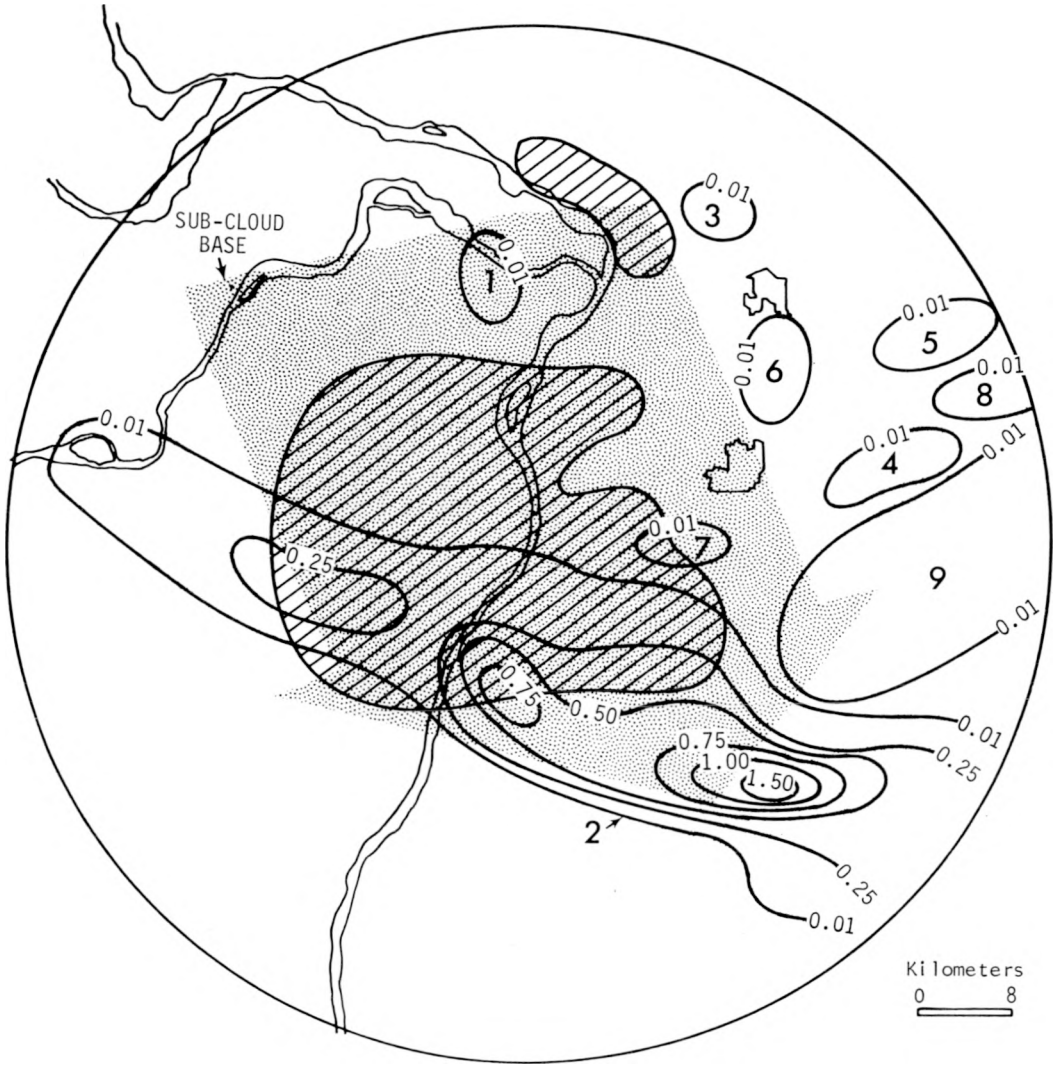

Figure D-14. Total rainfall from all raincells on 14 July 1973 between 1500 and 2000 CDT

The first appearance of cell 2 as a well-defined entity on the network is shown at 1605 on figure D-15a. The short duration, isolated cell 3 is also shown in proximity to the Wood River refinery complex. It is interesting to note that cells 1 and 3 were both stationary and related to known sources of anomalous cloud behavior. The major cell, 2, was migratory with movement to the ESE.

During the next 15 min, the isolated cell 3 dissipated while cell 2 intensified and moved to the SE (figure D-15b). In the subsequent 15 min a new cell appeared directly S of the city (shown as cell 2a on figure D-15c). This stationary cell merged with the main storm system within 15 min and the first thunder was recorded at SLU coincident with this event. An additional new cell (4) was observed E of Collinsville at this time, but it cannot be physically related to the major system passing S of St. Louis.

Continued new cell development was also observed in advance of the moving system as shown at 1645 on figure D-15d. The new cells, coincident with the sub-cloud base zone of convergence, 2b and 2c (echo D), remained stationary while awaiting the approach of the major system from the WNW.

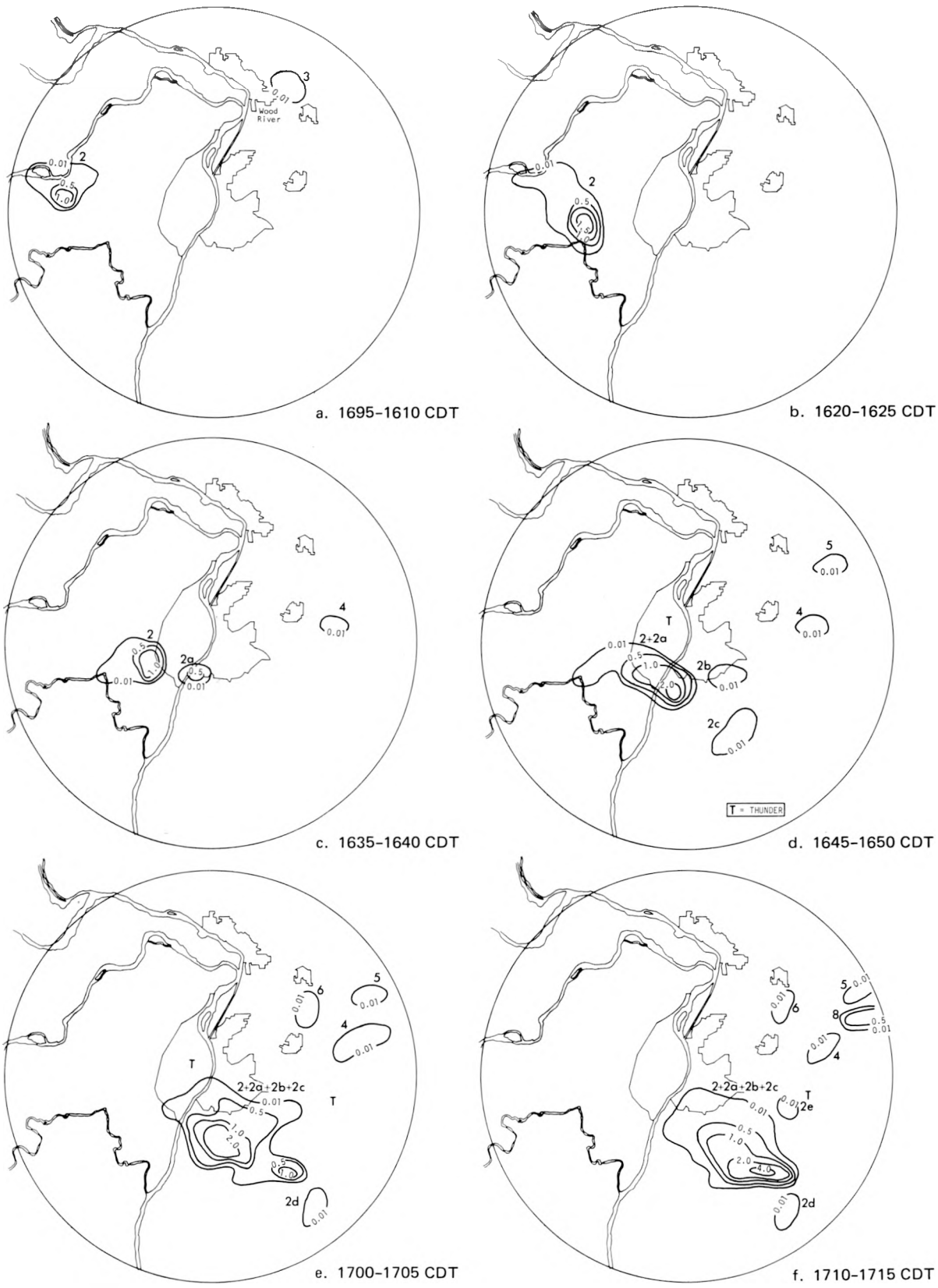

Figure D-15. Raincell development depicted by 5-min rainfall rates (in/hr) at selected times between 1605 and 1715 CDT

Several mergers occurred between the moving system and new cell development E and SE of the storm track. Cell 2 was involved in at least 4 merger events during its lifetime while all other cells remained individual entities. The mergers contributed to an apparent movement of the primary storm, but such mergers cannot be responsible for the observed advection of the storm at an average speed of 20 mi/hr which was likely moving with winds at the 700-mb level. Additional isolated cells developed NE of the East St. Louis area, but they did not contribute to the major storm intensification (figure D-15e).

The storm system reached its peak point rainfall rate at 1710 after at least 4 mergers had occurred. The maximum rainfall rate of 5.61 in/hr (figure D-15f), which has an expected return frequency of once in 9 years, indicates the intensity of this small-area, isolated thunderstorm.

The production of rainfall as a function of time is shown on figure D-16. The rapid increase of rainfall is extremely well related to the rapid growth of the associated radar echo top. A comparison between the rainfall (figure D-16) and the radar echoes (figure D-12) suggests that an acceleration of the echo top resulted following the merger of echoes A and C and a corresponding rapid release of precipitation was observed 10 min later. This temporal relationship between echo top growth and precipitation growth was maintained throughout the period of storm intensification. The symmetry of the rainfall production may be due, in part, to the fact that the 5-min storm rainfall was not totally measured at each of the temporal extremes because of lack of complete data at network edges. However, a closed 0.01-inch isohyet for the storm was observed between 1625 and 1740 and this portion of the rainfall produced the observed symmetry.

The time of merger events between raincells is indicated by M on figure D-16. It is of interest that 4 of 5 new cell mergers occurred during the intensification of the storm, and the fifth merger occurred during the 5 min of the observed maximum precipitation production from the system. The previous discussion established that the new cells developed and remained stationary, essentially waiting in the path of the approaching primary cell 2. The development of these new cells also occurred in the region estimated by the low level airflow to be under urban influence. This region of maximum potential urban influence is depicted by the stippled area on figure D-16.

The new cell developments all occurred in time and space such that urban influences could have led to their development and modified their behavior. Consequently, their interactions with an approaching storm, and the subsequent increases in rainfall, provide interesting evidence of how an urban area can lead to added rainfall.

STORM SUMMARY

The total rainfall for the afternoon (1400-2000) of 14 July is shown on figure D-17. It is obvious that cell 2 dominated the rainfall pattern. The occurrence of thunder in association with this storm is also indicated.

The pattern of relatively light rainfall E of a line from Edwardsville to Belleville came with middle cloudiness associated in time with the maximum development of the primary convective storm. The only convective rain observed outside the region of the main storm and embedded in the stratiform middle clouds appears to be related to the isolated industrial areas or specific physiographic (bottomlands) sources of warm, moist air. These observations exemplify the tenuous stability of the atmosphere and the possible role of localized surface sources of heat, moisture, and aerosols to initiate showers.

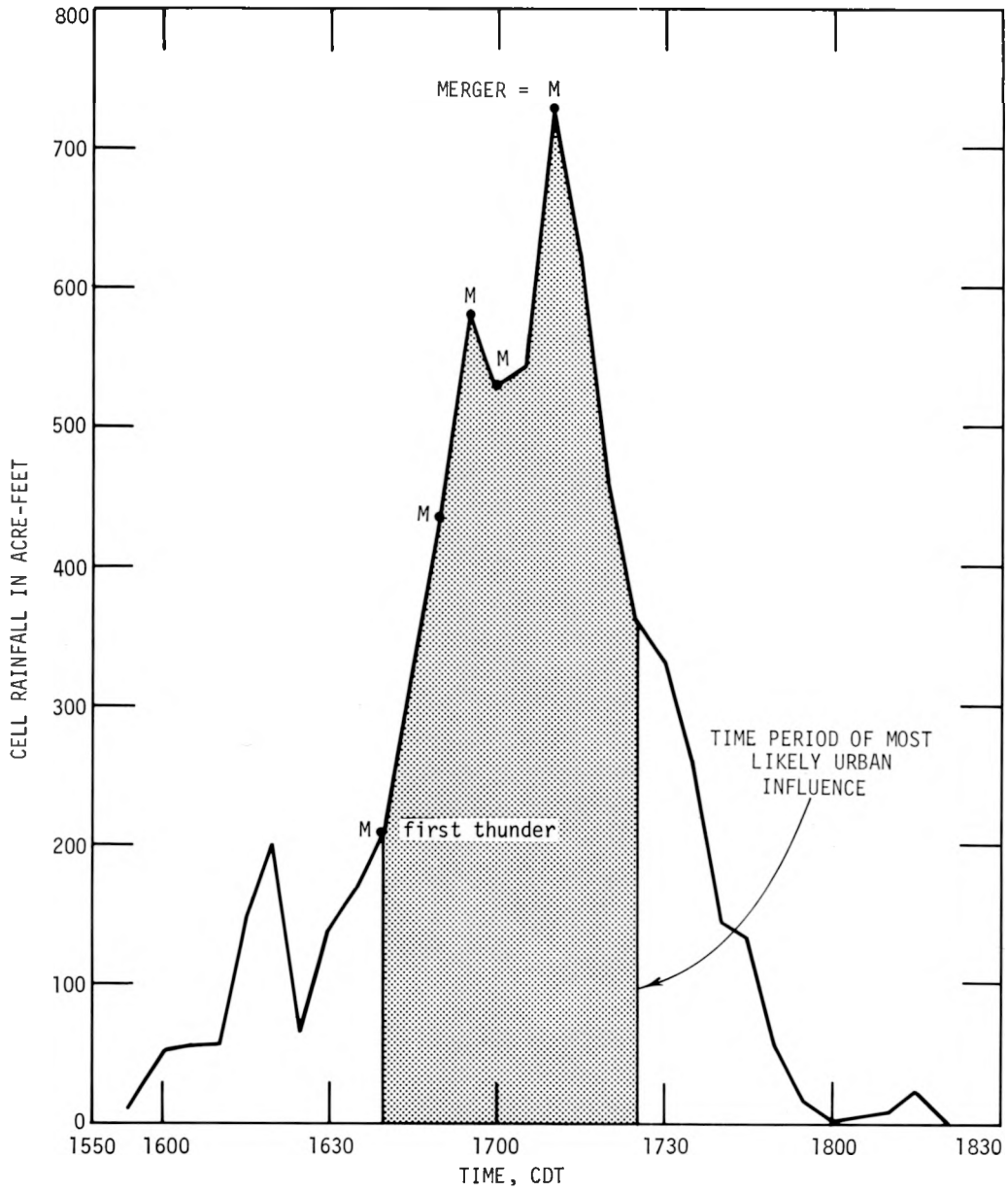

Figure D-16. The rainfall production (ac-ft) from raincell 2 as a function of time

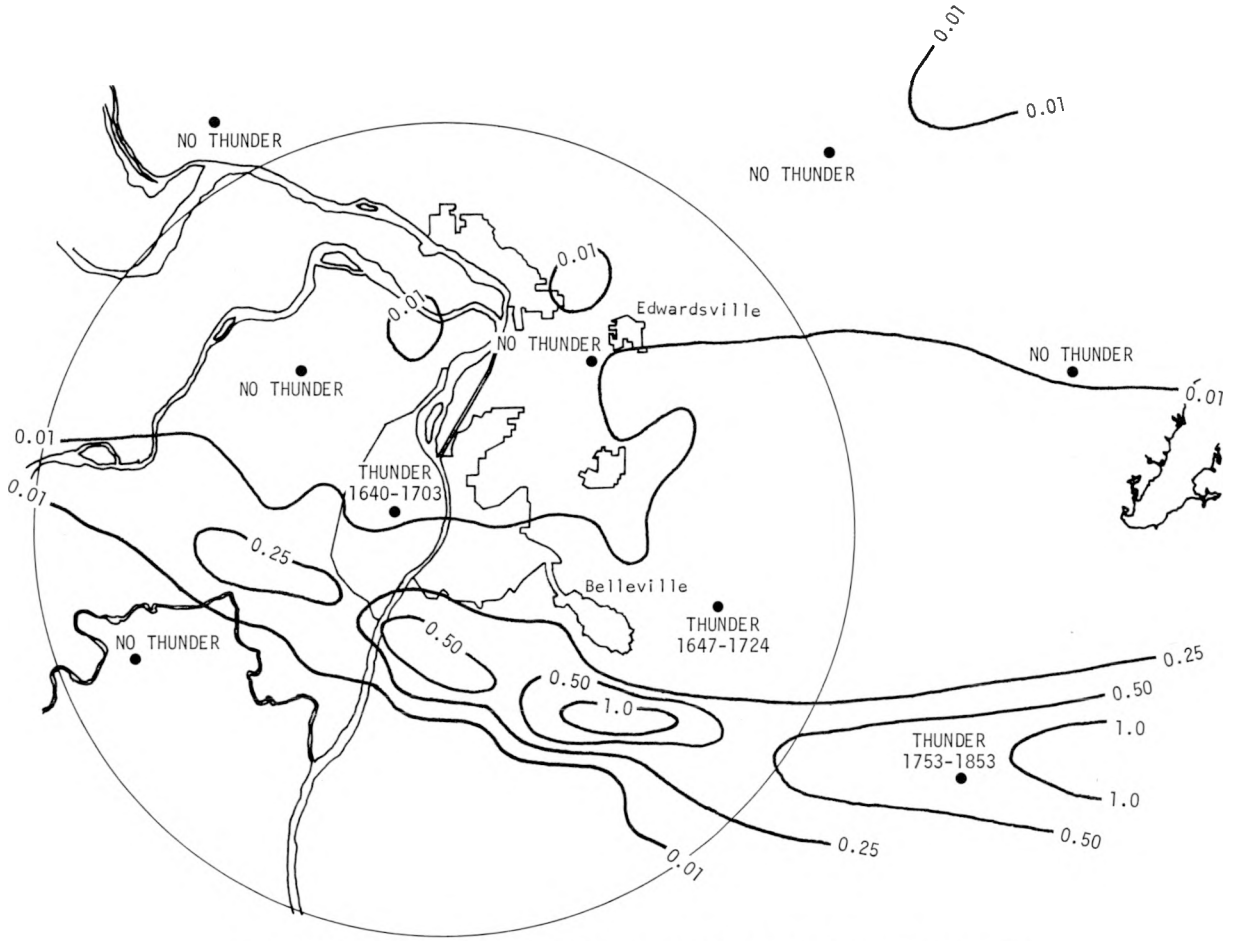

Figure D-17. Total network rainfall between 1400 and 2000 CDT on 14 July 1973

The first thunder was recorded at SLU at the time of the first merger of the migratory system (figure D-15d) and the stationary new raincell S of St. Louis. This event also coincided with the initiation of the rapid production of rainfall (figure D-16). No hail was recorded from this storm, although heavy point rainfalls were measured.

CONCLUSIONS

Unfortunately, certain key data were not available for this case study. The aircraft was not flown and surface chemistry data were not collected because the synoptic situation suggested post-frontal conditions not conducive to good convective activity. This reflects the need for careful updating in forecasts for mesoscale areas. The lack of aircraft observations is a particularly severe handicap in attempting to link this storm directly to urban effects.

Even with these difficulties, the analysis of available data indicates a possible role of the city in producing the observed precipitation pattern. The early, isolated showers that developed N and E of St. Louis appeared to be qualitatively related to nearby urban or industrial areas. These showers, for the most part, remained quasi-stationary and existed for relatively brief intervals of

time. Only one shower within the same macroscale environment developed into a thunderstorm and persisted longer than 2 hr.

The question to be resolved is not why only one major convective cloud developed, but rather, how the St. Louis urban complex might have contributed to its development, lifetime, or intensification. Preceding the initiation of the major rain system, the surface temperature, dew point, and wind patterns all reflected local conditions that could support convection. The temperatures and dew points were both relatively high, although the temperatures at 1600 already reflected cooling due to advecting cloudiness. The winds at the surface showed a convergence–divergence couple in proximity to the first observed precipitation. None of these features, however, can be directly related to the St. Louis urban area. It is concluded that the initial development of the isolated thunderstorm event was an atmospheric response to a locally unstable region and that the cell was due to a combination of temperature, moisture, and low-level wind patterns unrelated to man's activities.

The movement of the storm corresponds quite well to the mean-layer wind between 850 and 700 mb, that is 300° at 20 mi/hr. Perhaps by coincidence, this direction of movement corresponds approximately to the orientation of the low-level convergence zone induced by the increased roughness of the urban center. This low-level convergence contributed to where four new raincells embedded in the urban aerosol plume developed.

The link between this storm and the urban area resides in the growth and development of these new cells in advance of a migratory natural storm. These new cells appeared in proximity to the convergence zone downwind of the city. The convergence zone was a response of the atmosphere to the change in surface roughness and was consistent with the findings of Angell et al. (1973).

This case study is representative of a simple isolated storm and may be considered a building block for understanding effects on more complicated thunderstorm systems. The apparent urban effect on the boundary layer airflow and the possible microphysical alteration of clouds by urban aerosols were not complicated by nearby convective storms. Conceptually, the superpositioning of several of these isolated storms perpendicular to the line of their motion would have constituted an organized convective system. The obvious interaction of neighboring cells would lessen the ability to discern the direct effect of local atmospheric perturbations on storm behavior.

The results of this study suggest four factors that can lead to effects on isolated storms, such as the one on 14 July, or on multicellular systems:

1) Down-city development of a convergence zone in the sub-cloud layer
2) Development of relatively slow moving or stationary convective cells in proximity to the urban-caused convergence zone
3) Alteration of the microphysical structure of the urban-enhanced convective activity by the introduction of aerosol, in particular, 'giant' aerosols
4) Merger of the urban-modified clouds with a migratory mesoscale cloud system and the subsequent release of stored water through an enhanced warm-rain process

This four-point hypothesis suggests additional areas of emphasis for future work and a need for examination of past data with these points in mind. The most important of these points is the confirmation of the urban-related convergence zone and its dependence upon low-level wind speed, direction, and vertical shear. The location and strength of the convergence could be a determining factor in the location and magnitude of the urban rainfall anomaly.

The second point deserving additional scrutiny is the location of point and small area sources of giant cloud CN because these play an important role in the alteration of urban-enhanced convective clouds. The low-level trajectory of the urban aerosol containing giant nuclei to the convergence zone could be a decisive factor for precipitation alteration.

The scenario proposed by the four-point hypothesis is dependent on the pre-existence of macroscale conditions conducive to the formation of convective clouds. The urban effects are then involved in controlling the temporal and spatial initiation and inadvertent modification of precipitation. This hypothesis, after verification with independent data, can form a basis for transferral of results from St. Louis to other urban areas. The convergence zones can be predicted by judicious use of available numerical models. Only a minimal field observation program to assess the giant nuclei production over the area of interest would be required to predict the location and relative magnitude of a precipitation anomaly.

REFERENCES

Angell, J. K., W. H. Hoecker, C. R. Dickson, and D. H. Pack. 1973. *Urban influence on a strong daytime air flow as determined from Tetroon flights.* Journal Applied Meteorology, v. 12(6):924-936.

Huff, F. A., Editor. 1974. *Interim report of Metromex studies: 1971-1973.* Illinois State Water Survey.

Huff, F. A., and S. A. Changnon. 1972. *Climatological assessment of urban effects on precipitation at St. Louis.* Journal Applied Meteorology, v. 11:823-842.

Jones, D. M. A. and P. T. Schickedanz. 1974. *Surface temperature, moisture and wind studies. In* Interim Report of Metromex Studies: 1971-1973, F. A. Huff, Editor. Illinois State Water Survey, pp. 98-120.

Semonin, R. G., and S. A. Changnon, Jr. 1974. *METROMEX: Summary of 1971-1972 results.* Bulletin American Meteorological Society, v. 55(2):95-100.

E. SEVERE STORMS OF 23 JULY 1973

Paul T. Schickedanz and Donald F. Gatz

CONTENTS

E. SEVERE STORMS OF 23 JULY 1973

INTRODUCTION

This was a day of very severe weather in the St. Louis area, when the heaviest rain occurred W and NW of the city. The main purpose of this investigation was to learn whether the city contributed to either the severe weather, or to the W to E decrease in heavy rain across the MMX circle.

SYNOPTIC WEATHER CONDITIONS

Macroscale

Conditions at 0700. The most important synoptic feature for the St. Louis area was a stationary front, oriented approximately E-W across the E-central United States. Its precise position is not clear. NWS operational facsimile charts placed the front approximately over St. Louis at 2200 CDT on 22 July, along the Missouri-Arkansas border at 0700 on 23 July, and just N of St. Louis at 1000 on the 23rd. Subsequent analysis of satellite data by Purdom (1974) placed a warm front across E-central Missouri, but N of St. Louis, at about 0900 on 23 July. The two positions were not greatly different at mid-morning on the 23rd. However, the position inferred from the satellite data is probably more accurate, in view of the lack of any strong discontinuities in surface weather parameters.

The 850 mb map at 0700 showed extensive areas of moisture (dew point depressions of $\leqslant$ 5.0C) in the E United States covering all of Missouri and the S half of Illinois. Winds were SW with little temperature advection.

The 500 mb chart for 0700 showed a pressure ridge from Georgia to James Bay and a major trough situated near the West Coast. Winds in the St. Louis area (figure E-1) were SW at 500 mb, with a slight tendency for warm advection. A short wave trough was oriented from Wyoming to Oklahoma in the SW flow.

The 200 mb chart indicated a NE course of the jet stream from Amarillo to Madison, and the jet's closest approach was NW of the St. Louis area across Iowa.

Synoptic conditions were generally favorable for convective activity, with warm temperatures and ample moisture in the lower layers. Severe weather would probably not have been expected, however, in the absence of warm air advection at low altitudes, cold air advection aloft, and only moderate wind shear.

Afternoon. The surface map for 1300 (figure E-2) shows a line of thunderstorm activity across central Missouri associated with the front and an approaching squall line. This analysis is based heavily on Purdom's (1974) detailed analysis of this case with satellite data.

The satellite photograph at 1159 (figure E-3a) shows the squall line approaching the front from the W. By 1526 (figure E-3b) the squall line had overtaken the front and produced a large convective cloud mass across central Missouri.

The cloud mass in SE Missouri at 1526 is another important feature of Purdom's analysis. Subsequent satellite photographs (figure E-3c) show that that cloud mass grew (or moved) toward the NNW and eventually intersected with the advancing squall line. Heavy rain and severe weather in the St. Louis area followed the intersection of these two systems.

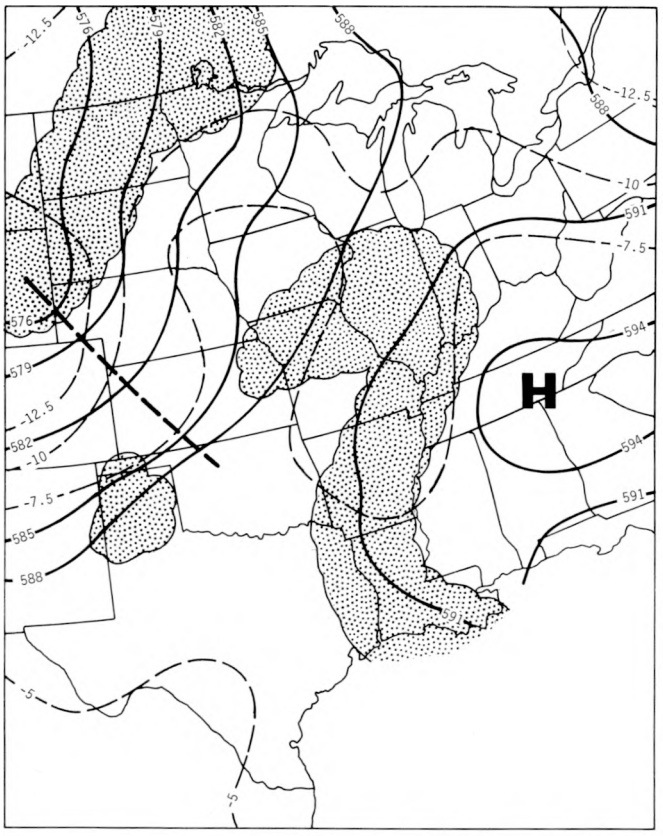

Figure E-1. 500 mb chart for 0700 on 23 July

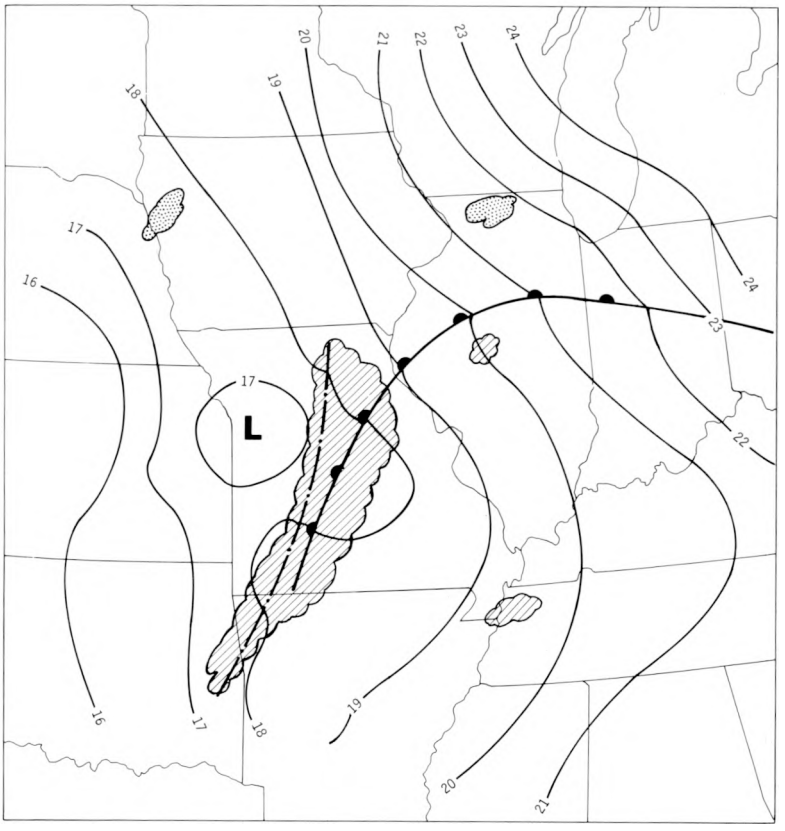

Figure E-2. Surface weather map for 1300 on 23 July

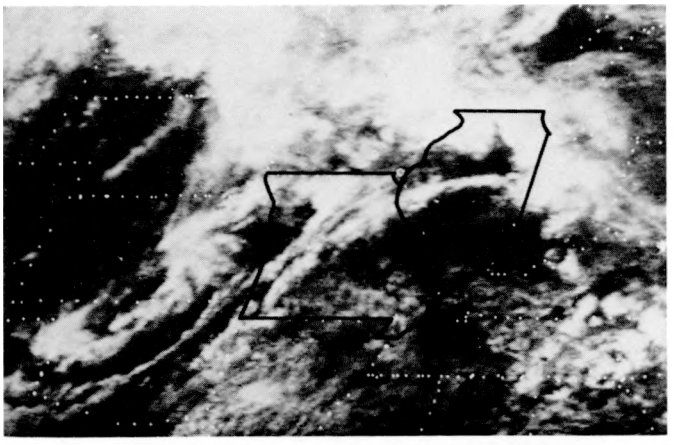

a. Squall line approaching warm front at 1159

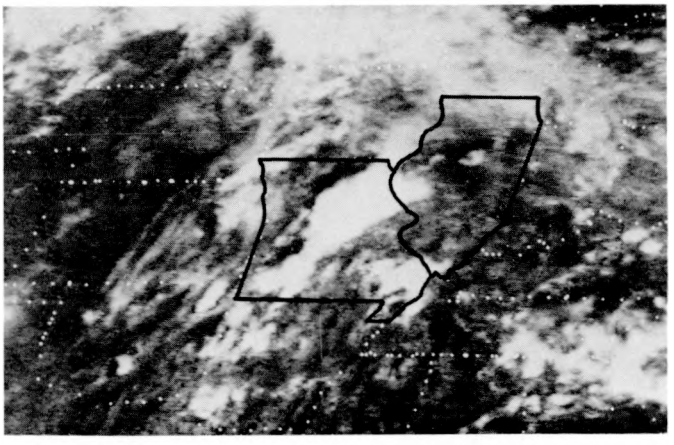

b. Merged cloud mass (central Missouri)
and new cloud development to SE

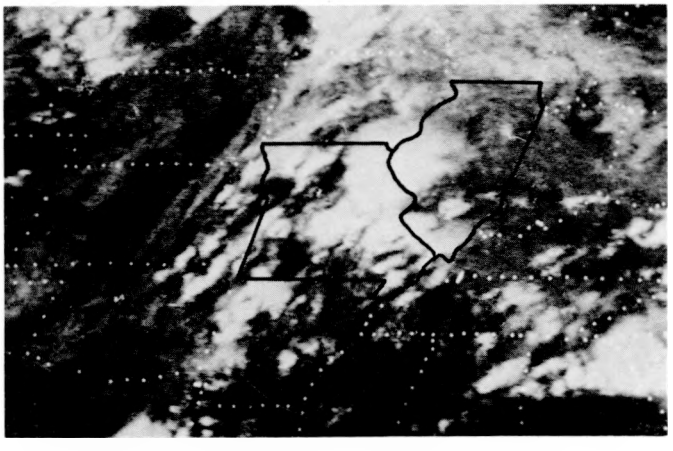

c. Merger of two cloud systems (separate in b)

Figure E-3. Satellite views of weather events affecting the St. Louis area on 23 July

Mesoscale

Although most attention is centered on the afternoon events, the day actually had two periods of precipitation. Light rain occurred in the St. Louis area for several hours during the early morning. Surface weather conditions just prior to both precipitation periods are presented.

Early Morning Rain. The surface temperature distribution at 0000 on 23 July is shown on figure E-4. The highest temperatures occurred over St. Louis, with a broad zone of relatively high temperatures along the Mississippi and Missouri Rivers. Figure E-5 shows a 5F range of dew point temperatures in the MMX circle, with maximum values occurring in the S portion of the circle and in a narrow zone along the E bank of the Mississippi.

Compared with weather observations at the nearest surrounding synoptic stations, the city was about 5F warmer and also somewhat drier (2 to 3F dew point differences).

The surface wind chart for 0000 (figure E-6) shows wind directions varying from NE to SE over the MMX circle, with most speeds less than 5 m/sec. These winds match those to the N of the front, indicating that the front lay S of St. Louis at this time.

The distribution of θ_e at 0000 is shown in figure E-7. Except for a small pocket of low values just S of the city, the highest values were located in a broad band along the Mississippi S of Alton.

Squall Line Rain. The surface temperature distribution at 1500, prior to the squall line rain, is shown on figure E-8. Temperatures ranged from 87 to 95F within the network, with the highest temperatures occurring in the S sections and the lowest in the SW. There is weak evidence that the city area was slightly cooler than the surrounding area. The moisture (dew point) distribution at 1500 (figure E-9) shows very high dew points (79F) at PMQ and in the S part of the circle. Low values occurred over and W of St. Louis and in the Alton-Wood River area. Both temperatures and dew points in the rural areas of the MMX circle agreed closely with those measured at nearby synoptic stations that were unaffected by rain. Winds at 1500, ahead of the squall line, were SE over the MMX circle at speeds mostly between 5 and 10 m/sec (figure E-10).

The θ_e distribution at 1500 (figure E-11) shows some strong gradients, with very high values located NW and S, and a broad zone of low values running across the circle from W to NE.

Pre-squall line atmospheric stability conditions in the St. Louis area are presented on figure E-12. The data show a substantial difference in moisture in the surface to 500-mb layer between PMQ and ARC at about 1330, but substantial agreement between the 1335 and 1611 soundings at PMQ. The moisture deficiency over the city resulted in a much more stable lifted index at ARC than at PMQ at about 1340 (+1 as opposed to -6).

The moisture deficiency over St. Louis that appears in the sounding data (figure E-12) agrees with the surface dew point distribution at 1500 (figure E-9), except the difference between the city and the outlying areas is far greater aloft than at the surface. These differences are so great, even at 500 mb, that they raise questions regarding the validity of the moisture data. Relative values within a given sounding could be valid, but comparisons between sites cannot be made with confidence.

Low-Level Airflow. Airflow data are presented for 1400 and 1600, in the pre-rain environment. Flow is depicted for 500 m, 1000 m, and 1500 m MSL, by streamlines and isotachs.

The 500 m flow at 1400 (figure E-13a) was uniformly SE over the whole circle. Isotach maxima and minima suggest local areas of convergence and divergence, but no strongly organized pattern. At 1000 m (figure E-13b), the flow was almost directly from the S, with a slight suggestion of convergence in the N portion of the circle in both the streamline and isotach analyses. At 1500 m (figure E-13c) a few stations are missing because the pilot balloon was lost from sight in the clouds. Over the E half of the circle, where data are available, flow was still uniform from the S.

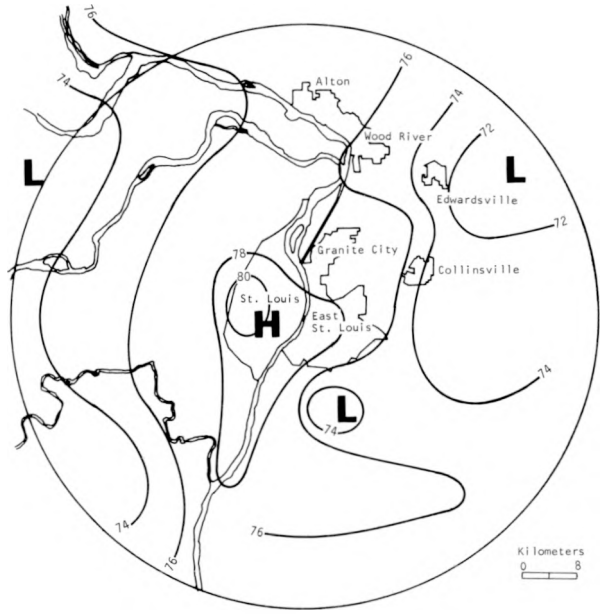

Figure E-4. Surface temperature distribution at 0000 CDT before morning rain

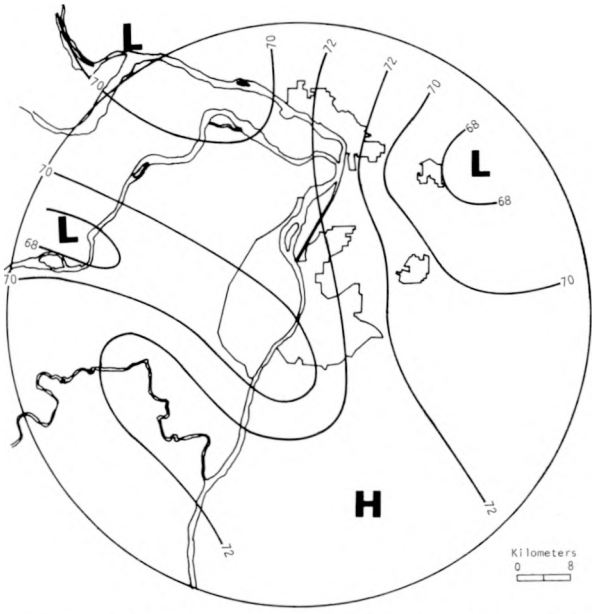

Figure E-5. Surface dew point distribution at 0000 CDT

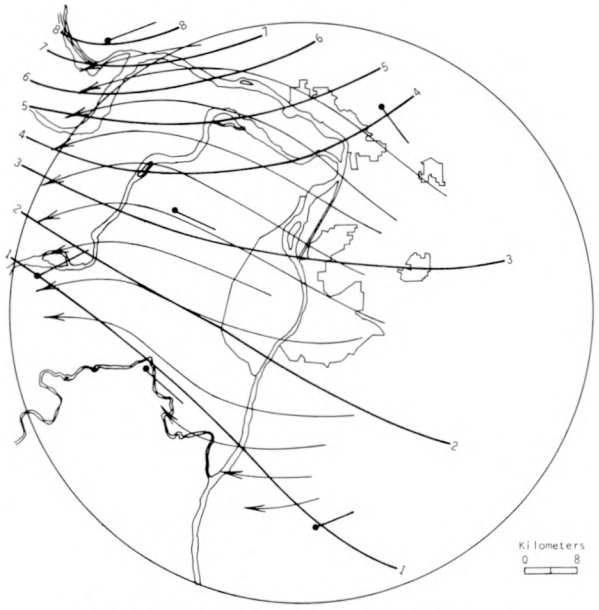

Figure E-6. Surface wind chart for 0000 CDT (Isotachs in m/sec)

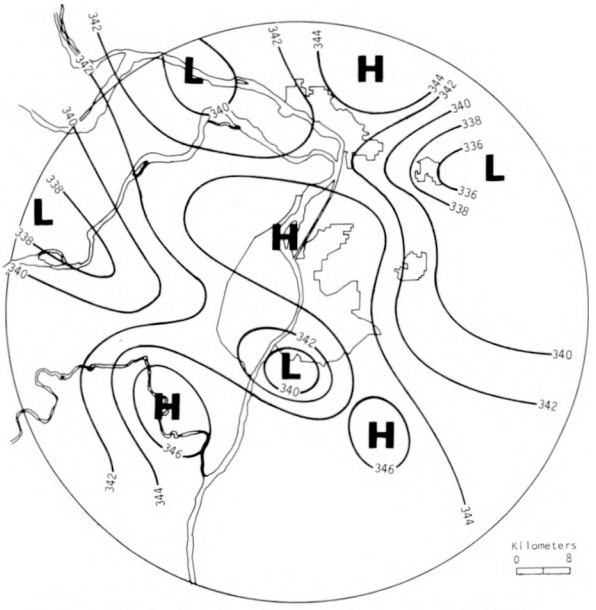

Figure E-7. Surface θ_e (°K) distribution at 0000 CDT

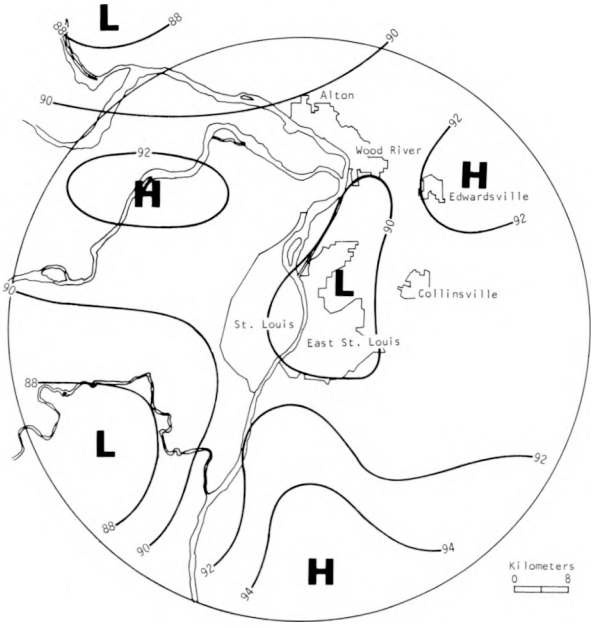

Figure E-8. Surface temperature distribution at 1500 CDT

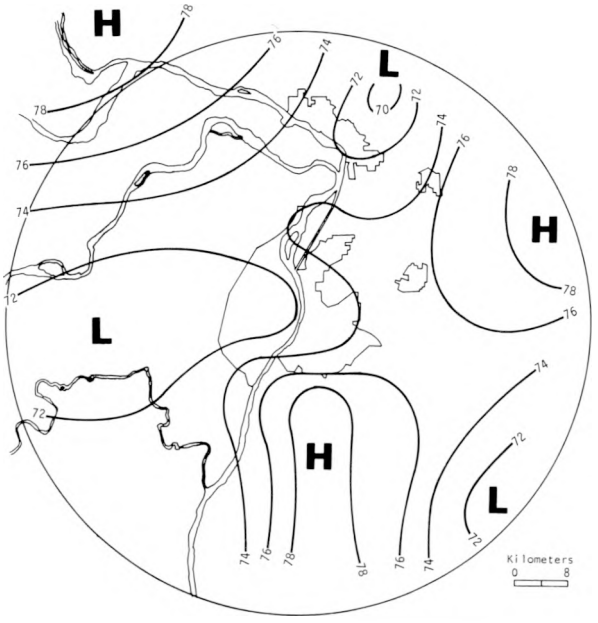

Figure E-9. Surface dew point distribution at 1500 CDT

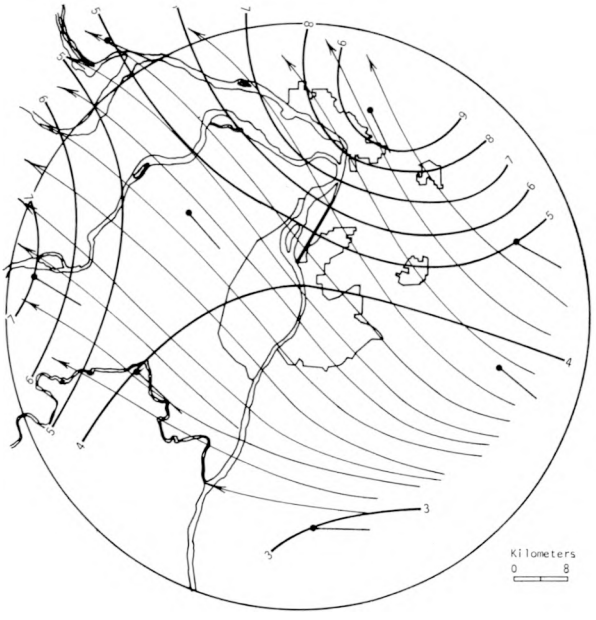

Figure E-10. Surface airflow at 1500 CDT
(Isotachs in m/sec)

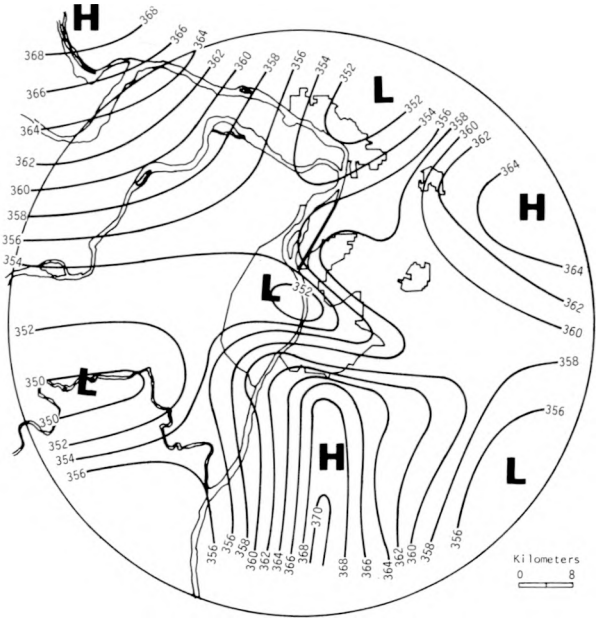

Figure E-11. Surface θ_e (°K) distribution at 1500 CDT

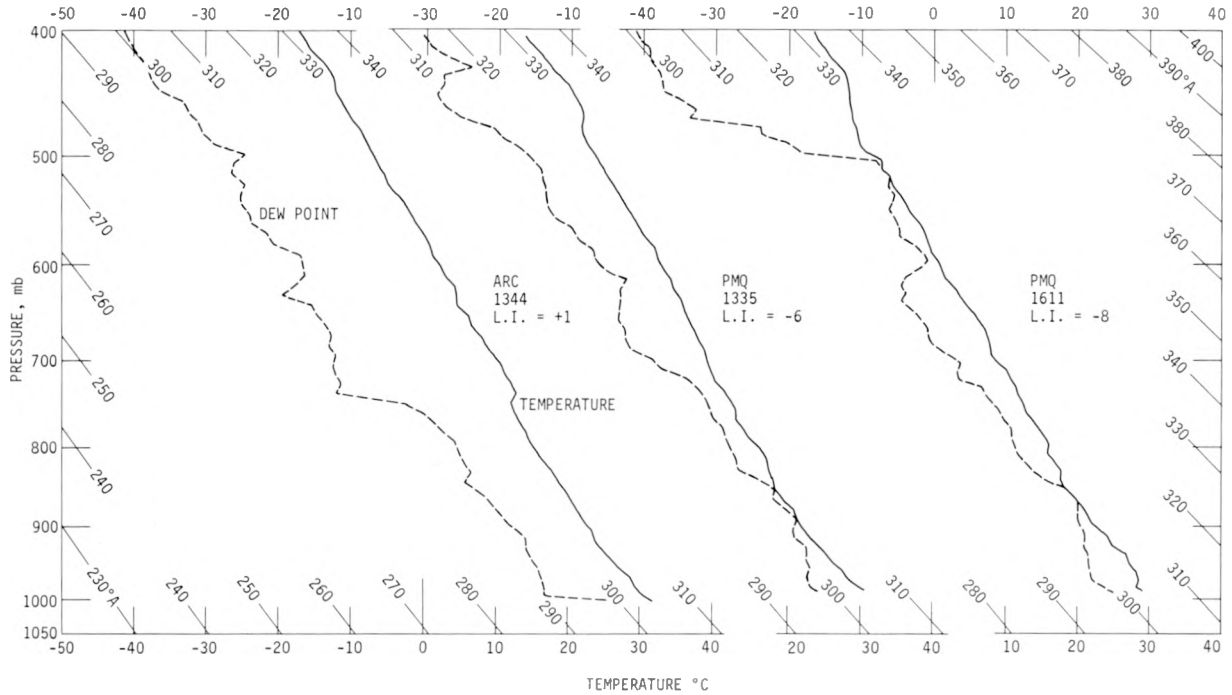

Figure E-12. Temperature and moisture soundings in the St. Louis area on 23 July

By 1600, both 500 m and 1000 m (figures E-14a and b) flow had backed somewhat, to a SE direction. At 1000 m accelerating winds upstream of ARC and decelerating winds downstream, with mostly parallel streamlines, suggest divergence in the SE and convergence in the NW portions of the circle. At 1500 m (figure E-14c) mostly S winds still prevailed. No strong patterns of convergence or divergence were evident at this height.

PRECIPITATION MORPHOLOGY

The precipitation events on 23 July were associated with two different synoptic conditions. The first situation was an E-W stationary front, associated with precipitation occurring from 0000 to 0600. The second was a complex squall system associated with precipitation occurring from 1400 to 2300. Because these synoptic cases produced different conditions that both led to rain, and the two events occurred at separate times, the two cases and their corresponding precipitation events are treated and discussed separately.

E-W Stationary Front Case

Macroscale Precipitation Elements. To demonstrate the macroscale conditions associated with the development of precipitation elements and the relationship of these elements to the mesoscale precipitation elements, the precipitation over the general area shown on figure E-15 was investigated. Hourly precipitation data from recording raingage stations of the NWS were plotted for each hour in which rain fell in the area. The precipitation system was followed by the hourly maps as it approached and passed through the MMX circle. An isolated maximum of precipitation

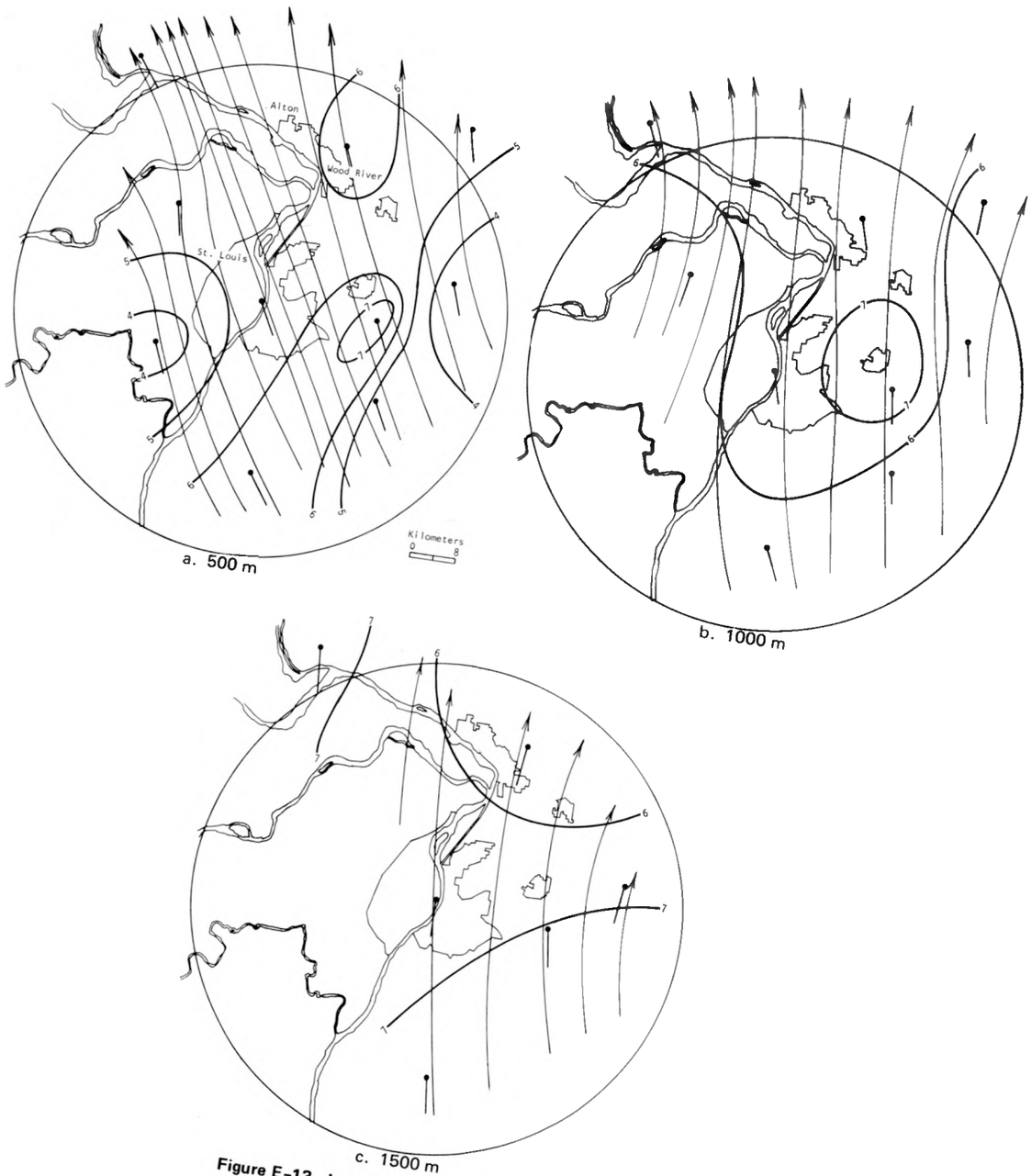

Figure E-13. Low-level airflow at 1400 CDT

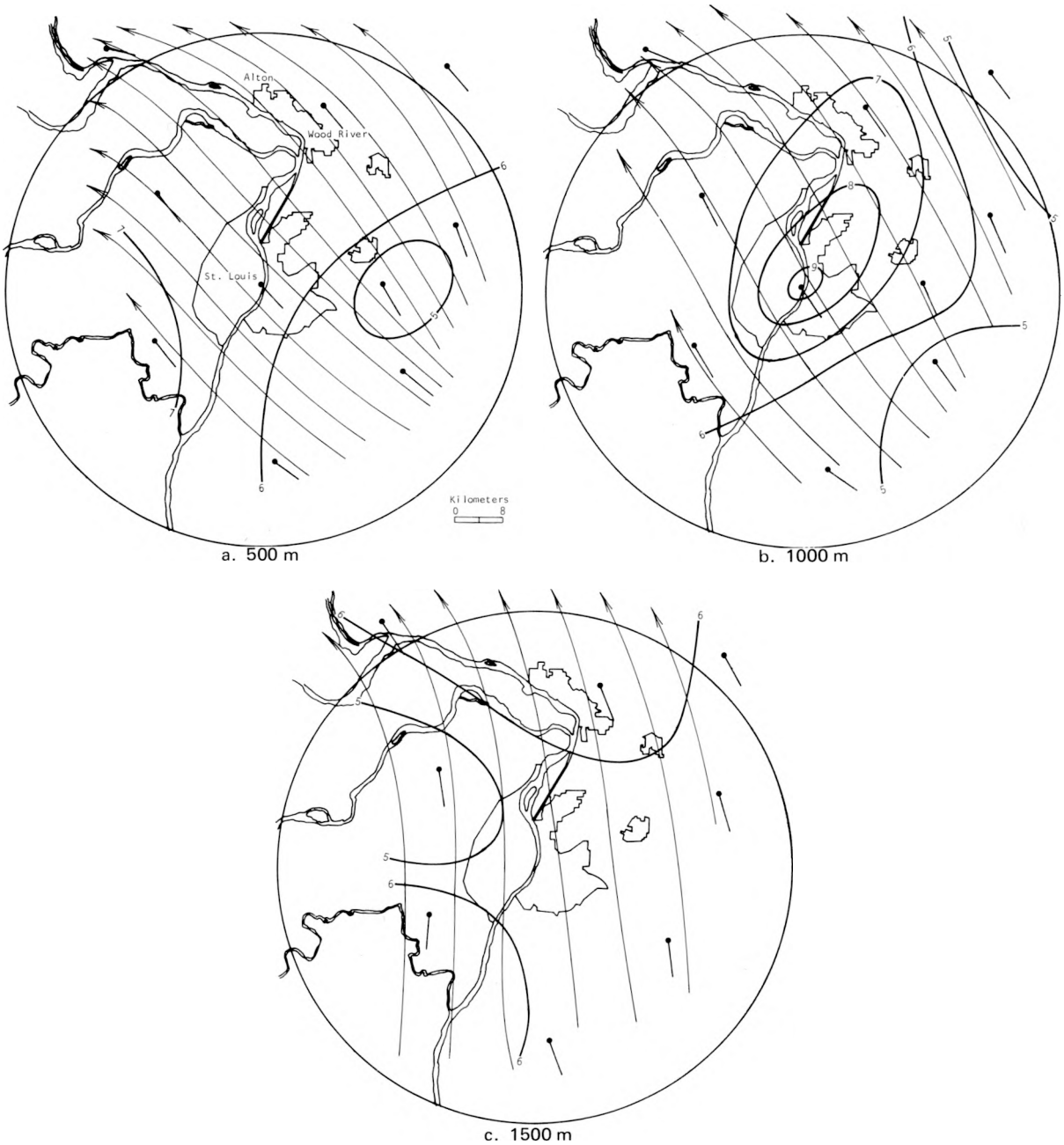

Figure E-14. Low-level airflow at 1600 CDT

Figure E-15. Total rainfall pattern (macroscale) for the frontal rain case

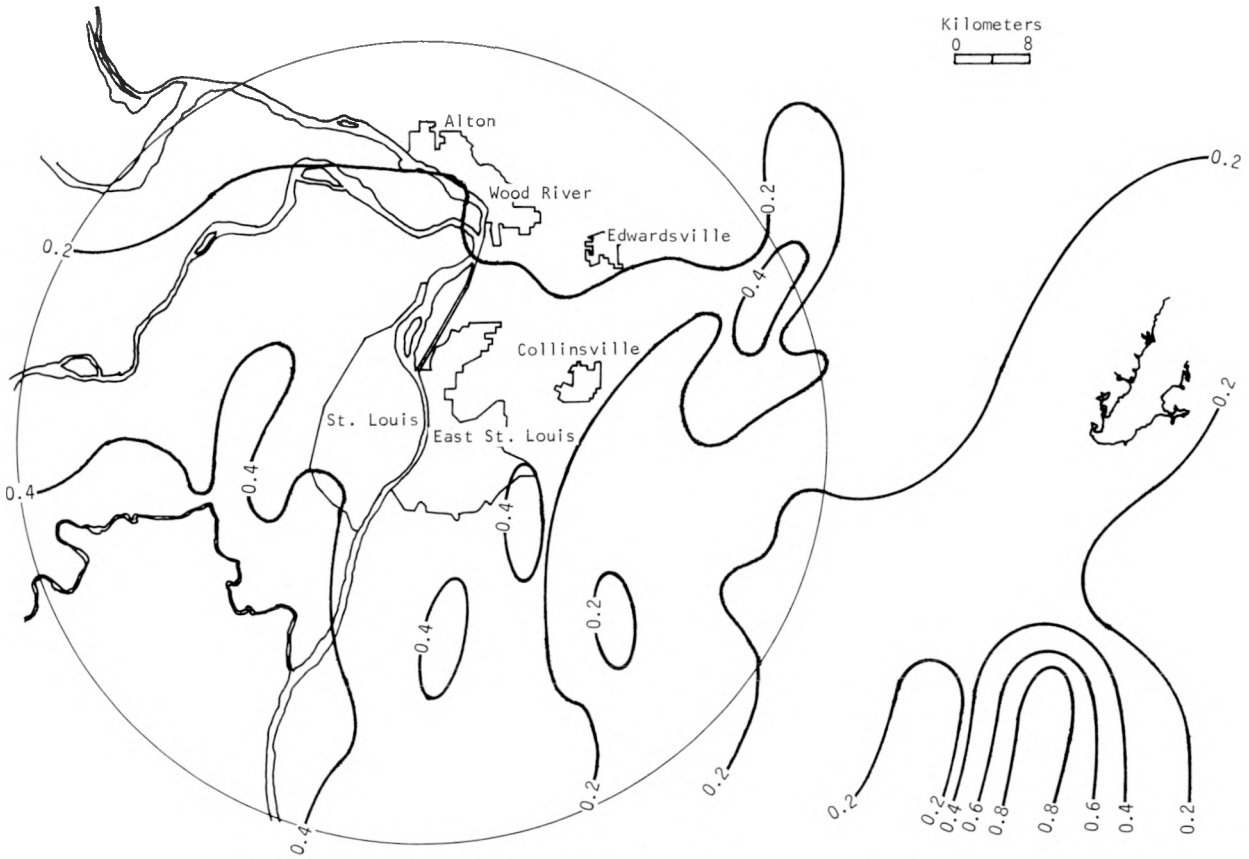

Figure E-16. Distribution of rainfall in the MMX circle and extended network for the frontal rain case

occurred in the circle between 0100 and 0200, but it was extremely small (0.01 inch). The heaviest precipitation occurred outside the MMX circle.

The total rainfall pattern during the rain period is depicted on figure E-15. The MMX circle did not have an isolated rainfall maximum and the 0.25-inch isoline indicates that the precipitation in the circle represents part of the general macroscale pattern. There is insufficient evidence to suggest either an increase or a decrease in precipitation due to the urban effects of St. Louis.

Mesoscale Precipitation Elements. The total rainfall in the MMX circle (0000 to 0600) is shown on figure E-16. There was a relatively uniform distribution of rainfall throughout the W half of the MMX circle and some isolated highs in the E half. The maximum rainfall (0.85 inch) occurred in the extended (E) network. This high is also reflected in the macroscale precipitation pattern (figure E-15).

No hail fell in the MMX circle during the period of precipitation associated with the frontal case, and no thunder was reported at the observing sites. No aircraft or chemistry data were collected in this nocturnal case.

Raincells. During the frontal case there were 38 cells with complete life histories in the network and 12 cells with incomplete life histories (i.e., 'edge of network cells'). The rainfall pattern of the 11 cells that produced more than 100 ac-ft are shown on figure E-17. Most of the cells occurred within or near the 17.0 g/kg mixing ratio isoline. Overall, there is a good correspondence between cells producing over 100 ac-ft of precipitation and the region of high surface moisture.

Raincell locations were also compared to the surface temperature distribution (figure E-4). Six of the 11 raincells occurred in areas where temperatures exceeded 76F. In general, there was some

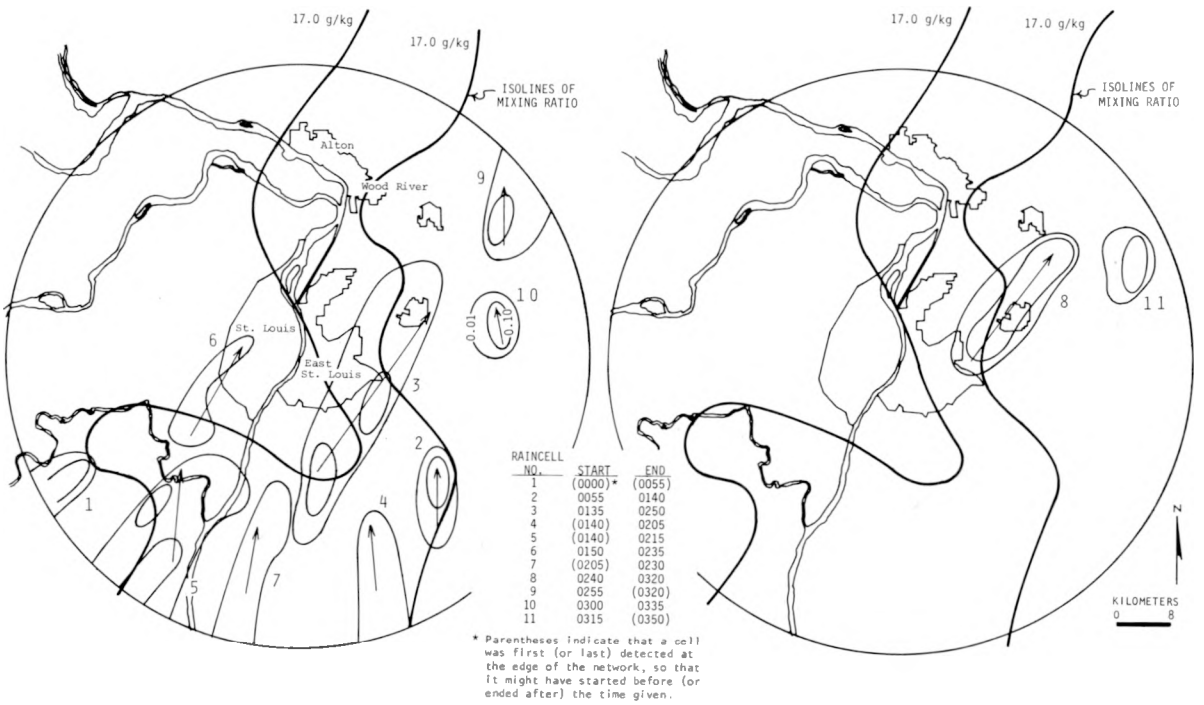

RAINCELL NO.	START	END
1	(0000)*	(0055)
2	0055	0140
3	0135	0250
4	(0140)	0205
5	(0140)	0215
6	0150	0235
7	(0205)	0230
8	0240	0320
9	0255	(0320)
10	0300	0335
11	0315	(0350)

* Parentheses indicate that a cell was first (or last) detected at the edge of the network, so that it might have started before (or ended after) the time given.

Figure E-17. Comparison of rainfall for frontal raincells with volumes > 100 ac-ft and the surface moisture pattern

correspondence between the raincells producing > 100 ac-ft and the regions of high surface temperature, but the agreement was not as good as with moisture.

There is also a low in the θ_e pattern (figure E-7) in the St. Louis-Centreville area indicating that the θ_e pattern was dominated more by the low moisture values than by the higher temperatures. In general, the locations of the cells correspond to higher values of surface θ_e.

The surface wind data for 0000 (figure E-6) show that the airflow was generally from the E. These very limited airflow data indicate that the convective activity was not downwind of the major nuclei sources. The contribution of moisture appears to be more important than the contribution of urban and industrial nuclei to the development and history of the raincells. Unfortunately pibal wind, aircraft, and radar data were not available during this precipitation period. Therefore, it was not possible to make a further assessment of the possible contribution of nuclei to the development and history of these raincells.

The initiation frequency (i.e., the number of times that each gage was within a cell initiation) of all 50 cells during the frontal case is shown on figure E-18. For comparison, the 17.0 g/kg mixing ratio lines are superimposed on the initiation patterns. A considerable portion of the 1-isoline of cell initiation lies outside of the 17.0 lines. However, all of the 2-cell initiations occurred within or near the 17.0 mixing ratio lines except one SE of St. Charles. Thus, there is some agreement between cell initiations and the surface moisture pattern. There was no precipitation on the previous day to examine for a relationship with the surface moisture pattern.

A comparison of the surface temperature pattern (figure E-4) with the initiation pattern (figure E-18) revealed some correspondence between the two. However, just as with the raincells of more than 100 ac-ft, the relationship is not as strong as that between initiations and surface moisture. Raincell initiations also showed some tendency to occur in areas of higher than average θ_e values.

An interesting characteristic of the 0000-0600 period is that even though there were a considerable number of cells (50), the individual raincells did not produce large amounts of precipitation and the total rainfall was not high.

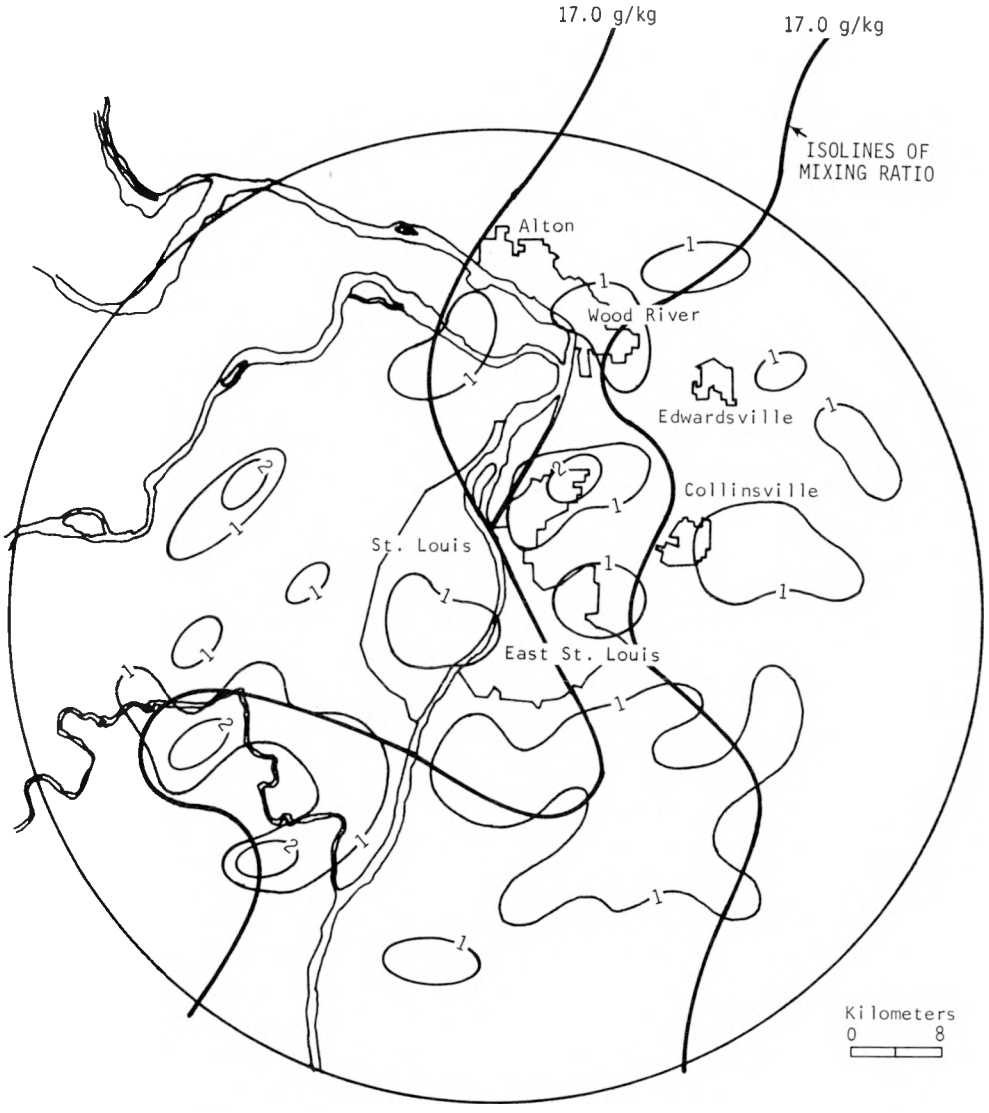

Figure E-18. Initiations of raincells during the frontal case compared with the surface mixing ratio distribution at 0000 on 23 July

Overall, it appears that local moisture sources influenced the location of convective activity somewhat in the early morning case. This raises the important question: "What produced the prior moisture pattern and is it linked to the urban area?"

It was noted that rainfall did not occur in the MMX circle on the previous day. Thus, it is doubtful that the local moisture pattern can be explained on the basis of prior rainfall. However, the higher moisture values generally correspond to the Mississippi amd Meramec River Valleys. The exception to this general correspondence is the low in the St. Louis–Centreville area. This general pattern is similar to the average 1973 moisture pattern prior to the onset of storm precipitation (Jones and Schickedanz, 1974).

If the river valleys were the major sources of moisture, the distribution of convective activity might then be attributed to natural causes and not to the presence of the city. There is little evidence to suggest that the city was the cause of the convective activity, but the local moisture sources indicate that the river valleys may have played an important role. This concept is supported by the fact that the convective activity did not occur within the urban plume.

There is no evidence to suggest a decrease in convective activity due to the presence of the city or to surface moisture and temperature. The mesoscale precipitation pattern (figure E-16) appears to be merely a reflection of the general macroscale precipitation pattern (figure E-15).

Squall-Line Case

Macroscale Precipitation Elements. The purpose of this investigation was to determine whether the city contributed to either the severe weather or to the W to E decrease in precipitation within the MMX circle (see figure E-22). Because the severe weather followed the intersection of the two squall lines, the 10-cm PPI radar film data were used to determine more precisely 1) the movement of the two systems and their associated precipitation, and 2) the location of the merger area. In addition, the hourly precipitation distributions were investigated in the manner described for the frontal case to determine whether the squall system dissipated as it passed through the MMX circle, and to compare the severity of precipitation elements in the MMX circle with those in the general area.

The 10-cm PPI echoes (0° antenna tilt) for 1633, 1714, 1726, and 1828 are shown in figure E-19a and b. The radar echoes (figure E-19a) show the merger of the E- and N-moving squall lines. The echo merger occurred along a line extending SSW from a point immediately outside the W edge of the MMX circle. The merger occurred during the period 1644–1714 and the resulting echo mass moved ENE through the circle. The echoes at 1828 indicate that the squall line did not dissipate after moving through the MMX circle although the area of echo coverage is somewhat less than that at 1726.

Further insight is gained by investigating the hourly precipitation patterns (1500–2300) shown in figures E-20 and E-21. Temporal changes in both the radar echo and the satellite cloud patterns indicate that the movement of the precipitation systems was as shown in figure E-20a, b, and c. The time of merger was near 1700 and occurred SW of the MMX circle. After the merger, the precipitation intensified and heavy rainfall occurred as the system passed through the circle.

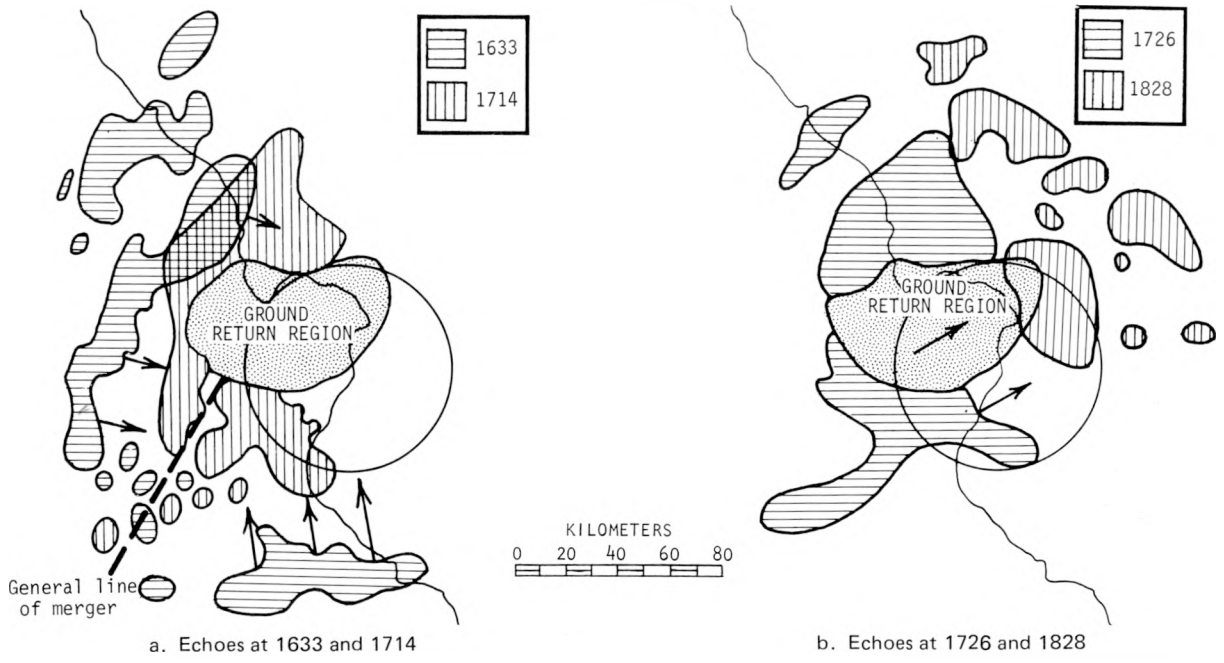

Figure E-19. Locations and movement of 10-cm PPI radar echoes (0° antenna tilt) prior to and after the intersection of the two squall systems

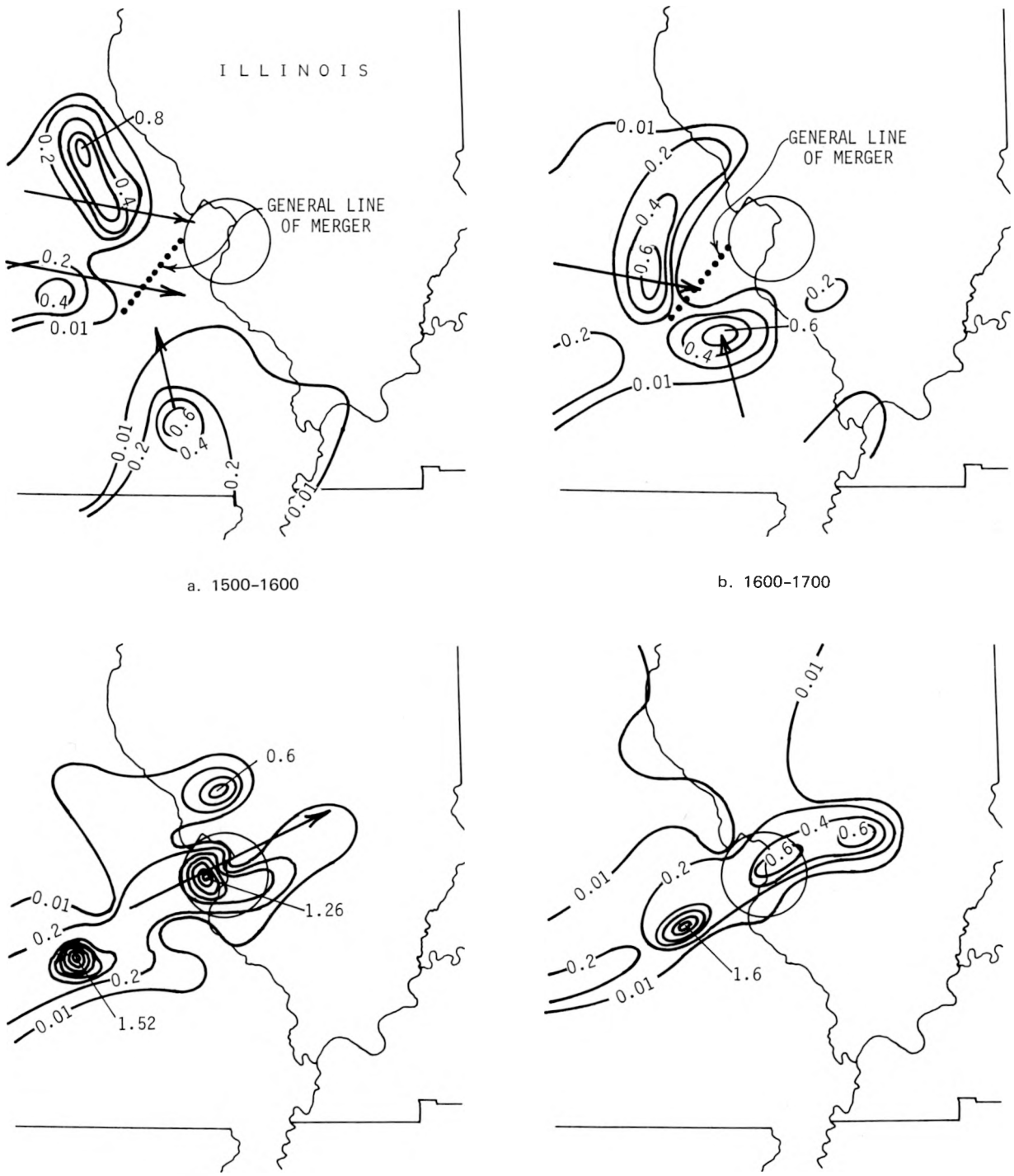

a. 1500-1600

b. 1600-1700

c. 1700-1800

d. 1800-1900

Figure E-20. Hourly macroscale precipitation distributions during the squall-line case, 1500-1900

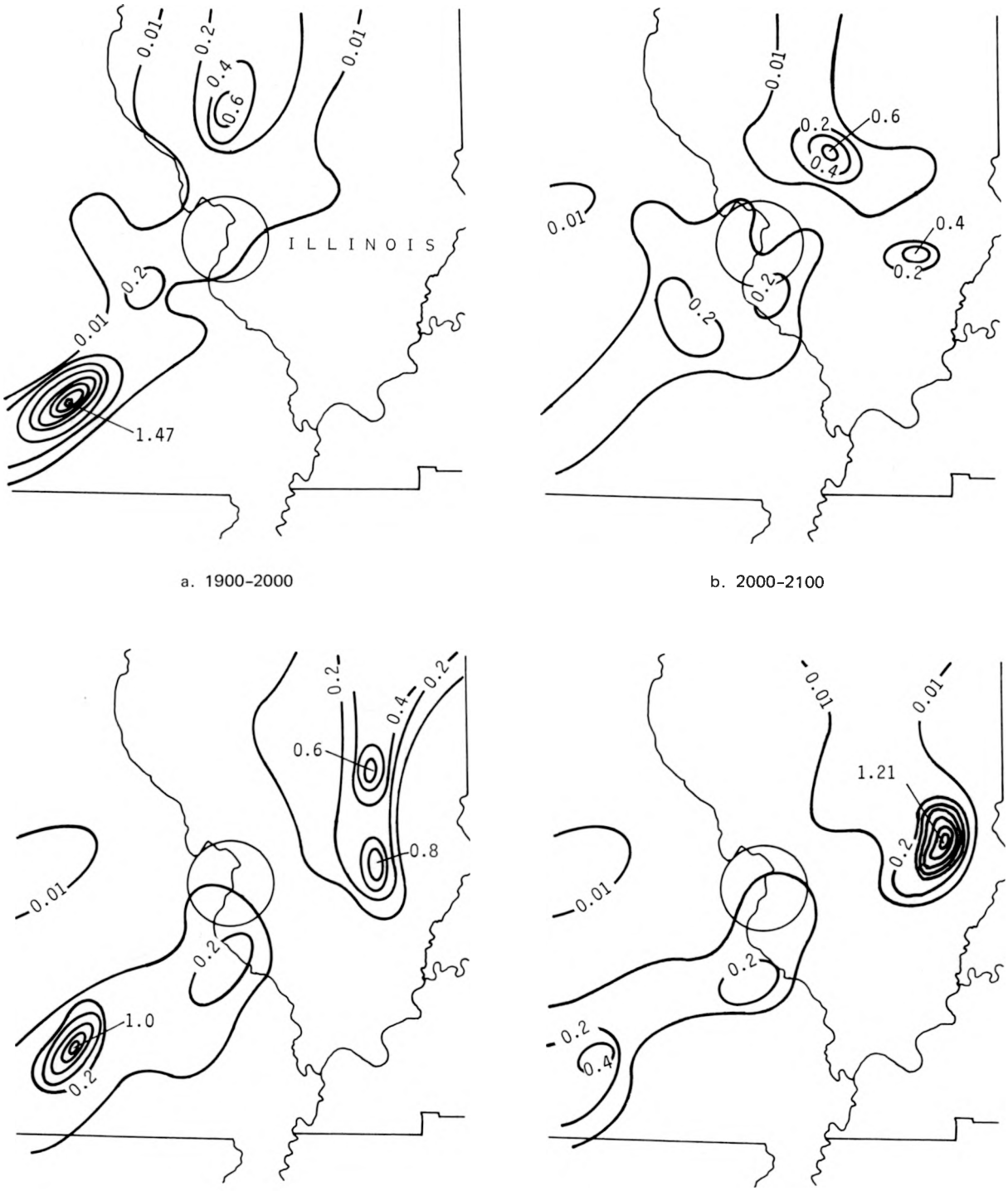

a. 1900–2000

b. 2000–2100

c. 2100–2200

d. 2200–2300

Figure E-21. Hourly macroscale precipitation distributions during the squall-line case, 1900–2300

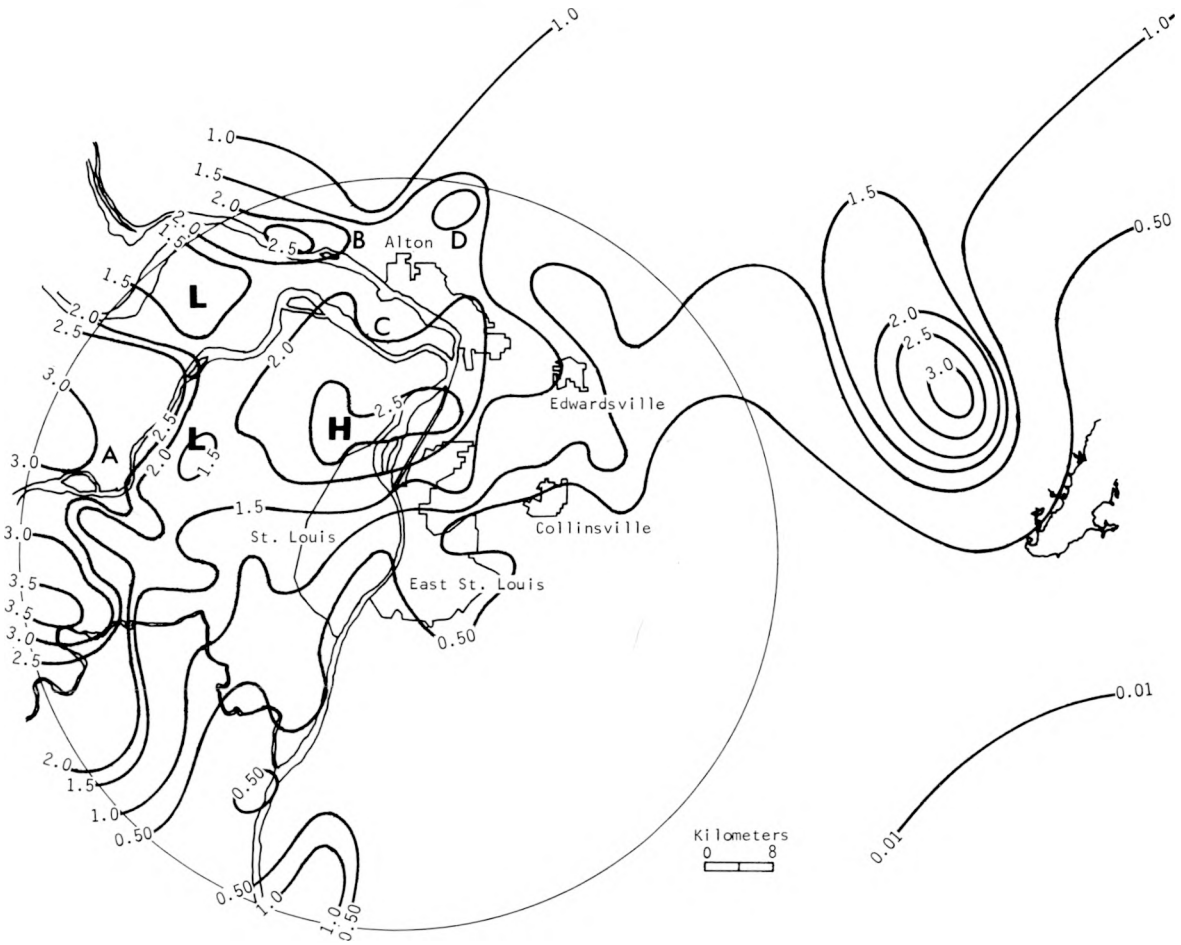

Figure E-22. Distribution of rainfall in the MMX circle and extended network for the squall-line rain, 1445-2100

The precipitation system intensified as heavy rain (1.26 inches) fell within the MMX circle (figure E-20b, c). Heavy rain also occurred SW of the merger area during the period 1700–1800 (1.52 inches) and in the SW and NE portion of the general area during the periods 2100–2200 and 2200–2300. The precipitation patterns after 2000–2100 indicate that the macroscale precipitation system split apart and the N portion of the squall line moved E while the S portion became quasi-stationary. This stationary system continued to produce light intermittent precipitation in the MMX circle until 0500 on 24 July, and an intensification of the system later occurred in the S portion of the general area.

The characteristics of the macroscale precipitation patterns after 1800 did not indicate that the overall squall line precipitation dissipated after passing through the MMX circle. In fact, the squall line precipitation at 2100–2200 (2-3 hr after passage) is similar to the precipitation at 1500–1600 (1-2 hr prior to passage) except the locations of the two systems are different. There is much evidence on figures E-19 through E-21 to indicate that the heavy rainfall in the MMX circle was a result of intensification due to the intersection of the two squall lines.

Mesoscale Precipitation Elements. The total rainfall from the squall line in the MMX circle and extended network from 1445 to 2100 is shown on figure E-22. A broad band of precipitation exceeding 1.0 inch extended across the NW part of the circle and into the extended network. Within this broad band there were 5 areas where rainfall exceeded 2.0 inches and 3 of these areas had rainfall > 3.0 inches. The major maxima in the circle, based on 2-inch isohyets, are labeled A, B, C, and D.

The mean motion of the heavy rain was determined to be from 240° at 13 m/sec. The vector mean of 700 and 500 mb winds at Monet, Missouri, at 1900 was 228° at 12 m/sec. The close agreement between storm motion and the steering flow at middle levels suggests that the movement of the heavy rain was determined by large scale, rather than local conditions. This general movement agrees with radar echo movement as shown on figure E-19.

Extrapolation back along the direction of motion at the speed of the system places the heavy rain system in the vicinity of the squall-line merger at about 1700. Thus, both the motion and the timing of the heavy rain suggest that the heavy rain system was a result of dynamic interactions produced by the merger of the squall lines.

Hailstreaks are shown on figure E-23 along with the times of occurrence, number of hailstones per square foot, and maximum stone sizes. The hailstreaks all occurred with rainfall

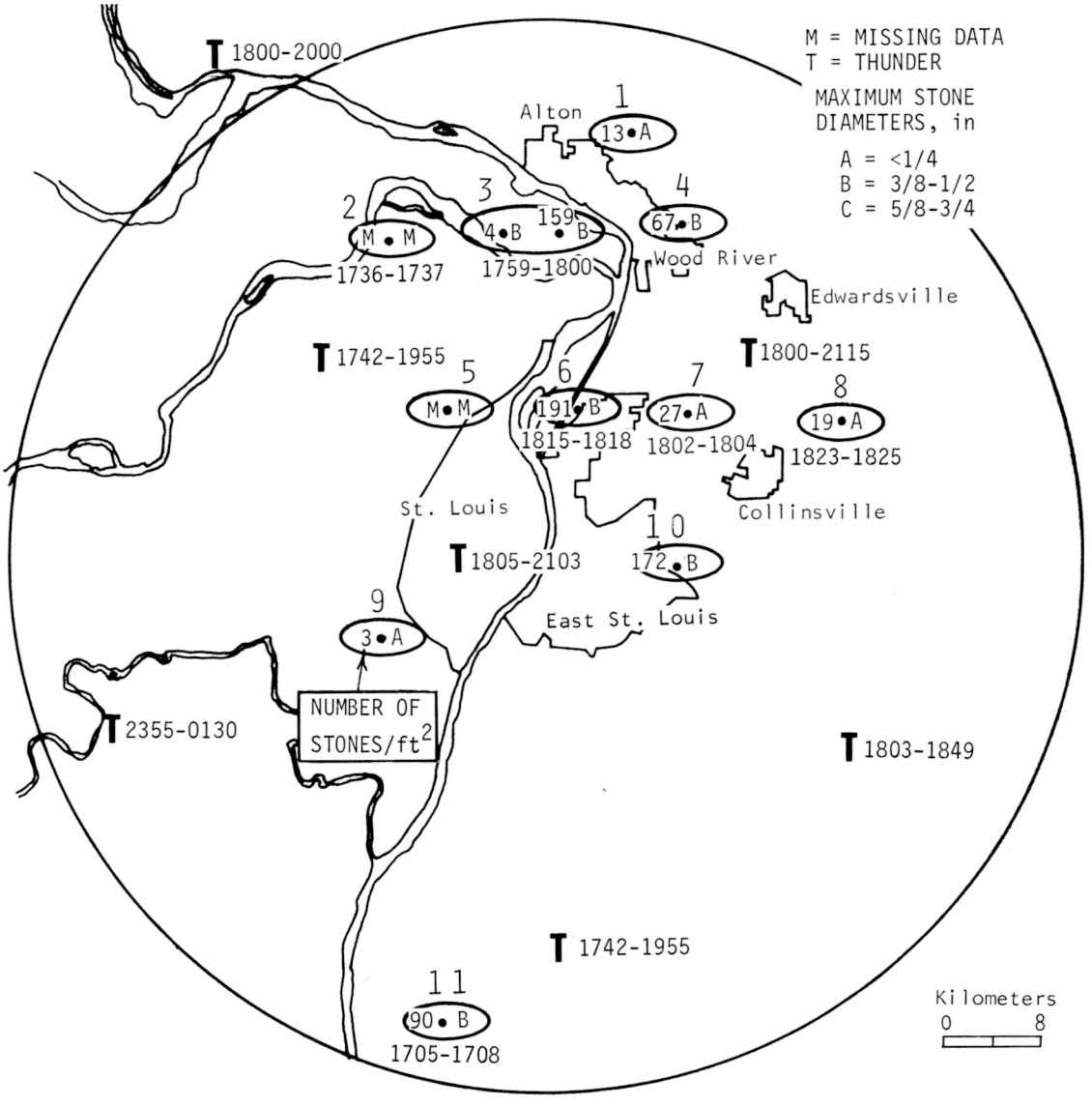

Figure E-23. Hailstreaks and thunder periods associated with the squall line

greater than 0.50 inch. Seven of the hailstreaks (numbers 1-7) were located in or near the 2.0-inch line of area C (figure E-22). However, there was no hail near area A which had rainfall exceeding 3.0 inches. Hailstreaks 8, 9, and 10 were near the 1.0-inch rainfall line across the center of the network. Although not shown on figure E-23, there were two hailfalls near the 3.0-inch high in the extended network. Hailstreak 3 was the largest in areal extent and hailstreak 6 produced the most stones, 191/ft^2. Hailstreak 6 was close to the 2.5-inch isoline of rainfall immediately N of Granite City. However, hailstreak 10, which produced the next largest number of stones (172/ft^2), was in an area of only 0.5 inch of rainfall. Thus, the most intense hailstreaks did not necessarily occur in the region of heaviest rainfall.

The times and locations of thunder periods are also shown on figure E-23. Thunder was present at all observing sites in the network, indicating that the storms were of the thunderstorm category during the squall-line period. The longest thunder periods were those over the city and to the NE of the city.

Raincells. During the squall-line period there were 39 raincells with complete life histories within the MMX circle and 15 cells with incomplete life histories. The raincell patterns associated with those cells which produced $\geq$ 1000 ac-ft, 500-1000 ac-ft, and $<$ 500 ac-ft were compared with the patterns for hailstreaks, surface temperature, and surface moisture.

The raincells with volumes $>$ 1000 ac-ft occurred in the area where total rainfall was $>$ 0.50 inch, and most of the cells with volumes between 500 and 1000 ac-ft also occurred in this area. Eight of the 11 hailstreaks were associated with cells having volumes $>$ 500 ac-ft.

Comparison of the cells in all three categories with the pre-rain surface temperature pattern (figure E-8) indicated that the cells did not occur preferentially in areas of high surface temperatures. That is, the cells were located in the cool regions as well as in the warm regions.

The comparisons of the cells in all three categories with the pre-rain surface moisture pattern showed that there was a tendency for the heavy raincells to occur in the areas of low surface moisture (figure E-9). Although this tendency was strongest in cells with volumes $>$ 1000 ac-ft, it was also present in cells with smaller volumes. There was a similar tendency for heavy raincells to occur in areas of low θ_e.

The initiation frequency (i.e., the number of times cells began at each gage) for all 54 cells during the squall-line period was compared with the prior temperature and moisture patterns. No relationship was found between the initiation frequency and the patterns of surface moisture, temperature, or θ_e.

The tendency for heavy cells to occur preferentially in areas of low surface moisture raises the possibility of a decrease in rainfall in the high moisture areas. Such a decrease within the MMX circle appears unlikely since it is not suggested in the macroscale pattern. Also, it is difficult to conceive how the addition of high moisture would decrease the rainfall. Further investigation reveals that the surface θ_e pattern is dominated by the surface moisture pattern rather than the surface temperature pattern (figures E-7, E-8, and E-11). Thus, areas of low moisture values were also areas of low θ_e. Boatman and Auer (1974) have shown that there were other days during August 1972 and August 1973 in which low moisture values often over-shadowed higher temperature values to produce lower θ_e values.

Under these conditions, weakening of thunderstorm updrafts may occur with the ingestion of near surface air having relatively low θ_e values. This weakening could be associated with the lower latent and sensible heat energies represented by the lower θ_e air. The weakening leads to an increase in rainfall rates if large amounts of condensed water have been supported by strong updrafts prior to ingestion of the low θ_e air. Thus, it is conceivable that rainfall may be increased in regions of low θ_e as a result of updraft weakening. The possible role of this mechanism in relation to the occurrence of heavy rainfall in the low θ_e regions on 23 July is investigated in the following section.

Rainfall Rates and Associated θ_e Patterns. The progression of heavy rainfall during the periods 1710–1750 and 1750–1840 is shown on figures E-24 and E-25, respectively. The surface pattern of θ_e was superimposed on the rainfall rates so that comparisons could be made. Although some of the heavy precipitation occurred in regions with θ_e values of 350–360K, most occurred in regions with $\theta_e < 356$K.

As the precipitation entered the network, the first heavy rainfall rate cores occurred within the region of $\theta_e < 352$K on the W side of the network (figure E-24b). During the period 1730–1740 (figure E-24c) there was a 4 in/hr maximum (core A) immediately N of the low θ_e region of 352K. Although not in the W region of $\theta_e < 352$K, this rate core could have ingested some of this air as the airflow at 1000 to 1500 m (figure E-14b and c) was from the SSE. Boatman and Auer (1974) stated that the average near-surface origin point for Cu cloud updraft air on several study days in August 1972 and 1973 was 2-3 miles toward the direction of the sub-cloud transport winds.

The rainfall pattern during 1740–1750 (figure E-24d) includes heavy rate cores located

1) within the low θ_e region on the W side of the network (B)
2) N of the low θ_e region (A)
3) 3-4 mi NNW of the θ_e low in the urban area (C)

The core in the N part of the city is of particular interest because it represents a 'quick advance' of the heavy rainfall compared with the pattern during 1730–1740. Comparisons of the positions and times of rainfall rates during the period 1730–1740 with the low θ_e region in St. Louis suggest that this 'quick advance' may have been influenced by a sudden ingestion of low θ_e air from the city region. Severe weather events associated with the crash of a commerical airliner (discussed later) suggest that this 'advance' may have played an important role in the crash.

During 1750–1800 (figure E-25a) core D developed along the 356K isoline on the side toward the lower θ_e values and facing the sub-cloud transport winds. Core E also developed in a region where surface θ_e values were in the range from 356 to 360K prior to the rain. Core E represents another 'quick advance' core, but does not appear to have been as closely associated with the lower θ_e values as was core C. During 1800–1810 (figure E-25b), core D merged with core F as they moved toward the low θ_e region in the Alton-Wood River area. Core G initiated in the vicinity of the low θ_e region in St. Louis.

By the end of the 1810–1820 period (figure E-25c), DF and E had merged to form DFE in the low θ_e region at Alton-Wood River. Core G intensified as it moved into the Granite City area. The final stage of the heavy rain system on the network (figure E-25d and e) indicates that heavy rain did not occur in the high values of θ_e SE of Alton-Wood River.

It is informative to compare the patterns of rainfall rate and θ_e to the updraft positions shown on figure E-30f (see page 119). The updraft positions in the two more northerly regions, N of St. Louis, reveal that the updraft areas were situated on the SE side of the heavy rain area. This indicates that low θ_e air could have been ingested into the cores in the W low θ_e region (figure E-24b) and into the quick advance core C (figure E-24d). It is assumed that there is a time lag of 10-20 min between the ingestion of low θ_e air and the occurrence of heavy rain rates at the surface (Boatman and Auer, 1974).

The updrafts in the Alton-Wood River area also indicate possible ingestion of low θ_e air in the merger region of cores D, E, F, and DF (figure E-25a, b, c). The more southerly region of updrafts is of special interest because it passed through areas of high θ_e but never produced the heavy rainfall rates that were associated with the other tracks (figures E-22, 24, and 25).

The comparisons of certain updraft tracks, rainfall rates, and θ_e patterns suggest a relationship between the low θ_e values and the occurrence of heavy rain that is consistent with the mech-

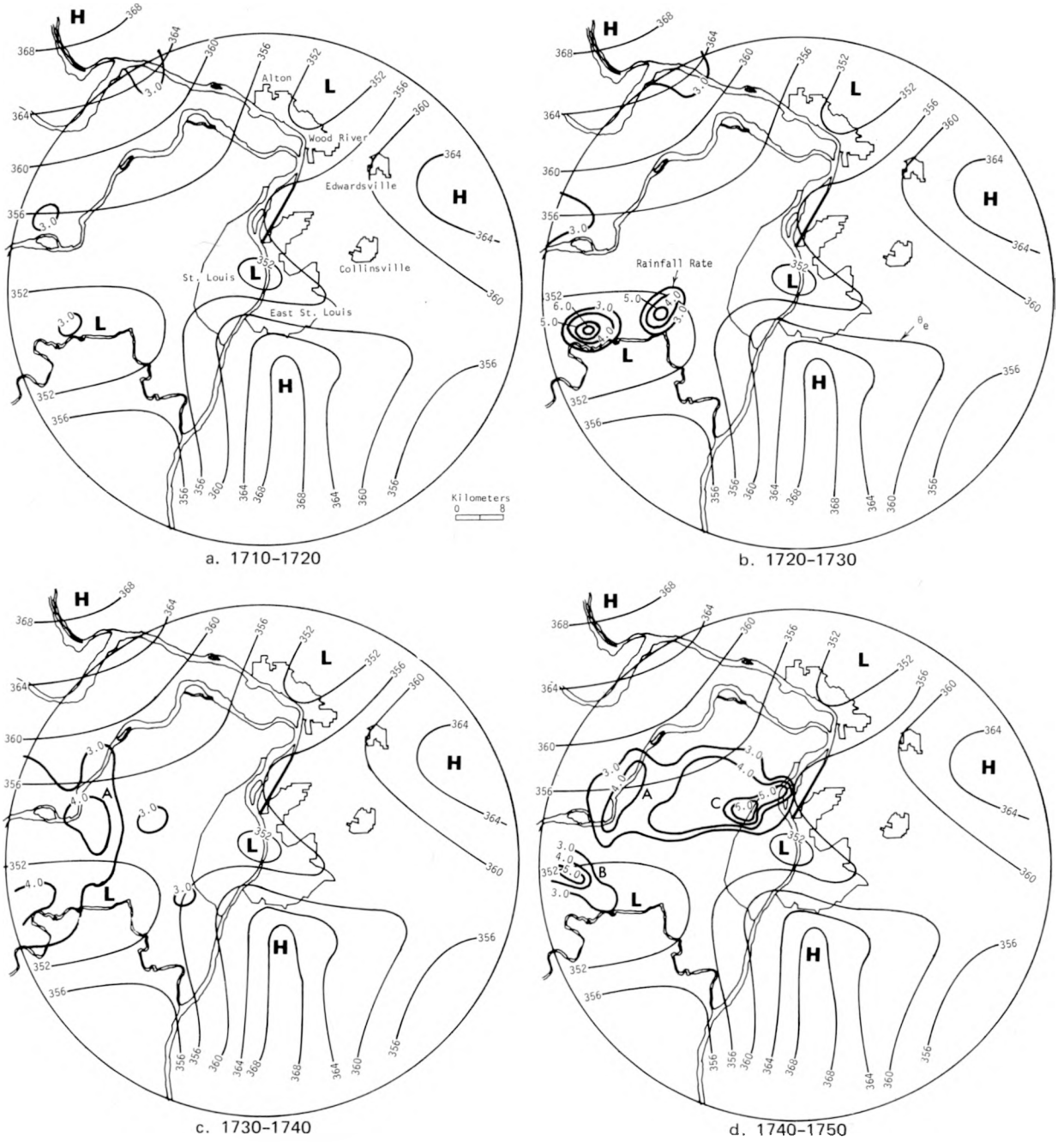

Figure E-24. Comparison of the distribution of surface θ_e (°K) at 1500 m with subsequent heavy rainfall rates ($\geq$ 3.0 in/hr), 1710-1750

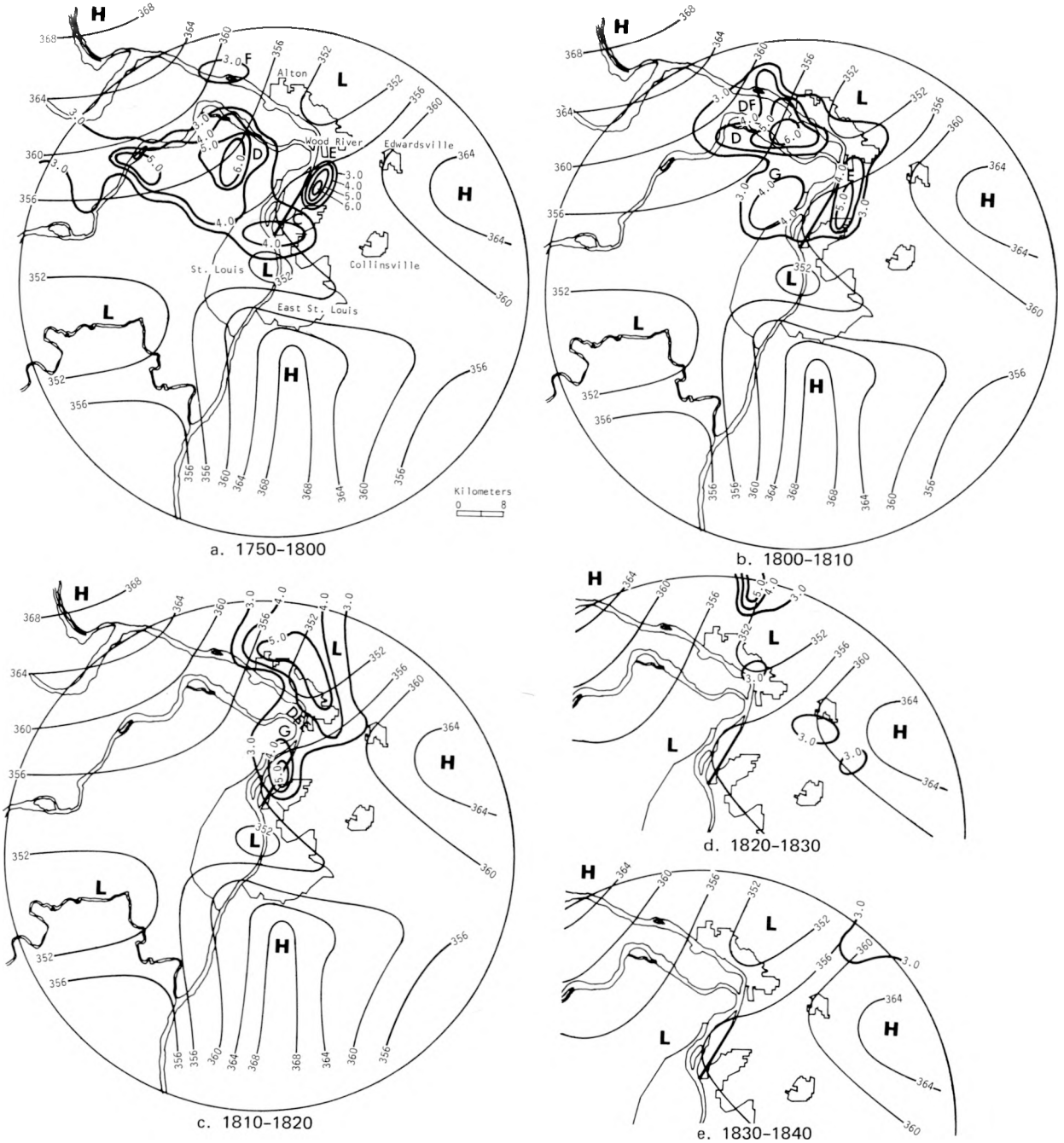

Figure E-25. Comparison of the distribution of surface θ_e (°K) at 1500 m with subsequent heavy rainfall rates ($\geq$ 3.0 in/hr), 1750-1840

anism proposed by Boatman and Auer. In addition, the heavy rain is generally confined within areas of $\theta_e \geq 356$K. It appears that the 356K isoline may be close to the critical value at which lower θ_e values would inhibit convection. Further, the relatively higher rainfall rates within the 356K region appear to be associated with the relatively lower θ_e values (352K).

Boatman and Auer (1974) analyzed soundings in the St. Louis area by using parcel theory to determine the critical values of θ_e. Our analyses of the soundings for 1610 at PMQ and 1735 at ARC indicated that air with θ_e values $\leq$ 355K (PMQ) or 354K (ARC) would inhibit convection, and could thus lead to increased rainfall rates 10-20 min later.

Because airflow was from the SE, part of the heavy rain area was also downwind of the city and may have experienced effects from nuclei sources and/or low level convergence. To check this possibility, attention is again directed to figures E-13, E-14, E-22, and E-24. Rainfall maximum C is located in the N St. Louis-Granite City area (figure E-22). At 1400, airflow at the surface and at 500 m was from the SE and the airflow at 1000 and 1500 m was from the S (figure E-13). Thus, air motion was suitable for bringing city aerosols to the location of this rain maximum. Although the 1000 m wind field at 1600 (the last available data) suggests possible convergence in the NW section of the network, it is unlikely that these conditions would apply to the period of the observed rainfall.

Additional information was gained from the research aircraft (AI) flights made on this day. In the aircraft data of the first flight (figure E-26) CN maxima were present

1) in the vicinity of Portage des Sioux (20,000/cc)
2) in East St. Louis (20,000 to 25,000/cc)
3) in the Granite City area (47,200/cc)

During the second flight (figure E-27), the counts were generally lower than they had been earlier in the area E of the river, but maxima of 10,000 to 30,000/cc occurred NE of the major industrial areas at East St. Louis and Granite City, as well as at a few other locations.

Further analyses of the aircraft data indicated that CN from Granite City and East St. Louis were probably transported by the low level airflow into the region of cores D, F, and DF. Also, the position of the 'quick advance' rate core (E) N of Granite City (figure E-25a) with respect to the local CN peak indicates that it could have ingested high CN concentrations.

The analyses suggest that some of the heavy rain could have been the result of the ingestion of low θ_e air. However, some of this rain occurred from convective cells that probably also ingested high concentrations of CN. One 'quick advance' core (C) occurred in a position where it could have been strongly affected by low θ_e air while another core (E) probably ingested high concentrations of CN from Granite City. It is impossible from the available information to determine unequivocally the relative roles of these potential influences.

A very important question is: "What is the dominant influence when air containing both low θ_e values and high CN is ingested into sub-cloud updrafts?" The weakening of the updraft and subsequent rainfall might negate the influence of the nuclei because there would be insufficient time for micro-physical processes to operate. This is an important consideration because high CN concentrations often occur simultaneously with low θ_e air in urban areas.

Radar Echoes and Mesoscale Precipitation Elements. All RHI echoes during the squall-line period were plotted along with their maximum heights. However, because of the excessive rainfall rates on this day, the radar data became badly attenuated by 1600 and it was impossible to perform meaningful analyses after that time. There were a few distinguishable echoes prior to 1600 in the SW portion of the network, but most of these did not produce precipitation at the surface and are of little interest. The 10-cm PPI integrator data were missing because a stroke of lightning had badly damaged the system on 9 July.

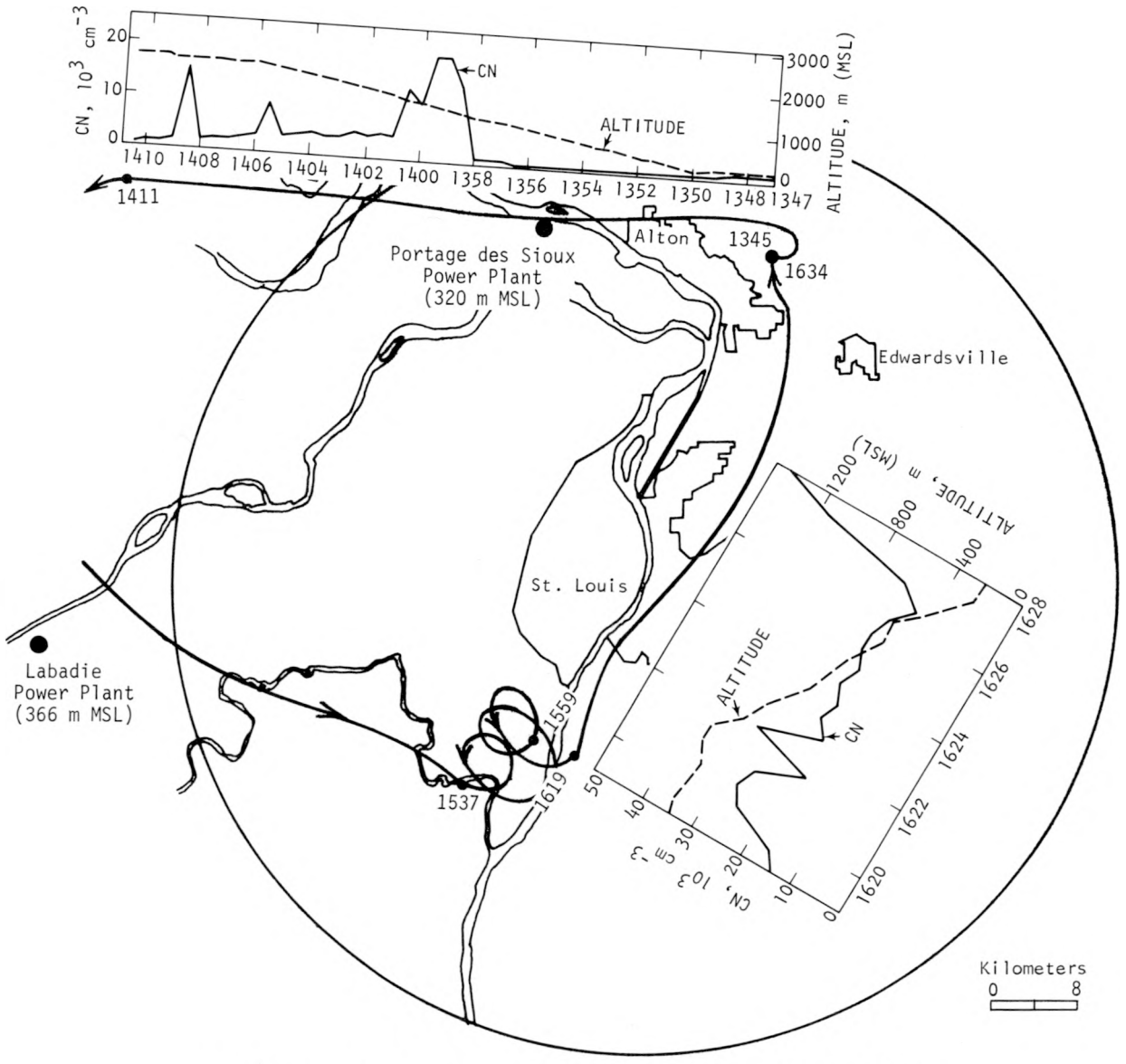

Figure E-26. Flight track of first AI flight on 23 July with selected CN observations (Power plant stack heights in parentheses)

Excessive Rainfall Rates and Associated Events. At approximately 1600 on 23 July, an extremely intense rainstorm entered the W edge of the MMX circle, moved to the ENE, and left the circle at 1900.

There were 30-min amounts exceeding 2 inches in N St. Louis and in the Granite City area from this storm. Rainfall amounts of this magnitude have a return period of 25 years. Furthermore, during the period 1725–1810 there were many 5-min rainfall amounts corresponding to hourly rates from 4.6 to 9.9 in/hr. A rainfall rate of 9.9 in/hr represents a 5-min amount of 0.8 inch which has a return period of 50 years.

During these severe weather conditions, a commercial airliner crashed in its approach to Lambert Field from the SE (National Transportation Safety Board, 1974). The plane crashed into a residential area approximately 2.3 mi SE of the outer airport edge marker at 1743:24 (figure

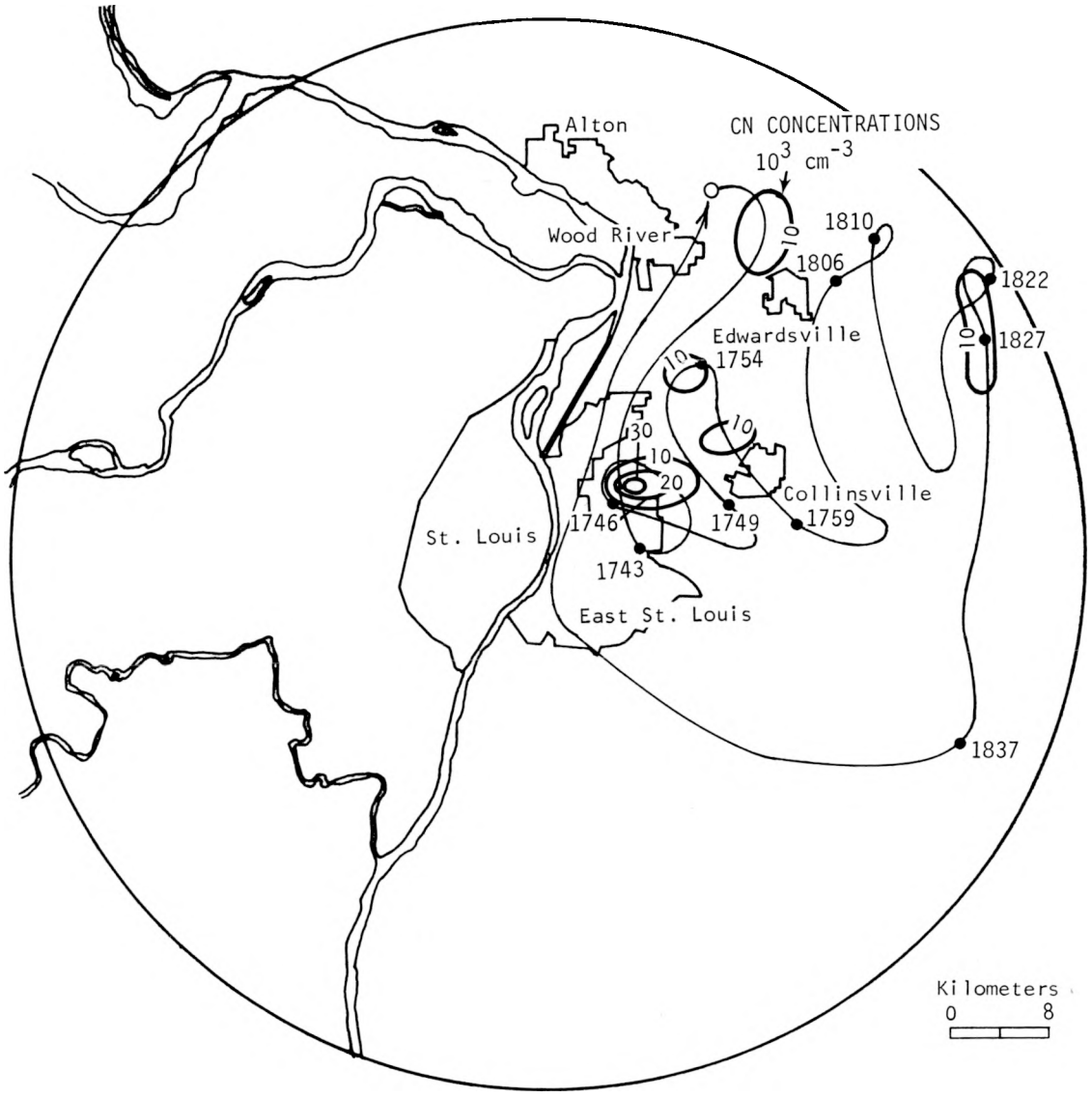

Figure E-27. Flight track of second AI flight on 23 July with measured CN concentrations shown in plan view

E-28). The Safety Board determined that the probable cause of the accident was the aircraft's encounter with a strong downdraft of a thunderstorm. Prior to the crash, a light plane that landed on the same approach at 1740 encountered a severe downdraft (the plane dropped at a rate of at least 3500 ft/min) at approximately the location shown on figure E-28.

Rain core C, immediately E of the crash site, is the first 'quick advance' rain core discussed previously. The rain core is enclosed by a rate isohyet of 5.0 in/hr. The 5-min rates measured at the two gages within this core were 5.97 and 6.13 in/hr. Less intense but still very heavy rain was occurring in the general area between this core and the airport during the 1740–1750 period. It is noteworthy that this heavy rain core existed for only 10 min (1740–1750) or less, and that it occurred in a location where there had been only light rain or none very shortly before.

The close proximity of the severe downdraft reported by the light plane to the area of very heavy rain strongly suggests that the two were associated. Furthermore, the position of the

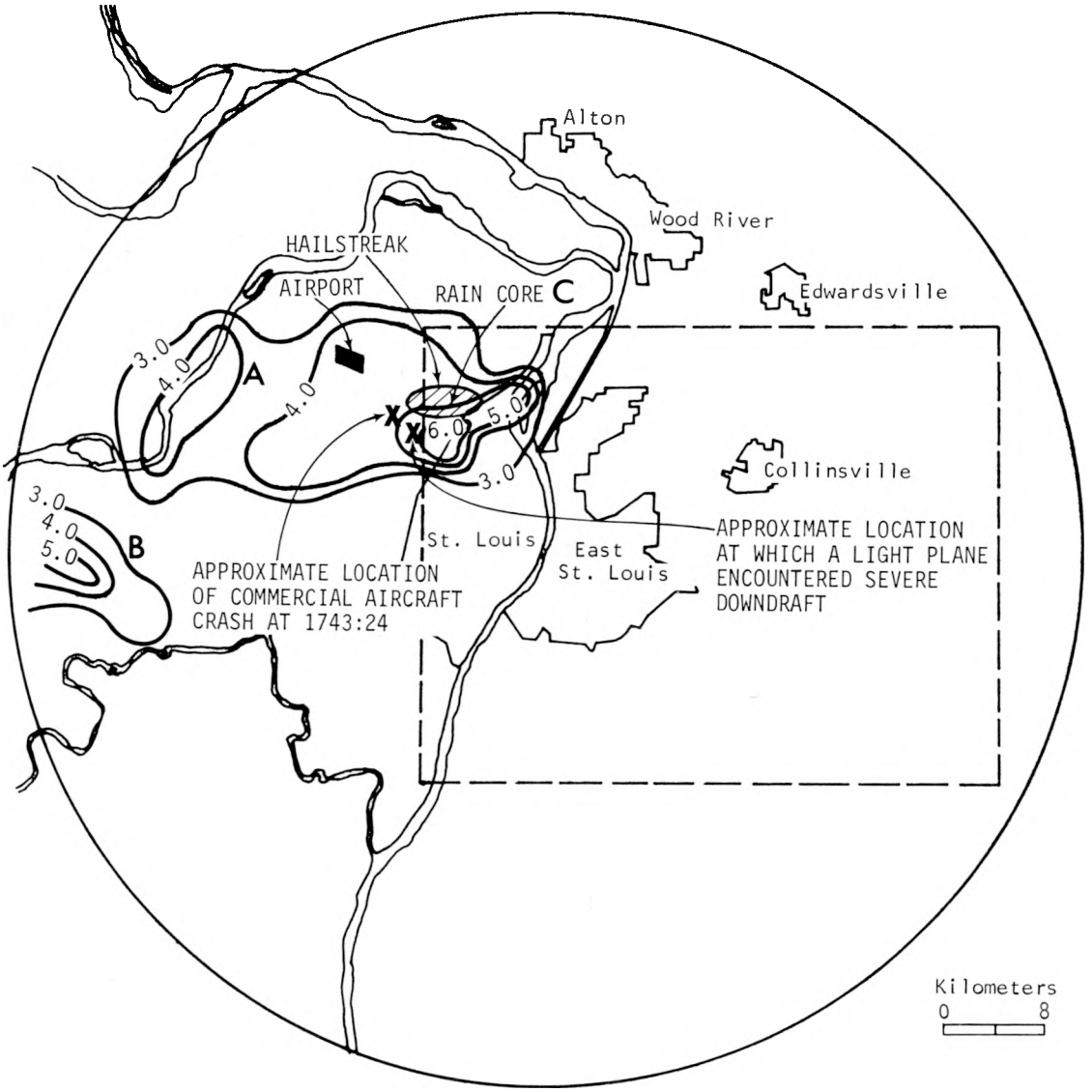

Figure E-28. Distribution of heavy rainfall rates ($\geq$ 3.0 in/hr) from 1740 to 1750 and location of airplane crash

core with respect to the glide path and the crash site makes it very likely that the plane encountered this core shortly before the crash.

Figure E-28 also shows a hailstreak close to the rain core, but the exact time of the hail is unknown, and it is uncertain that the hail and the raincell were related. Rain core C shown on figure E-25 produced point rainfalls of 1.0 inch in 10 min. A point rainfall amount of this magnitude in 10 min has an average return period of only once in 20 years.

An inspection of figures E-24 and E-25 indicates that this rain core (C) and the 'quick advance' rain core (E) in the Granite City area are the only cores of similar timing and magnitude within the network. Both of these cells could have been influenced by urban and industrial factors. Thus, it is conceivable that the plane crash could have been indirectly associated with urban effects on the precipitation process.

AIRCRAFT OBSERVATIONS

The aircraft used for research and tracer missions made two flights on 23 July. Both In and Li tracers were released during the second flight.

Flight 1 began at 1345 and, after a counter-clockwise flight around St. Louis, ended at 1634. The flight path is shown on figure E-26, along with CN concentrations encountered on the leg W of the Alton airport and that from S of St. Louis to the airport. Flight altitude is shown to aid interpretation of the CN data.

Airflow during the flight may be inferred from the measurements at 1400 and 1600 (figures E-13 and E-14). The altitude range of the W leg was from 213 to 2256 m MSL. The main CN peak was encountered at about 1400 at an altitude of about 1280 m. Figure E-13 shows that flow at both 1000 and 1500 m was almost directly from the S at the location of the high concentrations.

The width of the main peak [~ 3 min, or about 11 km at a speed of 61.8 m/sec (120 kt)] was too wide to be accounted for entirely by the nearby Portage des Sioux power plant (see location on figure E-26). Consideration of the E winds at the surface (figure E-10) and 500 m (figure E-13a) suggests that the Granite City industrial area was a possible contributor to the main peak. This is supported by the broad 'elevated baseline' W of the main peak, which could be the effluent of the St. Louis metropolitan 'area source.' The substantial peak observed at about 1408 at a height of about 2000 m is probably the flume from the Labadie power plant (see plant location, figure E-26, and wind flow, figure E-13c).

The northward leg E of the Mississippi River shows, in general, substantially higher CN concentrations. Almost all concentrations encountered exceed the *highest* observed on the W leg. This is not surprising since the plane was over industrial areas for most of the N-S leg. The peak concentrations of over 40,000/cc were encountered at an altitude of < 1000 ft MSL in the Granite City area. Although the aircraft track in figure E-26 shows that the plane passed upwind of Granite City, there is sufficient uncertainty in the determination of the track to suggest that the flight could have passed directly over Granite City. In view of the low-level wind direction, this observation of maximum CN is strong support for the earlier suggestion that the Granite City area contributed to the main peak on the E-W leg.

The path of the second flight is shown on figure E-27. The temporally closest available low-level winds are those for 1600 (figure E-14). CN concentration isopleths are depicted on figure E-27 in plan view. The flight altitude is not shown, but operations were conducted at about 1220 m MSL until 1825, and near 610 m afterward. Peak CN concentrations (30,000/cc) were observed in the East St. Louis area, and smaller peaks (10,000/cc) were noted downwind of Collinsville and Edwardsville.

The flight path during tracer releases is shown in detail on figure E-29. The In release took place over East St. Louis for a short time (1.5 min beginning at 1746), whereas the Li release extended over 44 min (beginning at 1743) and covered an extensive area of the rain chemistry network.

RAIN WATER CHEMISTRY

This section deals with the deposition of chemical elements in the rain. It is divided into two parts dealing with the tracer and the non-tracer constituents of the rain.

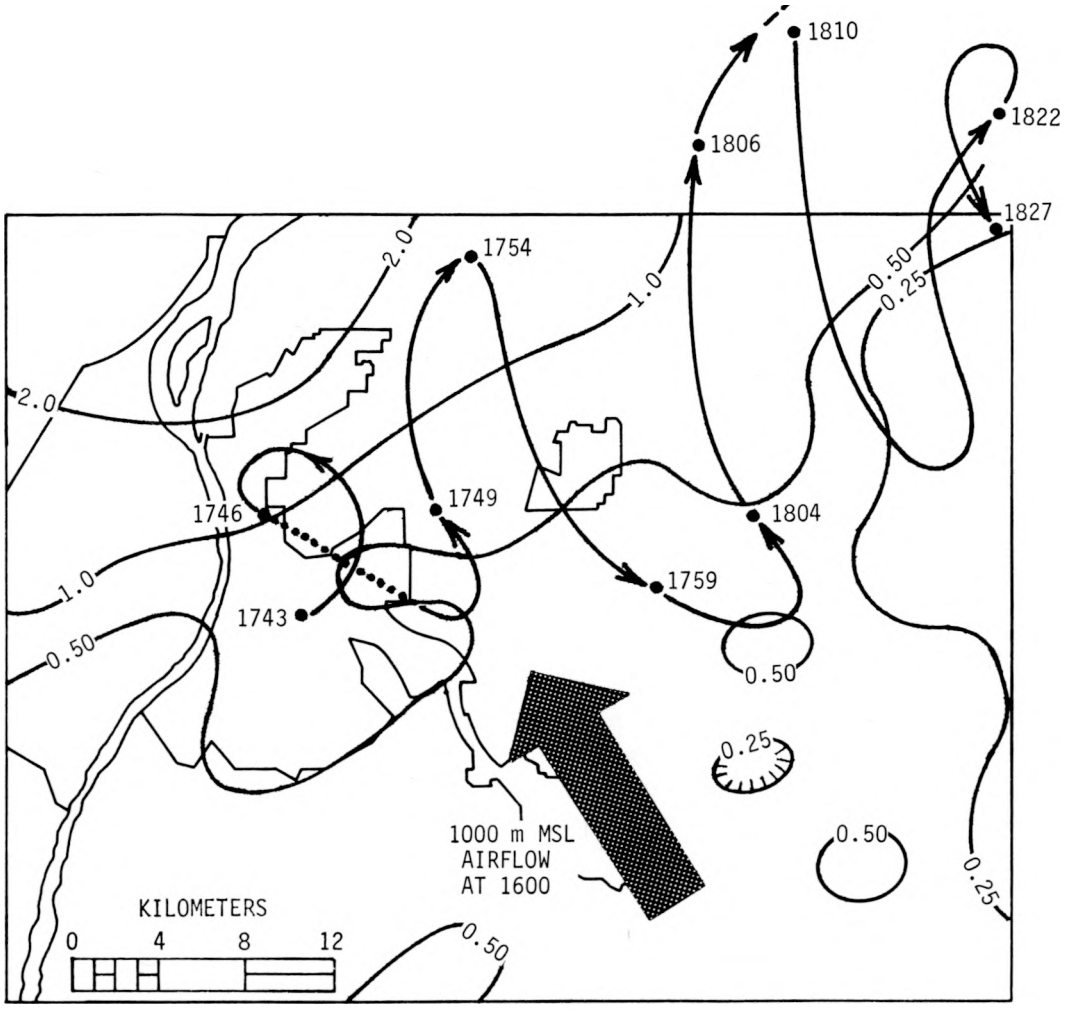

Figure E-29. Rainfall in the chemistry network after the start of tracer releases (Li was released along entire aircraft track and In was released over dotted portion only. The wind direction shown is approximately that of flight level, at 1600)

Tracer Deposition

Both In and Li tracers were released on 23 July. However, In analyses have not been completed, and only Li results are discussed in this report.

The aircraft track during tracer releases is shown on figure E-29, along with total rainfall after the beginning of the tracer burn and airflow information. Rainfall $\geq$ 0.3 inch was quite general throughout the rain chemistry network, and the heaviest rain (> 2 inches) fell in the NW corner.

The relationships between airplane location, updrafts, and the rainfall rate field are explored in figure E-30. This figure shows a series of 10-min average rainfall rate fields and the Li release path over each 10-min period. Beginning with the 1800–1810 period, the aircraft path 20-min before each period is also shown as dashed lines.

Reasonable estimates of updraft speed, the height of rain generation, and raindrop fall speeds suggest a 20-30 min interval between water vapor entering a convective cloud in the updraft and its subsequent deposition as rain. The occurrence of heavy rain downwind (with respect to

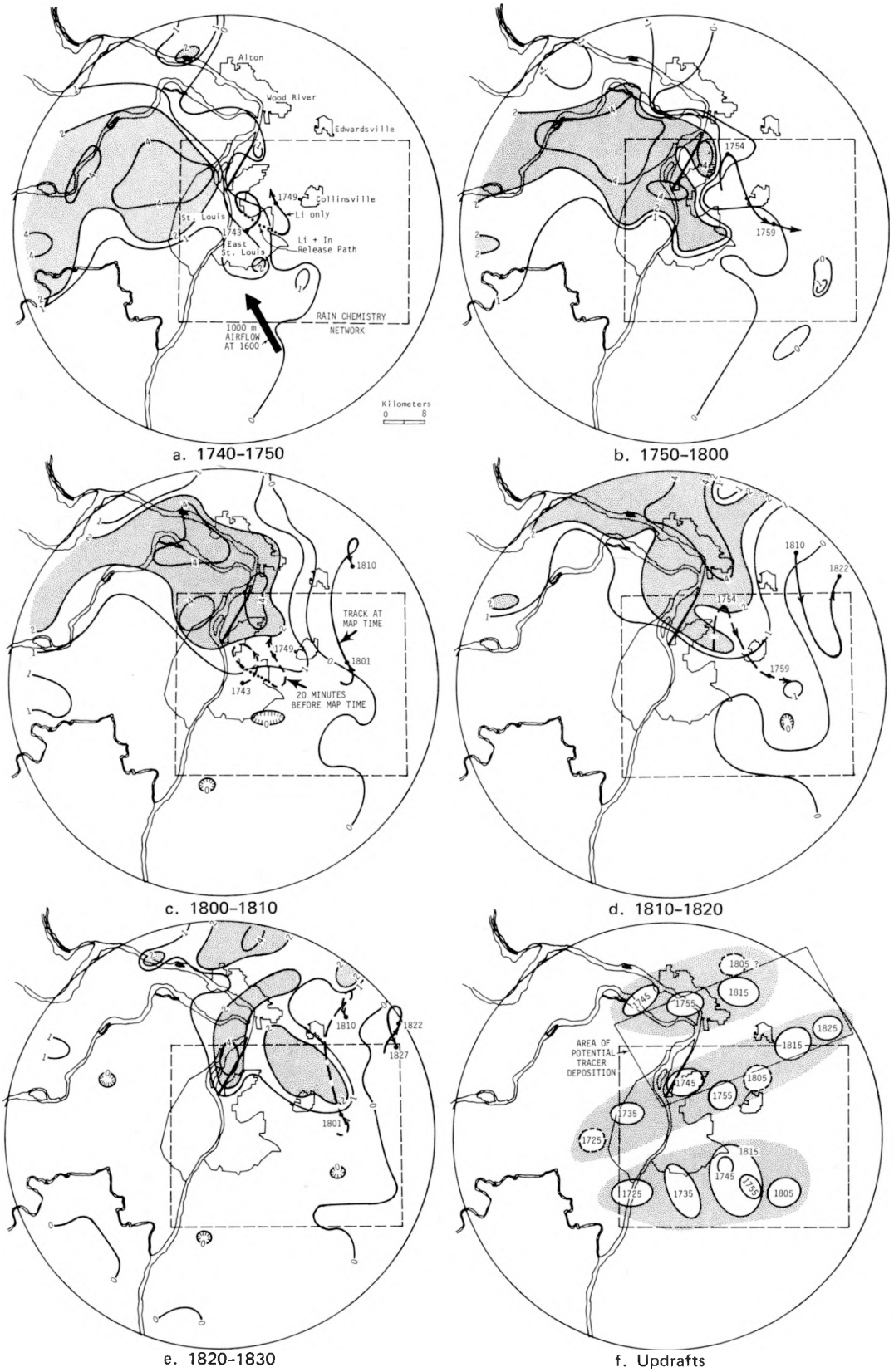

Figure E-30. Rainfall rate (in/hr) distributions for successive 10-min periods during the squall line, and updraft positions inferred from the rainfall rate distributions

wind at flight level) of the airplane track (presumably flying in the updraft) 20 min earlier, for several of the time periods shown on figure E-30, confirms the estimated cycling time for water vapor. Furthermore, it suggests that the tracer should have been deposited over the extreme N portion of the network and N of the MMX circle.

Figure E-30 provides evidence that the airplane actually was flying in, and following, a strong updraft. Updraft locations were inferred from the configuration of the 0-rainfall rate isoline on figure E-30a-e. Updrafts were inferred to exist in a 'notch' or 'indentation' in this isoline, especially if there was a strong gradient in the rainfall rate nearby. This method of inferring updraft locations is consistent with the concept that updrafts are located in regions of weak radar echoes (Marwitz, 1973). It presumes that vigorous updrafts prevent precipitation from reaching the ground beneath them. Two examples of inferred updraft locations shown on figure E-30a are 1) immediately SW of Alton, and 2) over Granite City. In both cases, notches in the 0-isoline of rainfall rate occur near strong rainfall rate gradients. Note that rain core D (figure E-25a) developed in the position of the Alton updraft at 1740–1750 (figure E-30a), with a 10-min lag. Also, a merger of rain cores (figure E-25b) occurred in the position of the Alton updraft at 1750–1800 (figure E-30b) with a 10-min lag. These events support the concept that low θ_e ingestion leads to the production of heavy rainfall rates.

In figure E-30f, inferred updraft locations have been plotted for the 5 periods shown on figure E-30a through e and for two prior periods (not shown). The time label on each inferred updraft is the mid-point of the time period in which it was detected. Dashed updrafts indicate that the updraft's existence or location is less certain.

Figure E-30f shows three distinct updrafts traversing the MMX circle during the period of tracer release. Comparison of the airplane track with the successive positions of the updraft that crossed St. Louis and Granite City indicates that the plane was following, and frequently in, this updraft. It is interesting to compare the behavior of the two updrafts farthest N, both associated with heavy rain, with the updrafts farthest S. Although the S updrafts traveled across a region of high θ_e values, and died as they apparently ingested successively lower θ_e air, they produced no heavy rainfall.

Soluble Li deposition per unit area (pg/cm^2) was computed at each collector from measured concentrations and the respective sample volumes. These gross deposition values were corrected only for dry deposition of soluble natural Li. This correction was made separately for each sample by using the duration of sampler exposure and the median deposition rate (mass/cm^2/hr) at the respective sites found in about 20 cases in 1972.

The wet deposition of soluble Li (pg/cm^2) remaining after subtracting the dry deposited fraction from the total is shown on figure E-31. In general, the deposition pattern follows the pattern of post-burn rainfall (figure E-29), with high values in the NW quadrant of the network. The maximum deposition values occurred close to the tracer release track of the airplane.

On the basis of the information on figure E-30, tracer Li would be expected in the heavy rain that fell in the N portions of the rain chemistry network, and the greatest deposition did occur there. Still unanswered, however, is the question of how much of this amount was natural Li and how much was tracer.

For a general idea of how much tracer deposition to expect, the following calculation was considered. All 236 g of tracer Li are assumed to have been deposited in the rain that fell downwind of the tracer release path between the two updraft regions shown on figure E-30f. The box shown on the figure has an area of 444 km^2; thus, the average deposition would be:

$$\frac{236\ \text{g}}{444\ \text{km}^2} = \frac{2.36 \times 10^{14}\ \text{pg}}{4.44 \times 10^{12}\ \text{cm}^2} = 53\ \text{pg/cm}^2$$

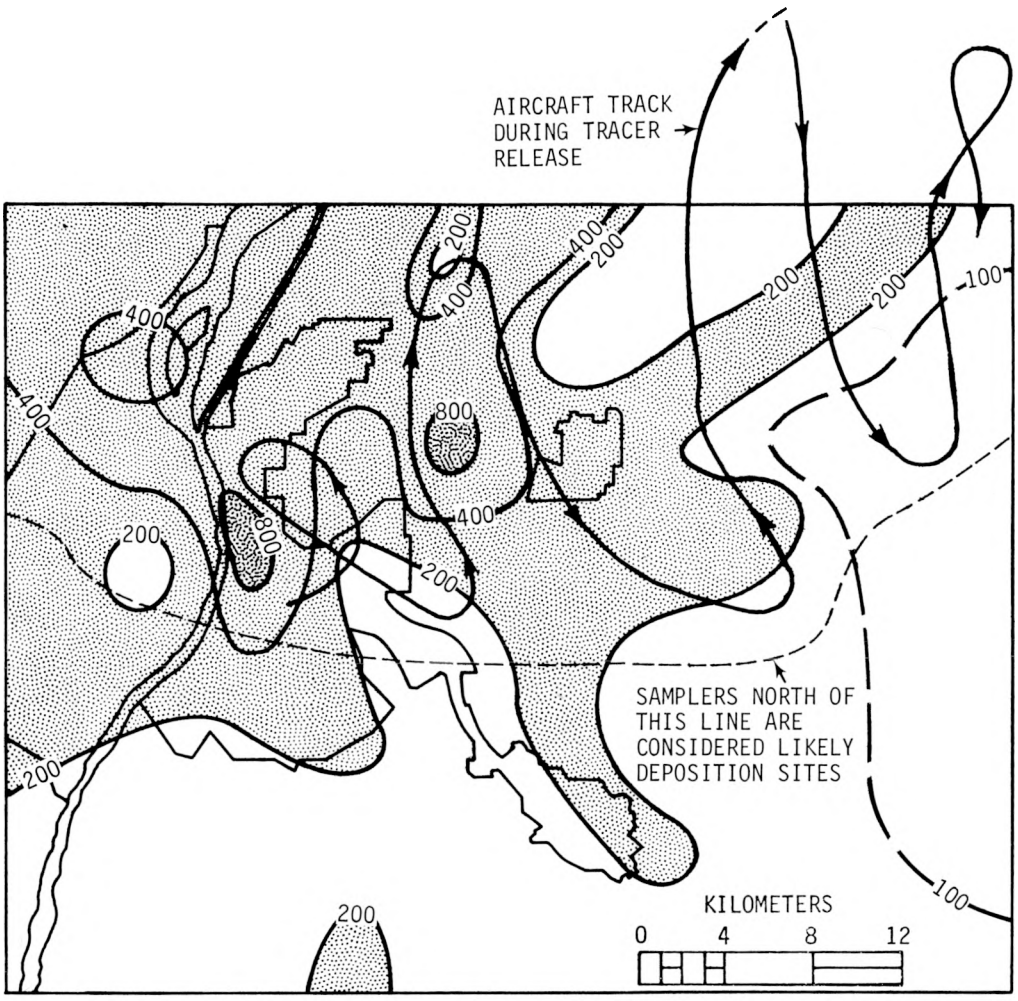

Figure E-31. Soluble Li deposition (pg/cm^2) corrected for dry deposition

Clearly, tracer deposition was not uniform, and this calculation is intended only to provide general background information relevant to the problem of distinguishing tracer Li from natural Li. The results suggest that this task may be difficult in view of measured depositions between 200 and 1300 pg/cm^2 in the expected target area.

The investigation was pursued along two separate lines. First, Li deposition (corrected for dry contribution) was plotted against the rain amount that occurred after the tracer release was begun. Samples in the N section of the network, where tracer deposition was thought likely, were identified differently in the graph from those where tracer deposition was unlikely. This made it possible to look for different relationships between deposition and rainfall between the two groups of samples. As a control, the same analysis was performed on K which is thought to be predominantly soil-derived.

This investigation showed no discernable difference in deposition–rainfall relations between the two groups of samples, but it identified two samplers near the tracer release track where Li deposition was 2 to 3 times what would have been expected from the rainfall amounts.

The second method of investigation was to compute Li/K deposition ratios and compare them with the earth's crust ratio. The results showed that the computed ratios did not exceed the

earth's crust ratio nor was there a pattern of higher ratios in the area of expected tracer depositions.

Overall, it must be concluded that it has not be possible to reliably separate tracer and natural Li for this case study.

Non-Tracer Elements

This section concerns measurements of the deposition of *soluble* elements in precipitation. Again, dry deposited materials have been subtracted in the same way as was done for Li.

Deposition patterns of Na, Mg, K, Ca, and Zn are shown on figure E-32 along with rainfall for the time the samples were exposed. All values have been normalized to their respective network means. All elements show a strong relationship between deposition and rainfall, except Zn which has a strong maximum elsewhere (E of Granite City). A Zn maximum was found in the same locale on 13 August 1973, suggesting a source in the Granite City industrial area. A consistent distance of the maxima from the source sets limits on aerosol trajectories and in-cloud cycling times. If the source is in the Granite City area, as the data suggest, then the gap between the source and the maximum deposition suggests an in-cloud trajectory and a scavenging mechanism for a major portion of the Zn aerosol.

The elements other than Zn are known to have large, rather fixed, natural sources (such as soil dust) but varying urban and industrial source strengths. These differences are not readily apparent in deposition patterns because of the strong influence of rainfall amount on the amount of deposition. However, it is possible to remove the variability connected with the varying rainfall amounts by comparing elements by their ratios.

Ratios of each element to K (as an index of the soil source) are shown on figure E-33. Maxima common to all elements are found in the E, S, and SW portions of the network. Since these maxima are away from their individual maxima (figure E-32), an abnormal *deficiency* of K is indicated in these areas. Because these maxima are common to Na, Mg, Ca, and Zn, they do not suggest a non-soil source, unless it were a source of all these elements. The ratio maps do suggest non-soil sources for two elements. A Zn source is suggested in the Granite City area. In addition, a Ca source may exist in the area S of East St. Louis. Several limestone quarries operate in that region.

SUMMARY AND DISCUSSION

Frontal Precipitation System, 0000-0600

The macroscale synoptic conditions associated with the early morning rainfall include an E to W quasi-stationary front in the St. Louis vicinity. The location and movement of the front are difficult to state precisely from the data available, but it is quite likely that the precipitation was somehow associated with the front.

Mesoscale surface conditions at 0000 featured relatively warm, dry air over the city area and generally airflow to the E.

Rainfall in the MMX circle during this period was less than 0.55 inch at all sites, and there was no severe weather. Neither hail nor thunder occurred during the precipitation period.

Raincells showed preference for areas of high surface moisture, weak preference for areas of high θ_e, and little or no preference for areas of high surface temperatures. Raincell initiations

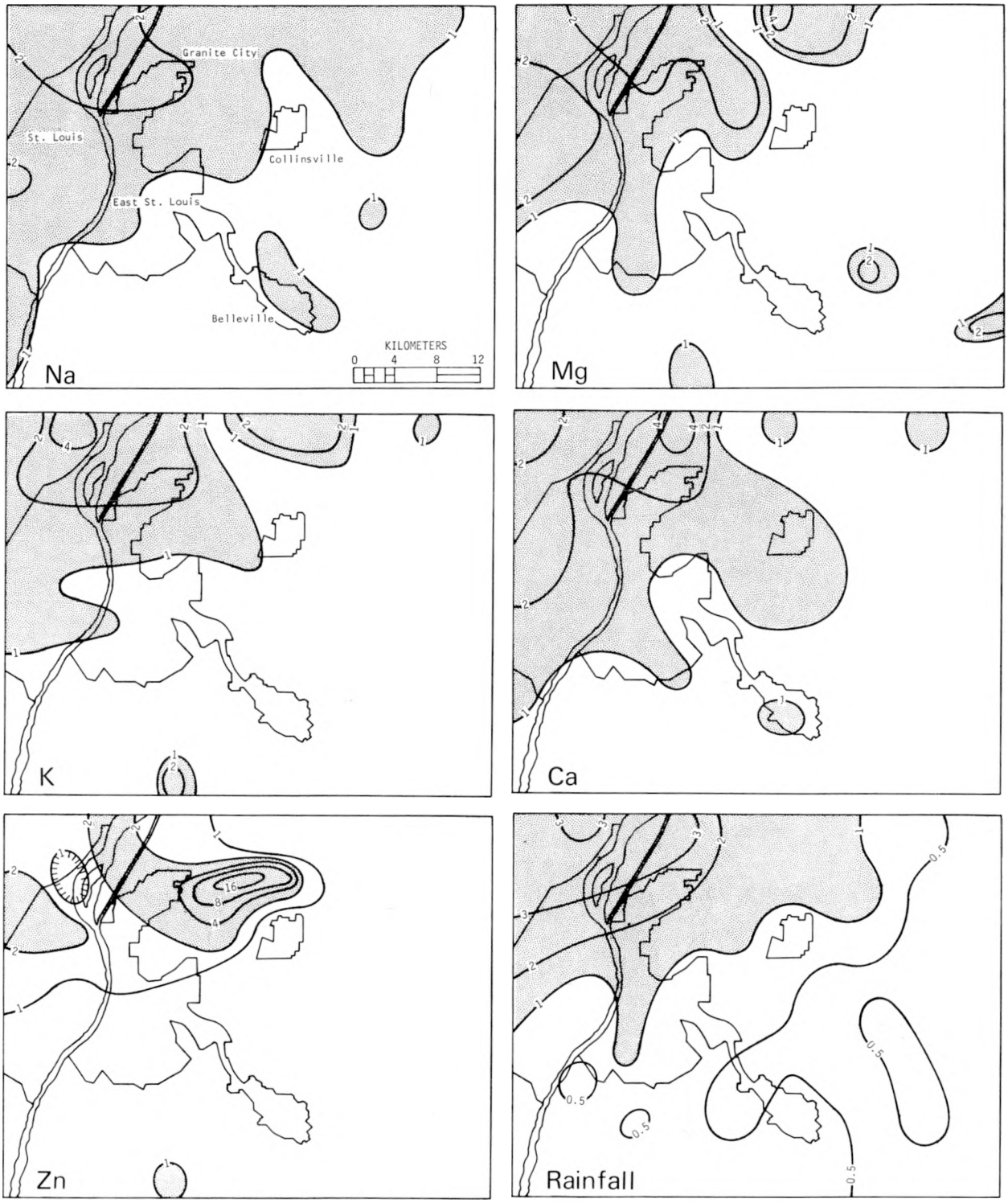

Figure E-32. Deposition (mass/area) of non-tracer elements and rain, each normalized to its network mean

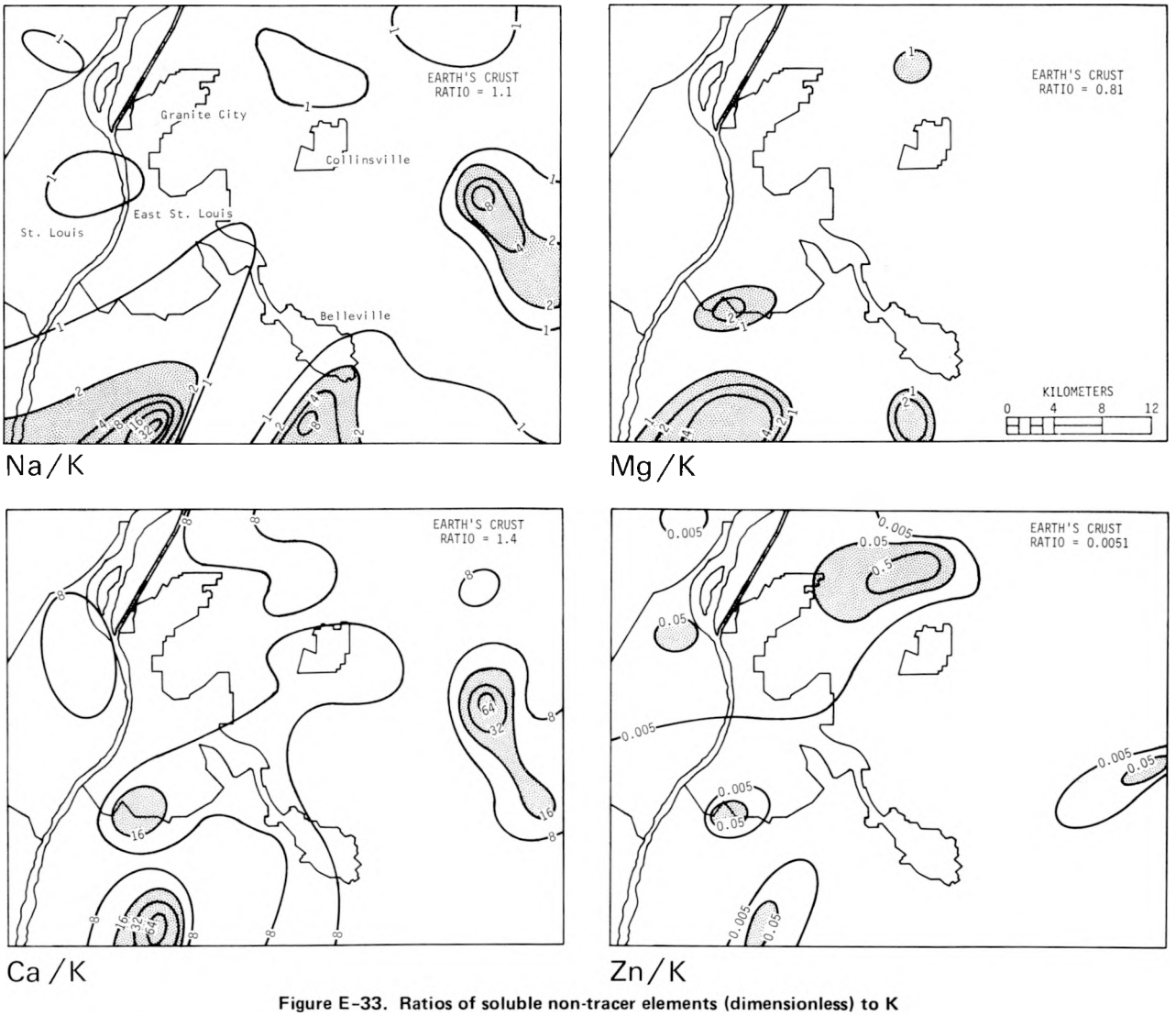

Figure E-33. Ratios of soluble non-tracer elements (dimensionless) to K

showed considerable correspondence with areas of high moisture, but only weak correspondence to areas of high temperatures. The period can be characterized by many weak raincells with low rainfall rates.

Thus, it appears that local moisture sources influenced the location of convective activity in the early morning case. There is little evidence to suggest that the city was the cause of the convective activity, but the pattern of surface moisture indicates that the river valleys may have been the main local sources. No aircraft or rain chemistry data were collected for this portion of the case.

Squall Line Precipitation System, 1400–2300

A squall line formed in W Missouri, along the leading edge of outflow from prior thunderstorms in Kansas. As the squall line moved E, it intersected a warm front that curved NE across central Missouri. Heavy thunderstorms were generated along the intersection. The squall line later intersected an area of precipitation moving N from the Cape Girardeau area, and the severe storms generated as this intersection moved NE across the St. Louis metropolitan area.

Mesoscale surface data prior to the squall line show surface temperatures in the low to middle 90's across much of the network. Slightly cooler air was present in the SW (hills) and NW portions of the MMX circle. Surface dew points were in the middle to upper 70's across much of the network except for a swath of relatively drier air (dew points in low 70's) running from the W to the NE edge of the MMX circle. Surface winds were generally SE, veering to S at the 1000 m level. The pre-rain sounding at PMQ indicated an unstable atmosphere with a lifted index of -6.

The hourly macroscale precipitation patterns show the intersection of the two squall lines also seen in the satellite and radar data. During the hour in which the merger occurred, heavy precipitation occurred within the MMX circle. The analyses of the movement and direction of the macroscale precipitation systems prior to and after the merger indicate that 1) the heavy rainfall in the MMX circle was probably the result of intensification due to the intersection of the two squall lines, and 2) the large-scale squall system did not dissipate after passing through the circle.

The severity of the storm is illustrated by extremely high rainfall rates which occurred during the squall-line period. Thirty-min amounts exceeding 2 inches occurred at several raingages in the N St. Louis and Granite City areas. These events have an average return period of 25 years. The total storm rainfall was $>$ 1 inch across the NW portion of the network. Rainfall of 2 to 3 inches occurred in several locations, but principally in the W, NW, and N sections.

Raincells were not located preferentially in areas of high surface moisture or in areas of high surface temperatures. Similarly, cell initiations did not occur preferentially in areas of high surface moisture or in areas of high surface temperatures. However, there was a tendency for the heavy raincells to occur near areas of low surface moisture.

Further investigation revealed that the surface θ_e pattern was dominated by moisture rather than temperature. Thus, areas of low moisture were also areas of low θ_e. Boatman and Auer (1974) have proposed a mechanism whereby heavy rain can occur following the ingestion of low θ_e air in an updraft. This concept was investigated by an analysis of 10-min rainfall patterns in conjunction with the θ_e pattern prior to the onset of precipitation. Since the heavy rainfall was generally caused by macroscale conditions independent of the urban area, the above concept was investigated from the viewpoint of possible redistribution of the precipitation within the MMX circle.

Most of the heavy rainfall occurred in areas with surface $\theta_e < 356$K. An analysis of upper air soundings at PMQ and ARC indicated that values of $\theta_e < 354$-355K would inhibit convection and could lead to a weakening of the storm with subsequent heavy rainfall. Within the 356K region, the higher rainfall rates appeared to be associated with lower θ_e values (352K).

The overall analyses suggest that some of the heavy rain could have been the result of the ingestion of low θ_e air. However, analyses of aircraft and airflow data indicate that low θ_e values were frequently accompanied by high CN concentrations.

Analyses of tracer chemistry data were unable to separate tracer Li from natural Li in the rain. There appears to be a strong source of Zn in the Granite City area, and the deposition pattern of soluble Zn suggests rapid wet collection and deposition of aerosols with a near-surface source by an in-cloud process.

CONCLUSIONS

The main objectives in this study were to determine whether the city modified the precipitation systems to cause or contribute to 1) the W to E decrease in heavy rain, and 2) the severe weather events.

The timing and motion of the heavy rain system strongly indicate that it was generated by the merger of two squall systems SW of the MMX circle at about 1700. From there, the upper level steering flow determined its path. Thus, the general location and W to E decrease of the heavy rain was determined by synoptic and mesoscale conditions that were tens of miles upwind of the city.

Within the area of heavy rain, there is evidence that the ingestion by the storm system of low θ_e air may have caused some redistribution of rainfall. The same mechanism probably caused some degree of increase in the rainfall rate and, thus, downdraft intensity (two measures of storm severity).

If this mechanism did increase the storm intensity, then it is important to determine how often it occurs, and how much of the observed E-side anomaly can be accounted for by it. It would appear that such a mechanism can operate only in rainstorms strong enough to accumulate water aloft. This is consistent with the observation that much of the observed urban anomaly is produced by heavy rainstorms (Huff and Changnon, 1972).

Low θ_e values were probably accompanied by high CN concentrations. In such a situation, it is impossible to determine unequivocally the relative roles of these two potential influences. Additional research, particularly case studies, will be needed to solve this problem.

Our work has suggested that additional analyses are needed for a better understanding of the storm on 23 July. Other radar data should be examined for details of the major convective cells in the heavy rain system that was attenuated on the PMQ radar. The southernmost updraft region shown on figure E-30f behaved contrary to what would be expected from the updraft-weakening mechanism discussed earlier and should be examined in more detail. The calculation of water budgets for each of the major updrafts should help determine whether condensed water from the S updraft could have fallen in the heavy rain to the N.

This study uncovered a potentially useful tool for other studies, namely the method of locating updrafts based on rainfall rate distribution. This tool should help to determine if urban areas are preferred locations for convective updrafts. Finally, satellite data were found to be a valuable tool for these kinds of investigations.

REFERENCES

Boatman, J. F., and A. H. Auer. 1974. *Inadvertent thunderstorm modification by an urban area.* Preprints, 4th Conference on Weather Modification, Fort Lauderdale, Florida; AMS, Boston, pp. 366-373.

Huff, F. A., and S. A. Changnon, Jr. 1972. *Climatological assessment of urban effects on precipitation at St. Louis.* Journal of Applied Meteorology, v. 11:823-843.

Jones, D. M. A., and P. T. Schickedanz. 1974. *Surface temperature, moisture, and wind studies. In* Interim Report of METROMEX Studies: 1971-1973, F. A. Huff, Editor, Illinois State Water Survey for NSF Grant GI-38317, pp. 98-120.

Marwitz, J. D. 1973. *Trajectories within the weak echo regions of hailstorms.* Journal Applied Meteorology, v. 12(7):1174-1182.

National Transportation Safety Board. 1974. Aircraft Accident Report No. NTSB-AAR-74-5, Washington, D.C.

Purdom, J. F. W. 1974. *Satellite imagery applied to the mesoscale surface analysis and forecast.* Preprints, 5th Conference on Weather Analysis and Forecasting, St. Louis, Missouri; AMS, Boston, pp. 63-68.

F. SQUALL ZONE STORMS ON 25-26 JULY 1973

S. A. Changnon, Jr., and F. A. Huff

CONTENTS

F. SQUALL ZONE STORMS ON 25-26 JULY 1973

INTRODUCTION

During the evening of 25 July and the early morning of 26 July 1973, a severe rainstorm accompanied by thunderstorms and hail developed in the Alton–Wood River area. At the center of this storm just north of Alton, 1-hr and 2-hr rainfall amounts were of an intensity expected to occur on the average of once in 10 years at any given point in this area (Illinois State Water Survey, 1970). The rainfall in this storm occurred during the period from 2000 to 0230, but most of the downpour in the center of the storm was recorded between 2000 and 2200. Some rainfall occurred in all regions of the MMX circle between 1640 and 0250, but heavy rains were recorded only in the Alton–Wood River area.

The storm of 25-26 July was selected for detailed study for three reasons. First, it was potentially indicative of urban-industrial effects on precipitation at Alton–Wood River when there was none at St. Louis. Second, its close examination might provide some clues as to the 1971–1972 raincell differences noted between the two areas (Schickedanz, 1974). Finally, it was a nocturnal storm.

Preliminary analysis of the precipitation, aircraft soundings, and wind data indicated that the severe rainstorm was a potentially urban-affected event because of 1) its position with respect to Alton–Wood River, 2) a relatively large number of raincell initiations within and immediately downwind of the urban-industrial area, 3) good mixing extending from the surface to cloud base that permitted surface effluents and atmospheric penetrations to reach cloud level, and 4) intense rainfall rates that were apparently produced by mergers of individual raincells over the urban area.

Unfortunately, certain MMX data found to be very helpful in most of the case studies were not available for this storm, primarily because it occurred at night. The pibal and rain chemistry networks were not in operation during the storm. Operation of the Survey's 3-cm RHI radar ceased shortly before initiation of the storm rainfall, and the 10-cm PPI radar was out of operation due to malfunctions during two critical periods of the storm. Aircraft sampling operation also ceased about the time the storm started. Consequently, evaluation of the potential urban effect in this storm had to be accomplished primarily from the synoptic weather information, raincell data, severe weather observations, surface temperature and humidity measurements, and limited radar data.

SYNOPTIC ANALYSES

The convective activity in the MMX circle on 25-26 July was associated with the approach and passage of a cold front. The severe rainstorm in the Alton–Wood River area during the evening of 25 July was associated with a prefrontal squall zone. Convective activity in the zone was intensified by a minor wave traveling along the cold front W of the MMX circle.

Surface Weather Maps

Examination of the surface maps at 3-hr intervals showed that the front was approaching the W edge of the MMX circle at 1900 CDT on the 25th and a wave on the cold front was located

in S-central Missouri. Most of the storm rainfall occurred in the 2000–2200 period. Figure F-1 shows the surface map at 2200 when the small wave was passing through the St. Louis region. Thus, the heaviest rainfall apparently occurred shortly in advance of the cold front wave. A moisture ridge with dew point temperatures in the 70-75F range extended to the N in advance of the surface front.

Upper Air Data

Figure F-2 shows the 850-mb height contours and dew point temperature patterns at 1900 CDT on 25 July, approximately 1 hr before the start of the heavy storm period, and when scattered convective activity was present in the SE part of the MMX circle (figure F-9). A trough accompanying the surface cold front extended in a N-S direction through E Iowa and central Missouri and then SW. Relatively high dew points (15-16C) extended to the E from St. Louis. Differences between the air and dew point temperatures were relatively small, less than 2C, over most of Illinois including the MMX circle.

The 700-mb and 500-mb contours for 1900 (figures F-3 and F-4) show typical patterns associated with a cold frontal system. The 700-mb trough extended through W Missouri behind the surface front, and the 500 mb trough was centered in E to central Nebraska and Kansas. Overall, the surface and upper air patterns were favorable for rather extensive convective activity to occur with the approach and passage of the cold front.

Radiosonde observations were available from PMQ and ARC at approximately 0700 and 1400 on 25 July. The PMQ sounding was taken about 20 mi WNW of the Alton-Wood River storm center and the ARC sounding about 20 mi S of the storm core. Soundings were also available at 0700 and 1900 CDT from the NWS station at Salem, 60 mi E of the MMX circle. The early afternoon sounding for PMQ and the early evening sounding for Salem are shown in figure F-5. The PMQ and ARC soundings indicated relatively unstable conditions in the lower 100 to 150 mb in the afternoon with Cu bases most likely in the vicinity of 2000 to 3000 ft. Relatively unstable conditions were indicated to 850 mb by the Salem sounding at 1900. Both soundings in figure F-5 show several alternating layers of relatively moist and dry air aloft.

The early afternoon soundings showed a Showalter stability index of +5 at PMQ and +3 at ARC. However, by 1900 CDT the Salem sounding showed a relatively unstable -2. No rain occurred on the MMX circle during the afternoon. The first rain of significance was not recorded until after 1800 CDT, when showers occurred in the SE quadrant of the circle. The soundings also indicated an increase in low-level moisture from early afternoon to early evening. At PMQ, the sounding at 1345 indicated an average mixing ratio of 14 g/kg in the lower 850 mb. At 1900, the Salem sounding indicated a surface mixing ratio of approximately 18 g/kg with an average of 16 g/kg in the lower 850 mb. Thus, as could be expected with an approaching cold front and upper level trough, the atmosphere was becoming more moist and less stable with time, and by mid-evening relatively heavy convective activity was recorded in the circle. As indicated earlier, this activity was along a prefrontal squall line or zone.

REGIONAL RADAR AND RAINFALL ANALYSES

Radar Echo Distribution

NWS radar summaries were used to obtain a measure of the areal extent, duration, and intensity of the mesoscale convective activity in the vicinity of the MMX circle. These showed

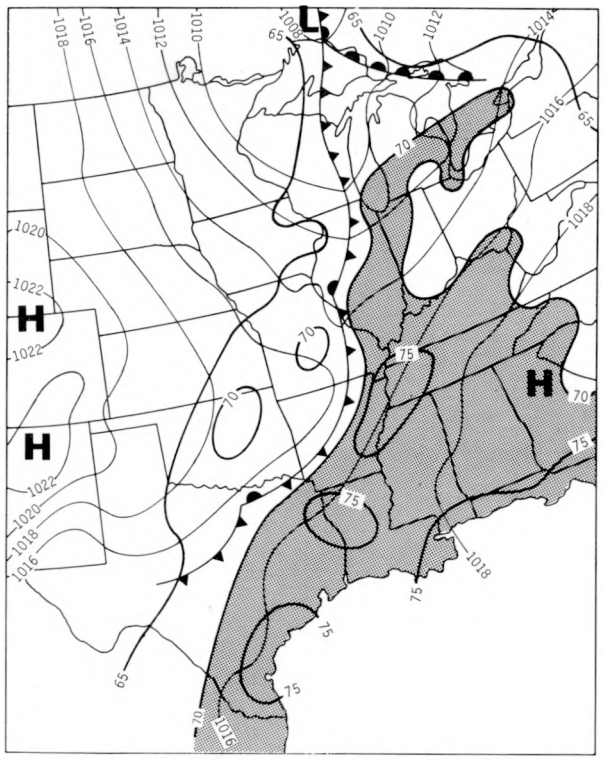

Figure F-1. Surface map at 2200 CDT

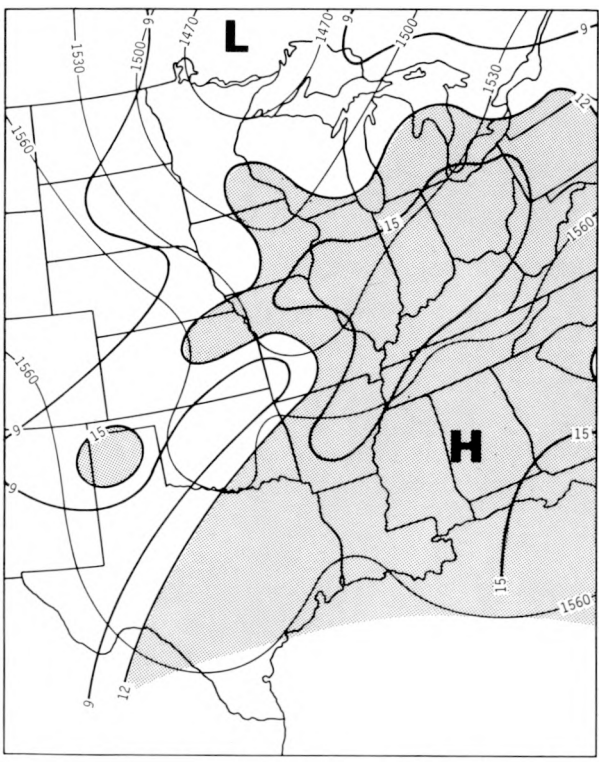

Figure F-2. 850-mb map at 1900 CDT

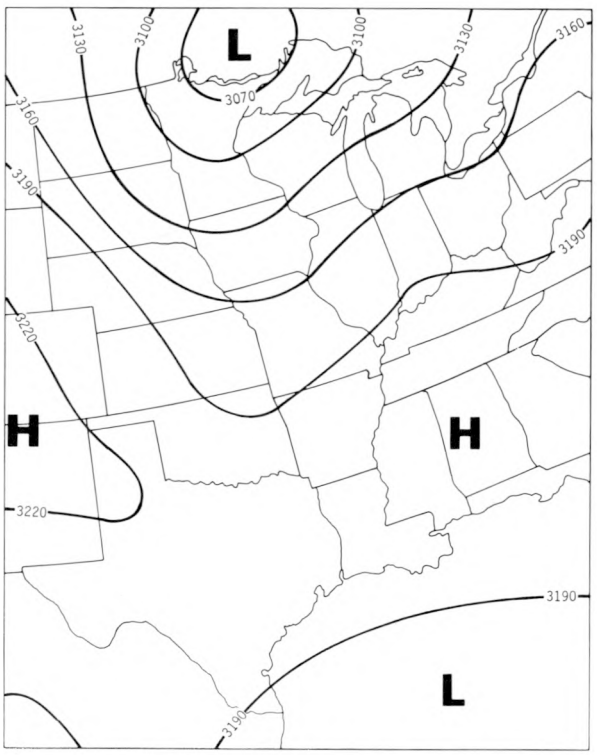

Figure F-3. 700-mb map at 1900 CDT

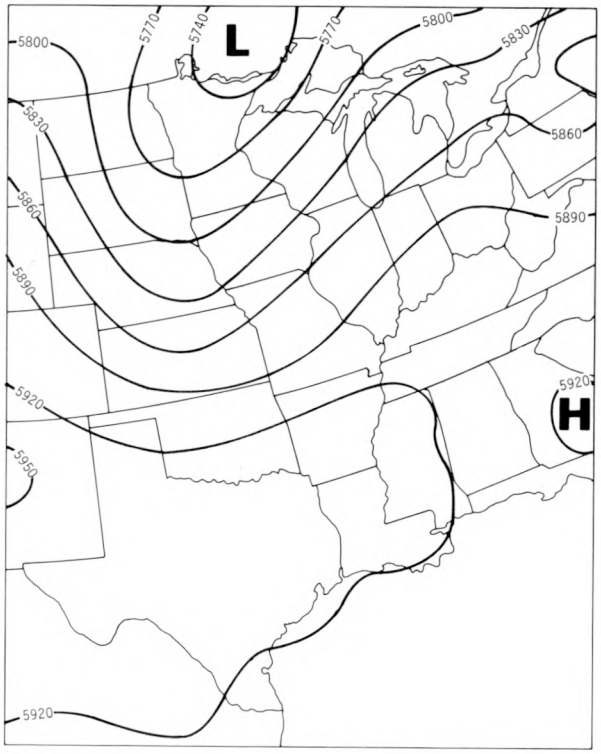

Figure F-4. 500-mb map at 1900 CDT

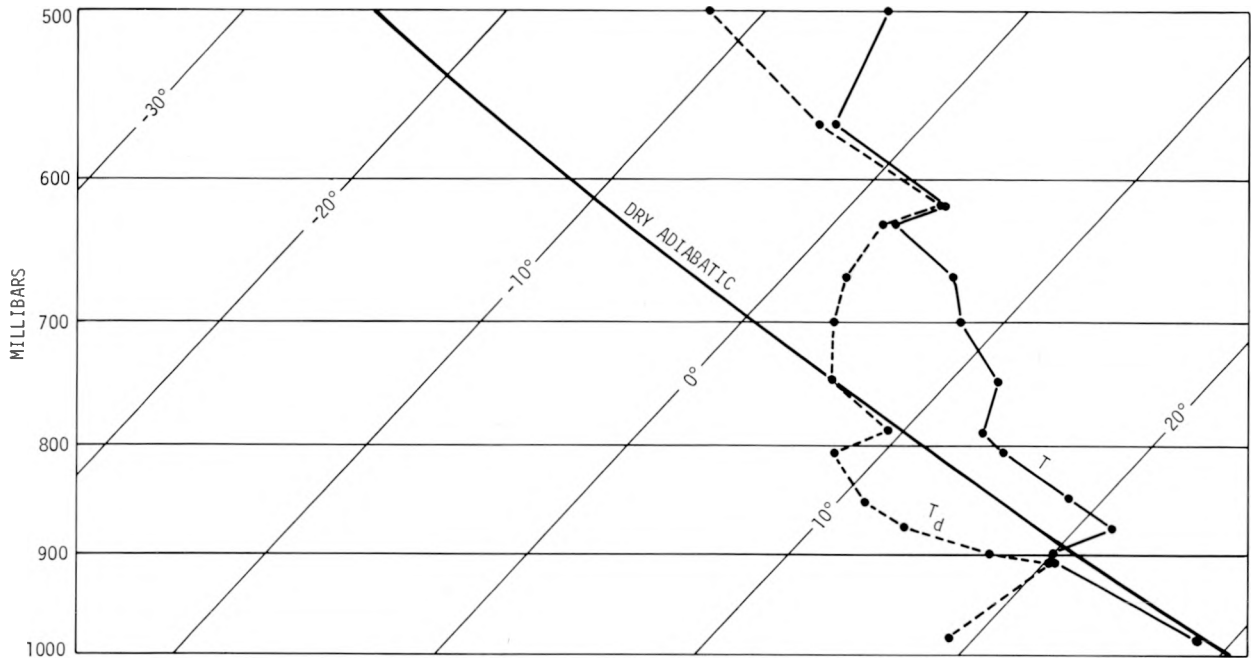

a. PMQ at 1345 CDT

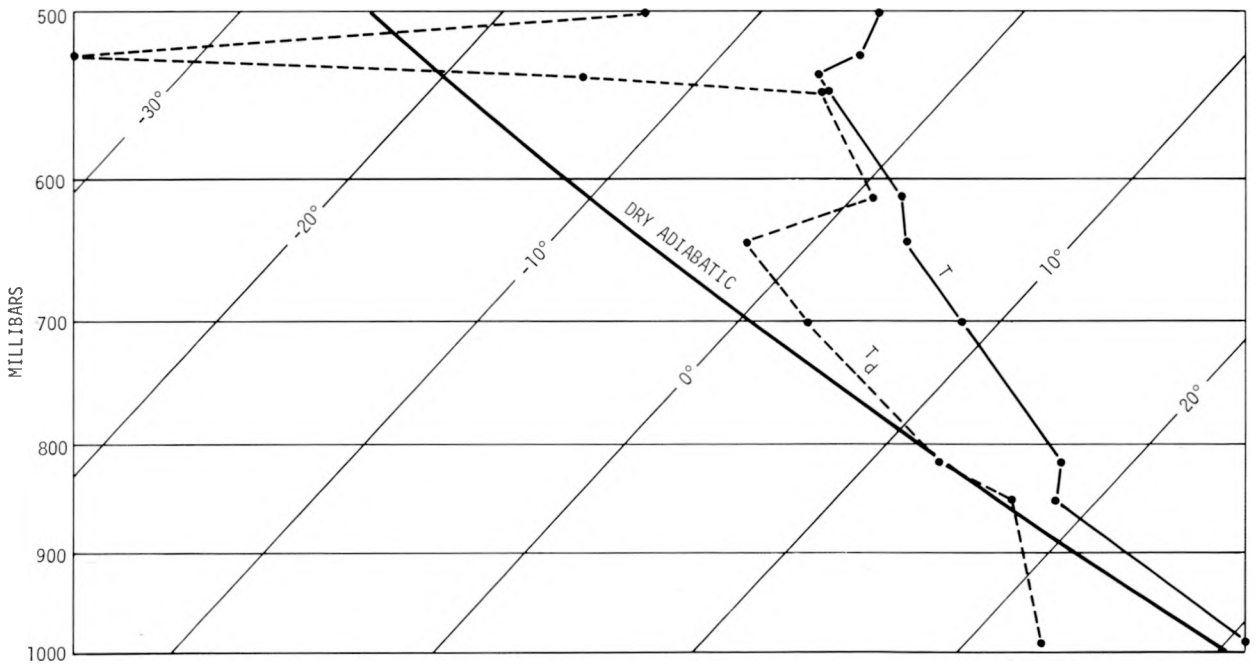

b. Salem at 1900 CDT

Figure F-5. Radiosondes at 1345 and 1900 CDT

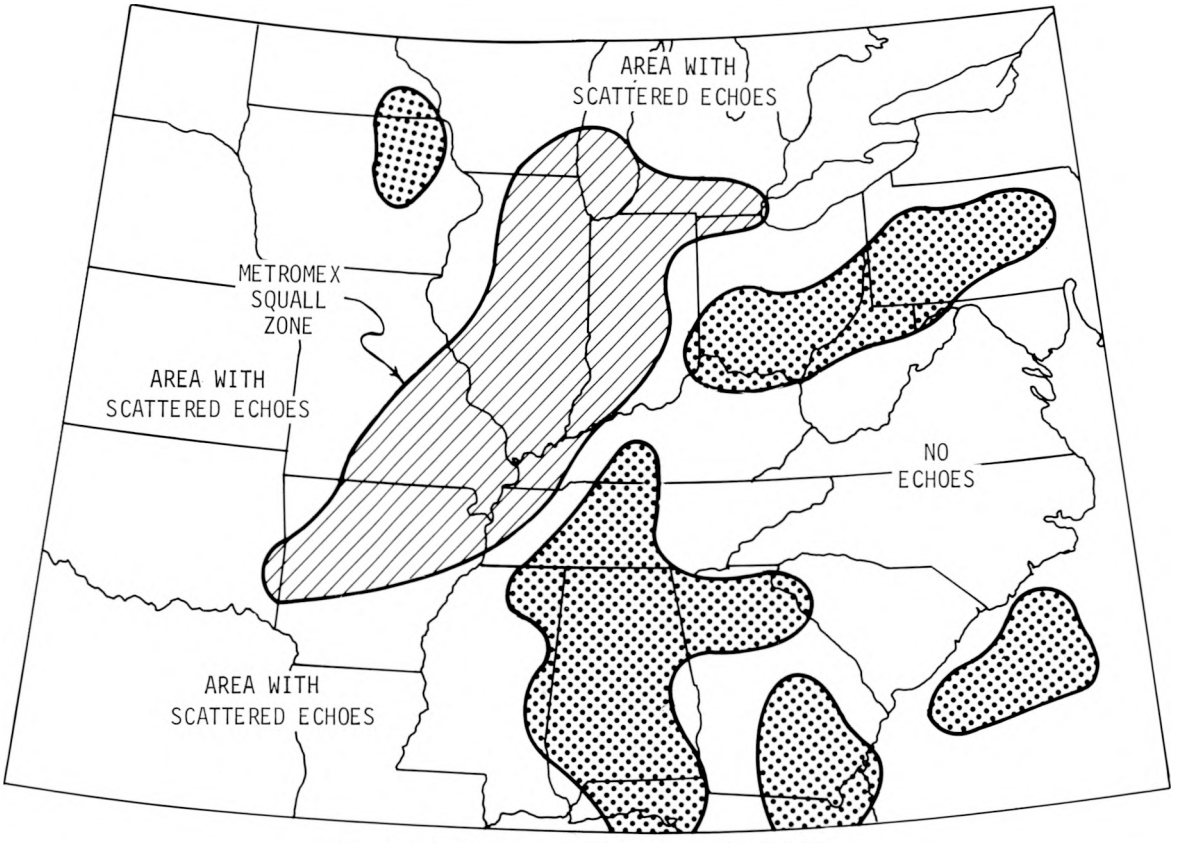

Figure F-6. Envelopes of radar echoes at 2140 CDT

widespread scattered RW and TRW throughout much of the 25th and the morning of the 26th in the region from the E part of the Great Plains to the East Coast. The intensity and density of this activity maximized from mid-afternoon to midnight on the 25th in the Missouri–Illinois–Indiana region.

The radar summary map for 1450, approximately 1 hr before the initial rainfall on the MMX circle, showed scattered RW and TRW activity across most of Missouri, Iowa, and W to NW Illinois. Echo tops were mostly in the range from 30,000 to 50,000 ft. Two regions of radar echoes were about to merge in the St. Louis region. By 1640 these echo areas had merged, and echo tops of 48,000 to 50,000 ft were indicated SW of St. Louis.

Convective activity was continuous in the Missouri–Illinois area during the next few hours with echo tops frequently reaching levels of 40,000 to 50,000 ft, and occasionally higher. The envelope of the large squall zone associated with the MMX rainfall under study is shown in figure F-6 for 2140 CDT. At that time, intense rain rates were being recorded in the Alton–Wood River region. At 2140, echo tops were reported in the range of 20,000 to 25,000 ft in NE Illinois, increasing to 35,000 to 50,000 ft over S-central and S Illinois and SE Missouri.

By 2340 CDT, the squall zone associated with the MMX rainfall had moved slightly to the E, decreased somewhat in areal extent, and most tops were under 40,000 ft. At 0040, the squall zone was decreasing in echo tops and areal extent. However, convective activity continued in E Illinois and extreme SE Missouri throughout the night. At 0740 on 26 July, echo tops of 30,000 to 48,000 ft existed at scattered locations in the above regions. At that time, scattered convective activity also continued to the E from Indiana to New York.

During the evening–morning period of rainfall on the MMX circle, the areal extent and intensity of the convective activity was most pronounced in E Missouri and Illinois. With echo tops reported to 50,000 ft or higher in scattered locations, the potential for heavy rainfall was present. Similar to the case of 11 August 1972, the convective activity had a relatively long duration, with some activity in or near this region throughout the afternoon and evening of the 25th into the early morning of the 26th.

Rainfall Distribution

Figure F–7 shows the regional rainfall pattern for Illinois and E Missouri during the period of rainfall on the MMX circle. This map provides a generalized measure of the intensity and areal extent of rainfall resulting from the convective activity identified by the NWS radar summaries. The map was constructed from the NWS climatic network data only, and does not include any MMX measurements. The climatic network averages only about 1 raingage per 250 mi^2, and will not record many small-area, intense events that may be centered between raingages.

Figure F–7 shows that the rainfall was widespread over the two states, but was very 'spotty' with storm amounts ranging from 0.01 to over 3 inches among the Missouri–Illinois stations. In general, the heaviest storm rainfall occurred along a NE–SW zone extending from SW to E-central Illinois. Several stations in this zone received 1 inch or more of rain, and Mt. Olive, approximately 25 mi NE of the MMX circle, recorded the largest 2-state total, 3.09 inches, between 2100 and 2300. Other stations in the zone with amounts of 1 inch or more received their rainfall from late evening to early morning, similar to the heavy storm centers on the MMX circle discussed later. As shown in figure F–7, the N part of the circle was in the zone described above.

TOTAL STORM RAINFALL

Figure F–8 shows the distribution of total storm rainfall on the extended MMX study area for the period 1640 to 0250 CDT. This incorporates the entire period of rainfall on the area. The heaviest rainfall occurred in the Alton–Wood River area and NE of the MMX circle at Mt. Olive. Rainfall in this region occurred in the evening between 2000 and 2300 CDT. The 0.5-inch high in the SW part of the circle occurred in the same period. The minor highs (> 0.25) on the E edge of the St. Louis urban area resulted from showers in the 1830–1900 period. The highs farther E in the circle were from late evening showers.

The heavy rainfall in the Alton–Wood River area was part of the heavy rainfall zone extending NE–SW from E-central to SW Illinois (figure F–7). Since other heavy rainfall NE of the MMX circle occurred at approximately the same time (late evening), the MMX area storms could not have been responsible for any of the rains to the NE. However, they did occur within the same storm system which apparently was a squall line within the squall zone shown in figure F–6.

RAINCELL ANALYSES

Raincell data were analyzed to investigate for any potential urban effect upon the rainfall. Emphasis was placed on the storm activity in the Alton–Wood River area where the potential for

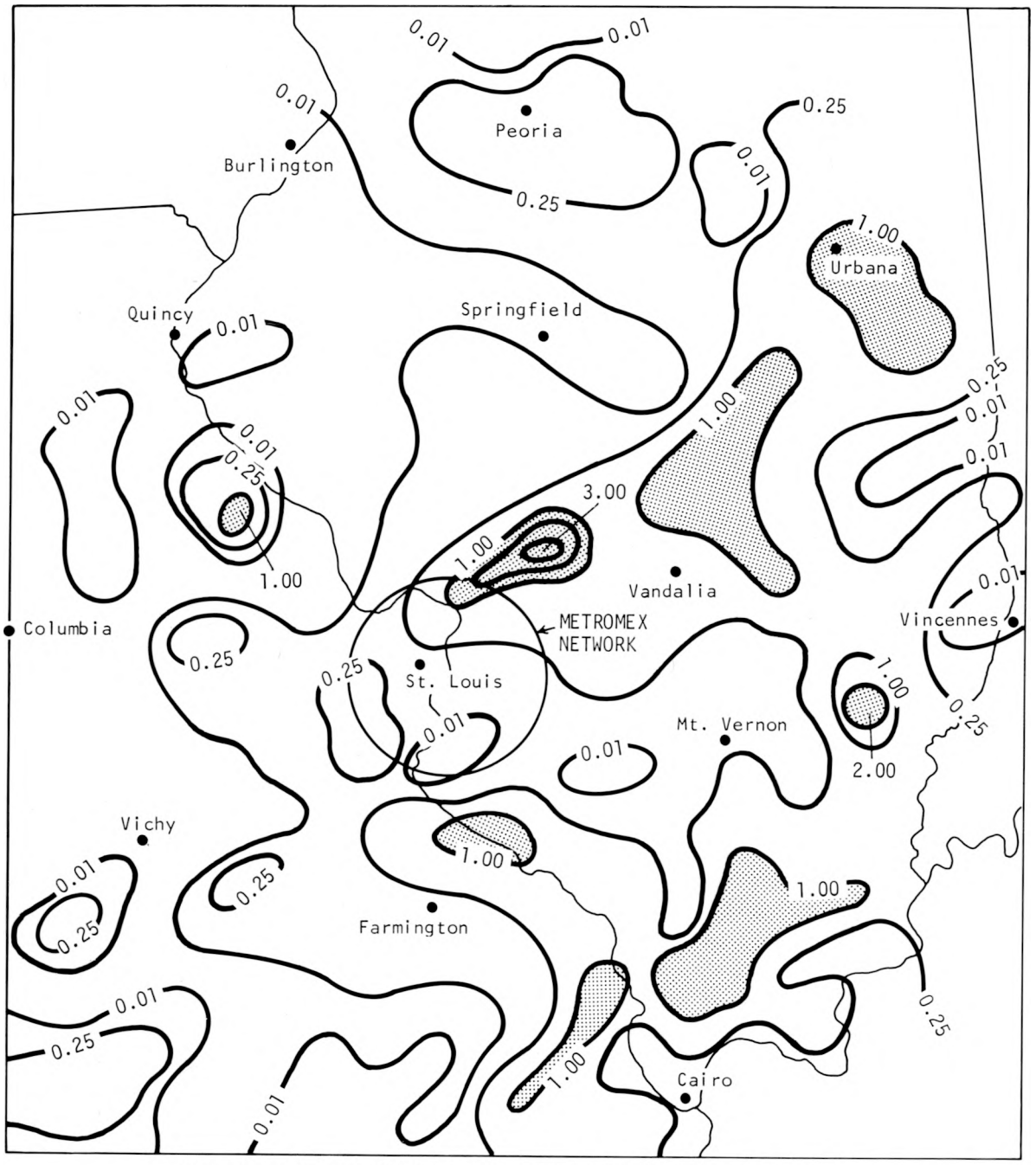

Figure F-7. Regional rainfall pattern for 1630 to 0300 CDT on 25-26 July 1973

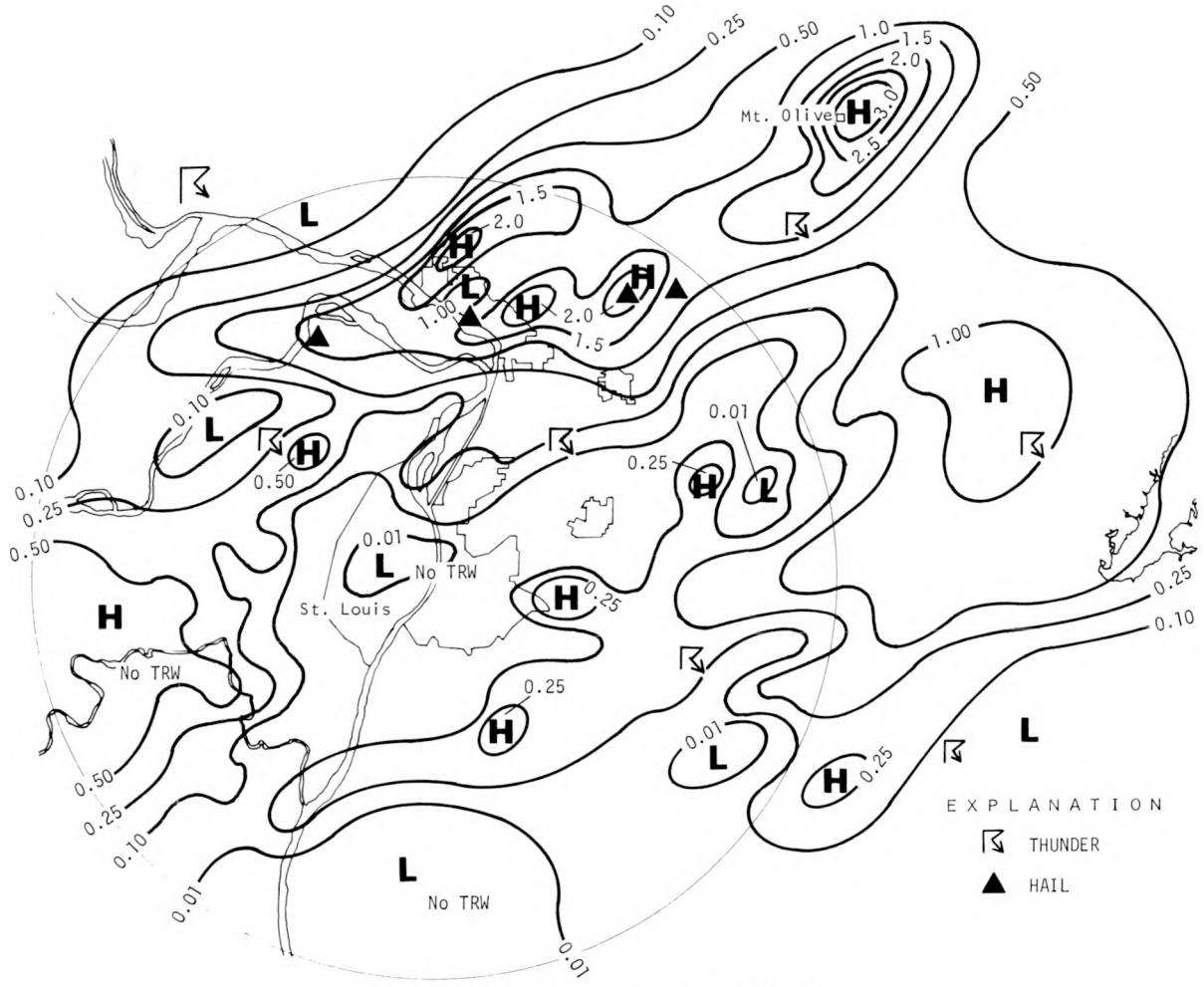

Figure F-8. Total storm rainfall on MMX circle

urban enhancement of RW and TRW appeared to be greatest. Although potential urban effects upon the relatively light rainfall downwind of St. Louis cannot be ignored, a sizeable rain increase was not there in this case. Any effects from St. Louis, if present, did not produce major storms, nor did that area have widespread convective activity to initiate or support rain enhancement to the degree that occurred in the Alton-Wood River area. As will be shown in later sections, this area was favored by one or possibly two conditions. First and foremost, a favorable area for Cu development existed several miles upwind of Alton-Wood River as the result of a pre-rain temperature and dew point (moisture) maximum in the river bottomlands. With existing flow conditions, the bottomland clouds would have moved toward Alton-Wood River where urban factors could then have enhanced their rain production. Another factor possibly contributing to the heavy storms was the movement of a weak wave on a cold front through the MMX area; however, there is no reason to suspect that the wave effect would have been greater in the Alton-Wood River area than in the St. Louis region.

Raincell Histories

The first raincell was not detected in the MMX area until 1640 when a small, nearly stationary cell produced 0.12 inch in the 1640–1720 period. This cell was associated with an air mass shower that developed in the Mississippi River Valley about 8 mi S of St. Louis. The maximum 5-min rate was 0.85 in/hr, and the cell encompassed an area of only 10 mi^2. Raincell 2 was also a quasi-stationary air mass shower that formed about 5 mi SE of the urban area at 1715 and dissipated at 1740 in nearly the same location. It produced only 0.02 inch of rainfall.

Raincell 3 developed at 1815 in the same location as raincell 2. Raincell 4 formed about 6 mi W of raincell 3 at 1825. Neither appeared to be urban-related since low-level flow (surface to cloud base) was from WSW and inflow to these storms was rural air. These two cells moved very slowly NE and merged at 1855 about 3 mi SE of the urban area (figure F-9).

Raincell 5 was the first raincell developing in a position to be urban-related. It developed at the E portion of the urban area at 1840 in a locally warm, moist zone and moved to the E. It reached its peak intensity with a maximum 5-min rate of 2.43 in/hr in its center at 1845–1850. Figure F-9a shows the network rainfall distribution at that time. Raincell 5 eventually merged with the previously merged non-urban cells (3 and 4) at 1905. Updraft data and CN measurements going into raincells 3, 4, and 5 at 1910–1915 (described in more detail later) indicate they were ingesting urban surface air with very high CN concentrations. Thus, the rain output from this merged combination could have been urban-modified and the rain high (> 0.25 inch) just E of the St. Louis area (figure F-8) could have been due in part to urban effects.

Raincell 6 was first detected at the E extremity of the small mesoscale rain system resulting from the merger of raincells 3, 4, and 5, and cell 6 quickly merged with them into a single center. This mesoscale system drifted slowly to the E and eventually dissipated by 2040. The total rainfall associated with the system is shown in figure F-9b. Two major centers existed. The center SE of St. Louis had a recorded maximum of 0.34 inch that was produced entirely by raincell 4. The center just E of the urban area of St. Louis had a maximum of 0.34 inch which resulted from raincell 5 (that was exposed to urban effects) and the merger with 3 and 4. However, the most intense rainfall in both centers occurred prior to the mergers discussed above.

Raincell 7 was a very weak cell that produced only 0.02 inch. However, it developed almost exactly in the same position as raincell 5 at the E side of the urban area. Raincell 8 was first detected at 1955 in the E part of Granite City and, therefore, also could have been urban-affected. It drifted northward for approximately 3 mi and then dissipated. The heaviest amount was 0.06 inch recorded just N of Granite City at Site 62.

Raincells 1-8 were the N extremities of an isolated area of afternoon shower and thunderstorm activity centered 50 mi S of St. Louis. This activity developed in the early afternoon and slowly moved to the E. Much of the Survey's aircraft cloud data collected on 25 July was associated with the showers in this area and included data from several of the cells (1-8) discussed above.

The preceding paragraphs have discussed the raincell distributions up to the beginning of the heavy storm that was to be centered in the Alton–Wood River area. During the afternoon and evening storms, a total of 69 raincells were identified and analyzed within the 26-mi radius of the research circle. Analyses showed that 23 of these cells combined to be responsible for the Alton–Wood River storm centers. The total rainfall contributed by the 23 cells is shown in figure F-10. In the following paragraphs, we will discuss these 23 cells with regard to initiation, movement through the area, intensification through mergers, and combinations of these events.

Raincell 9 was the first cell involved in production of the heavy rainfall in the Alton–Wood River area. It was first detected just SE of Wood River at 2005 (figure F-11a). This cell formed downwind of raincell 8 and merged with it almost immediately; after this merger raincell 8 dissipated.

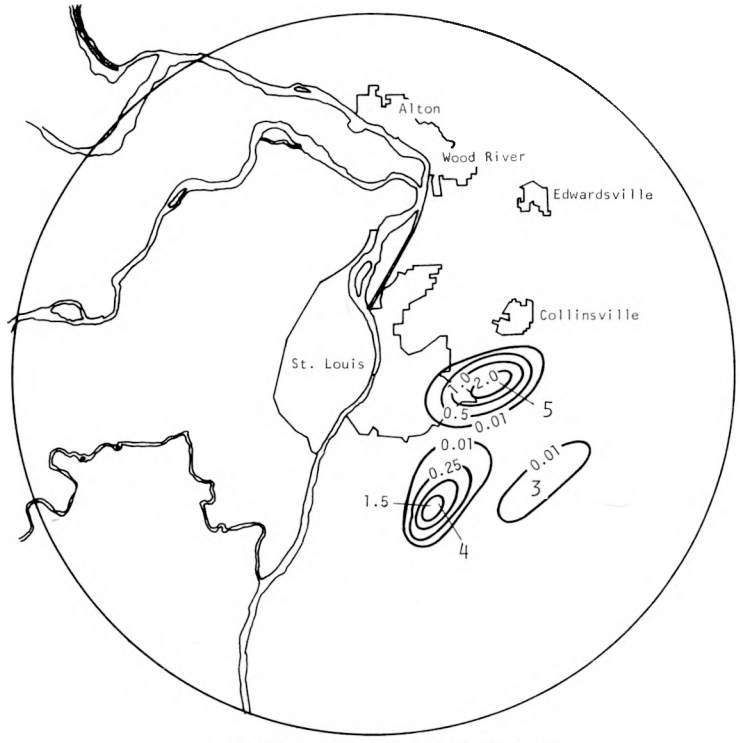

a. Network raincells at 1845-1850 CDT

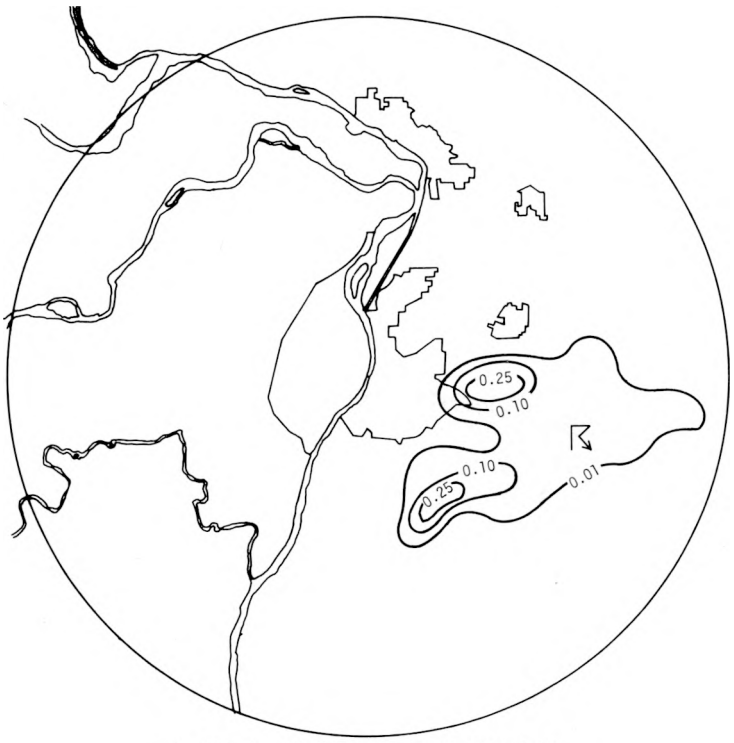

b. Total rainfall from raincells 3+4+5+6

Figure F-9. Early evening mesoscale system

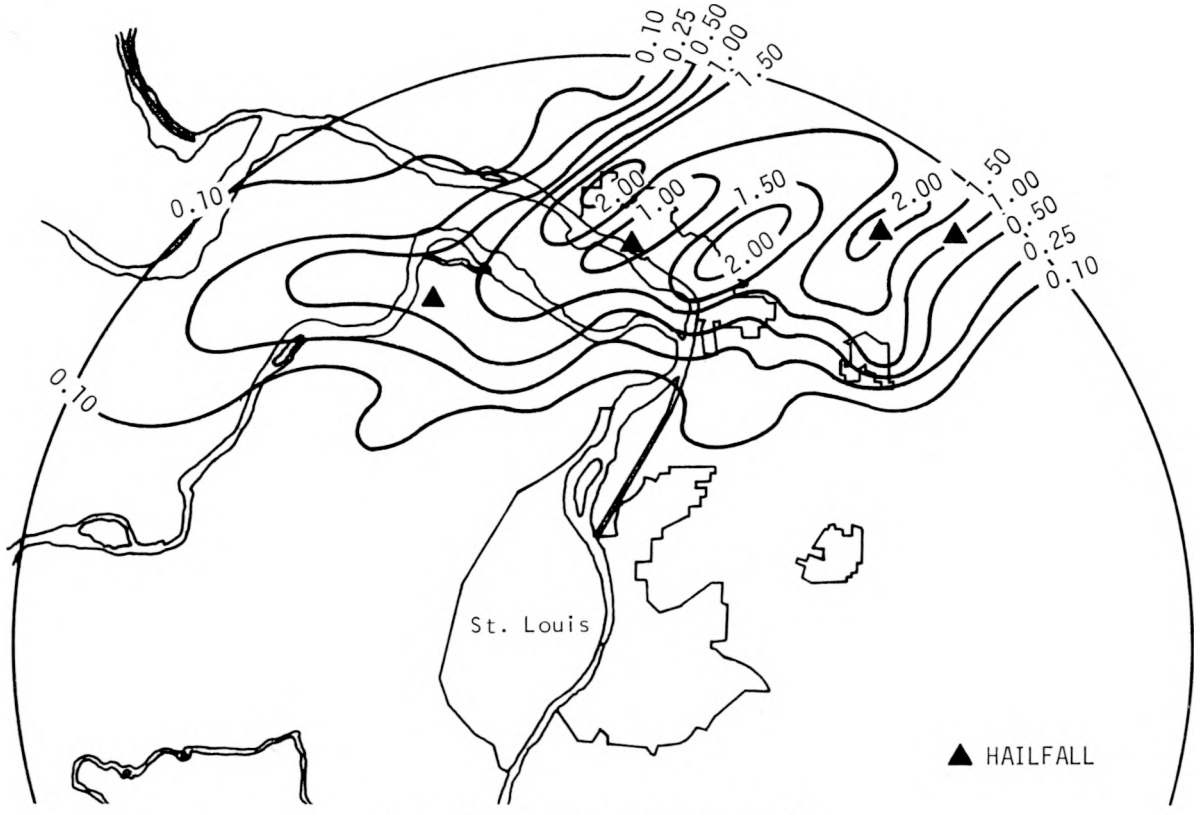

Figure F-10. Total rainfall and hail distribution from 23 raincells producing Alton-Wood River centers

However, the development of cell 9 may also have been related to favorable atmospheric conditions produced by the earlier apparent urban-related cell (raincell 8). Raincell 9 moved NE at approximately 20 kt and left the network at 2040. This raincell could have been urban-affected because of its relationship with raincell 8 and its development near the Wood River industrial area. For example, oil refineries are located about 1 mi W of the rain initiation point. It also initiated in a relatively moist area (figure F-18).

Raincell 11 was detected at 2030 approximately 5 mi SW of raincell 9 and 2 mi E of Alton. This cell moved NE off the study area and merged with raincell 9 near the MMX border. Thus, raincells 8, 9, and 11 formed a mesosystem related to urban effects, and their total rainfall is shown in figure F-11b. Rainfall maximized 6-7 mi NE of Wood River as the result of the combined output from raincells 9 and 11. The extended network rain amounts for 30-min periods indicate that this mesosystem may have contributed to the heavy rainstorm that produced 3.09 inches farther NE at Mt. Olive (figure F-8). Limited radar data from the 10-cm PPI and hourly radar reports from the NWS station at St. Louis provide some additional support for this theory, as discussed later.

Raincells 12 and 13, detected at 2035 CDT, were the next to affect this area. Cell 12 developed in the bottomlands of the Missouri River, SW of Alton, and cell 13 formed just N of Alton. Raincell 13 remained quasi-stationary and merged with raincell 12 over Alton by 2050 CDT. Raincell 14 was detected in the W portion of the circle at 2045. This cell moved NE and eventually merged with raincell 20 which also formed in the bottomlands SW of Alton.

Merged cells 12 and 13 remained quasi-stationary over Alton for about 20 min after merger before moving NE. During this period, raincell 16, which formed in the bottomlands SW of Alton,

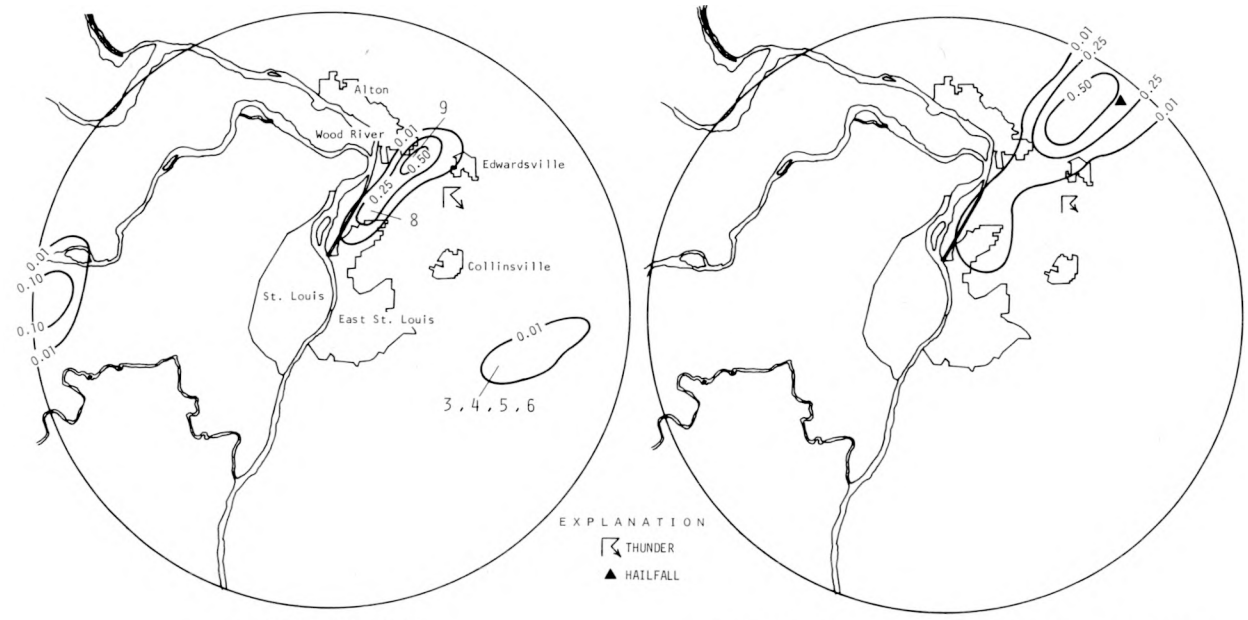

a. 2005–2010 CDT

b. Total rainfall and hailfall from raincells 8+9+11

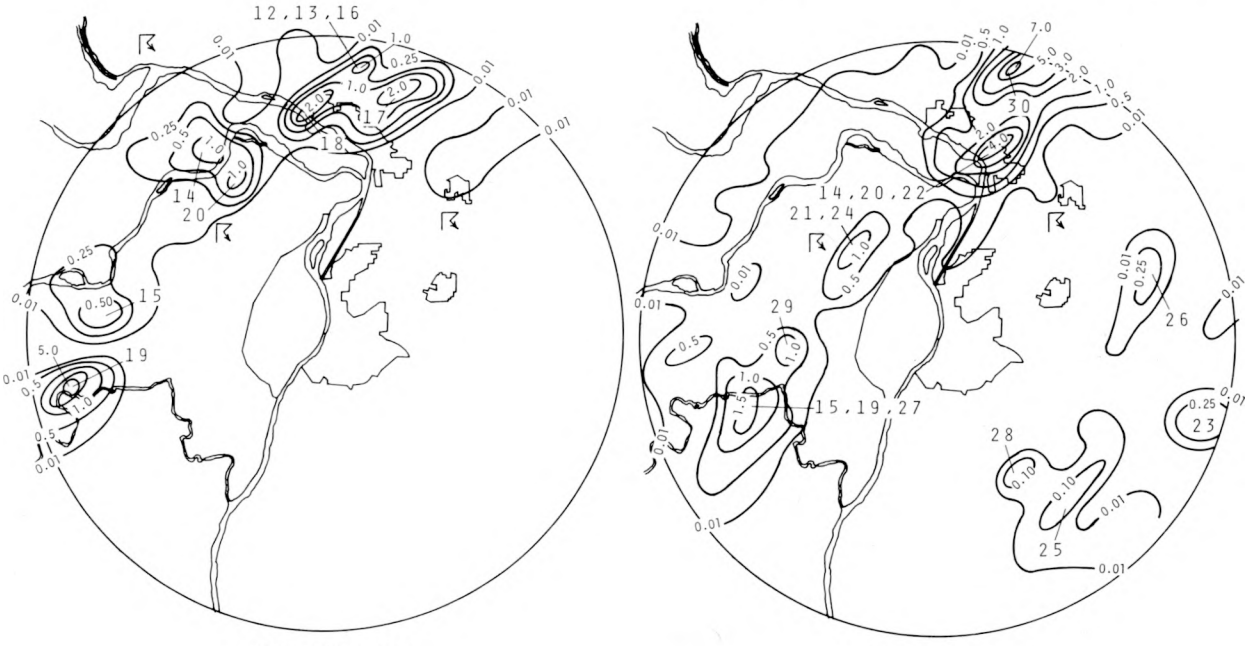

c. 2110–2115 CDT

d. 2140–2145 CDT

Figure F-11. Selected raincell, rainfall, and hailfall periods during Alton–Wood River storm

also merged with the combined raincells 12 and 13. Raincell 17 formed about 5 mi NE of East Alton at 2105 and moved NE. Raincell 18 developed about 2110 on the W edge of Alton, SW of the merged complex (raincells 12, 13, 16) which was near the N edge of the circle.

Figure F-11c shows the raincell distribution at 2110–2115 CDT. Seven of the cells which contributed to the Alton–Wood River high (12, 13, 14, 16, 17, 18, and 19) are shown on this map. Raincells 12, 13, 16, and 18 were primarily responsible for the storm raincell center located just N of Alton (figure F-8). The heaviest rates occurred after the merger of raincell 18 with the merged combination of 12, 13, and 16. Mean 5-min rates of 5 to 6 in/hr were recorded N of Alton in the 2120–2130 period. The raincells, which were arranged in an approximate NE–SW line in figure F-11c, were associated with a prefrontal squall line (discussed later).

Raincell 22 was the next development that affected the Alton–Wood River area. This cell formed over East Alton near 2120 and combined with the merged raincells 14 and 20 at about 2130 in the same area. The 3-cell complex then remained quasi-stationary over the East Alton–Wood River area until 2150 when it moved to the E. Mean 5-min rates reached 4 to 5 in/hr at the core of this cell complex when it was in the urban area.

Figure F-11d shows the raincell distribution at 2140–2145 CDT. A very intense cell (raincell 30) had developed about 6 mi NE of Alton at that time. Also, raincells were scattered throughout the MMX circle by 2140, but none appeared in the immediate St. Louis urban area. Several were location 15-20 mi E of the city, and, conceivably, these cells could have been urban-related. However, if an urban-increase mechanism was operative in the St. Louis urban-industrial area, its rainfall effects were not being asserted in the immediate urban area or within several miles downwind, as was observed in other case studies and as was indicated by an earlier climatic study by Huff and Changnon (1972).

As shown in figure F-11d, the most intense raincells at 2140 remained in the Alton–Wood River area. Raincell 33, the next development in the area, formed about 5 mi NE of Alton, drifted SE, lasted about 20 min, and produced a maximum 5-min rate of 5.84 in/hr at 2200–2205.

The remaining raincells in the Alton–Wood River area were generally much weaker than the earlier cells and contributed only small amounts to the storm total. Raincells 41, 44, and 45 developed in the heavy rainfall region at 2200, 2210, and 2215, respectively. Raincell 41 developed SW of Edwardsville, raincell 44 on the SE edge of Wood River, and raincell 45 about 3 mi NE of the center of Wood River. Raincells 44 and 45 were weak and short-lived. Raincell 41 was of moderate intensity with central rates of 1 to 2 in/hr. This cell moved ENE and merged with raincell 40 before leaving the study area.

Raincell 48 was a weak, short-duration cell that developed in the bottomlands SW of East Alton, and contributed an insignificant amount to the Alton–Wood River storm. Raincell 57 was a small cell of weak to moderate intensity that developed between Edwardsville and Granite City and remained stationary during most of its 40-min life. Raincell 59 was a small, weak, short-lived cell that developed E of Edwardsville. Raincell 63 was a weak, quasi-stationary cell that developed over the Alton area. Raincells 64, 66, and 67 moved into the Alton–Wood River area from the SW, but were decreasing in intensity by their arrival time. Raincell 69, the last of the 23 cells involved in the Alton–Wood River storm, developed just NE of Alton and produced a maximum of 0.11 inch at Site 11.

Raincell Initiations and Mergers

The locations of the initiation of rainfall from each of the 69 raincells were determined to ascertain the trends for cell development in urban or other obvious non-urban effect areas. The

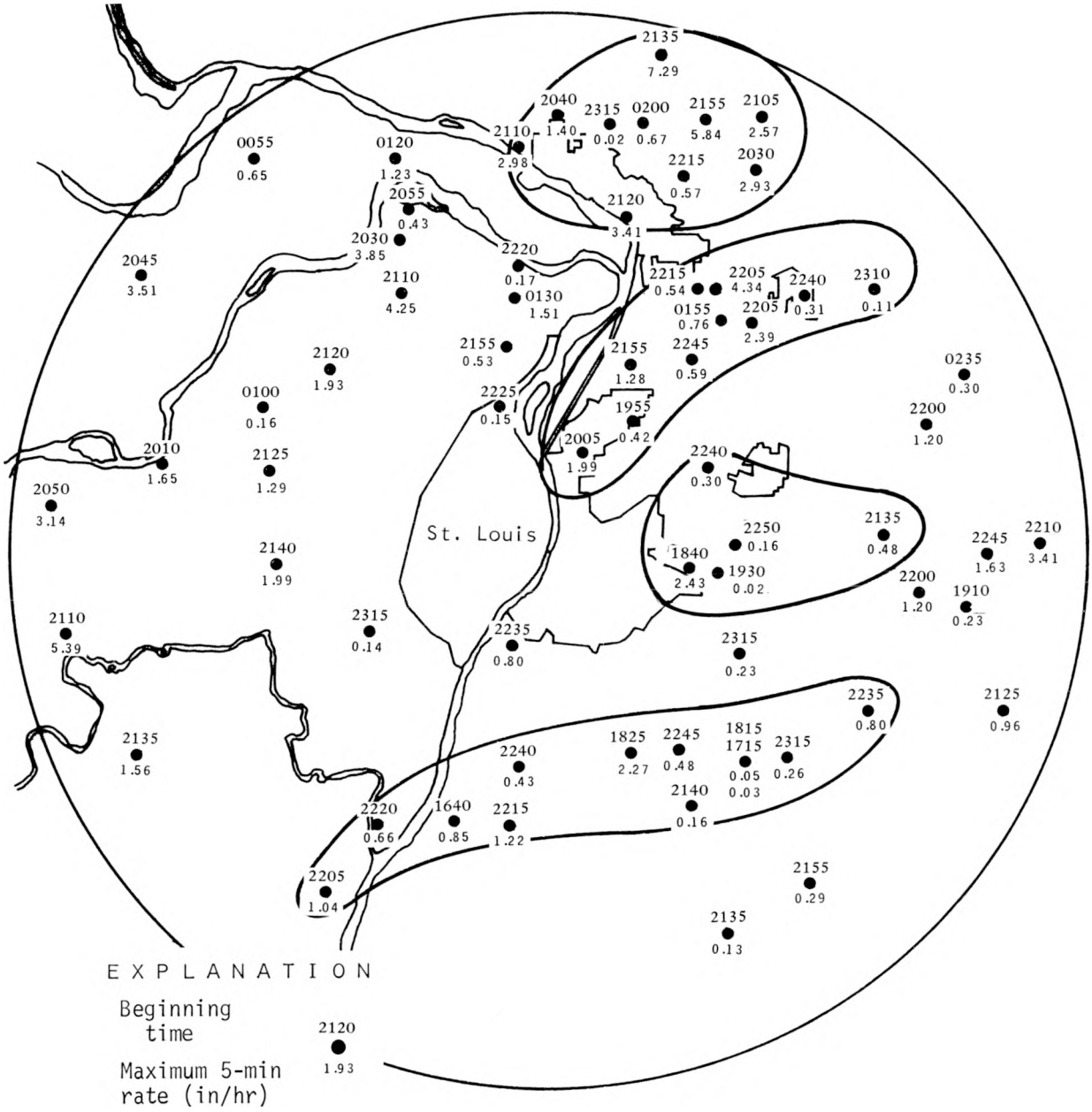

Figure F-12. Raincell initiation points and 5-min maximum rates (anytime during cell life)

times of initiation and 5-min maximum rates in each raincell are shown in figure F-12. Initiations in four areas of particular interest are encircled.

It is apparent from figure F-12 that raincell initiations in the immediate urban area of St. Louis were less than the MMX circle average of approximately 1 initiation per 30 mi^2. However, a region of above-average occurrences was located directly E of the city, as indicated by the line enclosing 5 cells. A WSW low-level flow indicates that these are potential urban-effect cells. Most cell movements were from the WSW to W in this region, implying that the clouds from which these raincells developed originated in the urban-industrial region or the plume therefrom. Further-

more, as pointed out earlier, several of these cell developments were the N extremities of an afternoon system that aircraft updraft and aerosol measurements indicated were being subjected to urban surface effects during portions of their lifetimes.

Another area of above-average initiation frequencies extended from Granite City NE to Edwardsville (figure F-12), and this area contained cells likely related to urban conditions. With raincells moving from the SW to W in this area, the convective clouds could have originated over Granite City or Wood River; if so, they could have been related to nuclei sources, such as the steel plant at Granite City or the oil refineries in the S part of Wood River (also a moisture source).

Figure F-12 also has an envelope around 10 raincell initiations in the Alton-Wood River area and these are also considered to reflect potential urban-industrial effects of the area. Six of these cells had 5-min rates exceeding 2 in/hr. These six cells were major contributors to the three high centers shown on figure F-8. The other area of concentration of raincell initiations indicated in figure F-12, was in the S part of the circle, and these cells were quite possibly associated with convective cloud developments over the Ozark Hills to the SW and W.

Of the 69 raincells initiating on the network, 30 or 43% were classed as potential urban-effect cells. With SW to W cell movements, the urban-effect area involved approximately 39% of the network area. The frequency of raincell initiations in the potential urban-effect region was 1 cell per 25 mi^2 compared with 1 per 36 mi^2 in the no-effect areas. Thus, the urban-effect frequency was above average for the area, but the bias toward potential urban-effect developments was not strong. However, the effect from urban sources at night was probably considerably less than during afternoon storms. The urban destabilizing effect would be superimposed on the diurnal heating in the late afternoon storms, which would tend to maximize the destabilizing of the lower atmosphere. As pointed out in the 11 August 1972 study, this would favor both thermal and nuclei effects from urban-industrial areas because the mixing layer would deepen.

An analysis was made of the time of initiation and of the location and time of maximization of the more intense raincells. All cells with maximum 5-min rates of 1.80 in/hr (0.15 in/5 min) were included in the analysis. The results showed that of the 20 intense raincells, 7 maximized in or within several miles downwind of Alton-Wood River; 5 maximized in or downwind of the St. Louis urban area; and the other 8 (40%) maximized upwind of both urban areas, mostly along or to the E of the Missouri River Valley. Thus, there was a slight trend, at least, for the more intense cells to maximize in the potential urban-effect areas, since 60% of the cells were in the urban areas (39% of the total network area) on July 25.

Since merger of convective elements was shown to intensify storm rainfall intensities (Huff, 1967; Simpson et al., 1972), the distribution pattern of raincell mergers was determined for the storm of 25-26 July. The network distribution is shown in figure F-13 and locations and times are shown for each of 17 mergers detected from the raincell analyses. There were 6 mergers within or several miles upwind of Alton-Wood River and 5 of these (at 2050, 2100, 2120, 2125, and 2130) were major causes of the high centers N of Alton and NE of East Alton (figure F-8).

Four of the 5 important mergers mentioned above occurred within the urban area of Alton-Wood River or in the immediate vicinity. The raincell patterns indicate that these mergers were probably caused by horizontal growth in one or more raincells situated over the urban area. Thus, the greater concentration of mergers in the Alton-Wood River area appears to have resulted from urban intensification effects. The other mergers shown in figure F-13 did not result in any significant increase in rainfall intensity; in fact, in several cases rainfall decreased after merger.

Although mergers undoubtedly are extremely important in the intensification of rainfall, single raincells often exhibit heavy intensities and provide major contributions to the total rainfall in heavy rainstorms. This is illustrated in figure F-14 with mass curves for Sites 10, 22, and 24

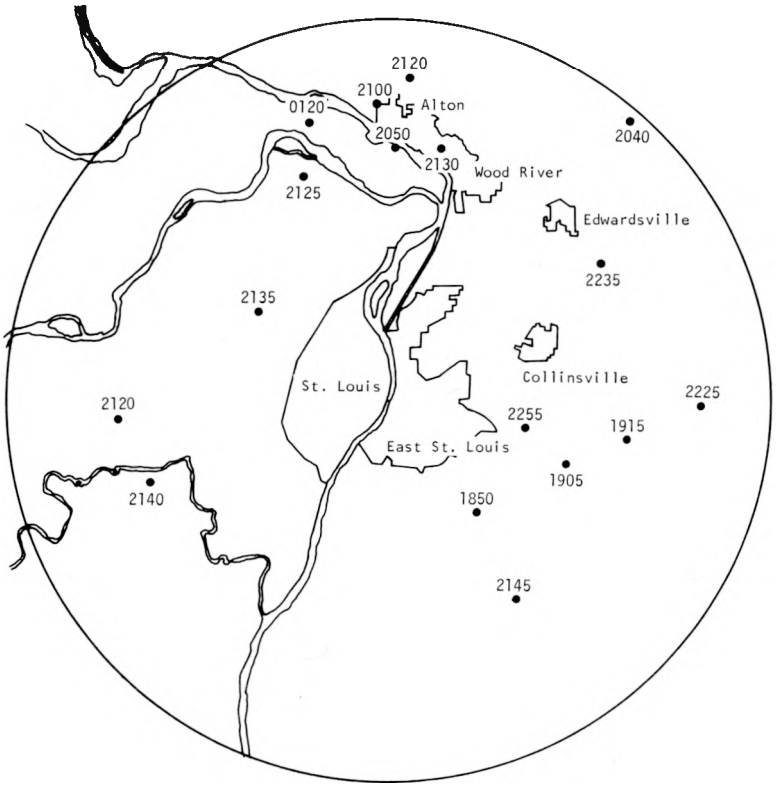

Figure F-13. Mergers of surface raincells

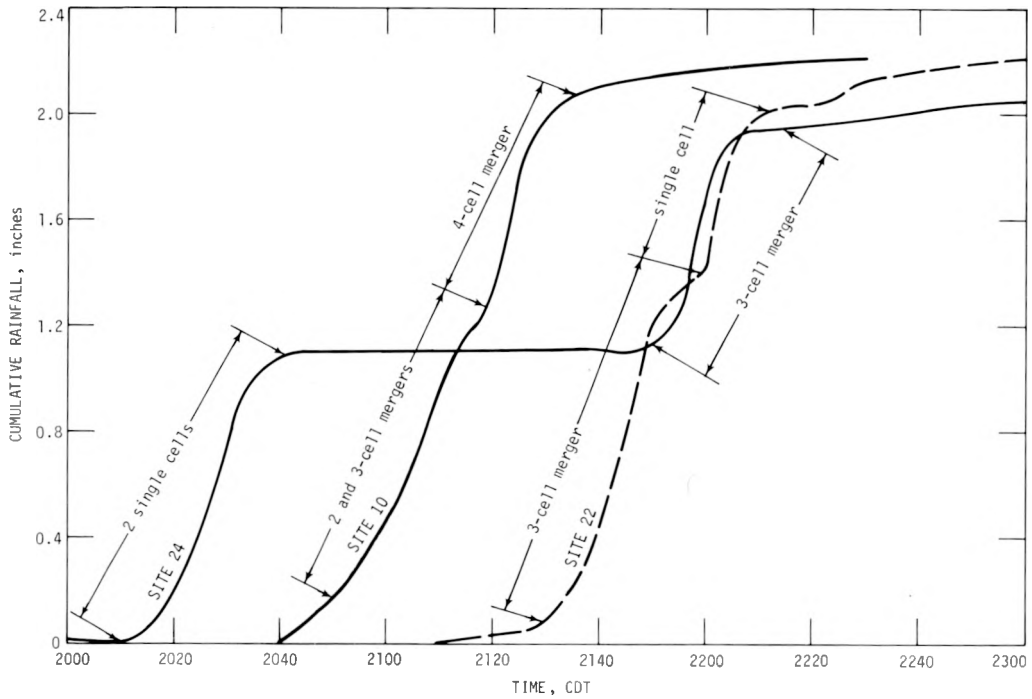

Figure F-14. Mass rainfall curves for three sites on 25 July 1973

that were located at the center of each of the three highs in the Alton–Wood River area (figure F–8). At Site 10, N of Alton, 88% of the total storm rainfall (2.22 in) was associated with raincell mergers. At Site 22, NE of East Alton, 60% of the storm total (2.21 in) occurred with mergers. However, at Site 24, NE of Wood River, only 41% of the 2.05-inch total occurred as the result of cell mergers. Overall, 64% of the rainfall at these three raingages occurred after raincell mergers had taken place. Thus, mergers were a dominant factor in producing two of the three high centers.

The severe rain storm of 25 July was of the same general magnitude as the storm of 11 August 1972. The most intense short-period rates occurred at Site 10 near the center of the high located N of Alton. At Site 10, a total of 1.50 inches fell during the 30 min from 2055–2125, and 2.12 inches was recorded in the 1 hr from 2040–2140. These values represent point rainfall amounts expected to occur on the average of once in 10 years at any given point in this area (Illinois State Water Survey, 1970). This heavy rainfall was associated with a 2-cell merger that later ingested 2 other raincells to eventually become a 4-cell merger. As pointed out in the discussion of the 11 August 1972 storm, the multicellular merger is a common characteristic of severe rainstorms in Illinois (Huff and Changnon, 1964).

Movement and Duration of Raincells

Raincell analyses indicated that most of the cells moved from a SW to W direction, although a few of the weaker cells moved from the WNW late in the storm period. Figure F–15 illustrates typical movements with a sample of 14 raincells that include both single cells and merger combinations. During the storm period, the speed ranged from near 0 with a few short-lived weak cells to approximately 25 kt with strong cells. However, most of the cells had speeds in the range of 11 to 22 kt. The median for the 14 raincell movements shown in figure F–15 was 18 kt. Thus, the direction of movement was typical of summer convective raincells, and speeds were generally moderate.

The average duration of the 69 raincells was 20 min with individual cell durations ranging from 5 to 40 min. These durations are less than average for summer raincells. The average duration of 1475 raincells measured on the MMX circle in 1971–1972 was 25 min and the average for the 100 raincells with heaviest mean rainfall was 45 min (Huff, 1974). Examination of the data indicates that raincell durations in the Alton–Wood River area were similar to those over the remainder of the circle. The distinguishing characteristic of the cells in the severe rainstorm center was greater intensity, with raincell mergers preceding the heavy intensities in the majority of the occurrences. Schickedanz (1973) has shown from the 1971–1972 raincell studies that the major urban effect in the Alton–Wood River area appears to be associated with intensification of existing raincells (rather than increase in areal extent) and, consequently, longer cell durations.

RADAR ECHO ANALYSES

The 10-cm PPI radar indicated the first activity in the Alton–Wood River area at about 1815 CDT when weak echoes were observed in the vicinity of the oil refineries in S Wood River, near a power plant along the river in East Alton, and between Edwardsville and Collinsville. Echoes were also noted in the SE quadrant of the MMX circle, and they were associated with a squall line to the S that had extended into the circle. This squall activity extended to approximately 125 mi S of St. Louis according to the NWS radar report at 1835.

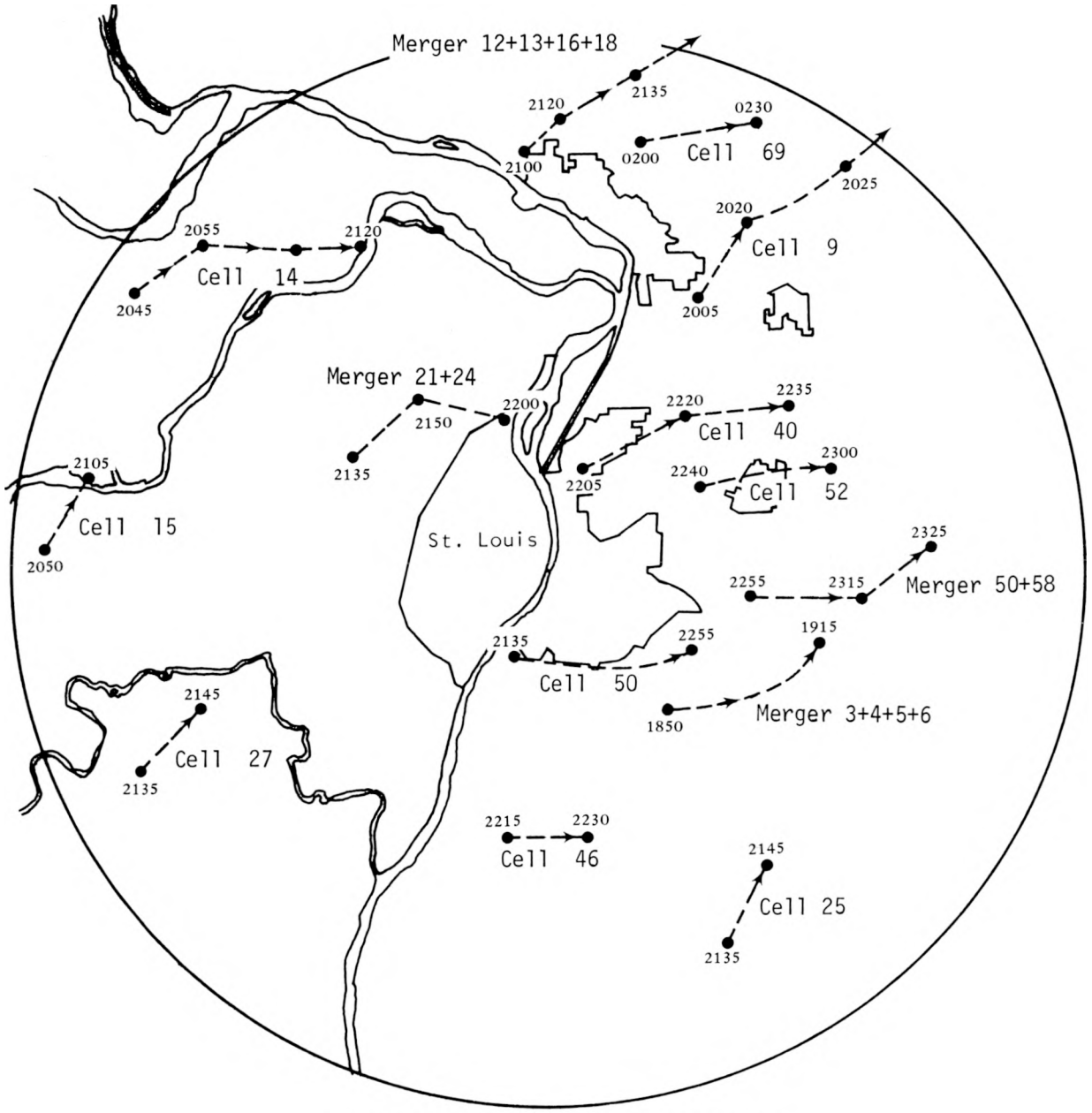

Figure F-15. Movement of single and merged raincells

Scattered echoes with little or no movement continued to develop in the region from Alton to Collinsville until 1938 CDT when the radar was shut down because of maintenance problems. It appeared that the light echoes formed over or downwind of urban initiation points, such as the Wood River refineries, but dissipated rapidly as they moved from the initiation source. No measurable rainfall was recorded in the MMX circle with these echoes.

The radar was back in operation by 2020 CDT. At that time, a line of scattered echoes was oriented WNW-ESE from Alton to Edwardsville. However, major echoes of greater areal extent and intensity were located about 8 and 20 mi NE of Wood River and were approaching a merger stage.

The closest echo appeared to have originated in the Wood River area (oil refineries), according to the raincell analyses discussed earlier, and it intensified as it moved NE. It is difficult to ascertain whether the other, more distant cell originated in the Wood River area or was associated with the N extremity of the squall zone mentioned above. The NWS radar report at 2030 CDT suggests a merger between the progressing Wood River cell and a cell on the NW edge of the old system moving to the E that had produced some relatively heavy, short-duration rainfall rates in the SE quadrant of the MMX circle in the 1830–1900 period.

Unfortunately, the radar was again off the air for approximately 1 hr beginning at 2055 CDT, and this prevented observations of echo behavior during a major portion of the heaviest rainfall in the Alton–Wood River area. However, the limited 10-cm PPI data, the NWS radar reports, and the MMX raincell analyses do indicate that the convective storms which initiated and/or intensified in the Alton–Wood River area also contributed to the severe rainstorm in the Mt. Olive region about 25 mi NE of Wood River. The NWS radar reports indicate the Alton–Wood River and Mt. Olive storms eventually formed the S extremity of a squall zone that later reached into E-central Illinois and produced moderate to heavy rainfall amounts at scattered locations.

THUNDERSTORMS AND HAILSTORMS

Thunder

Seven of the 10 thunder stations recorded thunderstorms on 25 July. These locations and the 3 non-thunder (no TRW) sites are denoted on figure F–8. Clearly, the thunderstorms and the major convective activity were in the N and E portions of the MMX circle. The lack of thunder activity in the 0.5-inch rain area W of St. Louis is probably related to the fact that this rain was largely produced by dissipating storms that, if they were thunderstorms earlier, had become light rainshowers before they entered the circle.

The 62 raincells up to 2400 on 25 July were classified, whenever possible, as to whether they became thunderstorms. Some were 'unknown' because directional analyses of the thunder data did not allow clear identification, or because the raincells were in 'null areas,' that is, they were too distant from an observation point (> 8 mi) to allow identification. This analysis showed that 6 raincells were unknown, 30 were thunderstorms, and 26 were just showers.

The 62 raincells were in turn also classified as to whether they were potentially 'urban affected' by crossing or developing over the two urban-industrial areas. Others were placed in a separate class if they were clearly located above the floodplain of the Mississippi–Missouri Rivers, an area suspected to have effects on raincells (Huff, 1973). The remaining cells were classed as 'no-effect' cells with no urban or valley effects. The origin pattern of the 62 raincells and their thunderstorm classifications appear in figure F–16. Three areas are noted: 1) the N portion where all known cells were thunderstorms and classed as either urban (Alton–Wood River) affected or bottomland affected; 2) the E–W central region of mixed thunderstorms and showers; and 3) the S portion where all known cells were showers.

The resulting raincell division is summarized in table F–1. This shows that 19 of the 22 known urban-effect cells (86%) and 4 of the 5 bottomland-effect cells (80%) became thunderstorms, whereas only 7 of the 20 known no-effect cells (35%) became thunderstorms.

The raincells also became thunderstorms rather rapidly after rain appeared. Time of first thunder could be accurately determined for 34 of the cells. Twenty-three cells produced thunder within 5 min after rain at the ground, and eight within 6 to 10 min after rain. Only three took 11 or more

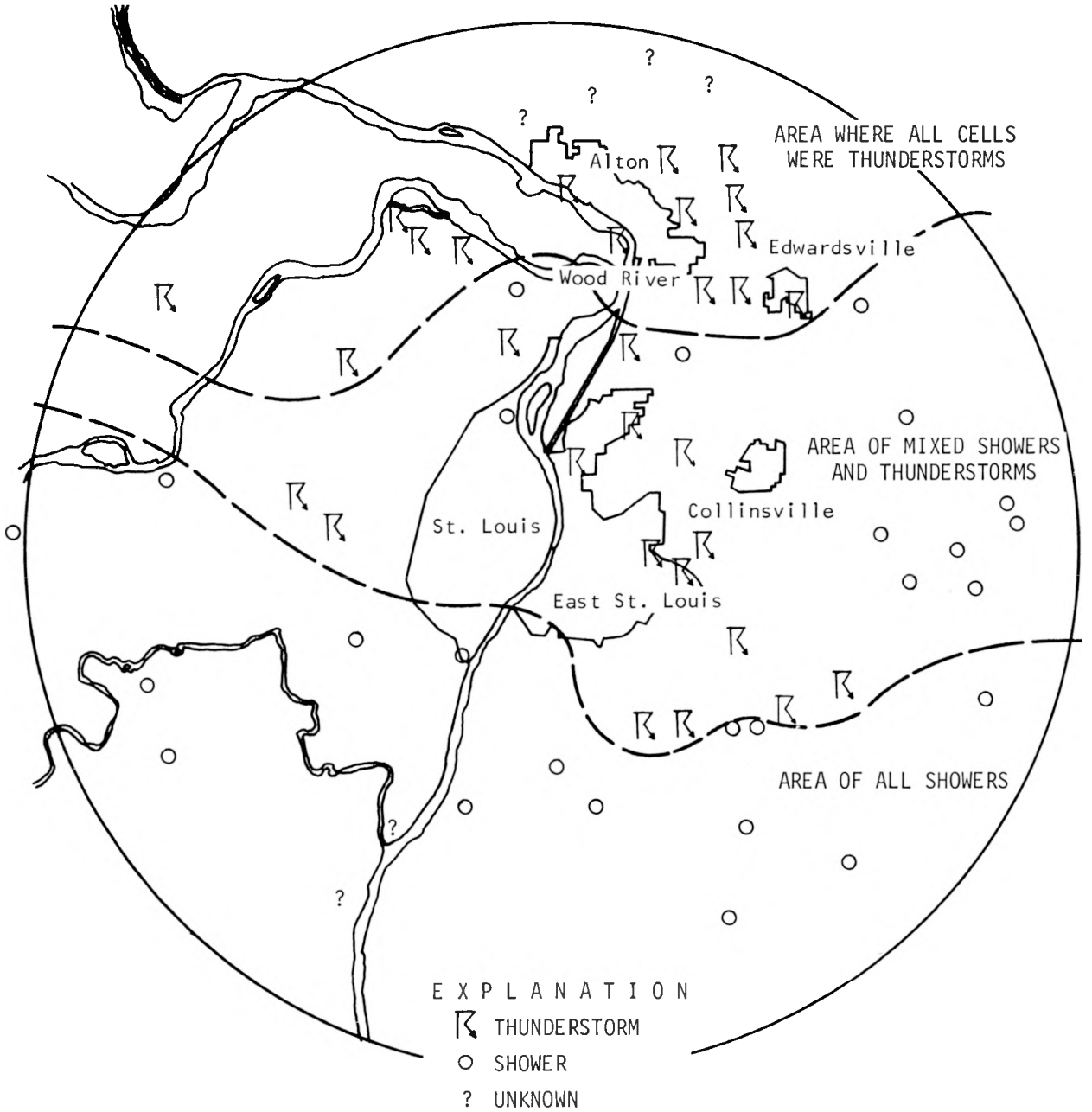

Figure F-16. Origin of thunderstorms and rainshowers

minutes. Two of these 'late' thunder cells became thunderstorms after they merged with other cells E of St. Louis.

The point durations of thunder activity are also of interest. PMQ had 16 min of thunder; STL reported 72 min; EDW had 165 min; BLV recorded 182 min; BVK had 13 min; LVT had 37 min; and OKV recorded 110 min. The OKV thunder activity came with the afternoon (1745-1936 CDT) cells that developed primarily S of the MMX circle and moved ENE (cells 1 through 6 of figure F-9 were the N end of this area of activity).

Importantly, the two stations E of St. Louis that had the greatest number of thunder days and longest durations in 1971-1972 and thus indicated the presence of urban effects on storm activity (Huff and Changnon, 1972), also had the longest thunder durations on 25 July.

Table F-1. Thunderstorm Status and Location of Raincells

	Number of cells			
	Potential urban effect	*No effect*	*Potential bottomland effect*	*Total*
Became thunderstorm	19	7	4	30
Did not become thunderstorm	3	13	1	26
Unknown status	3	3	0	6
	25	23	5	62

There were two periods of intense (peals $\geqslant$ 1 per min) thunder activity at Edwardsville. The first was associated with raincell 9 (figure F-11a), and the other with raincells 40 and 41. All were urban-effect cells.

In summary, there were two thunderstorm periods (storm groups) on 25 July. One was in the afternoon and occurred largely to the S of the MMX circle, but this system also produced thunderstorms at BLV and OKV. The second and major period of thunderstorms began in the late afternoon and produced thunderstorms throughout the N half of the MMX circle. No thunderstorms occurred in the SW portion, even though rain occurred there.

Urban effects on thunder activity were indicated in two ways. First, 85% of all potential urban-effect raincells became thunderstorms. Second, the stations just E of the urban areas had 1) longer thunder periods than any others, and 2) one station had 42 min of intense thunder frequency, more than at any other locale.

Hail

Hailfalls on 25 July were interesting but not exceptional. The first hailfall began at Site 29 (in the bottomlands – see figure B-2b) at 2025 CDT, and the last hail ended at 2158 CDT at Site 24, about 8 mi E of Alton. Five hailfalls occurred, two at Site 29 in the bottomlands, one in Alton, and two E of Alton (see figure F-8 for hail locations). Hailfall characteristics are displayed in table F-2 according to the types of storms (raincells) from which they originated.

Table F-2. Hailfall Characteristics on 25 July

	From storms over the bottomlands	*From urban effect storms*	*Mean from large Illinois sample*
Number of hailfalls	2	3	
Average duration, minutes	1.5	3.0	3.2
Largest stone size, diameter inches	0.25	0.40	0.5
Average number of stones/ft^2	11	24	25
Average rain with hail, inches	0.15	0.51	0.40
Average energy, ft lbs/ft^2	0.191	0.2286	0.2247

Two conclusions seem clear. First, the urban-effect hailfalls were longer, produced more stones, had larger hail, fell with more rain, and resulted in more impact energy than did the hailfalls from bottomland related storms. Second, the values in both cases were less than the means calculated

from a large sample of Illinois data (Changnon, 1970). Thus, the point hail on 25 July was not significant. The five hailfalls indicated that five hailstreaks occurred, but their areal extent could not be defined well.

The hailfalls were all associated with the conglomerate of heavy rain producing cells that developed and merged in the Alton area (figure F-8). The first two hailfalls occurred with raincell 12 at Site 29, located near the bend of the river SW of Alton. The first hail fell during 2031-2032 CDT in the rain core of newly initiated cell 12. The second hailfall came at 2049-2051 CDT, also from raincell 12, but along its rear (W) edge. The location of merged raincells 12, 13, and 16 at a later time (2110) are shown in figure F-11c.

The next hailfall came during 2046-2050 CDT at Site 25 (figure F-11c). The hail fell in the 5-min rain core (rate of 0.72 in/hr) of cell 11 that had developed 15 min earlier on the rear (W) side of raincell 9. Raincell 11 had merged with raincell 9 and the hail fell within 10 min after the merger.

The fourth and most intense hailfall came during 2056-2058 CDT at Site 20 in the S part of Alton where raincells 12 and 13 had merged. It was in a heavy rain core (rate $>$ 1.5 in/hr), and the merger occurred 6 min before the hail began.

The final hail fell from 2155 to 2157 CDT at Site 24. It also fell in a heavy rain core ($>$ 5.0 in/hr) resulting from the merger of cells 14, 20, and 22 (figure F-11d). These cells had initiated over the bottomlands and they merged 20 min before the hail fell.

In summary, the hail from the urban-affected raincells (Alton) was more intense than that from the non-urban (bottomland) cells. The urban-effect hailfalls all occurred 1) in heavy rain cores, 2) in later storm stages than those from the bottomland cells, and 3) in 5 to 10 min after mergers of two or more major raincells. In many respects, these and other hail results were similar to those on 11 August 1972. Most of the hailfall characteristics were less than average. Furthermore, the first hail occurred in bottomland cells and in the early stages of storm development. As on 11 August, the hail results for 25 July 1973 suggest that the apparent urban-related hail increases, noted in prior climatic studies (Huff and Changnon, 1973), were related to mergers of major large raincells that had resulted from or had been enhanced by urban-related conditions.

CLOUD ANALYSES

The sources of data on clouds, including the types, when and where they formed, and their important characteristics (base heights, updrafts, liquid water content, etc.) were limited for 25 July. The afternoon photographs from the cloud camera at St. Louis were not usable due to development errors. There were three AI aircraft flights between 1339 and 2030, but the clouds of importance to the major rain in the study area were not studied in detail. However, some useful cloud information was gleaned from these flights. The third and only other source of cloud data was the visual surface observations taken at PMQ, STL, and BLV. These data, as they reflect the important cumuliform clouds, were limited because of persistent low (Sc) and middle level (Ac) cloud decks during much of the Cu development time. Hense, most of the possible questions about the important rain-producing clouds on 25 July cannot be answered with the available data.

Cloud Conditions from Surface Observations

The hourly observations of cloud types, cloud heights, sky cover, and visibility for PMQ (W), STL (center of circle), and BLV (E) were analyzed. Visibility varied greatly from W to E. It was

excellent (15 to 20 mi) all day at PMQ; at STL it was 12 mi until 1600 CDT when it decreased to 6 to 8 mi; and at BLV it was approximately 7 mi throughout the day. AI flight notes from 1400 to 1500 reported considerable haze over the metropolitan area.

There were three cloud layers during the afternoon on 25 July, but the first and most persistent clouds were Ac. An Ac deck existed during the night of 24-25 July and persisted all day throughout the area. These were generally at 10,000 ft and provided an overcast until 1000 when they became scattered (0.4 to 0.5 sky cover). Importantly, the Ac cover diminished greatly at PMQ and STL (W area) between 1700 and 1900 but remained broken to overcast at BLV.

Sc and a few CuFra began developing between 1200 and 1300 CDT. Their bases were at 3000 ft at PMQ and STL, but 1600 increased to 4000 ft at STL. Their bases at BLV remained at 2500 ft all day. The base of a thunderstorm over STL at 2112 CDT was estimated at 1800 ft. At 2000 the cumuliform (lowest) clouds had increased from scattered to broken *only* at STL; they remained scattered at PMQ and BLV until 2300 when all became overcast. The third and highest cloud deck consisted of scattered Cs that appeared over the entire area at 1300. This became broken and then overcast from 1500 to 1600. It disappeared between 1900 and 2000.

The cloud history for 25 July reveals several interesting facts that are potentially relevant to the localized buildup of heavy raincells in the Alton–Wood River area. Clearly, the clouds all developed because of macroscale atmospheric processes and were not apparently relatable to urban processes. However, the 1000 ft rise in Cu bases over the city compared with rural heights between 1500 and 1600 CDT suggests urban effects on the condensation level. The area in the W part of the MMX circle was generally clearer during most of the day than the central and E areas. Hence, greater surface heating was possible. Important to this process was the W area's decrease in the Ac coverage after 1700 which largely dissipated at 1900. This was related to an increase in Cu reported at STL at 2000. This change is also confirmed by aircraft observations at 1910–1930 of an area of developing Cu along the Missouri River W and NW of St. Louis. Area cloud cover became overcast by 2000 CDT with broken Cu and Sc at 3000 ft and scattered Ac at 10,000 ft. The major raincells in the 2000–2100 CDT period developed only in the network area where the Ac deck cleared and Cu development had occurred in the prior 2 to 3 hr.

Cloud Information from Aircraft Data

There were three cloud related flights on 25 July. A flight of the Aerocommander aircraft leased by the Survey from Pennsylvania State University, for a study of mid-level congestus clouds, began at 1339 CDT and ended at 1800. An AI flight, designed to be a tracer mission, began at 1604 CDT and ended at 1810 CDT. A second AI flight, again for a potential tracer release, began at 1850 and ended at 2030. Hence, aircraft were airborne and were collecting meteorological data most of the time between 1345 and 2030, the 7-hr period prior to the development of the heavy rainfall. Unfortunately, much of the flying was not in areas where storm development crucial to understanding the major rain circumstances occurred. The tracer missions never took place, although suitable clouds occurred in the 1800–1900 period when the AI aircraft had been directed to land. As an alternative, the AI airplane attempted to perform several cloud base updraft measurements on both flights.

The flight of the Aerocommander furnished several useful facts. At approximately 1400, the sky was overcast in and around St. Louis with Sc located at 3000 ft AGL. Visibility was very poor because of haze, and plumes of smoke rose nearly vertically and indicated light S winds.

Shortly before 1400, an area of CuCong located about 30 to 50 mi S and SSW of St. Louis began to develop, and the Aerocommander made several cloud penetrations in the 12,000 to 14,000

ft level between 1430 and 1550 CDT. These showers that later merged to form thunderstorms never reached the St. Louis area, but passed just to the S of the MMX circle. This activity resulted in thunderstorms at OKV (figure F-16) in the late afternoon. Raincells 1 through 6 were the N extension of this group (see figures F-9a and 9b). The important aspects of these clouds were: 1) they were 'wet' (high liquid water content) clouds, and 2) they had strong updrafts (1000 to 2000 ft/min) at mid-levels. Subsequent cloud base updraft measurements by AI among several clouds of this same group, but done 40 to 60 min later, revealed updrafts of 200, 500, 600, 1000, and 1200 ft/min. These were much lower than the mid-level values, but still relatively strong cloud base values. The AI flight between 1604 and 1810 was largely in this same cloud complex which contained a meso-cluster (not line) of showers and thundershowers. This elongated area was oriented NE-SW and slowly drifted to the ENE.

The first AI flight studied several clouds in this cluster. Cloud base updrafts were not found in some showers, but when found, they occurred in various positions from the rear (W) side, to the right front flank, and to the left front flank. The bases of these clouds, including those in the SE portion of the circle at 1720-1745, were generally between 2500 and 3200 ft AGL. This meso-cloud cluster does not appear to have played any role in the later heavy rainstorms in the network. The clouds did appear to be rather 'tropical' in nature (wet with strong updrafts). Their importance relates to Survey studies in purposeful rain enhancement because the development of meso-cloud clusters through enhancement by their mergers, such as occurred on 25 July, is seen as one potential rain augmentation technique to pursue (Semonin and Changnon, 1975). Further study of this cluster with the Aerocommander and AI data are recommended for this purpose.

The second AI flight (third flight of the day) began at 1850. The aircraft in search of a tracer mission (having earlier missed potential raincells 3, 4, and 5) first flew to the Belleville area. There it circled on the back side of merged raincells 3-4-5 in a weak (200 ft/min) rear (W) side updraft. The cloud base was lower than earlier ones at 2300 ft AGL, and for some undefined reason tracers were not released into these cells.

At this time (1910-1915 CDT) the aircraft reported a line of developing Cu to the W and NW, and thus flew WNW to investigate. These clouds were along the Missouri River, and they formed a rough NE-SW line. The radar operator directed the aircraft farther W to a thunderstorm located 35 to 45 mi W of St. Louis. Front side (E) updrafts of this storm were weak (200 ft/min) and the storm was classed as dissipating at 1952 CDT. At 2001 CDT, the aircraft was directed to return to base as "radar advised system not too active for a cold front or squall line" (pilot log). The aircraft flew ENE passing just S of St. Charles and on to Alton between 2001 and 2030 CDT, flying among the growing Cu that quickly became the important storms of 25 July.

Listed below are conclusions concerning the Cu cloud properties, based upon the limited cloud information available.

1) Their bases were relatively low, varying from 2300 to 3300 ft AGL.
2) Updrafts were in various positions around the cloud bases, and there were no preferred locations.
3) Merged cells 3-4-5 developed on the rear side of the clouds and were entraining urban source air.
4) Important storms on the MMX circle developed from clouds that formed around 1900 CDT over the bottomlands of the Missouri-Mississippi Rivers, although storms farther to the SW suggest there also was a WSW-ENE zone of mesoscale instability across the circle at that time.
5) Cloud movements were not fast, less than 15 mi/hr.
6) Clouds contained moderate to strong base updrafts at their bases and at mid-levels (12,000 to 14,000 ft).

7) Cloud merging was common and led to thunderstorms.
8) Very hazy conditions existed from the surface to low cloud deck bases in the afternoon, suggesting urban source air could reach cloud bases for ingestion.
9) The radar detection and direction, and the short-term forecasting both of cells for tracer missions and of storm activity, were not of high quality. The aircraft was directed to land during a period of moderate-to-good cell formation over the rain chemistry network. When the aircraft approached these merged cells at 1910, they were not selected, possibly because of aircraft crew opinions. Finally, the developing system at 2030 was judged as weak. As in the case of 14 July 1973, the question is, "Were the poor visibility, uncertain synoptic conditions, and overcast conditions a deterrent to belief in the development of good convective activity?"

Interactions of Surface Conditions with Clouds

The second AI flight on 25 July began with takeoff at 1850 CDT at Alton. A track toward the S was followed at about 3000 ft MSL to the Belleville area, arriving at 1912. The aircraft circled in a weak updraft of cells 3-4-5, proceeded W at 3500 ft across the East St. Louis and St. Louis area in the 1915–1930 period, and passed by the Labadie Power Plant 30 mi W of St. Louis. Winds at flight levels were generally from the WSW.

Select locales along this 45-min flight were chosen to demonstrate the cloud nuclei variations in the area (table F-3). Comparable rural area values (5000-6000/cc) existed E and W of the city. Also, values were high over the city revealing that surface origin CN were reaching the cloud base level at 3000 to 4000 ft. The highest CN value was measured in the updraft of cells 3-4-5. These results strongly indicate that 1) urban surface air was feeding into merged cells 3-4-5, indicating they should be classed as urban-effect cells; and 2) surface air was reaching cloud base heights at the time (1900–1930) when cloud and subsequent storm development began over the bottomlands and then over the Alton–Wood River area.

Table F-3. Cloud Nuclei Variations

Location	*Elevation (ft MSL)*	*Time*	*Cloud nuclei (No/cc)*
Alton	surface	1850	26,000
Rural area between Wood River and Granite City	3100	1902	5,000
Granite City	3000	1907	14,000
Belleville–East St. Louis	2900	1912	17,500
Belleville–East St. Louis	2900	1914	19,000 (air in storm updraft)
St. Louis	3100	1920	16,300
St. Louis suburbs	3450	1923	17,000
West rural area	3500	1926	6,400
Labadie Power Plant	3700	1929	12,000
West rural area	3800	1931	5,100

The storm on 25 July was a test case to investigate what effects Alton–Wood River produced when St. Louis apparently had little or no effect on rainfall. It would seem that the storm maxima over and beyond Alton–Wood River (with little over St. Louis) was due to three possible conditions:

1) The entire cloud inception and rain maxima over Alton–Wood River were due to natural macroscale conditions (chance)
2) The bottomlands produced sufficient moisture–heating effects to initiate clouds that, in turn, were enhanced by industrial effects in the Alton–Wood River area

3) The bottomlands produced a sufficient effect to initiate clouds that in turn maximized over Alton-Wood River by natural causes (accident).

The lack of clouds and heavy rain over and ENE of St. Louis suggests the importance of the bottomland effect. If 25 July is judged to reflect an Alton-Wood River effect, this case may further suggest that the Alton-Wood River effect on rain cells noted by Schickedanz (1974) is intimately related to bottomland effects on cloud and shower inception.

TEMPERATURE, DEW POINT, AND SURFACE WIND ANALYSES

Air and Dew Point Temperatures

The Survey's hygrothermograph network data on 25 July shows a peak in both the air and dew point temperatures in the bottomlands SW of Alton-Wood River preceding the severe rainstorm which started at approximately 2000 CDT. Figure F-17a shows a peak in the surface temperature at 1800 CDT S of the Missouri River and SSW-SW of Alton-Wood River. Figure F-17b shows the air temperature distribution at the start of the rainstorm at 2000, and again a peak in the air temperature pattern is indicated even closer to Alton-Wood River in the bottomlands at the bend of the Missouri River. Approximately a 5F difference between the urban area of Alton-Wood River and and the bottomlands high is indicated in figure F-17b. Thus, the excessive surface heat in this region could have stimulated the formation of Cu. With the raincell analyses indicating storm movements from the SW to W, convective clouds could very well have developed in this area,moved into the Alton-Wood River area, and intensified from urban effects as the rain process began. The center of the air temperature high near Alton-Wood River in figure F-17b is only 9-12 mi from the urban area, and with speeds of 15-20 kt as indicated in the raincell study, the bottomland clouds would reach the urban area in a period of 30-35 min as they were reaching or closely approaching the rain stage.

Figures F-18a and b show the dew point temperatures at 1800 and 2000 CDT. A peak in the dew point temperature of 76F was located in the bottomlands SW and W of Alton-Wood River at 1800 CDT, and this was the highest dew point in the MMX circle. This high in the dew point distribution was maintained at 2000 CDT when the storm was just starting in the Alton-Wood River area. Thus, both the air and dew point temperatures were relatively favorable (in comparison with other areas of the 2000 mi^2 circle) for the development of Cu a few miles upwind of Alton-Wood River. It is likely that these bottomlands serve as a preferred initiation area for summer Cu and that many of these Cu then move into the Alton-Wood River urban-industrial area with the prevailing steering winds. Intensification of these convective clouds then occurs under favorable conditions because of the output of additional heat superimposed on diurnal destabilization (afternoon and early evening storms) and to industrial nuclei discharges that are probably the major urban-industrial input in night storms over the Alton-Wood River area.

Surface Winds

Winds were relatively light and variable during the forenoon and early afternoon of 25 July. Directions varied from SE through S to SW with speeds of 2 to 8 kt in the anemometer network within the MMX circle. During mid-afternoon, the passage of a mesoscale disturbance across the circle was indicated by the progressive shifting of winds from S to W-WNW in a W to E direction. This was likely related to the area of convective showers centered S of the circle. At 1500 CDT, the

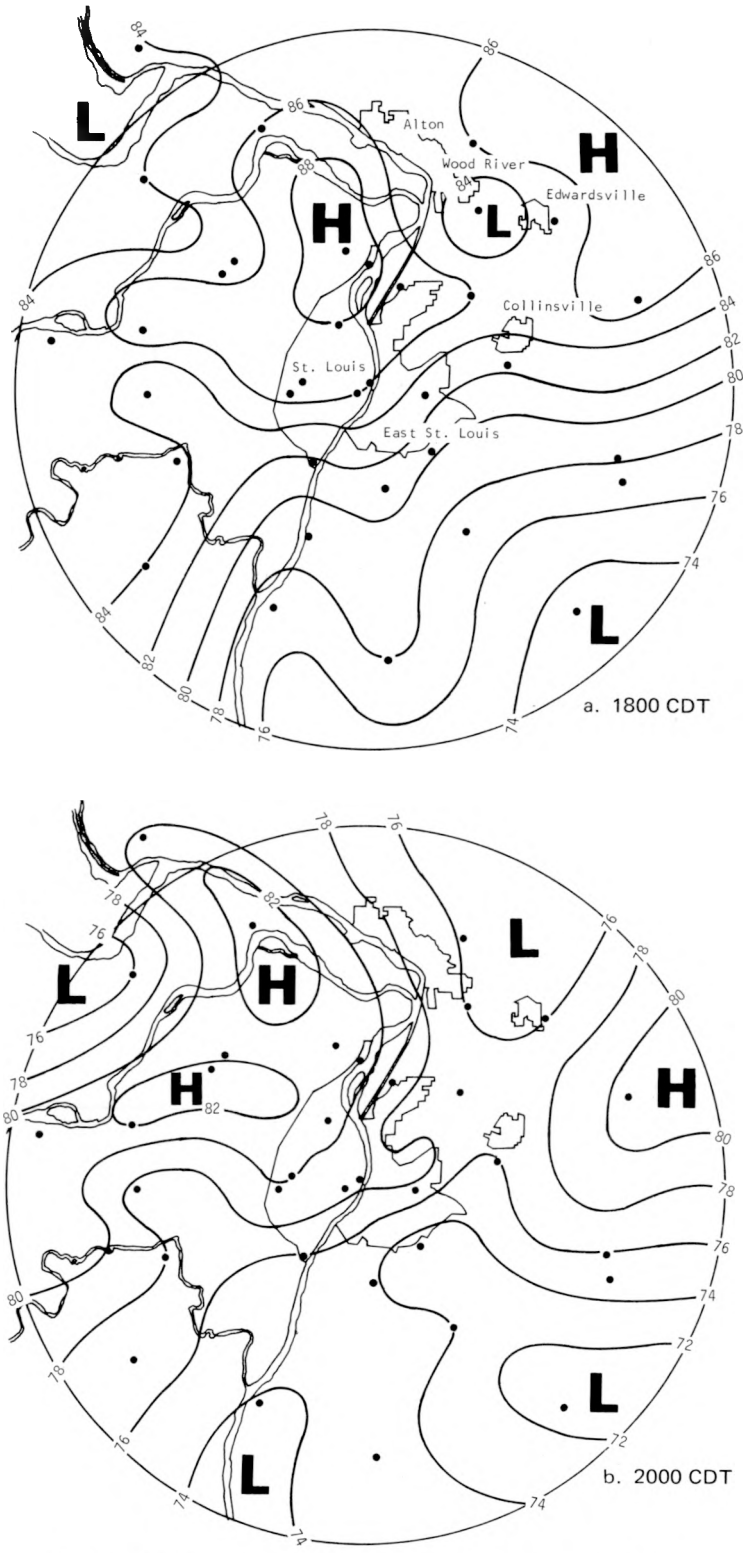

Figure F-17. Surface temperature patterns at 1800 and 2000 CDT

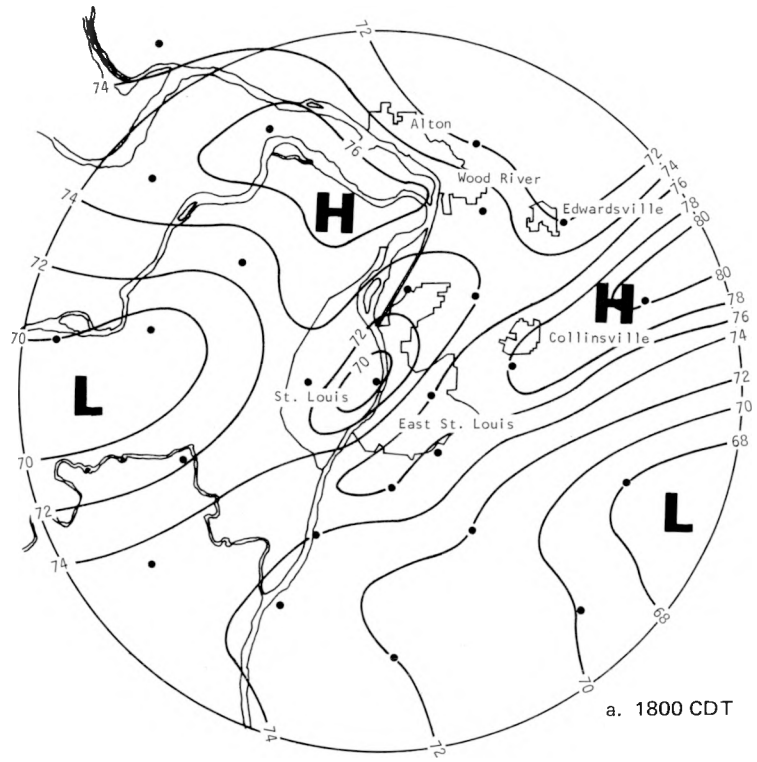

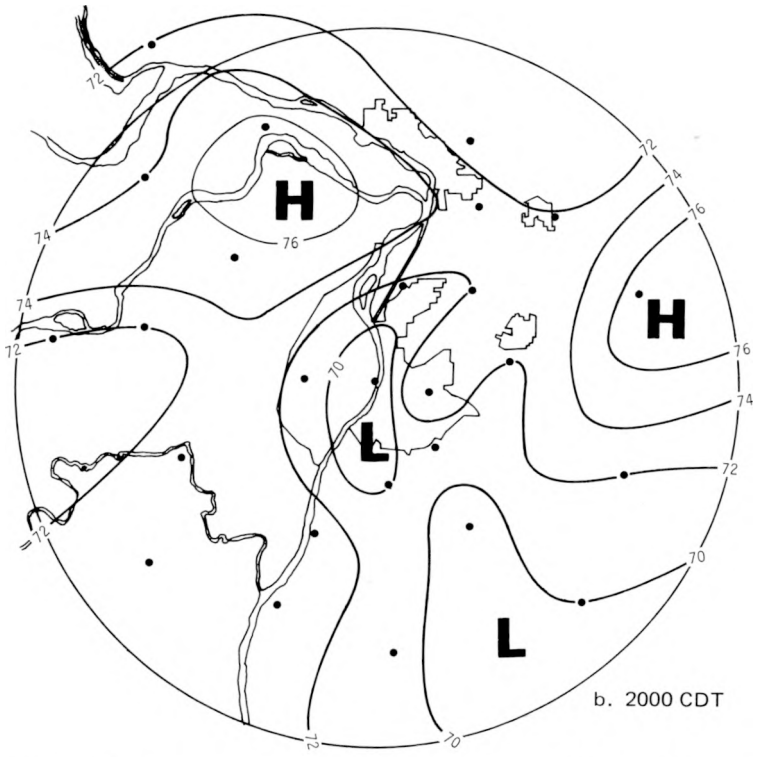

Figure F-18. Surface dew point temperature patterns at 1800 and 2000 CDT

winds had shifted from SW to WSW–W in the area W of the Mississippi. By 1600, the winds had shifted to the W, E of the river, and the wind shift line was oriented along a NNE–SSW line from Edwardsville to Waterloo, or from the NE part of the circle to the SSE portion (figure F–19a). At that time, the 3-cm RHI radar indicated an echo just protruding into the extreme S part of the circle, SW of Waterloo. Aircraft sampling flights at that time indicated thunderstorms farther S in conjunction with this mesosystem. No rainfall was recorded on the MMX circle with this system, but increased cloudiness was indicated at both STL and BLV. No significant changes in air or dew point temperatures were noted in the MMX circle.

Surface winds remained light throughout the afternoon and evening, and most stations showed a return to SE to SW flow by the start of the heavy rainstorm at 2000 CDT (figure F–19b). However, winds still remained from the W in the NW quadrant of the circle at that time, and some convergence was indicated in the Alton–Wood River region at the start of the storm. A cold front was approaching the circle at 2000 (see synoptic analyses), and all network winds backed to SW before the frontal passage later in the evening.

GENERAL SUMMARY AND CONCLUSIONS

Synoptic Weather

Basically, the Alton–Wood River and Mt. Olive storms were associated with the approach and passage of a cold front. They occurred in conjunction with a prefrontal squall zone in which convective activity was intensified by a minor wave on the front. The heaviest rainfall apparently occurred shortly in advance of the cold front wave within a surface moisture ridge with dew points in the 70-75F range. At 850 mb, relatively high dew points extended E from St. Louis, with air-dew point differences less than 2C over the MMX circle and surrounding region. Analyses of the 850 , 700, and 500 mb data in conjunction with surface maps indicated conditions favorable for rather extensive convective activity with the frontal system. Sounding analyses indicated an increase in low-level moisture and increasing atmospheric instability from afternoon to evening.

Rainfall

During the night of 25-26 July, a severe rainstorm accompanied by hail and thunderstorms was centered in the Alton–Wood River area of the MMX circle. A second and even more intense center was located about 15 mi NE of the circle at Mt. Olive. The general area of heavy rainfall ($\geqslant$ 1 inch) extended over an area of approximately 450 mi^2 ; 50% of this intense area was within the 26-mi radius of the MMX circle. Most of the rainfall occurred between 2000 and 2300 CDT, and 2-hr amounts in the storm centers reached values which occur at a given point on an average of only once in 10 years. The severe rainstorm occurred in conjunction with a squall line in advance of a cold front.

Although urban effects were quite likely involved in relatively light rain showers downwind of St. Louis, urban effects were more significant in the severe storm activity in the Alton–Wood River area. The initial raincells were detected in the late afternoon in the SW quadrant of the circle and produced cell means of a few hundredths of an inch, although 5-min moderate rates of 1-2 in/hr occurred in some of these late afternoon to early evening storms. During the total storm period, 69 raincells were identified and analyzed within the MMX circle. Of these, 23 were responsible for the Alton–Wood River storm centers in the 2000–0230 period.

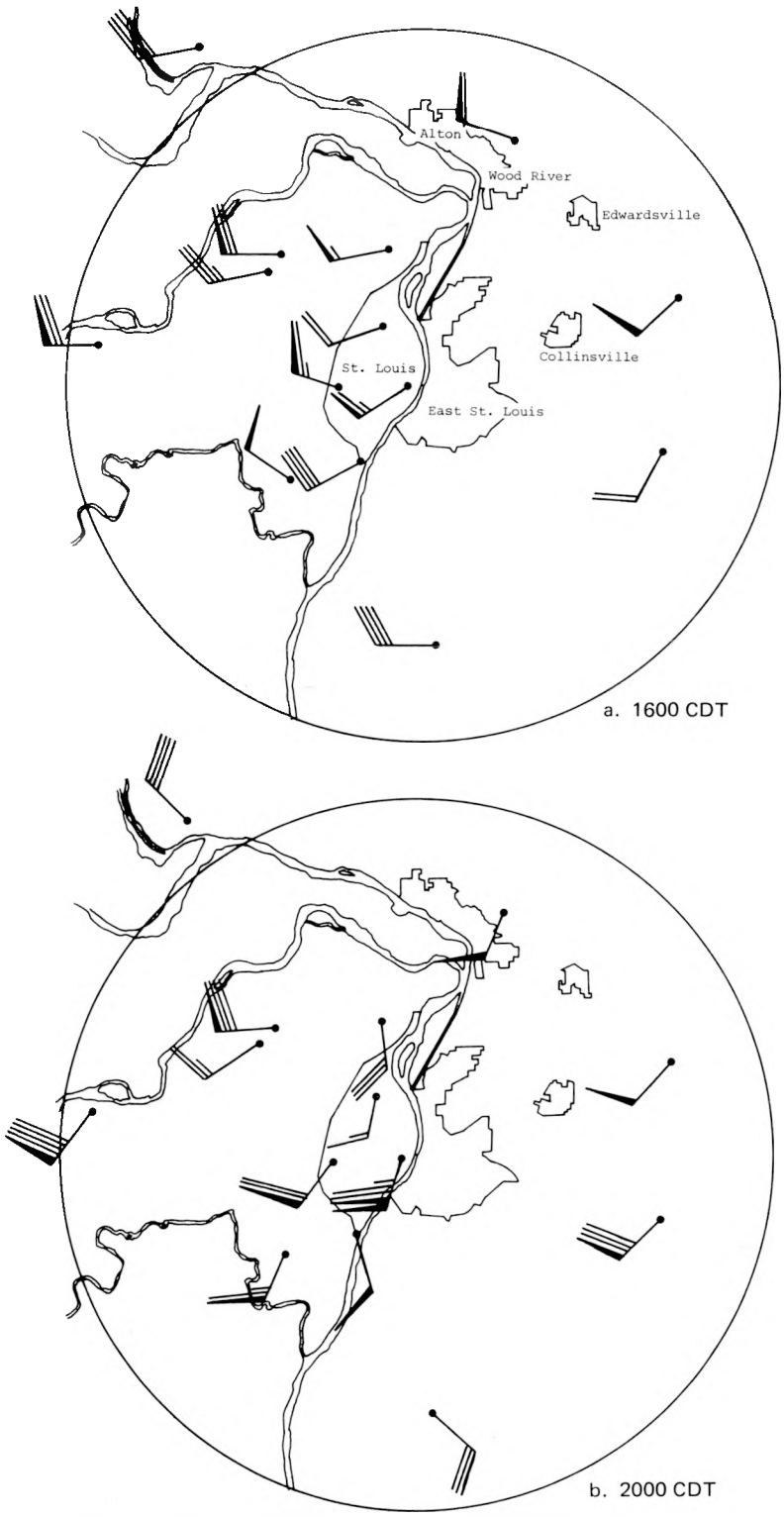

Figure F-19. Surface winds at 1600 and 2000 CDT

The initial raincells involved in the Alton–Wood River severe rainstorm were observed about 2000 CDT. The first of these (raincell 9), which later merged with raincells 10 and 11, was initiated in the vicinity of the Wood River oil refineries. The merged combination contributed to the Alton–Wood River center, and consideration of its movement and time indicates that this combination was also involved in the intense center at Mt. Olive. This indication was given additional support from limited 10-cm PPI radar data and hourly NWS radar reports plotted at St. Louis. Overall, a strong tendency for the rainfall to intensify in the Alton–Wood River area and the potential relationship between the Mt. Olive and Alton–Wood River storm centers suggest that urban intensification of existing raincells which had developed largely over the bottomlands was related to the development of the major storm centers.

In seeking further verification of the urban involvement, analyses were made of the location of 1) the initiation of the 69 raincells and 2) mergers of raincells that often result in surface rain intensification. Results indicated 10 potential urban-effect raincell initiations in the Alton–Wood River area, and 6 of these had 5-min rates exceeding 2 in/hr. Other areas of above-average raincell initiations in the MMX circle were located a few miles E of St. Louis, in the Granite City–Edwardsville region where they were under the possible effect of oil refinery and steel plant atmospheric discharges, and in the SW part of the circle where they were likely associated with the Ozark Hills.

Since there was no heat island over Alton–Wood River at the time of the rainstorm initiation, any urban enhancement of the natural precipitation processes would most likely have resulted from nuclei and/or moisture discharges from industrial sources. Analyses of raincell durations showed below average durations for the 69 network cells, and this further indicates that the severe rainstorm was enhanced by intensification of ongoing rain processes in the urban-industrial area of Alton–Wood River.

Of the 69 raincells initiated in the circle, 43% were potential urban-effect cells whereas the urban-effect area included only about 39% of the area; thus, some evidence of more frequent rain development in urban-effect areas existed. A slight trend was also noted for rain rates in the more intense raincells to maximize in potential urban-effect areas.

Analyses of raincell mergers revealed that 17 mergers occurred within the circle. Of these, 6 were within or slightly upwind of the Alton–Wood River area, and 5 of these were major causes of the high rainfall centers that occurred in the Alton–Wood River region. Four of these five mergers occurred within the immediate urban area, and analyses indicated they were probably caused by horizontal growth in one or more cells situated over the urban area. Thus, the greater concentration of mergers in the Alton–Wood River area appears to have resulted from urban intensification effects.

Most of the cells moved from SW to W with speeds ranging from near 0 to 30 mi/hr, and thus exhibited typical summer movements of convective storms. The average duration was 20 min, about 5 min less than the 1971–1972 MMX average. The major difference between the cells of the severe rainstorm center and other cells was greater than average intensity rather than longer duration. This supports earlier statistical analyses indicating that the major urban effect in the Alton–Wood River area is associated with intensification of existing raincells (Schickedanz, 1974).

Hail and Thunderstorms

Five hailfalls occurred on 25 July. Of these, three were from potential urban-effect storms. Analyses indicated that the hail from the urban-effect raincells was more intense than that from the non-urban cells. The urban-effect hailfalls all occurred in heavy rain cores, were recorded in later stages of their parent storms than those in the floodplain to the SW, and occurred 5 to 10 min after mergers of two major raincells. The results for 25 July suggest that urban-related hail increases are

associated frequently with mergers of major raincells that often develop in or are enhanced by urban atmospheric conditions. This supports earlier climatic findings in eight U.S. cities (Huff and Changnon, 1973).

There were two thunderstorm periods on 25 July. The major period began in late afternoon and produced thunderstorms throughout the N half of the circle. No thunderstorms accompanied the rain in the SW portion. Urban effects on thunder activity was indicated by the fact that 85% of all potential urban-effect raincells became thunderstorms. Furthermore, stations just downwind of the urban areas had longer thunder periods than those in the rest of the circle, and, in one case, 42 min of intense thunder occurred at a downwind station, more than reported at any other observation station.

Cloud Conditions

Surface cloud observations provided information relevant to the development of the heavy raincells in the Alton–Wood River area. All observed clouds developed because of the general synoptic conditions and apparently were not related to urban processes. Because of less cloudiness in the W part of the circle during the day, the development of Cu was more favorable in this region, and this theory was borne out by earlier Cu development and a more rapid increase in sky coverage during the early evening. Aircraft data also provided much pertinent information on cloud bases, updrafts, locations, and movements.

Overall, cloud analyses showed that the Cu had relatively low bases of 2300–3300 ft. Updrafts were moderate to strong at the bases and mid-levels, and there were no preferred locations around the bases. Cloud merging was common and observed to lead to thunderstorms. Cloud movements were relatively slow, less than 15 mi/hr. Hazy conditions existed from the surface to cloud bases indicating that urban source air was reaching cloud bases. Of major importance is the observation that some of the most intense raincells were apparently associated with clouds that developed about 1900 CDT over the Missouri–Mississippi bottomlands to the SW of Alton–Wood River area. This is a favored region of formation because of relatively high temperatures and low-level moisture in the bottomlands.

Air and Dew Point Temperatures and Surface Winds

The surface air temperature distribution just prior to initiation of the Alton–Wood River storm indicated a 5F increase between the urban area and the bottomlands 9-12 mi to the SW. This suggests that excessive heat in the bottomlands stimulated Cu formation. Furthermore, a peak in the dew point temperature was also located in the bottomlands in the 2 hr prior to storm initiations, and these dew points were the highest in the circle.

With raincell movements predominantly from SW to W and moving at 15-20 kt, the bottomlands clouds would have reached the urban area in 30-35 min. At that time they would likely have reached or closely approached the rain stage, and would have been exposed to urban intensification processes. As pointed out above, the analyses of raincells, hailfall, and thunder occurrences indicated intensification of the precipitation processes in the Alton–Wood River urban area. It is considered quite likely that the bottomlands serve as a preferred initiation region for summer Cu because of relatively high surface air and dew point conditions. Many of these clouds would then move into the Alton–Wood River area because of the prevailing steering winds, and urban intensification of the convective processes could then occur under favorable conditions for thermal and/or nuclei enhancement of the natural cloud processes.

Winds were generally weak throughout the day and evening. The wind field did indicate the passage of a mesoscale system with no significant rainfall in middle to late afternoon, but this system was not associated with the later severe storm system. Immediately prior to the start of the Alton-Wood River storms, most wind stations indicated SE to SW surface flow, but some convergence was indicated in the Alton-Wood River area at the start of the storm as a result of a combination of W winds in the NW quadrant of the circle with S flow over the remainder.

Major Conclusions

When all available data are taken into consideration, it appears that rather widespread convective activity was to be expected with the cold front approaching and passing St. Louis during the night of 25-26 July. However, it is also concluded that the *maximization* of rainfall in the Alton-Wood River area and quite likely the Mt. Olive area, resulted primarily from urban intensification of existing convective cloud systems. This conclusion is the end result of the combined analyses of all available data from MMX operations on 25 July. These included 1) raincell analyses from the dense raingage network; 2) analyses of data from the hail and thunder observation stations; 3) surface air temperature, dew point, and wind measurements from the hygrothermograph and wind measurement networks; 4) cloud observations from surface stations, and cloud observations and measurements from three sampling aircraft.

Furthermore, the MMX data analyses indicate that the main reason the urban enhancement was restricted primarily to the Alton-Wood River area was the favorable conditions for Cu development in the Missouri-Mississippi bottomalnds several miles upwind of the Alton-Wood River storm center. These favorable conditions resulted from both air and dew point temperature maxima at the surface in the bottomlands. In turn, these maxima were basically caused by less cloudiness in that part of the MMX circle during the daytime, which led to greater surface heating, and consequently accelerated evapotranspiration. Nature did not provide such favorable conditions for cloud development over and upwind of St. Louis, so that substantial rain enhancement by this urban-industrial region did not occur.

A finding common to this and two of the prior case studies in this report (11 August 1972 and 14 July 1973) was the presence of surface air-dew point maxima upwind of the storm centers prior to the start of the heavy rains. This suggests that naturally favorable conditions for Cu development in and/or slightly upwind of an urban-industrial area is an important prerequisite for effective urban enhancement of surface rainfall.

REFERENCES

Changnon, S. A., Jr. 1970. *Hailstreaks.* Journal Atmospheric Sciences, v. 27:109-125.

Huff, F. A. 1967. *Mesoscale structure of a severe rainstorm.* Preprints, 5th Conference on Severe Local Storms, St. Louis, Mo.; AMS, Boston, pp. 211-218.

Huff, F. A., Editor. 1973. *Summary report of Metromex studies, 1971-1972.* Illinois State Water Survey Report of Investigation 74, 169 pp.

Huff, F. A. 1974. *The distribution of heavy rainfall in a major urban area.* Preprints, National Symposium on Urban Hydrology and Runoff and Sediment Management, University of Kentucky, Lexington, July 29-31.

Huff, F. A., and S. A. Changnon, Jr. 1964. *A model 10-inch rainstorm.* Journal of Applied Meteorology, v. 3(5):587-589.

Huff, F. A., and S. A. Changnon, Jr. 1972. *Climatological assessment of urban effects on precipitation at St. Louis.* Journal of Applied Meteorology, v. 11(5):823-842.

Huff, F. A., and S. A. Changnon, Jr. 1973. *Precipitation modification by major urban areas.* Bulletin American Meteorological Society, v. 54(12):1220-1232.

Illinois State Water Survey. 1970. *Rainfall frequencies.* Technical Letter 13. 5 pp.

Schickedanz, P. T. 1973. *Use of surface raincells in evaluating inadvertent weather modification. In* Summary Report of Metromex Studies, 1971–1972, F. A. Huff, Editor, Illinois State Water Survey Report of Investigation 74, pp. 57-83.

Schickedanz, P. T. 1974. *Inadvertent rain modification as indicated by surface raincells.* Journal of Applied Meteorology, v. 13(8):891-900.

Semonin, R. G., and S. A. Changnon, Jr. 1975. *Metromex: lessons for precipitation enhancement in the Midwest.* Journal Weather Modification, v. 5:77-87.

Simpson, J., W. L. Woodley, and R. M. White. 1972. *Joint federal-state cumulus seeding program for mitigation of 1971 South Florida drought.* Bulletin American Meteorological Society, v. 53:334-343.

G. LOCAL SHOWERS ON 7 AUGUST 1973

Robert C. Cataneo and Douglas M. A. Jones

CONTENTS

G. LOCAL SHOWERS ON 7 AUGUST 1973

INTRODUCTION

This case concerns study of small convective showers that developed locally in and near the MMX circle. The day was chosen for investigation because it represented a typical marginal rainshower circumstance. Further, these showers appeared to be caused by local effects and were not related to any large-scale weather condition. No surface frontal zones nor upper air disturbances influenced the St. Louis region on this day. The radar located at PMQ indicated the presence of several small rainshowers in the area during the afternoon of 7 August, but the rain shafts were so small that they were not detected in the recording raingage network.

Because of the marginal convective nature of the day, several possible MMX field activities were not pursued. For example, no major atmospheric chemistry measurements were made. There was no aircraft release of tracers because potential clouds did not occur in or just W of the rain chemistry network (see figure B-1).

SYNOPTIC WEATHER CONDITIONS

Macroscale

At 0700 CDT on 7 August 1973, the upper air flow at the 500-mb level (figure G-1) was characterized by a weak ridge in the S, which had persisted for the previous two days. At the surface (figure G-2), a 1020-mb high over the mid-Atlantic coast brought weak S flow into the Midwest. This synoptic configuration resulted in a very stable situation in the St. Louis area with a 6F subsidence inversion present at approximately 780 mb, as may be seen in the PMQ sounding at 0700 (figure G-3). Because no surface fronts nor upper air disturbances were influencing the Midwest, no organized nor strong convective activity was expected in the area. However, the Survey forecasters for MMX predicted the inversion to dissipate by afternoon with isolated small air mass showers developing during the day as the low-level flow from the Gulf of Mexico increased.

Mesoscale

The three morning upper air soundings in the St. Louis region (shown in figure G-3) all exhibited a 3-9F inversion at the 780-800 mb height with very dry air above this level. The early afternoon (1300) soundings at the same location indicated a substantial weakening of the inversion with no significant change in the dew point values (figure G-4). However, both morning and afternoon ARC (urban) temperature traces revealed slightly higher values (~ 2F) below 800 mb than did the other (rural) locations.

The surface temperature pattern during the late morning through mid-afternoon revealed that values in the part in the MMX circle bounded by the Missouri, Mississippi, and Meramec Rivers (the W-central area) were 2 to 3F higher than those elsewhere, except in the Belleville area. This generally warmer in the W situation existed in varying intensities throughout the day (figure G-5). Significantly cooler temperatures (~ 3-4F) were evident in the Alton-Wood River area between 1200 and 2000 CDT as illustrated by the 1400 pattern in figure G-5b.

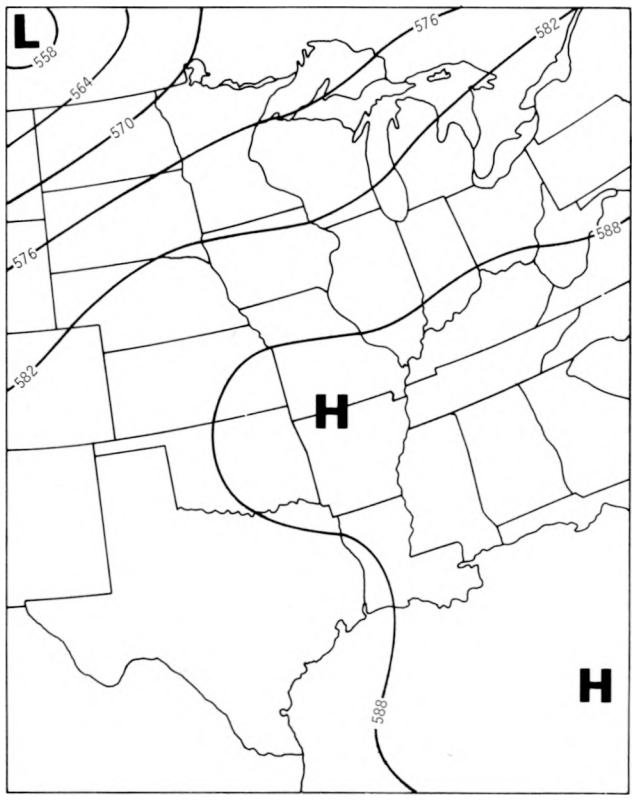

Figure G-1. 500 mb analysis at 0700 on 7 August

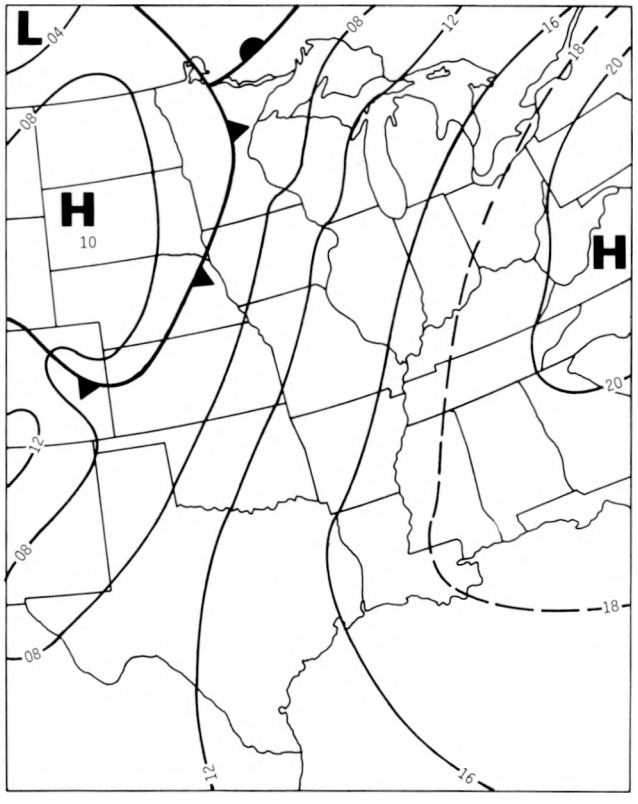

Figure G-2. Surface weather analysis at 0700 on 7 August

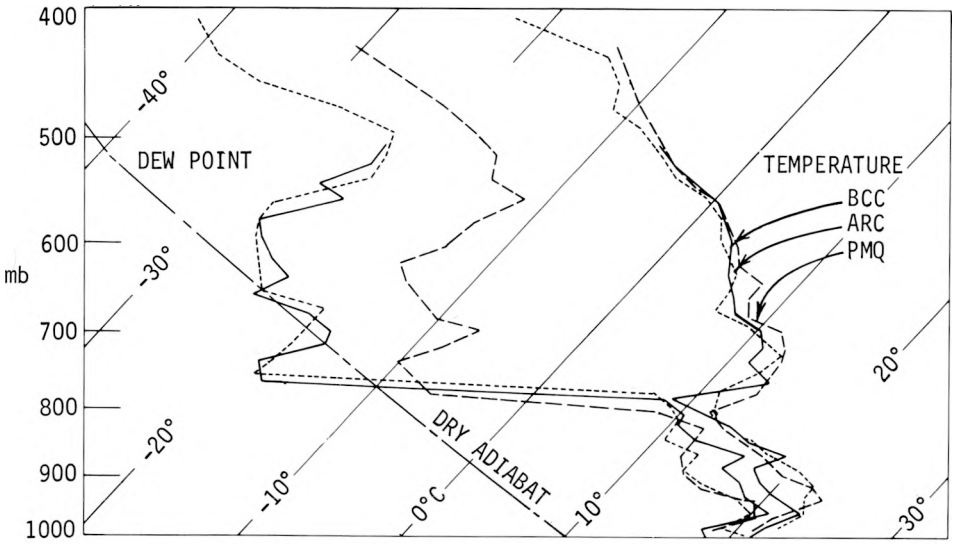

Figure G-3. 0700 soundings at PMQ, ARC, and BCC

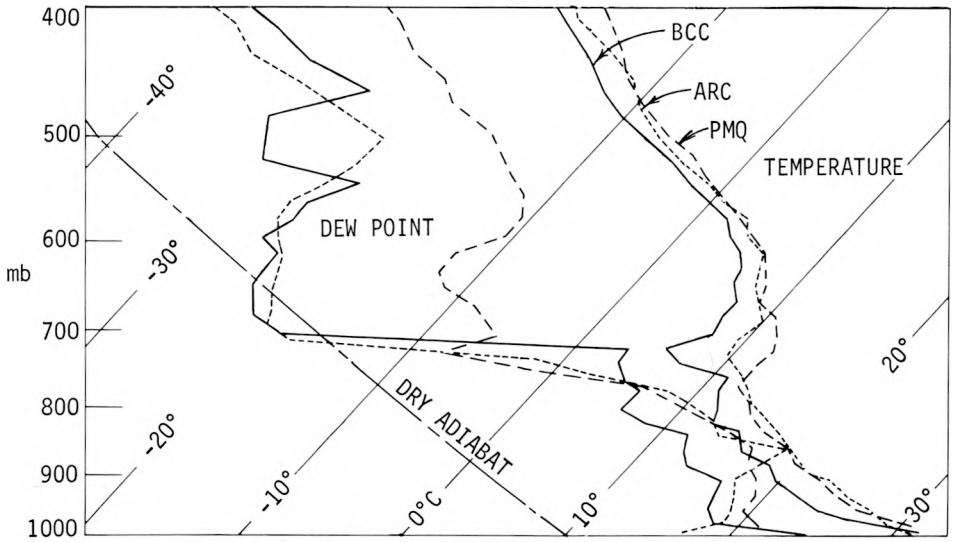

Figure G-4. 1300 soundings at PMQ, ARC, and BCC

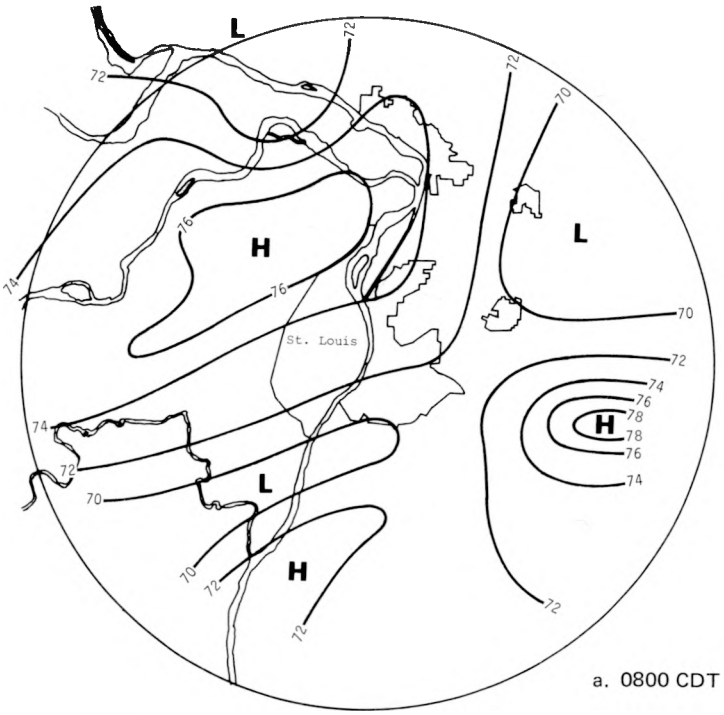

a. 0800 CDT

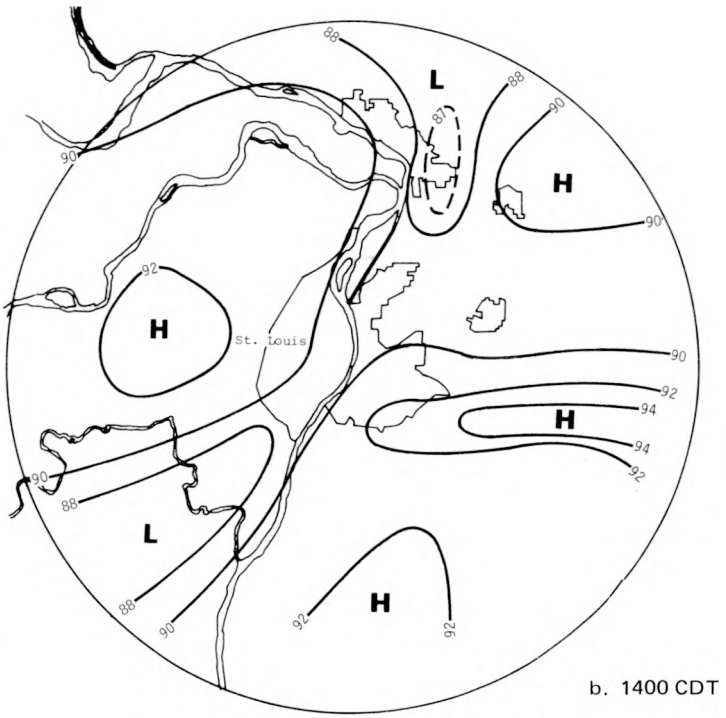

b. 1400 CDT

Figure G-5. Temperature field at 0800 and 1400

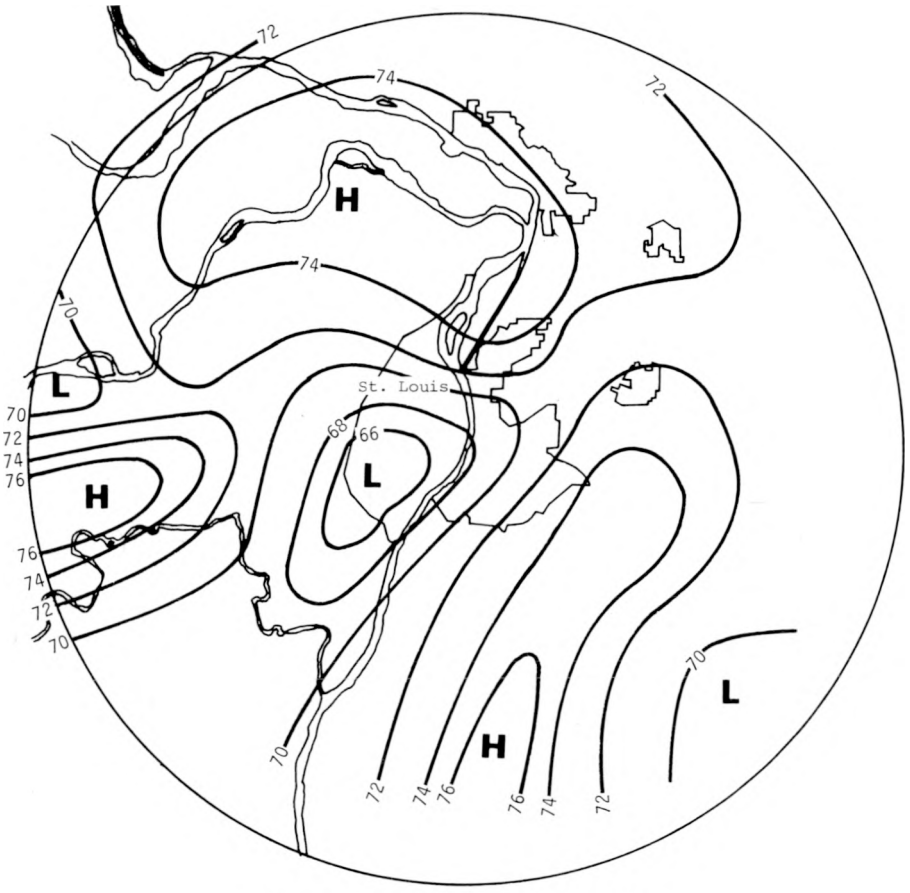

Figure G-6. Dew point field at 1400 CDT

The most significant feature in the surface dew point pattern (figure G-6) was a lower value area that existed from 1000 to 2200 in the St. Louis urban area. This was 8 to 10F below most others during the afternoon.

The surface wind flow was characterized by speeds in the urban area that were 4 to 8 mi/hr higher than rural values and this situation persisted through the 1200–2000 period (figure G-7). This flow pattern resulted in a zone of surface confluence N of the region with higher wind values and diffluence S of it. Another persistent surface weather feature was a tendency toward flow from the E in the E portion of the MMX circle, while the prevailing flow elsewhere in the circle was from the SSW.

The pibal data for 100 m and 250 m AGL for 1200, 1400, and 1600 also indicated convergence, as was suggested by the surface data, N of St. Louis. This occurred in the general vicinity of the Alton–Wood River area, as reflected in the 1600 patterns (figure G-8).

Forecast for the Day

The MMX forecast for 7 August, based on analysis of the general synoptic weather data and the 0700 soundings, called for possible isolated small showers by mid-afternoon. This forecast was based on the following conditions: 1) no large scale synoptic disturbance (surface frontal system or upper air disturbance) was affecting the area; 2) a decrease in the 3 to 9F inversion aloft was expected; 3) a lifted index of 0 to −1 existed in the St. Louis area; and 4) very dry air aloft,

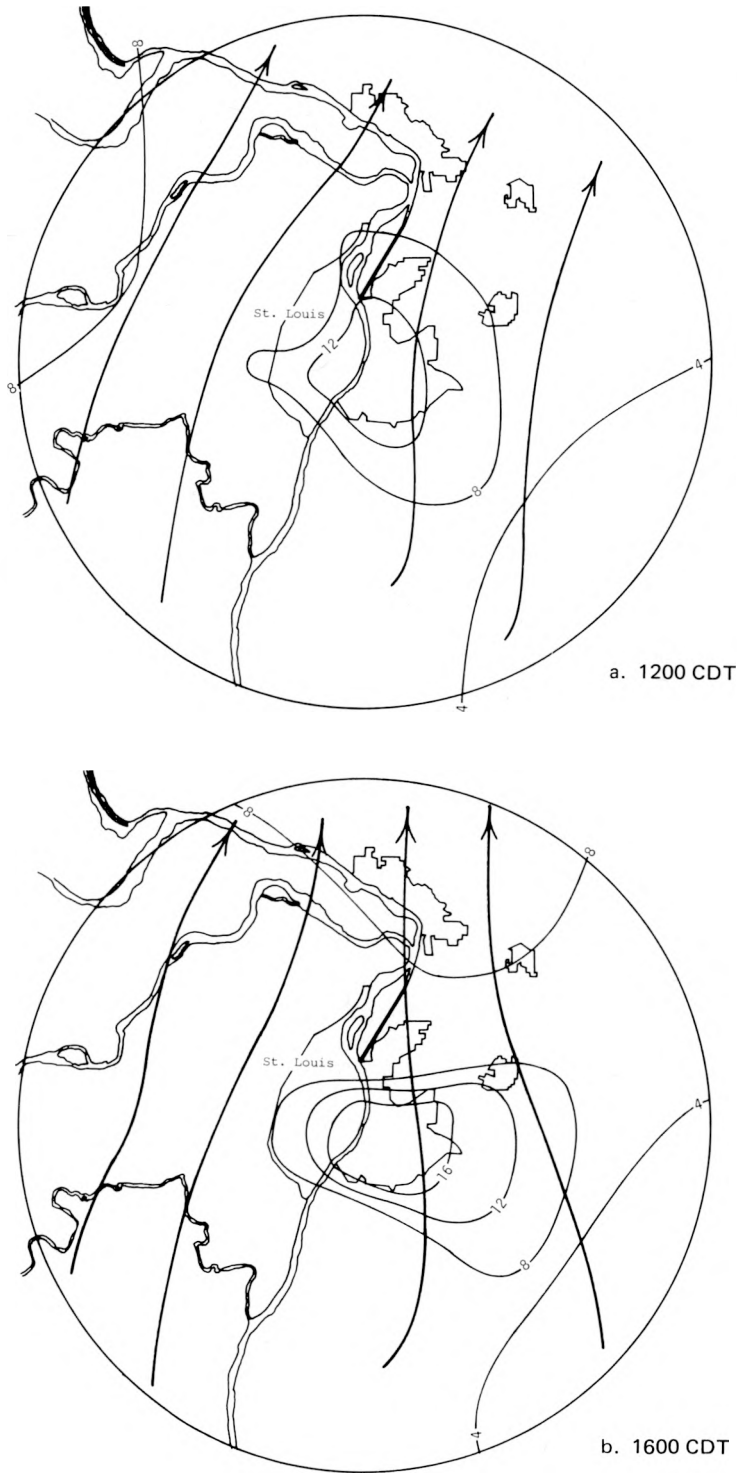

Figure G-7. Surface streamlines and isotachs (mi/hr) at 1200 and 1600 CDT

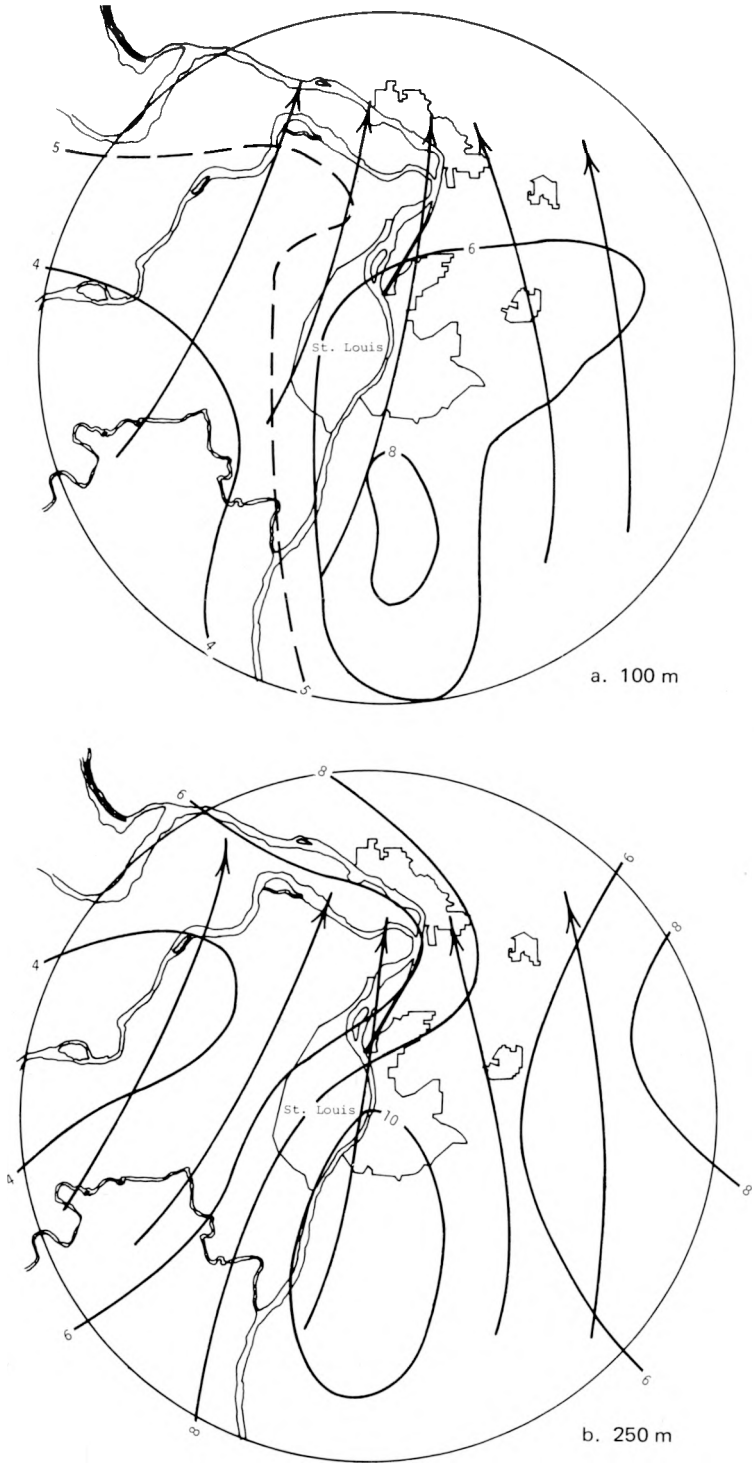

Figure G-8. 100 and 250 m streamlines and isotachs (m/sec) at 1600 CDT

above 750 mb, was present and expected to continue. The weather situation that developed followed the forecast closely. The 13 small afternoon showers that developed within radar range (60 mi of PMQ) are the principal features of this case analysis.

PRECIPITATION MORPHOLOGY

Aircraft Observations

The AI aircraft was instructed to fly a cross-sectional sampling pattern across the St. Louis urban area at certain prescribed low-level altitudes. Their goal was to map the CN, temperature, and moisture values. Air temperature, wet bulb temperature, and CN values for portions of the two aircraft flights on this day are shown in figure G-9, and the related flight tracks are shown in figure G-10. From these data, plus comments in the aircraft logs made during the flight (1404–1751), the following conclusions were obtained:

1) The top of the haze layer was at approximately 8000 ft AGL.
2) The tops of scattered small Cu did not reach the top of the haze layer.
3) A few CuCong had turrets extending slightly above the haze layer.
4) A very sharp rise in CN was noted when the aircraft passed over the urban-industrial complex (figure G-9).
5) The width of the urban plume was about 17 mi, as determined from the nuclei profile from track 6.
6) The atmosphere at 1800 ft MSL was warmer SW of the city than over the city.
7) Cloud-base levels in the Alton-Wood River region were approximately 300 ft lower than those over the city
8) No precipitation was falling from any of the clouds observed.
9) There seemed to be fewer clouds over St. Louis than there were NW and SE of the city.
10) The air over St. Louis was warmer and slightly more moist than that over most rural areas.

Clearly, the afternoon clouds that existed in the rural and urban areas had access to surface effluents and effects (heating and moisture).

Radar Observations

No measurable rain was recorded in any of the MMX circle raingages, although a number of small short-lived rain echoes were observed on both the 10-cm PPI and 3-cm RHI radars of the Survey. There was no hail detected in the MMX circle and no thunder was reported.

A summary of the first echo locations is shown in figure G-11. The initial echo of the day was observed at 1226 CDT on the 3-cm RHI. This echo was located W of St. Louis as shown in figure G-11. It is in an area envelope labeled group 1 where six subsequent echoes developed. These were observed in that part of the MMX circle W and WSW of St. Louis that is largely in the foothills of the Ozarks (see figure A-1). Five other echoes formed in and N of Alton-Wood River and these are labeled as group 2 on figure G-11.

The duration of the echoes in both groups was limited to 15 min or less (with one exception). The echoes had average tops of approximately 12,000 ft, and they moved from the SSW at 15 mi/hr. The major exception was an echo that developed just N of Alton in group 2 (figure

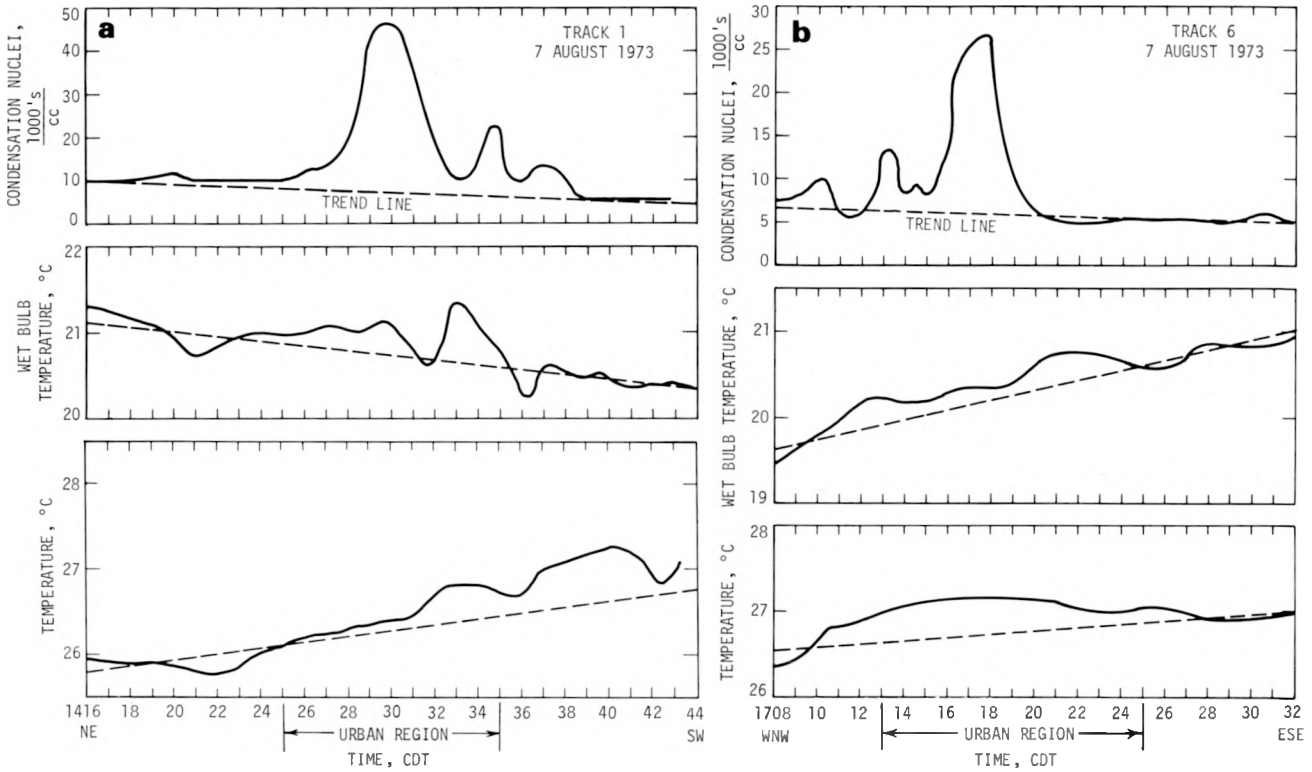

Figure G-9. Atmospheric parameters and aerosols versus time and location for two aircraft flights at 1800 ft MSL

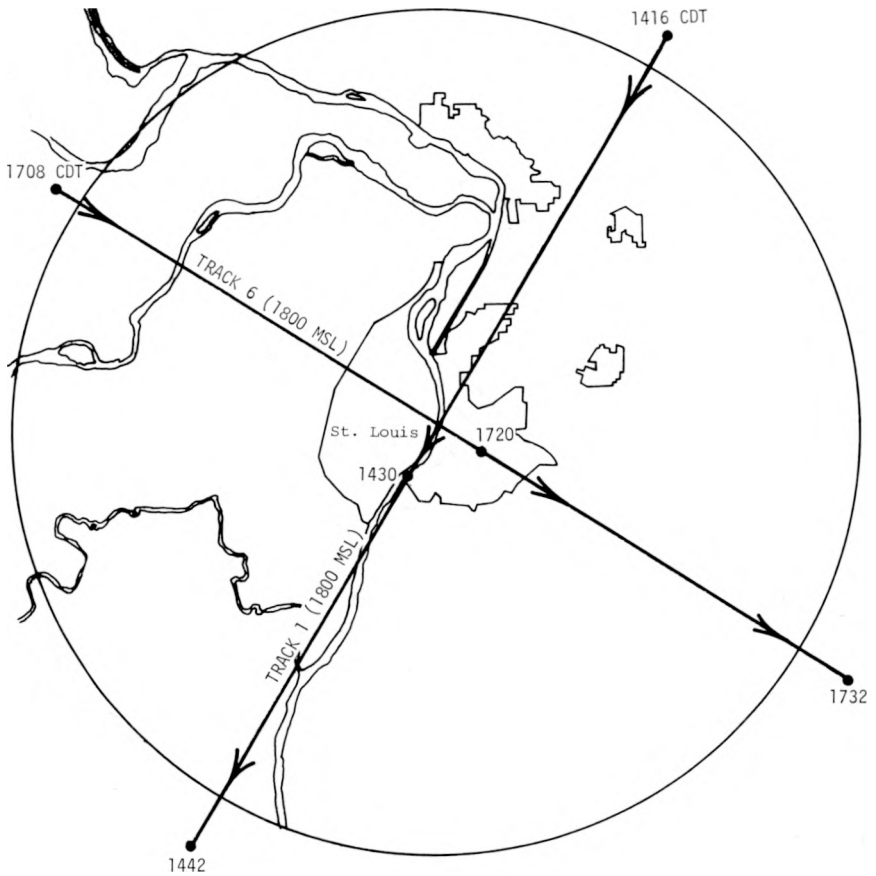

Figure G-10. Flight tracks for data shown in figure G-9

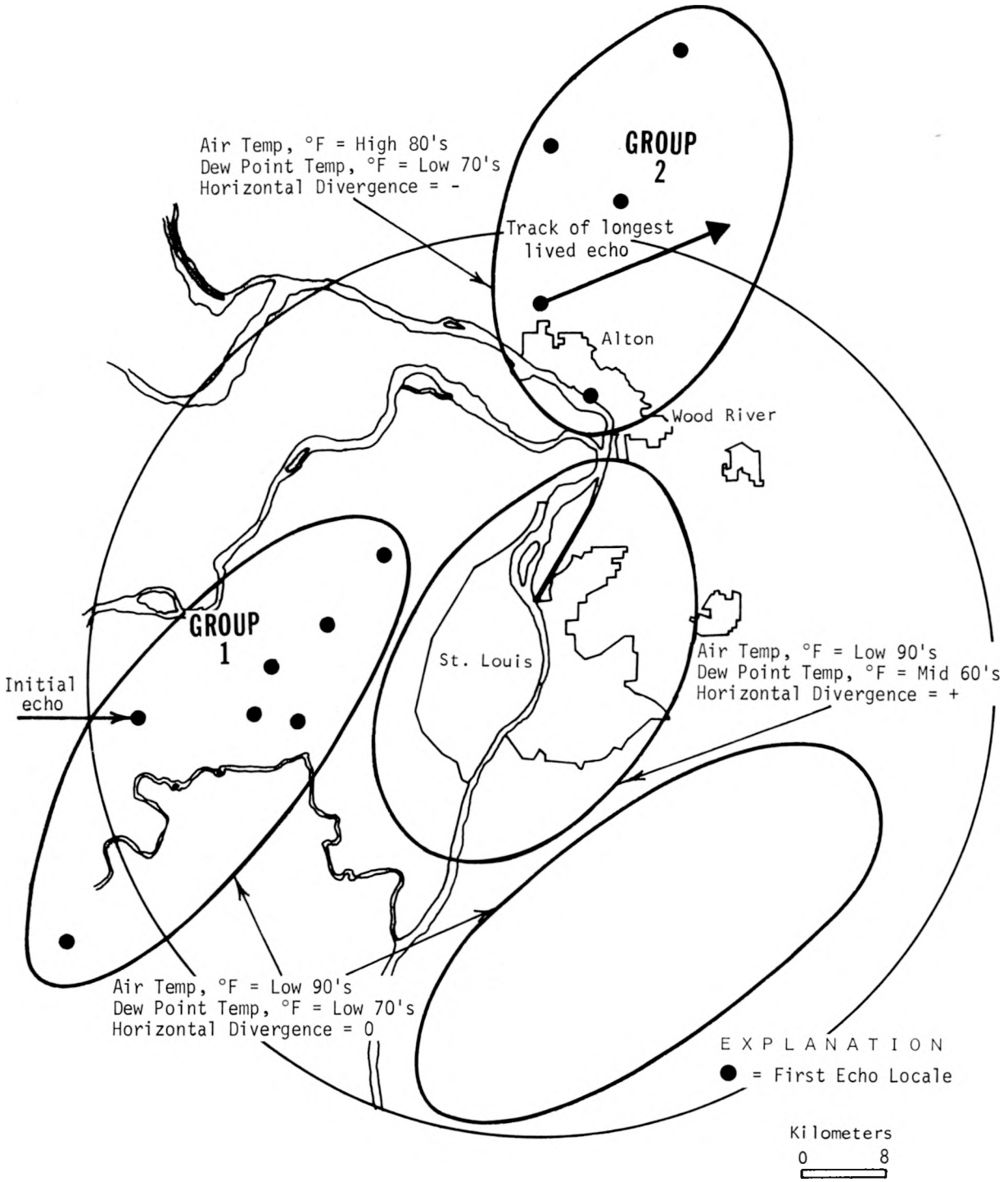

Figure G-11. First echo locations and generalized areal ambient conditions in the early afternoon

G-11). It persisted for 40 min while moving NE at 15 mi/hr, and its maximum top was 20,000 ft. Thus, this echo lasted considerably longer and had a significantly higher top than all others observed by the PMQ radars. The 7 echoes in group 1 had average durations of 9 min, and echoes in group 2, exclusive of the long-lived echo, had average durations of 12 min.

INTERPRETATION

Small isolated showers formed on 7 August as forecast, and there were two areas of echo formation in the MMX circle. Table G-1 summarizes various atmospheric conditions related to the two echo areas and to the St. Louis industrial area where no echoes occurred. The group 1 echoes, which first appeared at approximately 1230 CDT, developed in a local 'hot spot' region characterized by 2-3F warmer temperatures (see figure G-5). This surface heat anomaly might explain their inception since the flight data suggest it extended above 2000 ft (about midway up to cloud bases which were at 5000 ft). In contrast, the group 2 echoes, which appeared later with their first development at 1520, occurred in a region that was approximately 3 to 6F cooler at the surface than where the group 1 echoes developed.

Table G-1. Comparison of Weather Conditions in Three Areas

	Area of group 1 echoes	*Area of group 2 echoes*	*St. Louis area, no echoes*
Echo time	early afternoon	late afternoon	
Surface dew point temperatures, °F	70-73	70-73	65-68
Cloud nuclei at 1000 to 2000 ft AGL	little or no urban source nuclei (5,000 to 10,000/cc)	urban nuclei evident (15,000 to 50,000/cc)	urban nuclei evident (15,000 to 50,000/cc)
Surface temperatures in afternoon, °F	91-94	87-90	90-93
Low-level horizontal wind condition	no convergence or divergence	convergence	divergence
Cloud cover	scattered Cu	scattered Cu	less coverage than in other areas
Cloud base level, ft MSL	~ 5000	~ 5000	~ 5300

An important question to be answered is, "Would the echoes observed on this day have occurred in the absence of the St. Louis urban area or Alton-Wood River area?" Regarding group 1 echoes, the local factors that appeared to have possibly influenced the meager shower development were the local moisture and temperature anomalies. However, these anomalies could not be related to the urban area, and the cause of the temperature anomaly has not been established. No echoes were reported over the St. Louis area which had similar surface air temperature regime but much lower surface moisture values (table G-1). Thus, the thermal effect alone does not appear to be the sole causative agent for the formation of cells W of St. Louis. The effect of the forested Ozark Hills, largely in the release of moisture through evapotranspiration, and possibly in the development of upward air motions because of their rougher terrain, appear to have helped initiate the showers in the group 1 area.

In the area of the group 2 echoes, large concentrations of urban-industrial nuclei were found to exist at 2000 ft and these were likely available to the clouds. However, surface air temperatures in that area were lower than in the other regions of the circle. The later formation of the group 2 echoes may have been due to these lower temperatures. The low-level convergence produced by St. Louis N of the city, as indicated by the pibal wind data, was likely an important factor in the shower development. The absence of echo development in St. Louis may have been related to the significantly lower available moisture. Comparison of the afternoon ARC sounding with that at PMQ showed that the low surface dew points of the urban area extended to 1000 ft AGL. The aircraft observations of fewer clouds over the urban area also substantiate this condition.

CONCLUSIONS

The following conclusions have been reached about the cloud and shower developments on 7 August:

1) The significantly lower surface moisture in the city prevented the formation of cells in that region.
2) Higher surface temperatures related to the urban heat island did not cause group 2 echo formation, nor did the presence of large quantities of urban nuclei.
3) The showers in and just downwind of the Ozark Hills (group 1) probably formed as a result of local heating (cause unknown) and to hill effects on the atmosphere resulting in localized moisture and roughness-produced vertical motions.
4) The three rural echoes N of Alton (group 2) may have been influenced by the Alton–Wood River industrial area, although the temperature–moisture fields and nuclei plume are not known for this region.
5) The two showers in the Alton–Wood River region probably formed *a)* because of the presence of its industrial area (a nuclei and moisture source), and *b)* because of the area of convergence in the N-central portion of the MMX circle that was likely related to St. Louis.
6) The greater convective intensity (longer lifetime and higher maximum top) of one of the two Alton-area showers indicates that these urban factors helped initiate and sustain more vigorous convection on a very marginal convective day.

H. RAIN PERIODS ON 9 AUGUST 1973

Robert C. Cataneo

CONTENTS

H. RAIN PERIODS ON 9 AUGUST 1973

INTRODUCTION

The day of 9 August 1973 was chosen for a detailed investigation largely because an approaching late afternoon–early evening convective system had dissipated in the MMX circle and a release of tracers was performed in the updraft of a storm well W of the rain chemistry network and St. Louis. The primary goal of the study was to ascertain whether the urban area had led to a diminishment of the convective activity and associated rainfall.

Initial analysis showed that to understand this rain event meant including analyses of two earlier rain periods on 9 August. Although both of these were largely stratiform rains, one in the early morning and the second at mid-day, they influenced the atmospheric conditions prior to the principal convective storms desired for study.

Data available for study of the 9 August events were extensive. All standard MMX networks were in operation, and the Survey's radars were operational. The pibal network also was in operation and one AI aircraft flight in the late afternoon furnished cloud and atmospheric data.

SYNOPTIC CONDITIONS

Macroscale

The upper air pattern at 0700 CDT, as characterized by the 500-mb level (figure H–1), featured a long wave trough with its axis extending S into E Oklahoma from a closed low N of Minnesota. A surface cold front at 0700 CDT (figure H–2), associated with the upper trough, extended S from a low in N Minnesota to NW Missouri. This situation resulted in moisture advection into the Midwest, coupled with the dynamics necessary for organized convective activity. Some scattered shower activity had occurred along and ahead of this system during the 24 hr prior to 0700 on 9 August. After several rain periods in St. Louis on 9 August the surface frontal position was still approximately 100 mi NW of St. Louis.

Mesoscale

The first period of rain in the St. Louis research circle occurred between 0300 and 0600 in the N-central area. Two additional rain periods occurred during the day, one at 0725–1445 and one at 1710–2125. All three periods were prefrontal squall areas.

The surface temperature patterns prior to each rain period (at 0200, 0600, and 1600 are indicated in figure H–3. A very distinct warm area (heat island) persisted in the urban area between 0000 and 0800, as reflected in the 0200 and 0600 patterns. Thereafter, the surface temperature pattern became confused and was often dominated by the presence or absence of clouds and/or precipitation. An urban heat island was clearly re-established by 1800, and was maintained for the remainder of 9 August.

The surface dew point temperatures throughout the day varied from the high 60's (F) to mid 70's. They were also strongly influenced by the presence or absence of precipitation. The dew point patterns were similarly confused throughout the day with areas of distinct high and low values appearing in different locales with the passage of time and rain elements (figure H–4). Sur-

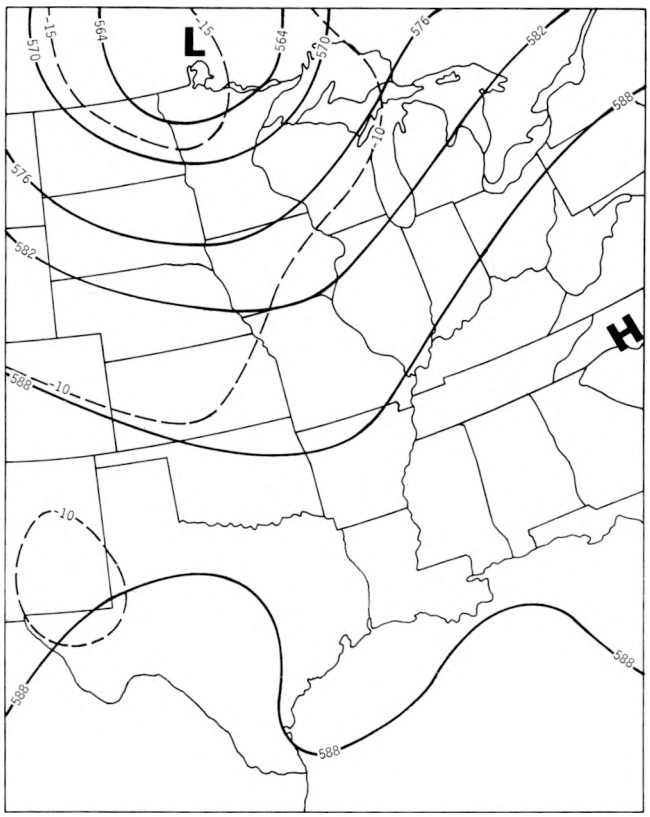

Figure H-1. 500-mb analysis at 0700 CDT

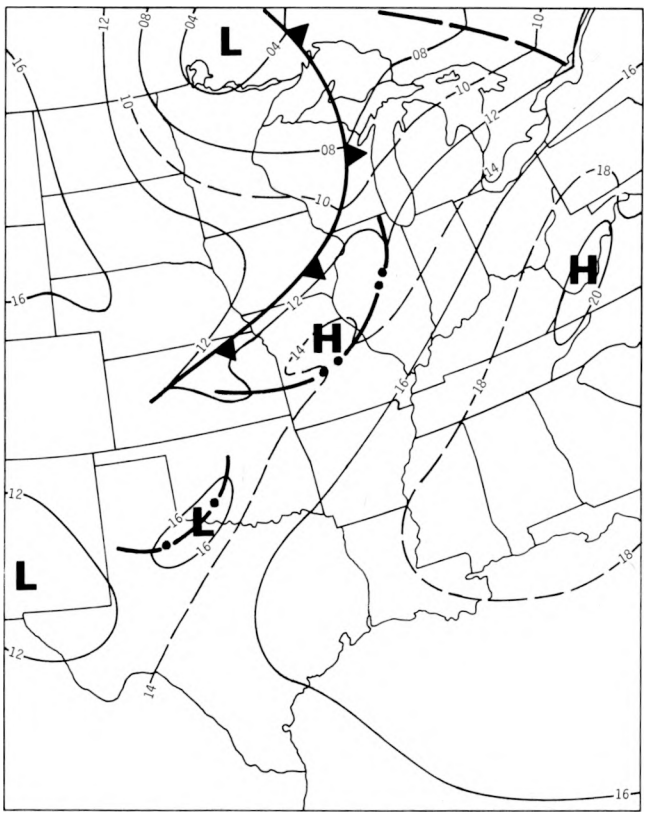

Figure H-2. Surface analysis at 0700 CDT

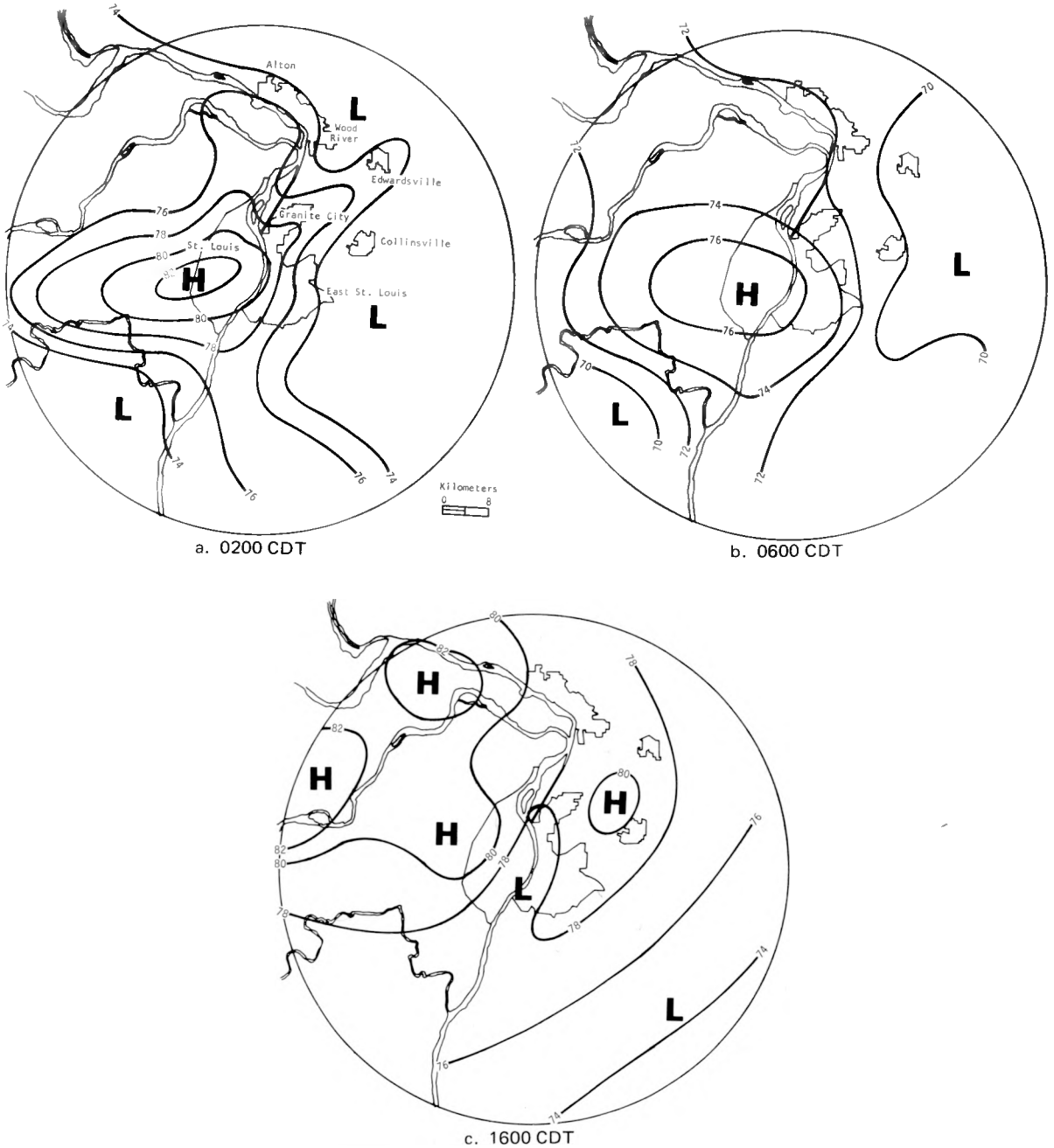

Figure H-3. Surface temperature pattern at 0200, 0600, and 1600 CDT

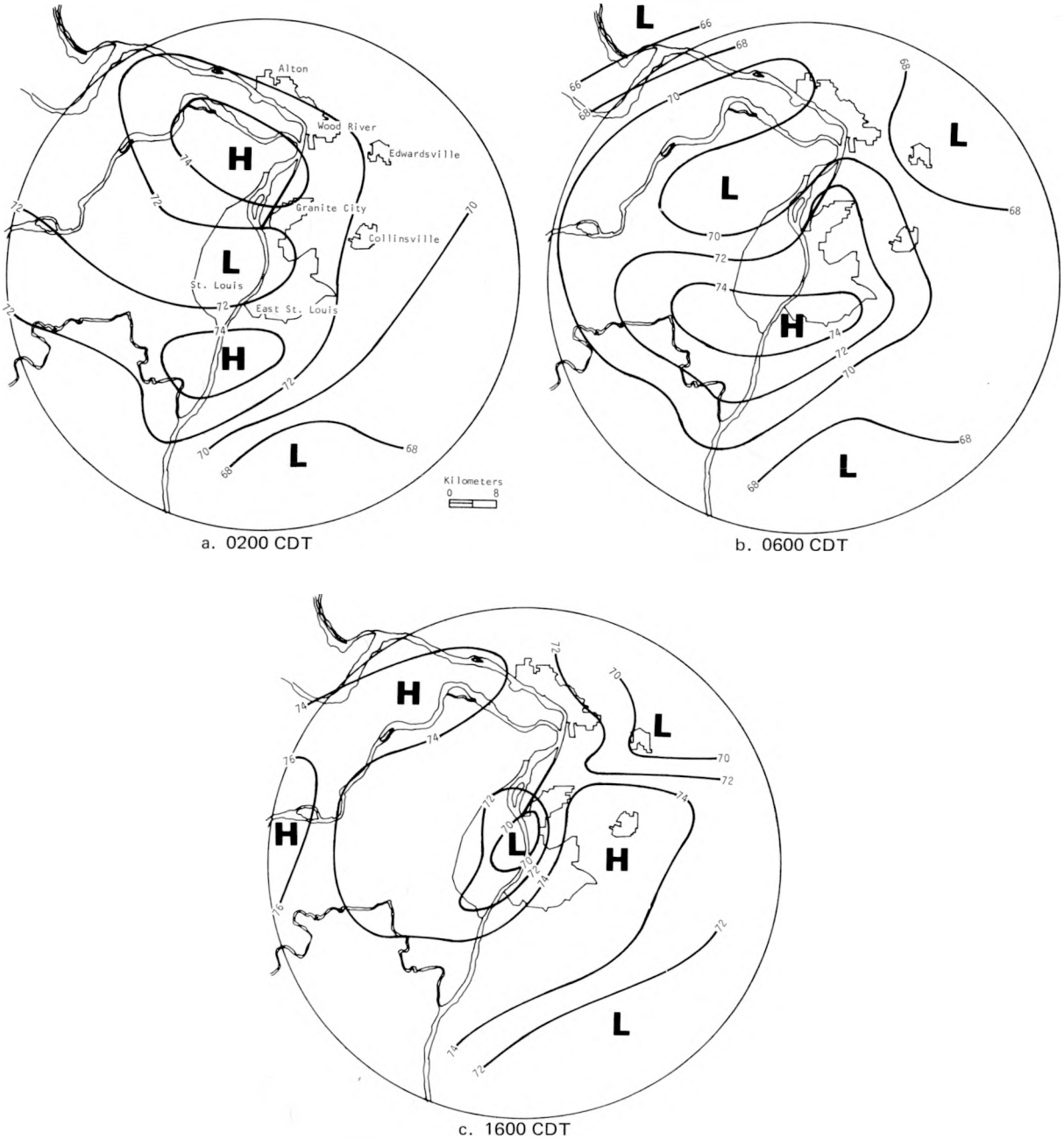

Figure H-4. Surface dew point temperatures at 0200, 0600, and 1600 CDT

face moisture over the urban area was relatively low prior to the 0200 and 1600 rain periods, but was relatively high prior to the rain period that began at 0600.

The surface wind data (figure H-5) revealed marked differences in the flow (speed and direction) as the day progressed. These changes often appeared to be related to the location of precipitation areas in the circle. For example, during the hour (0200) preceding the first period of precipitation (figure H-5a), the flow was from the E in the N third of the circle whereas S flow prevailed elsewhere. A surface convergence zone existed during this time (0200) just N of the urban area.

The morning (0700) and afternoon (1330) soundings at ARC (figure H-6) showed significantly warmer (approximately 3F) and more moist air (~ 1 g/kg) below 850 mb than that existing above the rural BCC site (figure H-7). In making the daily operational forecast at 0900 with the use of the 0700 data, plus a predicted afternoon surface temperature of 85F, both soundings indicated instability with lifted indices of -4 and -3 at ARC and BCC, respectively. The 1330 soundings at both locations revealed a considerable drying in the lower levels (below 600 mb), and the lifted indices still indicated unstable conditions. Another obvious feature is the significantly cooler and drier conditions evident at BCC between 950 and 650 mb, compared with the other location. The PMQ soundings (figure H-8), made in or near precipitation, show expected major fluctuations in the dew point values.

Low-level wind data based on pibal network measurements made at 1400 and 1600 CDT (figure H-9) do not show any indication of E flow near the surface, as observed in the surface wind pattern at 1300 (figure H-5). There is a marked veering of the wind with increasing height (S at 100 m to SW at 500 m) over the research area at both 1400 and 1600 (figure H-9). It is also evident that wind speeds decreased across the urban region at both times and at the 100 and 200 m AGL levels. This results in convergence over the urban area at these levels.

The mid-morning forecast was for organized convective activity to occur in the afternoon and evening as the cold front to the NW approached the local area; frontal passage was expected at approximately midnight. The morning soundings were moist and unstable. Since instability, moisture, and mesoscale dynamics were present, the situation appeared straight forward. Stratiform rain with imbedded showers was occurring at 0800 within radar range of PMQ and convective activity did occur later in the day. A tracer release into a convective cell in the W portion of the circle was made between 1816 and 1901. Unfortunately, the cell dissipated just as it reached the rain chemistry collection network.

Post analysis revealed that the surface cold front and associated long wave trough to the W moved very slowly to the E. The front moved at an average speed of approximately 10 mi/hr during the period from 0700 (9 August) to 0700 (10 August) and it was ill-defined with little air mass change for 200 mi on either side. The axis of the 500-mb trough at 0700 on 10 August was still to the W of St. Louis, oriented NE-SW through central Missouri (see 10 August case study).

Since convective temperatures were in the low 90's (F) and temperatures in the MMX circle did not exceed the low 80's on this day (figure H-3), large-scale vertical motions were necessary to release the instability observed in the soundings. The 1300 soundings revealed that air parcels had to be lifted approximately 5000 ft beyond the LCL to achieve positive buoyancy. It appears evident from the light precipitation and the lack of well-organized thunderstorms that sufficient vertical motions were not present to achieve the major lifting in the first two rain periods. However, there was sufficient lifting to cause the cloudiness and precipitation observed. Although there was evidence of convergence in the urban area (figure H-5) during the day, it apparently was not deep enough to release the potential instability observed in the soundings. It is equally evident that the evening convective activity was brought about by vertical motions sufficiently extensive to lift low-level air to regions of positive buoyancy.

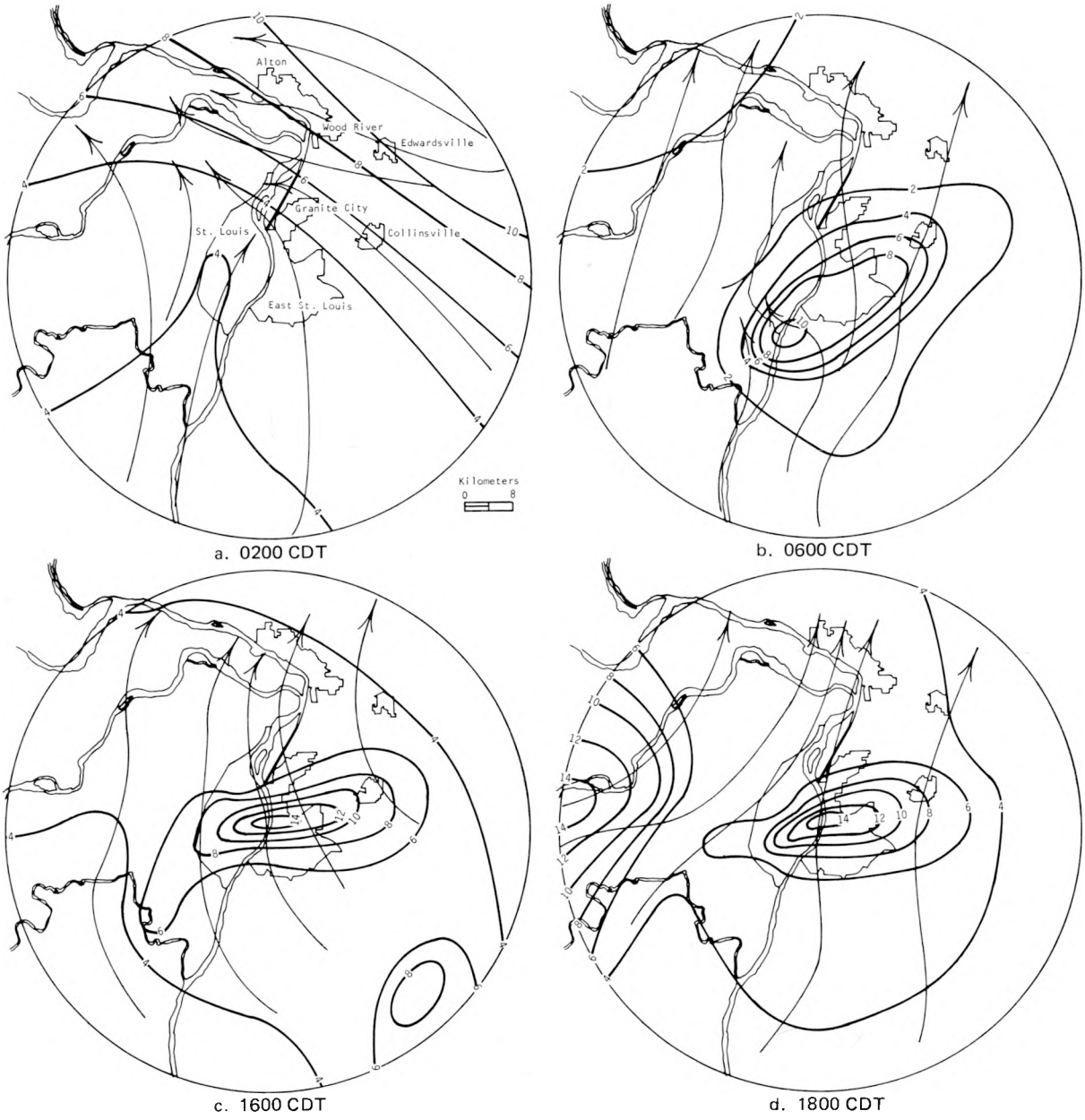

Figure H-5. Surface winds at 0200, 0600, 1600, and 1800 CDT

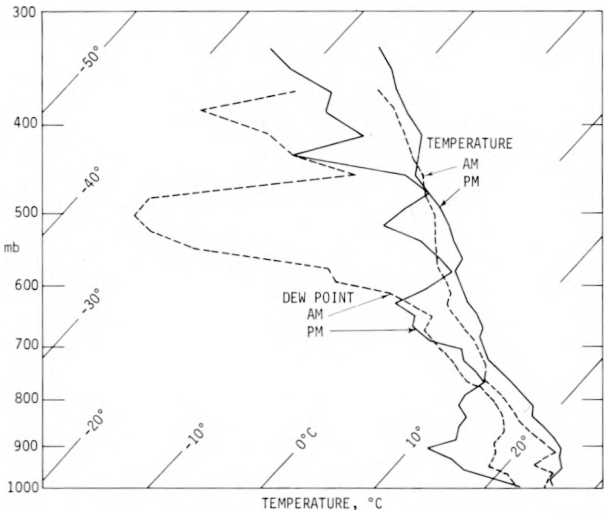

Figure H-6. Radiosondes at ARC for 0700 and 1330 CDT

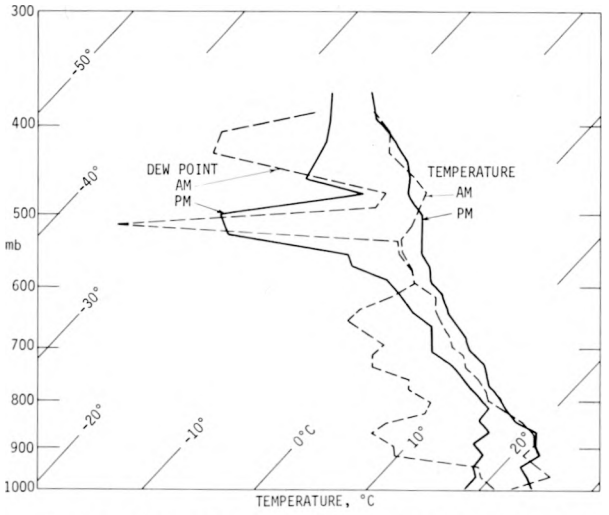

Figure H-7. Radiosondes at BCC for 0700 and 1330 CDT

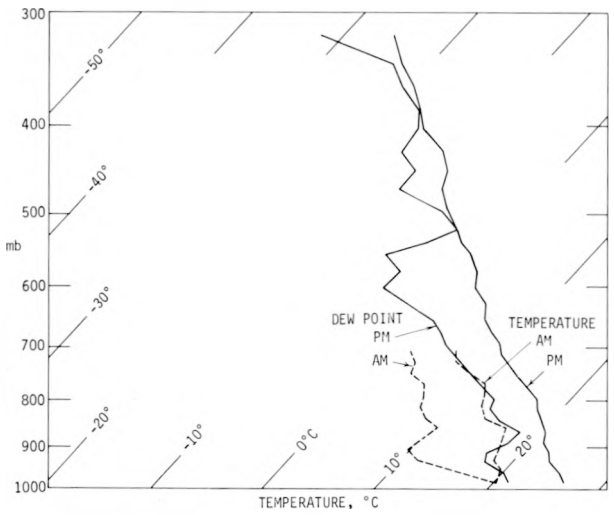

Figure H-8. Radiosondes at PMQ for 0700 and 1330 CDT

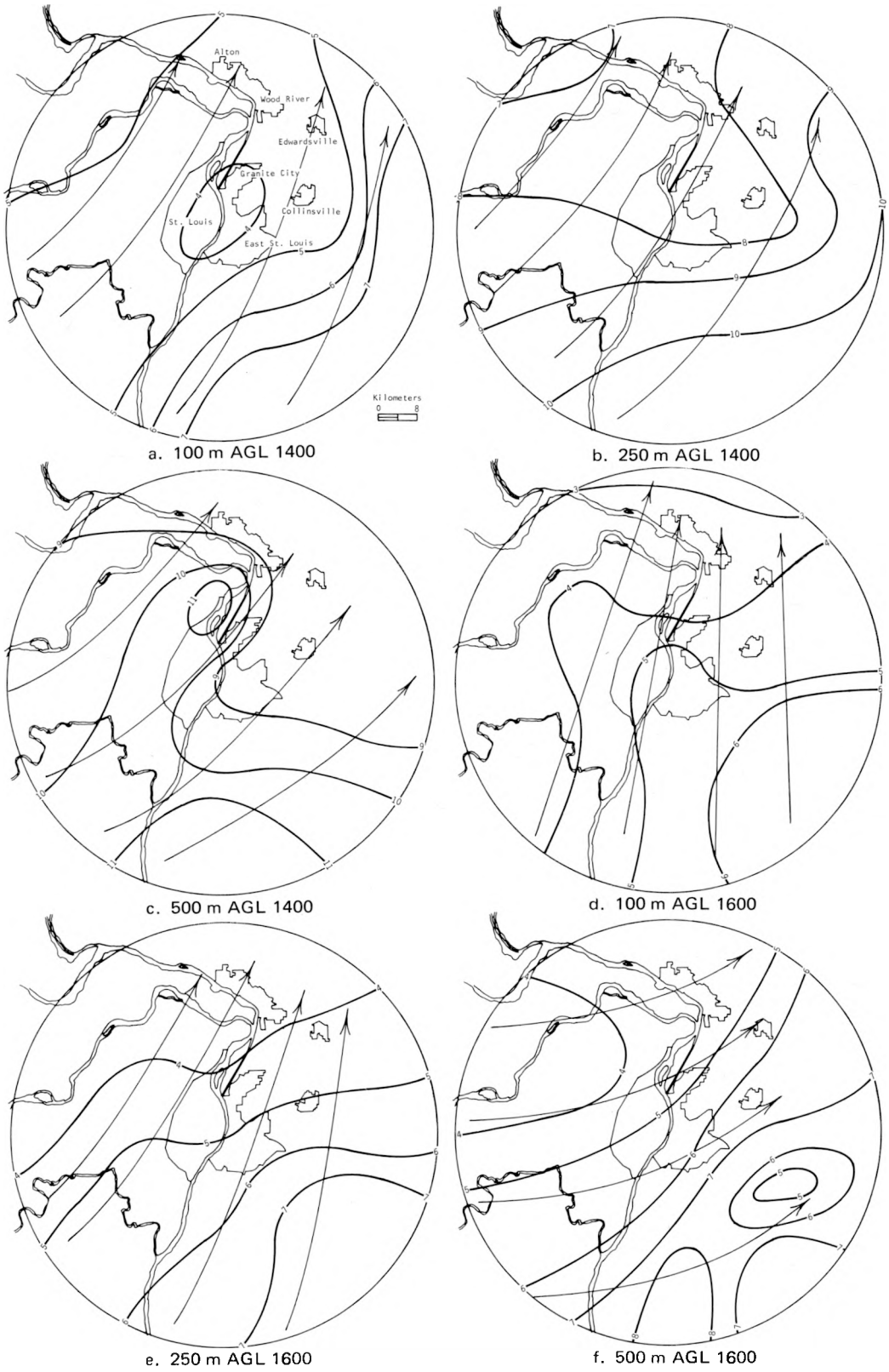

Figure H-9. Low-level wind data at 1400 and 1600 CDT

PRECIPITATION MORPHOLOGY

Raincells

There were three periods of precipitation on 9 August in the MMX circle, as observed from the raingage data. The periods were 0300–0600, 0725–1445, and 1710–2125. The first two periods were mainly stratiform rain with showers. However, light thundershowers occurred with the rain of the second period. Light frequency of thunder was recorded at all thunder observing sites during the second period, and light to moderate frequency of thunder occurred at three sites during the third period (table H-1). RHI 3-cm radar data indicated that the structure of much of the second rain period in the circle was stratiform. The third precipitation period was mainly convective in nature. The three periods will be discussed independently.

Table H-1. Locations and Times of Thunder

TYV	*SLU*	*EDW*	*STL*	*OKV*	*BLV*	*WLO*	*PMQ*
0900–0915	1010–1120	1130–1200	0800–0830, 0900, and 1728–1800	1100–1300	0901–1158	0900–1015 and 1800*	0900–1015 and 1800

**moderate intensity (frequency), all others are light*

Six raincells were observed during the early morning precipitation period (0300–0600), as determined from the raingage data. One of the six cells initiated 10 mi SW of Alton and moved to the NE over Alton–Wood River. The remaining 5 cells had no apparent movement. Table H-2 summarizes some cell characteristics and figure H-10 shows the total rainfall pattern for each cell. The cell which passed over Alton–Wood River (cell 1) lasted longer, had a higher maximum rain intensity, and covered a larger area than the other cells. The surface wind data preceding the precipitation (figure H-5) indicated that the bigger cell likely formed downwind of Alton–Wood River and St. Louis, as did cells 2 and 3. These wind data also indicated that there was low-level convergence in their initiation areas. The temperature and dew point patterns at 0200 (figures H-3 and H-4) indicate that the initiation area of the major cell was relatively cool and moist. These three cells, because of their location of initiation and motion over Alton (cell 1 only), are considered to be potentially 'urban affected' (table H-2), and other cells were apparently not urban affected. The total rainfall pattern for this period in shown in figure H-11a.

Table H-2. Raincell Characteristics Associated with 0300–0600 Rain Period

	Urban (3 cells)	*Non-urban (3 cells)*
Average duration, min	53	37
Average maximum intensity at initiation, in/hr	0.2	0.1
Average maximum intensity, in/hr	0.9	0.1
Average cell area, mi^2	41	9
Average water volume, ac-ft	248	24

Table H-3. Raincell Characteristics Associated with 0725–1445 Rain Period

	Urban (12 cells)	*Non-urban (84 cells)*
Average duration, min	47	22
Average maximum intensity at initiation, in/hr	0.5	0.6
Average maximum intensity, in/hr	1.5	1.1
Average cell area, mi^2	52	26
Average water volume, ac-ft	603	212

The second precipitation period of the day (0725–1445) included 97 raincells in the MMX circle, 12 of which initiated and/or passed over St. Louis or Alton–Wood River. Table H-3 summarizes the associated cell characteristics sorted on the basis of their locales and presumed effects.

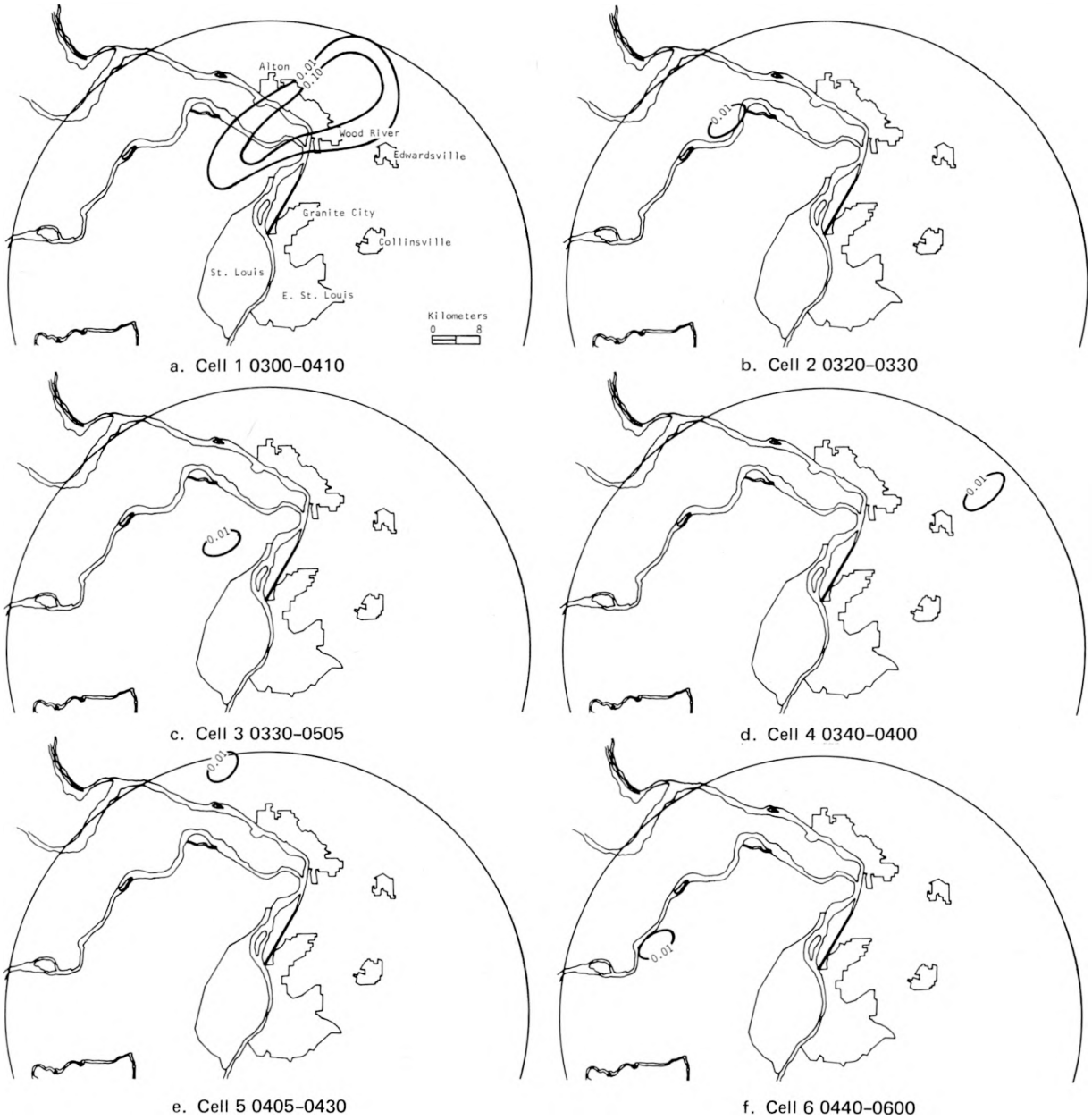

Figure H-10. Total rainfall for six cells in 0300-0600 rain period

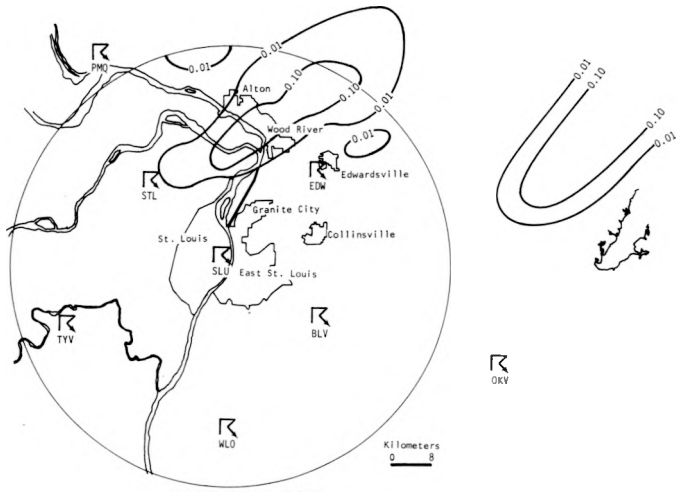

a. 0300-0600 CDT

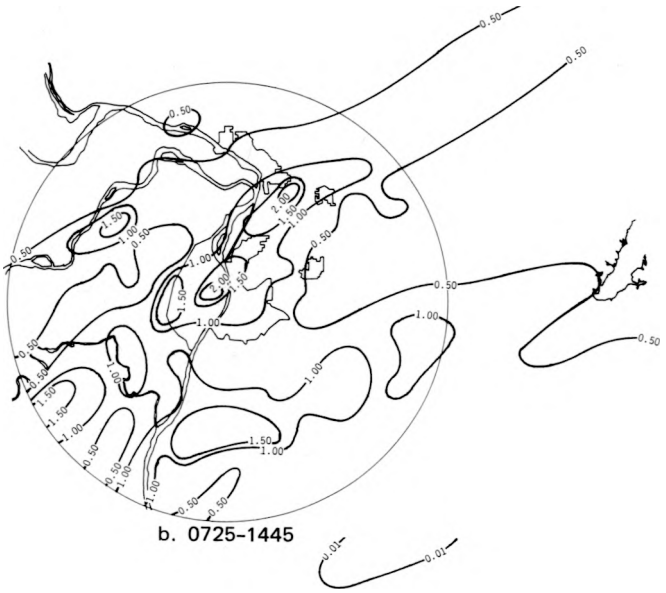

b. 0725-1445

c. 1710-2125

Figure H-11. Total rainfall for the three rain periods on 9 August

The cells initiating or passing over the urban regions during this rain period lasted considerably longer, achieved a higher maximum rain intensity, covered a larger area, and produced more rainfall than did the non-urban cells. The total rainfall pattern for this period is shown in figure H–11b.

The third precipitation period (1710–2125) included 25 raincells, one of which was treated with tracer material after it entered the MMX circle. The total rain pattern for the period appears in figure H–11c. The major cells during this period, including the 'tracer cell,' dissipated before reaching the urban area. Examination of low-level wind flows and the placement of these cells leads to the conclusion that the convective cells of the third system were neither enhanced nor dissipated by any urban conditions.

Total rainfall for the three precipitation periods is shown in figures H–11a, b, and c. Also shown are the locations of the thunder measuring stations referred to in table H–1. No hail was recorded in the MMX circle.

Radar Echoes

Much of the precipitation, as depicted by the 10-cm PPI radar, during the second rain period was stratiform in nature. Rain occurred over all of the MMX circle. Some moderate to heavy rain amounts occurred with thundershowers and associated shower activity. The echoes during the final rain period were mainly convective and were restricted to the W third of the MMX circle.

Prior to the final rain period in the circle, during which a tracer mission was completed, a few major cells had formed about 60 mi to the W of PMQ and moved from the WNW. All but one dissipated before reaching the MMX circle. The one storm echo that entered the circle was 'treated' with tracer material released W of St. Louis. The decision to release tracers into such a storm in its mature stage was based on one of the tracer study goals of 1973 which was to release material into a mature storm several miles W of the rain chemistry network to determine if the material ever appeared in that network. However, the treated cell dissipated before reaching the network and the hoped-for experiment failed. Table H–4 summarizes some characteristics of four of the more important echoes of the third period that initiated and dissipated well within range of the 10-cm radar. Figure H–12 shows the last radar-observed position of the 'tracer echo,' as well as the inception and dissipation locations of the major cells during this precipitation period. A radar power outage between 1834 and 1900 did not permit following the cell through its dissipation stage.

Table H–4. Summary of Major Cell Echo Characteristics Associated with 1710–2125 Rain Period

Cell number	*Duration (hr)*	*Inception time and locale*
1 (tracer cell)	4.1	1445 (W of network)
2	3.9	1540 (W of network)
3	1.1	1629 (W of network)
4	0.5	1657 (W of network)

Aircraft Observations of Clouds

The flight track of the aircraft during its tracer release is shown in figure H–12. The flight meteorologist observed strong 1000 ft/min updrafts in the inflow air at the leading (E) edge of the storm at the initiation of the tracer release (1816). However, the cell rapidly decreased in intensity shortly thereafter and dissipated by 1900. A maximum echo top of 35,000 ft was ob-

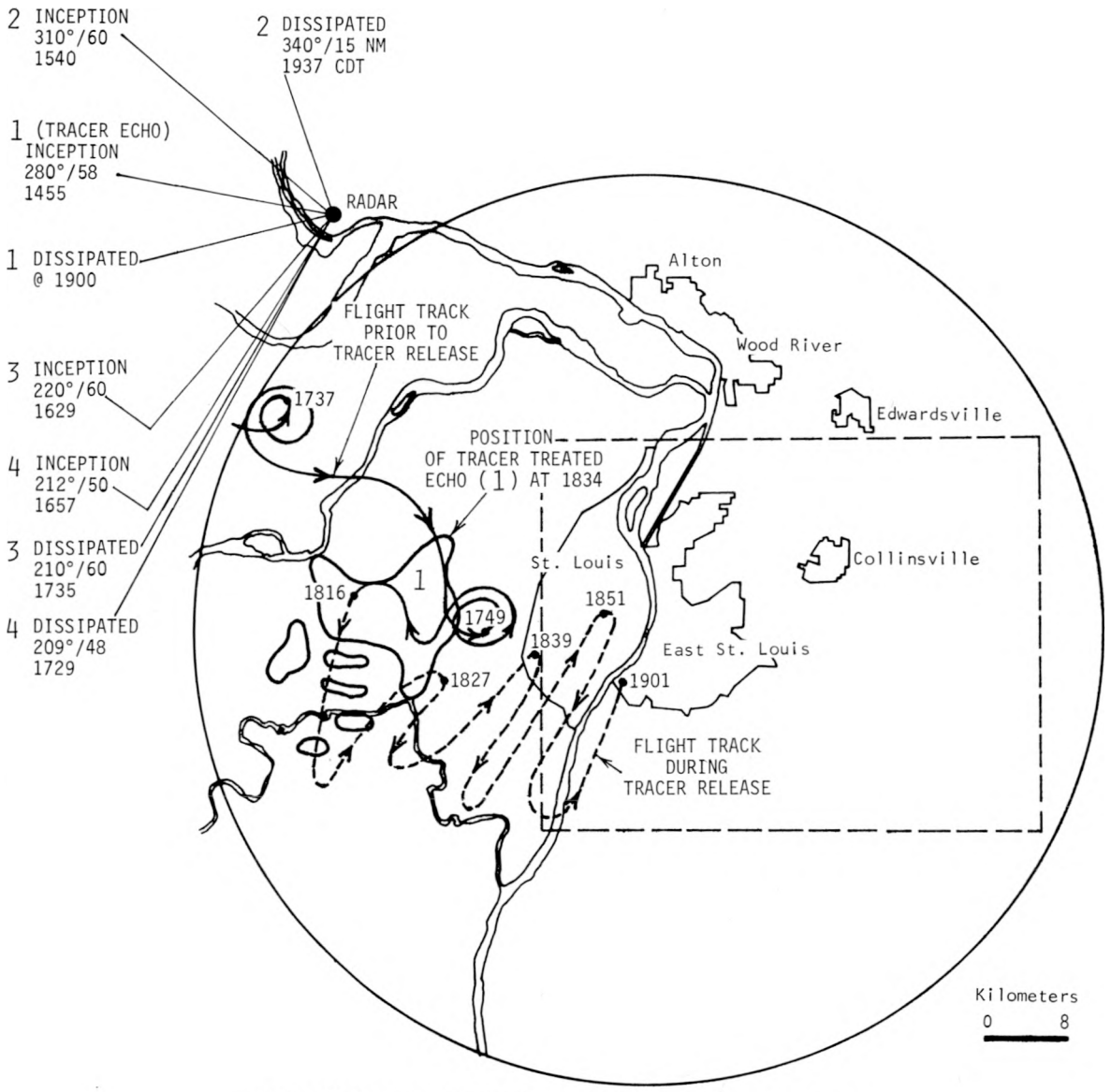

Figure H-12. Locations of echoes and flight track for tracer release

served by the 3-cm radar at the tracer initiation at 1816. During the 45-min period of tracer release, the flight meteorologist observed the maximum updrafts to decrease to < 200 ft/min, and clouds ahead of it all became diffuse. This cell was observed to have a height of approximately 45,000 ft 20 min earlier in its lifetime, and it had been slowly decreasing in height and intensity before reaching the circle. Much of the network rainfall in the third system (figure H-11c) was from the raincell in which the tracer was released. Inspection of figure H-11c reveals that the rain ended before it reached the rain chemistry network.

CONCLUSIONS

The first rain period (0300-0600) was mainly stratiform rain with six small cells that developed in the circle. Three cells initiated within or downwind of the urban area, as based on airflow data; these cells, on the average, lasted longer, were more intense, and covered a larger area than the 3 cells in the non-urban area. It is concluded that down-city cells may have been initiated and/or intensified by the Alton-Wood River industrial complex. The initiations and locations of the remaining cells indicate these were not influenced by the urban areas.

The second precipitation period (0725-1445), which was also stratiform rain but with a few thundershowers, produced rain over the entire circle. A comparison of raincells that initiated or passed over Alton-Wood River or St. Louis with those that did not indicates that the potential urban effect cells had a greater average maximum rain intensity, lasted longer, and produced more rain. The total rainfall pattern for this period corroborates these findings. The tentative conclusion for this precipitation period is the same as in the first period; raincells that appeared to be potentially influenced by the urban atmosphere were, on the average, greater rain producers.

The third precipitation period (1710-2125) was totally convective in nature. It was composed of storms that developed well to the W of the circle, moved to ESE and dissipated shortly before or just after entering the W side of the circle. One of the major cells during this period was treated with tracer material toward the end of its lifetime. The location of these cells, in reference to low-level flow, indicates that the urban factors likely did not play any role with the precipitation cells during this time. In fact, the system began dissipating 30 mi W of St. Louis and the urban area could not have had a role at that position. Furthermore, the prior rains had effectively scavenged out many aerosols and had so altered the surface and low-level patterns of heating, moisture, and airflow potentially related to the urban area so as to minimize the possibility of urban effects on clouds and precipitation processes.

It is evident from the raincell information presented that cells which initiated or passed over the urban region were quite different from those which did not. The crucial question to be answered is, "Can it be demonstrated that the urban atmosphere influenced the cells which passed over the region?" Table H-5 shows the lifting condensation level, convective condensation level, and mixing depths for various times during the day at three locations. Cloud bases on this day were represented more closely by the LCL rather than CCL since observed surface temperatures fell short of the convective temperature by approximately 10F.

Table H-5. Convective and Lifting Condensation Levels, and Mixing Depths (ft) in the St. Louis Region

	0700 CDT			*1000 CDT*			*1330 CDT*			*1800 CDT*		
	LCL	*CCL*	*OMD*	*LCL*	*CCL*	*OMD*	*LCL*	*CCL*	*OMD*	*LCL*	*CCL*	*OMD*
PMQ (west)				500	5000	SFC	3000	5500	2000	SFC	3000	SFC
ARC (city)	2000	5000	SFC				2500	6000	1000	500	1000	2000
BCC (east)	2500	5500	2000	1500	2500	1000	1500	5000	SFC	500	500	1800

Although the observed mixing depths indicate that near surface air parcels probably were not convected up to cloud base levels, it seems clear that near surface parcels were being lifted since extensive low cloudiness was observed throughout the day. As a result, it seems appropriate to conclude that the urban atmosphere was being lifted to the condensation level and became involved in the cloud systems that developed or passed over the urban region. In summary then, this case study suggests that the urban complexes were causative agents for increasing precipitation characteristics of some cells.

I. AIR MASS STORMS OF 10 AUGUST 1973

John L. Vogel

CONTENTS

I. AIR MASS STORMS OF 10 AUGUST 1973

INTRODUCTION

On the afternoon of 10 August four meso rain systems isolated in time and space occurred in the MMX circle. These systems on 10 August were chosen for an intensive investigation since they appeared to reflect a situation where 1) two isolated storm systems developed over St. Louis (indicating possible urban effects), and 2) two isolated storm systems developed over nearby rural areas. Hence, a comparative study of them should yield information on the reality and types of urban effects. The storms all developed in a warm air mass well S of any front. They were due to local instability and were true air mass storm systems unrelated to frontal activity.

Exceptional data collection was accomplished on 10 August. Useful aircraft flights were made and pibal and radiosonde operations were conducted at ideal times. Radar operations provided outstanding data on storm morphology.

The first mesosystem (I) on 10 August developed around 1400 over St. Louis and definitely had a relationship to urban conditions. This system lived 3 hr and drifted slowly to the SE before dissipating. Another mesosystem (II) developed just E of the SE corner of the MMX circle at around 1400. This rural system spread to the W and moved into the MMX circle at 1600. System III was first detected by NWS radar at 1440 CDT in the rural area about 50 mi NW of the MMX circle. This system moved slowly to the SE, and near its dissipating stage, it passed along the N edge of the circle. A fourth system (IV) developed because of apparent urban effects in N St. Louis shortly after 1600 and grew rapidly to the E and W over the urban area as it moved S over St. Louis.

SYNOPTIC WEATHER CONDITIONS

Macroscale

At 0700 the surface weather map (figure I-1) showed a cold front extending SW from a low near James Bay, Canada. The front was situated near the N edge of the MMX circle. There was very little thermal discontinuity in the immediate vicinity of the front; however, there was evidence of a moisture discontinuity. The midwestern area behind the front was characterized by dew point temperatures in the 50's to low 60's (°F), whereas the area S of the front had dew point temperatures in the upper 60's to low 70's, characteristic of its tropical air mass.

The SE corner of the United States and the Gulf States were dominated by the Bermuda High, but its influence had definitely weakened in the 24-48 hr prior to 10 August. The pressures over the SE fell 5 to 6 mb during this period, and stable air, associated with this high, was no longer evident over the MMX circle. Except for a 'bubble high' over W Nebraska, the region to the lee of the Rockies was dominated by a weak trough. There were lows over the Panhandle regions of Texas and Oklahoma and along the Kansas–Oklahoma border. The low along the Kansas–Oklahoma border was associated with a mesosystem that maintained itself throughout 10 August, and by 1900, this low had moved into SE Oklahoma.

The 850-mb chart at 0700 (figure I-2) showed a low N of Lake Superior, with a trough extending into S Illinois. A ridge extended N from a center of anticyclonic flow over S Louisiana to the W Dakotas. The thermal packing at this level gives supporting evidence of the location of the surface front. The flow over the MMX circle at 0700 CDT was from the WNW at 10 to 15 kt, but by 1900 the flow shifted and was from the WSW at 10 to 15 kt.

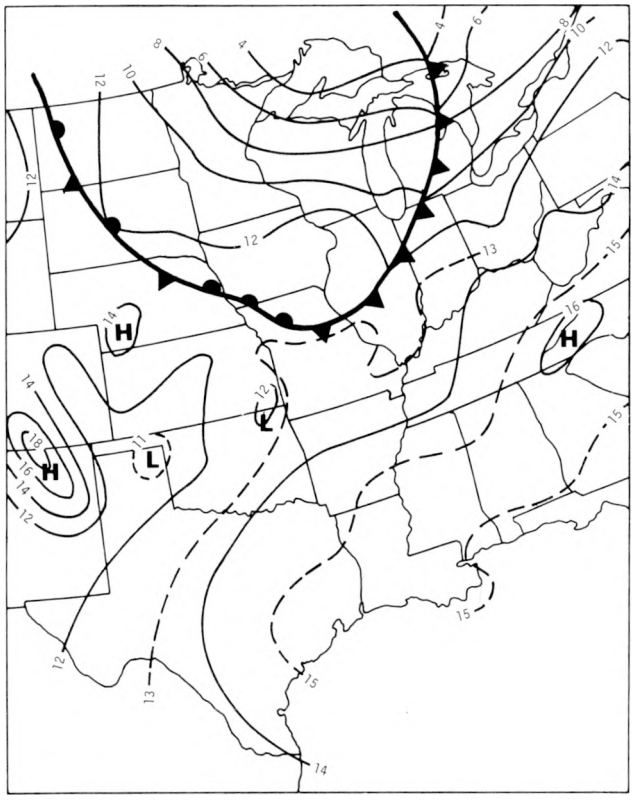

Figure I-1. Surface weather map at 0700

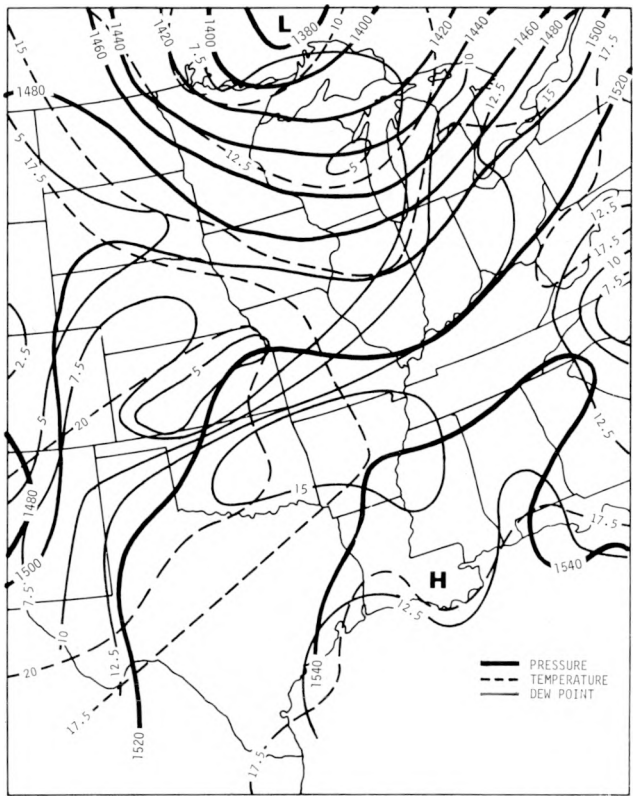

Figure I-2. 850-mb map at 0700

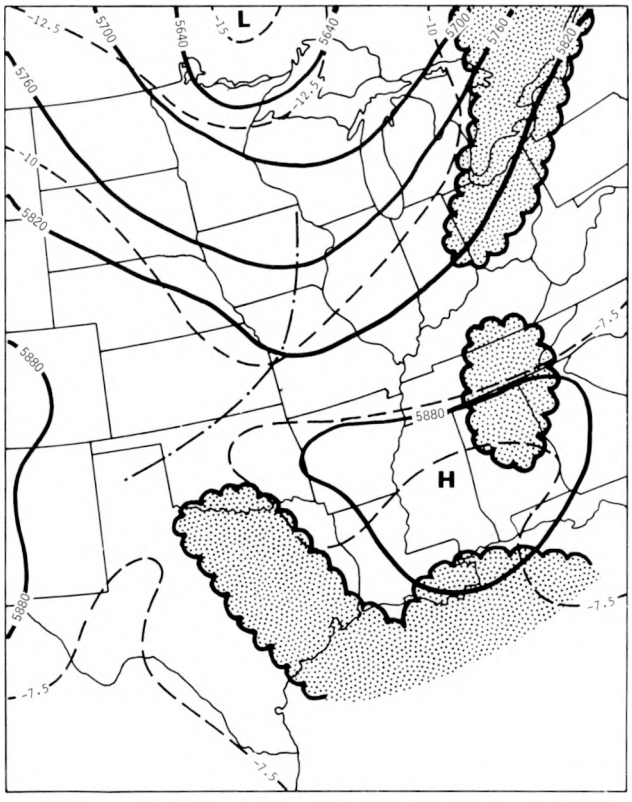

Figure I-3. 500-mb map at 0700

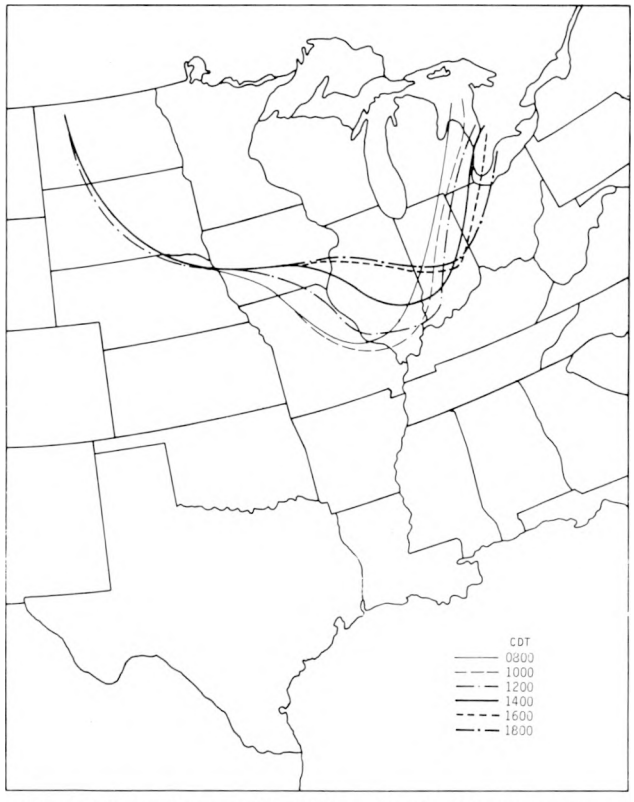

Figure I-4. Isochrones of frontal position for 2-hr intervals

The air over most of the upper Mississippi Valley appeared to have a continental polar origin, while the air to the lee of the Rockies and over Kansas and Nebraska was modified maritime polar air. The 10C isodrossotherm (figure I-2) marked the advance of the tropical air to the N at 850 mb. Another prominent feature was the intense moisture gradient from central Kansas to NE Oklahoma (10C over 2 degrees of latitude). This gradient was formed as a result of an extremely dry pocket of air over central Kansas, and apparently was the result of a subsidence zone behind the mesosystem over the Kansas-Oklahoma border. There was no evidence of this dry air later in the day, in fact, most of the Kansas-Nebraska area at 850 mb had dew points in excess of 10C by 1900.

At 0700 the 500-mb map for the S half of the United States (figure I-3) was dominated by light winds and general anticyclonic conditions. The circulation pattern over the N half of the nation was controlled by a trough with a low pressure area centered N of Lake Superior. The flow over the MMX circle at this level was from the WSW. By 1900 the anticyclonic flow over the S half of the United States was breaking down. The trough at 1900 extended from Lake Superior to the S tip of Texas and the flow over the Southern Great Plains, the lower Mississippi River Valley, and the Southeast was in an organized pattern.

Over most of the N reaches of the Midwest, the air at 500 mb was very dry with most dew point depressions at 30C or more. The only moist areas (dew point depressions $\leqslant$ 5C) were over the St. Lawrence River Valley and Ohio. Both of these areas were associated with active areas of convection that had moved across the MMX circle on 9 August 1973.

A feature of primary interest throughout the day of 10 August is the position of the front relative to the MMX circle. Figure I-4 shows the surface frontal positions as a function of time. Isochrones of frontal position are given for 2-hr intervals beginning at 0800. The frontal positions shown on figure I-4 differ radically from the NWS analysis after 1000. The NWS analysis maintained the front to the S of St. Louis during the entire day of 10 August. However, detailed analyses of all the available synoptic and mesoscale data from the NWS and METROMEX networks indicated that the front moved back across the St. Louis area at approximately 1200.

By 1400 the front was well to the N and E of St. Louis, and by early evening it moved N into the central portions of Illinois and Iowa. The timing of the surface position of the front is very important because the first precipitation that fell over the MMX circle began at 1416 over East St. Louis. At this time, the front was about 70 mi NE of the center of the circle, and the front did not appear to be a factor in the initiation of this precipitation. Additional evidence of the movement of the front to the N was provided by the thermal packing and the general configuration of the contour pattern on the 850-mb map at 1900.

Mesoscale

Figures I-5 through I-8 are composite temperature analyses of data from the MMX hygrothermograph network and from NWS surface reporting stations. They are combined so that one can readily see the large influence that an urban area and local heat and moisture sources exert on surface measurements of temperature and dew point.

The large-scale surface temperature pattern at 0700 (figure I-5) showed a trough of cooler temperatures from W-central Illinois to the vicinity of St. Louis. A second area of cooler air was evident over central Missouri. The thermal packing over E Illinois was characteristic of the packing one would expect along a front.

The 0700 surface temperatures across the MMX circle show three discrete maxima ($\geqslant$ 70F): 1) in the NW bottomlands between the Missouri and the Mississippi Rivers, 2) to the SW in the

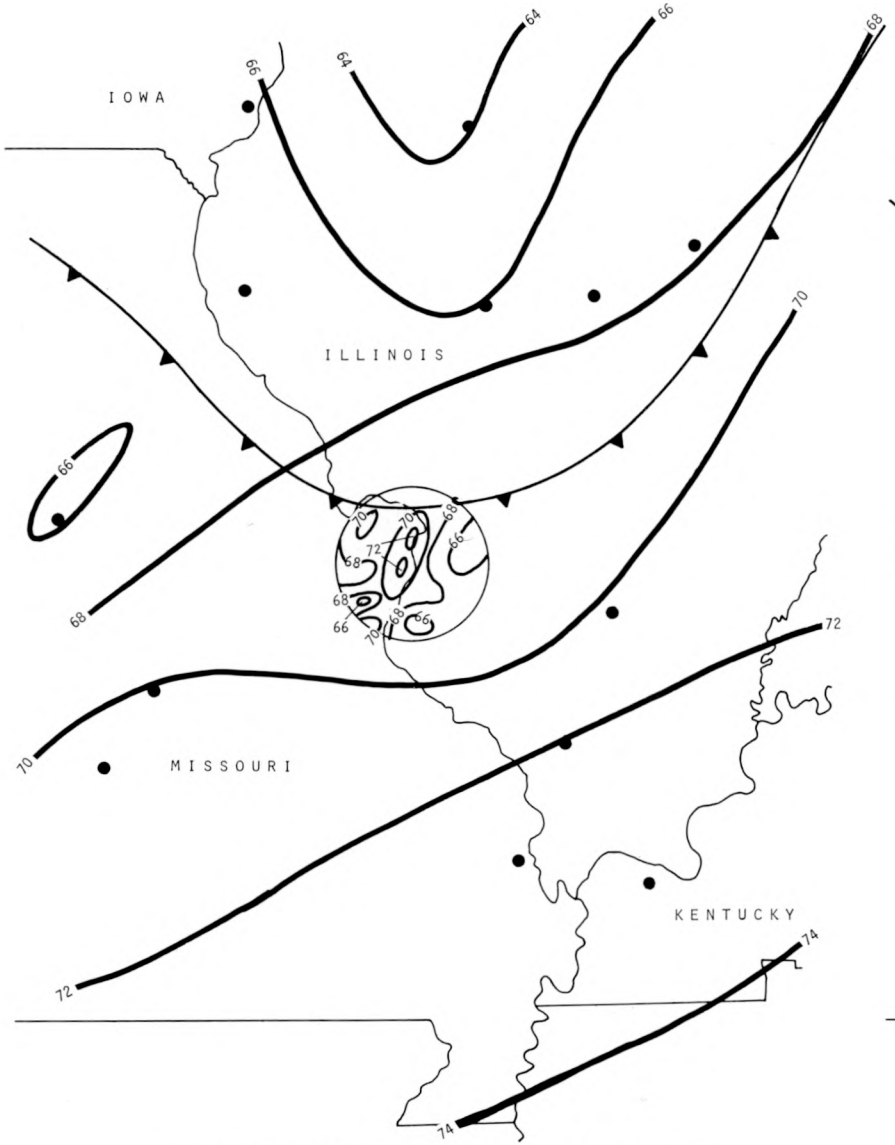

Figure I-5. Large-scale surface temperature pattern at 0700

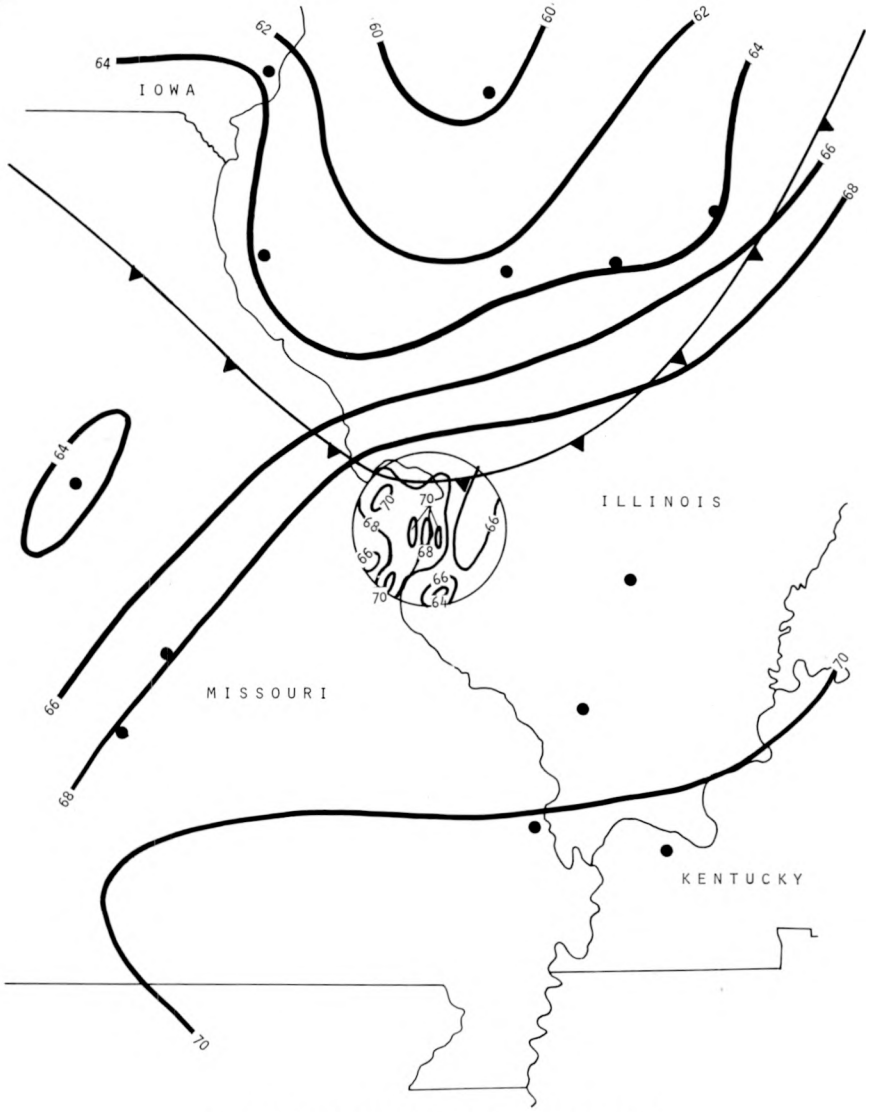

Figure I-6. Surface dew point pattern at 0700

foothills of the Ozarks, and 3) over the inner city of St. Louis. The coolest temperatures were located to the E of the Mississippi River, in a region that is essentially rural. The warmest surface temperatures observed were in the center of the city (73F), while 15 mi to the E of the city, the temperatures dropped to 65F. The 0700 temperature pattern was chosen because it was representative of the thermal pattern observed over the MMX circle from 0100 to 0700.

The surface dew point pattern at 0700 (figure I-6) shows a large-scale pattern with extensive packing of the surface isodrossotherms delineating the surface front over central Illinois and NW Missouri. A moisture gradient of 8F over 100 mi existed from W-central Illinois to just N of St. Louis. The dew point pattern over the MMX circle was quite complex. The lowest dew points were E of the Mississippi River, where the relative humidity was nearly 100%. Over the heavily congested areas on either side of downtown St. Louis, two 70F dew point maxima were observed, while over downtown St. Louis, a 68F minimum was observed. The station which measured this minimum was located in the Mississippi River Valley. Other river valley observing stations showed relatively low ambient temperatures at this hour compared with surrounding stations, while the air at these stations was either saturated or only a 1F spread existed between the temperature and the dew point. However the temperature was relatively warm at ARC and the spread between the temperature and the dew point was 5F. This suggests that the moisture pattern over the central portion of the city at this time was highly complex, and that the air over this region of the MMX circle was modified somewhat by the urban area.

Heating became noticeable at 0800 as temperatures rose 3-5F from 0700. The 0900 thermal pattern over the MMX circle remained relatively constant until 1400, 16 min before the first rain began over East St. Louis on 10 August.

Figure I-7 presents the temperature pattern at 1400 in the MMX circle and the surrounding 2-state area. The general area features a temperature minimum to the SW associated with an area of showers and thunderstorms. The MMX circle was in a broad band of relatively warm temperatures, but there were three discrete maxima within the circle at 1400. They were concentrated over the bottomlands between the Missouri and Mississippi Rivers, over St. Louis, and over East St. Louis. Another maximum lay over the SE edge of the MMX circle. This maximum was established by 0800 and maintained itself throughout the day.

The dew point pattern and frontal position at 1400 (figure I-8) shows a trough of low dew points over E Illinois where the lowest temperatures were observed (figure I-7). The highest dew points ($\geqslant$ 72F) reported by NWS stations were over SE Missouri. The dew point pattern over central Illinois seemed to indicate that the frontal position was located a little farther to the S. However, the warm front was moving quite rapidly to the N and the dew points in the vicinity of the front did not have time to respond to the warm, moist air being advected to the N. By 1500 the dew points in this region rose another 1-3F as tropical air continued to push to the N. The pattern in the MMX circle showed a maximum (72 to 75F) E of the Mississippi, a dramatic change from the minimum which was observed in this region at 0700 (figure I-6). Another maximum (72F) to the W was in the bottomlands of the Missouri River. The surface dew points over downtown St. Louis showed a relative minimum. Examination of the 1400 temperature and dew point patterns shows that a broad, warm, moist zone existed over the region E of the Mississippi River into the extreme SE edge of the circle. Another warm, moist zone was located over the bottomlands N of St. Louis.

One of the important conclusions from figures I-5—I-8 is that the NWS network of observing stations is not sufficiently dense to describe the pattern over the urban area. This is critical because if warm, moist zones are a key in the production of inadvertent urban rainfall, they must be known for forecasting such rains.

The temperature and humidity patterns over the MMX circle during the remainder of the afternoon were largely determined by the presence of convective activity. Some of this activity

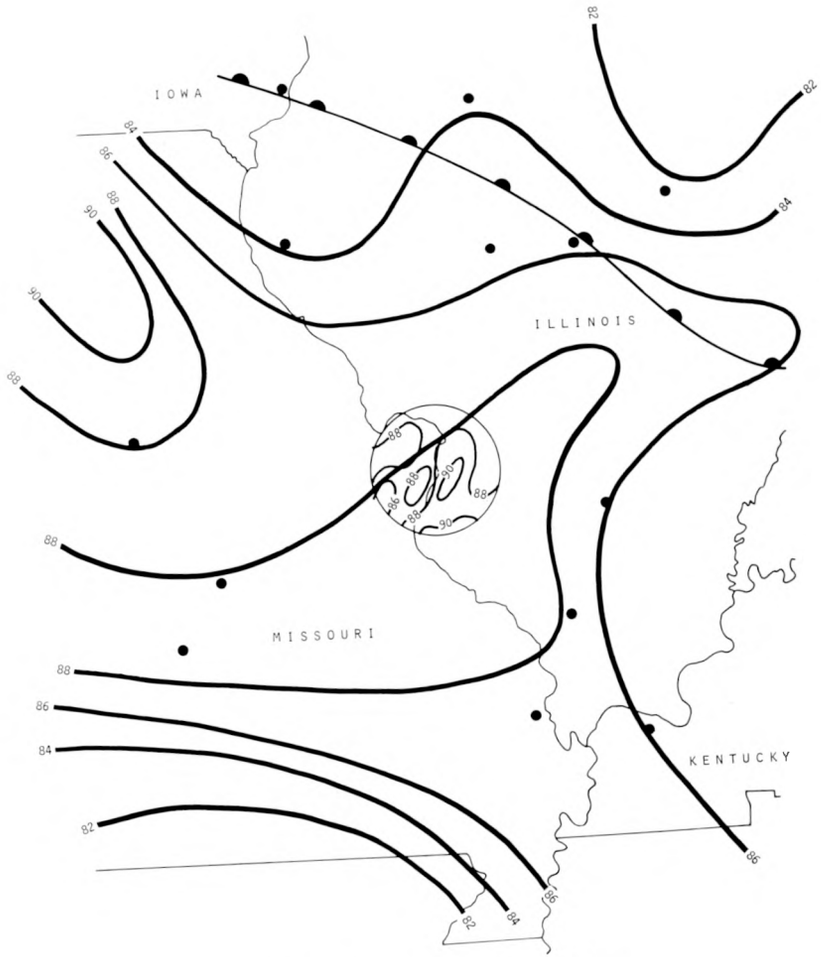

Figure I-7. Temperature pattern at 1400

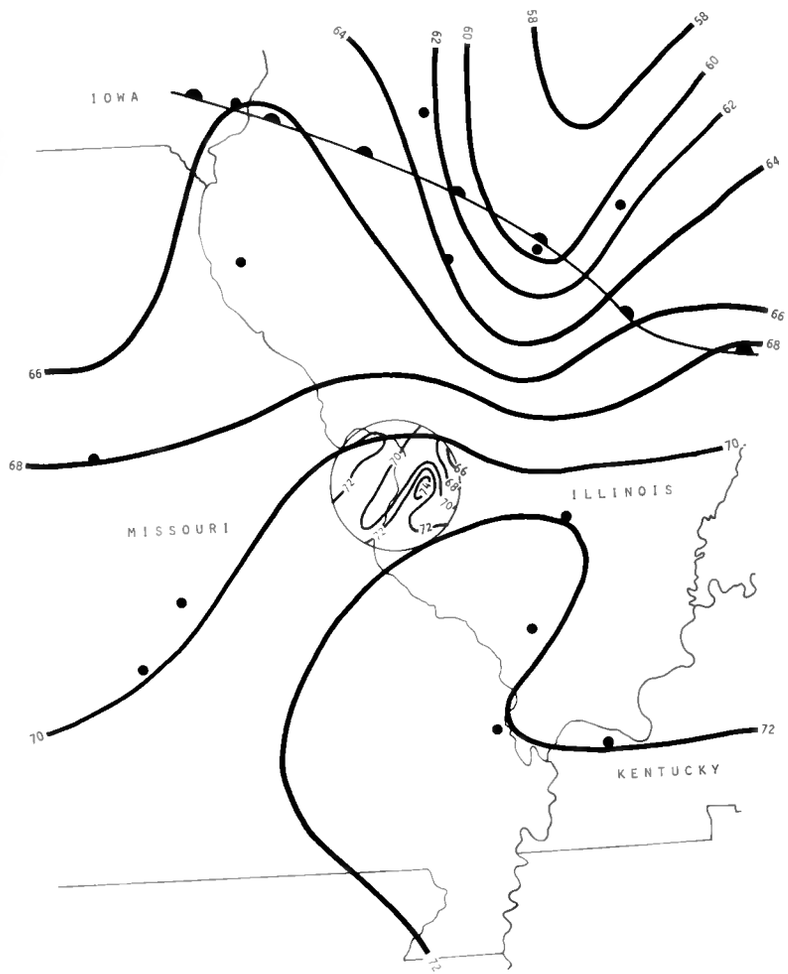

Figure I-8. Dew point pattern and frontal position at 1400

developed at 1416 (systems I and II). Systems III and IV began to affect the circle at about 1600, and the pertinent temperature analysis of that time period will be discussed later.

Soundings Analysis

Soundings over and in the vicinity of the MMX circle were scheduled at 0700 and again in the early afternoon at 1330. Unfortunately, there were no soundings or low-level wind observations scheduled during the forenoon hours to prove that the front had passed. The soundings indicate that the air masses sampled at approximately 0700 and 1330 were very similar and showed no real effect due to the frontal passages.

The PMQ sounding at 0736 (figure I-9a) shows an inversion from the surface to about 910 mb. The higher temperature profile shows that the atmosphere was conditionally unstable. The convective condensation level and the LCL were coincident at 885 mb (3800 ft). The convective temperature was 82F, and it was predicted that this temperature would be reached between 1100 and 1200. As will be shown later, this is about the time Cu clouds formed over a large part of the circle.

At 0736 the Showalter stability index was -1, and the lifted index was -4. Both indices indicated that the air mass was unstable and capable of convective activity, provided that enough heating or additional lift was obtained. The dew point profile indicated that the air mass was relatively moist up to 400 mb. This was in good agreement with soundings taken at nearby NWS radiosonde stations.

The 1340 soundings (figure I-9b) indicated that a superadiabatic lapse rate developed in the low levels (surface to 930 mb) at PMQ. The Showalter stability and lifted indices were relatively unchanged from the morning sounding. The convective condensation level and the LCL had raised from 3800 to 5000 ft. There was some advection of moisture in the middle layer from 700 to 5000 mb, and the radiosonde went through a thin layer of Ac clouds at about 600 mb (13,000 ft). These clouds moved over the W edge of the MMX circle between 1200 and 1300.

The afternoon sounding at PMQ shows that there was sufficient heating within the air mass for convective activity to form. Apparently, the movement of the front back and forth across the region had little overall effect on the structure of the air mass which encompassed the St. Louis area on the afternoon of 10 August.

Airflow

The surface winds throughout the morning hours were confused. There was no consistent wind direction because the frontal zone remained in the vicinity of St. Louis. However, even in this situation with the front moving across and then backing to the N, the city surface stations seemed to be disturbed by some local circulation. The rural sites indicated that the front passed, but the city stations did not. It was hard to determine if the frontal zone was disturbing the winds in the lower kilometer during the morning over the city, or if a local circulation caused by the urban area was perturbing the winds over the city. By 1200 the front was moving across the metropolitan St. Louis area. Figure I-10 shows the 1200 streamline and isotach fields of the averaged wind at 300, 750, and 1500 m MSL. These winds are the average of single theodolite balloon runs released at 1130 and 1200.

The flow through approximately the first kilometer was disturbed and showed the influence of the frontal zone as it moved to the N. At this time the synoptic analysis placed the S boundary of the front over the St. Louis area. The flow at 300 m was very similar to that at the surface.

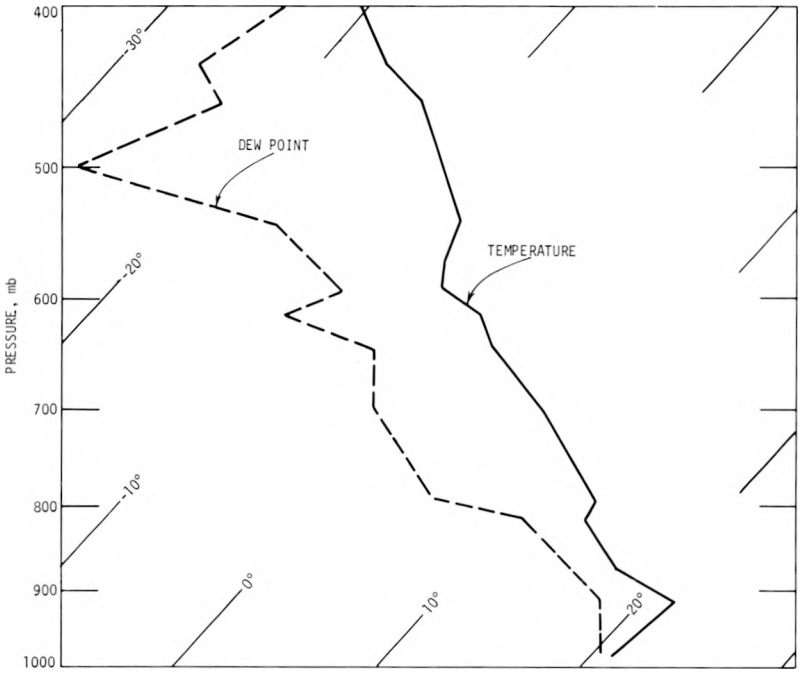

a. 0736 CDT

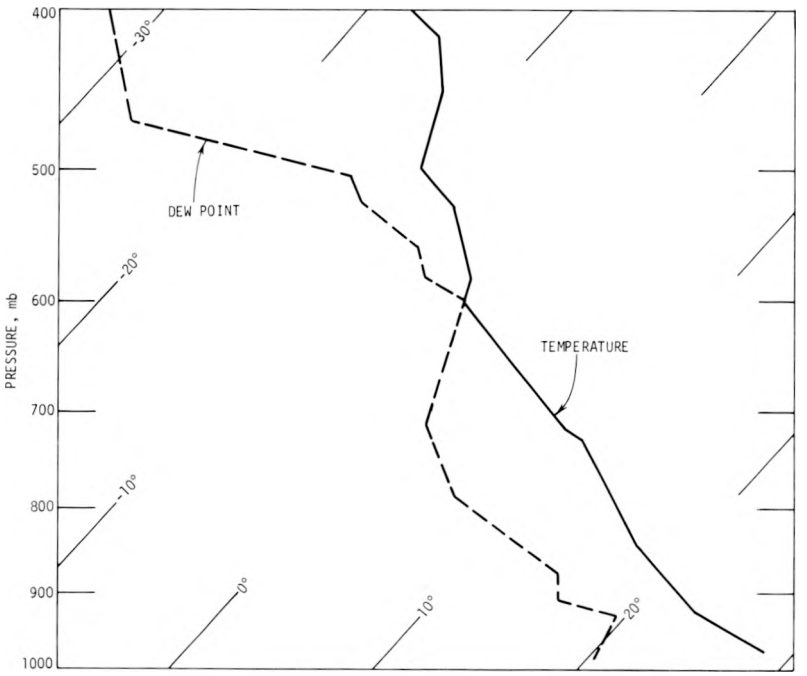

b. 1340 CDT

Figure I-9. Soundings at PMQ

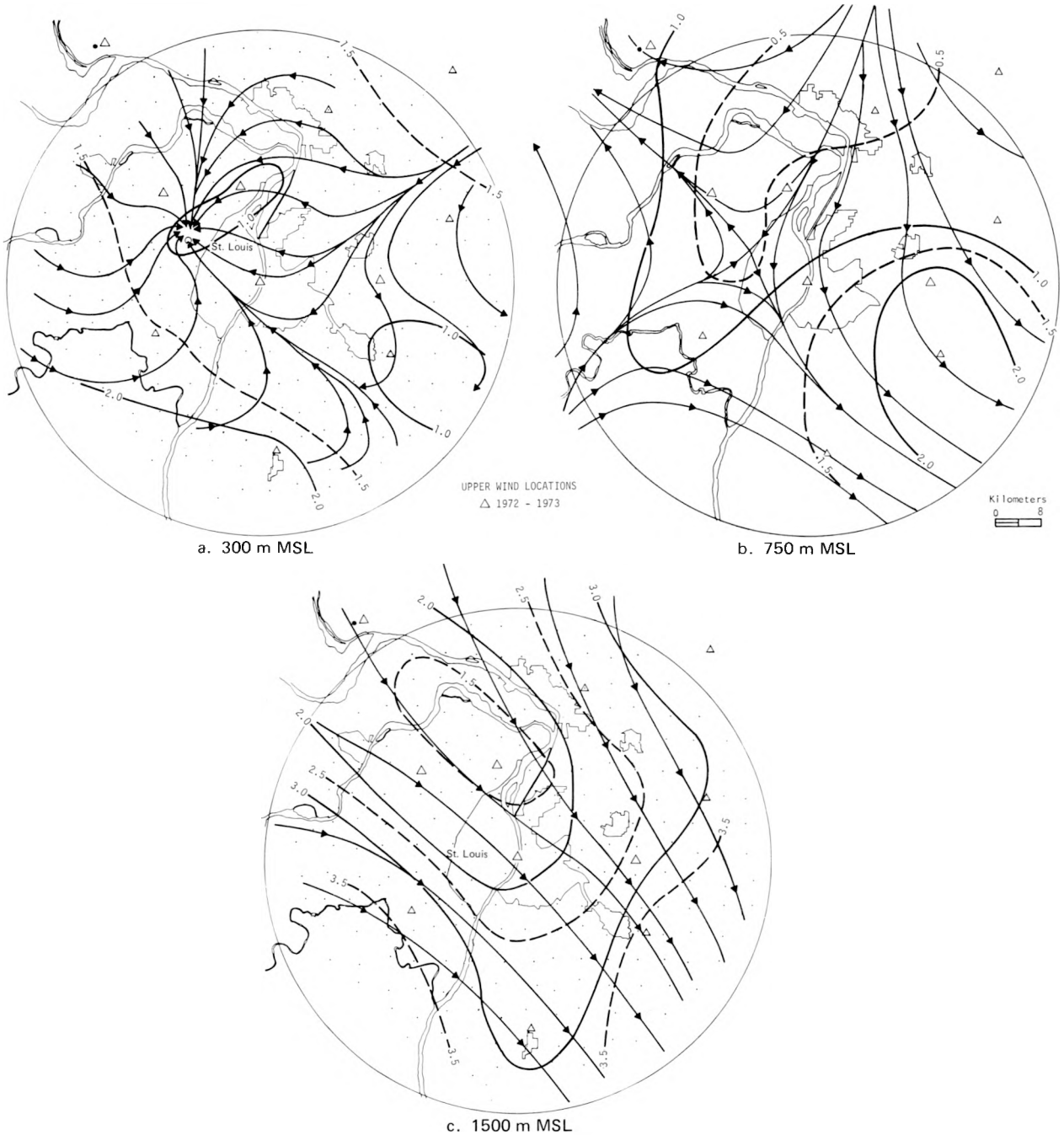

a. 300 m MSL

b. 750 m MSL

c. 1500 m MSL

Figure I-10. Streamline and isotach (m/sec) fields of the averaged wind at 1200

At 1200 the 300-m level (figure I-10a) showed two asymptotes of confluence. One extended from the bottomlands to W of St. Louis, and the other extended from the SE edge of the MMX circle to a small organized vortex to the W of St. Louis where both asymptotes met. Winds from the N were noted over the N two-thirds of the circle. The only winds from the S were over the extreme S sections of the network. At 750 m (figure I-10b), a neutral point (col) was evident and the streamline field showed that the flow was being perturbed by the frontal zone even to this level. Once again the predominant wind direction over the network was from the N, with winds from the S only over the SW edge of the circle. The influence of the frontal zone as it moved to the N across St. Louis was noted in approximately the first kilometer MSL over the MMX circle. The flow at 1500 m (figure I-10c) was from the NW across the whole network. There was a zone of confluence S of the Missouri River at 1500 m and confluence was noted at all levels from the surface to 1500 m in this region.

By 1400 the front was located 70 mi N of St. Louis (figure I-4). Figure I-11 shows the streamline and isotach (m/sec) patterns at 1400 for 300, 750, and 1500 m MSL. Once again the surface flow pattern and the 300-m pattern were well correlated. The flow through the first 1200 m was now generally from the S. An asymptote of confluence was noted over the N section of the network (figures I-11a and b). This zone was located in the same area through the first kilometer. There was little evidence of any confluence in the average winds over East St. Louis at the lower levels even though the first rainstorm began at 1416 in this area (system I). By 1500 m (figure I-11c) the flow had shifted and was from the WSW or WNW. There was anticyclonic turning of the wind over the W side of the Mississippi and cyclonic turning of the wind over the E side. This wave-like structure might be correlated with the advection of the mid-level moisture seen in figure I-9.

A dramatic change occurred in the overall low-level flow over the MMX circle in only 2 hr. At 1200 the lower kilometer of the wind field was perturbed by the passage of a frontal zone and the wind direction was highly variable across the circle. In contrast, by 1400 the low-level winds through the first 1200 m were from the S. At the 1500-m level, the winds changed from NW to nearly W in the same 2-hr period. Thus, in 2 hr the winds switched 180° in some locations and the frontal zone moved well to the N, no longer exerting any apparent influence over the metropolitan St. Louis area.

PRECIPITATION MORPHOLOGY

Clouds

During the early morning hours of 10 August 1973, the skies over St. Louis were either clear or covered by thin Ci or Cs (0.2 to 0.3 cover). Fog was observed in the Mississippi and Illinois River Valleys on the extreme W edge of the MMX circle and to the E of Belleville and Alton, where high relative humidities were previously noted (figures I-5 and I-6). No fog was reported at STL in the NW part of St. Louis County or at ARC in the Mississippi River Valley. The lack of fog at ARC corresponds well with the earlier observation concerning the temperature and humidity distribution in this area.

There were some scattered Ac in the area from 0800 to 1000. The first Cu were reported over the Wood River refineries just prior to 1000 and to the E of Belleville by the BLV observer at 1000. Figure I-12 was taken at 0940 from EDW and shows the area's first Cu which developed over Wood River. The remaining observing station reported the formation of Cu about 1 hr later

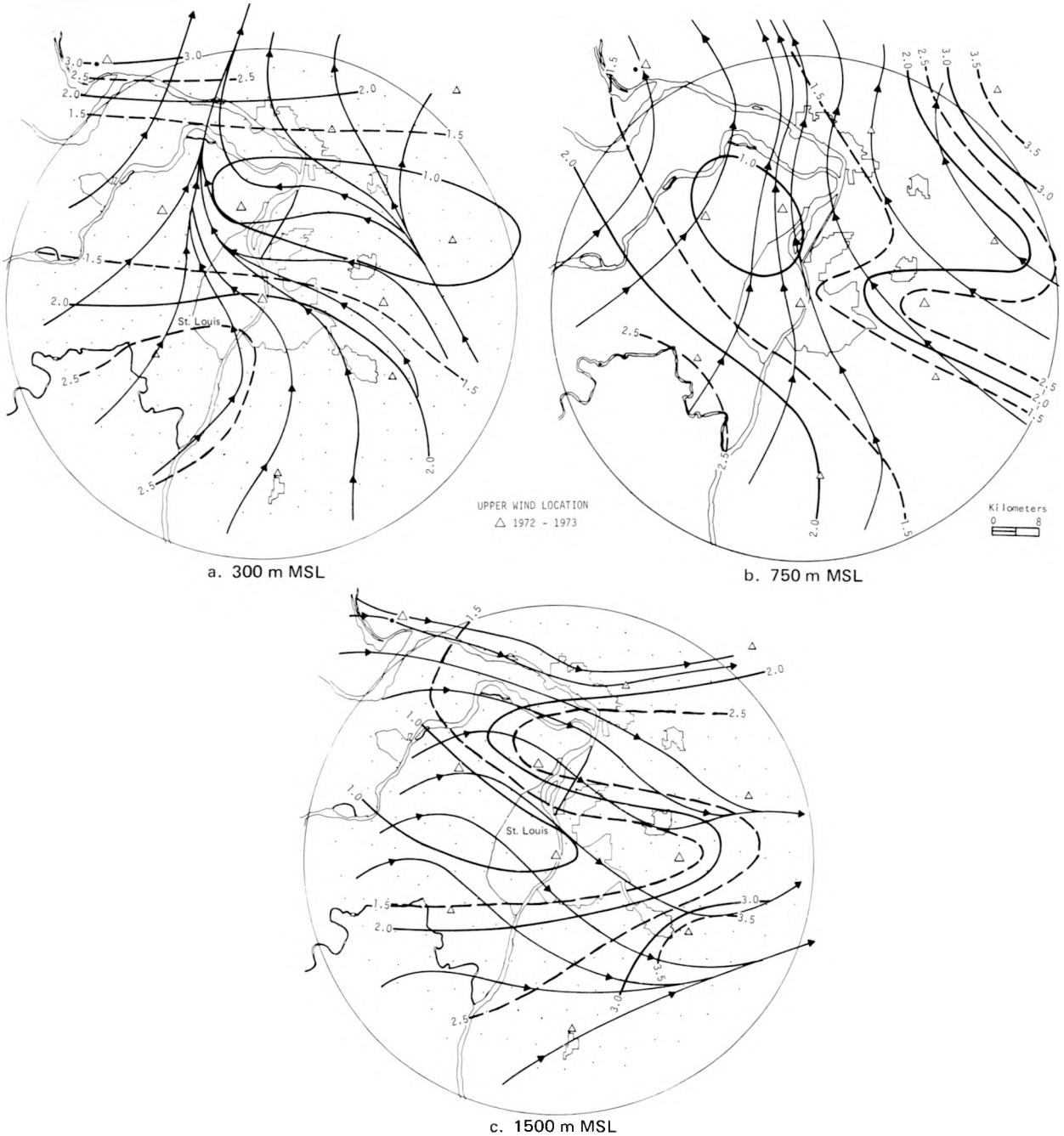

a. 300 m MSL

b. 750 m MSL

c. 1500 m MSL

Figure I-11. Streamline and isotach (m/sec) patterns at 1400

Figure I-12. First Cu at 0940 from Edwardsville

Figure I-13. Towering Cu over W St. Louis at 1549

(1100), and this corresponds rather closely with the time predicted. Thus, the first Cu on the morning of 10 August formed within the broad, warm, moist maxima that had developed on the E side of the Mississippi River by 0900. Therefore, the warm, moist zone which developed within the MMX circle was a preferential Cu initiation area (see figures I-7 and I-8 for the general configuration of temperature and dew point which prevailed from 0900 to 1400).

Towering Cu were being observed by 1400 throughout the metropolitan area. However, two areas were pinpointed by surface observers as having the greatest vertical development. One was just E of St. Louis and the other over the SE corner of the MMX circle. Both of these areas were characterized by relatively warm, moist air (see figures I-7 and I-8). Verification of more vigorous convective developments within these areas were supplied by the 10-cm PPI radar data. The initial echoes of 10 August formed within these same regions. This indicates that the warm, moist zones not only were initiators of convective activity, but also tended to increase the intensity of the Cu vertical development on 10 August.

A scattered layer of Ac was observed at 1400 on the W and NW edge of the circle. Figure I-9b indicates that the bases of these clouds were at 13,000 ft.

For the period from 1416 to 1600 there were only two thunderstorm complexes (systems I and II) over or near the MMX network. System I was located over East St. Louis, and it drifted slowly to the SE. System II was situated beyond the extreme SE edge of the MMX circle, but it built to the W so that it edged onto the circle by 1600.

System III formed NW of PMQ and moved over this station at 1500. This convective system was dissipating as it grazed the N portion of the circle. Some light rains occurred in the N third of the circle from 1645 to 1740.

Between 1400 and 1700 towering Cu dominated the rest of the network; a typical Cu of this period is shown in figure I-13. This airborne photo was taken over W St. Louis at 1549 CDT when these Cu were exhibiting considerable shear in their upper layers. In fact, at this time the directional shear over the W end of the network between 4000 and 5000 ft varied from 55°/1000 ft

in the S portion to 140°/1000 ft to the N. With such shear, clouds cannot be expected to develop to the thunderstorm stage, unless they find a preferential area of growth (Bates, 1967; Madigan, 1967). At 1600 an isolated thunderstorm (system IV) began to develop NW of St. Louis and it became the keystone convective entity for an intense mesosystem which intensified over the St. Louis metropolitan area and moved SE over the circle. Additional convective elements subsequently formed along the W and E flanks of the initial storm. The heaviest rains from this system fell over the W portion of the circle.

Precipitation Elements

Extensive study was made of the 3-cm RHI and 10-cm PPI radars and 5-min plots of rain data over the circle. The echoes depicted by the 3-cm RHI radar were labeled by numbers (1, 2, 3, . . .), while the echoes observed by the 10-cm PPI were denoted by letters (A, B, C, . . .). Each 5-min plot of rainfall was analyzed for rainfall centers, termed raincells. These were identified and labeled by numbers. For convenience, all raincells in each of the four systems and the various radar echoes that they correspond and refer to in the text are presented in table I-1.

Table I-1. Raincells and Echoes

	3-cm RHI echo	10-cm PPI echo	Raincell
System I			
	1	A	1
		B	2
		C	3
System II			
	2	G, H	4
		J, K, L	8
		L, K, O	4 + 8
System III			
			10
			12
System IV			
	7		7
			9
			13
			14
			16
			17
			18
			19
			20
			23
			25
			26

Radar Echoes, Systems I and II

The first echoes on 10 August reported by the NWS radar at STL formed an area of isolated showers and thunderstorms 75 to 200 n mi SSW of the circle at 1240. This system moved E at 15

to 20 kt during the afternoon and passed far to the S of the MMX circle. It reached its maximum intensity between 1540 and 1640 and then dissipated.

Another area of isolated showers and thunderstorms (system III) formed 50 n mi N and NW of STL between 1340 and 1440. This area drifted slowly SE for about 3 hr. As it approached the N edge of the MMX circle, its movement became more from the W. This system reached its maximum intensity just before entering the circle and only grazed the N edge of the MMX circle between 1645 and 1740.

The NWS radar at STL showed very little detail of the showers and thunderstorms that formed over the MMX circle during the afternoon of 10 August because much of this activity was obscured by ground clutter. The NWS radar at STL was not well located to monitor storms in the St. Louis area.

The 10-cm PPI radar at PMQ scanned continuously with an 80-mi range, and the first echo activity within the circle formed at 1416. The 3-cm RHI radar also detected this first echo centered just E of ARC at 1416. This echo had a maximum top of 22,000 ft at 1416 and was probably in existence 2 min before it was first measured by the slowly scanning RHI radar. The echo grew quickly and moved very slowly to the ESE for 2 hr. The echo appeared to have its initial roots over the city (i.e., the individual new cells which made up this convective element grew on its W flank and above the city and then moved into the storm core to the SE). However, the net result was that the storm center moved very slowly.

Figure I-14 depicts a 2-hr time sequence of vertical cross sections through echo 1 constructed from the 3-cm RHI data. Each slice shown in figure I-14 was taken through the center or the highest point of the storm. The first cross section at 1416 shows the base of the echo at 3000 ft and a top of 22,000 ft. This is the first active turret recorded, and in this sequence is labeled 1. By 1418 a second turret (convective cell) appeared to the NW (rear) of the first one. Both of these turrets moved to the SE and eventually decayed, but at 1429 a third turret developed to the NW (rear) of the main activity. The third turret reached a maximum height of nearly 30,000 ft at 1436. Prior to the development of the third turret, this convective element was only a rainshower. The first thunder of the day began at 1433 at the SLU thunder site, about 2 mi W of the radar echo, coincident with the vigorous vertical development of turret 3. This thunder activity was classified as light (4 to 11 peals per hour) and was heard from 1433 to 1437.

The maximum height of this convective element changed little over the next 20 to 30 min, even though a fourth turret appeared on the NW side of the storm at 1440. None of these first four turrets grew beyond 30,000 ft. A fifth new turret became evident at 1448, and by 1452 this cell was the most active region of the storm. By 1458 this turret attained a height of 30,000 ft and it continued to grow to a maximum height of 47,000 ft at 1519. The total growth was 27,000 ft in 31 min.

The fifth turret dominated the thunderstorm complex until 1522, when turret 6, which moved S of turret 5 at 1519, became the main convective impulse of this complex. However, after 1519, the thunderstorm complex began to decrease in height and showed signs of decaying. Figures I-14 and I-15 show that the height of the convective element decreased from 1519 until the complex completely disappeared from the radar view at 1619. Two other turrets became evident and, like turret 6, they all moved along the S periphery of the dominating turret. (As will be shown in the raincell analysis, some very light rains continued to fall in the vicinity of Belleville.) It is quite probable that the source air which the last three turrets (6, 7, and 8) were ingesting was coming from the rain cooled area over East St. Louis (see figure I-19a), and as a result this thunderstorm complex lost much of its buoyancy and intensity. The thunderstorm complex no longer drew air from the hotter, more polluted air over the city, but now drew air cooled by its own rain, and hence, dissipated.

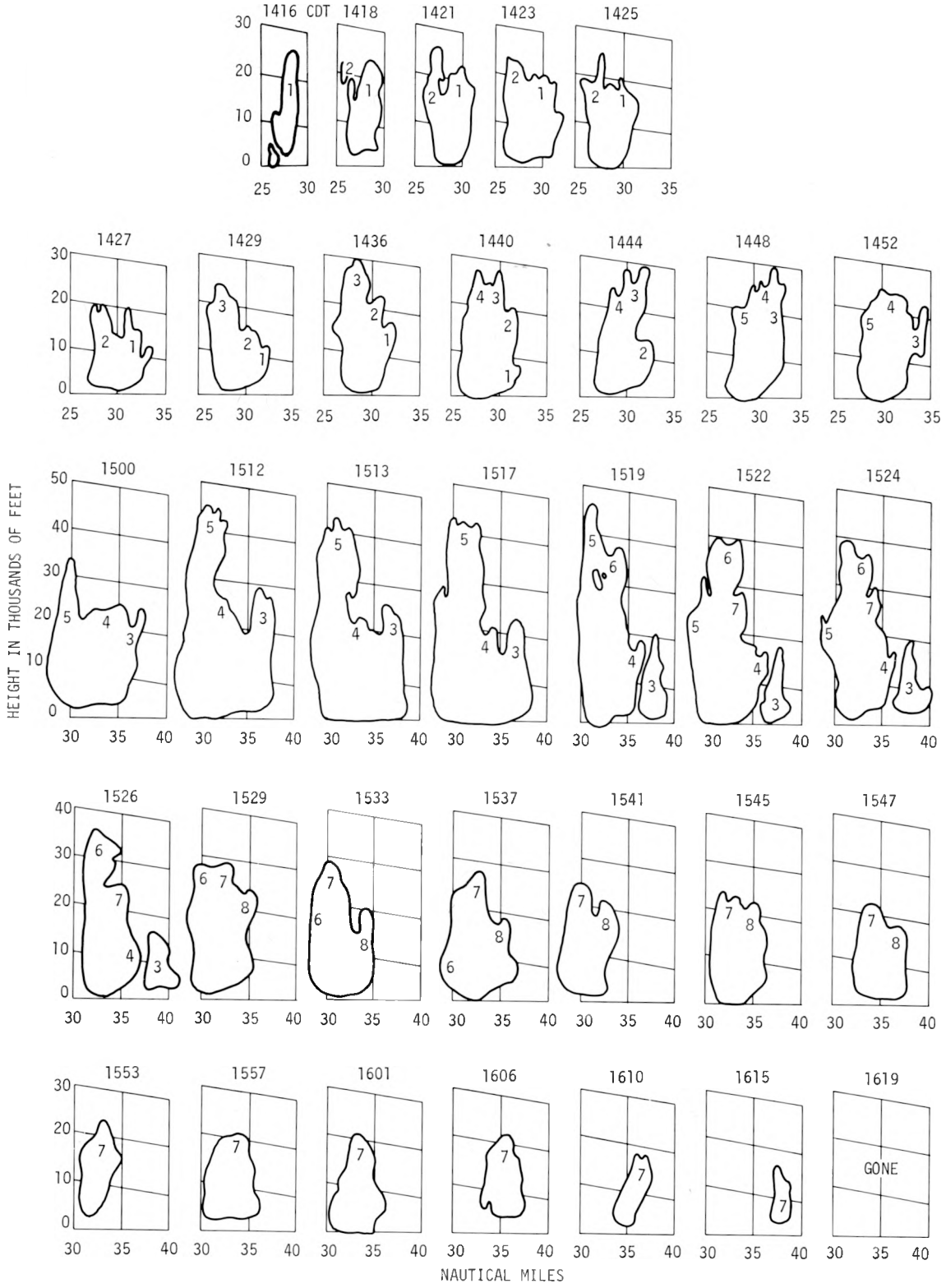

Figure I-14. A 2-hr sequence of vertical cross sections through echo 1 from 3-cm RHI data

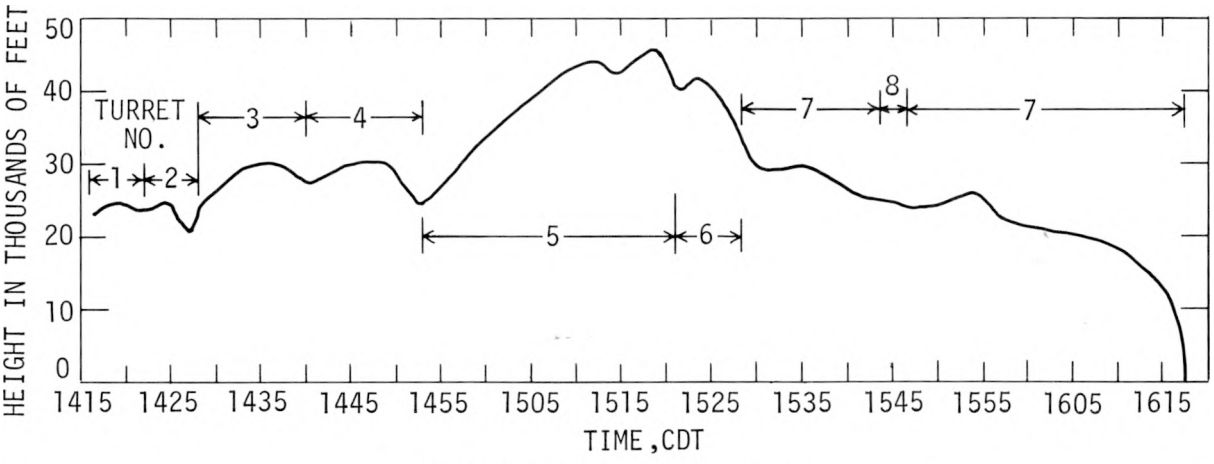

Figure I-15. Height of convective element

Thunder was again detected at SLU, beginning at 1457 and continuing to 1531. The thunder activity at this time was moderate (rates of 12 to 60 peals per hour) and the beginning of this thunder activity coincided with the explosive growth of turret 5 (16,000 ft in 12 min). After 1531, the thunder detector at SLU was no longer able to hear thunder, even though thunder with the storm was now being heard at BLV. It is quite possible that these data may give an idea of the range of audibility of the thunder instrumentation on this day.

The tracks of individual echo intensity centers within this convective element, as recorded by the 10-cm PPI are shown in figure I-16. The first echo center (A) formed at 1431, moved to the E for about 10 min, and then moved to the SE and disappeared at 1452. It reached its maximum intensity at 1439. A second intensity center (B) was noted at 1439 about 3 mi E of A's initial position, and it moved to the E during its 13 min of existence, paralleling A's motion. A third radar intensity center (C) formed at 1452 on the S edge of the thunderstorm complex over East St. Louis and it moved due E until it dissipated at 1535.

The minimum detectable intensity of the 10-cm PPI was 42 dbz and the antenna was elevated only 1/2°, so that the echo intensity tracks on 10 August represent heavy rains near the ground. It is assumed that the 10-cm PPI echoes reflect the downdrafts associated with the storm and it was found that the downdrafts were located on the S edge of the storm. From the 3-cm RHI data it would appear that the new echoes formed on the W (rear) side of the storm, ingesting city-origin air in their early stages of development. From the RHI slices taken through the storm center (figure I-14), it can be inferred that these new drafts moved on the N edge of the thunderstorm complex for the first hour, and on the S edge for the last hour. It seems that the early storms were 'back feeders,' i.e., the source or environmental air ingested by new cells was upwind at cloud level.

Additional information which further substantiates the new growth of turrets on the W part of this thunderstorm complex was obtained from the aircraft flight in this vicinity from 1420 to 1600. Updrafts of 300 to 700 ft/min were observed to the W of the main rain core. The aircraft crew also noted "various industrial smokes coming from steel mills, power houses, chemical plants and so forth being ingested into this cloud system" (Henderson and Duckering, 1973). In addition, large ice nuclei counts were obtained in the vicinity of these updrafts with the use of a modified cold box. Measurements in the region of the updrafts were as high as 1000 nuclei/cc, while the background measurements varied from 2-20 nuclei/cc. Clearly, the updraft air going into this storm was 'urbanized.'

A series of cloud photographs were taken at 5500 ft MSL from the W of this thunderstorm complex, and one of these is presented in figure I-17. This photograph was taken at 1512 looking

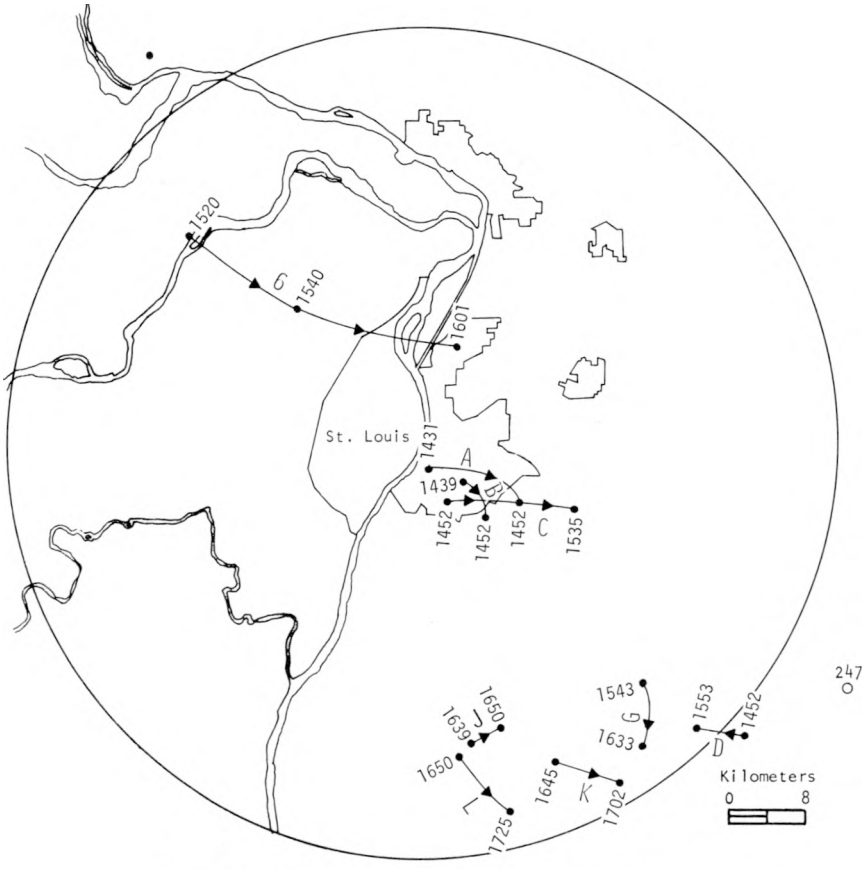

Figure I-16. Tracks of individual echo intensity centers

Figure I-17. Developing turrets at 1512 CDT on SW edge of thunderstorm over East St. Louis, taken from NW of storm looking SE

to the E. It shows the inflow area on the W edge of the thunderstorm complex. New turrets were developing to the W of the main rain core at this time.

A second radar echo (system II) formed at 1416 just beyond the SE edge of the MMX circle. This echo remained in this area for 1 hr, and drifted slightly to the S. Beginning at 1520, this echo started to develop to the W, and by 1645 new cells extended as far W as Waterloo. The 10-cm PPI radar first detected a 42-dbz intensity center with this storm at 1452. This center (D) tended to move slowly to the W as is illustrated in figure I-16. A second intensity center (G) was detected at 1543, about 7 mi to the NW of D. About 1 hr later, intensity centers J, K, and L formed, again further to the W. Centers J and L formed in the vicinity of Waterloo, while K formed about half-way between G and Waterloo. All of these intensity centers were associated with the cold air outflow to the W from the main storm. By 1730, system II began to drift to the S and soon dissipated.

The 3-cm RHI radar detected other echoes between 1400 and 1500, as shown in figure I-18. These echoes formed to the S of the MMX circle and they either dissipated or moved beyond the range of the radars. At 1520, the 3-cm RHI radar detected an echo (6) which formed in the vicinity of St. Charles. This echo initiated over the bottomlands between the Mississippi and the Missouri Rivers, a warm, moist zone, as shown by the temperature and dew point patterns at 1400 CDT (see figures I-7 and I-8). Echo 6 tracked to the ESE (figure I-16), and at 1601 it was located over Granite City where it dissipated. By 1600 the surface and low-level temperatures in the vicinity of Granite City had been cooled from the cold air downdrafts of the earlier storm over East St. Louis (see figure I-19). As this cell ingested air from the surface over Granite City the storm lost its thermal buoyancy.

Transition Period

The only change in the temperature and dew point fields over the MMX circle from 1400 to 1500 was their lowering in the vicinity of East St. Louis and on the extreme SE portion of the hygrothermograph network as a result of cold air outflow and/or rain from systems I and II. However, dramatic changes in the temperature and humidity fields occurred by 1600 across the network. The temperature field and the dew point configuration are shown in figure I-19a along with raincells which existed between 1555 and 1600.

There were pronounced minima over the center of the network and on the NW and SE corners. The minimum located over the SE edge of the circle became apparent at 1550 and was associated with the thunderstorm to the E of the circle. Another temperature minimum over the NW section of the network was a result of cold air outflow from a mesosystem which developed 50 to 60 mi NW of the MMX circle and moved SE. The temperature at St. Charles airport, located in the bottomlands between the Missouri and Mississippi Rivers, fell 8F (87 to 79F) in 1 hr. By 1600 the system was apparently past its maximum intensity, for when it moved onto the MMX circle only light rains accompanied it.

The pronounced minimum over the center of the MMX circle was caused by system I which originated over East St. Louis at 1416. The 84F isotherm surrounding this minimum shows the maximum extent of the cold air outflow from this thunderstorm complex. This outflow was elongated with a NE-SW axis and extended from Edwardsville to the vicinity of the confluence of the Meramec and Mississippi Rivers, a distance of 38 mi. This suggests that there was considerable outflow to the S. The outflow from this thunderstorm complex did not extend as far in the E-W direction. It reached from Collinsville to the center of the city of St. Louis, a distance of 18 mi.

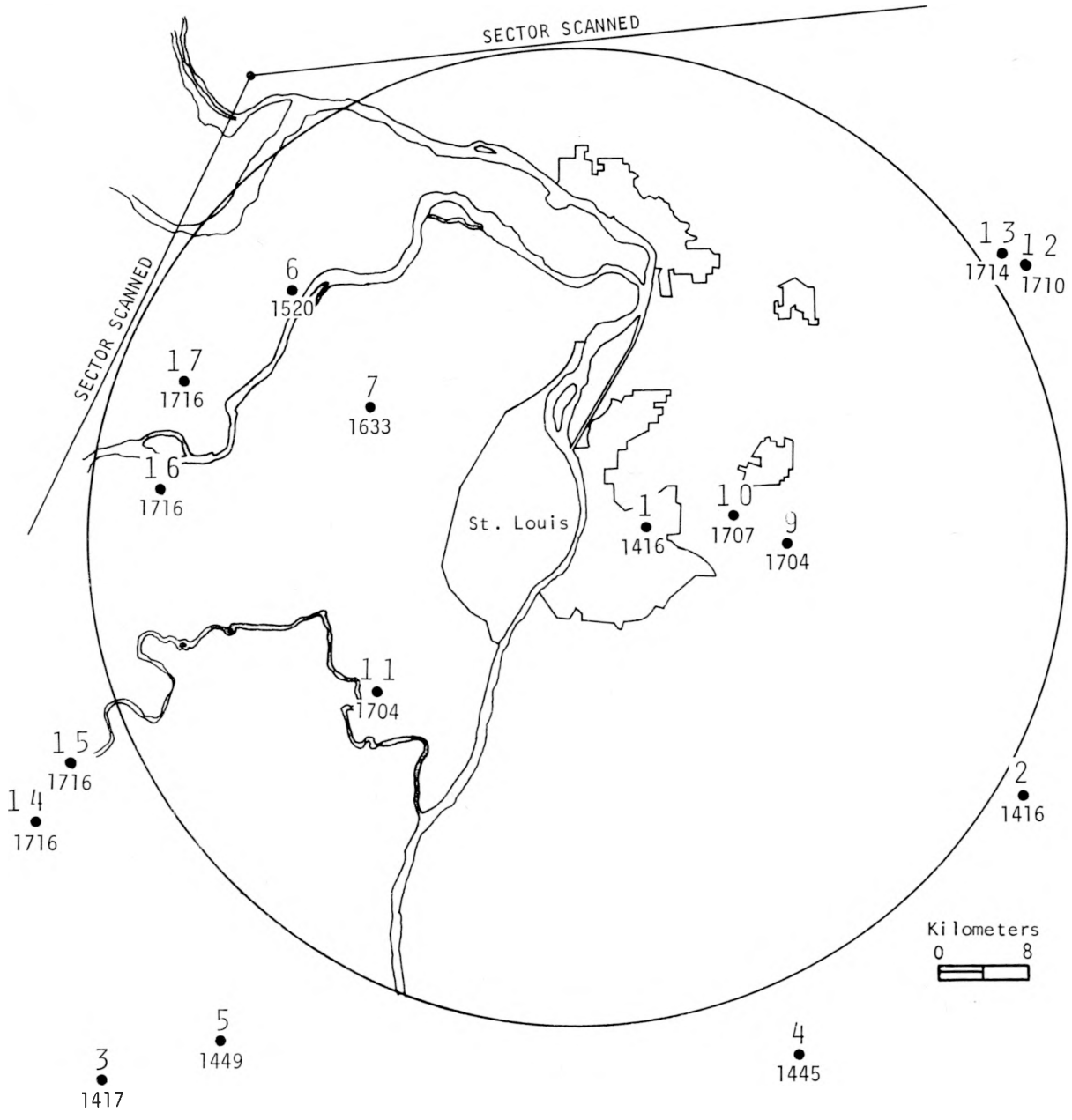

Figure I-18. Times of first echoes as depicted by 10-cm RHI radar

A fourth minimum appeared over the N portion of St. Louis County in the vicinity of STL, and this was the first evidence of the development of system IV. Within the next 45 min, this convective activity became the keystone cloud in the meso-squall system which eventually developed over the central portions of the MMX circle. The dew point pattern at 1600 showed a similar configuration of minima.

The history of the cold air outflows from the three mesosystems (II, III, and IV) which either formed or moved onto the MMX circle after 1500 on the afternoon of 10 August is shown in figure I-19b. The first region of the circle to be invaded by cold air was the SE section. This invasion of cold air began at 1500. The most rapid displacement of this cold air outflow occurred between 1500 and 1600, but the cold air outflow from system III continued to propagate to the N

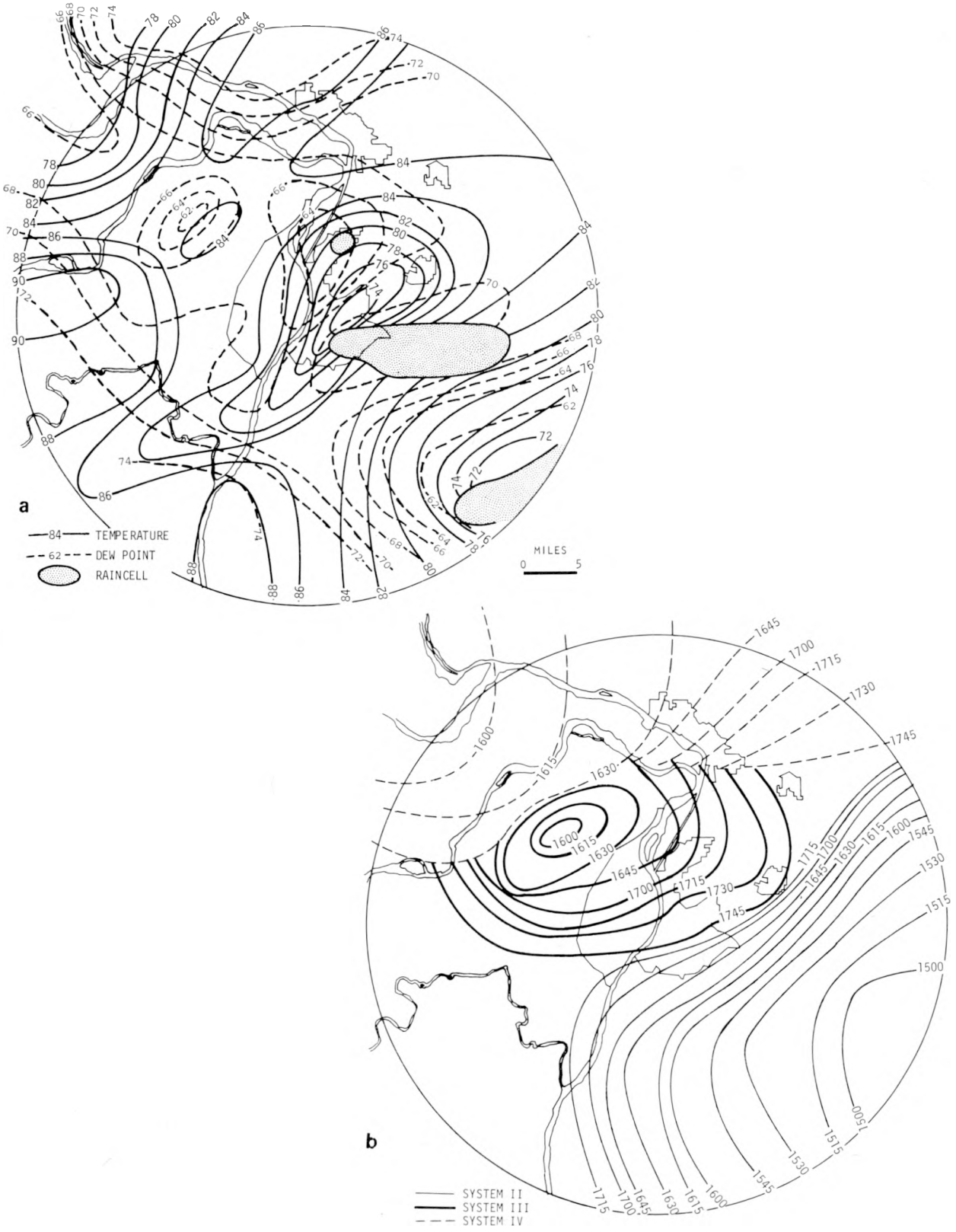

Figure I-19. a) Temperature, dew points, and raincells at 1555-1600 and b) isochrones of cold air outflows from systems I, II, and III after 1500

and W over the circle until 1715. The 3-cm RHI radar indicated that new convection continued to gro to the W during the afternoon in this region. Also, new intensity centers were noted by the 10-cm PPI radar during this time. The paths of these echoes are depicted in figure I-16. They seem to indicate that intense showers and thunderstorms were forming to the W as a result of uplift from the cold air outflow emanating from system II. Apparently, this cold air outflow forced the warm, moist air up and new convective clouds formed on the leading edge of these outflows. Formation of new thunderstorms in this manner has been noted by Byers and Braham (1949), Fujita (1963), and Purdom (1974), and was observed in another case study for 12 August 1973.

By 1600 a surge of cold air was noted over the NW sector of the network and system III and another new center of cold air outflow was apparently forming in the vicinity of system IV at STL. The surge of cold air from system III moved rapidly onto the circle, but its continued movement to the SE was thwarted over NW St. Louis County by the newly formed convective system (IV) in the vicinity of STL. System III did move across the N sections of the circle, but the intense mesosystem (IV) which formed and intensified over the central section of the network dominated this area, as is shown in figure I-19b. There is a possibility that the NW cold air surge from III helped to intensify the keystone cloud of IV over the NW section of the city of St. Louis between 1630 and 1645; however, careful analysis of the situation does not substantiate this possibility.

Radar Echoes, Systems III and IV

The first hint of any new convective development over the NW St. Louis area was the cold, dry area in the vicinity of STL at 1600 (see figure I-19a). By 1633 the 3-cm RHI radar detected echo 7 just to the S of STL (figure I-18). The horizontal and vertical dimensions of this echo increased rapidly. Its top, when first detected, was 17,000 ft and its areal extent near the ground was 3 mi^2. By 1647 (15 min later) the echo's top was at 35,000 ft and it was covering an area of 33 mi^2 near the ground. The volume of the storm increased from about 9 cubic miles to 180, a 20-fold increase in 15 minutes.

The first substantial precipitation from this cell was at 1645. Intense lightning and thunder activity (more than 30 peals per hour) were noted at the SLU thunder site beginning at 1648 and continuing until 1806.

This echo entity moved to the SE, as had echo 6, but, unlike echo 6, it did not move over the rain-cooled area of Granite City. Rather, it moved over the warm, relatively moist area that was now situated over the city of St. Louis (figure I-19a) and grew rapidly.

Figure I-20 depicts the radar life history of mesosystem IV which developed, intensified, and dissipated within the confines of the circle, as shown by the 3-cm RHI radar. The radar entity is shown at eight selected stages of its life history. Figure I-20a shows the surface position of the echo at 1637 about 3 mi SE of STL.

Between 1637 and 1656 the echo grew rapidly to the E toward the circle of warmer, moister air over the central city and industrial area. By 1656 (figure I-20b) several new echoes had formed on the W end of the system. Considerable horizontal development on the flanks of this echo continued to the E and the W as the storm was astride the metropolitan area. The development on the W periphery of the radar was more vigorous. The growth on the E side of the Mississippi River, where the surface had been previously cooled (figure I-19a) by the system I rainfall which occurred over East St. Louis in the 1416 to 1600 period, became less rapid as the storm moved over East St. Louis between 1656 and 1720, and the E portion of system IV tended to remain on the N edge of the rain cooled area of system I.

Figure I-20c shows the echo at 1723 when it measured 27 mi in length. In the next 17 min,

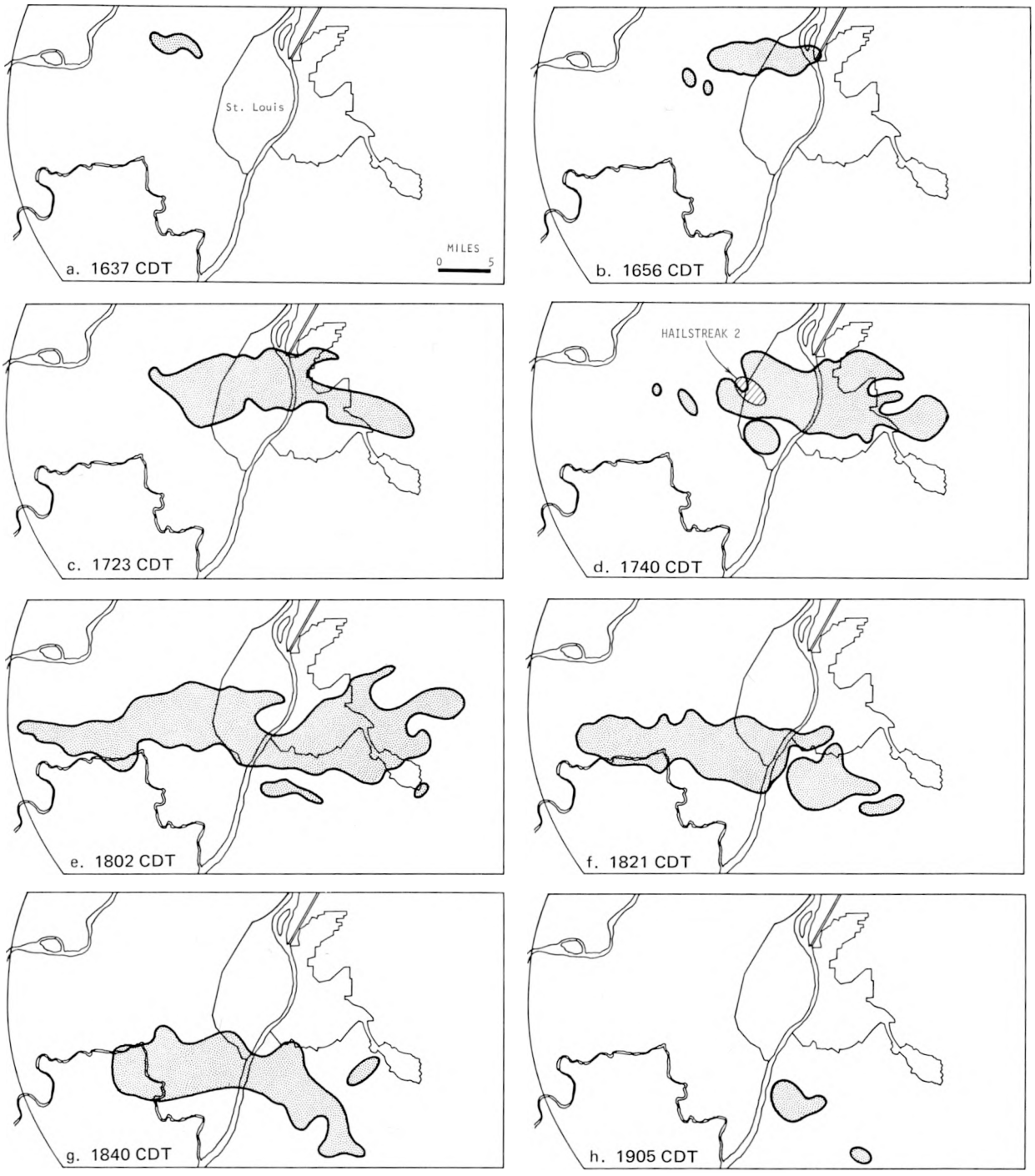

Figure I-20. Radar life history of mesosystem IV as shown by 3-cm RHI radar

the echo continued to grow and intensify on the E side of the metropolitan area, but very little additional activity formed on the W side until 1740. Additional growth of the echo over S St. Louis was noticeable between 1723 and 1740. It will be shown later in the raincell analysis that a merger of two cells took place in this area at 1730, probably several minutes after the cloud (radar echo) elements had merged.

The temperatures due W of system IV prior to 1740 were relatively cool. As system IV moved S, the air over S St. Louis and immediately N of the Meramec River was relatively warm, moist, and more conducive to further growth. At 1740 (figure I-20d) two new convective elements were initiated W of the main radar echo. Hail fell between 1748 and 1755 over the W edge of St. Louis, and the resultant hailstreak is depicted on figure I-20d.

After 1740, rapid development occurred on the W flank of the mesosystem. The echo grew from a length of 23 mi to 43 mi between 1740 and 1802, a period of 22 min. The maximum horizontal extent of the 3-cm RHI radar echo is shown in figure I-20e. The echo at this time stretched from Belleville to the W edge of the MMX circle. Several intense radar echoes formed just N of the Meramec River on the W extremity of the radar entity. There, centers were accompanied by intense thunder activity as recorded at the TYV thunder detector.

By 1821 (figure I-20f) the E and W edges of the radar entity began to erode. The W extreme of the echo appeared to fall apart as it encountered the Ozark foothills just to the S of the Meramec River, and as it spread beyond the influence of the W edge of the St. Louis metropolitan area. The Ozark foothills at this time were relatively cool. The E edge of system IV dissipated as it moved over the rain-cooled area where rains from system I were last recorded.

The echo continued to move to the SE, and it decreased in strength. By 1840 the echo's decrease is evident (figure I-20g) and after 1840 the echo began to dissipate rapidly as the E portion of the radar echo moved SE over the rain cooled area of a previous mesosystem. By 1905 (figure I-20h) very little remained of the mesosystem which originated over NW St. Louis County.

Raincells

Raincells were identified for each 5-min period from 1415 to 2035. For the purposes of this investigation it was necessary for a rain intensity center to be identifiable on at least two consecutive 5-min rain-rate maps over the MMX circle before it could be called a raincell. In this way it was hoped that each raincell would represent a localized circulation pattern. All rainfall on each 5-min map was identified with a raincell. Hence, no objective restraints were applied, and every 5-min rainfall pattern was analyzed.

Figure I-21 indicates the tracks of some of the major raincells which formed or moved onto the MMX circle on 10 August from systems I, II, III, and IV. Raincell 1 formed over the East St. Louis area between 1415 and 1420 and moved to the E. Two other raincells (2 and 3) were generated in this area. All three of these raincells formed just to the E of the Mississippi River and moved to the ESE as part of system I. Hailstreak 1 (figure I-21) was associated with raincell 2. Each subsequent cell within this system moved to the E and covered a larger area. The last cell, 3, lasted the longest, beginning at 1455 and dissipating at 1715.

At 1555 raincell 4 appeared on the SE corner of the network. This raincell grew to the W (figure I-21) and was associated with system II. One other raincell formed to the W of this initial intrusion at 1635 (raincell 8) and at 1700 cells 4 and 8 merged. These raincells formed near the boundary of the cold air outflow in regions of strong temperature gradient, as shown previously in figure I-19a. Hailstreak 5 was coupled with raincell 4, and hailstreak 3 fell to the E of the MMX circle before the rains moved onto the circle. These cells dropped rain $\geqslant$ 2-yr point frequencies

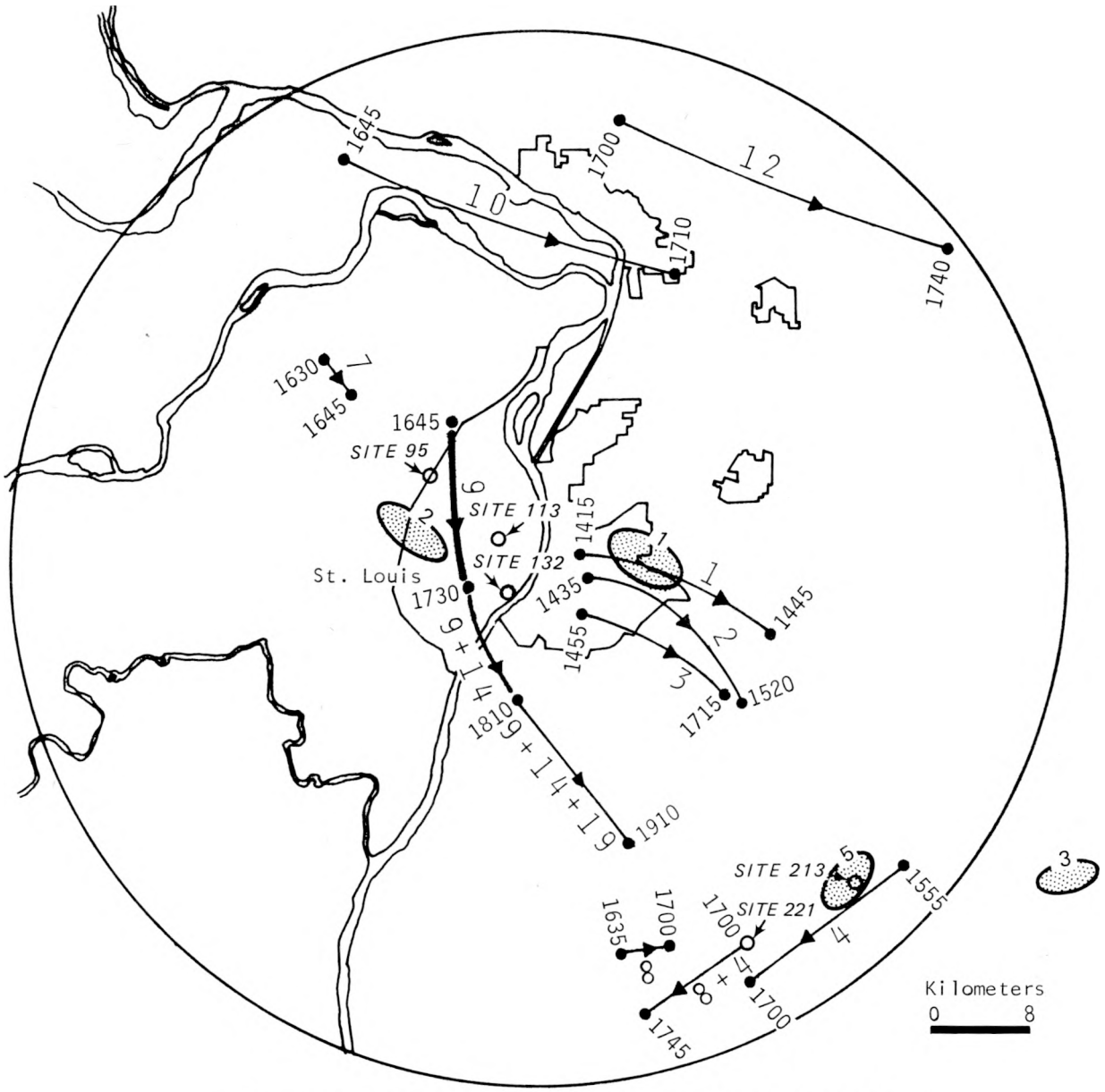

Figure I-21. Tracks of raincells which formed or moved onto the MMX circle

(for durations up to 60 min) at two different raingage sites (213 and 221) indicated by open circles on figure I-21. Table I-2 indicates the amount of rain and the point recurrence intervals that were equaled or exceeded at these and other sites having heavy point rainfalls on 10 August.

The next raincell (7) formed over STL at 1630 and lasted 15 min before it seemingly dissipated. However, the 3-cm RHI radar indicated (see figure I-20) that this raincell moved SE, apparently missing all raingages. When reaching the N part of St. Louis, it intensified and grew rapidly, forming raincell 9 at 1645 (figure I-21). This was the keystone raincell and a number of adjacent raincells formed E and W of it (these tracks are shown in figure I-22). Cell 9 moved almost due S from 1645 to 1730. At 1730 raincell 14 merged with 9, after forming to the S of 9 over the city. The combined raincell 9 + 14 intensified after this merger and moved SE. Hailstreak 2 was recorded

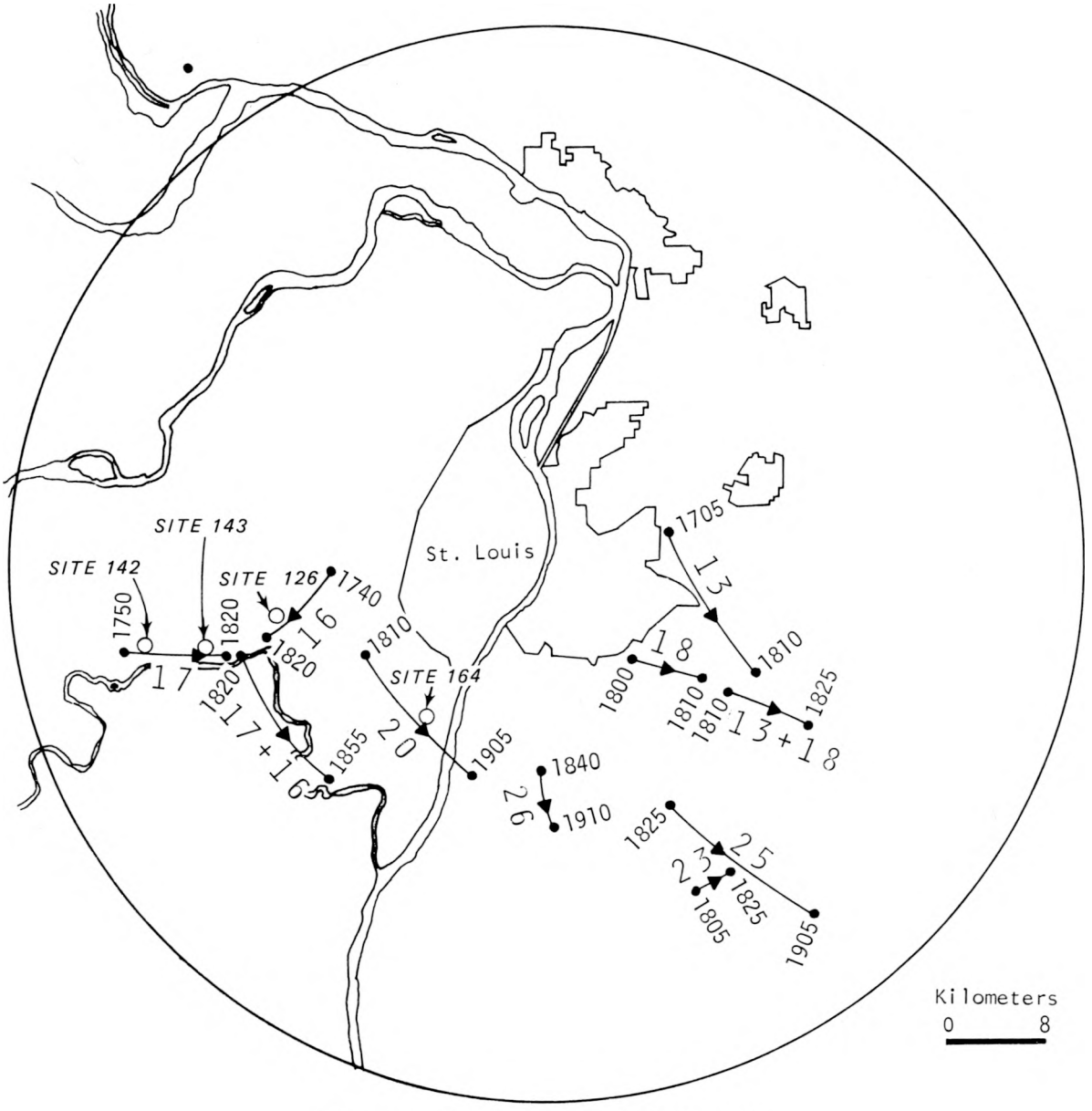

Figure I-22. Tracks of raincells from 1705 to 1910

between 1748 and 1755 and was associated with raincell 9 + 14. As raincell 9+14 moved E of the Mississippi, it decreased in intensity and merged with raincell 19 at 1810. After this merger, raincell 9+14+19 intensified again. This combined raincell continued to move to the SE and dissipated at 1910. Excessive point rainfall from raincell 9 was recorded at three different raingage sites (95, 113, and 132). The locations of these raingages are delineated on figure I-21 by circles.

As the keystone cell dissipated so did the rest of the organized mesosystem that had formed over STL. The individual convective elements within this mesosystem gave the heaviest rains of the day. Figure I-22 shows the paths taken by other raincells within mesosystem IV. Additional raincells formed both to the E and to the W of the keystone cell.

The heaviest rains of the day occurred with system IV, and all of the rain with a recurrence value of $\geq$ 2 yr associated with this system fell on the W side of the Mississippi River. Seven of the

Table I-2. Significant Point Frequency Rainfalls for 10 August 1973

	5 min	*10 min*	*15 min*	*20 min*	*30 min*	*40 min*	*50 min*	*60 min*	*2 hr*	*3 hr*
Site 164, cell 20										
Rain amount, inches		0.61	0.77	1.04	1.52	1.64	1.80	1.80	1.80	1.80
Recurrence interval, years		3	3	5	10	10	10	8	4	2+
Site 132, cell 9 + 14										
Rain amount, inches			0.77	0.94	1.14	1.15				
Recurrence interval, years			3	4	4	2				
Site 95, cell 9										
Rain amount, inches	0.35									
Recurrence interval, years	2									
Site 113, cell 9										
Rain amount, inches		0.60								
Recurrence interval, years		3								
Site 142, cell 17 + 16										
Rain amount, inches	0.62	1.12	1.34	1.53	1.61	1.75	1.75	1.75	1.75	1.75
Recurrence interval, years	22	26	25	22	24	13	9	7	3	2
Site 143, cell 17+16										
Rain amount, inches		0.55								
Recurrence interval, years		2								
Site 126, cell 16										
Rain amount, inches	0.41	0.70	0.81							
Recurrence interval, years	5	5	2							
Site 221, cell 4 + 8										
Rain amount, inches		0.57	0.74	0.86						
Recurrence interval, years		2	2	2						
Site 213, cell 4										
Rain amount, inches		0.62	0.77	0.94	1.12	1.20	1.25	1.26		
Recurrence interval, years		3	3	4	3	3	2	2		

nine sites that had notable rainfalls on this day (table I-2) were located on the W side of the Mississippi (figures I-21 and I-22) and all seven of these occurrences were associated with system IV.

The heaviest burst over the network occurred at Site 142 (table I-2) just to the N of the Meramec River. For a 20-min period from 1800 to 1820, this gage recorded rainfall amounts in excess of 20-yr point frequencies (Illinois State Water Survey, 1970). The total gage rainfall over a 40-min period equaled the 13-yr point frequency to be expected. The next most notable rainfall occurred at Site 164 from 1810 to 1900. The rainfall at this gage was not as dramatic in its early stages, but a total of 1.80 inches of rain fell at this site in 50 min, while 1.75 inches of rain fell at Site 142 in only 40 min. The largest 30-, 40-, and 50-min rainfall amounts at Site 164 equaled the 10-yr point frequencies.

Figure I-23 shows the 5-min rainfall rate patterns for four important times in the life history of the late afternoon mesosystem which formed over STL, intensified over the urban area, and dissipated just N of Waterloo. The 5-min rainfalls are expressed in units of inches per hour.

At 1650 (figure I-23a) system I, which formed over East St. Louis at 1416, had almost dissipated and raincell 3, the last remnant of system I, had a maximum hourly rainfall rate of 0.04 in/hr. Raincells 4 and 8 of system II were active in the SE portion of the network. The N portion of the network had rain from cell 10, part of system III which had been moving SE along the Mississippi River and only grazed the N portion of the circle. Keystone raincell 9 of system IV was just forming over N St. Louis.

By 1730 (figure I-23b), cell 3 had dissipated and the mesosystem over the metropolitan area was well developed. Cell 14 formed at 1710 to the S of the keystone raincell and remained relatively stationary until it merged with cell 9 during this 5-min period. The rain activity to the N and SE had greatly decreased. Raincell 13 formed at 1705 and was quasi-stationary over East St. Louis. During this 5-min period, a total of 605 ac-ft of water fell, mostly within the urban areas.

During the 5-min period from 1810 to 1815 (figure I-23c), the rainfall from system III reached its maximum intensity over the network, and a total of 1385 ac-ft of rain fell during this period. The convective line measured nearly 45 mi in length, and some of the maximum 5-min rains that fell on this day occurred just to the N of the Meramec River. There was some light spotty rainfall from showers to the N and S of the mesosystem. During this time, there were five distinct rain intensity centers. Raincell 17 on the extreme W edge of this system was raining at a rate of 6.02 in/hr. In the 5-min period previous to this, the rate at this gage (Site 142) maximized at 7.42 in/hr, giving a 5-min rain total of nearly 0.62 inch in 5 min, a point recurrence value of 22 years (table I-2). At the same time, raincell 16 to the E was dropping 0.30 inch of rain in 5 min at another gage. The rainfall intensity center of cell 9+14 had moved E of the Mississippi River at 1805-1810, and at 1810-1815, raincell 9+14 merged with raincell 19. The keystone raincell intensified for the third time just S of East St. Louis. Cell 13, which formed over East St. Louis at 1705, merged with cell 18 during this 5-min period. The western flank of the meso-system began to slowly dissipate after this period; thus, system IV maximized 1.5 hr after it began. The temperatures and dew points S of the Meramec River were relatively cool, and they were not conducive to continued development of convective activity.

By 1905-1910 (figure I-23d) all that remained of raincells 16 and 17 was a very small intensity center which was moving down the Meramec River after merging at 1820. After raincell 9+14 merged with raincell 19, this cell intensified again. However, by 1845-1850 the total system was dissipating rapidly (a decrease from 1385 to 360 ac-ft) after it moved over the region of the MMX circle which had been cooled by cold air outflow from system II. Figure I-19b defines the boundary of the cold air outflow which pushed onto the MMX circle, and it was into this region that system IV moved. Very little rain was falling over the network by 1905, and the last rains recorded over the network from this mesosystem were at 1940.

Overall, system IV initiated, developed, and dissipated in 3.5 hr totally within the confines of the MMX circle. The system's dissipation can be attributed to several causes which are all likely and possibly related. These causes are 1) loss of solar insulation, 2) advection over an area which had recently been cooled by rain, 3) the end of the natural lifetime of the system, and 4) the system's loss of the invigorating conditions of the city.

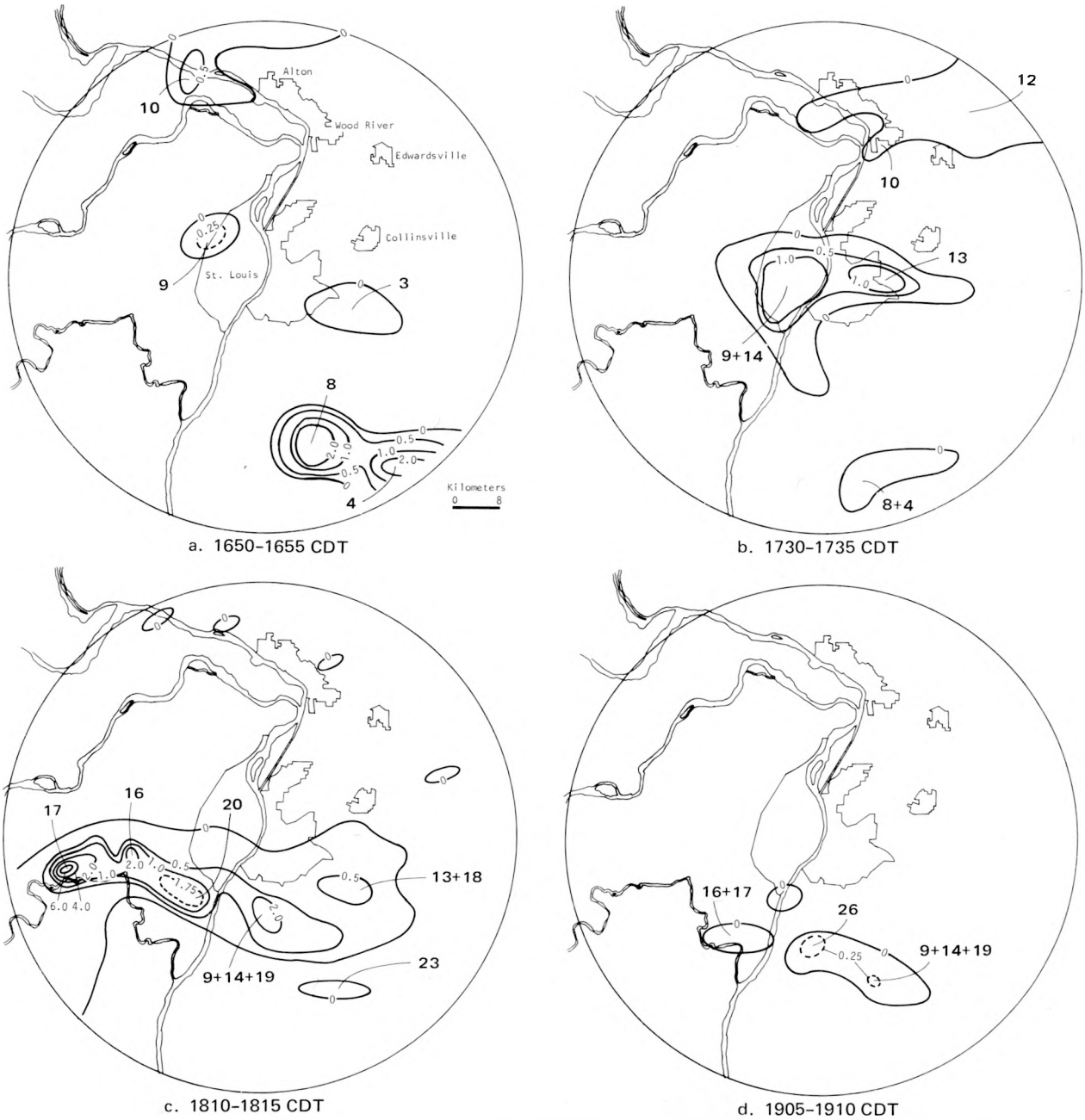

Figure I-23. 5-min rainfall rate patterns for mesosystem IV

Figure I-24. Total rainfall (inches) for 1415-2035

STORM SUMMARY

The total rainfall on 10 August for 1415-2035 is shown on figure I-24. A broad high of precipitation extended due W from the maximum values in East St. Louis to the W edge of the MMX circle (systems I and IV). Embedded in this region are four rainfall maxima $\geq$ 1 inch. Two additional 1-inch maxima occurred over the extreme SE and S edge of the circle (system II). The light rains over the N third of the circle were associated with system III.

Systems I, II, and IV dropped a total rainfall volume of 23,484 ac-ft over the S portion of the network. Over 80% of this total volume was the direct result of systems I and IV, which were definitely under the influence of urban air. More significant were the differences in the average rainfall over the urban and rural regions. The urban area had an average rainfall of 0.79 inch, compared with 0.40 inch over the rural areas. Thus, the average rainfall rate over the urban area was nearly twice the rain rate over the rural area. This seems to indicate that the urban-affected rain was more intense and quite likely the urban effects such as anthropogenic nuclei or added heat may well have augmented the intensity and, hence, the final rainfall of systems I and IV. System II, all rural, also had an average rainfall of 0.80 inch. This system was not affected by anthropogenic nuclei, but it did form within a similar hot, moist region. This would indicate that surface temperature and humidity exerted a profound influence upon the structure of convective rain on 10 August.

The rainfall in the E-W maximum fell at two distinctly different times. The first was associated with system I which formed at 1416, moved to the ESE, and ended about 1700. The rain from system I maximized over the Belleville area, as is shown in figure I-25a, and it dropped 2090 ac-ft. In the climatically defined anomaly area (Huff and Changnon, 1972), 70 to 100% of the total rainfall for 10 August was a direct result of this first isolated rain system that had urban roots. One hailstreak accompanied this system.

The second period of rainfall which made up the broad E-W maximum (figure I-24) fell as a result of system IV, which initiated and intensified over the urban area and then dissipated within the rural areas. The initial convective element of system IV, raincell 9, formed over N St. Louis at 1645, intensified as it moved SE over St. Louis, intensified further as it merged with two other urban related convective entities (raincells 14 and 19), and dissipated at 1910 over the rural area SE of St. Louis which was cool and dry (figure I-19b). The total rain from these raincells is shown in figure I-25b. The merger points are marked with X's. Hailstreak 2 was associated with raincell 9+14.

As system IV expanded to the E, there was a tendency for the radar echoes and the major raincell (13) over this area to remain on the N periphery of the rain-cooled area of system I. The N section of system I had the least rainfall (figure I-25a) and it received this rainfall early in its developmental stage. As the E edge of system IV moved S, much of its intensity was lost (figures I-25b and c). This evidence, coupled with the earlier findings of the radar and raincell behavior in this region, indicates that system IV lost much of its vigor due to the earlier rains of system I over East St. Louis.

The remainder of the rain which was associated with system IV is illustrated in figure I-25c. The rain to the E and to the W of the major rain element showed maxima just N of the Meramec River and over East St. Louis. The heaviest rains on 10 August were associated with system IV and the keystone storm which shows up as a minimum on figure I-25c.

Some of the heaviest rains recorded over E Missouri and W Illinois on the afternoon of 10 August, according to the NWS raingage reporting stations, were in the St. Louis area. Figure I-26 presents an analysis of the precipitation that fell on 10 August after 0700 CDT based solely on NWS station data.

There were four precipitation maxima reported on this day, and three were associated with squall systems which developed during the afternoon. The first shower activity according to the NWS radar data (labeled A on figure I-26) developed over S Missouri and N Arkansas at mid-day, and these scattered showers and thunderstorms moved to the E during the afternoon. An air mass thundershower (B on figure I-26) apparently produced 0.5 inch amounts over E-central Missouri.

The remaining 0.5-inch maxima were aligned along the Mississippi River Valley. The northern-most area (C) was part of system III which developed about 50 mi NW of St. Louis. This squall system maximized along the Mississippi River Valley and started to dissipate before reaching the MMX circle.

The most intense rainfall of the afternoon (D) occurred over the metropolitan St. Louis area where 1-inch rains were recorded at three different NWS sites. This rainfall was associated with systems I, II, and IV. The general configuration over the metropolitan St. Louis area, as depicted by the NWS raingage network, agrees well with the MMX pattern presented in figure I-24.

The general pattern presented in figure I-26 suggests that the squall system which developed over the St. Louis urban area may well have been influenced and made more intense by the St. Louis urban region. On this NWS data scale (which is the most detailed permitted in earlier climatic studies) initiation of rain related to urban effects is not suggested. However, the details shown by the dense network data and radar data strongly indicate urban-related initiation of large cells (and subsequent feeder cells) on 10 August, as well as urban-related intensification of existing rain systems.

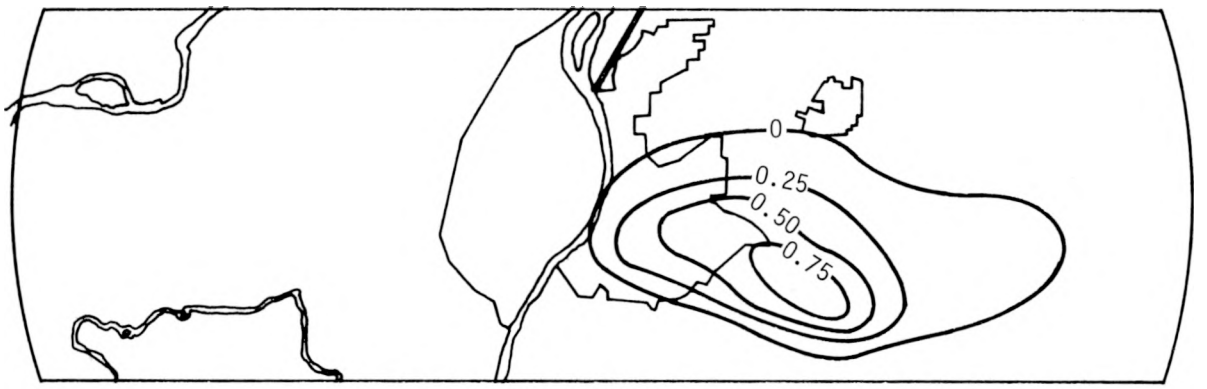

a. 1420-1700 CDT

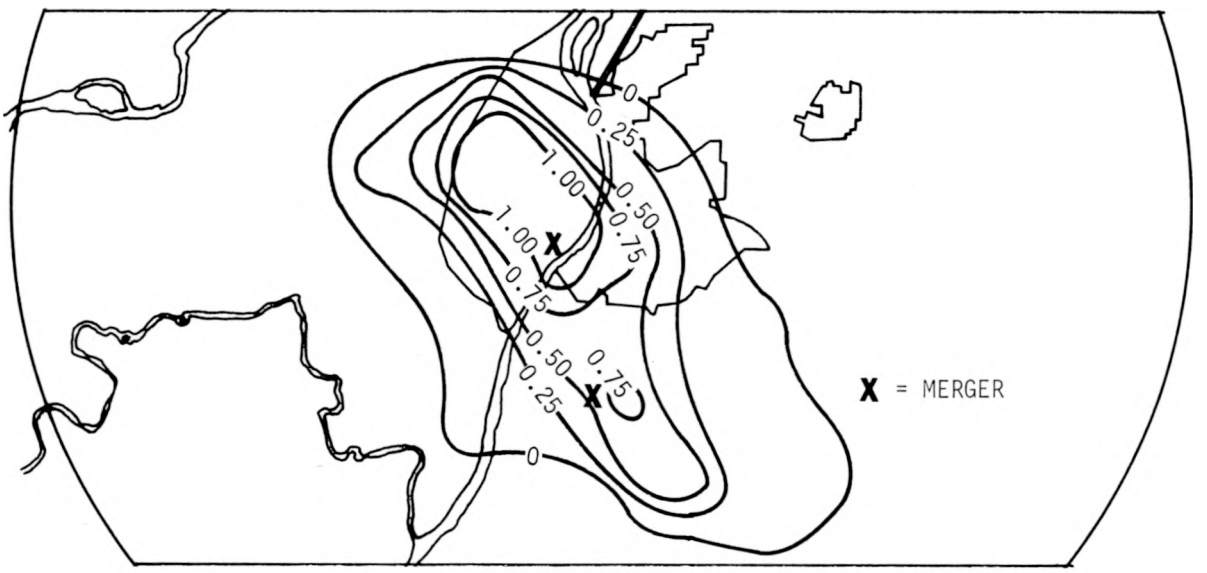

b. 1645-1910 CDT

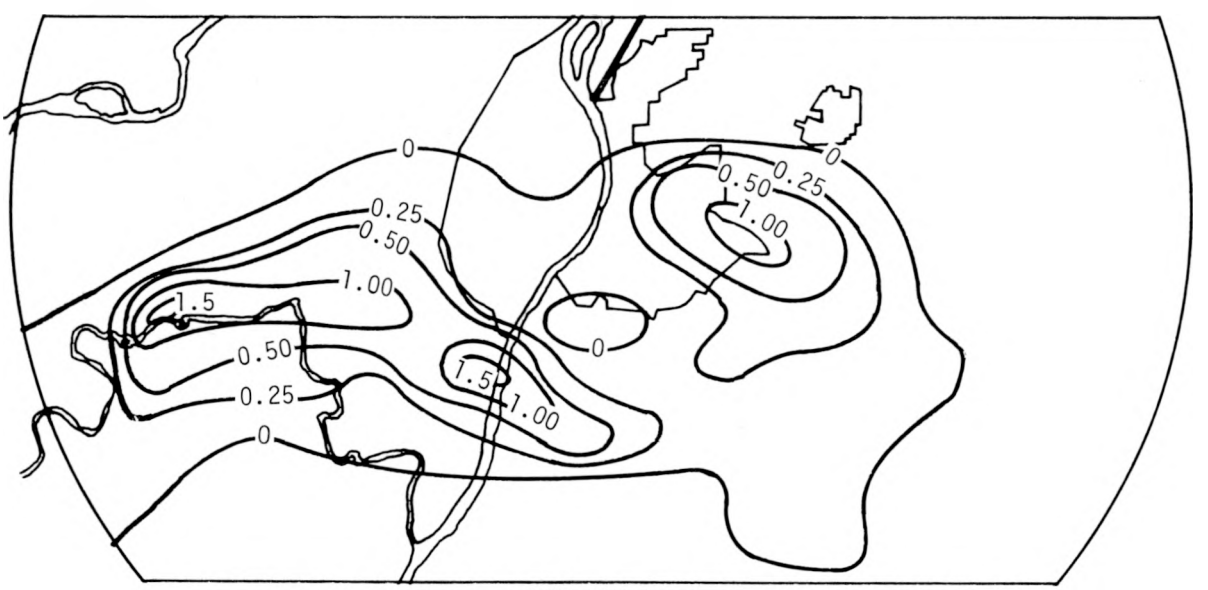

c. 1705-1940 CDT

Figure I-25. Rainfall associated with systems I and IV

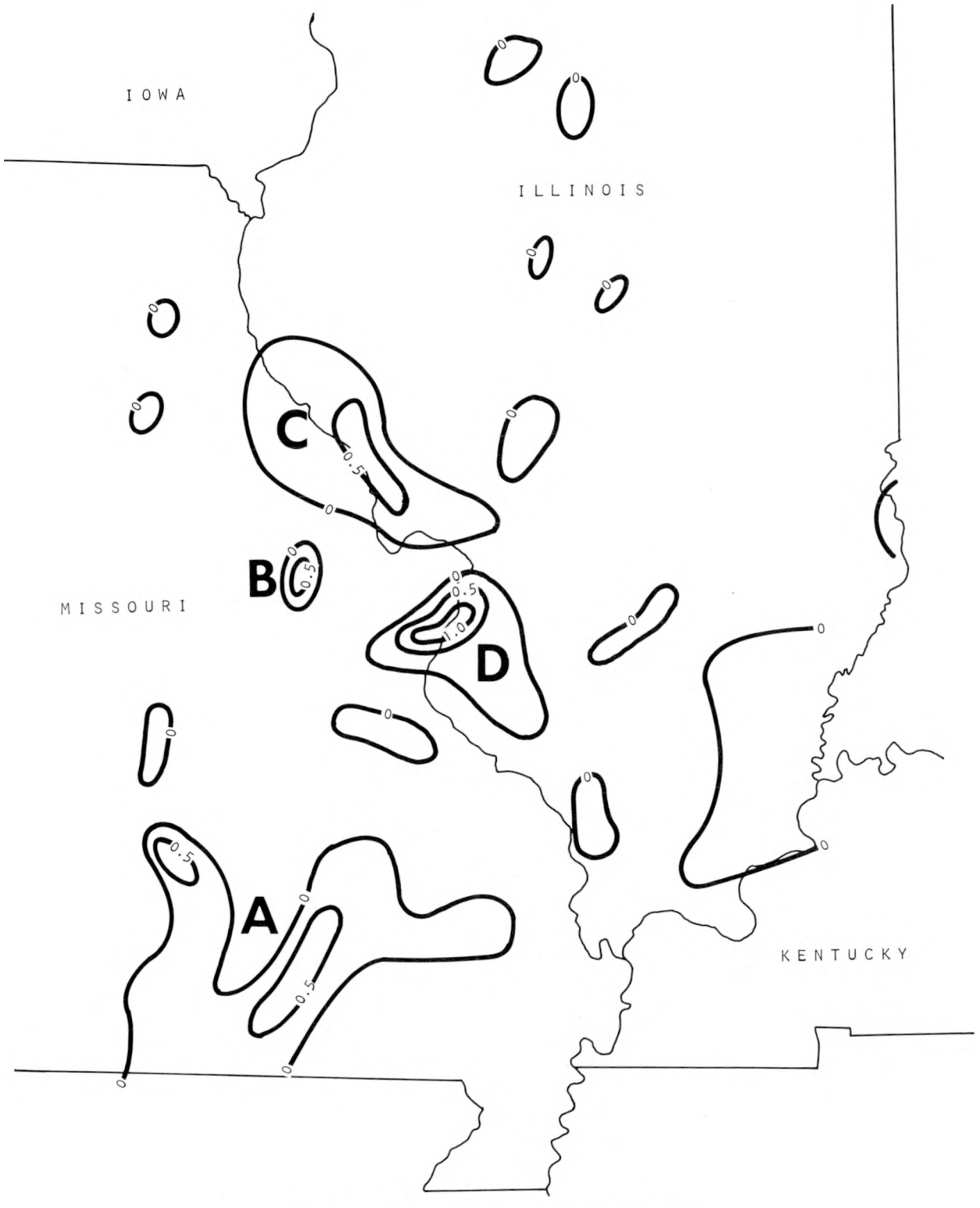

Figure I-26. Analysis of precipitation that fell after 0700

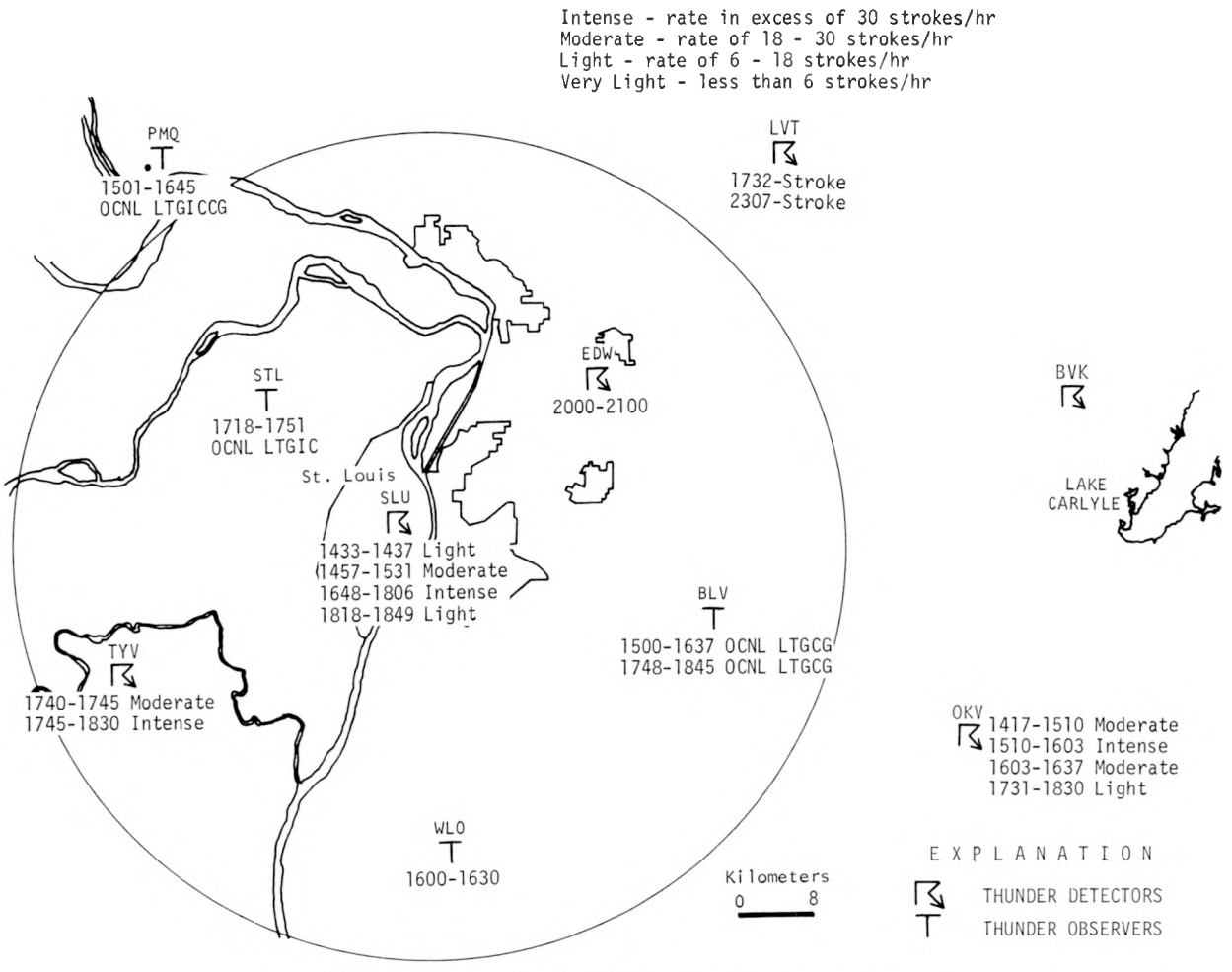

Figure I-27. Thunder and lightning observations and hailstreaks

Thunder and Hail

On 10 August, 9 of the 10 thunder reporting stations had thunder or lightning. Figure I-27 presents the thunder and lightning observations, and it also shows the hailstreaks on 10 August.

The SLU station detected two distinct periods of electrical activity during the afternoon of 10 August. The first began at 1443 and continued to 1531, and two separate intervals of different intensities were observed. Light thunder activity was observed at SLU from 1433 to 1437, at the time system I over East St. Louis first approached 30,000 ft (see figure I-14 and I-15). After this shower began to dissipate, the thunder activity ceased. Moderate thunder activity occurred between 1457 and 1531. This moderate activity accompanied the period of maximum development of system I. The thunder activity at SLU ceased, as the maximum top of system I dropped rapidly (figure I-15). Thunder was heard by the weather observer at BLV at 1500 as system I moved slowly to the SE. According to the observer, this activity continued until 1637.

A second period of thunder recorded at SLU began at 1648 and it was classified as intense. This activity lasted until 1806. It was during this period that system IV developed and intensified over the central portion of the MMX circle. As system IV moved to the S, the thunder intensity became light.

The TYV site recorded moderate thunder activity beginning at 1740. This activity lasted 5 min, and became intense from 1745 to 1830. During this time, the W portion of system IV grew explosively to the W (figure I-20). The most intense short-duration rainfall of the afternoon fell just N of TYV between 1800 and 1830.

The observer at BLV heard thunder and observed some occasional cloud to ground lightning (OCNL LTGCG) activity from 1748 to 1845. This thunder and lightning was generated by the E portion of system IV which was moving to the S across the central portion of the circle.

The OKV thunder station began to record moderate thunder activity at 1417. This moderate activity lasted until 1510 when it became intense. The intense electrical activity lasted almost 1 hr, and it was during this time that system II built to the W and invaded the SE section of the circle. By 1600, thunderstorms moved as far W as WLO. It is quite likely that hailstreak 3 (figure I-27) fell during this period of intense thunder activity. Hailstreak 5 fell during this intense activity between 1600 and 1603. Moderate electrical activity continued at OKV until 1637.

The PMQ observers heard thunder for the first time at 1501 and it lasted until 1645. This thunder was being generated by system III. Hail was observed at PMQ between 1625 and 1630 and is labeled as hailstreak 4. LVT, in the NE part of the extended raingage network, recorded a single stroke of lightning at 1732. At this time, system III was dissipating and moving ESE.

Table I-3 presents a compilation of data on the five hailstreaks on 10 August. The first hail occurred at Site 115 (in East St. Louis) when 12 small hailstones fell at 1450 with system I. Hail fell at Site 134 between 1503 and 1507 as hailstreak 1 moved SE inside echo A on the left flank (shown in figure I-16). However, the hailstones on this pad could not be measured because hail also fell there on 12 August, and it was impossible to separate the markings of the two hail occurrences.

Table I-3. Hail Statistics

Hailstreak	*Time*	*Site*	*Number of stones*	*Maximum size (inch)*
1	1450	115	12	all < 0.25
	1503-1507	134	unknown	unknown
2	1748-1750	111	unknown	unknown
	1755	112	5	0.3
3	uncertain			
	~1500-1700	247	63	0.4
4	1625-1630	000	301	0.5
5	1600-1603	213	708	0.8

Hailstreaks 3 and 5 were associated with system II which formed SE of the circle at 1416. Hail was observed at only two sites, 213 and 247. The largest and the greatest number of hailstones observed at any point on 10 August fell at Site 213 between 1600 and 1603. Over 330 of the 708 stones at that site had diameters > 0.4 inch. The largest stone that fell at this location was 0.8 inch. A total of 63 stones fell at Site 247, and the largest stone was 0.4 inch.

Between 1625 and 1630, system III dropped a total of 301 stones at PMQ. The largest stone observed from this hailstorm measured 0.5 inch, and no additional hail was observed as this system cut across the N sections of the circle.

Hail from system IV, which developed and intensified over STL was observed at two hail pad sites. One of these, Site 111, also received hail on 13 August, and since the same pad was exposed from the 9th through the 15th it was impossible to separate the two hailstorm markings. However, hail was observed at Site 111 between 1748 and 1750. At Site 112 a total of 5 hailstones fell. The largest stone had a diameter of 0.3 inch.

Tracer Mission

The AI aircraft took off at 1403, and began to measure updrafts and other parameters of convective clouds over the circle. A suitable convective cloud for the release of tracers was being sought. The isolated storm of system I which formed over East St. Louis during the early part of the afternoon was unfortunately rejected.

System IV began to develop rapidly over N St. Louis at 1645 and was monitored by the AI aircraft as it intensified. The aircraft found strong inflow regions on the S and SW front of this mesosystem and began to release LiCl in a region of vigorous updrafts at 1729. Between 1729 and 1800, the AI aircraft made a series of E–W passes over the S or leading edge of system IV. The release was ended at 1817 (Henderson and Duckering, 1973). However, for the most part, the tracer release was completed by 1802, except the aircraft crew were unable to extinguish the LiCl generator on the left wing until they landed at Alton Civic Memorial Airport.

This storm complex was a 'front feeder,' i.e., the source air flowing into the base of the updraft was being supplied from air in advance of the storm. This is supported by new cell growth and mergers shown in figures I–25 and I–26, and by the updraft data supplied by the AI aircraft flight in the vicinity of system IV.

Figure I–28 shows the rain rate pattern at four separate times during the release of LiCl into the base of system IV. The four periods shown are every other 5-min period from 1725–1730 to 1755–1800. Superimposed upon each raincell analysis are the AI flight paths for 10-min intervals.

At the beginning of the tracer release, system IV was situated over the central part of St. Louis and was growing explosively to the W (figure I–28a). During the 5-min period from 1725–1730 (figure I–28a) the mesosystem extended some 28 mi in an E–W direction. Near the end of the tracer period 1755–1800, the mesosystem grew some 10 mi to the W. System IV maximized at its greatest length and highest rainfall rates only 10-min later at 1810–1815 (figure I–23c).

The Li deposition on 10 August is presented in figure I–29. Isolines are drawn for every 100 pg/cm^2. This figure shows that there were three distinct highs of Li deposition on this day. The major high was concentrated just N of the Belleville area. Two minor maxima were noted, one on the extreme W edge of the rain chemistry network (over the city of St. Louis) and the other about 3 mi S of the E side of the metropolitan area. Superimposed upon figure I–29 is the AI flight path during the burn period.

Two of the Li maxima were to the N of the release track and the third was just to the S. There is a definite tendency for a ridge of high values to extend to the W from Belleville, across East St. Louis, to the W portion of the network. The portion of the rainfall from 1730 to the end of the rain period, or that rain which could have been affected by the tracer release beginning at 1729, is shown in figure I–30. The rainfall pattern showed a maximum over S St. Louis and the E side of the metropolitan area. The potentially affected rain pattern and the deposition pattern shown in figure I–29 agree only about a general maximum region across the S sections of the metropolitan area.

During the tracer release, system IV developed very rapidly to the W. The rainfall and deposition patterns shown in figure I–28 and I–29 suggest that the Li may have been diffused through the total rain system, and a good portion of the total Li may have been exchanged between cells W of the rain chemistry network.

In an effort to determine the validity of the Li deposition, the potentially affected rain amounts were plotted against the Li deposition at each collection point in the rain chemistry network in figure I–31. This scattergram shows two groupings: 1) The 'background group' seems to be concentrated between 500 and 600 pg/cm^2, while a singular point shows a deposition close to 1000 pg/cm^2 with just slightly more than 0.25 inch of rain. This point was either a spurious event (contamination), or it was definitely affected by the tracer release. 2) The group that might be potentially affected includes

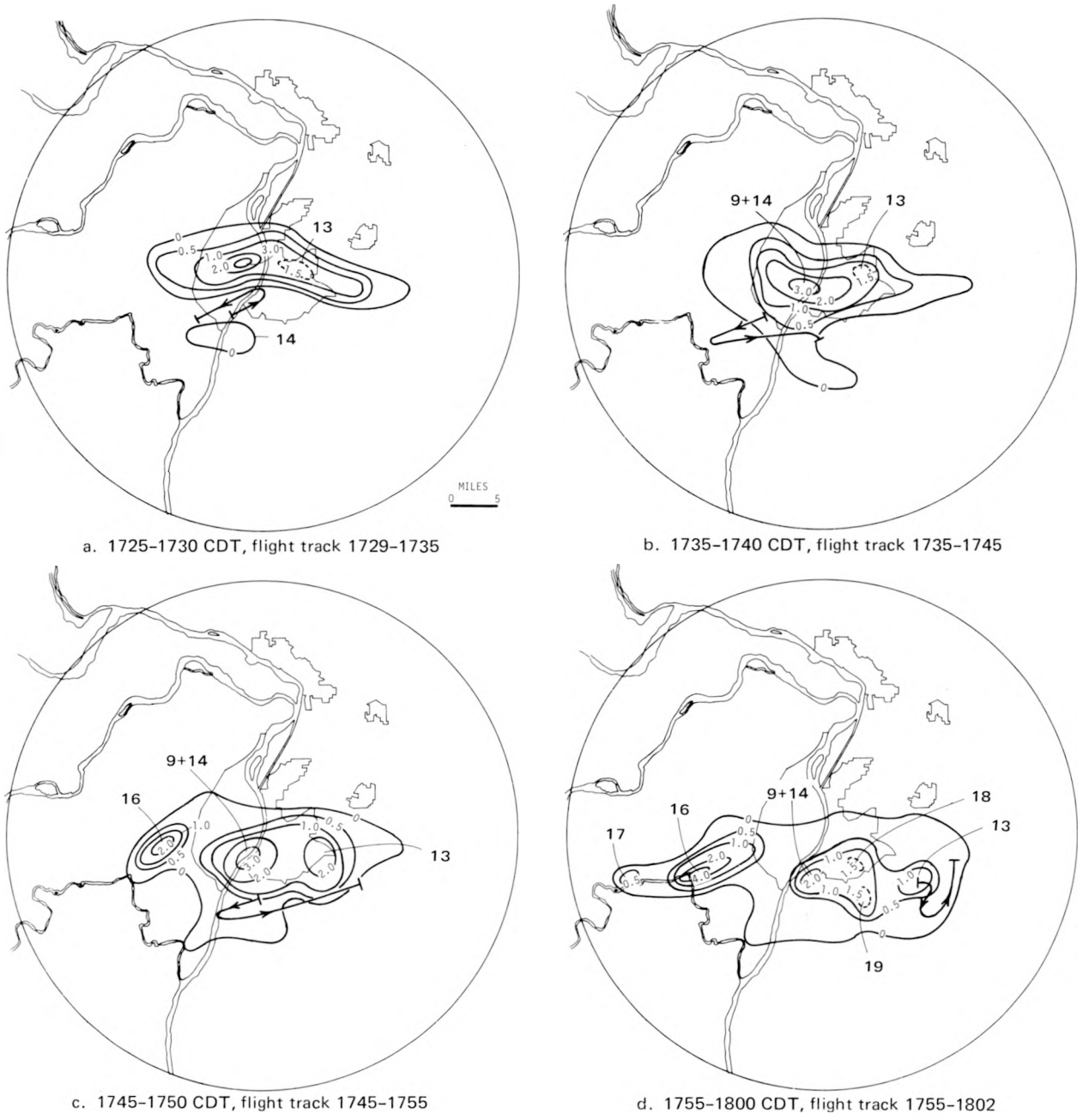

a. 1725–1730 CDT, flight track 1729–1735

b. 1735–1740 CDT, flight track 1735–1745

c. 1745–1750 CDT, flight track 1745–1755

d. 1755–1800 CDT, flight track 1755–1802

Figure I-28. Rain rate pattern during the LiCl release into the base of system IV

points taken within the three Li maximum depicted on figure I-29. Therefore, it is felt that the overall Li pattern in figure I-29 accurately represents the deposition pattern resulting from the tracer release on 10 August.

Because the overall pattern of the rainfall and the Li deposition suggests that a substantial portion of the tracer released on this day was swept out of the network, it is believed that a budget study of the Li should be made in an effort to determine how much of an interaction there was between the keystone and E raincells and the rains that developed on the W portion of system IV.

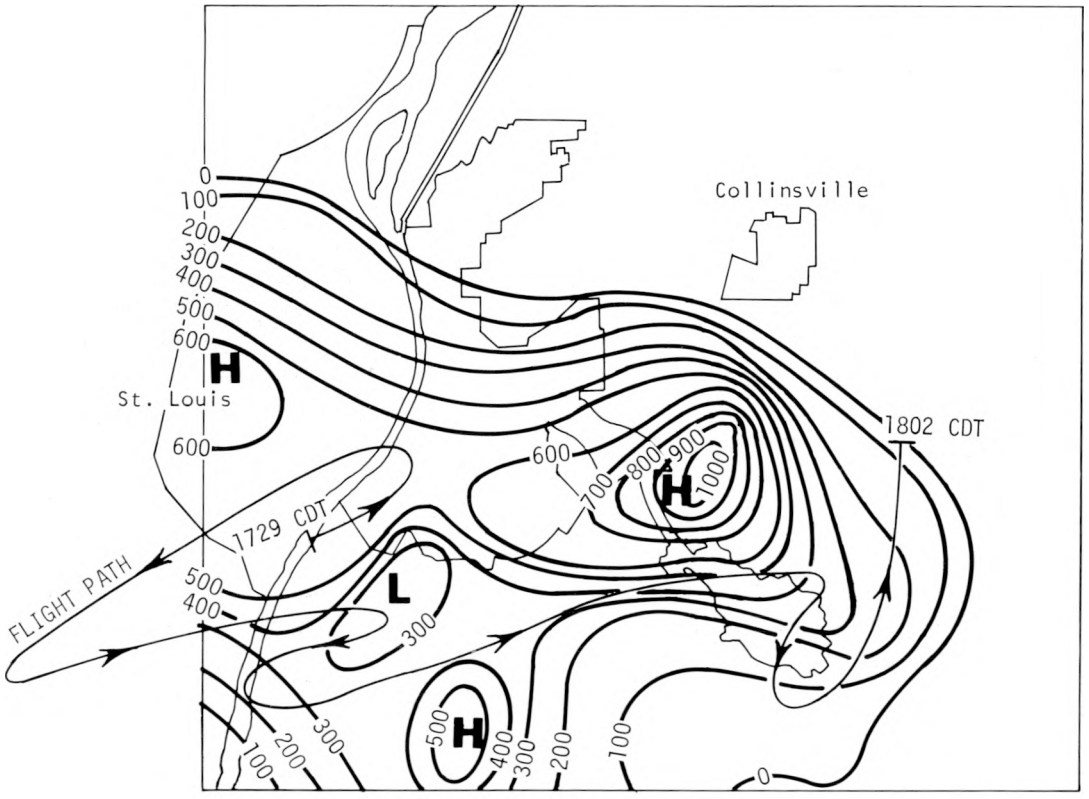

Figure I-29. Li deposition on 10 August 1973

CONCLUSIONS

On 10 August 1973, four meso-rain systems formed and intensified in or near the St. Louis urban area. None was a result of the cold front which moved S through the metropolitan area at about 0800 and then passed back N across the area near noon. Hot and moist zones on the surface influenced the development of the first Cu clouds of the day, and it was in these same regions that the first vigorous convective clouds developed. These zones were partly due to urban effects and partly due to natural conditions.

System I, which developed over East St. Louis formed in urban air. The radar analyses indicated that the turrets (new cells) of this convective system repeatedly formed over the W side of the system which was located over St. Louis.

Additional evidence to support the urban-relationship is data from the AI aircraft flights in the vicinity of the updrafts. These data indicated that updrafts of 300 to 500 ft/min were observed on the W edge of the mesosystem, and aircraft measurements showed that industrial effluents including large numbers of CN and ice nuclei were being ingested into the cloud base.

Rain systems II and III developed in rural areas and moved into the MMX circle from totally different directions. Motions of these, as with urban-related systems I and IV, were largely a result of where growth of their new cells occurred. This growth in every case was dictated by areas of relatively warm-moist surface air. System I moved little because its new cells developed on its upwind or W (urban) side and the system dissipated when its cold downdraft air finally terminated the urban source air. Cells of system II grew to the W into a warm-moist zone in the SE part of the circle. System III grew to the E, apparently into the warm-moist air of the Mississippi

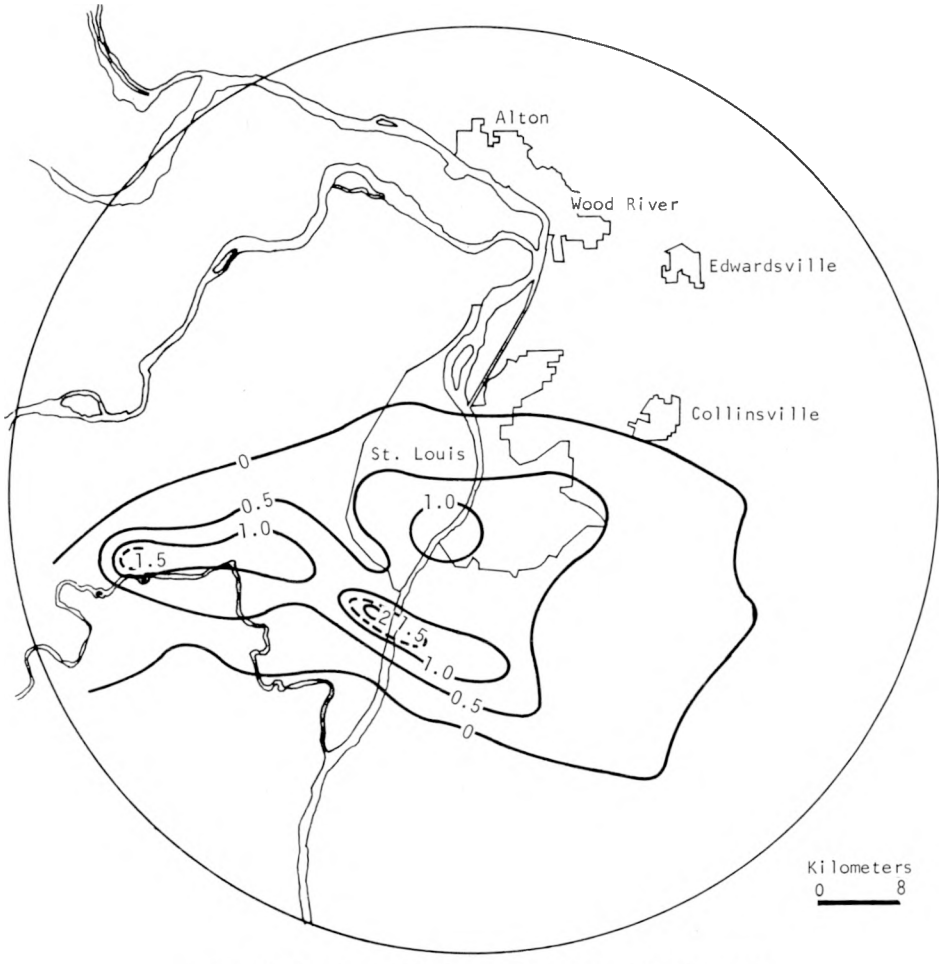

Figure I-30. Total rainfall potentially affected by the tracer

and Illinois River Valleys NW of St. Louis, and it ended just after it passed these areas. System IV developed over a warm part of the city, and flanking storms to the W and E grew into the warm-moist air over the entire metropolitan area. Growth to the E was limited when the cells fed on the colder and drier air remaining from system I. After this urban-related system migrated S of St. Louis, it was in a zone of less moist air and it dissipated.

System IV was first noted over the vicinity of STL. This urban-related system moved SE and subsequently intensified over N St. Louis. The growth to the E of the keystone cell was seemingly impeded by the cold air from the rainfall over the E side of the metropolitan area in system I. Vigorous growth to the W did not develop until system IV encountered a relatively warm, moist zone 5-10 mi N of the Meramec River. System IV then grew to the W rapidly (figure I-20), and some of the most intense rainfall rates of the day were experienced just N of the Meramec River.

The tracer experiment suggests that there was a great deal of interaction between convective elements in system IV. The tracer showed a secondary maximum of LiCl over St. Louis and the rainfall possibly affected by the tracers suggests that much of the LiCl was swept W of the rain chemistry network.

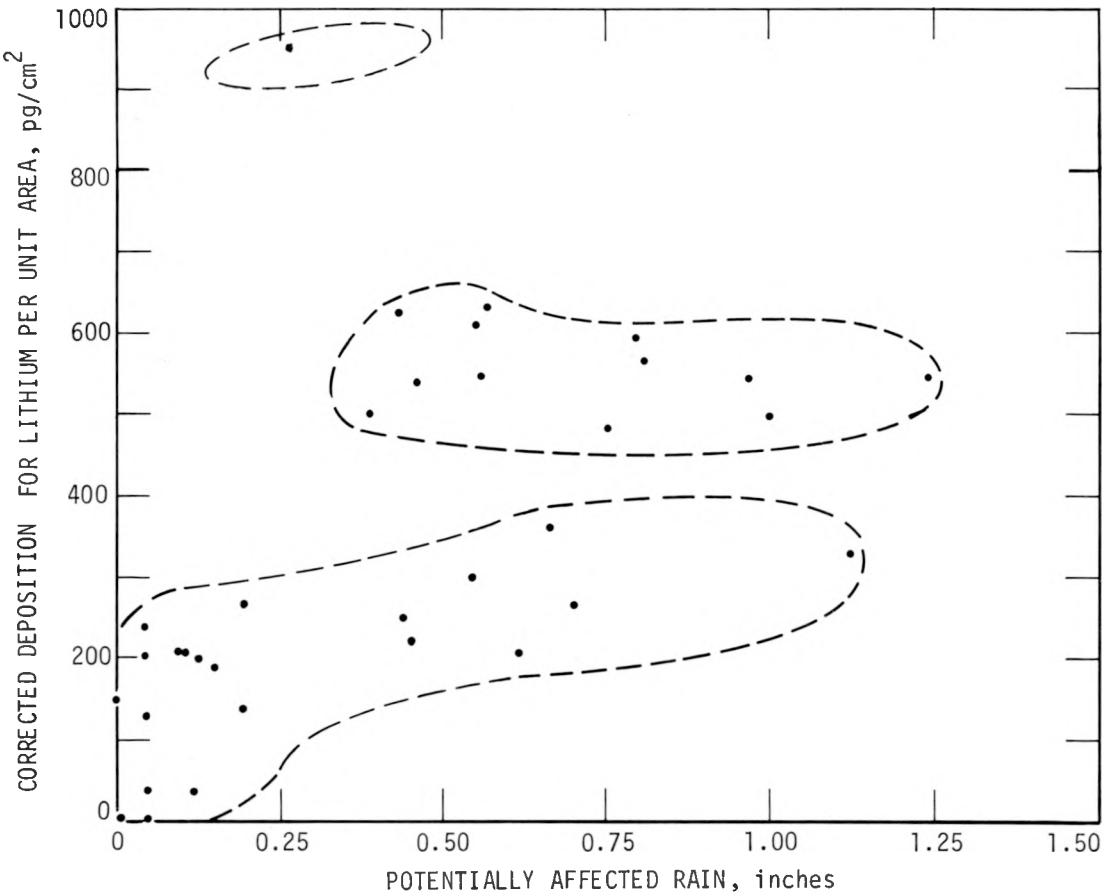

Figure I-31. Potentially affected rain amounts versus Li deposition

Nine raingages over the MMX circle recorded amounts, of various durations, that were in excess of 2-yr point recurrence values for the St. Louis region (see table I-2). There is the possibility that the urban areas are intensifying the various rain systems which move across the area (Huff and Changnon, 1972) and that the recurrence values of point rainfall, especially intervals of $\leq$ 1 hr, are being underestimated. This would have dire consequence to many city planners, because sewer systems, transportation facilities (highways), and other facilities are usually designed and constructed to withstand only 2- to 5-yr point recurrence rainfall values. If these recurrence values are being exceeded, it is necessary to revise these standards.

REFERENCES

Bates, F. C. 1967. *On the structure and mechanics of the severe thunderstorm.* Unpublished manuscript, St. Louis University.

Byers, H. R., and R. R. Braham. 1949. *The thunderstorm.* U.S. Government Printing Office, Washington, D.C.

Fujita, T. 1963. *Analytical mesometeorology: a review.* Meteorological Monographs v. 5(27): 77-125.

Henderson, T. J., and D. W. Duckering. 1973. *A summary of operations, 7 July–19 August 1973.* Atmospherics Incorporated, Fresno, California.

Huff, F. A., and S. A. Changnon. 1972. *Climatological assessment of urban effects on precipitation at St. Louis.* Journal Applied Meteorology v. 11:823-842.

Illinois State Water Survey. 1970. *Rainfall frequencies.* Technical Letter 13.

Madigan, T. D. 1967. *The squall line thunderstorm: preferred formation region.* M.S. thesis, St. Louis University.

Purdom, J. F. W. 1974. *Satellite imagery applied to the mesoscale surface analysis and forecast.* 5th Conference on Weather Forecasting and Analysis, AMS, Boston, pp. 63-68.

J. SQUALL LINE OF 12 AUGUST 1973

G. M. Morgan, Jr., G. L. Achtemeier, and H. T. Ochs, III

CONTENTS

J. SQUALL LINE OF 12 AUGUST 1973

INTRODUCTION

The storms in the MMX circle on 12 August 1973 were initially chosen for an intensive study because a squall line developed over the urban area and possible urban effects on this formation existed. The synoptic and mesosynoptic analysis for this day presented all of the complex problems associated with summertime meteorology of Illinois (as well as most of the United States E of the Rockies). This case was also chosen to be a pilot effort to test and evaluate the objective weather analysis procedures developed for another Survey project, the Design of an Experiment to Suppress Hail (DESH). Computer analysis techniques being developed in pursuit of the DESH goals will also be available for application to METROMEX and other eventual studies.

A wave of very severe weather occurred in the St. Louis area on the afternoon of 12 August. The morning and early afternoon of 12 August were locally hot and humid, conditions common at St. Louis in August. Project forecasters indicated thunderstorms were expected. Large, rapidly growing thunderstorms indeed began developing after 1400. These reached peak intensity shortly after 1500 as a colossal rain and hailstorm struck in the Granite City area. Hailstones 2 inches in diameter were accompanied by record short-duration rainfalls. Many areas of the MMX circle E of the river experienced hail during less than 2 hr of intense convection from the squall line that evolved. There were more thunderstorms in the area during the late evening of 12 August, but they were not included in this case analysis.

The following analysis of the storm period converges toward St. Louis through successively smaller motion scales. First, the large-scale synoptic picture is given, with an attempt to account for all mesoscale systems which can be identified. Then attention is focused on the MMX circle which lies in the scale between meso- and thunderstorm scales. An attempt has been made to take all data sources into consideration, although more emphasis has been placed on some types of data than others.

SYNOPTIC ANALYSIS

Macroscale and Mesoscale

Events in the St. Louis area after 1500 can be traced to the interaction of several aging mesosystems. Most of these systems were spawned the previous day or during the pre-daylight hours of the 12th. Synoptic scale influences were minimal throughout the period analyzed. Interpretation of synoptic scale upper air soundings was made difficult by contamination of some soundings by adjacent thunderstorms.

Large-scale surface patterns consisted of a broad low pressure trough running from Lake Erie WSW to Kansas and Oklahoma, between two weak high pressure ridges of the same orientation. In the 0200 CDT pressure field (figure J-1) a weak quasi-stationary frontal system extended along the N rim of the trough from Lake Erie to SW Iowa then SW into central Kansas. During the day, the front over Indiana and Ohio pushed slowly S into the central part of those states, while other portions of the system remained stationary. Its extension over Kansas weakened, but a well-defined pressure trough remained throughout the analysis period.

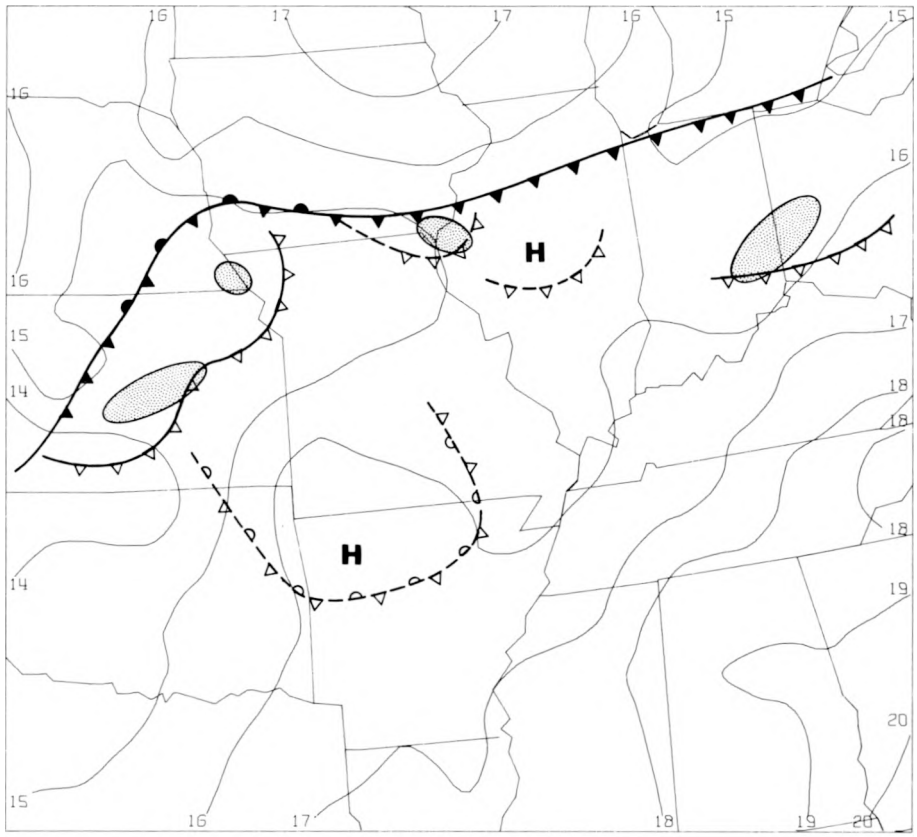

Figure J-1. Surface pressure pattern at 0200 CDT

Objective analysis of meteorological data was useful in identifying mesoscale systems of varying size, intensity, and age. Fields of accurate wind streamlines, θ_w, and divergence aided interpretation. From sets of computer-derived objective fields, mesosystems were identified and tracked in time and space.

Chronological placement for 5 major mesosystems active during the first 16 hours of 12 August are presented in figure J-2. Systems 3 and 4 were in the St. Louis area prior to and during the severe weather outbreak there. Systems 1 and 5, located over SW Missouri and Arkansas, *may* have played an indirect role by turning mid and lower tropospheric winds or by providing potentially unstable air masses that could be advected into the St. Louis area.

The mesosystems are labeled by decreasing age. System 1 was an old cold dome generated from intense convective activity that occurred during maximum insolation hours on 10 August. Cloudiness and some widely scattered shower activity over S Missouri and N Arkansas prevented air mass modification on 11 August. Although system 1 was mostly inactive for over 36 hours, its thermodynamic properties were sufficiently dissimilar from its surroundings to identify it as a mesosystem. In the θ_w chart for 0200 CDT (figure J-3), two tongues of high θ_w air, one over N Oklahoma and the other in the Mississippi basin, flanked the disturbance characterized by low θ_w (< 20C) over SW Missouri. Later, by 0600, a pressure trough had formed along the E and S boundary with a low center 1.5 mb deep over NE Arkansas. Two hours later, squall mesosystem 5 developed in the vicinity of this trough. Rapid approach of squall mesosystem 3 from the NW and intense development of system 5, combined with the rather sparse number of observations in the area, caused weaker system 1 to be lost as an independent mesosystem after 0900. The weak pressure trough running from W Arkansas to N Oklahoma remained and some convective activity developed along it during the afternoon hours.

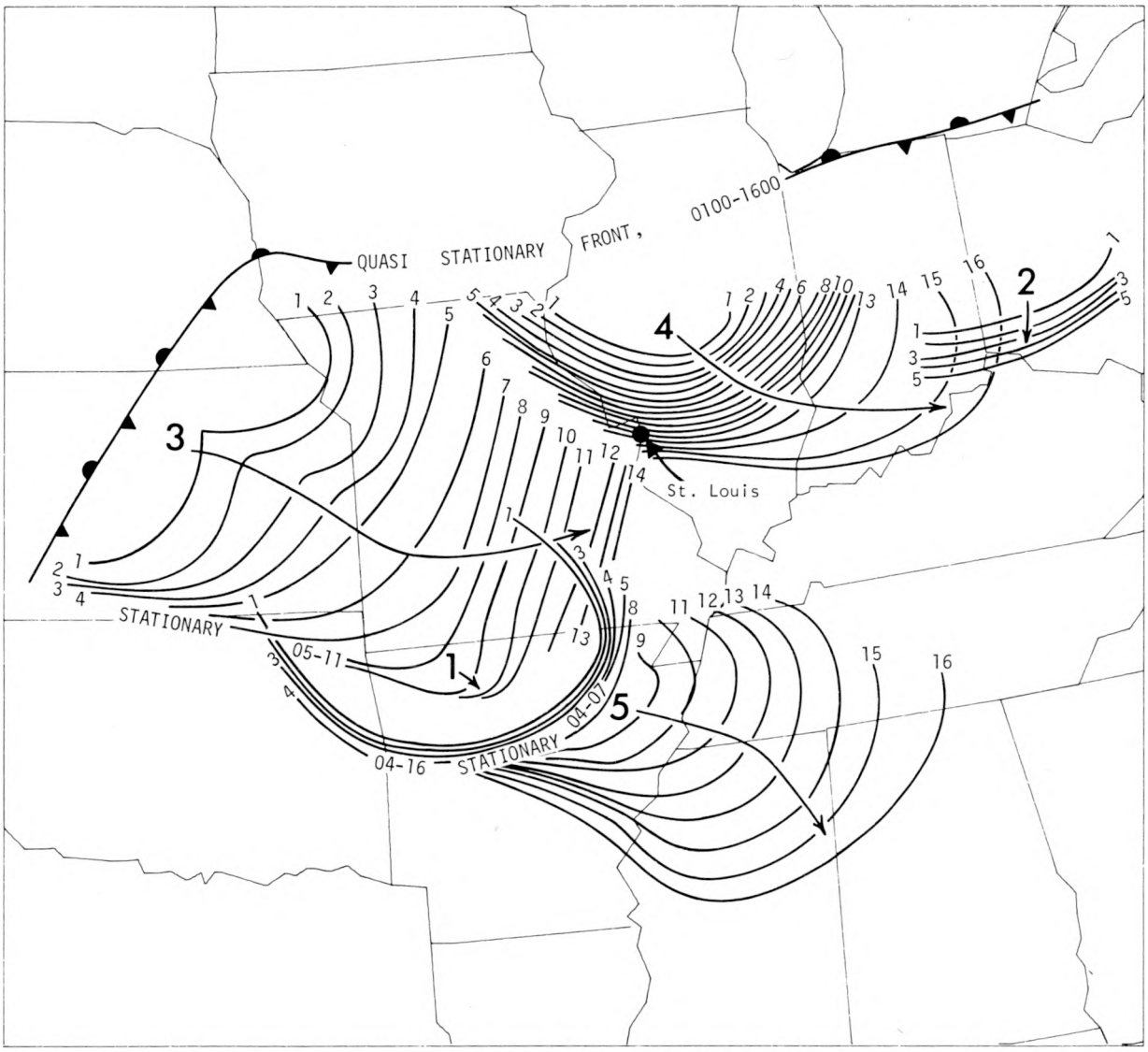

Figure J-2. Isochrones (in hours CDT) of leading edges of 5 mesosystems on 12 August

Squall mesosystem 2 dissipated over Indiana and Ohio during the pre-dawn hours of 12 August. Widespread thunderstorm activity was present from E Illinois to the E along and 200 mi S of the cold front as a short wave impulse passing through the area pushed the front toward the S. These storms and associated mesosystems weakened and disappeared from the study area after 0500 CDT.

Two areas of heavy thunderstorms merged over E Kansas to form system 3. This squall mesosystem progressed toward the E at about 30 kt until after 0600 when it diminished rapidly in intensity. The cold dome continued to spread and modify. By 1400 its leading edge could be defined as a weak pressure trough with slightly cooler temperatures behind it running from near St. Louis to the S into Arkansas.

Squall mesosystem 4 comprised several SE-moving groups of storms with overlapping trajectories. During the morning hours, the system expanded gradually under the weight of a cold dome that was intensified over roughly the same area by each passing echo group. A few of these storms were severe, producing 0.5 inch hail over the Survey's hail network in central Illinois.

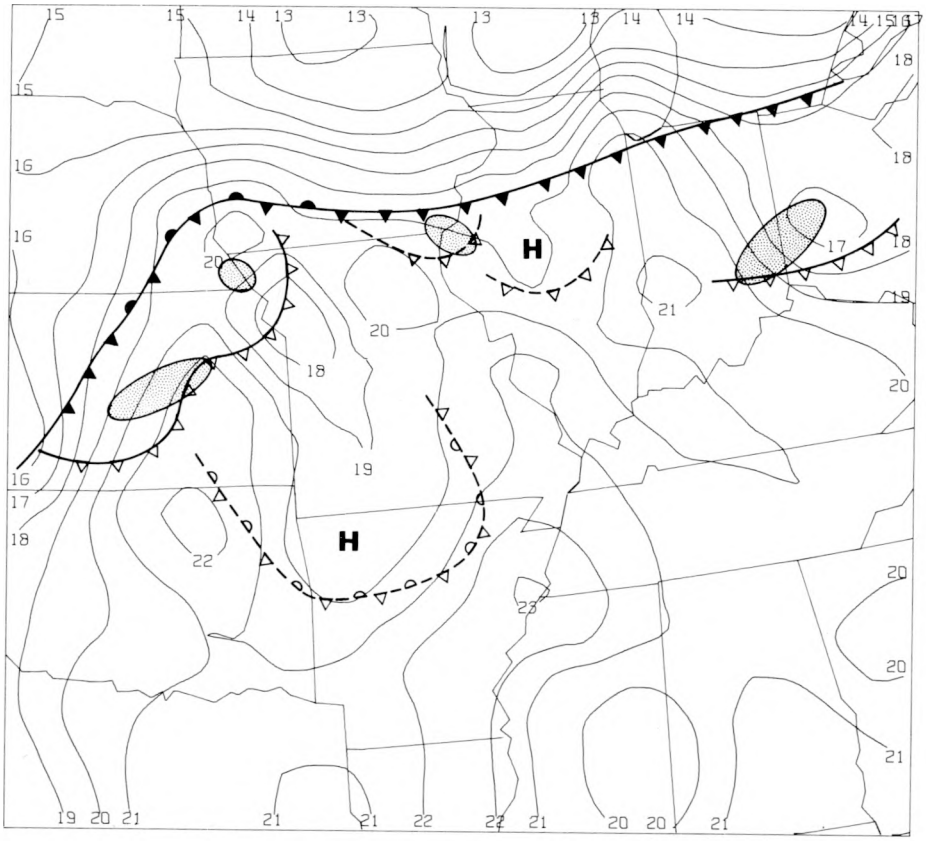

Figure J-3. Wet bulb potential temperature at 0200 CDT

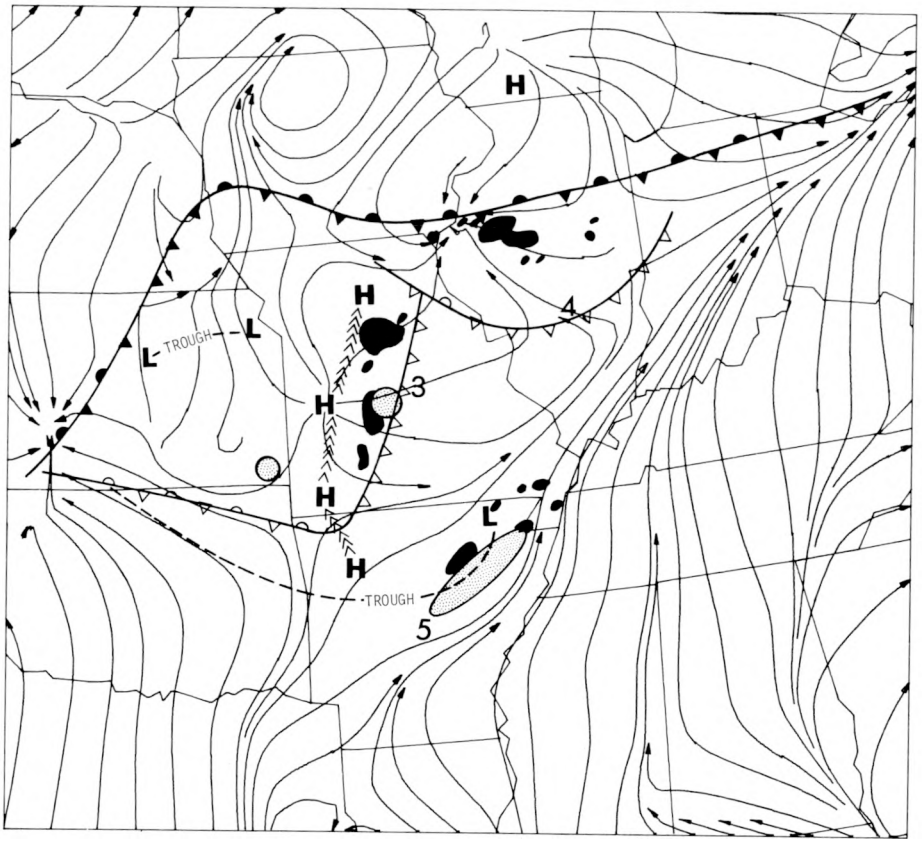

Figure J-4. Surface streamlines and positions of mesosystems at 0800 CDT

After 1200, the system intensified along the forward flank and moved to the E at 40 kt. Severe thunderstorms accompanied by tornadoes and wind storms occurred over E Illinois, central Indiana, and SW Ohio.

The W half of squall mesosystem 4 reactivated after 1530. Severe thunderstorms were reported at St. Louis and at Effingham in central Illinois. Maximum diurnal heating, plus the presence of squall mesosystem 3, helped intensify the thunderstorms in the St. Louis area.

Squall mesosystem 5 spawned at 0900 within the pressure trough associated with aged system 1. It expanded rapidly into Mississippi and Tennessee and became the day's most organized squall line with linear designation on two consecutive NSSFC radar charts. However, no severe weather reports were received with this system.

Movement of Mesoscale Systems into the St. Louis Area

Three important mesoscale systems were present in the St. Louis area just prior to and during the squall line development and severe weather outbreak of 12 August. The cold leading edge of the system 4 had entered the metropolitan area between 1100 and 1200 causing the wind at St. Louis to shift briefly to the NE. The system then became stationary along an E–W axis between St. Louis and Belleville.

The second possible mesoscale influence was the remnant of the old cold dome of system 3 which had passed Columbia and Vichy 40 mi W of St. Louis at 0900, a time when only a few isolated radar echoes defined the remains of the system 3 squall line. System 3 probably continued to expand and subside, increasing convergence farther E.

The third system providing convergence necessary to release convection over St. Louis was a mesocyclone not shown on figure J-2. It developed over NW Missouri at 0900 and moved rapidly SE to the general vicinity of St. Louis by 1500.

Figure J-4 shows streamlines and positions of mesosystems at 0800 CDT. Stippled areas indicate convective 'hot spots,' defined as areas with echo tops exceeding 40,000 ft as deduced from hourly radar summary charts, and the dark areas are approximate locations of radar echoes as taken from St. Louis NWS radar worksheets.

Mesosystem 3 was dissipating at this time, but radar indicated a broken line of showers and thunderstorms, several of which were fairly strong. By 1000 CDT these storms had dissipated. Farther W, a mesoscale trough, separate from the front, had developed over E Kansas. It probably developed as a 'wake low' when subsidence and adiabatic warming behind the major squall line caused pressure falls there.

Over Illinois, system 4 was active with several large echoes S and W of Peoria. Echoes over E Illinois were the remnants of a group of thunderstorms that had passed over roughly the same area several hours before. The area of echoes over NE Arkansas and SE Missouri developed into squall mesosystem 5 (see figure J-2).

Temperature, θ_w, pressure, and streamline fields for 1000 CDT (figure J-5) show distributions of dynamic and thermodynamic patterns 5 hours prior to the development of the storms in the St. Louis area. The double wind field trough over N-central and S-central Illinois locates the sataionary front and the leading edge of the mesosystem 4. Pushing to the SW, this mesosystem was in N Missouri and approaching the St. Louis area from the NE. Major precipitation areas were over central Illinois, but several new echoes had formed in the Quincy vicinity in W Illinois near the mesoscale front.

Because of cool air generation by the three squall mesosystems, the stationary front was lost in the temperature field (figure J-5a) but was placed well in the θ_w field separating moist con-

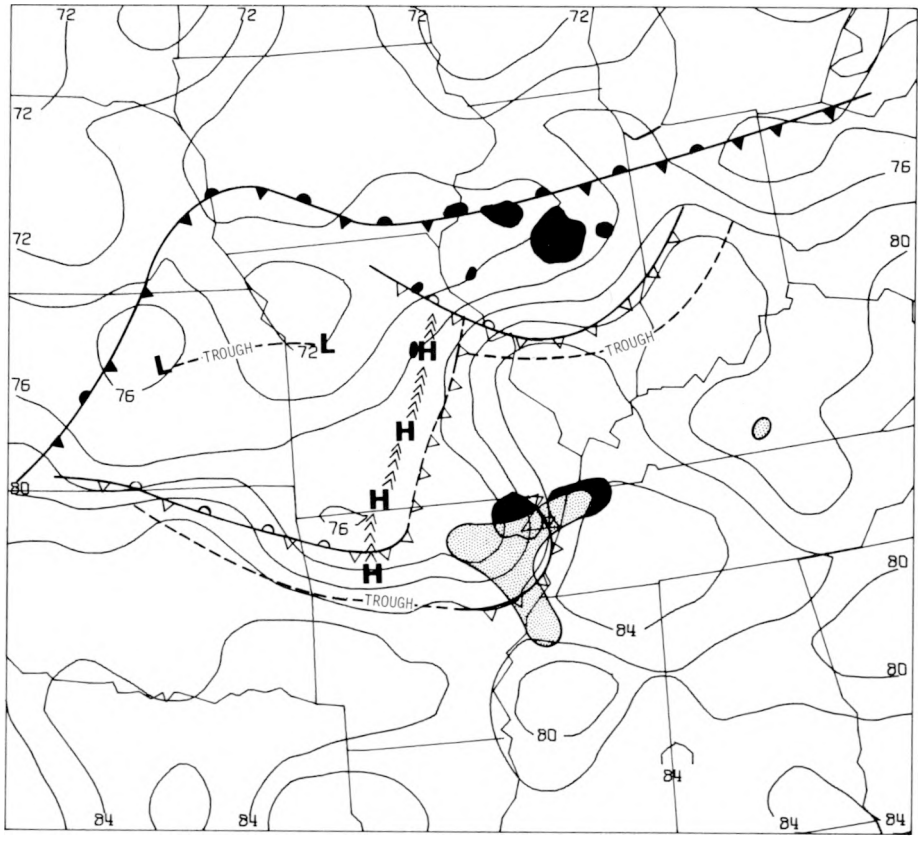

a. Surface temperature

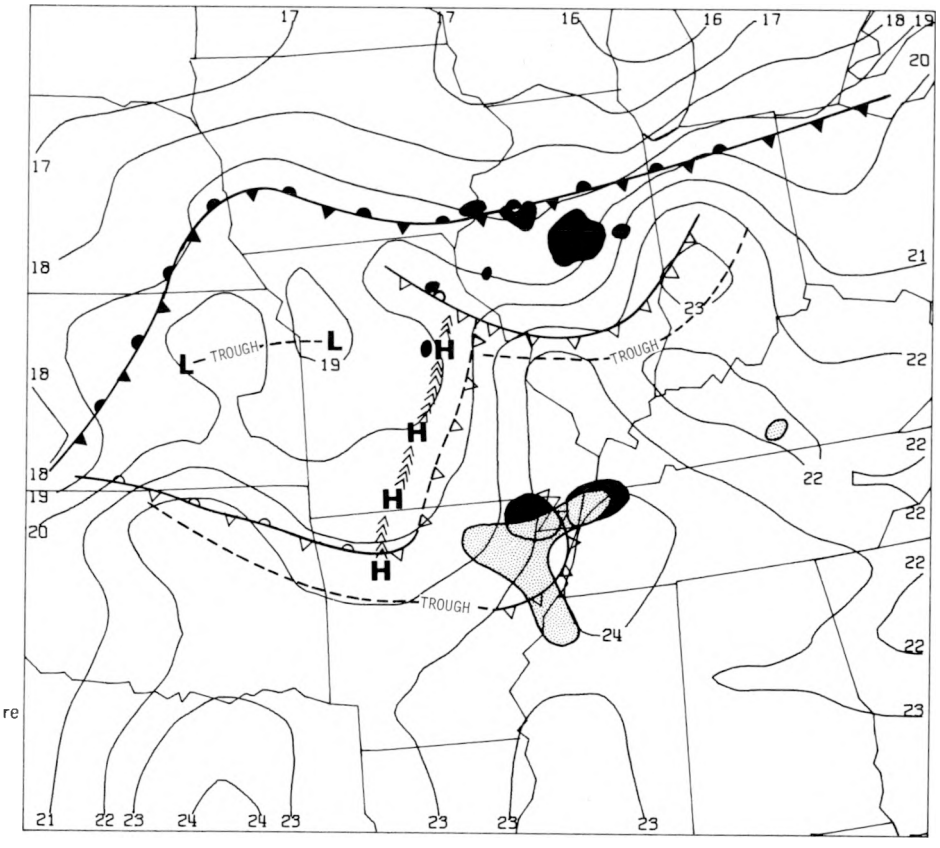

b. Wet bulb potential temperature

Figure J-5. Surface conditions at 1000 CDT

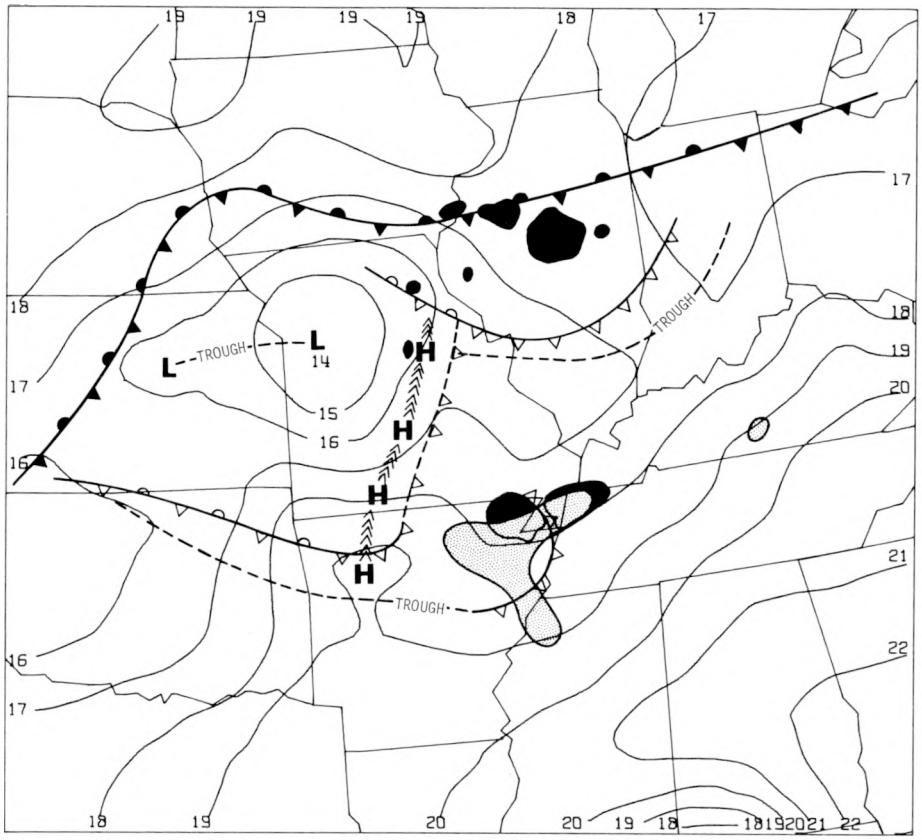

c. Surface pressure

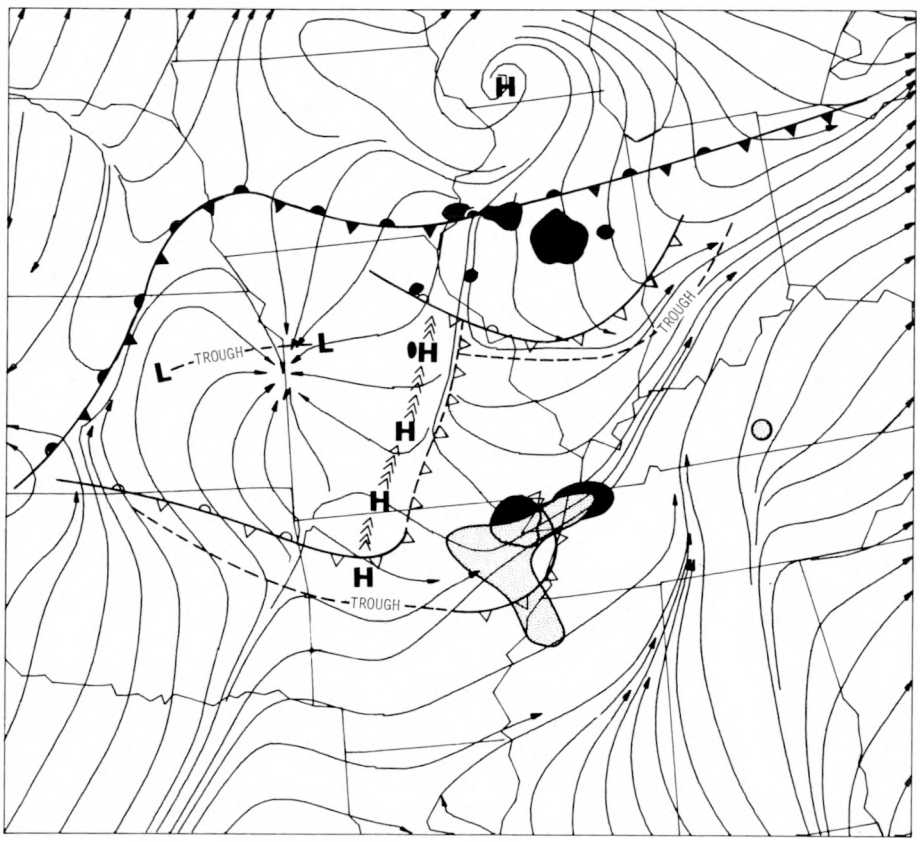

d. Surface streamlines

Figure J-5 (Continued)

vectively unstable air from drier air to the N. Both thermodynamic fields give good placement to squall mesosystems. System 3 was approximately 50 mi W of St. Louis and was still identifiable in the wind field by an elongated mesoscale ridge. Convective activitiy was rapidly diminishing.

System 5 was well established in the temperature field but had apparently not transferred sufficient quantities of low θ_w air downward from intermediate levels as this system was weakly shown in the θ_w field (figure J-5b)

The dominant feature of the pressure field was the mesoscale low over NW Missouri with a central pressure of less than 1014 mb. This low had reached sufficient intensity to accelerate winds over much of Missouri and E Kansas (see figure J-5d).

Farther E, a trough line appeared in the pressure field from E Missouri into central Indiana. This feature was relatively weak, yet was persistent in time and was of sufficient strength to influence the winds especially over Indiana where the trough appeared strongest. Increased convergence over central Indiana may have aided convective release there: severe weather reports from central Indiana and SW Ohio were received when system 4 intensified and pushed rapidly through the area.

Figures J-6 and J-7 show the continued development and propagation of the mesolow across Missouri to the E. At 1200 (figure J-6) convergence near the low was sufficient to initiate convective activity. This was relatively weak (echoes did not exceed 25,000 ft) and short lived because of the cool air mass over which the low moved. A weak mesoscale depression in the Springfield (Missouri) vicinity further complicated the analysis.

By 1400 (figure J-7) the mesolow was located approximately 50 m W of St. Louis. A weak pressure trough through E Missouri, S of St. Louis, marked the remains of the edge of system 3. Thermodynamic charts showed somewhat drier air W of this line that had warmed to temperatures typical of the undisturbed environment E of the trough.

A second trough extended SW from the mesolow. Had more observations been available, more complicated wind and pressure patterns might have been found. However, this trough line is the simplest representation of a pressure disturbance and was in agreement with winds and pressures at Springfield and Vichy.

The third pressure trough extended generally to the W from the mesolow into Kansas. It persisted through the remainder of the analysis period and was supported by more observations than the other troughs.

Farther E the trough line extending from Indiana to Missouri at 1200 was dropped from the 1400 chart when mesosystem 4 accelerated to the S to merge with it. At 1400 no radar echoes were associated with the W extension of mesosystem 4 or the approaching mesolow.

Fields of temperature, θ_w, pressure, and streamlines for 1500 are presented in figure J-8. This was when the storms in the St. Louis area were becoming well developed. An extensive baroclinic zone extends from the leading edge of system 4 in Indiana to the W into E Kansas. In Missouri, intensification of the baroclinic zone resulted from frontogenetical effects of the passage of the mesolow convergence field through the area.

Farther S, squall mesosystem 5 had developed an extensive cold dome over much of W Tennessee. A warm tongue extends NE across SE Missouri and then to the E ahead of the system 4 pseudo cold front.

The wet bulb potential temperature field (figure J-8b) retains support for the quasi-stationary front and, to an extent, for the trough extending S from St. Louis. In both thermodynamic fields, the mesolow located just W of St. Louis was embedded within zones of considerable contrast.

The pressure field (figure J-8c) shows system 4 lying within the trough which had been identified earlier as a separate entity. The mesolow is W of St. Louis. The three Missouri troughs present at 1200 still appeared in the pressure field and the main trough extending back into Okla-

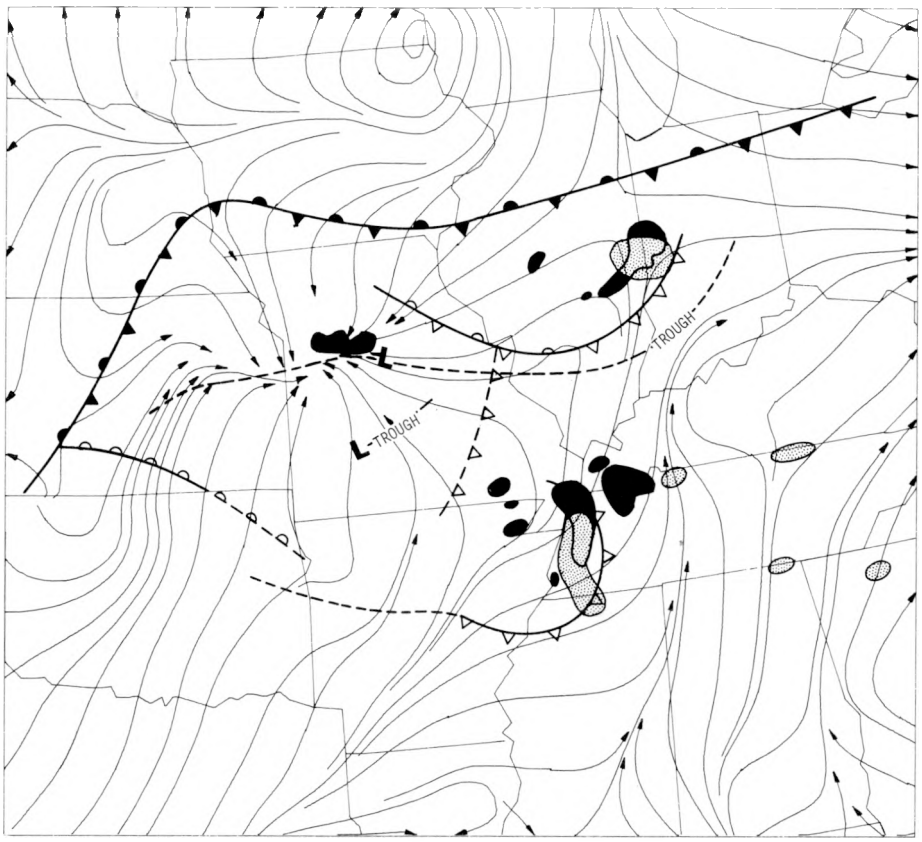

Figure J-6. Surface streamlines at 1200 CDT

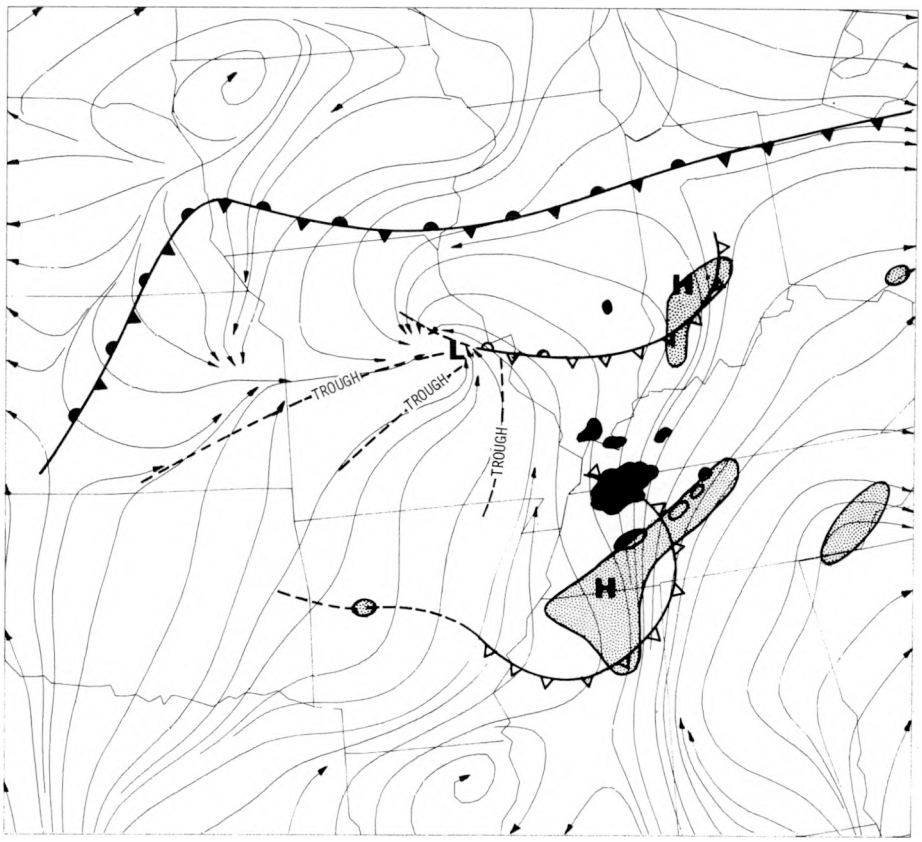

Figure J-7. Surface streamlines at 1400 CDT

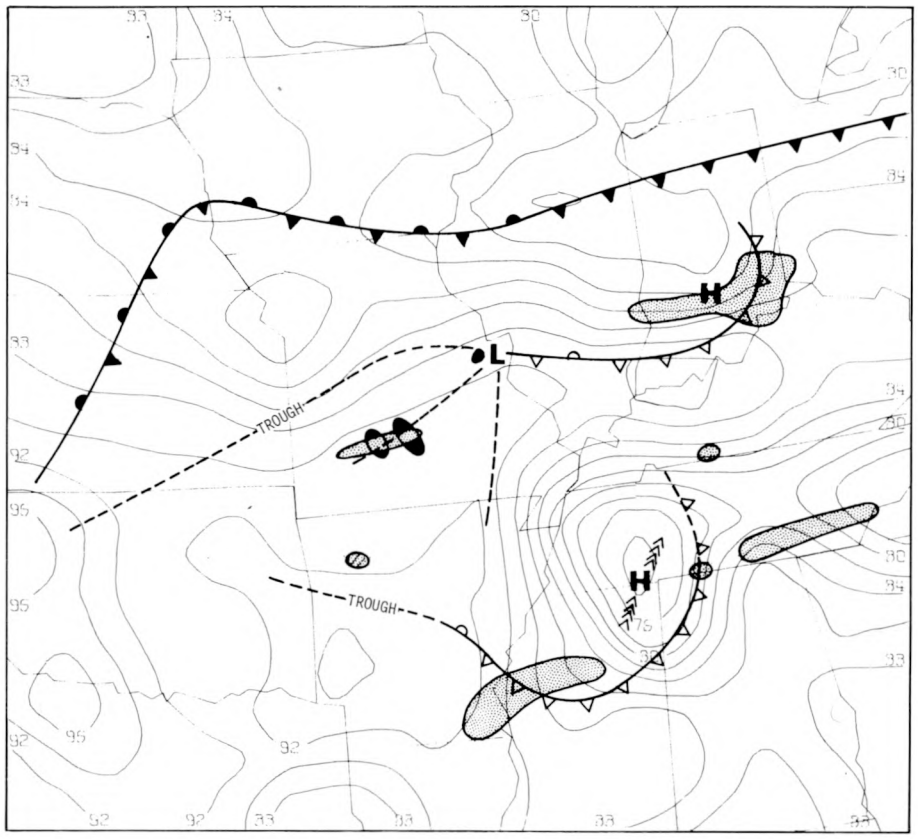

a. Surface temperature

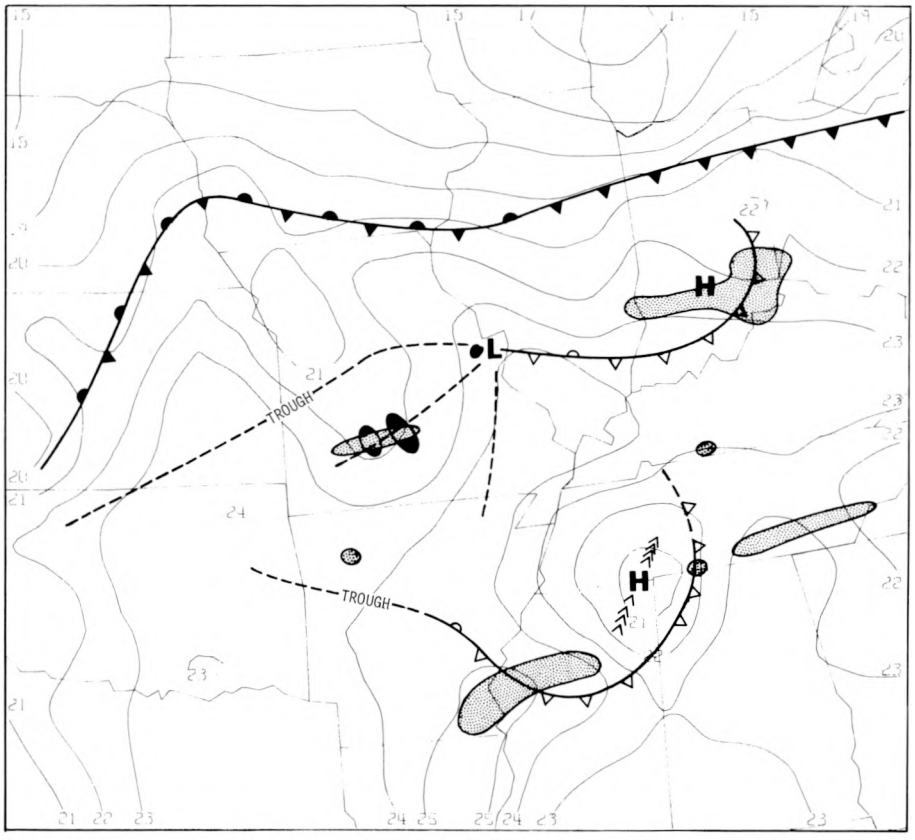

b. Wet bulb potential temperature

Figure J-8. Surface conditions at 1500 CDT

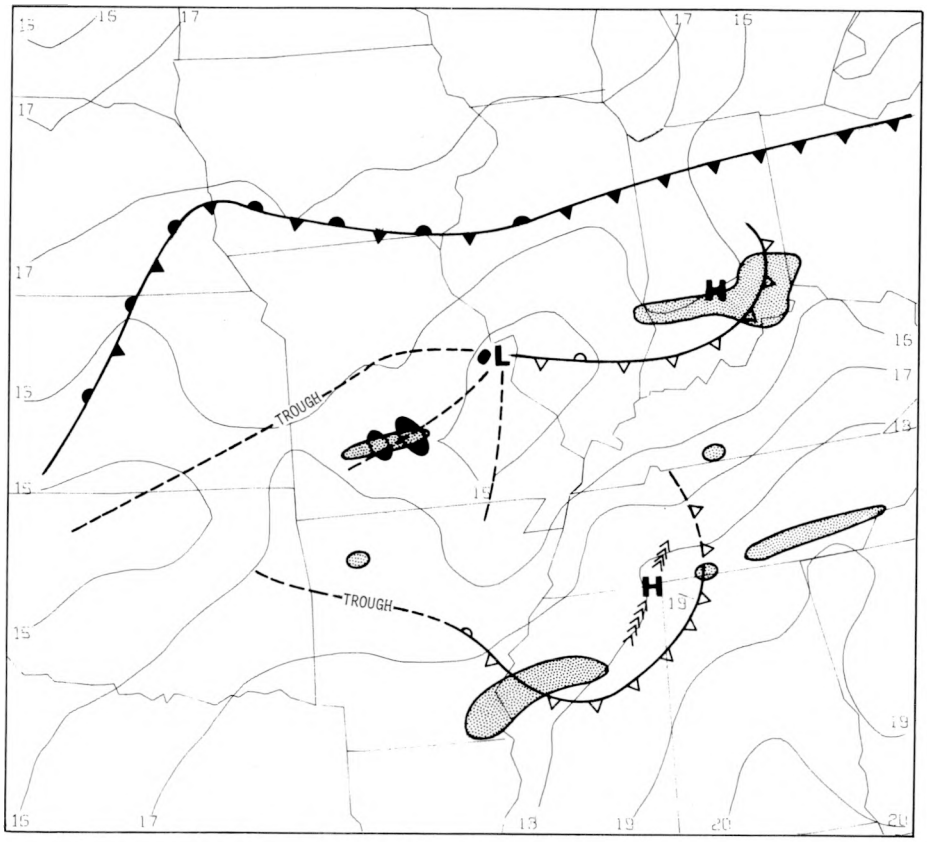

c. Surface pressure

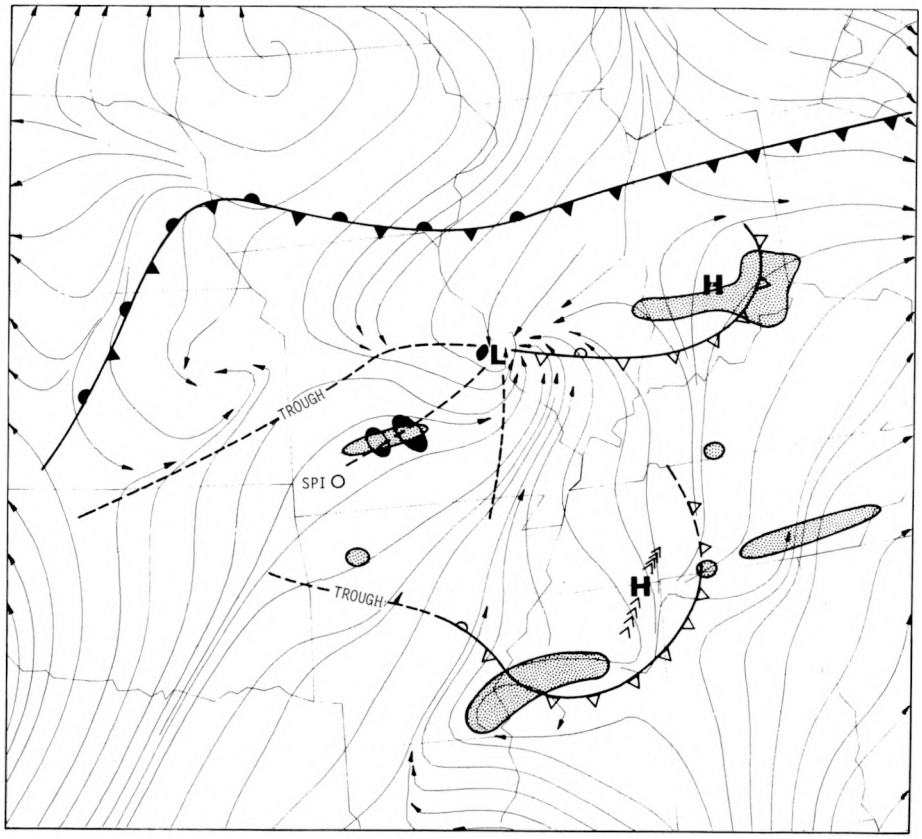

d. Surface streamlines

Figure J-8 (Continued)

homa was supported mainly by the wind field (figure J-8d). Several echoes have appeared along the second trough in SW Missouri. One small but strong echo is shown W of St. Louis near the mesolow center. The exact position of the low center cannot be determined on this scale so no inferences are made as to its position in relation to the echo just W of St. Louis.

Before 1500, the analyses showed the mesolow to have propagated within an air mass characteristic of a partially modified subsident cold dome. However, about 1500, the mesolow approached the forward boundary of this air mass, and for the first time its convergence field drew upon air with a higher degree of convective instability. *This occurred at or very near St. Louis.*

Air masses in the St. Louis area had been further destabilized through convergence and lifting during the 4-hr period prior to thunderstorm development. Figure J-9 shows patterns of accumulated convergence (from 1100 to 1500) occupying much of Missouri, S Illinois, and SE Kansas. Cumulative convergence values across S Missouri and SE Kansas were apparently a reactivation of old squall mesosystem 3. Convergence in S Illinois resulted from acceleration of winds into the pressure trough ahead of mesosystem 4. High convergence values over N-central Missouri were due to the mesolow that approached St. Louis.

Figure J-10 shows the cumulative convergence patterns for the 8-hr period ending at 1900. Increases from St. Louis to the E compare well with intense thunderstorm out-breaks over S Illinois after 1600. By 1800, the convergence zone had activated thunderstorms from E Illinois to N-central Oklahoma with numerous tops exceeding 50,000 ft.

Further, the tendency for the cumulative convergence zone to remain stationary accounted for the persistence of echoes with tops about 40,000 ft over SE Kansas and SW Missouri, while as the rejuvenated squall mesosystem 3 pushed SE into N Arkansas, echo tops fell below 40,000 ft.

After 1500, the mesolow moved through air masses favorable for intense convection, and coupled with favorable afternoon heating conditions, this movement led to rapid development of thunderstorms in and SW of St. Louis along the second pressure trough. This activity, along with positions of fronts and mesosystems for 1600, are shown in figure J-11. Stippled areas indicate convective 'hot areas' with echo tops above 40,000 ft. The mesolow is positioned between St. Louis and Belleville. A SW wind at St. Louis reflected outflow from nearby thunderstorms, not the mesolow circulation, and pushed the wind field circulation center to the NE into Illinois.

In summary, severe thunderstorms occurring in the St. Louis area between 1500–1600 could be ascribed to the chance combination of three mesosystems that increased convergence and destabilized the atmosphere to the extent that, in the presence of strong afternoon heating, they led to explosive convection. This event could have been predicted with the use of mesoscale objective analyses of several standard observed meteorological variables, attesting to the importance of these methods in providing short-range local thunderstorm forecasts.

Upper Air Synoptic Patterns

The closest major jet-stream axis lay over S Wisconsin at both 0700 and 1900 CDT with the maximum wind over Peoria and Salem slacking from 65 and 42 kt, respectively, to 49 kt at Peoria (Salem missing) during that time span. Tropopause pressures were less than 150 mb with temperatures near -67C throughout the period.

The morning 850-mb chart (figure J-12) showed the general frontal picture described by surface analyses with some irregularities in the field patterns which can be ascribed to the mesoscale systems.

The 700- and 500-mb charts (figures J-13 and J-14) show some interesting features which relate to the events at St. Louis later in the day. The 500-mb chart suggests a prominent area of

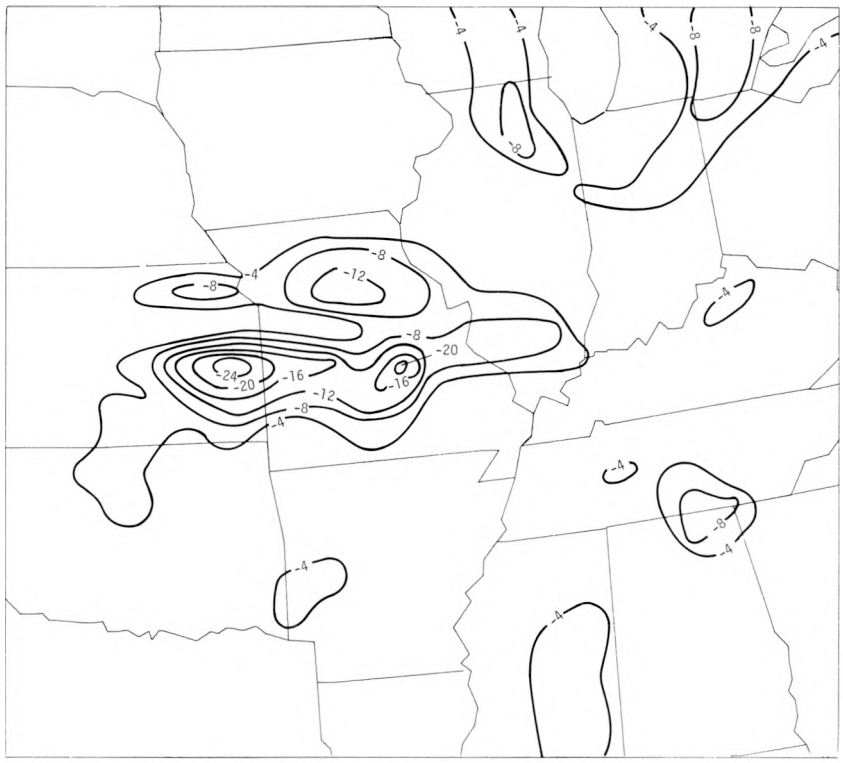

Figure J-9. Accumulated convergence values in 1100 to 1500 period

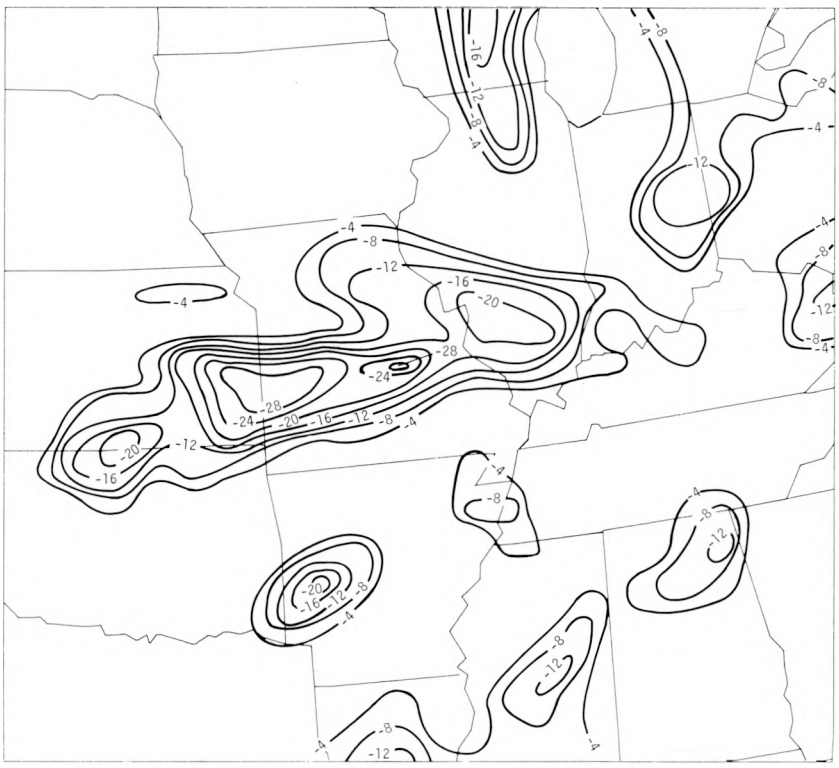

Figure J-10. Accumulated convergence values in 1100 to 1900 period

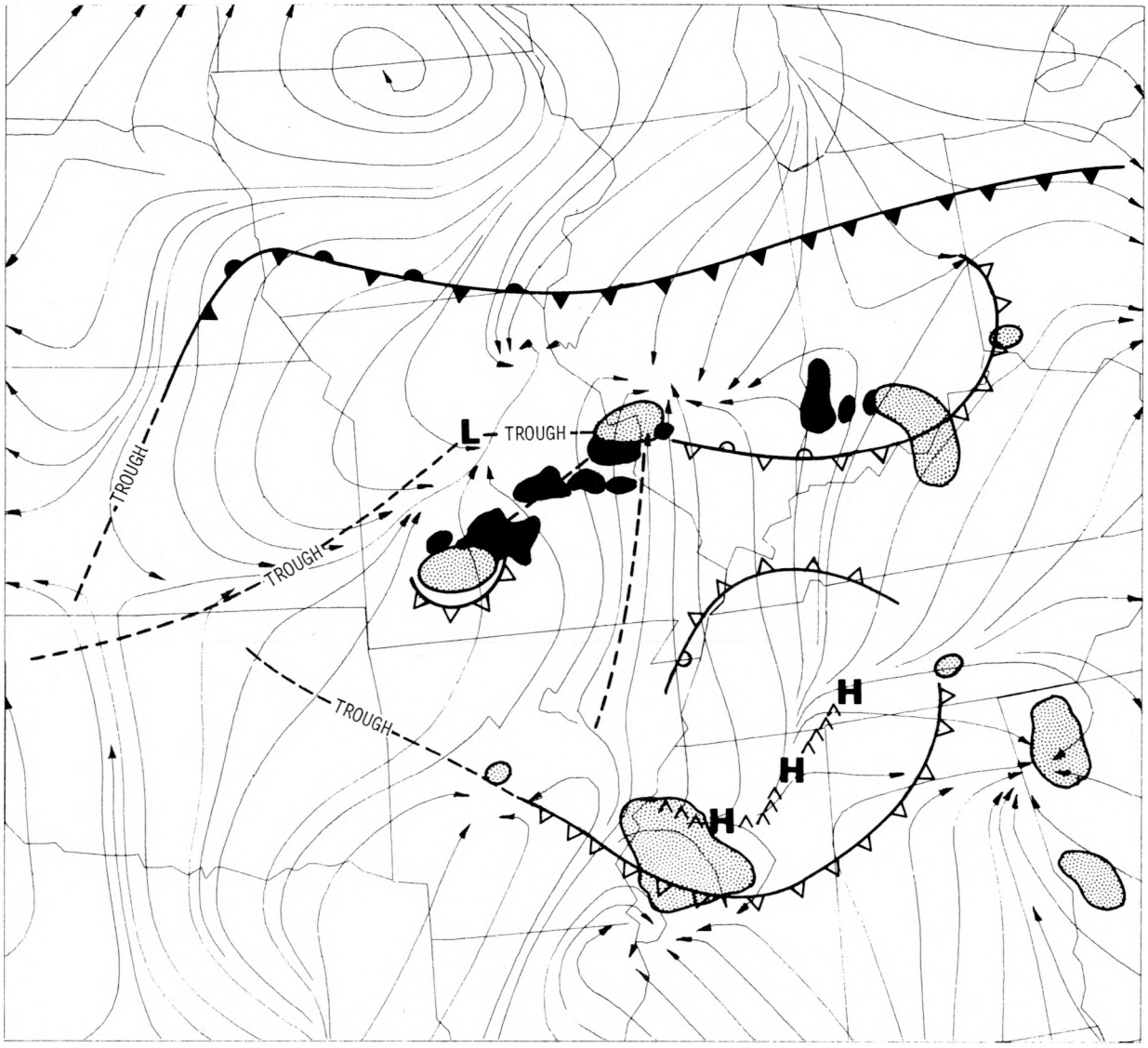

Figure J-11. Surface streamlines, synoptic weather conditions, and echoes at 1600 CDT

subsidence warming adjacent to and W of a cool area of high relative humidity that covers most of Illinois, Missouri, and SE Kansas. The wind observations show that the subsiding air behind the moist region may be a descending jet branch. Additional subsident air is apparent over Arkansas and Tennessee. At 700 mb, the warm dry subsident air is apparent over S Illinois and central Arkansas and to the W over W Iowa, Nebraska, and W Kansas. The moderately cool, moist sounding over E Kansas and SW Missouri may be partly due to contamination by convection, but the area is roughly in line with the cool moist area at 500 mb.

At 1900 just after the squall line period at St. Louis, the overall pattern at 850 mb (figure J-15) reveals little progression. A large area of low ($\leq$ 8C) dew points replaced the previous moist center astride the Mississippi. This reflects the passage of the mesoscale systems previously described. At 700 mb (figure J-16) the dry warm axis persists across Arkansas, S Illinois, and Kentucky, with the cool moist axis still identifiable across the St. Louis area. At 500 mb (figure

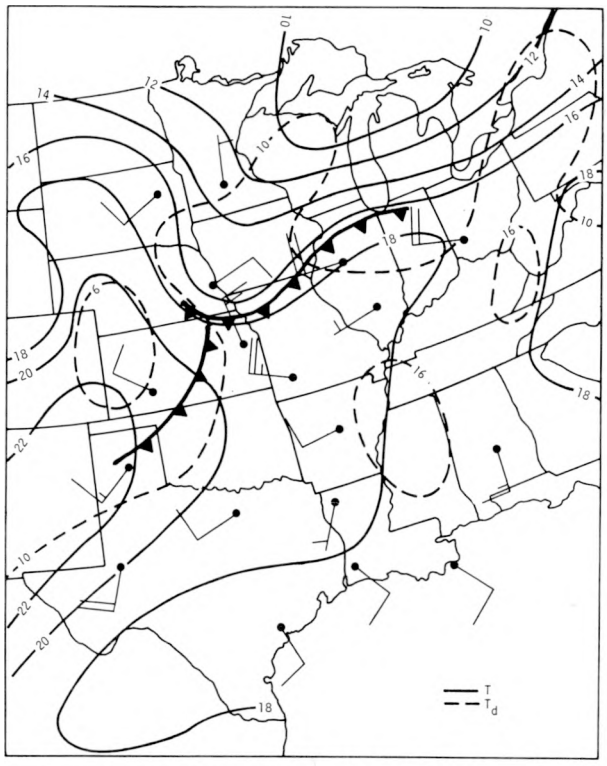

Figure J-12. Conditions at 850-mb level at 0700 CDT

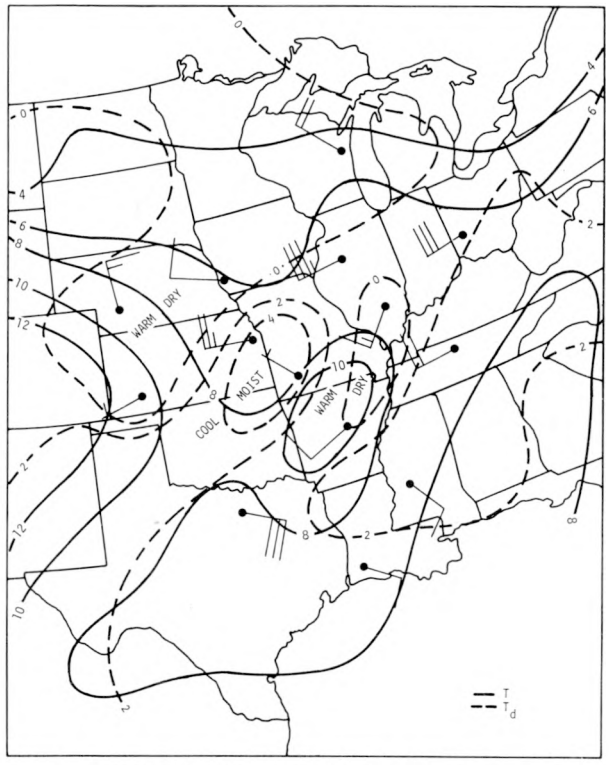

Figure J-13. Conditions at 700-mb level at 0700 CDT

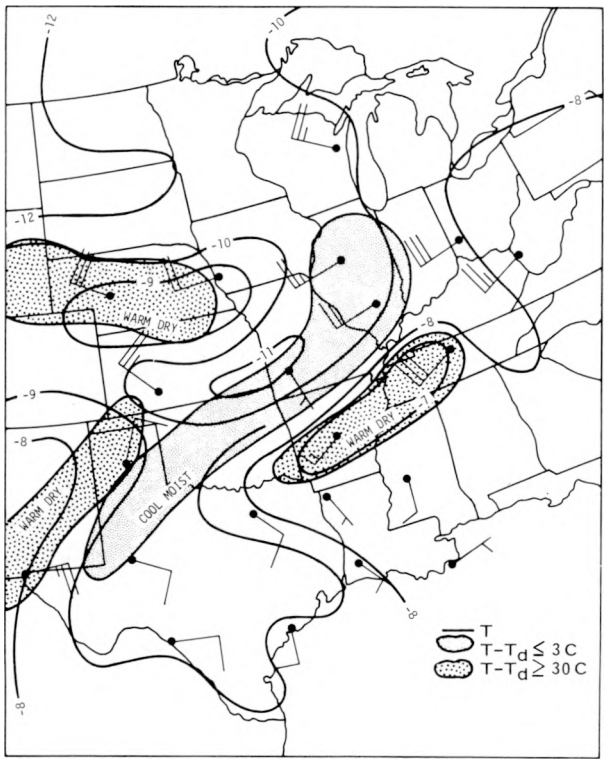

Figure J-14. Conditions at 500-mb level at 0700 CDT

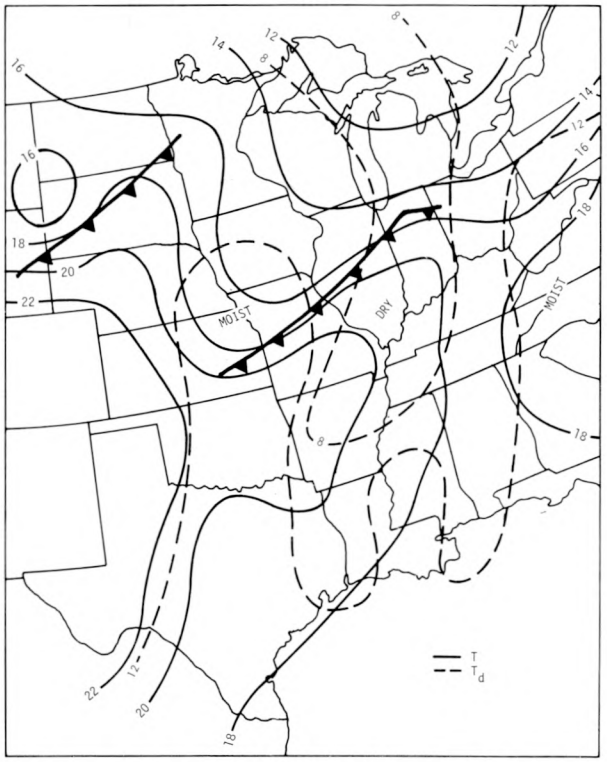

Figure J-15. Conditions at 850-mb level at 1900 CDT

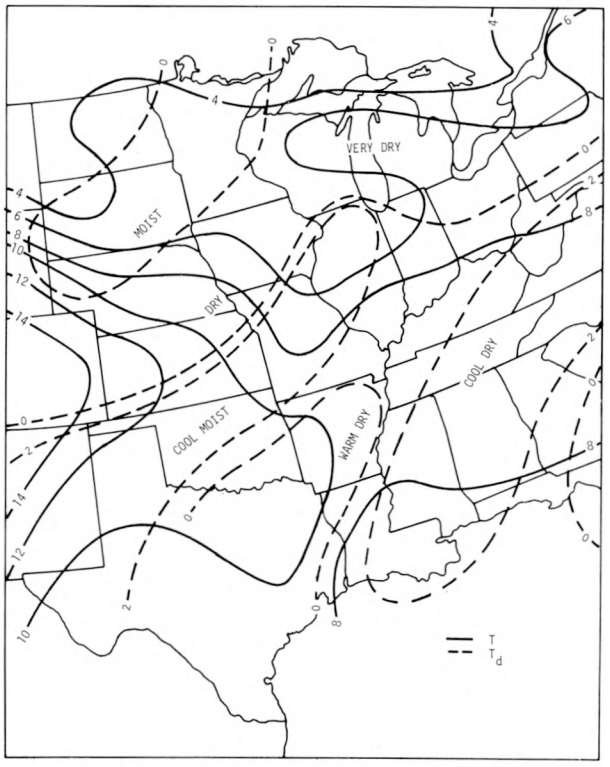

Figure J-16. Conditions at 700-mb level at 1900 CDT

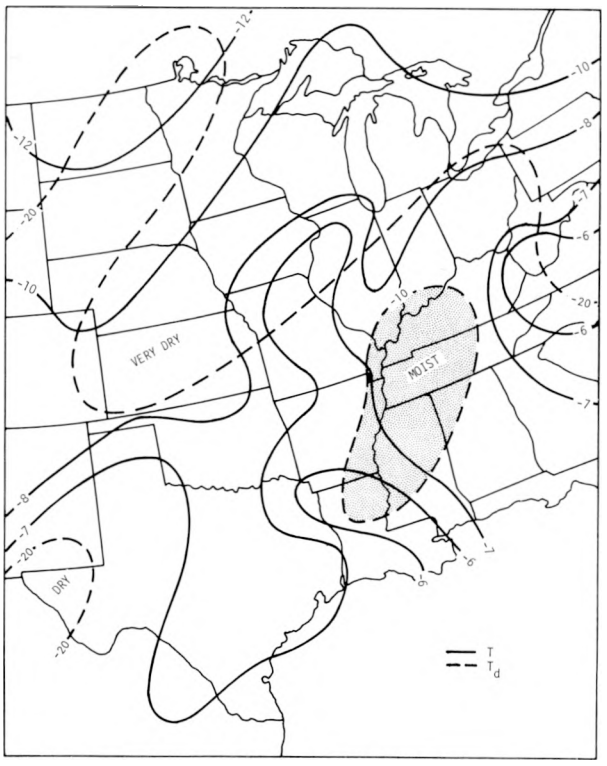

Figure J-17. Conditions at 500-mb level at 1900 CDT

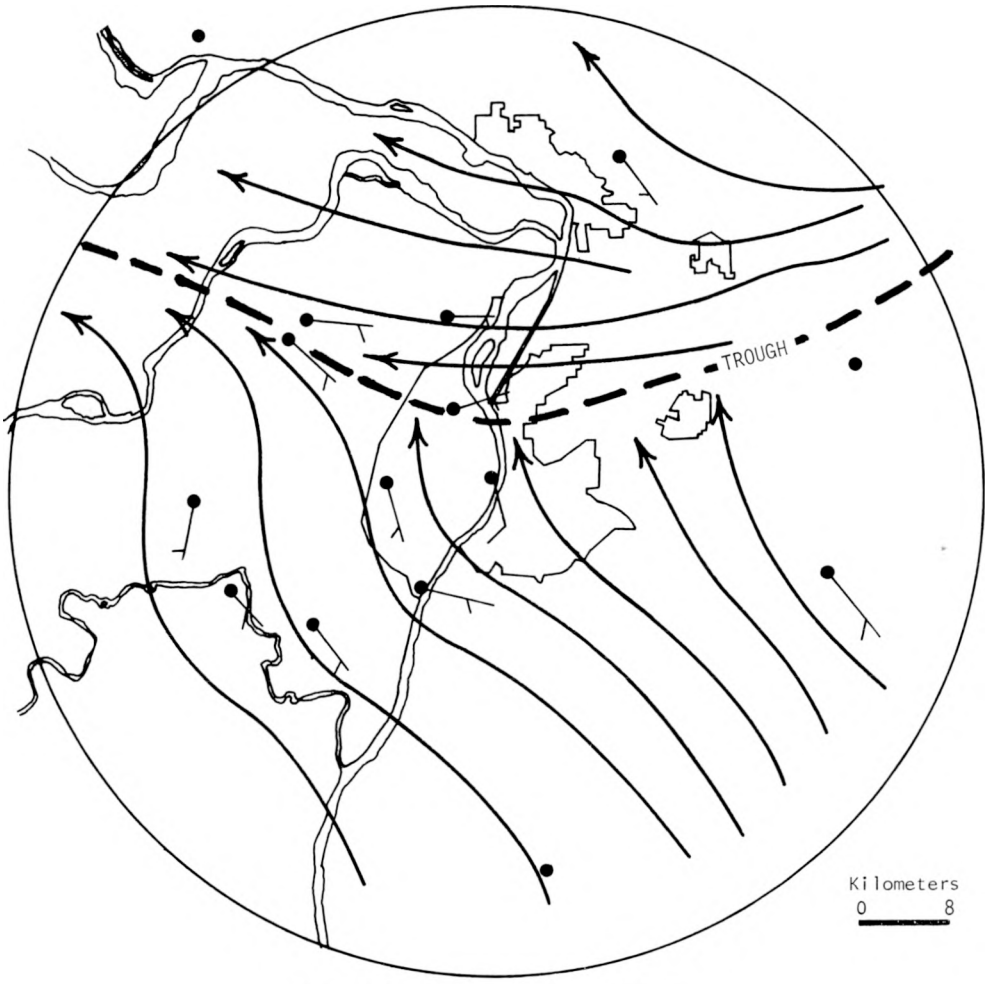

Figure J-18. Surface winds at 1300 CDT

J-17) the dry, possibly subsident air mass is located farther N over N Illinois, Iowa, N Missouri, Kansas, and Nebraska. Moist air implying rising motions or convective contamination is over Louisiana, Mississippi, Tennessee, Alabama, Kentucky, and S Illinois.

WEATHER CONDITIONS IN THE MMX CIRCLE

The period of greatest meteorological interest in the MMX circle began just prior to the first precipitation that began just before 1500. The general conditions in the area leading to the intense activity can be best understood by study of conditions in the 1200 to 1400 period.

The wind flow at the surface at 1300 (figure J-18) suggests that the trough, which marks the edge of mesosystem 4 centered to the NE, lies through the circle, with more or less SE winds to the S, and E flow in the N part. This trough is the location of the initial radar echo developments within the circle.

Sounding and Upper Air Analysis

Upper air soundings were made from PMQ at 1327 and 1600 CDT, from ARC at 1333, 1633, 1714, and 1811, and from BCC at 1330, 1720, and 1800. Our analysis of these soundings focuses on the stratification of the equivalent potential temperature, θ_e. The analysis of θ_e from soundings so close in space and time is illuminating not only for the case at hand but also for research on large-scale θ_e analysis such as that described by Morgan and Beebe (1971).

At 1330 (figure J-19) at both PMQ and ARC there are middle level quasi-adiabatic layers with near constant mixing ratios. This is usually the case just above the θ_e minimum level in subsiding layers of low θ_e air. The subsidence within the air mass steepens the lapse rate and enhances vertical mixing. Subsequent lifting will not rapidly alter this configuration. Atop this layer at approximately 4500 m above PMQ there is a saturated (probably cloud) layer of higher θ_e which appears to be of low-level origin. It may be a Cu residue or anvil, or, since the sounding indicates that the saturated air is in either a neutral or buoyant state, this layer may be rising Cu or Ac elements encountered by chance. The θ_e profiles at these two sites are, apart from this saturated layer, typical of summer over the continent. The lower layers (up to about 2500 m) are convectively unstable as indicated by the dry minimum in θ_e. The low values of θ_e are characteristic of polar air, while the layers nearer the surface have tropical characteristics.

At BCC the stratification is somewhat different. The dry θ_e minimum below 3000 m is present as in the other two soundings, but the layer of air with θ_e less than 330K is much deeper, extending to over 6000 m. This higher level low θ_e air has a higher relative humidity with height, not quite reaching saturation just above 5000 m. This indicates that this air mass has been lifted. Lifting low θ_e air produced very low temperatures; in fact, in this case the 500 mb temperatures are -7, -9, and -11C at PMQ, ARC, and BCC, respectively, a gradient of 4C in about 40 mi. *The fact that this gradient may or may not be real or representative has consequence mainly for the general problem of representativeness of widely spaced soundings.* The soundings at PMQ and ARC may be merely contaminated by the cloud layer which was discussed above. In that case the sounding at BCC would be more representative of the pre-storm environment over the MMX circle (figure J-14 shows a closed -11C isotherm at 500 mb in SW Missouri and SE Kansas).

The low level θ_e values are also interesting. The major feature is that θ_e values are lower than elsewhere in the lowest 1000 m at BCC, which is upwind with respect to the low-level flow. The explanation for this may lie in some old meso or sub-mesoscale system not apparent in the synoptic analyses, or it may be related to the cloud bands visible in a 1300 CDT satellite photograph. The cause of this cool air cannot be isolated with confidence.

Static instability indices for the three soundings at the cross section shown on figure J-19 show moderate to great instability (as great as 7C of buoyancy at 500 mb). However, the levels at which parcels from low levels become buoyant (LFC) are near or above 700 mb for all three soundings. In the light of possible contamination of the two soundings (not to mention the spatial proximity of the soundings), one might entertain the possibility of low-level air such as is present over ARC rising through a middle troposphere such as that at BCC. In this case the LFC drops to near or below 850 mb and the buoyancy at 500 mb becomes 9 or 10C.

Surface Weather Conditions

Figure J-20 shows S winds just penetrating an otherwise W pattern from the S at 1000 CDT. Even with such a gross change in flow there are very little time and space changes in the overall temperature or virtual temperature distribution 2 hr later (figure J-21). At 1200 the warmest temperature axis over the city is in its western part, and the locally coolest area lies to the N, but also over part of the city.

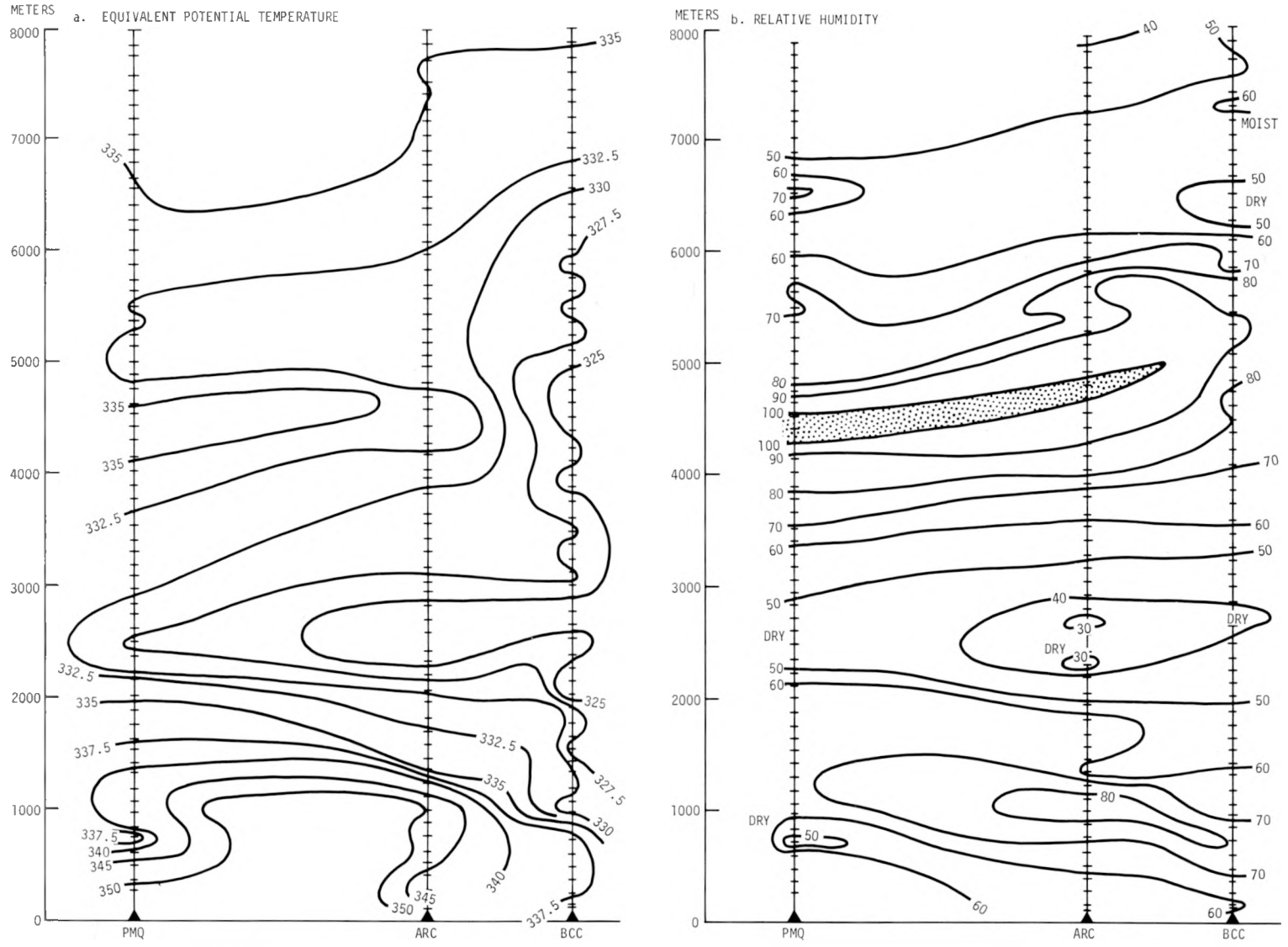

Figure J-19. Vertical cross section of equivalent potential temperature (°K) and relative humidity (%) at 1330 CDT

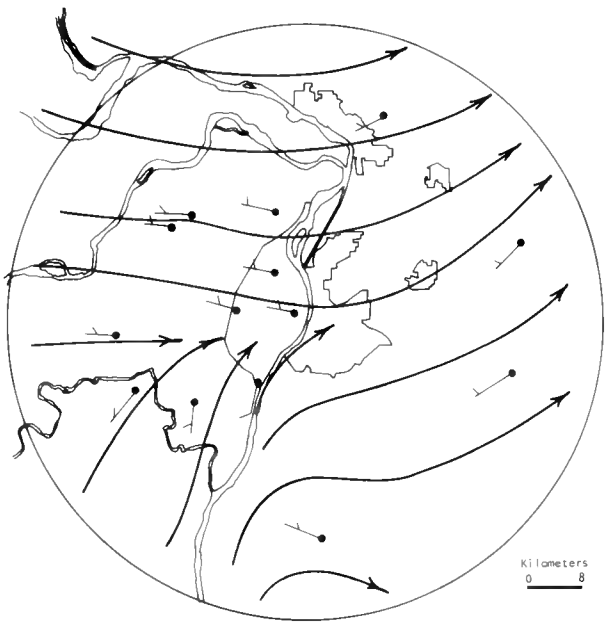

Figure J-20. Surface winds at 1000 CDT

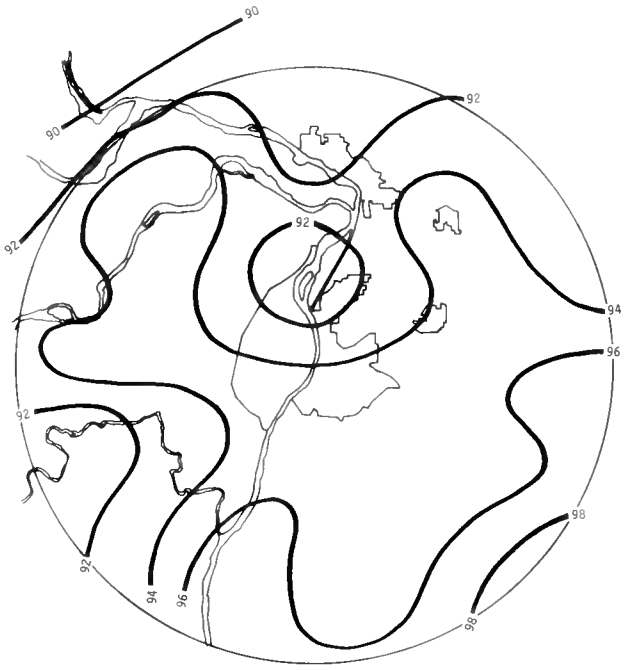

Figure J-21. Virtual temperature (°F) at 1200 CDT

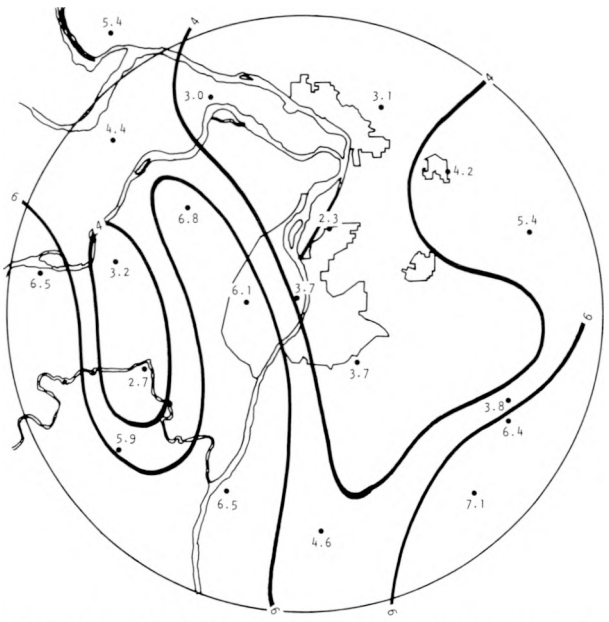

Figure J-22. Difference of 0600 temperatures on 12 August and 0600 average for August 1973

An examination of the 1200 average temperatures calculated for August 1973 (Jones and Schickedanz, 1974) showed that the cool area on the N is a persistent feature. To avoid the possibility that this feature might be due to either instrument bias or to particular site characteristics, it was decided to compare the montly averages (which are available for each hour) with the actual temperature changes on 12 August. The August means for 0600 have been subtracted from the values at all stations in figure J-22. This shows a warmer than average morning temperature distribution, and the greatest departures from the mean are along the river and over the W suburbs of St. Louis. The smallest departure is at Site 79 (Granite City). The same treatment for 1200 CDT (figure J-23) shows a similar pattern, with some differences (if the warming from 0600 to 1200 were normal at all stations, the maps would be identical in all respects). Figure J-24 shows the result of subtracting figure J-23 from figure J-24 which gives the departure of the 6-hr temperature change from its monthly average. These show that an abnormally high heating rate occurred over a large region to the NE of St. Louis (Alton, Edwardsville, Granite City); over a very small region just W of St. Louis; and in the vicinity of the juncture of the Meramec and Mississippi Rivers. A pronounced retardation of heating occurred in the vicinity of STL. The areas of least heating were where substantial rains had occurred on 10 August and evapotranspiration differences may help explain the high and low temperature areas.

It is interesting to consider the parallel that exists between this morning heating pattern and the locations of the major storm initiations which followed. The first major radar echo grew near the small intense anomaly S of St. Charles, and the second and more major storm activity of the day occurred in the more extensive area of anomalous heating which encompasses Granite City. The third area of anomalous heating was also subjected to low-level wind divergence (discussed below).

The major research problem is to assign a cause to the pattern of pre-rain heating. It could be due to 1) differences in incoming radiation (cloudiness, haze), 2) the effects of the thermal properties of the underlying surface, or 3) a combination of these and advection. It is important to stress that the patterns under discussion are free of any normal effects such as the persistent urban heat island. We suspect, from study of the radiosonde and pibal data, that some dramatic changes were occurring just above the surface. This suggests that the response of the surface layers to these changes is slower than is generally thought. All of the soundings showed a sharp drop in temperature and humidity just above the surface. However these may be due to an erroneous surface measurement by the operating crew because these surface values agree with the values derived from the hygrothermograph network. The suggestion is that the surface values reflect little more than the character of the local surface, at least on the space scale of our study.

This is a serious problem. Meteorologists commonly infer the state of the lowest kilometer of the atmosphere from surface observations. This usage is implicit in our METROMEX study, and our greatest hopes for short-range hail forecasting, under study as part of DESH, rely on it. One cannot arbitrarily say that the soundings are in error, nor can one abandon use of hourly surface reports. The subject merits very serious study.

Low-Level Airflow

The low-level winds from the pibal network show another interesting feature, in addition to the presence of the trough already noted in the surface data. At the 100-m level at 1330 CDT, the isotach pattern shows a strong speed (> 7 m/sec) maximum moving into the MMX circle from the SE (figure J-25). At 1400 (figure J-26) the maximum is in the circle with speeds > 5 m/sec. At 1530 intense convective activity was under way, and the flow pattern (not shown) was somewhat

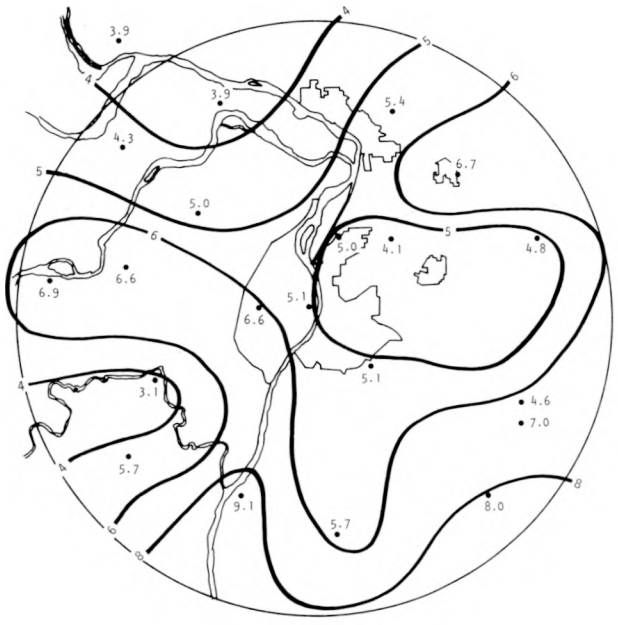

Figure J-23. Difference of 1200 temperature on 12 August and 1200 average for August 1973

Figure J-24. Departure of heating 1200–0600 on 12 August from the average heating for August 1973 (°F)

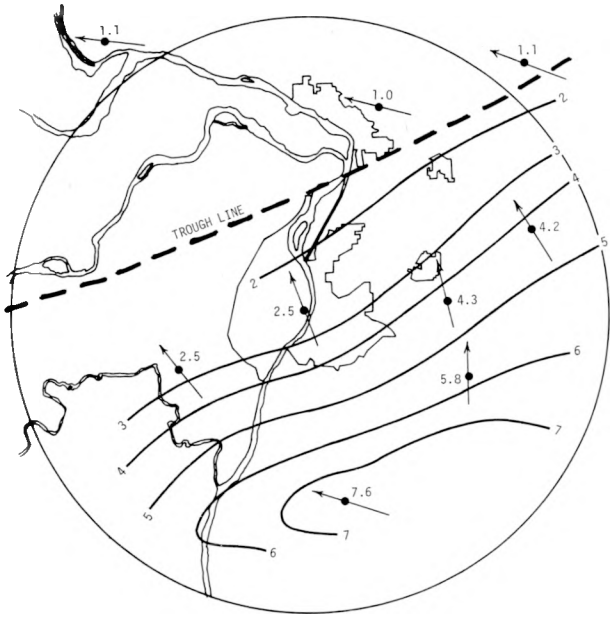

Figure J-25. Isotach (m/sec) pattern at 100-m level at 1330 CDT

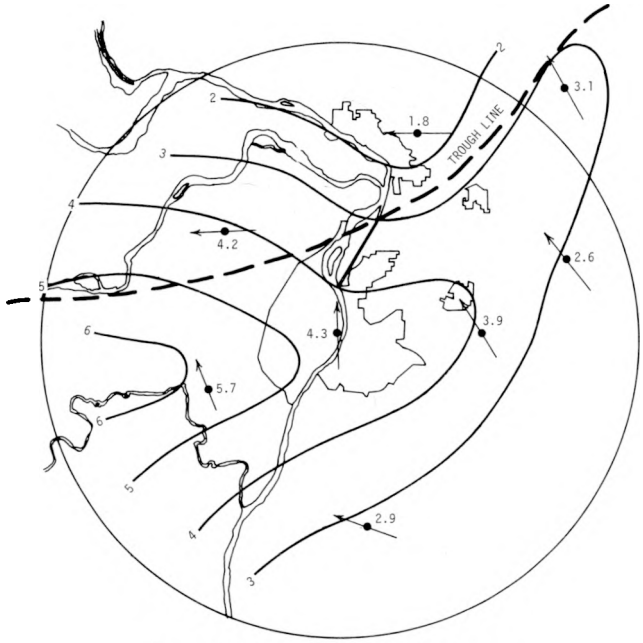

Figure J-26. Isotach (m/sec) pattern at 100-m level at 1400 CDT

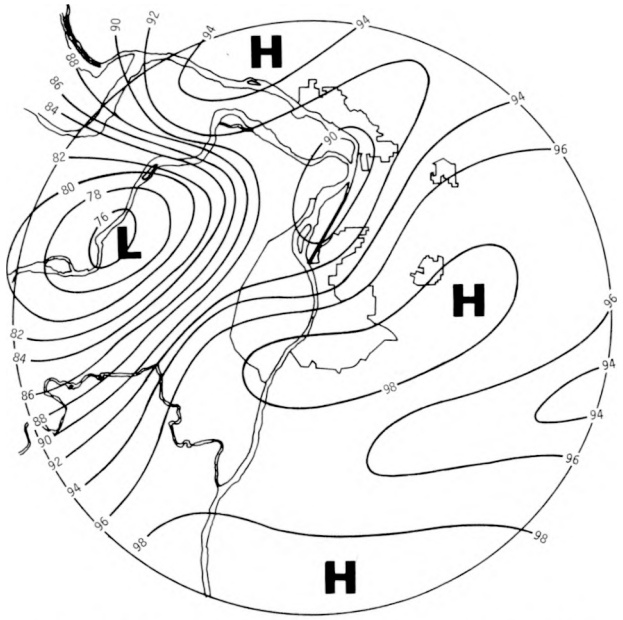

Figure J-27. Virtual temperature pattern at 1500 CDT

disturbed by the presence of cold outflow from the storms. The high-speed surge, if real, may be related to the cooler air apparent in the lower layers at BCC in the 1330 θ_e cross section (figure J-19). In one accepts the existence of this speed surge (allowing for the possible errors in the measurements), then it becomes a candidate for the role of 'trigger' in setting off the extreme convection which began along the trough on the W edge of the MMX circle just before 1430. The arrival of the surge at the position of the trough would produce local pre-storm convergence values in excess of any of those computed from the data by Bellamy's method. At 1330 the calculated 100-m peak convergence was 2.9×10^{-4} ; the 500-m peak convergence was 4.2×10^{-4} ; and at 1400 these became 2.3×10^{-4} and 2.8×10^{-4} at 100 and 500m, respectively. No estimates could be made near the W edge of the circle at either time.

The 1500 CDT virtual temperature distribution (figure J-27) shows the initial phase of cold air production by the first convective storm cell. The 100 m winds at 1600, shown in figure J-28 seem to catch the cold outflows from radar echo systems A and B (see figure J-32), and the cold outflow from a cell to the S of the MMX circle. This third development is indicated by the 13 m/sec SW wind near Waterloo, and the virtual temperature distribution at 1600 CDT (figure J-29). It was also indicated by the presence of a strong radar cell just S of the circle at 1540 according to the St. Louis radar. Since the cold air boundaries indicated in figure J-28 are purely schematic, perhaps a better picture of the cold outflow interactions can be given by figure J-30 which shows isochrones of the sharp temperature drops. At least three distinct sources of cold air are identifiable. A tendency is also readily observable for the cold flows to rapidly squeeze off the pool of remaining warm air (virtual temperature $\geqslant$ 90F), and in fact at 1700 (not shown) there was no warm surface air apparent within the circle. This rapid and convergent invasion of the MMX circle (which had been occupied by very warm moist air) by these thunderstorm-generated cold air flows can easily explain the rapid and violent convection, and then also the rapid decay of convective activity which followed.

The wind flow at 1500 m (figure J-31a-c) revealed a rather orderly progression from the S at 1330 to the WNW at 1830. This is unexpected from consideration of the morning or evening 850-mb flow pattern. The flow switched in a manner resembling a trough passage.

There was a speed maximum in the 1500-m flow from the W which seemed to follow the decaying line. It seems to be an acceleration of the flow due to a pressure disturbance accompanying the line (a wake depression). The peak values of speed were just over 9 m/sec (figure J-31a-c). The principal squall line echoes during the 1600–1700 period moved toward the SE of ESE at speeds of 9 to 12 m/sec so there is no evidence for back-side feeding at this time. The winds at and below 1500 m just ahead of the line flowed more or less parallel to the line so the relative front side flow toward the line was comparable to the speed of the line.

The last important feature discernible in the low-level winds was the entry from the NE of low-level cold outflow from a storm cell somewhere beyond the circle (figure J-31d). This cold flow was not very energetic, but the increased convergence associated with its arrival may have helped produce some light shower activity that took place E of the Mississippi River after the passage of the main line.

PRECIPITATION MORPHOLOGY

Radar Echoes

The storm evolution is difficult to establish with the 10-cm PPI radar data because of the very high threshold that existed on this day (40 dbz). The 3-cm RHI radar data provide much more information.

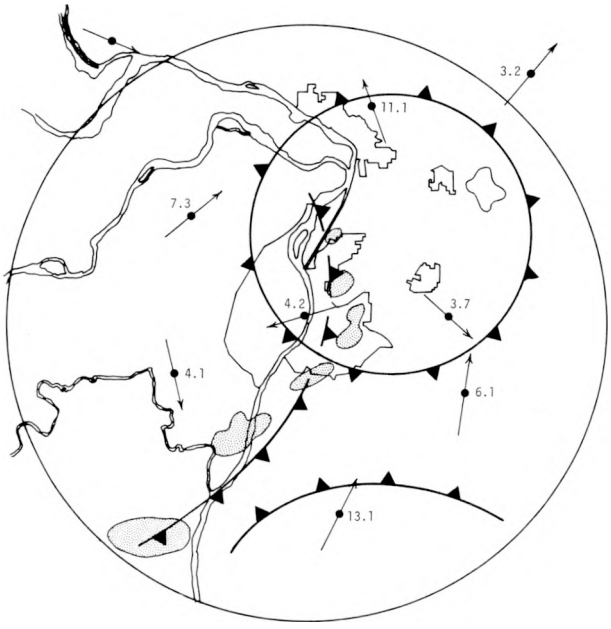

Figure J-28. 100-m winds and schematic picture of cold outflow boundaries and 10-cm (40 dbz) radar echoes (shaded) at 1600 CDT

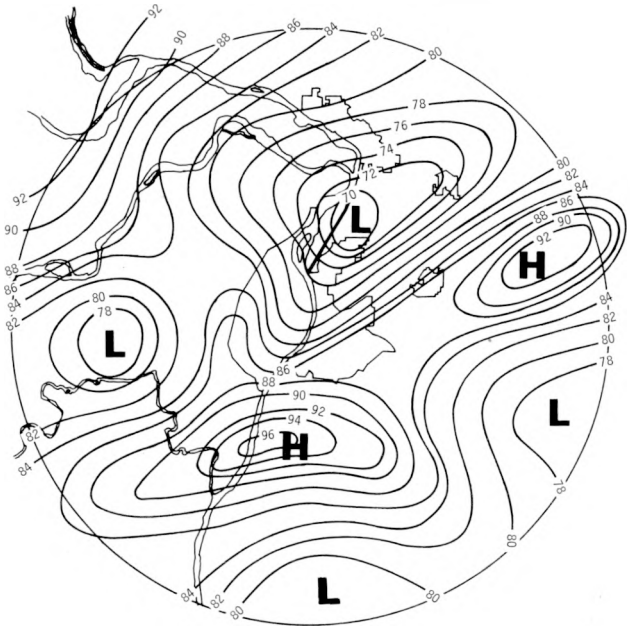

Figure J-29. Virtual temperature (°F) pattern at 1600 CDT

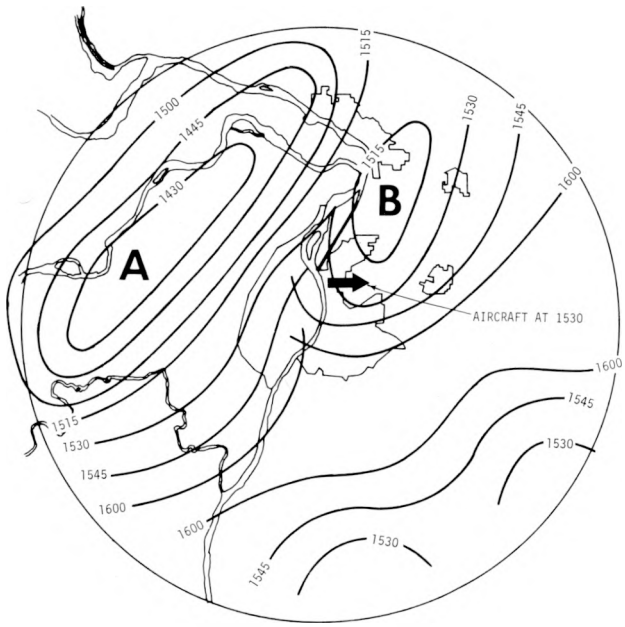

Figure J-30. Isochrones of sharp temperature drops

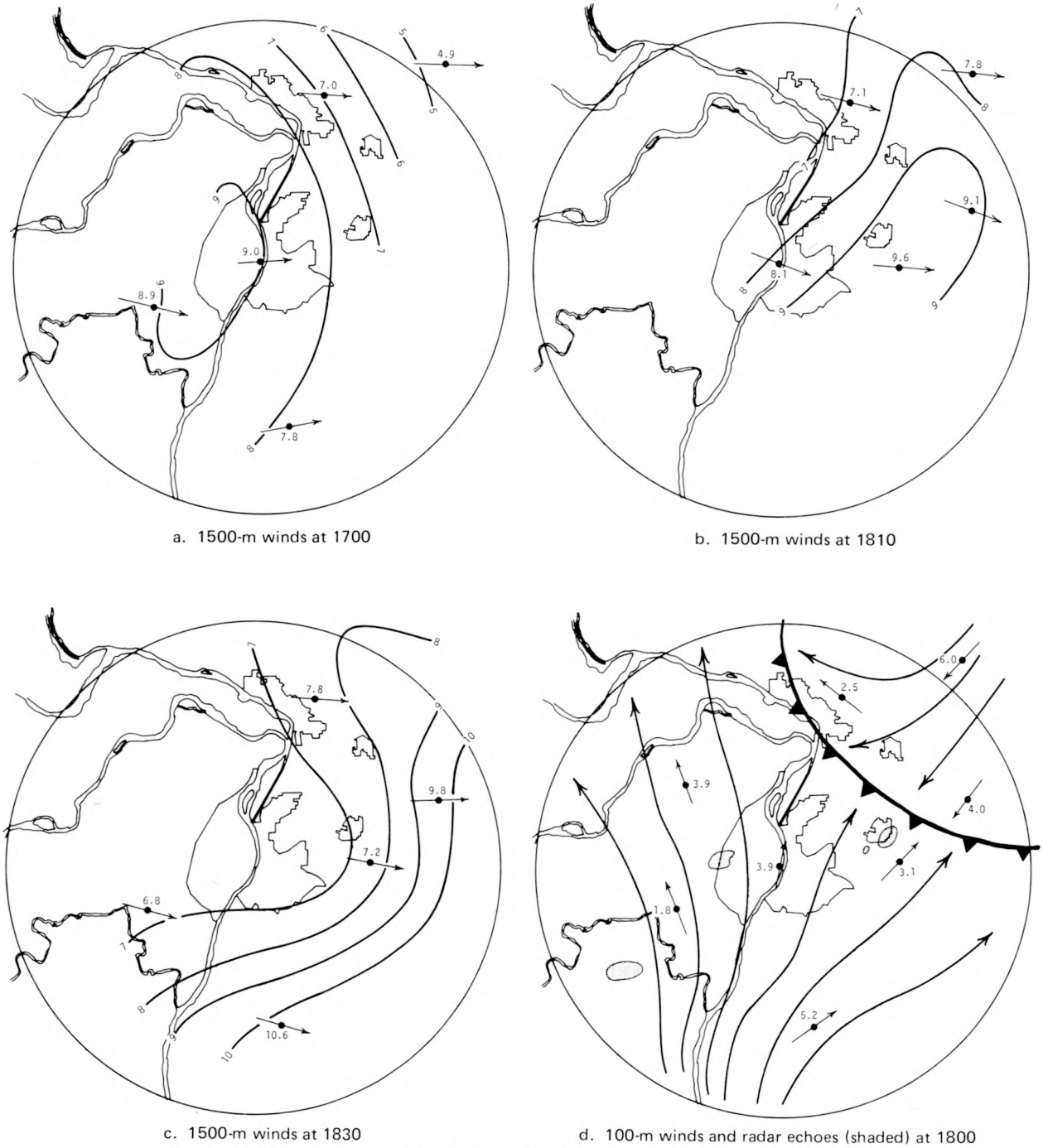

a. 1500-m winds at 1700

b. 1500-m winds at 1810

c. 1500-m winds at 1830

d. 100-m winds and radar echoes (shaded) at 1800

Figure J-31. Afternoon wind patterns (isotachs in m/sec)

Horizontal (CAPPI) sections were created from the RHI data for altitude levels of 10,000, 20,000, 30,000, 40,000, and 50,000 ft AGL. These were extremely useful for understanding the development of the echoes although the attenuation was a problem. For clarity and conciseness of display, these were assembled into pseudo-three-dimensional displays by plotting each successive CAPPI level with a northward offset, and one example is shown in figure J-32. The bottom level, considered ground level, contains the 10-cm PPI echo pattern (at 40 dbz).

Echo mass A was detectable at the time the RHI radar was first turned on at 1443. It then was a large storm with its top above 50,000 ft, although because of typical haze at that time, it was not readily visible at great distances. Echo A subsided slightly after 1443 but again exceeded 50,000 ft later, but it was not as large nor as vigorous after 1443 as cell B became. Cell A initially moved E at about 11 mi/hr as a large irregular mass with no 40 dbz (10 cm) echo beneath it.

A new development (A') grew rapidly on the rear (W) flank of A, well above 40,000 ft (see figure J-33). It briefly exhibited a 40 dbz surface echo between 1506 and 1528. The new development (A') appeared to merge with older echo A which in turn produced a very small 40 dbz surface echo at 1546 before decaying (see figure J-32).

Echo mass B first appeared at 1447 as a first echo from 6000 to 20,000 ft. It was located 4 mi NW of the reference point shown on figure J-32 (which is Site 98 on figure B-2b). It formed in the strong convergence along the trough. By 1458 it had grown 50,000 ft and had a marked notch or hook shape at the lower levels. Echo B was a rather complex echo with almost no net motion for 40 minutes, probably because of its vigorous development on all sides.

The systematic scanning of the 3-cm RHI radar was interrupted between about 1559 and 1609 because of some requests for guidance from the aircraft. By 1618, the FPS-18 PPI echo pattern showed a line oriented NE-SW with six large 40 dbz echo areas (see figure J-28). Tops were over 50,000 ft for the 4 echoes in the area just E of St. Louis.

At about 1530 the AI aircraft was in flight and had skirted to the E of the major rain-producing cloud (echo mass B) and had experienced a strong updraft (1200 ft/min) on the SW quadrant of the storm (see figure J-32). This inflow area must have been quite strongly sloped, and was associated with a pronounced 'notch' in the lower portions of the echo, with an overhang at 40,000 ft. Relatively high CN counts were found in the updraft air.

Just W of this updraft area, the aircraft experienced a severe jolt. At this point it may have come under the influence of the cold outflow in the region where it was undercutting the outflow from the large cell (A) to the W. The occlusion of these two cold outflows would have produced extreme vertical motions and turbulence, and was probably responsible for the development of the new cell marked C in figure J-32. Cell C grew very rapidly through 50,000 ft, merging with cell B and dominating that echo mass by 1546. It first appeared at 1511, at 10,000 and 20,000 ft, and began its rapid growth at 1528, passing through 30,000 ft at that time. It exceeded 40,000 ft at 1537 and 50,000 ft at 1546. At this time cell B began a 'dumping' phase, the 'notch' filling in at all heights, the top descending, and the echo moving rapidly over the fixed reference point. This could be the process of descent of the large hail.

Figure J-33 shows tops of some major echoes versus time. The inconsistent RHI data collection from about 1550 to 1620 is unfortunate, but it appears that all the storms in the entire line were in a decaying phase from about 1600 onward with rapid decay after 1636. From 1636 on, the variations were such that only the highest echo top in view is indicated on figure J-33.

Echo B has two peaks (figure J-33). The first sing of downdraft air at the ground from that echo occurred at 1515. At about that time the echo top was descending, but about 9 min later (1524) it started growing again. The arrival of cold air at the ground may have acted to re-invigorate the storm. The 1530 isochrone position on the echo B temperature drop (figure J-30) also related

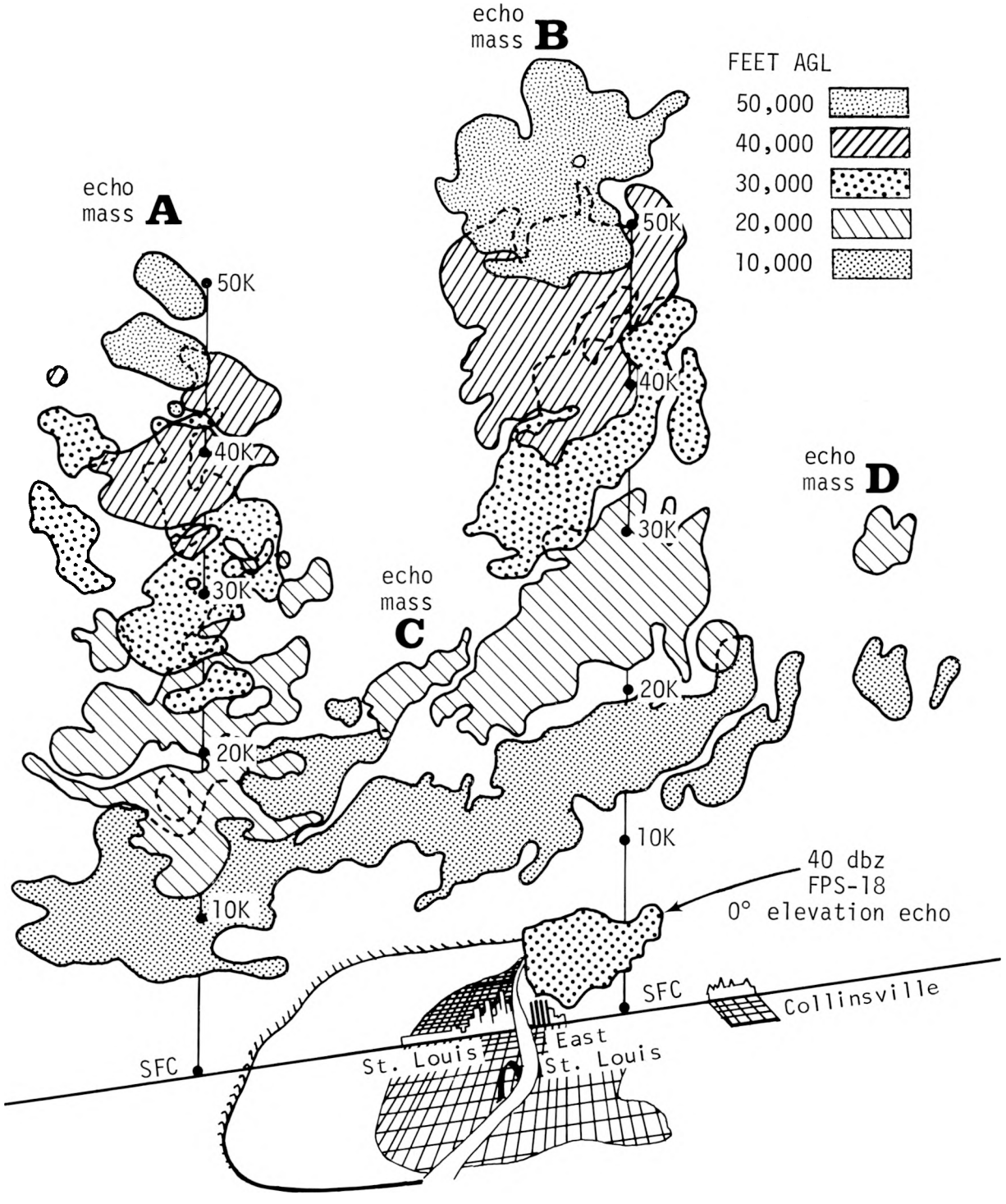

Figure J-32. Tilted CAPPI presentations for echoes A and B at 1500 CDT

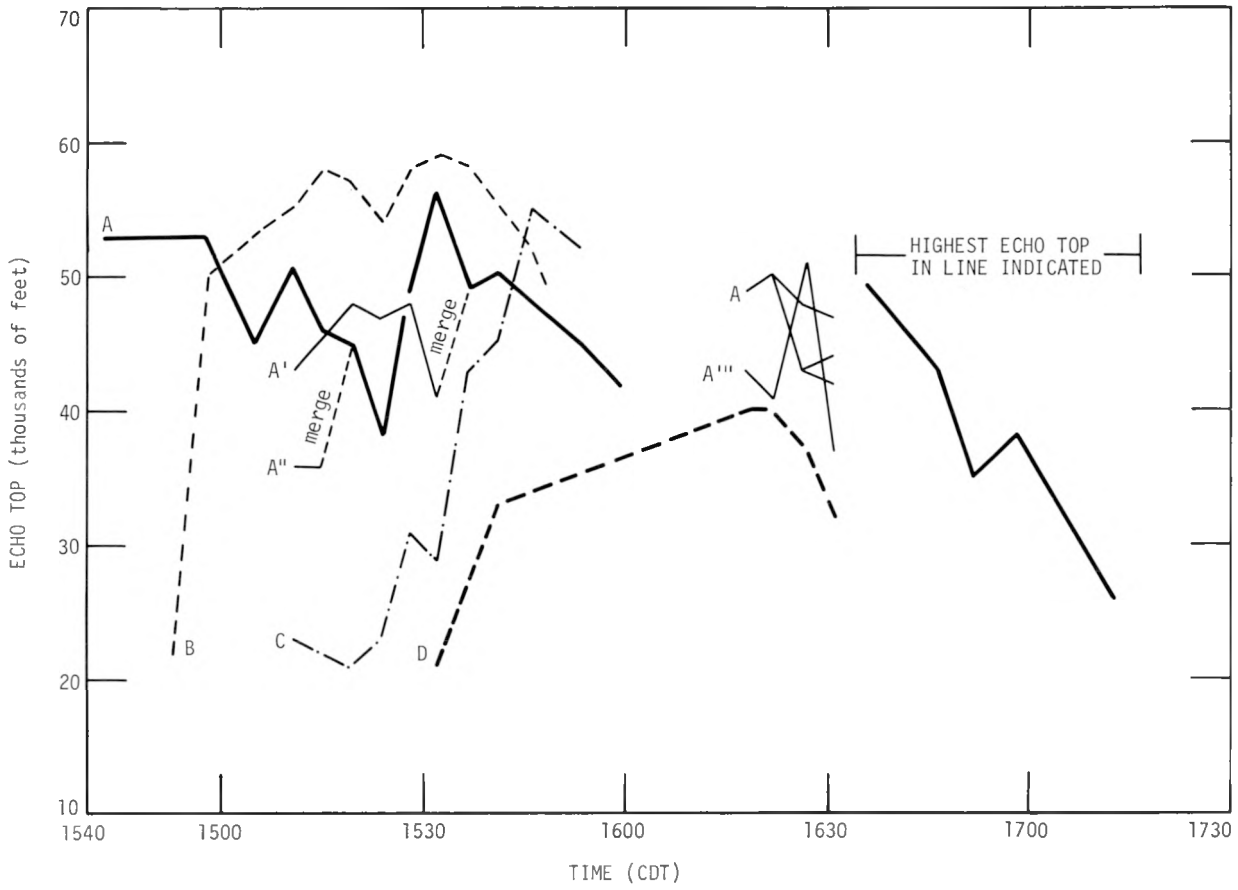

Figure J-33. Behavior of maximum echo top values for selected echoes

fairly well with the severe jolt experienced by the aircraft at 1529. The rain from echo B began at Site 79 (just prior to 1450) in Granite City, and the highest rate remained over that gage through 1515.

The flight logs indicate that the inflow to cells B and C after they were well developed was largely from the front or on the ESE side. Smoke plumes were observed blowing into the approaching line.

Rain and Hail

The map of total rain accumulation (figure J-34) shows that echo mass B was the dominant rain-producing entity of the day. The most intense rainfall occurred at Site 79, where the largest hail also fell. The highest 5-min rain rate at this gage was 20.5 in/hr at 1500 CDT, and the 100-yr 5-min rate in this area is approximately 13 in/hr. The rainfall pattern for echo mass A shows the result one would expect from its short but intense lifetime, as revealed by the radar analysis.

Data concerning hail and rainfall are of interest. Figure J-35 shows the number of raincell initiations during one-half hour intervals from 1400 to midnight, first for all raincells and then for those cells which also contained hailfalls. Three principal peaks in activity are discernible in the upper curve, one at 1600, one at 1800, and another at 2030. The first of these produced almost all of the hail, as shown by figure J-35b. Curve c indicates that, at the peak of activity, 55% of the

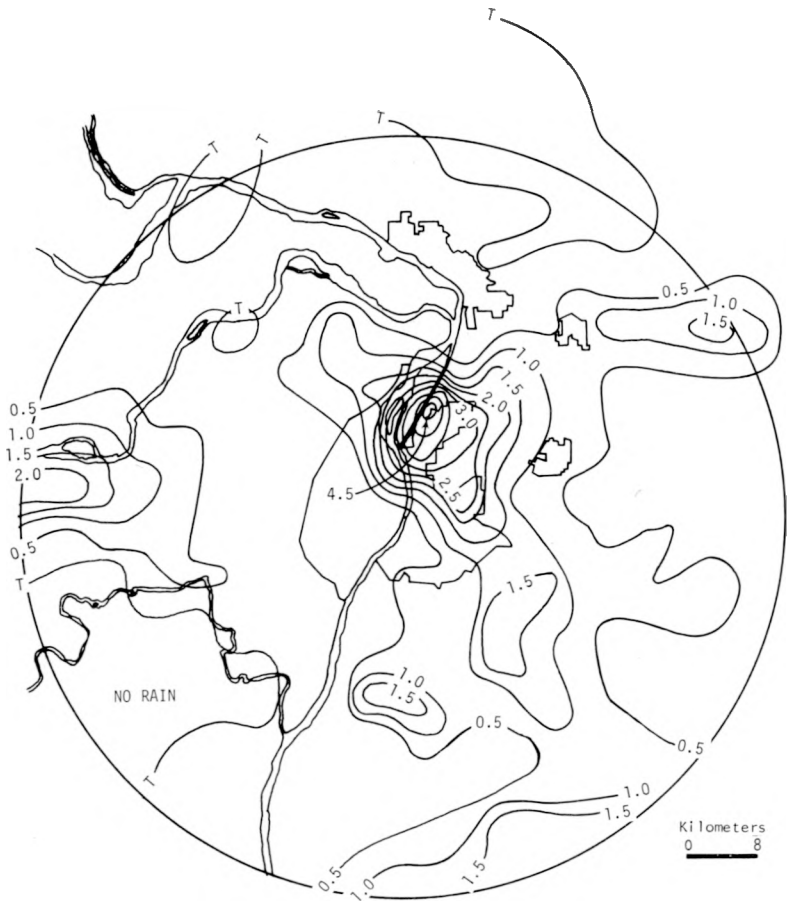

Figure J-34. Total rainfall on 12 August

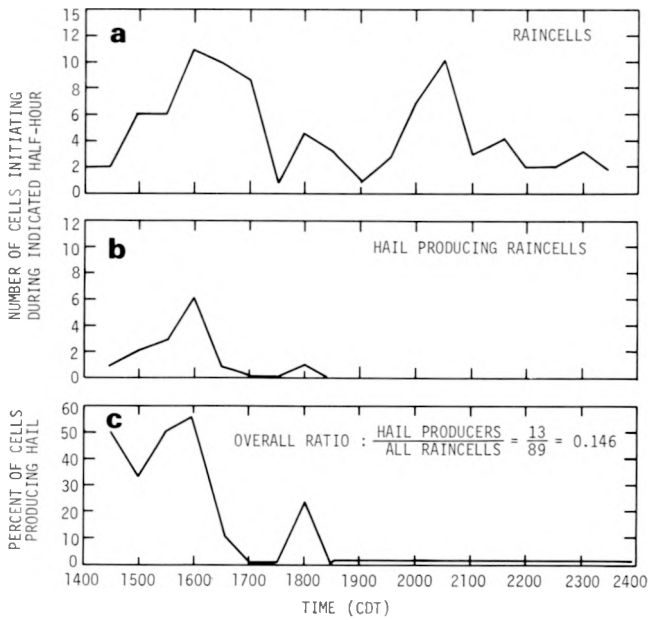

Figure J-35. Half-hour frequencies of initiation of a) raincells and b) hail producing raincells as a function of time and c) percent of raincells that produced hail

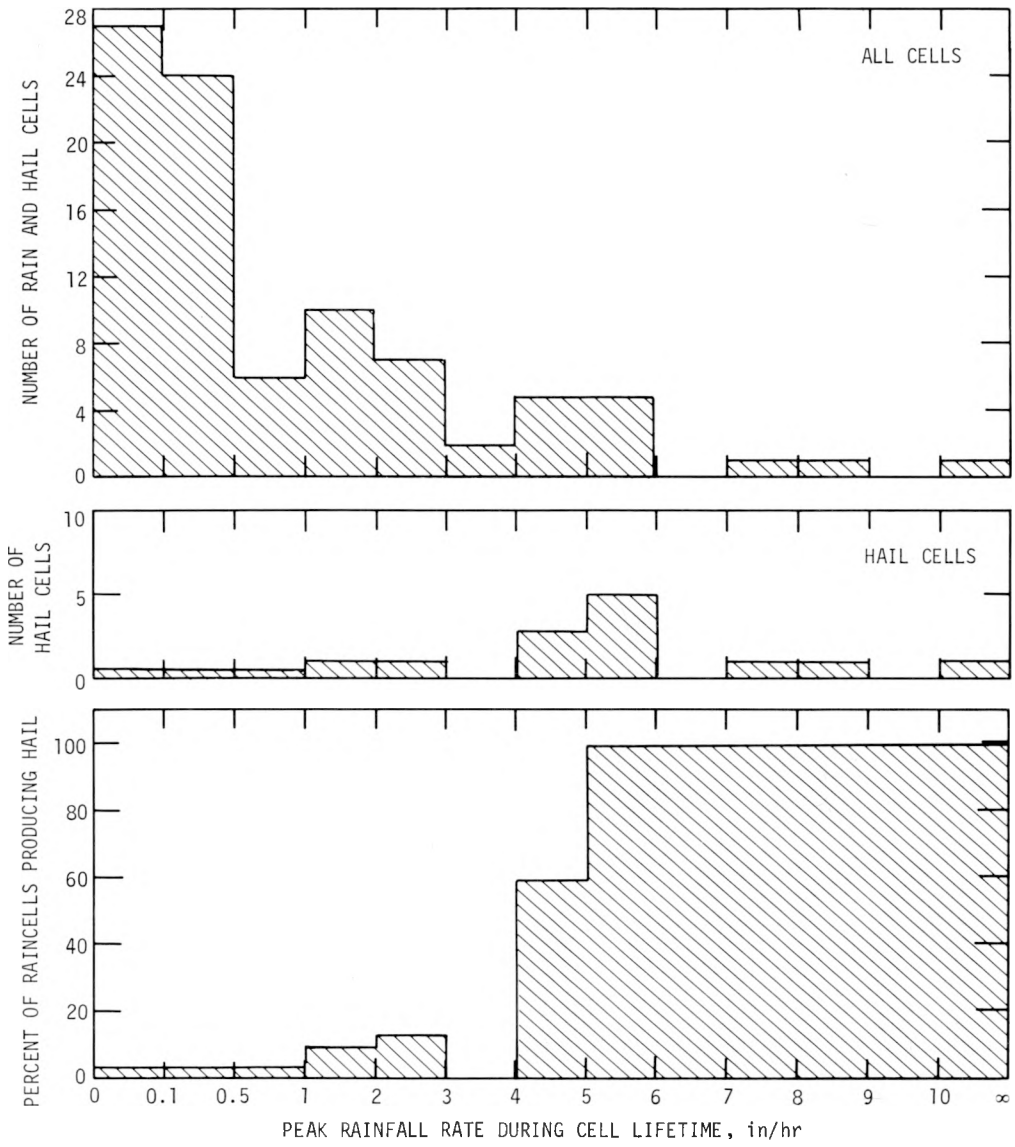

Figure J-36. Distribution of raincells, hail-producing raincells, and percentage of cells producing hail related to peak rainfall rate during raincell lifetime

new raincell initiations also produced hail. Figure J-36 shows the distribution of all raincells and and hail-producing cells as a function of peak rainfall rate during the cell lifetime. These figures show the association between hail and heavy rainfall as well as that between hail and high radar reflectivity. Eleven of 13 hail-producing raincells showed peak 5-min rates exceeding 4 in/hr, and all raincells producing 5-min rainfalls rates > 5 in/hr also contained hail.

The surface hail observations are shown in figure J-37. They are grouped according to the eight echo systems which produced them (indicated by large letters). The long arrows show the direction of motion of the radar echoes which could be tracked, but this was not practical for A, B, C, or D which had no motion. The short arrows through the observations points indicate the direction of arrival of the hailstones. We have recently begun the routine estimation from hailpads of the direction of arrival of the hailstones (Morgan and Towery, 1974). These measurements from

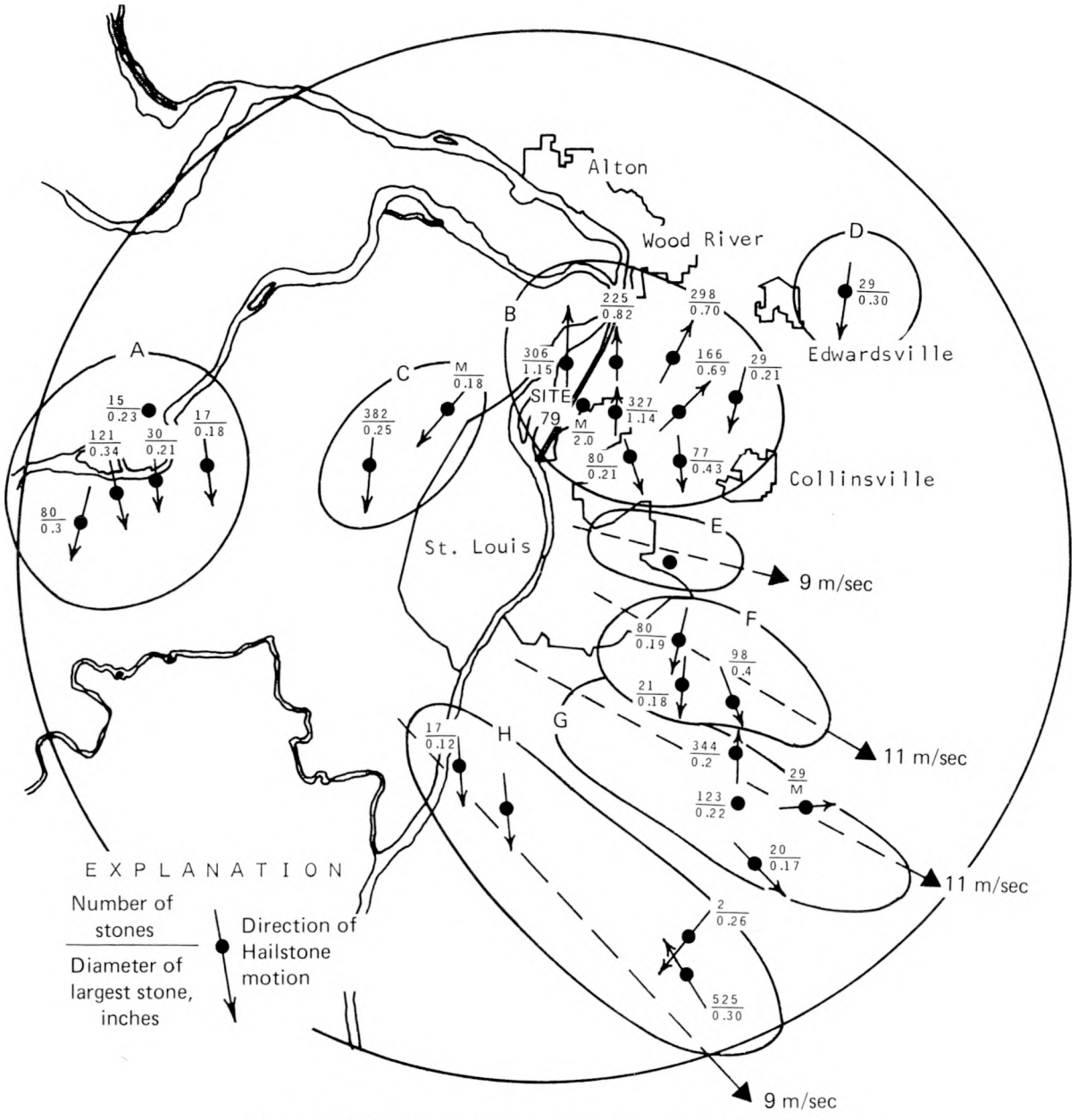

Figure J-37. Hailfall characteristics grouped by associated echo systems

12 August partially verify earlier observations that the hail most often blows out of the storm toward the right relative to the direction of storm movement. However, for the hail from echo B, which showed little net movement, the arrows show that the hail was blown outwards from the principal rain core, both to the N and to the S. This fits well with the character of the downdraft (discussed elsewhere).

The hail associated with echo mass B was quite remarkable. The largest hail stones fell at Sites 61, 62, 63, 79, 80, and 81. Stone diameters exceeded 1 inch at three of these and at one, Site 79, the hailpad was destroyed by stones over 2 inches in diameter. The largest hail appears to have been blown toward the N.

General Cloud Conditions

During the early morning hours, the local area was clear to scattered. Visibilities were moderately reduced by ground fog and haze, but in a patchy fashion (as low as 3 mi at ALN, 5 at BLV, not at all at STL). STL reported AcCas at 0555 and towering Cu the next hour. PMQ noted AcCas at 0600, 0700, 0800, and 0900, with towering Cu at 0800 and 0900. These would be expected with the cold moist axis of lifted air noted at 500 mb at that time and could have been the S limit of the precipitation system which had passed through N and central Illinois previously and dissipated in the Alton area. Cloudiness through the morning consisted of a scattered (occasionally broken) middle deck reported between 8000 and 12,000 ft and a scattered to broken upper deck. After 0500, the scattered sky condition developed everywhere, but with some differences in timing from station to station. PMQ had scattered clouds from 1100 through 1400, BLV from 0900 through 1200, and ALN from 1000 through 1200. SUS was scattered through the morning from 0516 through 1245 except for one report at 0649, and STL had scattered clouds through 1255, with broken conditions at 0455, 0655, and 0755. There was more overall cloudiness at East Alton and this may have contribued to retarding the warming there and to the SSW.

TRACER STUDIES

A tracer experiment was performed on this day and a sample of the results is shown in figures J-38a and b. The first shows the deposition of Zn, a natural or industrial contaminant in the rain, and the second shows the distribution of deposition of the artificial tracer, Li, and the aircraft release track. Both show a strong relationship to the distribution of total rainfall (figure J-34), but with some exceptions.

The release of 590 g of Li began at 1545 and contined for 36 min. The aircraft flew in a strong ($\geq$ 1000 ft/min) but smooth frontal updraft typical of those in organized developing squall lines. The aircraft flew a race track pattern (figure J-38b) along a 12-mi distance in front of the relatively straight front edge of the storm system. Comparison of the release track and the surface Li pattern suggests there were highs (deposition values $>$ 6) directly below and likely related to Li release and the subsequent rainfall in the track.

Although the inflow was relatively laminar and unchanging with time along the front edge of the line, the Li pattern is highly variable. In addition, high values ($\geq$ 5) exist at three locales N of the release track. Semonin (1975) evaluated the individual Li samples to estimate points where there was a 95% or better likelihood that the Li value contained tracer as well as natural background. There were 5 such locales, each marked with a star on figure J-38b. These were in areas where cells and heavy rain existed or developed during or after the release. Thus it appears the Li was being exchanged by in-cloud processes. The two significant Li values about 10 mi NW of the release area occurred where major cell B and C had merged, and this may indicate considerable exchange and flux of air into cell C.

Finally, the generally low Li values SE of the track ending locale (near Belleville), and the placement of the significant values near the start and behind the release area together suggest that there was rather rapid in-cloud processing of the Li, and that the Li was moving 3 to 5 mi horizontally before being deposited.

A release of In tracer was made in the 1532-1535 period into an updraft along the S side of cell B (see figure J-32). At this time, the analyses of In is incomplete, but should be studied when finished.

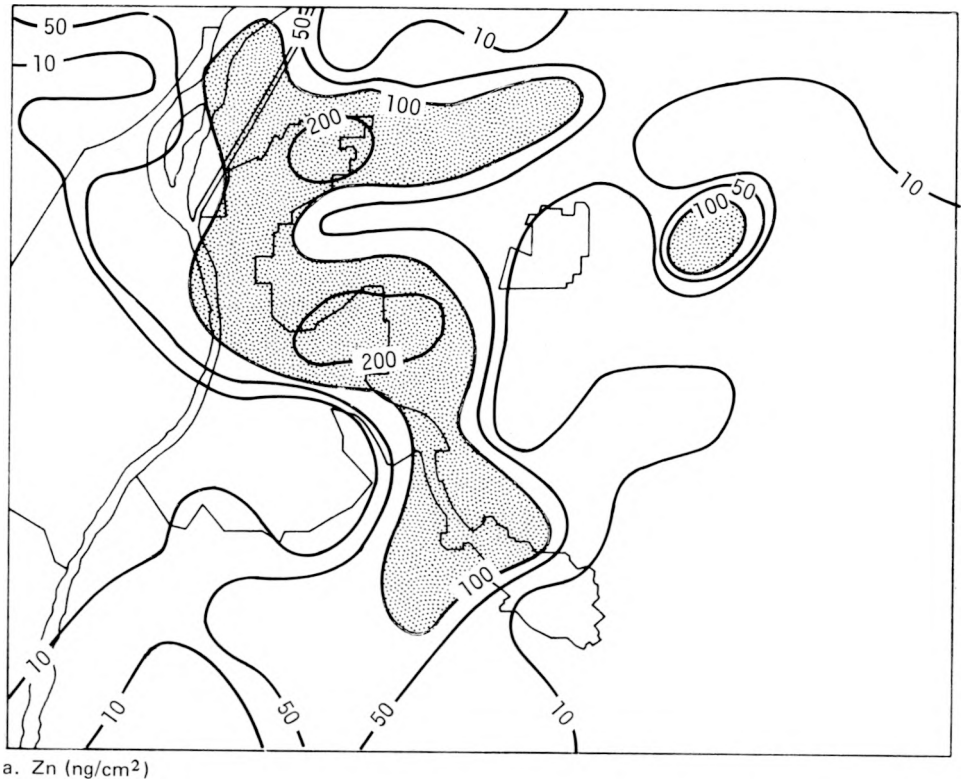

a. Zn (ng/cm²)

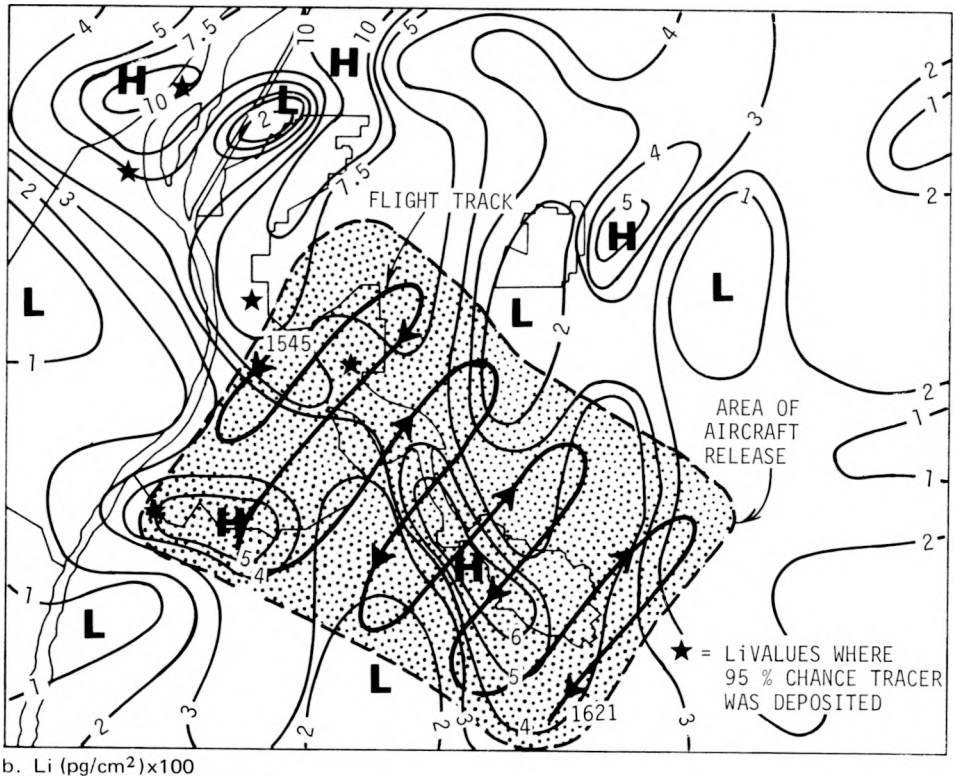

b. Li (pg/cm²)x100

Figure J-38. Corrected deposition of Zn and Li and aircraft release track

SUMMARY AND RECOMMENDATIONS

The severe thunderstorms of 12 August 1973 in the St. Louis area appear to have largely been the result of the interaction of mesoscale entities whose causes were quite remote from any local (urban) effects. These mesoscale entities (cold outflow boundaries, etc). created a regime of destabilizing vertical motion and high instability in the St. Louis area which was sufficient to explain the severity of the convection which took place there. In fact, the scale over which these conditions occurred was much greater than our research area and severe storms occurred over portions of Illinois and Missouri. The objective weather analysis procedures tested in this storm proved to be very useful and informative.

The actual placement of the storms that occurred within the circle, however, appears to have been influenced by local effects. In particular, zones of anomalous relatively great surface heating prior to storm development were situated at the locations of major cell development, and the heating pattern could be expected to reflect surface energy balance conditions. The heating differences may be related to the antecedent rainfall distribution.

An unexplained speed surge in the low-level winds preceded storm development and may have created small-scale convergences. The arrival of this surge may have influenced, above all, the timing of the storm development.

The peculiar, semi-stationary development of the largest storm to occur within the MMX circle may have been due to the shielding effect of the first large storm which was located upwind of the large storm. The intake air into this storm was from urban sources, as shown by the high CN values measured and the high Zn values found in its rainfall. Thus, it is potentially an urban-affected storm and its unusual severe character may be partially attributable to urban effects.

The rapid development and then decay (locally) of the violent phase of the activity would seem to be due to the interaction of fresh cold flows from several storm systems. These acted both to cut off the low-level warm moist air and to lift the warm air rapidly.

Studies such as this aimed at documenting specific storm events and determining their interaction with the urban area could benefit from an increase in the surface data network, especially in regard to winds. More pibal and radiosonde data would certainly be of great value. A special need was highlighted by our unsuccessful attempt to look for the effects of cloudiness on the heating distribution. Some increase in observations of cloudiness and visibility (haze, fog) would be of great value. Cloud camera data are useful, but satellite data would be more useful. Some simple device to record the total illumination at a number of points would be desirable. Radiometric or pyrheliometric observations have been too little explored in METROMEX.

REFERENCES

Jones, D. M. A., and P. T. Schickedanz. 1974. *Surface temperature, moisture, and wind studies. In* Interim Report of METROMEX Studies: 1971–1973, F. A. Huff, Editor, Illinois State Water Survey, pp. 98-120.

Morgan, G. M., Jr., and R. C. Beebe. 1971. *Analysis of the time-space behavior of the field of equivalent potential temperature during a severe weather situation.* Preprints, 7th Conference on Severe Local Storms, Kansas City; AMS, Boston. pp. 54-59.

Morgan, G. M., and N. G. Towery. 1974. *Microscale studies of surface hailfall.* Illinois State Water Survey for NCAR Subcontract No. 25-73, Final Report, March 1974, 33 pp.

Semonin, R. G., Editor. 1975. *Precipitation scavenging studies in METROMEX: 1971-1974.* U.S. Energy Research and Development Administration Research Report No. 4.

K. COMPLEX LINES OF 13 AUGUST 1973

Donald F. Gatz and Paul T. Schickedanz

CONTENTS

K. COMPLEX LINES OF 13 AUGUST 1973

INTRODUCTION

This day was selected for intensive study for three main reasons. First, it was a day of heavy rain and hail in the St. Louis area. Second, two synoptic weather types of precipitation of interest in connection with urban-related storms occurred on this day – a squall line and a cold front. Third, a single storm occurred in the climatological excess rain area E of the Mississippi River in advance of the squall line. In essence, these conditions offered an opportunity to examine for urban effects on a complex rain-producing situation.

This day was an excellent choice for study, not only because it provided an opportunity to to examine these various types of precipitation all occurring on the same day, but also because it led to the identification of a mechanism for urban precipitation enhancement, or redistribution, that had not been previously suggested.

SYNOPTIC WEATHER CONDITIONS

Macroscale

This discussion sets the broad-scale scene for the weather events that occurred locally in the St. Louis area. It begins with a description of conditions at 0700, looking first at the surface weather map and proceeding to successively higher levels. It then follows the development of surface weather conditions between 1300 and 2000.

Conditions at 0700. The surface weather map (figure K-1) featured high pressure centers located over lower Michigan (central pressure 1012 mb) and E Wyoming (1023 mb). Another high pressure center was located in the Atlantic Ocean off the Florida-Georgia coast ($\simeq$ 1021 mb). Three weak low pressure centers were present in the far W, one located in Washington (1009 mb) and two in California (1012 mb and 1008 mb).

A stationary front was located in a broad trough of low pressure running E-W between the two highs to the E. This front lay across central Missouri and was the approximate N boundary of a broad area of moist air (dew points $\geqslant$ 65F) covering the SE United States. A trough of low pressure moving to the S curved from upper Michigan across Wisconsin, Minnesota, and into South Dakota.

Light to moderate rain and showers were reported in N Wisconsin and Minnesota. Rain and thunderstorms were in progress near the W end of the stationary front, in E Kansas. Moderate to heavy fog was reported from many stations in the E half of the country, especially in the moist SE section.

The widespread moisture was also evident aloft. At 850 mb, dew point depressions of $\leqslant$ 5F were present across virtually the entire E half of the country, including all of Missouri. Winds at 850 mb were W at 10-20 kt (5-10 m/sec), and were advecting slightly warmer ($\leqslant$ 1F) air into the St. Louis area.

The moisture, again characterized by dew point depression $\leqslant$ 5F, was still present at the 500-mb level (figure K-2) but its extent was limited to a broad irregular swath from Texas to Virginia and the Carolinas. The N boundary of this zone lay just S of the Missouri-Arkansas border. The 500-mb height contours showed a major trough just upstream of the St. Louis area at the W

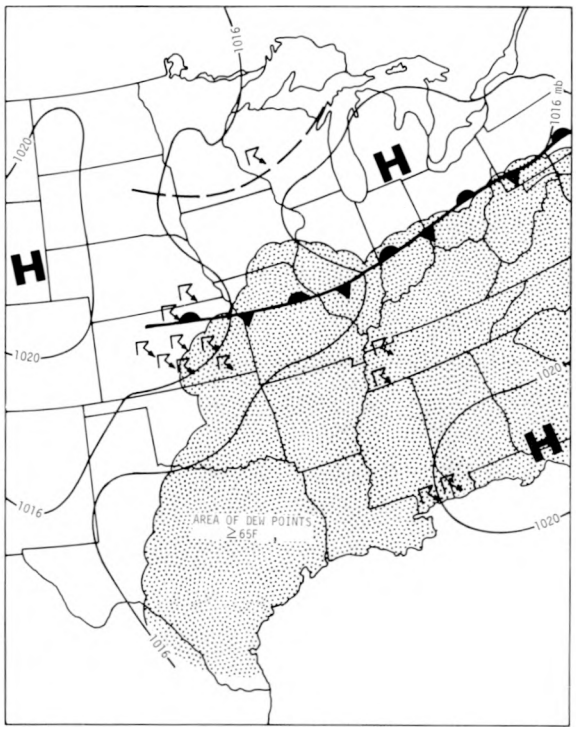

Figure K-1. Macroscale surface weather map for 0700

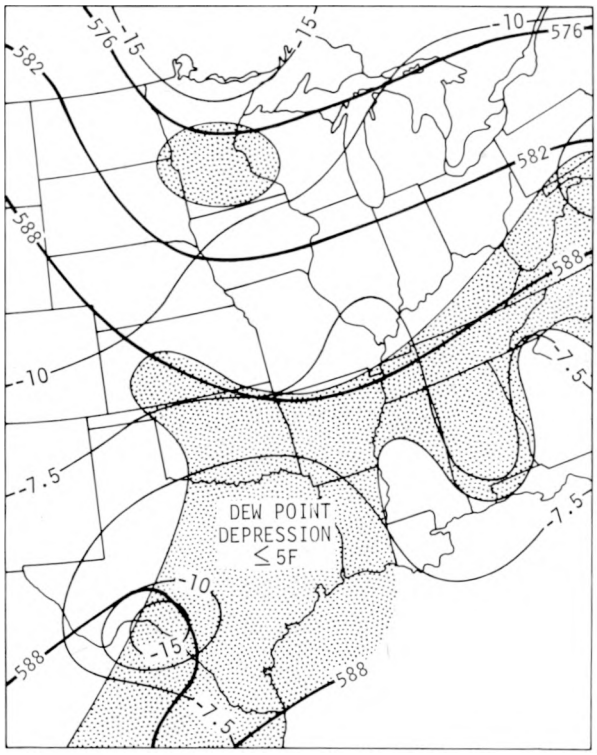

Figure K-2. 500-mb chart for 0700

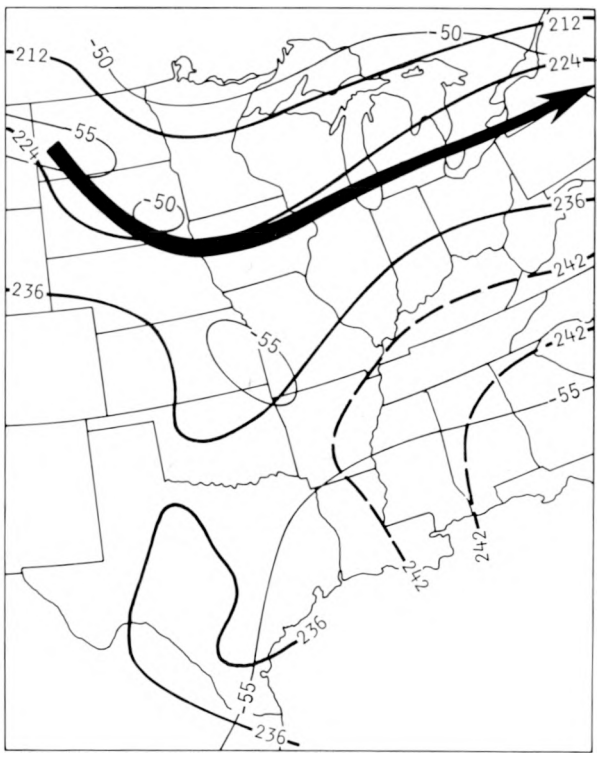

Figure K-3. 200-mb chart for 0700

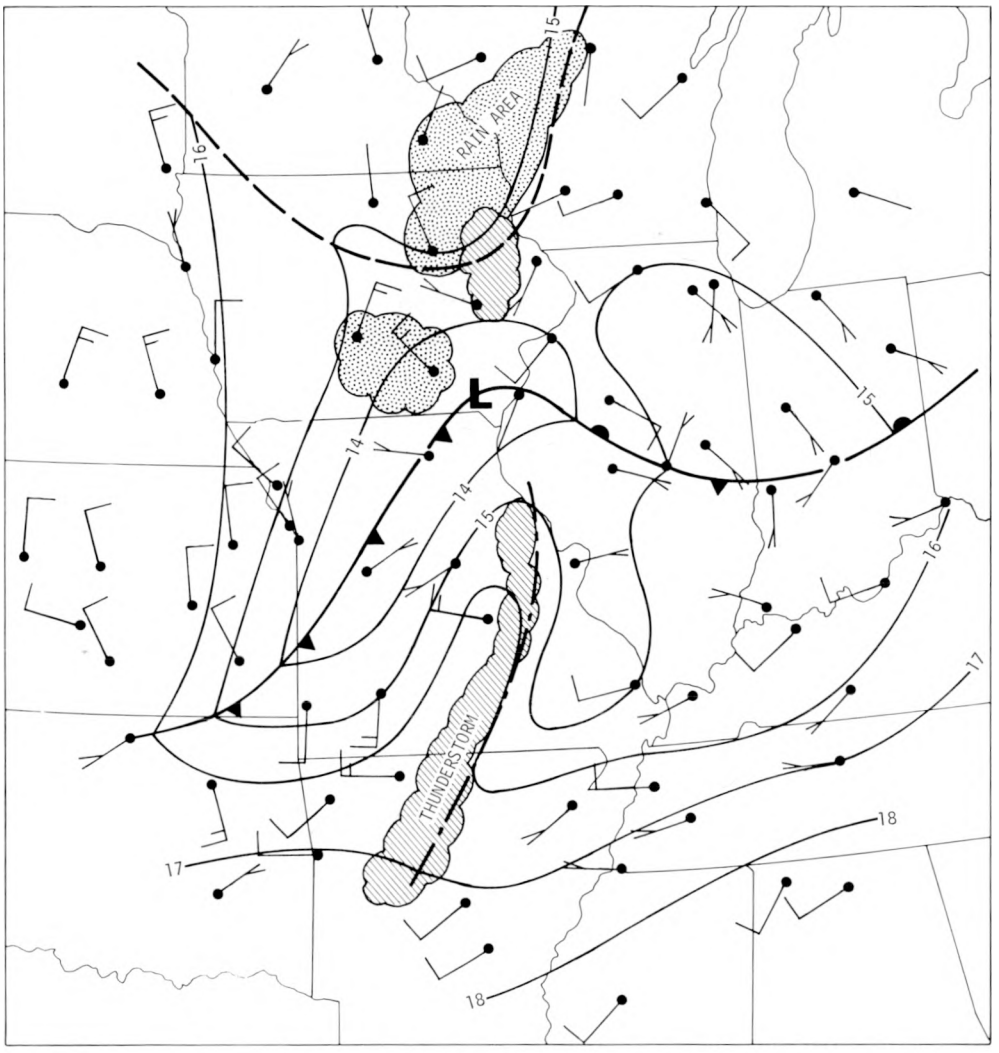

Figure K-4. Surface weather map for 1300

border of Missouri. A following ridge was oriented from Arizona to Montana. Winds across Missouri at 500 mb were from the W, from 15 to 30 kt (8-15 m/sec), with little tendency for immediate advection of either warmer or colder air. Colder air was associated with the W ridge, but its motion was not expected to bring it into the St. Louis area immediately.

Still higher, the 200-mb chart (figure K-3) also shows the approaching low-pressure trough. The jet stream, with maximum winds in the range of 50 to 70 kt (26-36 m/sec), was located across central Iowa at its closest approach to the St. Louis area.

Development of Surface Conditions, 1300-2000. By 1300 (figure K-4) a low pressure center had developed along the stationary front. The low center was located in NE Missouri. The front itself was now an open wave, with the warm front portion across central Illinois and the cold front trailing from the low center across NW Missouri.

A squall line was present in the warm sector, oriented approximately N-S, and approaching the St. Louis metropolitan area. Additional light to moderate rain and showers were occurring in Iowa, Minnesota, and Wisconsin, associated with either the low center or the advancing trough that by 1300 had reached central Iowa.

The map 1 hr later at 1400 (figure K-5a) shows the continued development of the low pressure center and the continued movement of the front, the squall line, and the N trough. By 1400 the squall line had reached the W edge of the MMX circle. Also at this time, a band of rain was associated with the cold front.

The 1500 map (figure K-5b) shows continued development and motion of the system. The front had reached central Missouri, and the S end of the squall line had advanced faster than the N end, so that at this time the line was oriented along the Mississippi River N of the St. Louis area, but extended directly S from the city.

By 1600 (figure K-5c) the low pressure center had deepened further and moved across the Mississippi River into Illinois. The cold front had passed Columbia, Missouri, and there were thunderstorms now associated with it. The squall line was oriented NW-SE from the low center. The leading edge was well into Illinois, but light rain was still falling in the MMX circle.

Four hours later at 2000 (figure K-5d), the low pressure center had moved into E-central Illinois, with the trailing cold front just E of the St. Louis metropolitan area. A thunderstorm associated with the front was still in progress at STL. Scattered rain and thunderstorms were present behind the front throughout Missouri, and additional rain and thunderstorms were occurring in Iowa and Wisconsin in association with the low pressure trough that had passed Milwaukee, Rockford, and Burlington by 2000. This sequence ended a 7-day period, 7-13 August 1973, of varied and interesting precipitation events, 5 of which were studied in detail for this report.

Mesoscale

Pre-Squall Line. In this section temperature, humidity, and wind conditions in the MMX circle at 1400, just before the first rain began, are presented. In addition to these measured parameters, the areal distribution of one derived parameter, equivalent potential temperature (θ_e), is also described because of its relation to the total energy available for convective processes.

Figure K-6 shows the distribution of surface temperatures in the MMX circle at 1400. There is a N-S gradient of 11F, with warmer temperatures in the S part of the network. According to the synoptic scale surface map at 1400 (figure K-5a), this gradient was not across the front that was located N of the St. Louis area.

The strong temperature gradient was probably caused by a variation in cloud cover. Observations of cloud cover at 1400 are available for five stations in the area: PMQ, STL, and ALN in the cooler air ($\leqslant$ 80F) region, and SUS and BLV in the warmer air ($\geqslant$ 84F) region. The three cooler stations all reported overcast conditions with ceilings at 1400, 1800, and 1000 ft, respectively. The two warmer stations reported broken clouds at 2000 or 2500 ft, with SUS also reporting broken clouds at 5000 ft and BLV an overcast at 25,000 ft. Thus, there is a strong possibility that the observed strong temperature gradient was caused by greater insulation in the S and W portions of the network.

The distribution of dew point temperatures at 1400 is shown in figure K-7. Values range from 69 to 76F. Maximum temperatures ($\geqslant$ 75F) occurred to the WNW of St. Louis and in a broad N-S zone through East St. Louis.

The surface wind fields at both 1300 and 1400 (figure K-8) are presented to show pre-rain conditions. Figure K-8a shows general E flow across the city with a marked confluence of streamlines toward an E-W line immediately S of the city. Figure K-8b shows similar features, except the confluence is even more evident. Also, by 1400 the general wind field had veered somewhat to a more SE direction. The existence of the confluence line was verified by its appearing on two successive hourly maps.

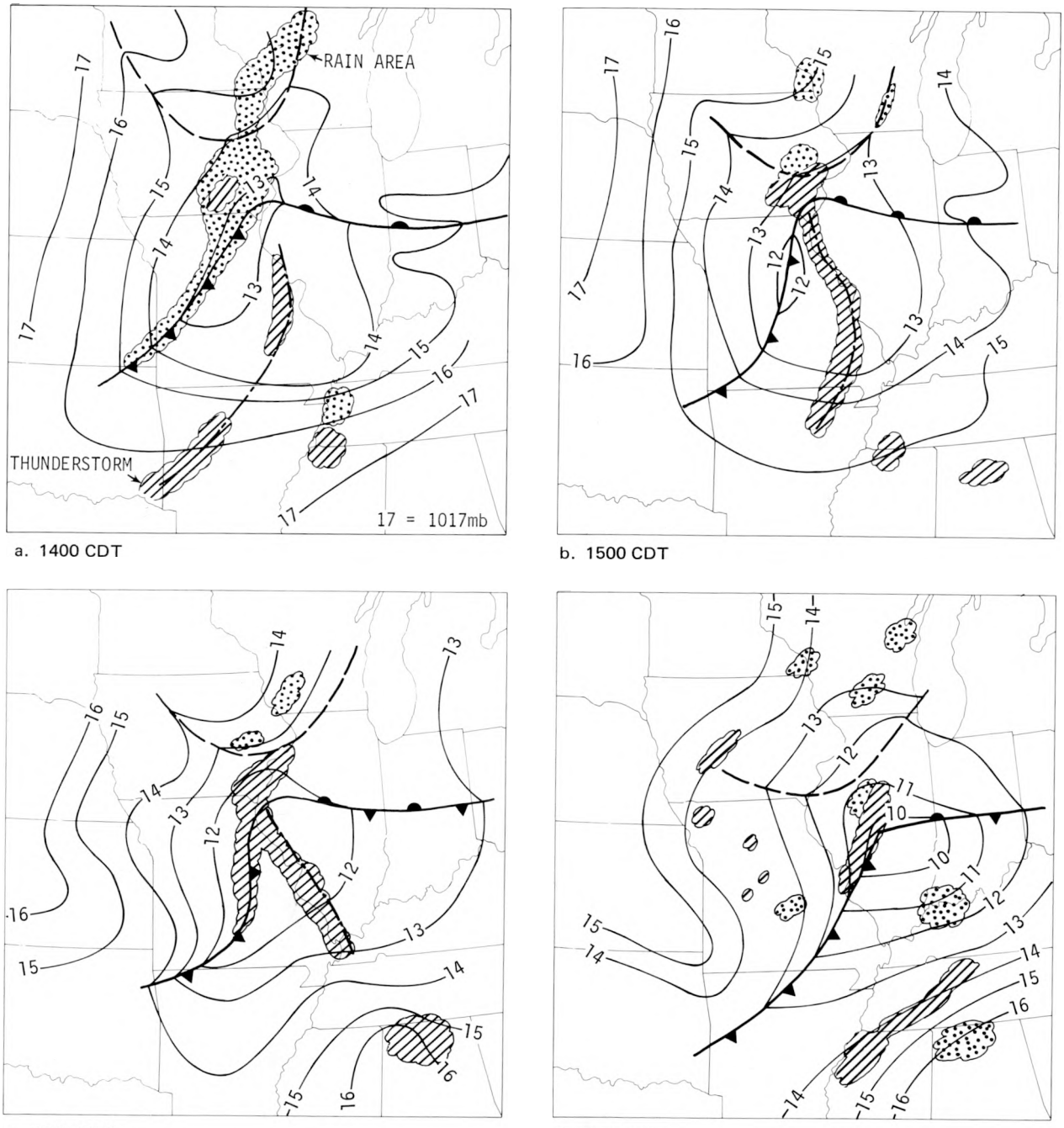

Figure K-5. Surface weather maps for afternoon and evening

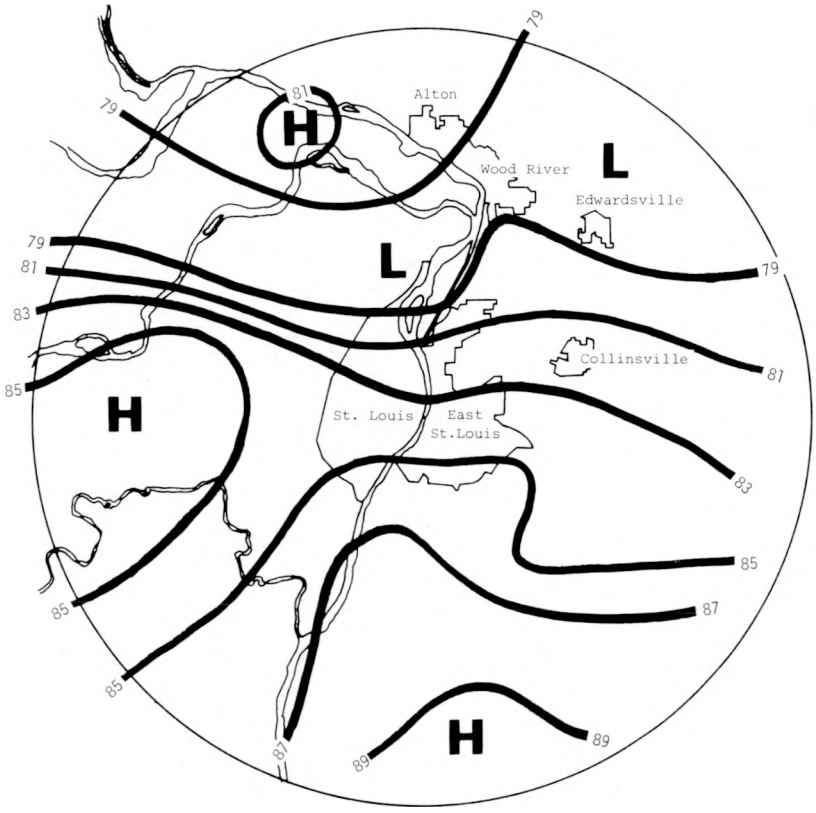

Figure K-6. Surface temperature field at 1400

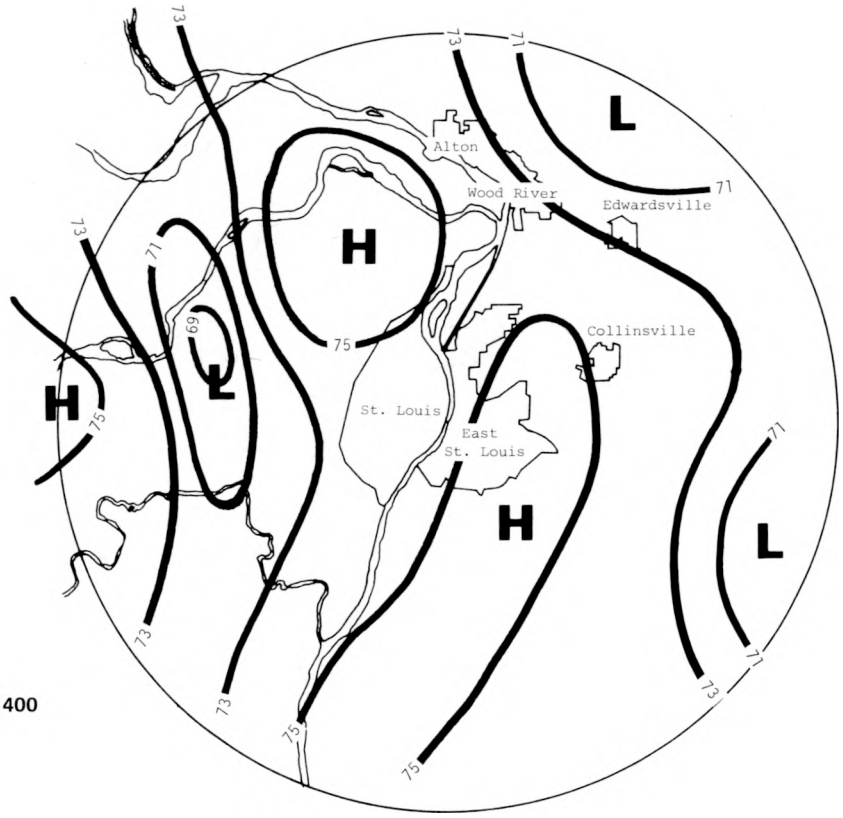

Figure K-7. Surface dew point field at 1400

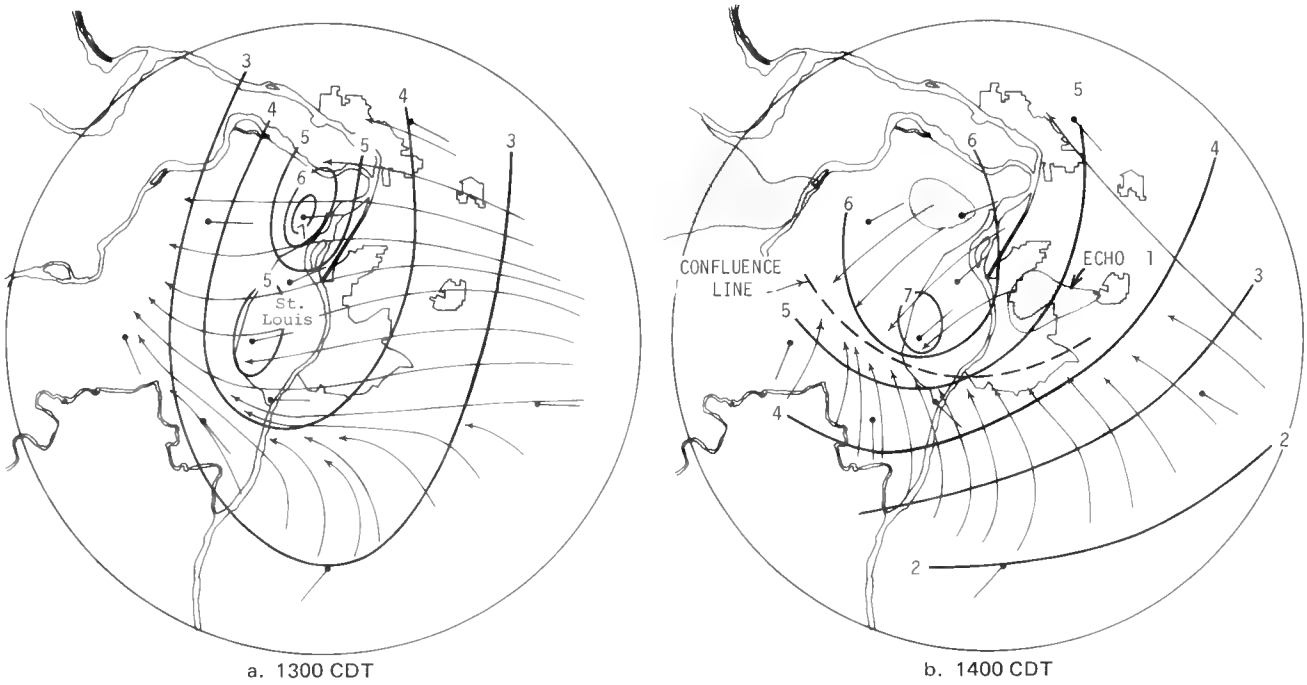

Figure K-8. Surface wind fields at 1300 and 1400 (Isotachs in m/sec)

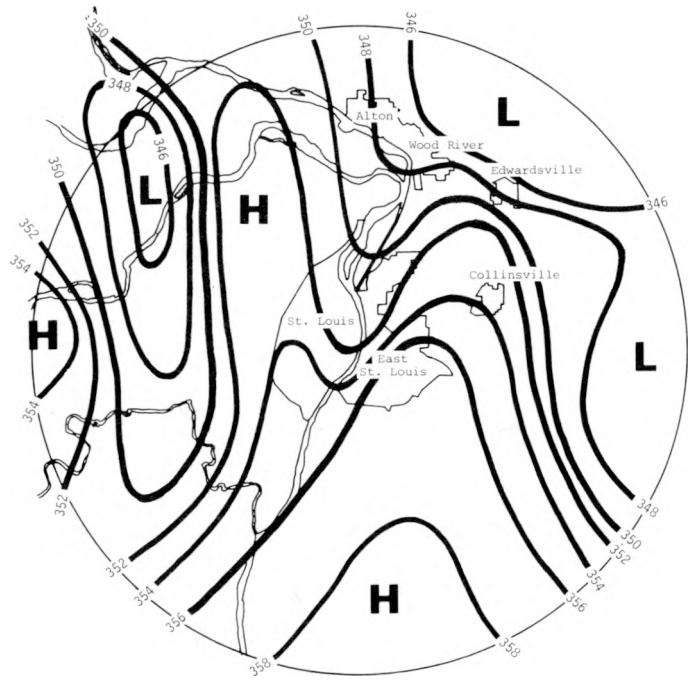

Figure K-9. Surface equivalent potential temperature (°K) field at 1400

The 1400 surface wind chart also shows radar echo positions derived from the 3-cm RHI display. These echoes were observed at 1409, when the day's RHI observations began. Additional observations from the 10-cm PPI display indicate that the first echo in the research circle (echo 1) was first observed at 1400. If echo 1 first appeared at 1400, the observed confluence line is unlikely to have resulted from an organized thunderstorm downdraft outflow, as the presence of radar echoes on the 1400 surface wind chart might at first suggest. If no echoes occurred before 1400, the confluence observed at 1300 could not have originated because of thunderstorm outflow either.

The cause of the observed confluence line and its relationship to the development of precipitation are potentially important subjects. If the line were caused by some feature of the urban environment and it could be shown to have contributed to the development of convective cells, this phenomenon, if also detected in other cases, could contribute to observed urban precipitation anomalies.

The role of the confluence line will be discussed further in the analyses of the winds aloft. However, the 1400 surface wind chart in figure K-8b shows that the line is immediately adjacent to the largest two of the three radar echoes that developed shortly after 1400.

The equivalent potential temperature (θ_e) is a measure of the total energy available for convective development from both sensible and latent heat. Therefore, the distribution of θ_e over the network may determine preferred locations for convective cells to develop or dissipate. The distribution of θ_e at 1400 is shown in figure K-9, and this field exhibits features that reflect a combination of the temperature and moisture distributions, with maxima far to the W and S in the MMX circle, and just W of St. Louis.

Temperatures in the S portion of the circle matched those at NWS stations farther S, and were generally in the upper 80's (F). Temperatures at NWS stations N of the MMX circle were generally in the low 80's. Temperatures in outlying areas in the N part of the circle were in the same range, but the lowest temperatures in the MMX circle (upper 70's) were lower than those found anywhere in the area surrounding St. Louis (except near the squall line). These low temperatures occurred primarily in association with low clouds (e.g., at STL and ALN).

Average moisture conditions in the MMX circle closely matched those at neighboring NWS stations, with dew points in the low 70's. However, the maximum dew points in the circle (middle 70's) were typical of those found much farther S (at Cape Girardeau and S).

A comparison of mesoscale and macroscale winds shows that the cyclonic circulation near the city evident on the MMX circle surface wind chart for 1300 (figure K-8a) is also seen in the winds at the surrounding synoptic stations (figure K-4). This suggests the presence of a mesocyclone associated with the advancing squall line. Synoptic scale pressure data are insufficient to confirm a feature of this small scale, but if a mesocyclone were present and attributable to some physical feature of the city (e.g., a heat island), it would be another physical link between the urban environment and the precipitation anomaly.

Pre-Cold Front. Surface weather observations at 1700, following the squall line and just prior to the rain associated with the cold front, provide a view of the environment encountered by the advancing precipitation system.

The temperature gradient at 1700 (figure K-10) was completely altered from that present at 1400. Maxima were located in the NW and SW portions of the MMX circle, with a minimum in the E portion. This is consistent with the movement to the E of the squall line and the earlier end of the rain in the warmer W sections. The range of temperatures was 10F.

Dew point temperatures at 1700 are shown in figure K-11, and again, the highest values were in the NW and SW sections with low values in a broad band across the center of the network

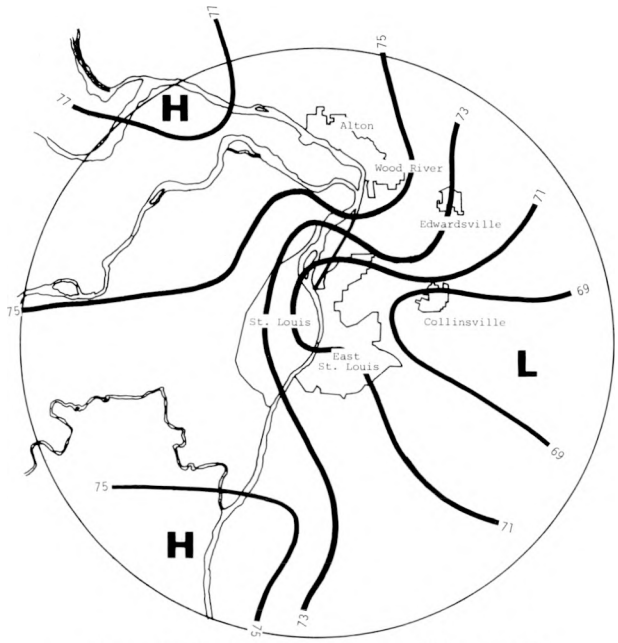

Figure K-10. Surface temperature field at 1700

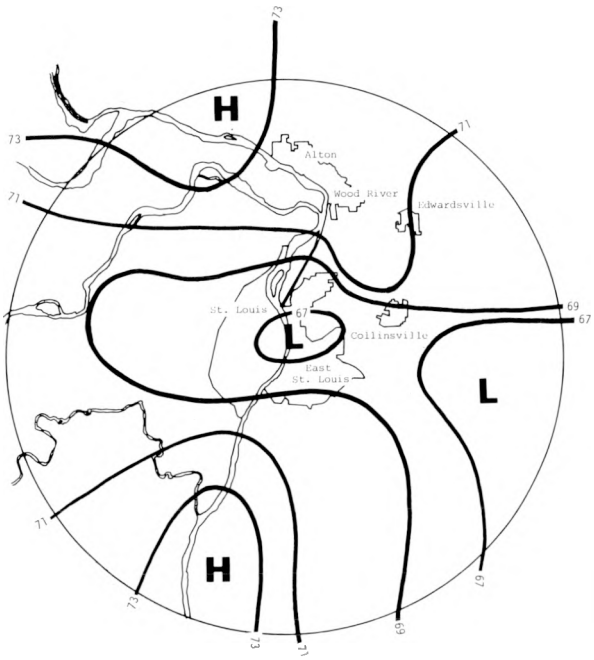

Figure K-11. Surface dew point field at 1700

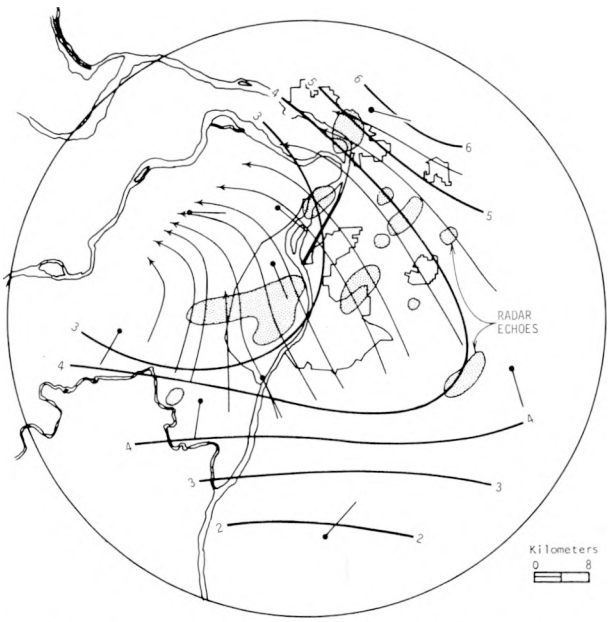

Figure K-12. Surface wind field at 1700 (Isotachs in m/sec)

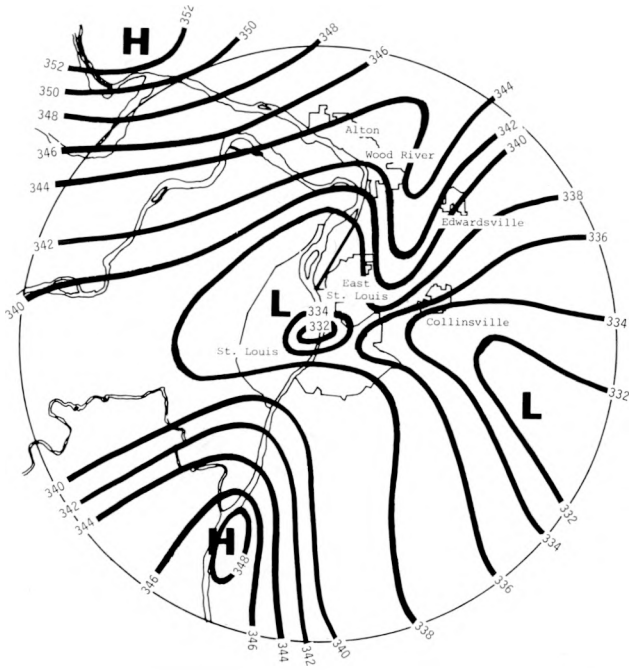

Figure K-13. Surface equivalent potential temperature (°K) field at 1700

and in the E section. This means that low dew points occurred where light rain was still in progress (see radar echoes in figure K-12). This is puzzling, but may reflect the presence of mid-tropospheric air brought to the surface in squall-line downdrafts.

Surface winds at 1700 (figure K-12) were primarily from S to SE over most of the MMX circle, with convergence suggested W and NW of the city. The radar echoes shown in figure K-12 were light showers between the squall line and the frontal rain.

The θ_e distribution is shown in figure K-13 and reflects the similar patterns of temperature and moisture. High values prevailed to the N and S of the city, with a broad band running E-W across the center of the MMX circle where values dropped from 340K at the W edge to near 330K at ARC, then increased slightly at East St. Louis before dropping off again toward the E edge of the circle.

Thermodynamic Structure of the Air Mass. These analyses included study of temperature and moisture variations with height on thermodynamic diagrams as well as time-height and space-height sections through the area of temperature and moisture parameters. Pre-squall-line conditions are stressed.

Soundings of temperature and dew point at ARC before rain began (1335) and after the cold front passage (2042) are shown on figure K-14. Before the rain, temperatures near the surface were in the upper 20's (C) with dew points in the low 20's. The lifted index at 1335 was -9C, indicating a very unstable condition. The sounding at 2042 shows cooling near the surface, with temperatures in the low to middle 20's and a large increase in moisture above 800 mb. At 2042 the lifted index was 1.0C, indicating that stable conditions were established.

Pre-storm conditions across the network are portrayed in the vertical section shown in figure K-15, which includes soundings from PMQ, ARC, and BCC at about 1330. Moisture, represented by the mixing ratio, increases from PMQ to ARC to BCC near the surface. The dew point gradient at the surface at 1400 (figure K-7) is in the same direction, but weaker. Aloft, the ARC sounding shows greater moisture than the outlying sites at all levels up to 700 mb.

The θ_e field shows that the air column over ARC was warmer at all pressure levels up to about 600 mb than either of the two non-city sites. This feature is not seen in the surface temperature field at 1400 (figure K-6), where ARC is 3F warmer than PMQ, but 1F cooler than BCC. The lack of a temperature maximum at ARC is probably due to local conditions, because that site was immediately downwind of the Mississippi River at the time. Also, the half-hour difference in the observations could have contributed to this difference.

Above 600 mb, a rapid cooling with height occurred at ARC, but was not seen at the other sites; this resulted in unstable conditions between 500 and 600 mb, with temperatures approximately 5C cooler over the city. The extreme instability of the ARC sounding has already been illustrated in terms of the lifted index, and is supported in the cross section by the number of superadiabatic layers present in the soundings, especially those at ARC and BCC.

The average depth of the observed mid-day mixed layer (by Wuerch's definition, 1970) determined from the 1330 soundings at PMQ, ARC, and BCC was 2730 m MSL. The mean CCL from the same soundings was 1075 m MSL. (For reference, the elevations of these sites are 273 m, 140 m, and 155 m MSL, respectively.)

The mixing depths observed at the individual stations were 2553, 3228, and 2409 m MSL, respectively. Thus, the urban mixing layer was almost 700 m deeper than the greater of the two non-urban sites. The CCL was highest at PMQ at 1342 m with heights of 1023 m and 860 m observed at ARC and BCC, respectively.

Low-Level Airflow. Airflow is depicted by streamline and isotach (in m/sec) analyses at 500 m, 1000 m, and 1500 m MSL. Thus the 1000 m and 500 m charts depict airflow at the ex-

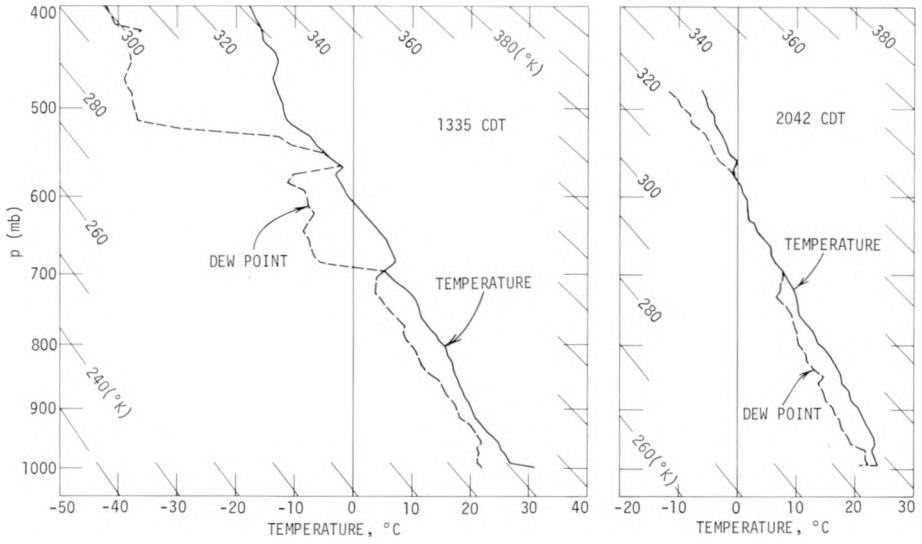

Figure K-14. Temperature and dew point soundings at ARC before and after the rain

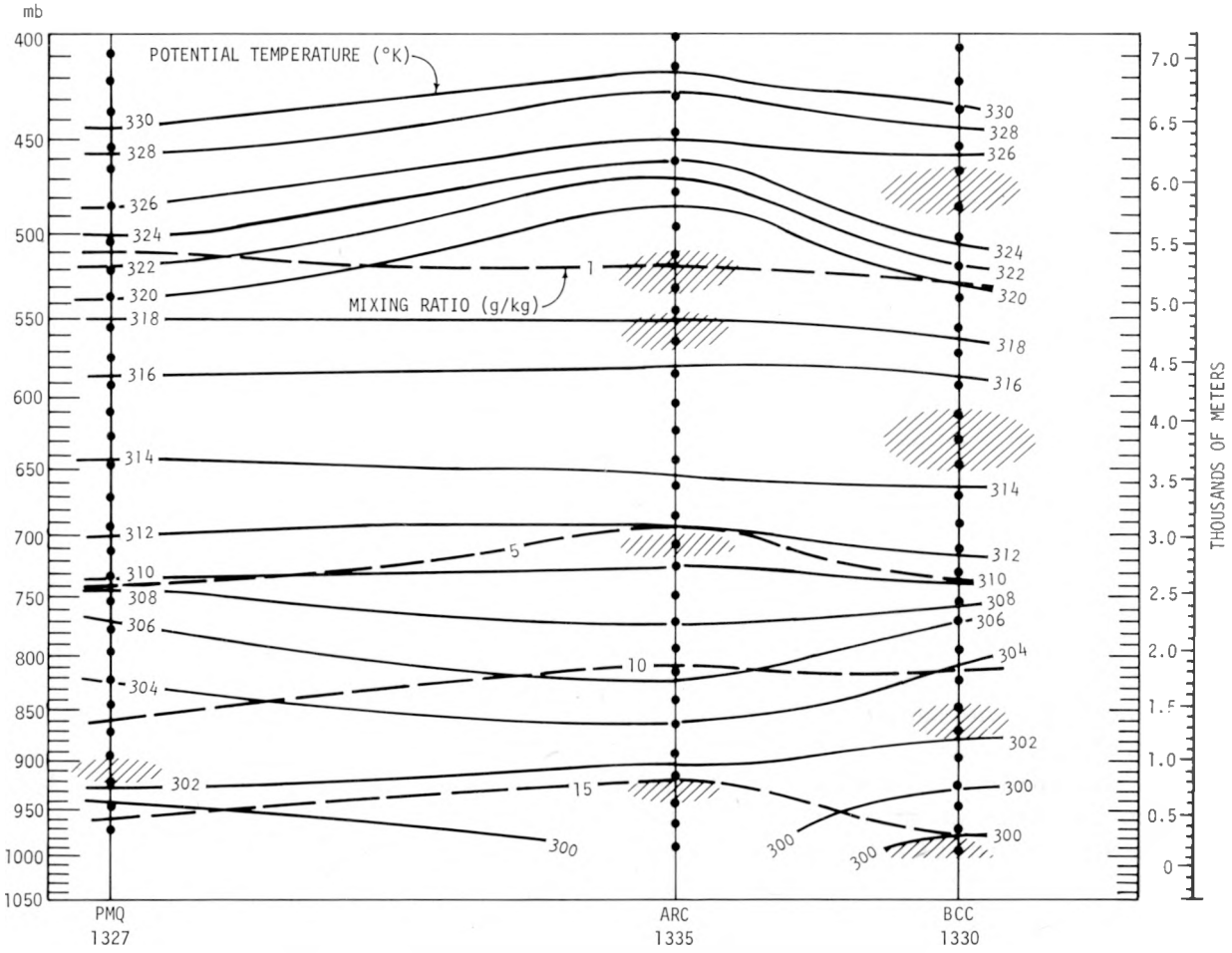

Figure K-15. Vertical cross section of potential temperature and mixing ratio
(Hatched areas are superadiabatic layers)

pected cloud base and about midway between the ground and cloud base, respectively. MMX circle winds for 1400, 1530, 1830, and 1930 are presented in figures K–16, K–17, K–18, and K–19, respectively. Radar echo positions at or near map times are also shown because of the potential influence of convective cells on airflow. The 3-cm RHI radar was the main source of these data, but 10-cm PPI data were also used. Echoes observed only on 10-cm PPI are so labeled.

At 1400 the 500-m flow (figure K–16a) was predominantly from the SE. Flow in the central portion of the network appears to have been somewhat distorted by incipient convective cells that appear as radar echoes (see other discussions of radar echo data). There is a zone of confluence in the S portion of the field that approximately matches that in the surface wind fields at 1300 and 1400 (figure K–8). However, the isotach analysis in figure K–16a shows speeds increasing downstream in the region of confluence. Thus, it is unclear whether there is a net convergence or divergence.

One level higher (1000 m) at 1400 (figure K–16b) there are fewer stations with data because some of the pilot balloons entered low clouds and could not be followed. Where a streamline analysis was possible, it was found that winds were from the S with some evidence at stations on the E of deviation around the incipient cell (echo 1) E of the Mississippi River. From the diffluence of the streamlines and increasing speeds downstream, divergence is apparent just upwind of that echo. The loss of additional stations with data at 1500 m (figure K–16c) hampered the wind analysis further, but a continued veering of the general wind with height is evident.

The next available set of low-level airflow observations occurred at 1530, about the time that the squall line reached ARC. The charts for 500 m, 1000 m, and 1500 m MSL are shown in figure K–17a-c.

At 500 m (figure K–17a) the flow was S to E over the portion of the network where rain was not falling and observations were made. There is strong evidence for convergence along the leading edge of the squall line (approximately the leading edge of the massive echo in the area between the city and PMQ in figure K–17a). Both confluence of the streamlines and decreasing wind speeds occurred along the streamlines from upstream to downstream. Similarly, the flow was convergent in the vicinity of the cell over Collinsville at 1530 (cell 1).

At 1000 m (figure K–17b), data from fewer stations indicate winds veering with height and little confluence of the streamlines. The data are too few and wind speeds too similar to speculate about speed convergence. At 1500 m (figure K–17c) continued veering appeared, with straight streamlines and some evidence for speed convergence near cell 1.

At 1830, still prior to frontal passage, 500 m winds (figure K–18a) were predominantly from the S over the entire network with strong streamline confluence in the N portions and a general speed convergence over the whole area.

The 1000 m chart at 1830 (figure K–18b) shows S winds prevailing to this level, with predominantly parallel streamlines. Speed convergence appeared generally over the network with a maximum in advance of the cell over the Meramec River to the SW. Some veering was evident at 1500 m (figure K–18c) but no strong evidence for large-scale convergence appeared.

At 1930, with the front somewhere in the network (the precise location is difficult to fix because of the effects of the precipitation), the 500 m winds (figure K–19a) had veered to the SW. The streamlines are nearly parallel, but indications of speed suggest convergence upwind of Collinsville and divergence downwind.

The 1000 m winds (figure K–19b) were also from the SW in the SE portion of the MMX circle, with cyclonic curvature to nearly S in the NE portion. Streamlines are nearly parallel, but the continuously decreasing speed in the direction of the wind suggests convergence. Since wind data were missing at all but one station at the 1500 m level at 1930, no chart is presented.

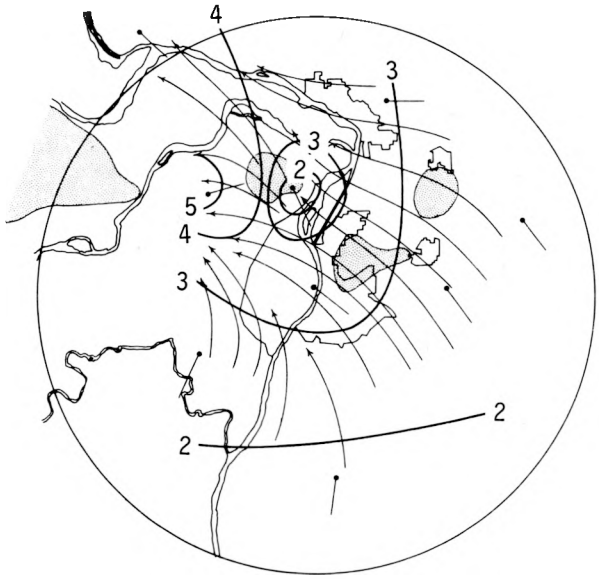

a. 500 m MSL

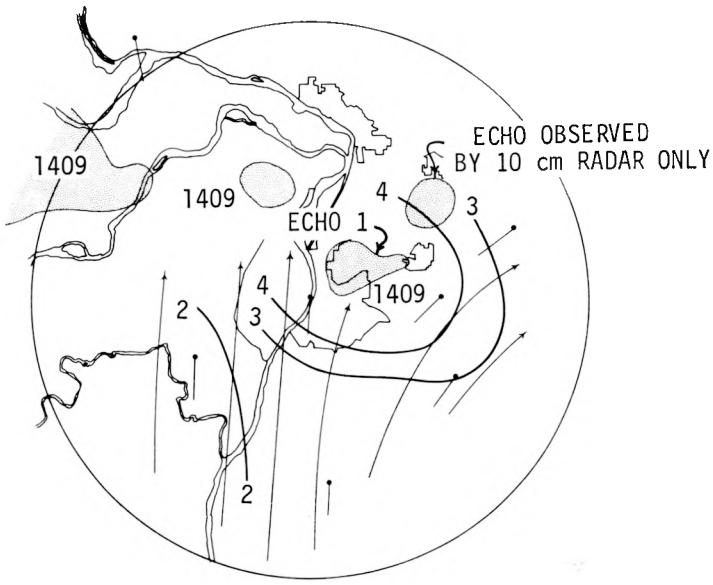

b. 1000 m MSL

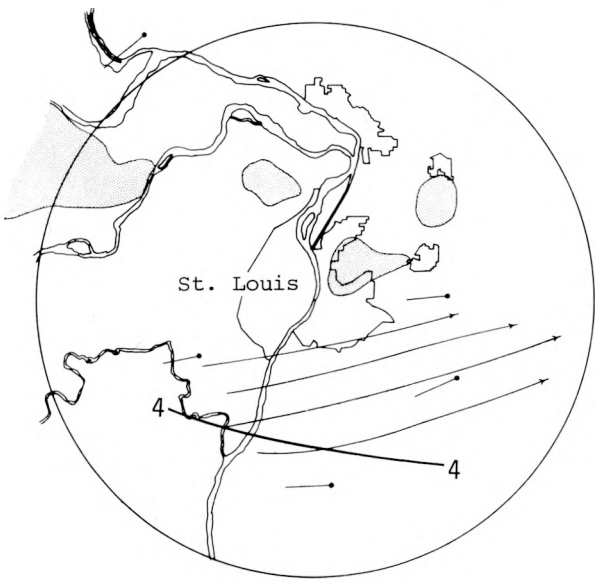

c. 1500 m MSL

Figure K-16. Low level airflow at 1400 (Isotachs in m/sec)

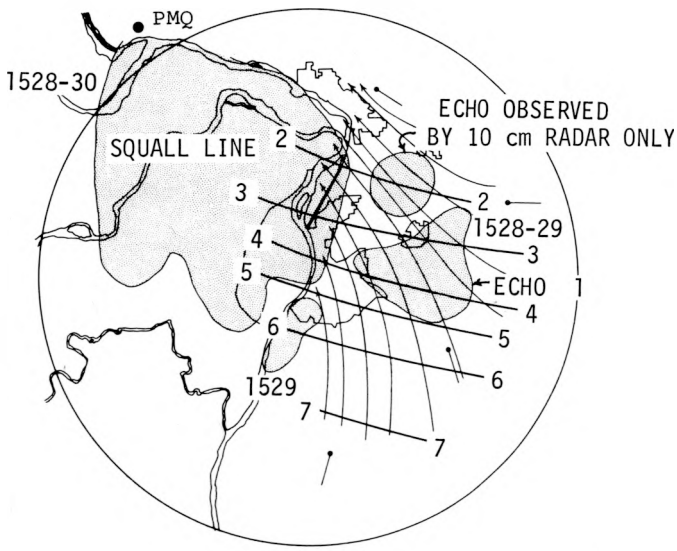

a. 500 m MSL

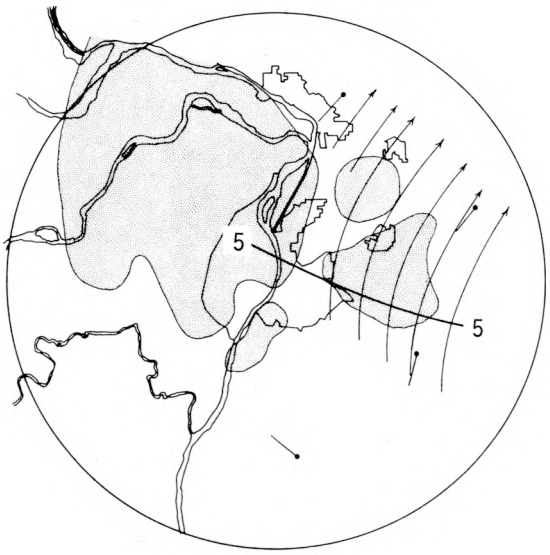

b. 1000 m MSL

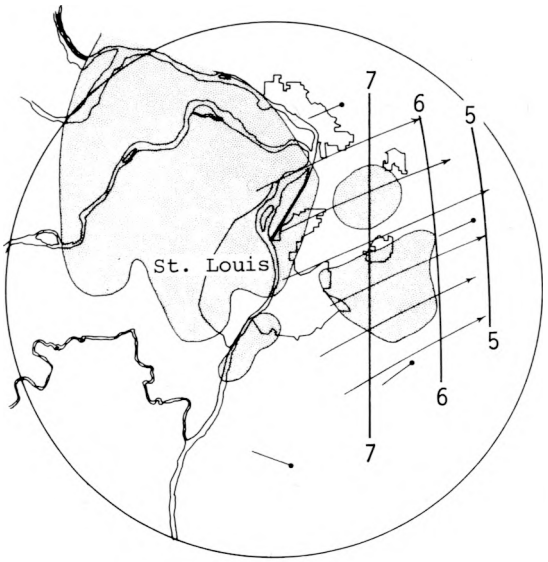

c. 1500 m MSL

Figure K-17. Low level airflow at 1530

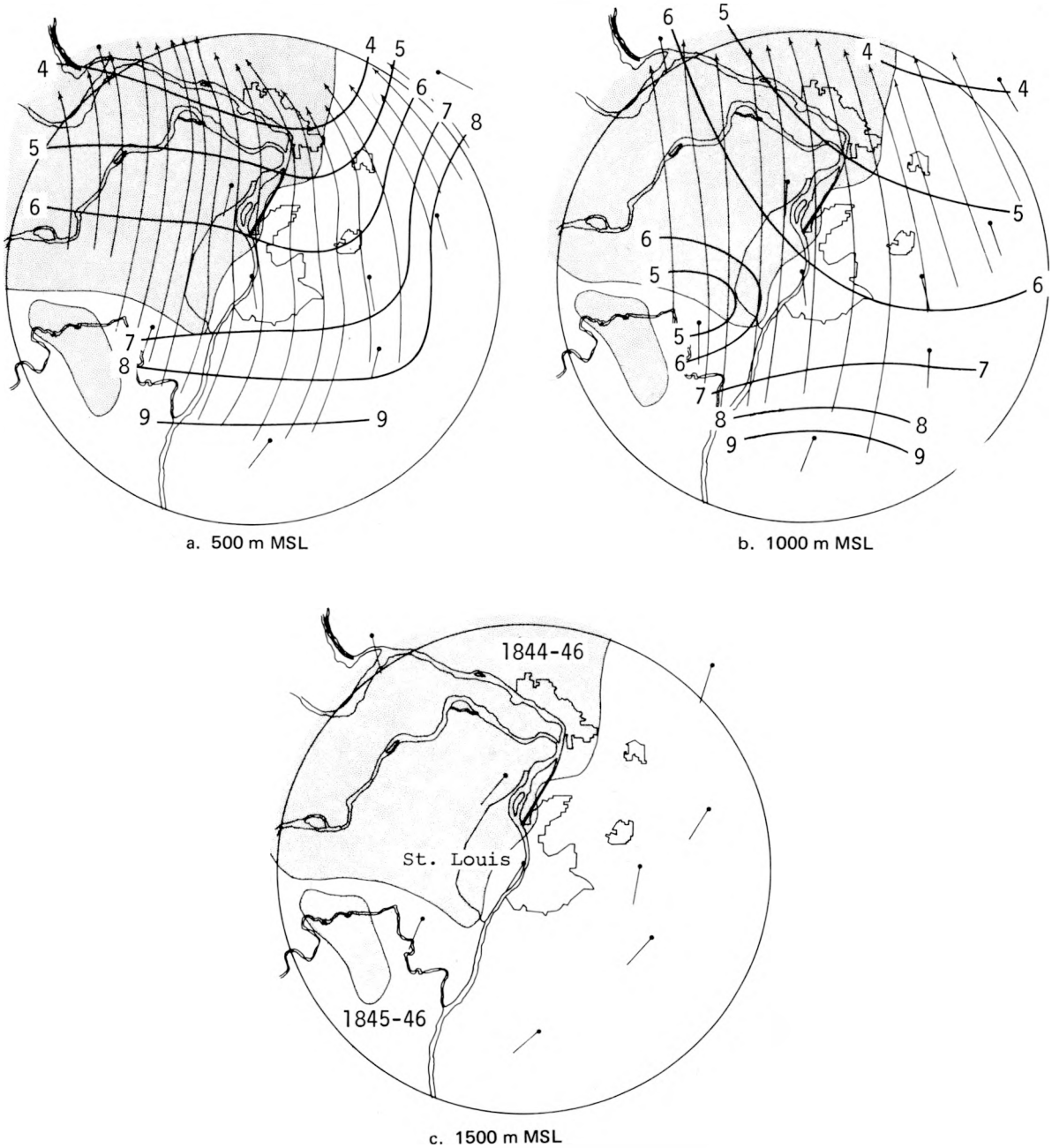

a. 500 m MSL

b. 1000 m MSL

c. 1500 m MSL

Figure K-18. Low level airflow at 1830

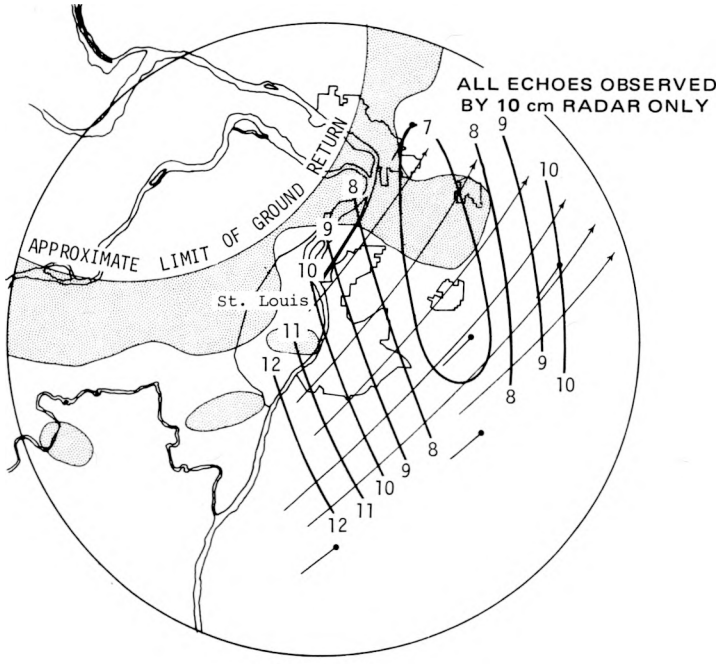

a. 500 m MSL

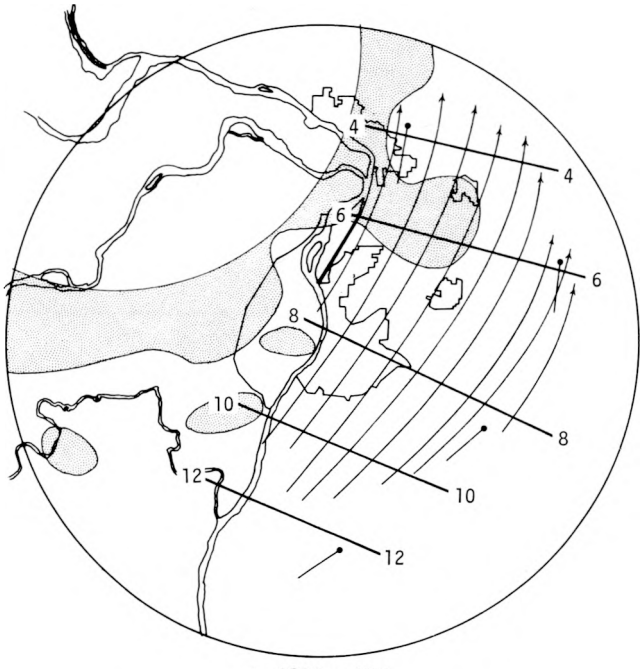

b. 1000 m MSL

Figure K-19. Low level airflow at 1930

PRECIPITATION MORPHOLOGY

The precipitation on 13 August was associated with two different synoptic conditions. The first was a squall line that produced precipitation in the MMX circle during the 1400–1730 period, and the second was a cold front that brought precipitation during the 1730–2400 period. Because the distributions of temperature and moisture parameters, at least at the surface, before the squall-line rain were different from those before the frontal rain, the two cases and their correspoinding precipitation elements are treated and discussed separately.

Squall-Line Case

Macroscale Precipitation Elements. To understand fully the precipitation events inside the MMX circle, it is helpful to first examine the associated broad-scale precipitation field. Hourly precipitation data from NWS recording raingage stations were plotted for each hour in which rain was present in S Illinois and SE Missouri. The squall line and the front were sufficiently separated in space and time to allow plotting separate hourly maps of 1) squall line rainfall and 2) frontal rainfall. The squall line rainfall during the hours ending at 1300, 1400, 1500, and 1600 is shown in figure K–20a-d.

The precipitation system is shown as it entered the W edge of the 2-state area, as it advanced toward the MMX circle, and as it passed through it. The striking feature of these patterns is the isolated maximum of 1.1 inches of rainfall that appeared within the circle during the hour ending at 1500. This maximum actually occurred in advance of the squall line (figure K–20c). As the general squall-line precipitation proceeded to the E, there was another isolated maximum in the pattern within the circle (figure K–20d). Both the mesoscale and macroscale synoptic data suggest the presence of a mesoscale low pressure system in the vicinity of the MMX circle. The total large-scale rainfall pattern associated with the squall line is depicted in figure K–21. A distinct maximum of rainfall was present within the circle and was the largest amount observed in the Missouri–Illinois study area.

Rainfall data presented thus far were from NWS recording raingages only. Data in the next section were observed in the Water Survey's 3-mi grid within the MMX circle and the 9-mi grid extended network.

Mesoscale Precipitation Totals and Severe Weather. The total rainfall from the squall line within the entire network (from 1400–1730) is shown on figure K–22. A 10-15 mi wide band of precipitation exceeding 0.25 inch extended 70 mi, from the W edge of the circle through St. Louis and out into the extended network. Within the MMX circle three areas had precipitation exceeding 1.0 inch. These maxima are labeled A, B, and C on figure K–22 and occurred, respectively, W of the city, in the city, and E of the city. Rainfall maximum C occurred in the same region as the climatological precipitation maximum (Huff and Changnon, 1972). Rainfall maximum C had the largest point value with 2.24 inches.

Hail observations are shown on figure K–23 along with times of hailfall, numbers of stones per ft^2, and maximum stone sizes. All hail fell within the area where rain exceeded 0.25 inch; furthermore, the larger and more intense streaks were either in or near 1-inch rain areas. The largest and most intense hailstreak occurred E of St. Louis, where precipitation exceeded 2.0 inches. In this hailstreak the number of stones reached 624/ft^2 and maximum stone diameters exceeded 0.75 inch. The point average stone frequency was 111/ft^2, a value 4 times the average (Changnon, 1970). The hailstones within the squall line generally were greater in size and frequency than average, and the heavier hail and larger streaks E of St. Louis support climatic findings on hail increases there (Changnon and Huff, 1973).

Figure K-20. Macroscale hourly rainfall (ending at times shown) with the squall line

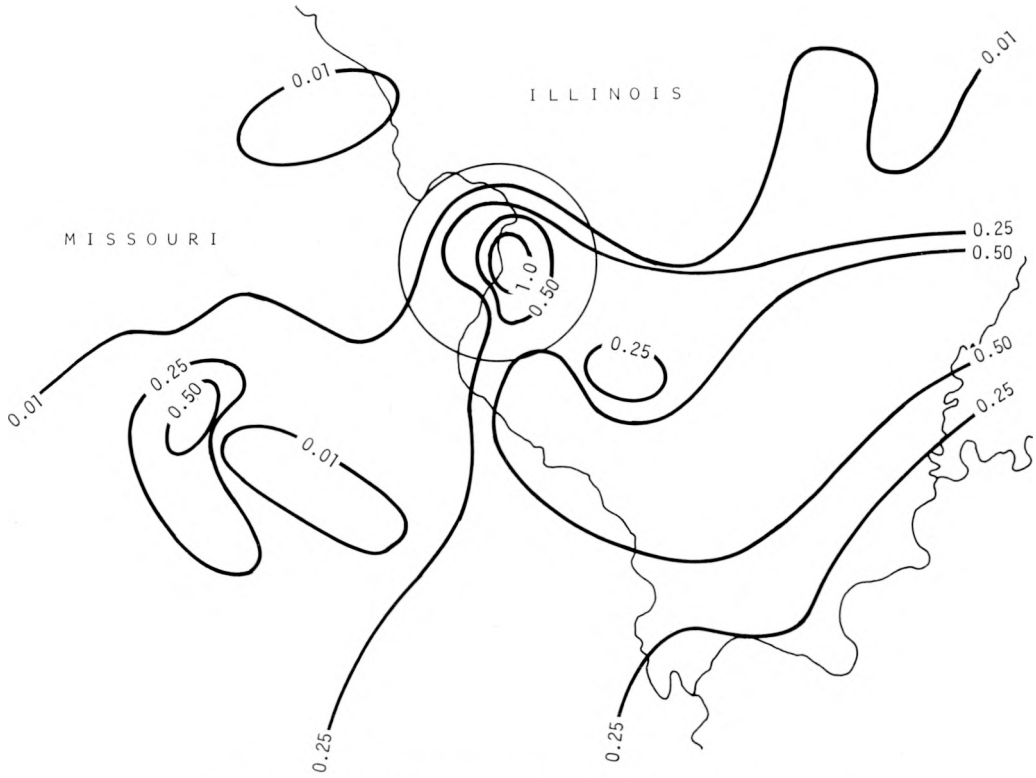

Figure K-21. Macroscale total rainfall pattern from the squall line

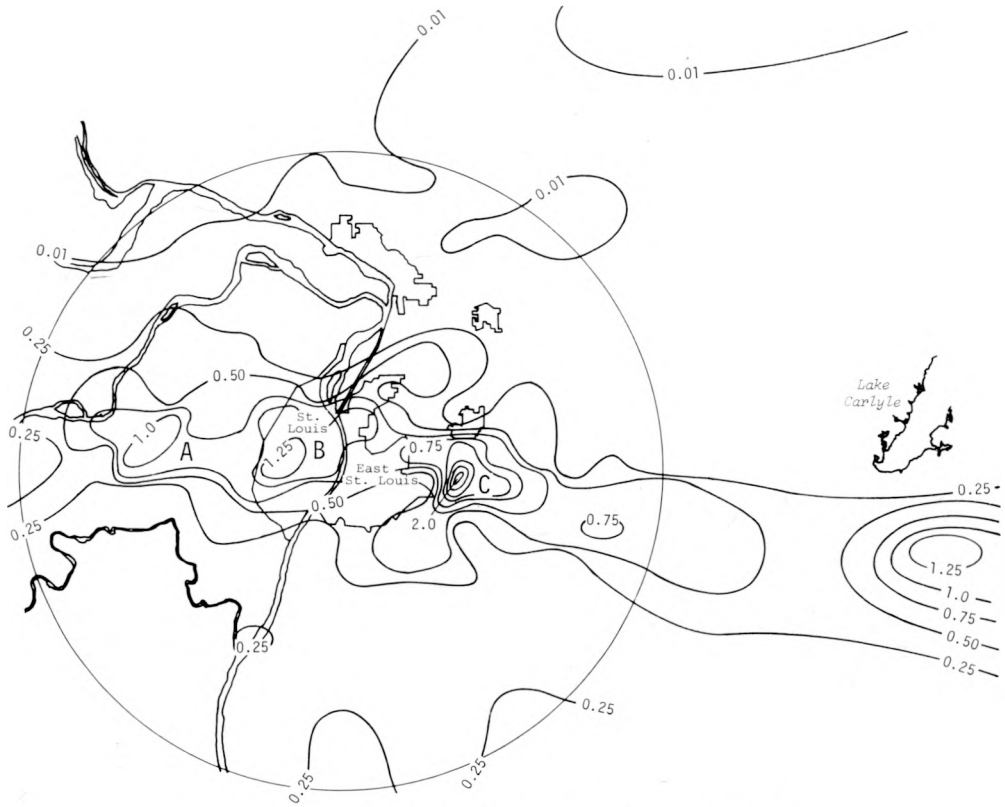

Figure K-22. Mesoscale rainfall from the squall line, 1400-1730

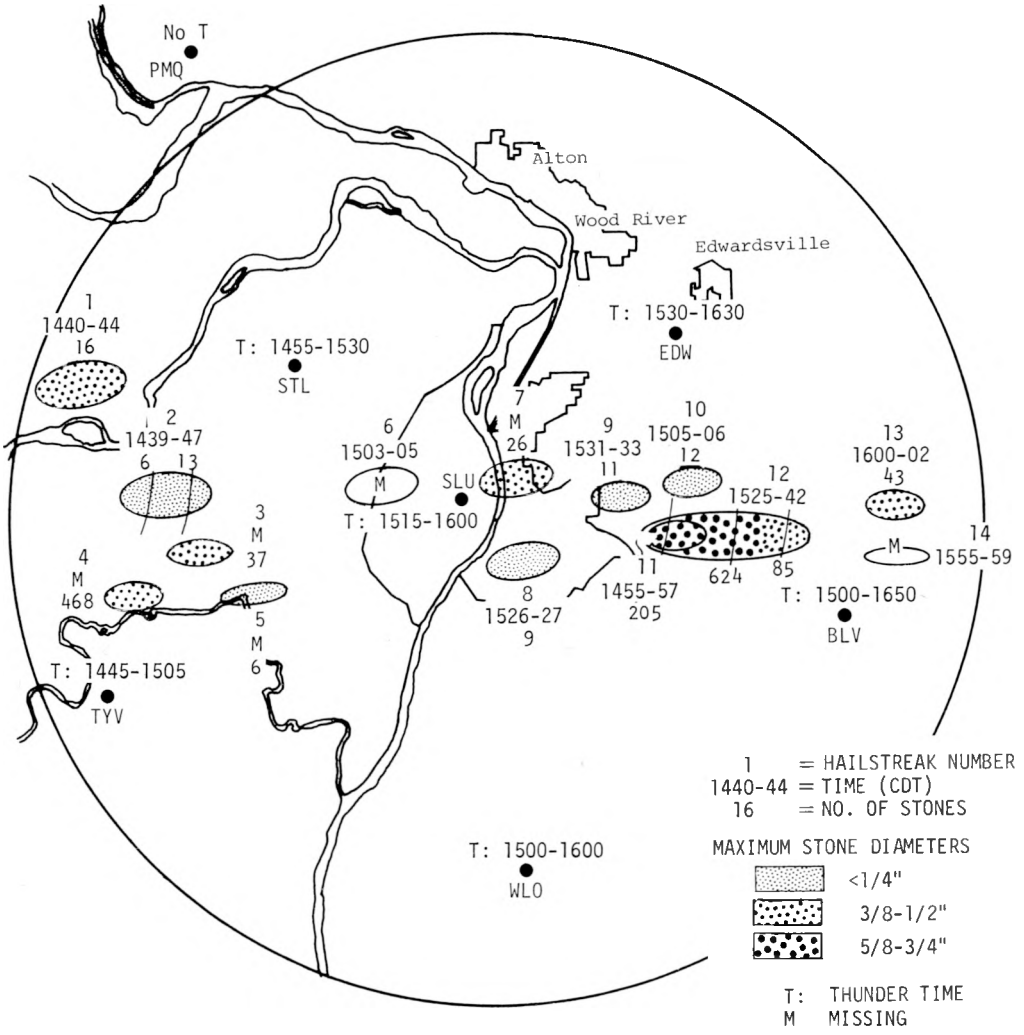

Figure K-23. Hail and thunder events associated with the squall line

The times and location of thunder are also shown in figure K-23. Thunder was heard at most observational sites indicating the rather general distribution and W-E motion of the thunderstorms within the squall line. Durations of thunder periods in the W were short (20 min at TYV, 35 min at STL), increasing from W to E (45 min at SLU, 60 min at EDW, and 110 min at BLV). This agrees with the tendency for longer thunder periods E of St. Louis (Changnon and Huff, 1973).

Raincells. During the squall-line period there were 25 raincells with complete life histories within the network, and 8 cells with incomplete life histories (i.e., 'edge' cells). The rainfall patterns associated with those cells that produced more than 100 ac-ft of rain are shown on figures K-24 and K-25. Cells 1 and 8 contributed to rainfall maximum C shown on figure K-21. Cell 6 contributed to rainfall maximum B, and cell 2 contributed to rainfall maximum A. The extension of the 0.5-inch isoline into the Granite City area was produced largely by cell 7, and the extension of the 0.5-inch isoline into the region W of Belleville was produced by cell 9. The isolated rainfall maxima in the S part of the MMX circle were produced by cells 4, 5, and 10. The hailstreaks associated with each cell are also shown on figures K-24 and K-25.

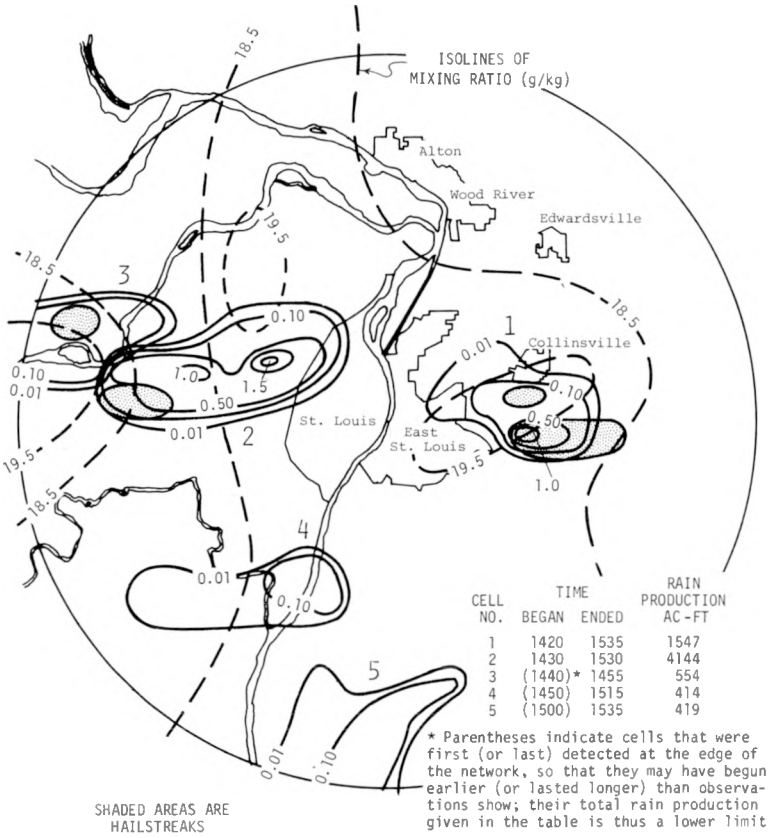

CELL NO.	TIME BEGAN	TIME ENDED	RAIN PRODUCTION AC-FT
1	1420	1535	1547
2	1430	1530	4144
3	(1440)*	1455	554
4	(1450)	1515	414
5	(1500)	1535	419

* Parentheses indicate cells that were first (or last) detected at the edge of the network, so that they may have begun earlier (or lasted longer) than observations show; their total rain production given in the table is thus a lower limit

Figure K-24. Rainfall and associate hailstreaks for squall-line raincells having volumes greater than 100 ac-ft, 1420-1500 CDT

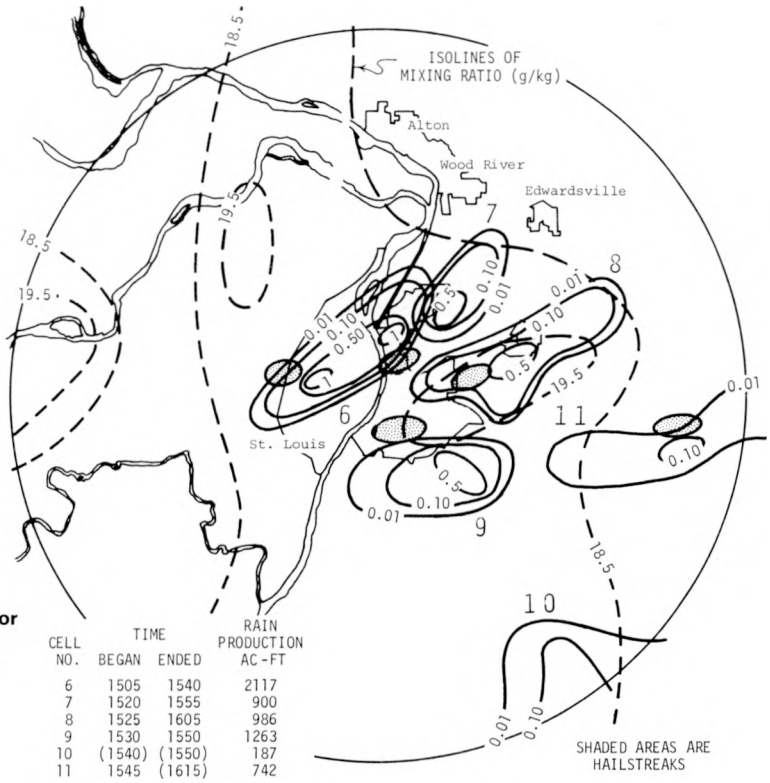

CELL NO.	TIME BEGAN	TIME ENDED	RAIN PRODUCTION AC-FT
6	1505	1540	2117
7	1520	1555	900
8	1525	1605	986
9	1530	1550	1263
10	(1540)	(1550)	187
11	1545	(1615)	742

Figure K-25. Rainfall and associated hailstreaks for squall-line raincells having volumes greater than 100 ac-ft, 1505-1545 CDT

All hailstreaks with the exception of 2 and 11 were point (single gage) occurrences only. Thus, direction could only be determined for hailstreaks 2 and 11, and these moved from directions between 260 and 280 degrees. This is the most frequent climatological movement of hailstreaks with 39% of all hailstreaks moving in this direction (Changnon, 1970). The duration of hailstreak 2 was 8 min and that of hailstreak 11 was 17 min. Climatologically, hailstreaks defined by two or more points have durations exceeding 11 min 45% of the time and durations exceeding 15 min 27% of the time. Hailstreak 12 began 65 min after raincell 1 and hailstreak 2 began 8 min after raincell 2. Hailstreak 12 initiated 8 min after two radar echoes merged. (Because no merger of raincells was observed at the surface, the observed echo merger implies a fusion of liquid water masses aloft.) Climatologically, the difference between initiation of rain and hail is 12-16 min (Changnon, 1970) for air mass storms, Thus, these hailstreaks possessed near-average characteristics.

The 18.5 and 19.5 g/kg isolines of mixing ratio (ω) at 1400 CDT are also shown on figure K-24 for comparison with cell positions. Particular attention will be paid to locations, with respect to the surface moisture pattern, of cell *initiations* (first rain) and *maximizations* (most rain). Raincell 2 initiated in the vicinity of the maximum in ω on the W edge of the network and then moved to the E where it maximized in the 18.5 isoline of ω near the 19.5 isoline. Cell 4 initiated on the SW edge of the circle and them moved to the E and maximized within the 18.5 isoline. Cell 1 initiated and maximized immediately E of the city and within the 19.5 isoline of ω. The other cells on figure K-24 also occurred within regions of relatively high mixing ratios.

The cells on figure K-25 are also in the vicinity of ω maxima. Cells 7, 8, and 9 completed their life histories in or near the 19.5 isoline and within the 18.5 isoline. Cells 6 and 10 occurred completely within the 18.5 isoline and cell 11 initiated within the 18.5 isoline. The ARC sounding at 1335 (figure K-14) indicated that there was an abundance of low-level moisture ($T_d \geqslant 65$F up to 920 mb). The implication is that there was ample moisture to sustain convection, and *the association of the larger cell rainfalls and surface moisture suggests that surface moisture was an important contributing factor in the initiation and development of the precipitation within these cells.* In contrast to the strong association with surface moisture, raincell precipitation does not appear to be related to the surface temperature field (figure K-6), with the exception of precipitation from cells 2, 3, and 5, which all occurred in the vicinity of temperature maxima.

The 11 raincells discussed all yielded more than 100 ac-ft of water. The rain that fell from the 22 smaller cells (those with less than 100 ac-ft) was accumulated and the rainfall pattern is depicted on figure K-26. The point amounts were small, indicating that most of the cell rainfall was produced by cells greater than 100 ac-ft.

The initiation frequency of all 33 cells (i.e., the number of times that each gage was within a cell initiation) during the squall line period is shown on figure K-27. For comparison, the 18.5 and 19.5 isolines of ω were superimposed on the initiation patterns. Ten of the 12 areas enclosed by 1-isolines of cell initiation lie largely within the 18.5 isoline of ω that encloses only 60% of the gages in the MMX circle. The exceptions are the 1-isolines along the Meramec River and in the Wood River area. The 2-isolines of cell initiation occur in the vicinity of 19.5 isolines. Thus, the initiation of raincells during the squall-line period appears to have been favored by high values of surface moisture.

Since the initiation and development of cell rainfall in the squall line occurred in the vicinity of surface moisture maxima, the *source* of this moisture is of obvious concern. One potential source is recent prior rainfall. Thus the surface moisture pattern at 1400 was compared with the precipitation that fell the day before. The pattern of rainfall $\geqslant$ 0.50 inch and the pattern of mixing ratios $\geqslant$ 18.5 g/kg are shown on figure K-28. The heavier rainfall from the previous day occurred largely in the area of the 18.5 isoline with the notable exception of the 1.0 isoline of rainfall E of

Figure K-26. Rainfall and associated hailstreaks for squall-line raincells having volumes less than 100 ac-ft

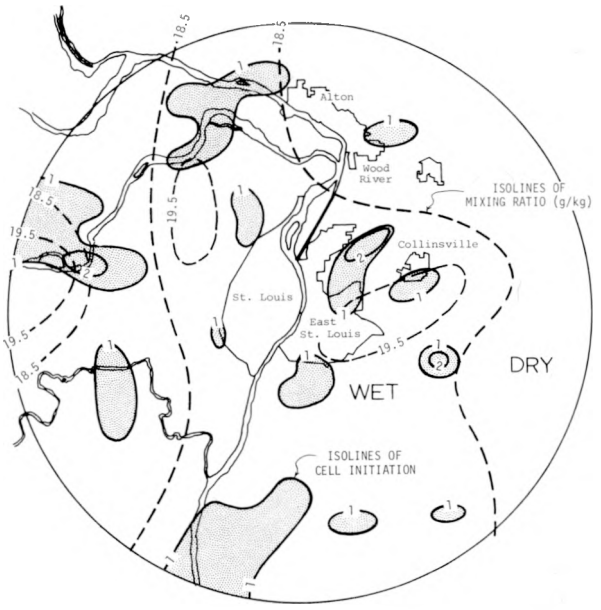

Figure K-27. Raincell initiations per gage during the squall line compared with the surface mixing ratio field prior to the rain

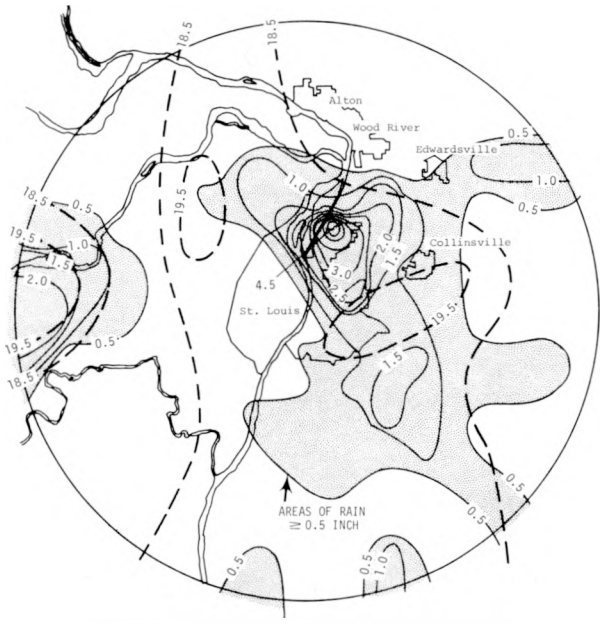

Figure K-28. Comparison of rainfall ⩾0.50 inch from 1445-0245 on 12-13 August and mixing ratios ⩾18.5 g/kg prior to the squall line on 13 August

Table K-1. Raincell Characteristics for Complete Cells Producing Volumes Greater than 100 Ac-Ft during the Squall Line

Cell	Initiation time, CDT	Volume (ac-ft)	Average rain (in)	Area (mi^2)	Duration (min)	Velocity (mi/hr)	Gradient (in/mi)
1	1420	1547	.44	66	75	3.5	.32
2	1430	4144	.64	122	60	13.9	.08
6	1505	2117	.71	56	35	20.3	.21
7	1520	900	.45	37	35	5.7	.06
8	1525	986	.28	66	40	18.0	.12
9	1530	1263	.36	66	20	19.5	.12

Edwardsville. The correspondence between the 19.5 isoline of ω and the prior precipitation on the W edge of the circle is excellent. Overall, there is considerable agreement between the ω pattern and the precipitation pattern on the prior day.

Selected cell characteristics for the complete cells shown on figures K-24 and K-25 are listed in table K-1. Cell 1 had the longest duration and produced the strongest gradients of precipitation. Cell 2 had the largest area and produced the heaviest volume of precipitation. Cell 6 had the highest average rainfall, the highest velocity, and a short duration. It is of interest that cells 1 and 2 spent much or all of their lives in regions of high surface moisture, whereas cell 6 crossed a region of low surface moisture, but high Aitken nuclei production rates. Auer and Dirks (1974) measured Aitken nuclei production rates of greater than 150×10^4 nuclei in the region shown on figure K-31. Thus, of the three largest rain volume producing cells in the squall-line period, cell 6 with the greatest probable nuclei intake had the shortest duration, was the fastest moving, and had the highest average rainfall but the smallest rainfall area. Its rain production and rainfall gradient figures were second among the three cells.

In contrast to the strong association between cell initiations and rain production with the surface moisture pattern, neither parameter shows a strong preference for temperature maxima at 1400 (see figure K-6). Nevertheless, both cell initiations and rain production show a definite preference for the warmer half of the MMX circle (mean temperature 83F). It is noteworthy that most of the cell activity associated with the squall line (also compare total squall-line rainfall, figure K-22) took place in a band across the middle of the circle. This band is closely associated with the maximum temperature gradient that probably delineates the S border of the area of low clouds.

Comparison of cell parameters in figure K-24 and K-25 with the pre-squall line (1400) distribution of θ_e reveals a definite preference for cells to initiate in areas of greater than average θ_e. Six out of eight cells that began within the circle (as opposed to those first detected at the edge of the circle) did so in areas of θ_e values equal to or greater than the circle average of 352K.

Radar Echoes and Mesoscale Precipitation Elements. First echoes during the squall-line period were determined from the 3-cm RHI radar data and are shown in figure K-29 as the hatched areas, along with their initiation times and maximum heights at initiation. The corresponding first raincells (shaded areas) of the period and their times of appearance as well as the 19.0 and 19.5 isolines of mixing ratio are also shown. There is a close spatial association between the first echoes and first raincells, indicating rapid precipitation processes, and the results show a tendency for the precipitation process to initiate in regions of high moisture.

Because radar signal integrator data were not available for 3-cm RHI radar echoes, an echo-frequency-coverage (EFC) representation was prepared in order to show the extent of the echoes. These representations were obtained by tabulating one count for each time an echo was above a raingage location. These counts were then accumulated over time at each gage location to obtain a total EFC representation of the echoes. The EFC for all echoes is shown on figure K-30.

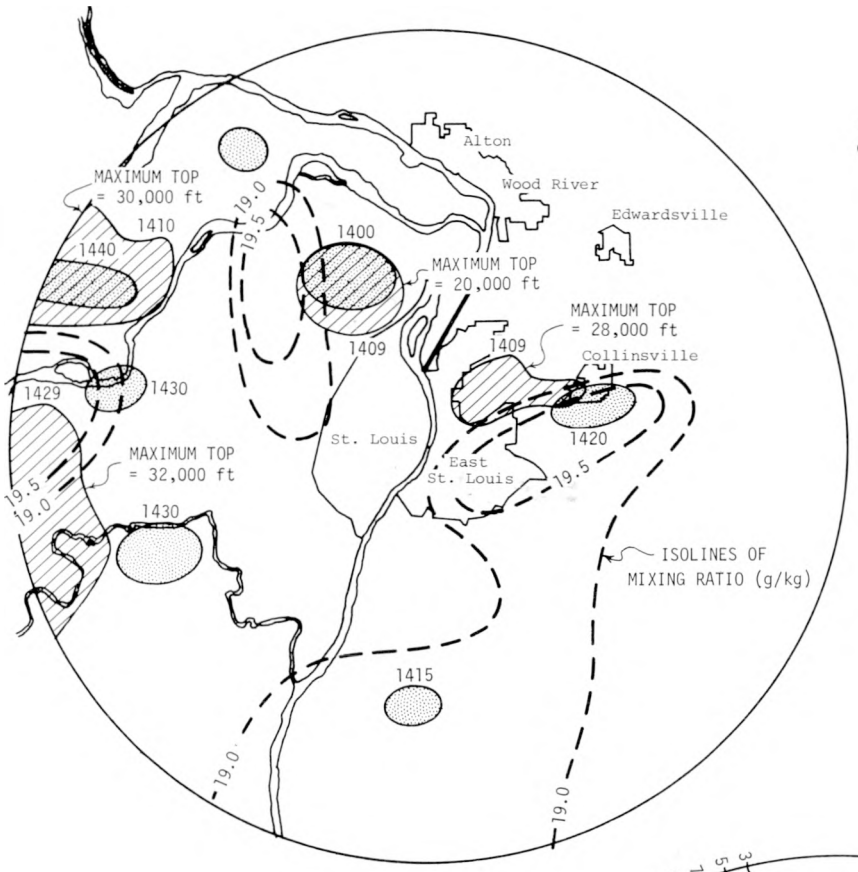

Figure K-29. Comparison of first radar echoes and first raincells during the squall line with the surface mixing ratio field before the rain

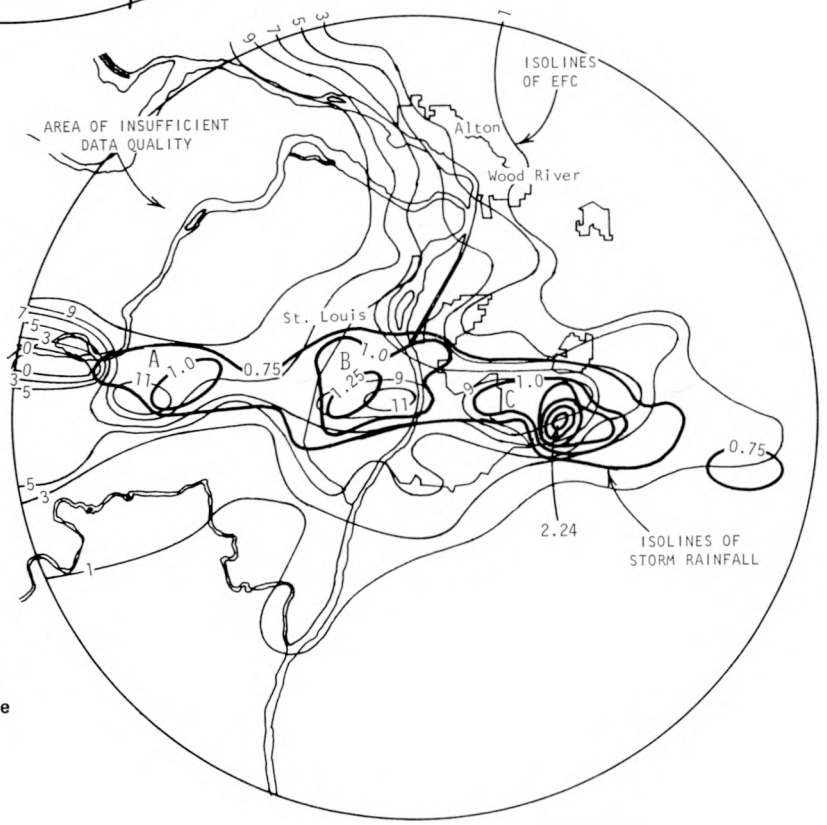

Figure K-30. Comparison of the EFC representation of 3-cm RHI radar echoes with rainfall ⩾0.75 inch from the squall line

The frequency maxima are labeled A, B, and C on the map. These maxima and their surrounding patterns correspond extremely well with the maxima on the total storm rainfall pattern shown on figure K-22. To illustrate this correspondence, isolines of rainfall greater than 0.75 inch were superimposed on figure K-30.

The excellent agreement between the total rainfall and the echo maxima suggested that EFCs for individual radar echoes could be useful. These were obtained for those echoes that could be delineated from the general echo mass in the NW part of the MMX circle. Echoes 1-5 were delineated and are represented on figures K-31 through K-36 as isolines of EFC.

Echo 1 on figure K-29 initiated on the E boundary of the St. Louis urban complex. In its subsequent development (figure K-31), this echo built to the W (backwards) across the river and into the St. Louis urban area. Thus, the echo had the time and opportunity to grow over the urban area and was present about 20 min before the associated raincell (cell 1) formed at 1420. (The 3-cm RHI data began at 1409, but 10-cm PPI radar data showed an echo in the same position beginning at about 1400.) At approximately 1515, echo 1 merged with echo 3 (figure K-31), thus forming echo 5, shown on figure K-33. Echo 3 had previously developed and moved through a region of high pollutant aerosol (Aitken nuclei) production rates, providing ample opportunity for it to entrain air with high aerosol concentrations. Thus cell 1, which produced heavy rain and the largest and most intense hailstreak, had an excellent opportunity to entrain pollutant aerosols through merger with echo 3 as well as from echo 1 which had its early growth over urban regions.

The airflow approaching cell 1 at 500 m was from the SE and of a non-urban nature, while the flow at 1500 m was from the SW with a trajectory over the city. The precise locations of the storm's inflow areas become an important factor in determining whether this cell was affected by the urban environment. This region is not clear from the RHI data, but the fact that the echo grew to the W (i.e., on the 'back side') strongly suggests an inflow area on the city side. The merger of echoes 1 and 3 provides another possible mechanism by which the city air could have been ingested into cell 1.

Raincell 8 formed in the high-moisture region of East St. Louis and moved NE through the moisture maximum (figure K-25). Furthermore, it initiated in the general merger region of echoes 1 and 3, but at 1525 (figure K-25), approximately 9 min after the merger (figure K-34). Echo 5, the associated post-merger radar echo, subsequently merged with the general echo mass at 1545-1549. Thus, cell 8 initiated in the city, in a maximum of surface moisture and in the merger region of two radar echoes. This cell and cell 1 were the major contributors to rainfall maximum C (figure K-22) located bewteen Belleville and Collinsville.

Echo 2 first appeared W of the MMX circle and moved to the NE where it merged with a general echo mass that covered most of the NW part of the circle at that time (figure K-35). Raincell 2 began in the region of the merger and then moved from the W edge of the circle into the city. Cell 2 initiated in the heat and moisture maxima (figures K-6 and K-7) and produced its maximum point rainfall when it moved into the 18.5 isoline of surface mixing ratio. This cell also produced hail near the merger (figures K-24, K-35) and the heat and moisture maxima on the W side of the circle (figure K-6).

There was flow from the E (figure K-8) at the surface with a trajectory across the city and toward the cell. Also in the proximity of cell 2, there was a line of confluence in the surface airflow. There is also an indication of the confluence in the 500 m airflow. Furthermore, according to the surface and 500 m airflow, cell 2 was 'downwind' of the city during part of its life history *and potentially experiencing urban effects.*

Echo 4 originated in the Meramec and Mississippi River bottoms, within the 18.5 isoline of surface mixing ratio (figure K-36). This echo then moved to the NE into the city region of high

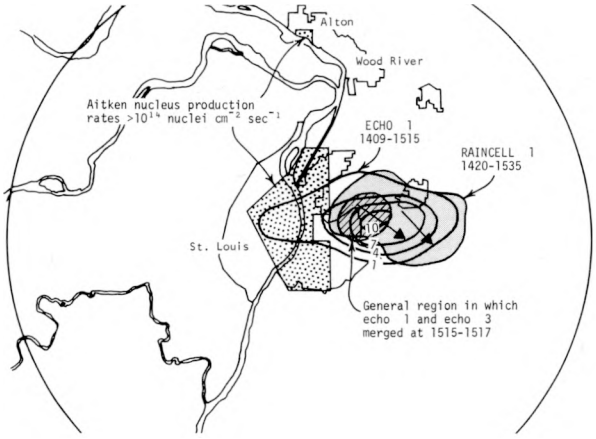

Figure K-31. Life histories of echo 1 and associated raincell 1

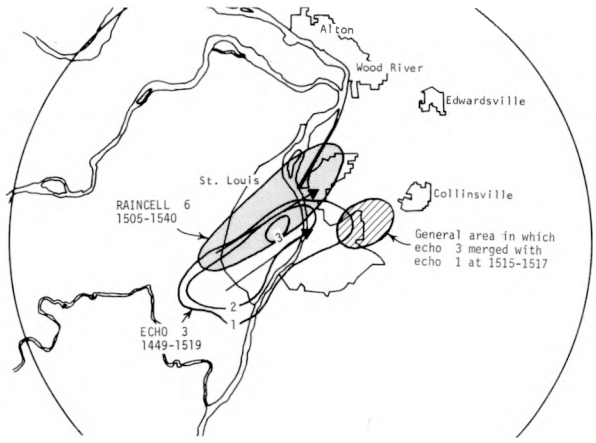

Figure K-32. Life histories of merged echo 5 and associated raincell 1

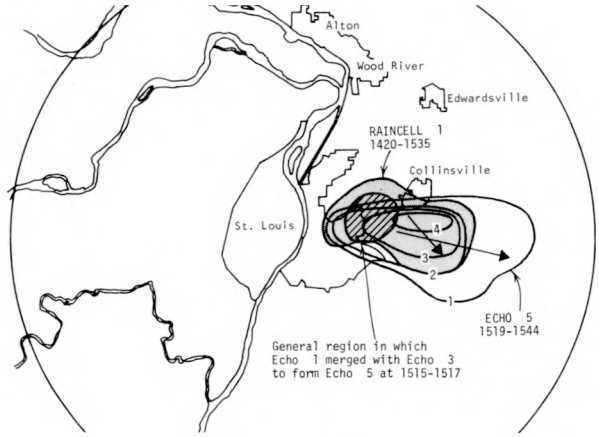

Figure K-33. Life histories of echo 3 and associated raincell 6

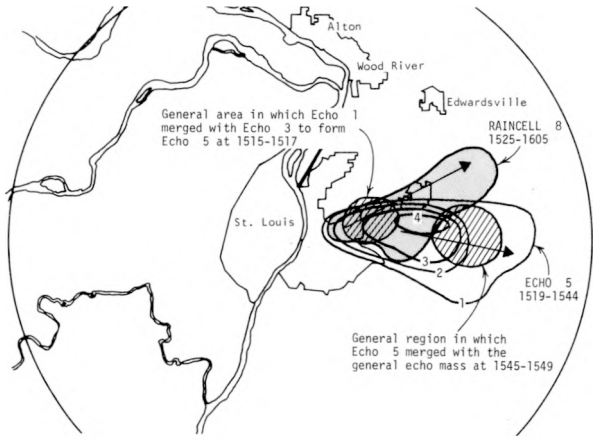

Figure K-34. Life histories of merged echo 5 and associated raincell 8

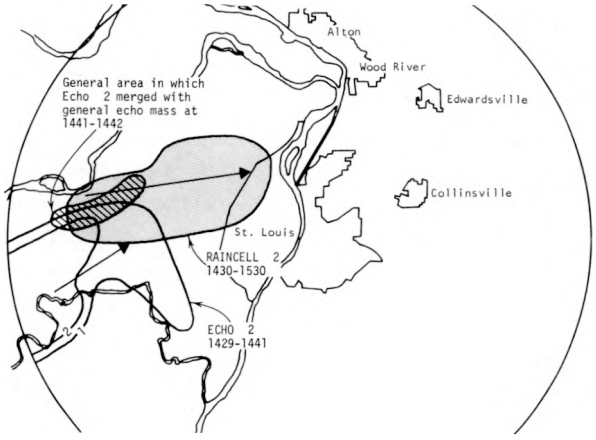

Figure K-35. Life histories of echo 2 and associated raincell 2

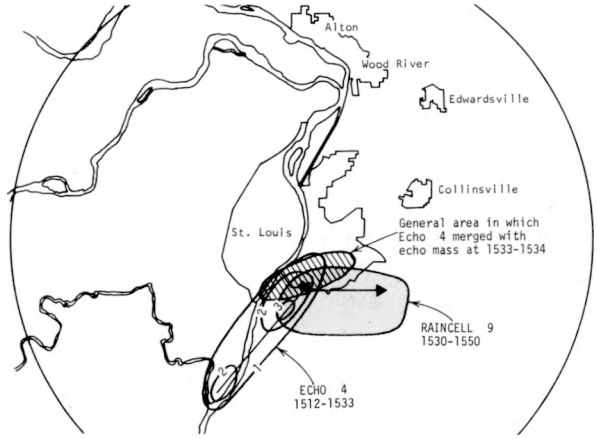

Figure K-36. Life histories of echo 4 and associated raincells 4 and 9

Aitken nuclei production rates (figure K-31) and merged with the general echo mass which was covering a large portion of the circle at that time. At the point of this merger, raincell 9 was spawned and then moved to the E into the Belleville area.

To demonstrate more clearly the time sequence of events associated with cell 1, a series of graphs were prepared to show the variation with time of several related raincell and radar echo parameters. These data are presented in figure K-37, to facilitate comparison of parameters before and after echo mergers.

[Note: Because of noise in the FPS-18 integrator recording system, data are available only for reflectivities > 42.5 db. However, other aspects of the FPS-18 data appear to be normal. For example, cell locations agree closely with those from the TPS-10 radar. Echo volume was approximated by multiplying the area of the 42.5 db reflectivity core by the maximum echo height from the TPS-10 data shown in figure K-37b.]

Figure K-37a shows time variations of both average radar reflectivity and echo volume for echoes 1 and 3 (and for echo 5, the echo resulting after the merger). For echoes 1 and 3, the echo volume reached a maximum 9 min after merger in the merged cell 5 and the reflectivity reached a maximum 5 min after merger.

Figure K-37b shows 3-cm RHI echo tops before and after the merger. The tops of both cells were increasing prior to the merger. The top of the merged echo 5 was about the same height as echo 1 prior to merger and higher than echo 3 prior to merger.

Figure K-37c and d shows two parameters of the raincells associated with the radar echoes just discussed. These parameters are rain volume (per 5-min period) and average rainfall (per 5-min period).

For raincell 1, which was associated with echo 1, there was an increase in cell volume prior to echo merger. After merger the volume increased further, reaching a maximum within approximately 13 min (figure K-37c). There was an increase in average rainfall prior to merger and a sharp increase after merger, with a maximum reached 13 min after merger (figure K-37d). For raincell 6, associated with echo 3, there was a large increase in cell volume just prior to echo merger, followed by a temporary decrease and then a secondary peak 13 min after merger (figure K-37d). Raincell 8 is not shown on figure K-37, but it initiated 8 min after echo merger. Thus, cell 8 initiated at approximately the same time after merger that the maximization was occurring in the other cells.

Hailstreak 12 began 8 min after the merger of radar echoes 1 and 3. This hailstreak had larger area, longer duration, larger hailstones, and produced more hail than any other hailstreak on 13 August. This hailstreak occurred a few minutes after merger in the vicinity of the city and in an area of high surface moisture.

The merger mechanism was an important contributing factor to rainfall intensification. Several raincells were either spawned or intensified in general merger regions and temporal data indicate that there was a tendency for echo heights and reflectivities to increase after echo merger and an intensification and/or initiation of raincells and hailstreaks after merger. Furthermore, the location of merger cells in relation to confluence in airflow patterns and their exposure to urban CN, heat, and moisture provide strong evidence for a link between rainfall intensification and properties of the urban area.

Frontal Case

Macroscale Precipitation Elements. The macroscale precipitation was investigated in the manner described earlier for the squall-line case. The frontal precipitation during the hours 1900,

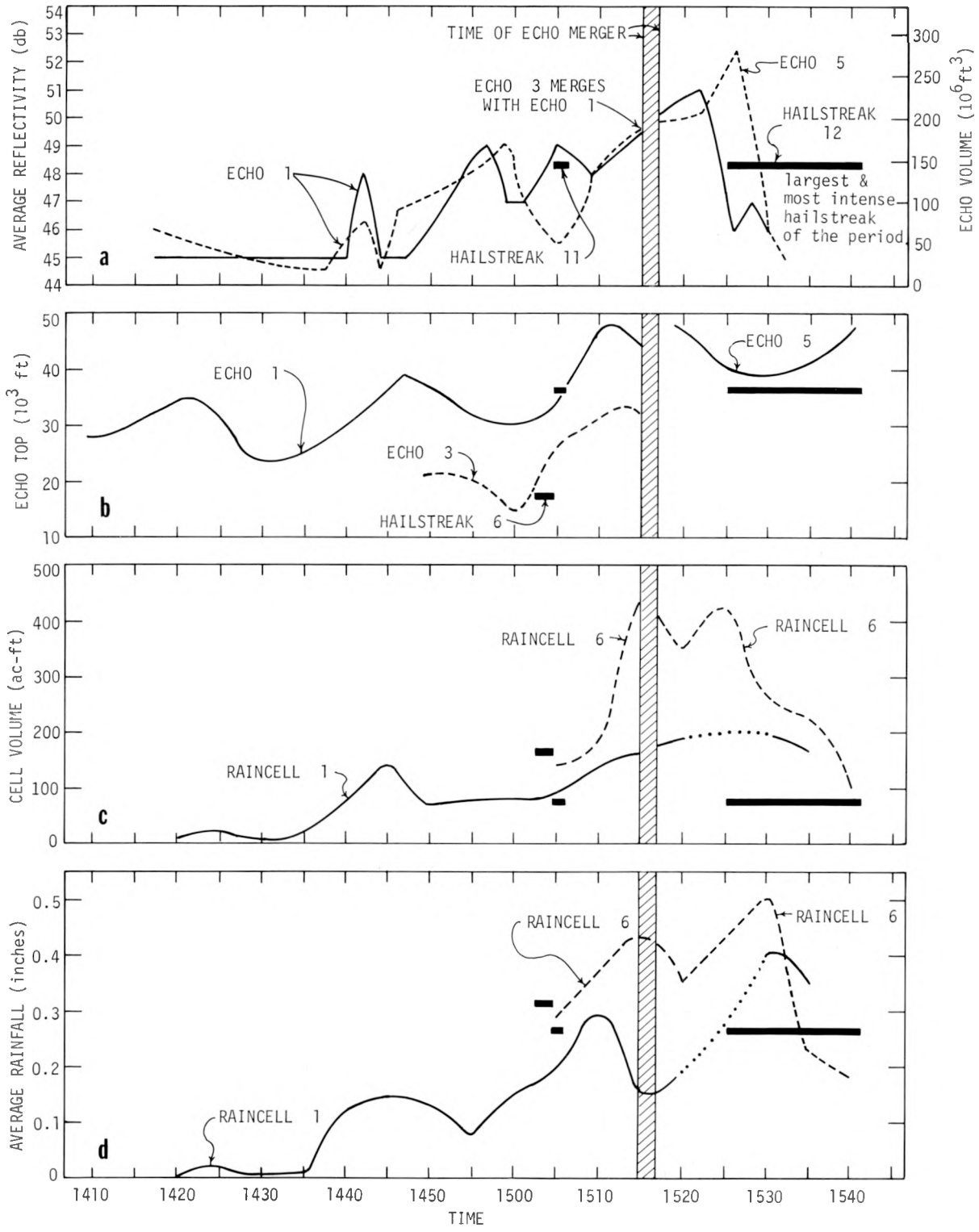

Figure K-37. Time changes of raincell and radar echo parameters before and after echo mergers

2000, 2100, and 2200 is shown on figure K-38. The precipitation system is shown as it approached and passed through the MMX circle. The striking feature of this pattern is that although the main core of the rainfall at 2000 is N of the MMX circle, there is an extension of the rainfall pattern into the circle. As the system passes through at 2100, there is an isolated rainfall maximum remaining in the circle. The rather isolated nature of the heavy rainfall in the MMX circle in relation to the major frontal activity is shown even more clearly on figure K-39 where the total rainfall pattern associated with the frontal system is depicted.

Mesoscale Precipitation Elements. The total rainfall from the frontal system on the MMX circle and the extended network (1730–2400 CDT) is shown on figure K-40. A broad band of precipitation exceeding 0.25 inch extends from the SW edge of the circle to the NE through Alton and out into the extended network. The 3-inch maximum 20 mi NE of Alton is within the broad frontal rain zone shown on figure K-39. However, due to the sparsity of NWS hourly stations, the 2- and 3-inch network maximums do not appear on figure K-39. Areas of rainfall exceeding 1 inch (figure K-40) lie roughly on a SW-NE line.

Hail did not fall on the network during the time of precipitation associated with the frontal passage. The times and locations of thunder are shown on figure K-40. Thunder was present at two observational sites in the MMX circle, indicating that the heavier rainfall came from thunderstorms.

Raincells. During the frontal passage there were 35 cells with complete life histories and 15 cells with incomplete life histories. The rainfall patterns of the 10 cells that produced more than 250 ac-ft are shown on figures K-41 and K-42. Several of these cells led to the 1-inch rainfall highs on figure K-40.

Isolines of surface temperature (figure K-10) were compared with the raincells shown on figures K-41 and K-42. All 10 of the raincells were located within the 73F isoline and 9 of these were within the 75F isoline. The striking feature of this comparison is the lack of raincells in regions where the surface temperatures were relatively low.

These 10 raincells are shown in relation to isolines of surface mixing ratio (ω) on figures K-41 and K-42. Most of the raincells are located within the 15.5 isolines of ω. The striking feature is the lack of raincells where the surface moisture content is low in relation to the overall pattern and less than 15.5 g/kg.

The rainfall from the cells producing less than 250 ac-ft was accumulated and the total pattern resulting from these cells was compared with isolines of surface temperature values (figure K-10). Most of the rainfall maxima were within the 75F isotherm. The exceptions were maxima in cell rainfall in the Granite City and Edwardsville areas. Thus, although the correspondence with temperature was not as close as it was for cells greater than 250 ac-ft, there was still considerable agreement.

A comparison was also made of the total pattern for raincells having volumes less than 250 ac-ft and the rainfall moisture pattern. The rainfall maxima were mostly within the 15.5 isoline with the exception of a few very small cells. Thus, both strong and weak raincells were generally located in regions where both surface temperature and moisture were high. The raincells also showed a rather strong preference for regions of high θ_e values at 1700.

The initiation frequency of all 50 cells (i.e., the number of times that each gage was within a cell initiation) during the frontal period is shown on figure K-43. For comparison, the 73F isotherm and the 15.5 g/kg mixing ratio isoline are superimposed on the initiation pattern. Most initiation areas, including all areas with 2 initiations, occurred within the 15.5 isoline of ω. Some of the cell initiations occurred at temperatures lower than 73F, notably in Granite City and E of Edwardsville. Still, the cell initiation appears to be associated with the wetter, warmer, higher θ_e surface regions.

Figure K-38. Macroscale hourly rainfall (ending at times shown) associated with the cold front

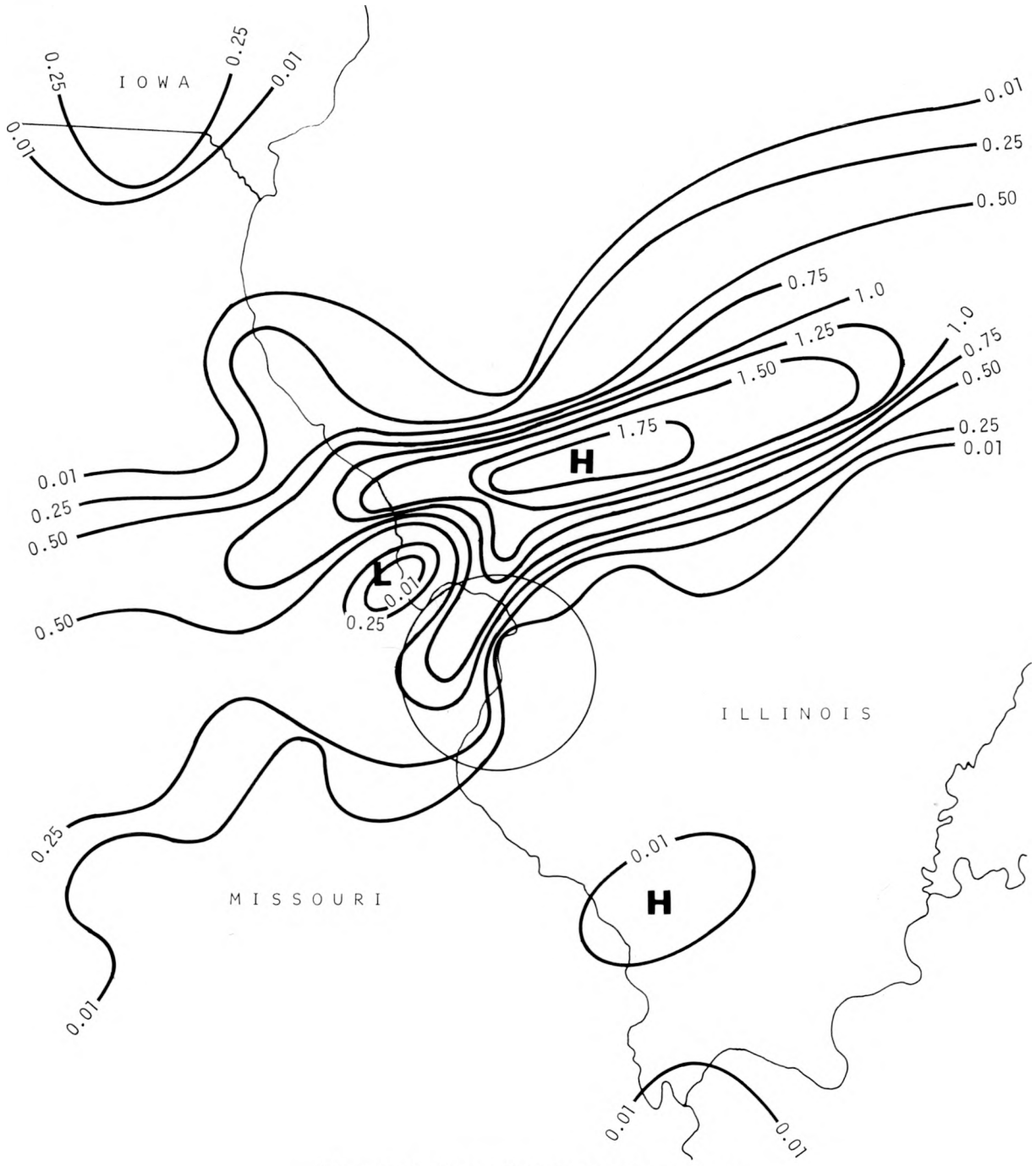

Figure K-39. Macroscale rainfall from the cold front

Figure K-40. Mesoscale rainfall from the cold front, 1730-2400

Because the initiation and development of cell rainfall may occur preferentially in the wetter regions, a comparison of the surface moisture pattern with the prior squall-line precipitation was made. Most of the prior squall-line precipitation (figure K-22) occurred in the drier portion of the moisture pattern at 1900 (figure K-43). However, the moisture maxima are located to the N and W of the prior precipitation. Thus, the maxima in the surface moisture patterns are generally in an area situated downwind of the prior precipitation.

The surface airflow was from the SE at 1600 (not shown), and was from the S with cyclonic turning toward the NW over the city region at 1700 (figure K-12). By 1800 the wind flow was largely from the S, and by 1900, largely from the SW. Thus, prior to the onset of precipitation the surface flow over the city was from the S or SE. The wind patterns are of particular interest when compared with the Aitken nuclei measurements along the flight track shown on figure K-44. The highest concentrations of Aitken nuclei are found NW of the city (maximum of 20,000/cc) and the lowest densities are found E of Alton-Wood River and E of St. Louis. Thus, the general area in which the frontal raincells were located was one in which high surface values of temperature and moisture were present as well as high Aitken nuclei concentrations aloft.

Furthermore, the surface winds at 1900 (not shown) and the 500 m flow at 1930 (figure K-19a) were from the SSW prior to the initiation of raincells 6, 8, and 9. These incomplete cells located on the N edge of the MMX circle may have contributed to the 3-inch rainfall maximum

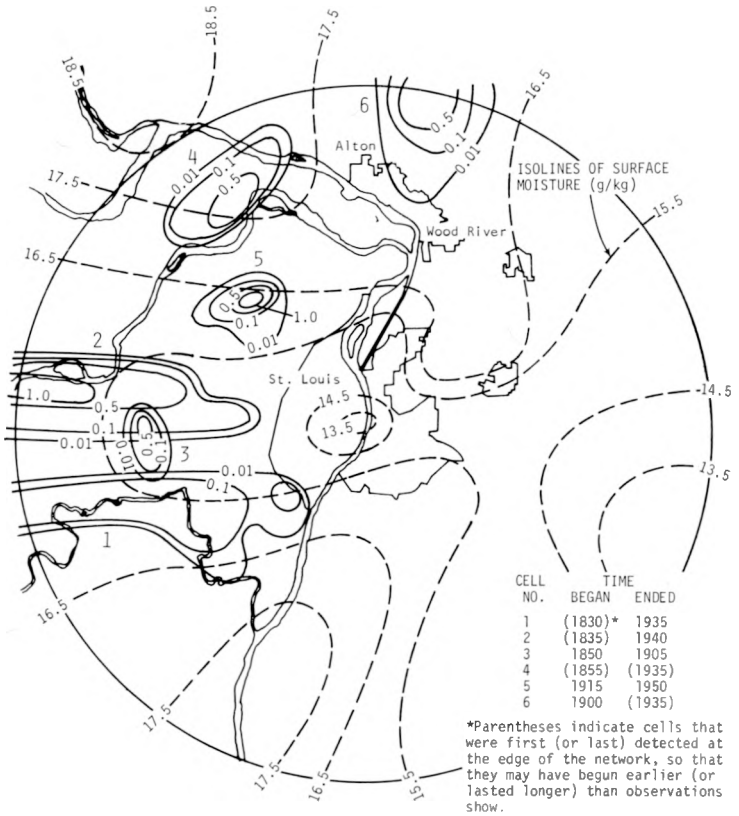

Figure K–41. Rainfall for frontal raincells 1-6 having volumes greater than 250 ac-ft, compared with the distribution of surface moisture before the rain

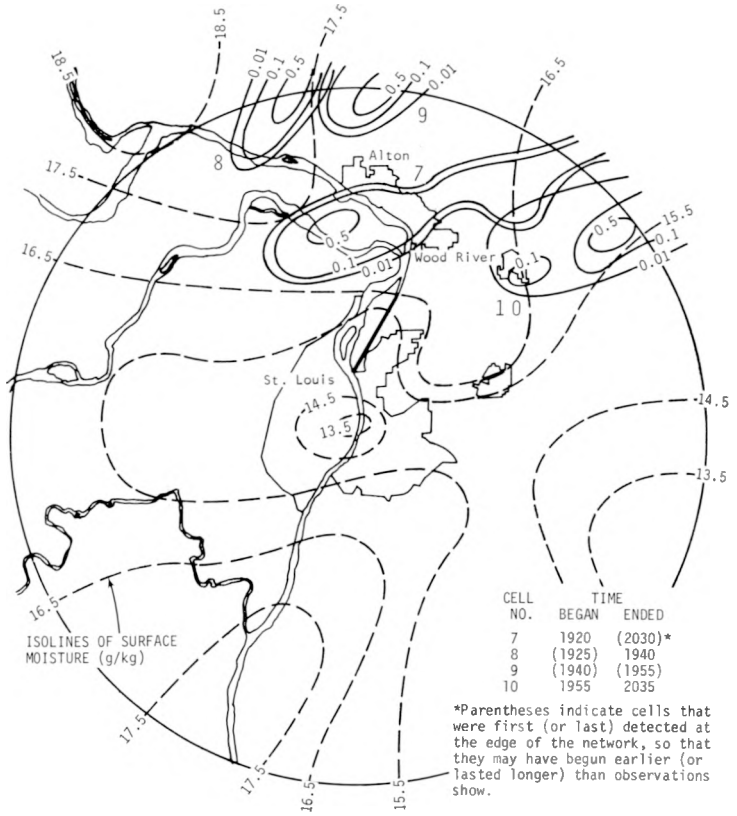

Figure K–42. Rainfall for frontal raincells 7-10 having volumes greater than 250 ac-ft, compared with the distribution of surface moisture before the rain

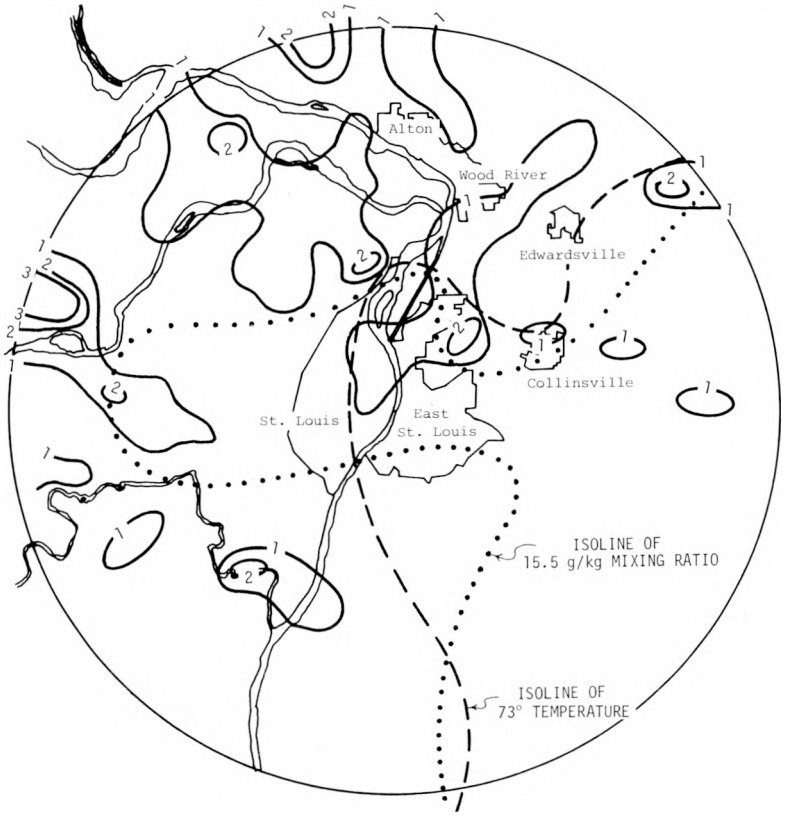

Figure K-43. Raincell initiations per gage (solid lines) compared with selected isolines of prior temperature and mixing ratio (higher values to the left of lines)

shown on figure K-40. This was the heaviest rainfall maximum and it was not far from the highest temperature and moisture values as well as downwind of the highest Aitken nuclei counts on the circle, as indicated by the aircraft data.

A major question is,"Was this a coincidental chain of events, or was there an underlying causal relationship between the rainfall and such parameters as surface temperature, surface moisture, and Aitken nuclei concentrations?" The extension of the rainfall maximum from the general core of frontal rainfall into the MMX circle as shown on figure K-38 is a suggestion that this chain of events was more than mere coincidence. It seems certain that the heavy frontal raincells had access to conditions produced or modified by the urban area.

Radar Echoes and Mesoscale Precipitation Elements. All 3-cm RHI echoes recorded during the frontal period were plotted along with their maximum heights. However, these data were available only from 1844 to 1918 and were not representative of the general frontal rain period. The 10-cm PPI integrator data were missing during most of the frontal period. Also, because of noise in the integrator recording system, data were available only for echoes that had reflectivities > 42.5 db. The storm on the MMX circle was not as severe as in the squall-line case (i.e., thunder at only 2 locations, and no hailfall), and echoes > 42.5 db did not occur.

Aircraft Observations

Because afternoon weather conditions at ALT were poor (restricted ceiling), the AI airplane was unable to take off until 1745, in the time period between the squall line and frontal rainfall.

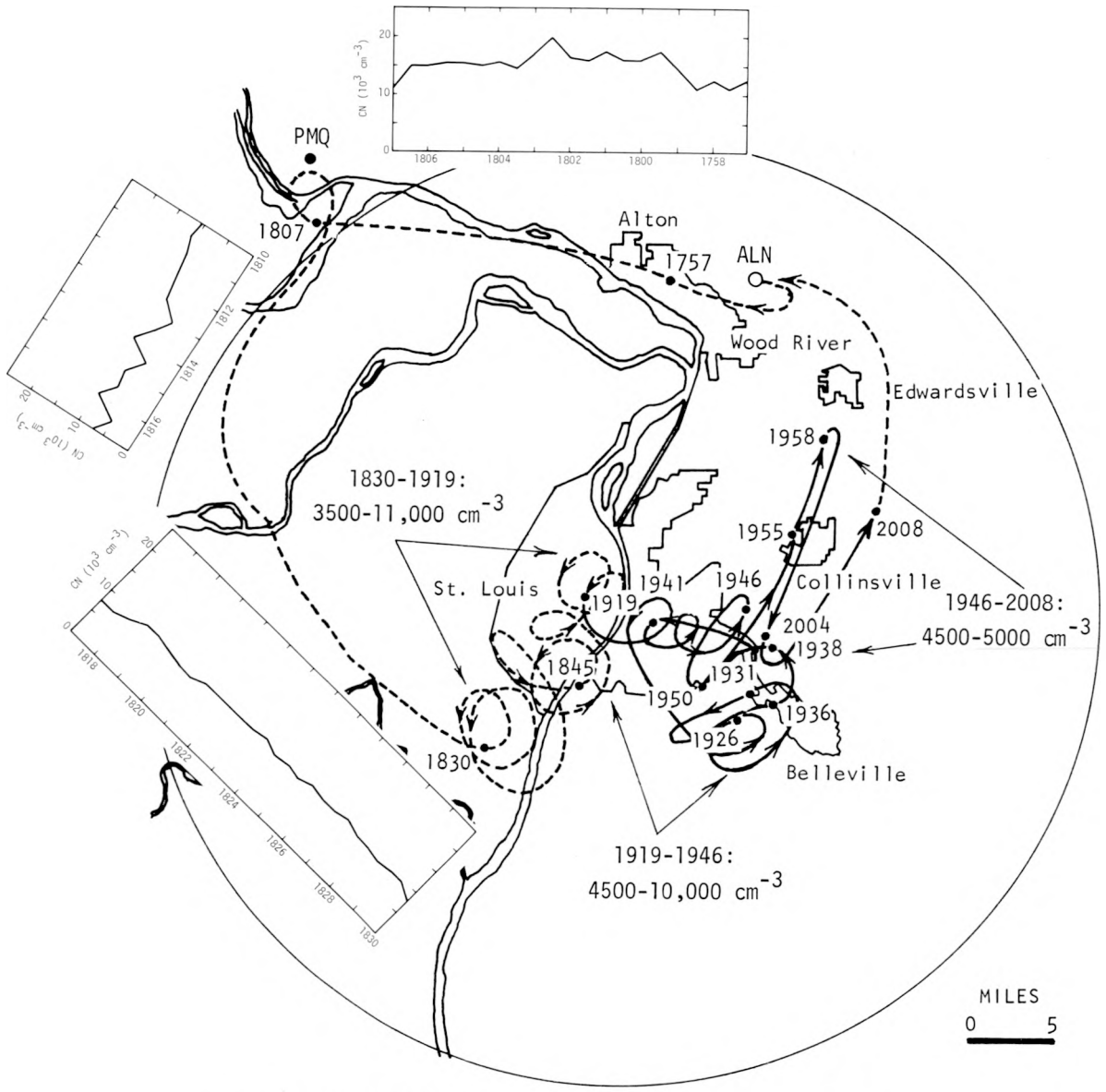

Figure K-44. Airplane flight path, showing CN concentrations encountered

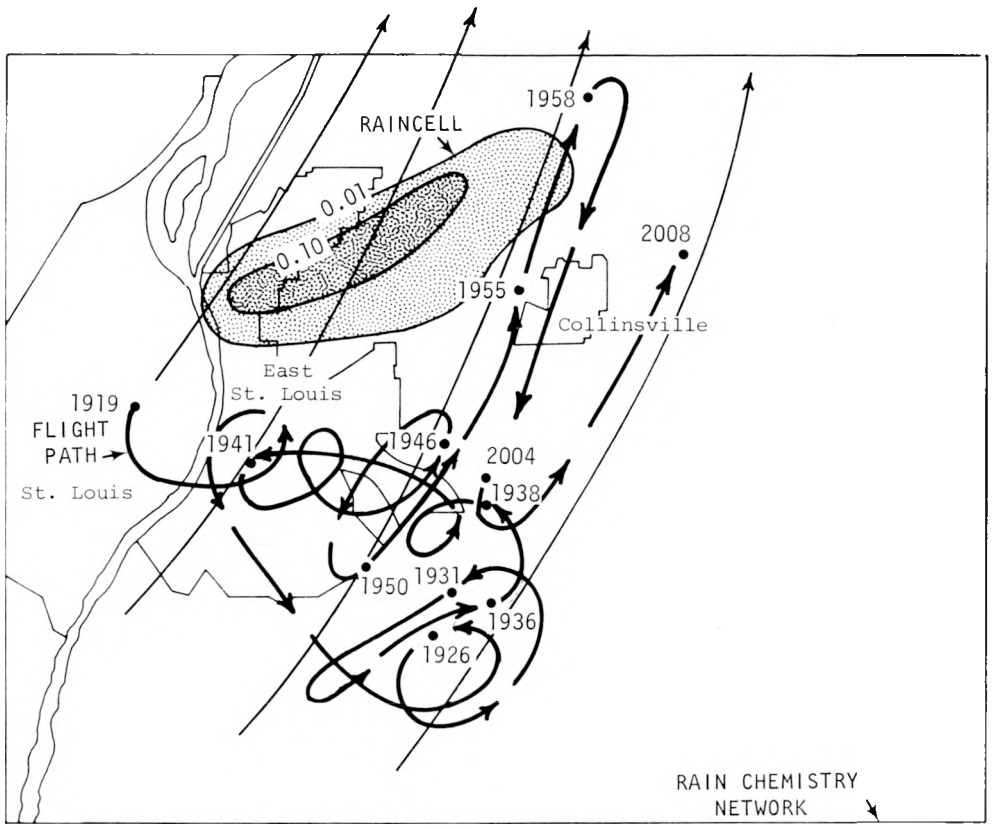

Figure K–45. Path of airplane during tracer release in relation to airflow near flight altitude (about 1000 m MSL) and rainfall from nearest raincell

The entire flight path from take-off to landing (at 2025) is shown in figure K–44 together with Aitken nuclei concentrations encountered during the flight. After take-off from ALN, the airplane flew W to the vicinity of PMQ, then S and SE along the W margin of the St. Louis metropolitan area, to the S boundary of St. Louis. From this point the plane began circling to wait for rain showers to the W to move into position for a tracer release. While circling, the plane moved generally along the Mississippi River over the urban area.

A release of tracer material began over St. Louis at 1919 CDT and continued for 49 minutes, until 2008. The flight path during tracer release is shown in detail on figure K–45. In general, the tracer was released between ARC and BLV, with one swing N to near Edwardsville. After the tracer release ended at 2008, the plane returned to ALN.

Figure K–45 also shows the streamlines at 1000 m MSL (approximate flight altitude) and the rainfall produced by the raincell closest in time and space to the tracer release. The streamlines indicate flow generally from the SW, so that winds were expected to carry the tracer material into the vicinity of the cell. Although only one cell was observed near the time and place of the tracer release, other non-cellular rain occurred during and after the release (a map of total post-burn rainfall will be presented later in the section on chemistry).

Compared with other cells and total rainfall on 13 August, the cell in question was a minor one, producing a maximum of 0.14 inch of rain at any gage site. Only three sites had rain of 0.10 inch or more, with two more receiving between 0.01 and 0.10 inch. The cell was first observed at Site 97 at 1940 and it ended at Site 82 at 2025. The lack of thunder at the SIE site indicates that the cell was only a shower.

Figure K–46 shows CN concentrations as a function of time when the plane was traveling along more or less straight legs to the N and W of the city, between 1757 and 1830. Altitude and

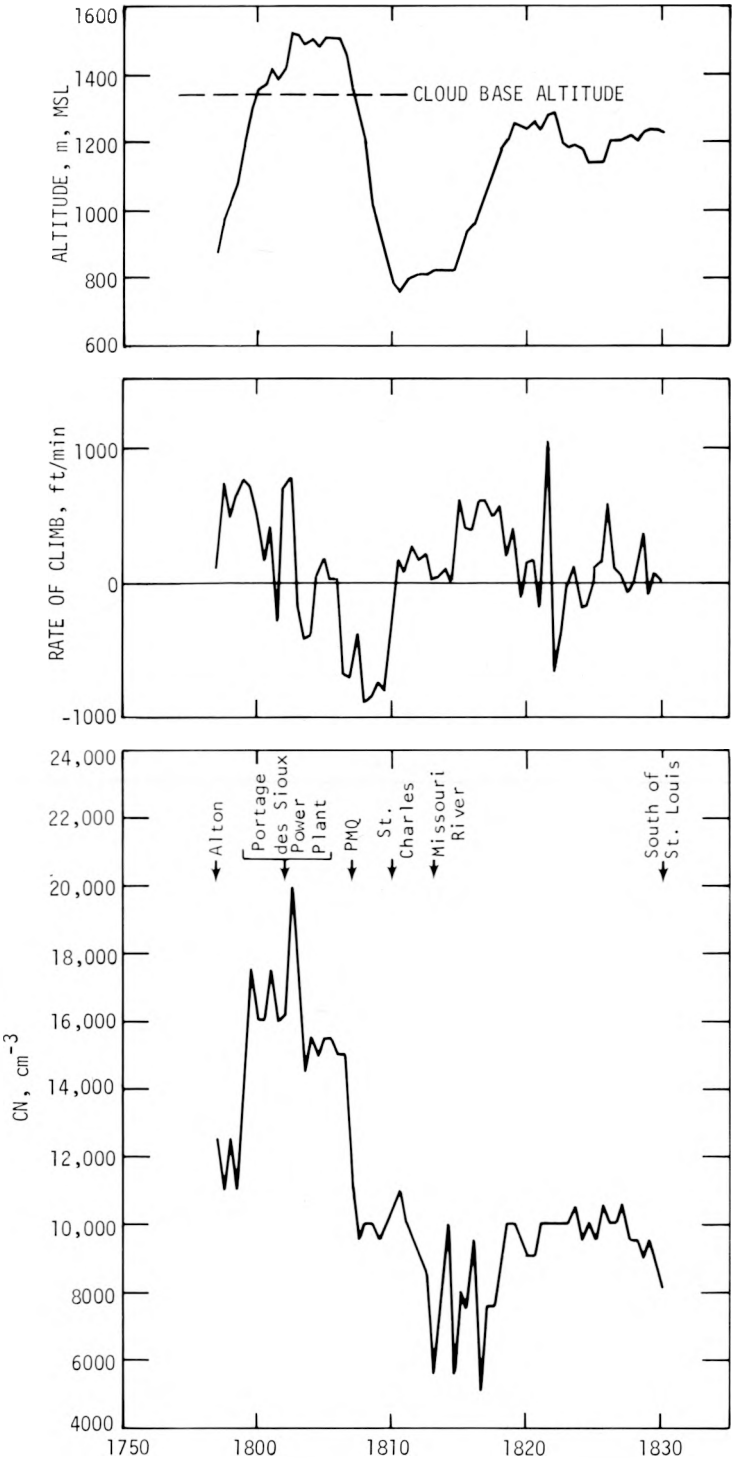

Figure K-46. Condensation nuclei, rate of climb, and altitude on flight legs N and W of St. Louis

rate of climb are also shown. Rate of climb is included to give a qualitative picture of the vertical motion encountered by the plane. Of course, this parameter will also reveal climbing and descending that is unrelated to air motion, but these occurrences are clear in the altitude record.

The altitude record indicates that the plane climbed to about 1350 m by 1800 after take-off at 1745, and then headed toward PMQ. The on-board observer's notes indicate that this was cloud altitude. The descent beginning at 1806 and the subsequent climb beginning at about 1815 were made in response to instructions from FAA control, to avoid airplane traffic around Lambert Field. The larger fluctuations in the rate-of-climb record appear to be related primarily to the controller-requested maneuvers.

The CN record shows a broad maximum between 1759 and 1807 when the plane was approximately between Alton and PMQ. Winds at 1000 m at 1830 (figure K–18b) do not suggest direct transport to the PMQ area by 1000 m winds, but inspection of the surface wind chart for 1800 (not shown) suggests an explanation. Surface winds in the city were generally from the E. Thus, urban effluents would have been carried to the W initially. Gradual upward diffusion of pollutants in winds veering with height implies a trajectory of anticyclonic curvature. This could, then, result in St. Louis pollutants reaching the vicinity of PMQ at 1000 m as observed in the CN peak.

During the period from 1807 to 1830, the plane flew to the S from the PMQ area to a point at the S end of St. Louis. On this leg of the flight, CN concentrations of about 10,000/cc were encountered, with several fluctuations down to about 5000/cc between 1813 and 1817. These concentrations are considerably lower than those observed in the E–W peak N of St. Louis, but they generally match the highest concentrations observed over and E of the city on figure K–47.

The CN concentrations, altitude, rate of climb, and θ_e for the portion of the flight E of the city, including the time of tracer release (1919–2008) are shown on figure K–47. The altitude record shows that the plane was descending at a rather uniform rate during the whole period shown in the figure. The rate of climb shows that rapid fluctuations of alternately rising and descending air were encountered.

The CN concentrations show large fluctuations between 1900 and 1938 with peaks in the vicinity of 10,000/cc and minima at or below 5000/cc. After 1938, concentrations stabilized between 4500 and 5000/cc. It is possible that the drop to an approximately constant 5000/cc in CN concentration occurred as the aircraft descended through the frontal surface. (Precise location of the front as it passed through the MMX circle was complicated by the presence of thunderstorms and associated downdrafts.) Although there is some uncertainty in the aircraft track between 1900 and 1919 CDT, these peaks were clearly measured over industrial areas (St. Louis or East St. Louis and Belleville), while the low concentrations were encountered primarily over rural areas.

The values of θ_e encountered by the aircraft between 1900 and 2008 are also shown on figure K–47. They range from 327.2 to 340.8. The θ_e parameter has been used as a tracer of air during convection because it is conservative for both adiabatic and condensation processes. To test whether the air encountered by the aircraft between 1900 and 2008 could have come from near the surface, vertical profiles of θ_e for the ARC and BCC soundings at about 1938 were plotted (figure K–48) and compared with the values encountered by the aircraft.

The figure shows that θ_e values between about 324 and 338K were present in the geographical area and within the altitude limits of the plane at about 1940. This accounts for all the θ_e values observed by the aircraft except a few about 338K at about 1900 and again at about 2007. These high values were observed when the plane was out of the general area between ARC and BCC and at least 25 min from sounding time. Furthermore, the rate-of-climb record shows no particular association of the high θ_e values with updrafts.

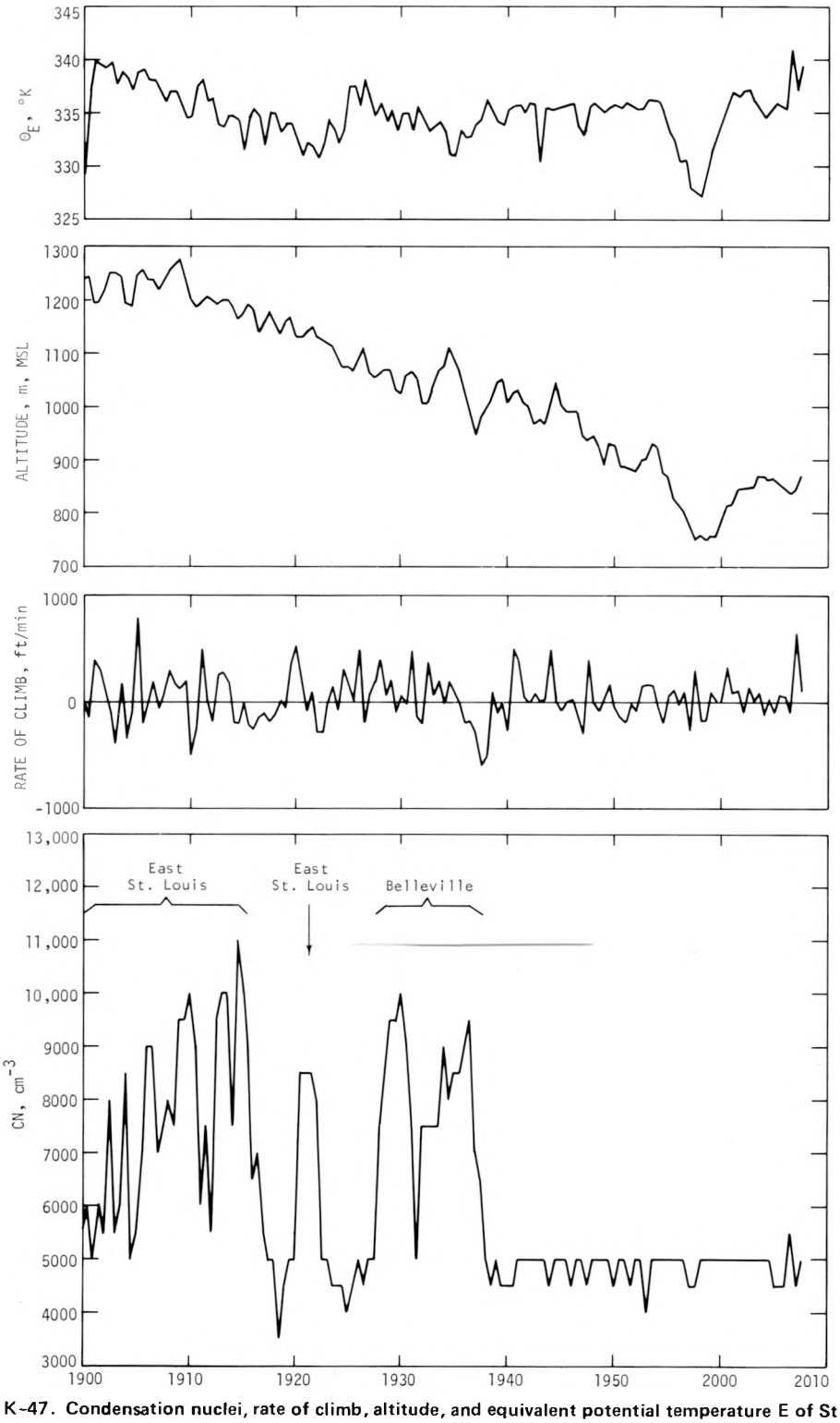

Figure K-47. Condensation nuclei, rate of climb, altitude, and equivalent potential temperature E of St. Louis

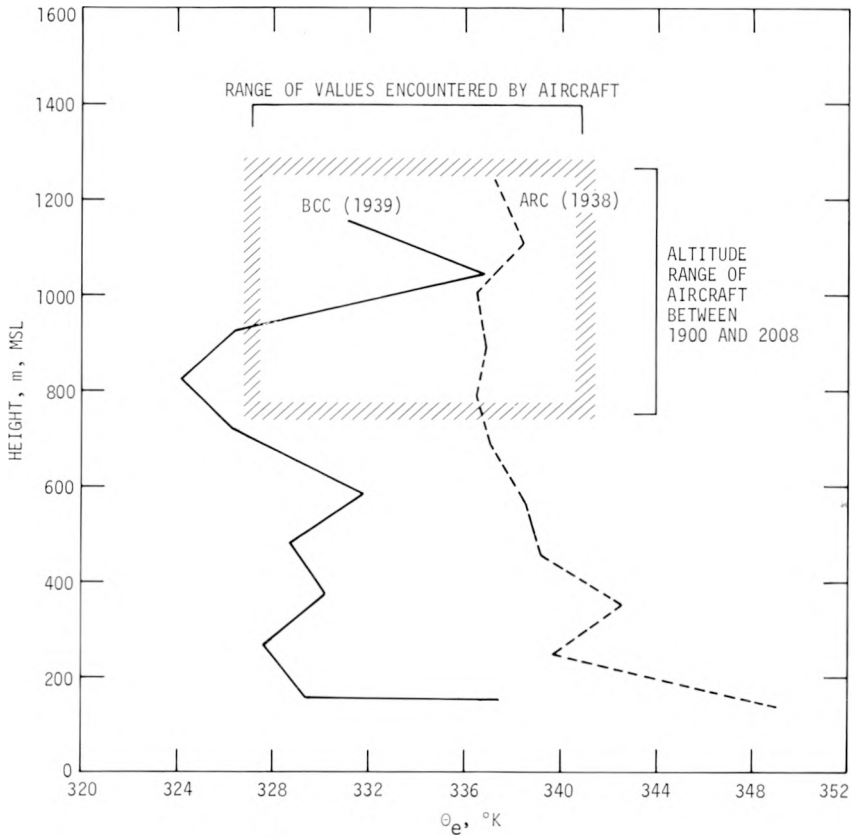

Figure K-48. Local equivalent potential temperature profiles, compared with values encountered by the airplane E of St. Louis

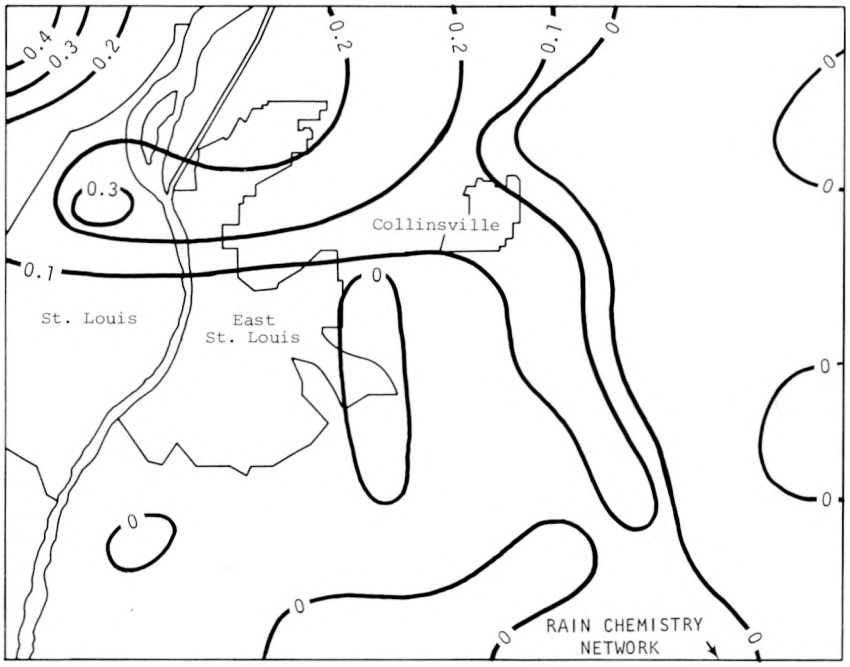

Figure K-49. Rainfall that occurred after the start of the tracer release

AIR AND RAIN CHEMISTRY

This section of the report is divided into three parts – one for each of the three kinds of data available for analysis. These are: 1) deposition of soluble tracer Li in the rain chemistry network, 2) deposition of soluble non-tracer elements in the rain chemistry network, and 3) results of source coefficient calculations made by using concentrations in air derived from Nuclepore filter samples.

Li Tracer Results

The path of the airplane during tracer release (between 1919 and 2008) was shown on figure K-45. The same figure included the rainfall amounts of the only nearby raincell during the release of the tracer and airflow streamlines at approximately the altitude of the plane.

Besides the cell rainfall shown in figure K-45, other rain occurred in the network after the tracer release began. The pattern of post-burn rainfall is shown on figure K-49. The most post-burn rain was recorded in the extreme NW corner of the rain chemistry network and amounts greater than 0.1 inch were mostly confined to that quadrant of the network also. This is in approximate agreement with the position of the cell rainfall shown on figure K-45, but indicates that most of the post-burn rain was non-cellular.

Li deposition per unit area (pg/cm^2) was computed at each collector site from measured concentrations in collected samples and the respective sample volumes. From these gross deposition figures, two corrections were made in an attempt to estimate net tracer deposition per unit area. The two corrections were for 1) dry deposition of natural Li and 2) wet deposition of natural Li.

The dry deposition correction was made separately for each sample, by using the time duration of sampler exposure and the median deposition rate ($mass/cm^2/hr$) at the respective sites found in about 20 cases in 1972.

In an attempt to tailor the correction for wet deposition of natural Li to this particular case, we took advantage of the fact that some samplers received rain before but not after the release of the tracer. An appropriate measure of the Li deposited in these samplers was used to correct the others for natural Li deposited wet. The details of this correction follow.

In many cases total deposition can be shown to be a function of total rainfall, so a relationship of this kind was sought by plotting Li deposition (corrected for dry deposition) against rainfall for those samples that received no post-burn rain. No systematic relationship was found for this case, so the median Li deposition ($mass/cm^2$) was computed for all samples where post-burn rain was 0, and this amount was used as a correction for natural wet deposition of Li.

The net tracer Li deposition ($mass/cm^2$) remaining after removal of natural Li from the total is shown on figure K-50. Values greater than 100 pg/cm^2 appear in St. Louis and at samplers in or near East St. Louis, Collinsville, Belleville, and at Site 135. The deposition maxima E of the Mississippi River are in or downwind (at flight altitude) of the location of the tracer release. However, neither these maxima nor the one in St. Louis correspond to either the total post-burn rain pattern or the pattern associated with the cell (figure K-45).

An independent assessment of the validity of the procedure used for correcting total Li deposition for dry and wet natural Li deposition may be made by using element ratios in precipitation samples. Because soil dust is a major source of natural Li, another soil element, K, was used as the index element. mass ratios of Li to K (corrected for dry deposition only and multiplied by 10^3 to produce numbers convenient to plot) are shown on figure K-51. Values greater than 1 appear along the St. Louis river front, from ARC to a point NE of Granite City, and also at Site 117. In these ratio units, the earth's crust ratio is about 2.5, so even the precipitation with the

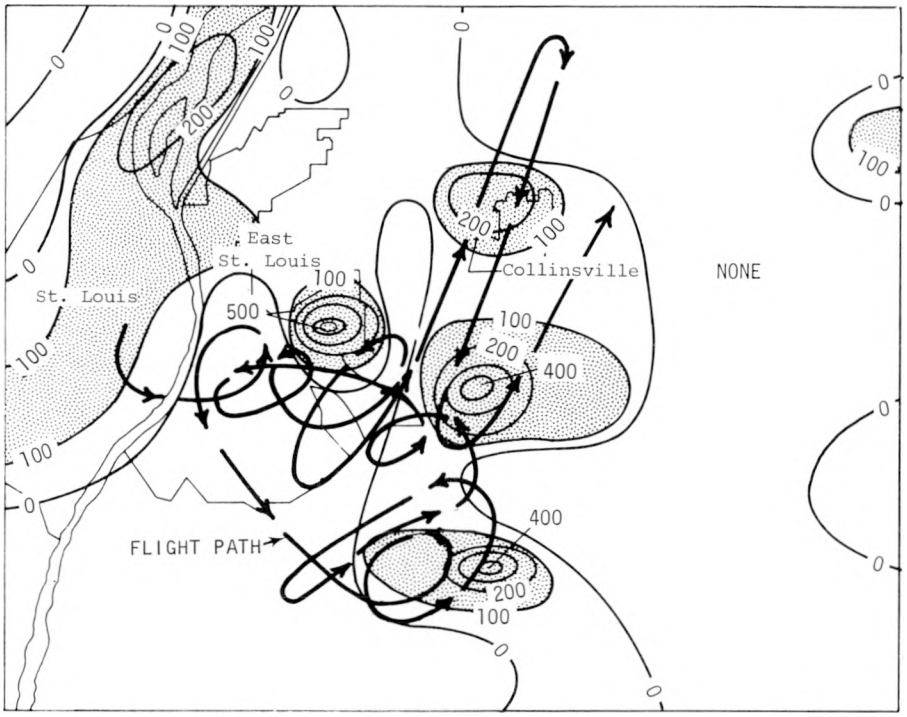

Figure K-50. Li deposition (pg/cm2) corrected for assumed contributions of natural Li from both wet and dry processes

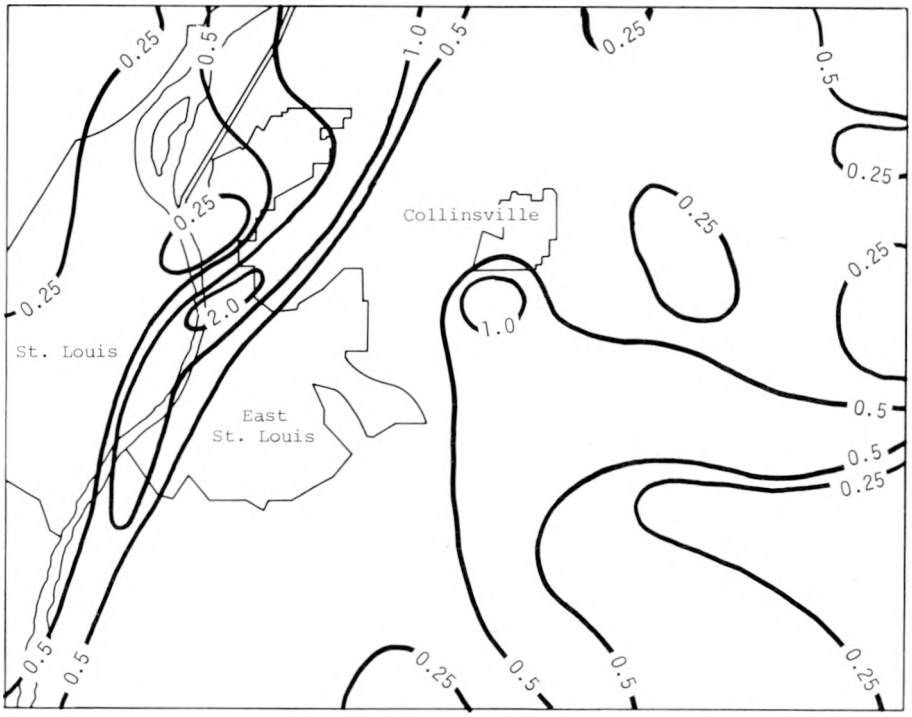

Figure K-51. Ratios of soluble Li to K in precipitation (corrected)

highest ratios was deficient in soluble Li relative to K with the earth's crust as a standard, and the maximum ratios did not match the maxima in the net tracer Li deposition pattern.

The ratio technique is admittedly crude because our ratios were computed only from soluble components, while the earth's crust ratio would include both soluble and insoluble components. Nevertheless, the extreme dissimilarity between the ratio pattern and the net deposition pattern calls for caution in interpreting the net Li deposition as tracer Li. The same caution would be suggested by the lack of correspondence between the net tracer deposition and either total post-burn rainfall or cell rainfall.

If the net Li deposition is not likely to represent tracer Li, one must ask what was wrong with the procedure used to calculate it. The deficiencies probably lie in the assumptions that deposition rates can be adequately extrapolated in time and space.

Non-Tracer Elements

The discussion in this section concerns measurements of *soluble* elemental concentrations in precipitation, or more precisely, parameters derived from these measurements, such as deposition. Here again, dry deposited materials have been subtracted from deposition values in the same way as done for Li.

Deposition patterns for Na, Mg, K, Ca, and Zn are shown on figure K-52 along with rainfall during the period when samplers were exposed. All patterns have been normalized to the mean value in the network to facilitate comparisons. Most elements show above average deposition in St. Louis and E to about Site 135 (in agreement with the rainfall pattern), but elsewhere in the network, deposition and rainfall patterns are dissimilar. The deposition of Zn is confined primarily to St. Louis and an area E of Granite City.

The differences in the deposition pattern between Zn and the other elements are large enough to suggest strongly that the urban area is the primary source of soluble Zn. The other elements are known to have large natural sources, such as soil dust, but varying urban and industrial source strengths. These differences are not readily observable in deposition patterns because of the strong influence of the amount of rainfall on deposition. Moreover, *concentration* patterns suffer from the same limitations and handicaps. However, it is possible to remove the variability connected with the amount of liquid water that happens to be associated with a sample by computing element ratios.

In the present case, the chemistry data are examined for evidence that air containing urban pollutants was involved in the formation of the rain that fell across the rain chemistry network. Thus, an index element that has no urban sources was chosen. Such an element exists in a relative rather than an absolute sense; however, K was chosen from the elements available to this study.

Mass ratios of Na, Mg, Ca, and Zn to K were computed and plotted on figure K-53. Precipitation that incorporated pollutants from urban air, by whatever physical mechanism, should thus have higher ratios (to K) for pollutant elements than precipitation that formed and fell entirely in non-urban air.

Thus, one might look for evidence of involvement of urban air with a particular convective cell by examining the elemental mass ratios in the rain from that cell and comparing them with the same ratios in rain from a part of the network where airflow patterns would indicate that urban air could not have been involved in the precipitation.

A number of features are common to the four ratio patterns. In each case, maxima occur along or near the river between St. Louis and East St. Louis, at Site 62 N of Granite City (except Ca/K), at Site 137, and S of Collinsville (Sites 117 or 135).

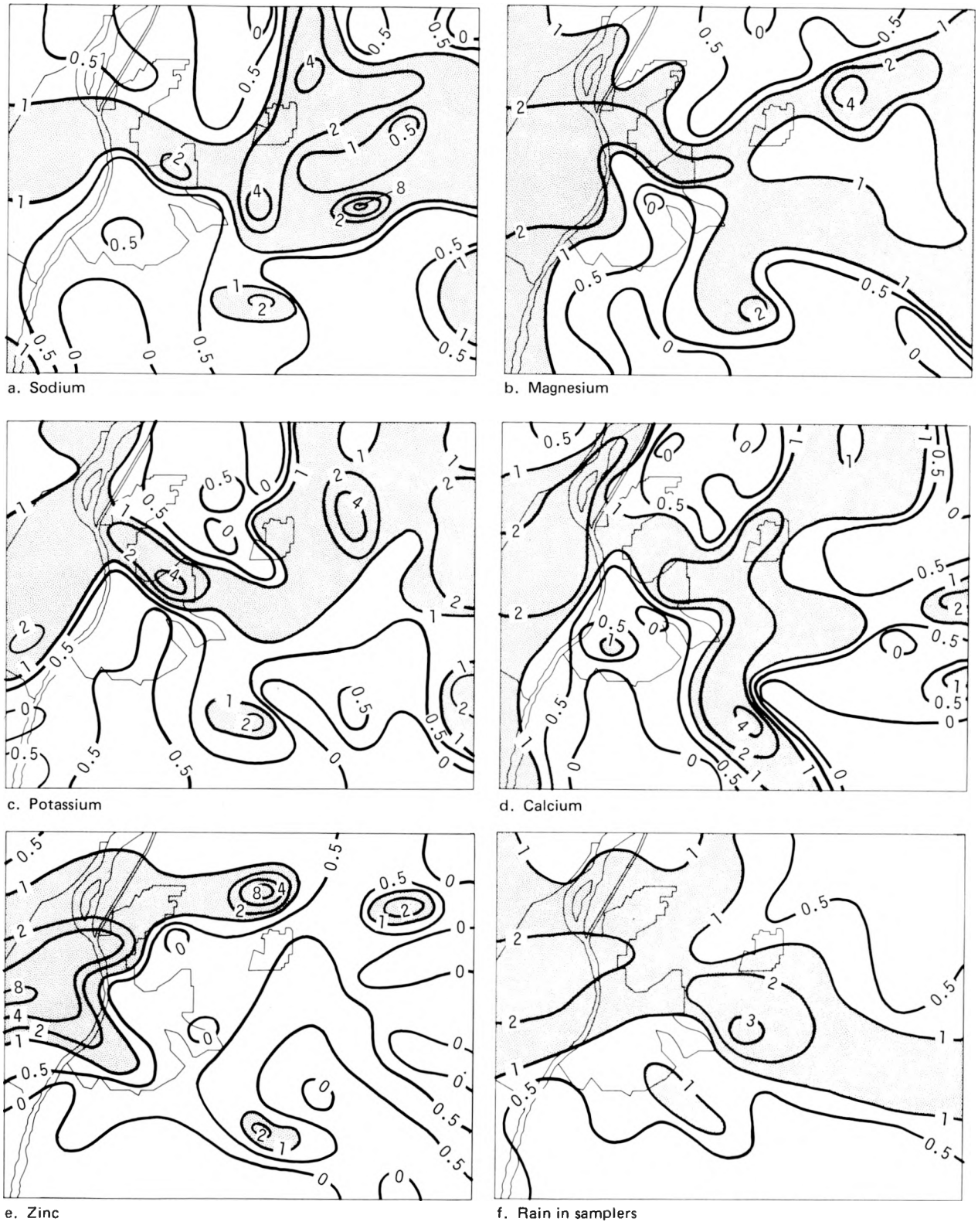

a. Sodium

b. Magnesium

c. Potassium

d. Calcium

e. Zinc

f. Rain in samplers

Figure K-52. Deposition of soluble trace elements and rainfall in the samplers, normalized to network mean value

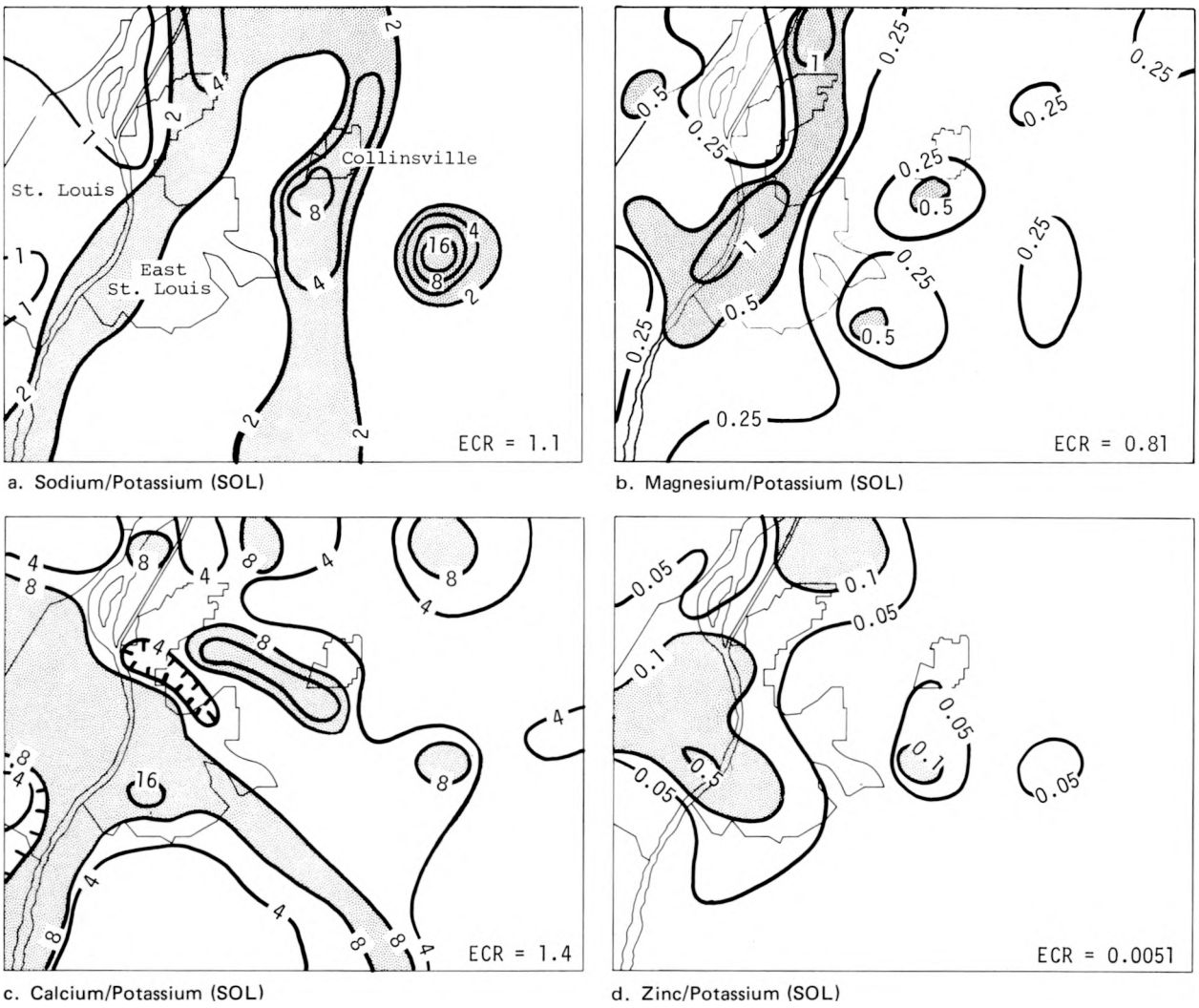

a. Sodium/Potassium (SOL)

b. Magnesium/Potassium (SOL)

c. Calcium/Potassium (SOL)

d. Zinc/Potassium (SOL)

Figure K-53. Ratios of soluble trace elements to soluble K in precipitation (Earth's crust ratio, ECR, of each element pair is also shown)

High ratios would be expected in and NW of urban and industrial regions in this case, from the generally SE winds at low levels in advance of both the squall line and frontal rainfall. However, the maxima S of Collinsville and at Site 137 cannot be explained this way, unless Scott Air Force Base is the source of the maximum at Site 137. The maximum S of Collinsville is of particular interest because that area was affected by the isolated cell ahead of the squall line. In fact, 23% of the afternoon's rain at Site 117 and 67% at Site 135 came from that cell. The occurrence of high mass ratios to K (especially Zn/K) at Sites 117 and 135 is evidence for involvement of urban air in that cell. Additional evidence for involvement of urban air in the early stages of radar echo development was presented earlier. Available data from air filter analyses offer additional evidence of the location of urban air in the MMX circle on 13 August.

Source Coefficients

Methods have recently been developed that allow computation of the relative contribution of various kinds of aerosol sources to the total aerosol concentration at a particular location. These

Table K-2. Source Coefficients for 13 August 1973

Site	C_{soil}(%)	C_{auto}/C_{soil}	C_{steel}/C_{soil}
0	8.9	0.22	0.51
22	8.5	0.18	0.40
81	8.5	0.42	0.49
113	20.0	0.42	0.31
151	9.4	0.59	0.36
159	0.8	0.41	0.98
300	7.8	0.43	0.54

relative contributions (known as source coefficients and expressed in percent) can be computed from the chemical composition of the ambient aerosol and knowledge of the chemical composition of emissions from the various kinds of sources considered. The details of the calculation method have been provided by Miller et al. (1972) and Friedlander (1973) and will not be repeated here. Gatz (1974) had computed mean source coefficients for auto exhaust, cement manufacturing (including limestone quarrying operations), fuel-oil fly ash, steel manufacturing, and wind-blown soil dust for 10 days during summer 1973 in the St. Louis area. One of the days included in that study was 13 August. Thus, source coefficients are available for this case at 7 locations in the St. Louis area.

The sampling sites are identified by number, and may be located on the map in figure B–2. The sites range from urban (Site 113) to suburban (22, 81, 151, 300), to remote (0, 159).

Source coefficients provide an objective means of evaluating whether the air sampled was 'city air' or 'country air.' Because sampling and operational requirements do not always permit confining sampling only to pre-rain air, this evaluation does not always identify 'upwind' and 'downwind' sites as clearly as would be preferred. Nevertheless, the information may provide a useful supplement to wind observations in assessing the source of air to the various convective precipitation systems under study.

The source coefficients for soil dust on 13 August are listed by site number in table K–2. The table also shows two source coefficient ratios (auto/soil, and steel/soil). These ratios were included as relative indices of 'urban effect.'

The table shows a relatively constant soil contribution at all sites except Site 113 in St. Louis (20%) and Site 159, a relatively remote site SW of the city (0.8%). In the city, abnormally high values for the soil contribution probably resulted from the inability of the method to distinguish between soil dust and coal fly ash (Gatz, 1974). Coal fly ash contributed at least half of the 20% 'soil' source coefficient at Site 113.

The abnormally low soil source coefficient at Site 159 is more difficult to explain, but may be related to the fact that the sample collected there was near the limits of detectability for many elements and for total mass on the filter.

Two different indices of urban effect are provided in table K–2 because auto exhaust and steel manufacturing represent area sources and a small number of point sources of pollution, respectively.

In terms of the auto/soil ratio, the various sites rank as follows from greatest to least urban effect: Sites 151, 300, 113 and 81 (tie), 159, 0, and 22. The steel/soil ratio yields another order: Sites 159, 300, 0, 81, 22, 151, and 113.

Site 159 could probably be eliminated as unreliable, and the differing urban effect rankings of the two indices explained by differences in source distribution, sampler location, and wind direction changes. In the final analysis, source coefficients did not provide much useful information on urban air versus non-urban sources to the various storms of interest on this day.

Improvement might possibly result if sampling could be confined to the time before rain began. With the usual time of the rain being late afternoon, and with 12-hr samples required for many sites, this would require visits to sampling sites either very early in the morning, or late on the *day before* rain was expected. Such requirements are probably not feasible in view of current operational procedures and precipitation forecasting capabilities.

CASE SUMMARY AND DISCUSSION

Macroscale Synoptic Conditions

At 0700, a stationary front across central Missouri was the macroscale feature most influencing St. Louis. The front marked the approximate N boundary (at the surface) of a vast area of moist air over the SE United States. Moist conditions extended upward as well, with large areas of small dew point depressions in the E half of the United States. Little temperature advection was occurring at 850 mb and 500 mb, but a major trough was present upstream of St. Louis at 500 mb.

By 1300 an open wave had developed on the front, with the low pressure center located in NE Missouri. The system center deepened and moved into E-central Illinois by 2000. A prefrontal squall line developed in the warm sector and moved E ahead of the front. Both the squall line and the front produced thunderstorms and considerable rain in the MMX circle during the afternoon and evening hours.

Mesoscale Synoptic Conditions

At 1400, just before squall-line rain began, there was an 11F gradient in surface temperatures across the MMX circle. Cooler temperatures in the N portion of the circle were accompanied by low clouds. Lesser cloud cover accompanied the higher temperatures in the S portion of the circle. The most moisture was present in a broad N–S band across the city and the extreme W portion of the circle. Surface winds were generally from the E, with an E–W line of confluence just S of the city.

At 1700, just before the frontal rain began, the warmest temperatures were in the N and W portions of the MMX circle. Moisture was high in both the N and S portions of the circle, and θ_e maxima existed to the NW and SW. Surface winds were generally from the S, with evidence for confluence of streamlines near the precipitation.

A comparison of two temperature and moisture soundings showed the expected warm, moist, unstable conditions before the squall line rain followed by surface cooling and overall stability after the frontal rain.

A cross section of potential temperature and mixing ratio from PMQ to BCC at 1330 showed surface moisture increasing from PMQ to ARC to BCC, but moisture aloft and overall instability were greatest over the city. This is significant because the isolated raincell (cell 1) that gave considerable rainfall on the E side of the city must have first developed as a cloud near the time and location of the ARC sounding that was much less stable than those taken simultaneously at PMQ and BCC. Here is direct evidence for city instability leading to a convective storm that produced considerable rain in the area of the anomalous maximum in the climatological rainfall distribution.

Squall-Line Precipitation, 1400–1730

Macroscale hourly precipitation patterns revealed an isolated high of 1.1 inches of rainfall for the hour ending at 1400. This high occurred ahead of the squall line. The total squall-line rainfall indicated a distinct maximum of rainfall within the MMX circle which was larger than any of the surrounding maxima.

The total storm on the network during the squall-line period produced three distinct highs in which the precipitation exceeded 1.0 inch. These highs were located W of the city, in the city, and E of the city between Collinsville and Belleville. The rainfall in the Collinsville–Belleville high was largely due to precipitation prior to the squall line and had amounts exceeding 2.24 inches. Furthermore, the largest and most intense hailstreak occurred within this high.

The heavy rain and hail from the squall line occurred in an E–W band across the MMX circle. This band coincides with a zone of high surface temperature gradient that probably marks the S boundary of the low clouds.

A comparison of raincells with the surface moisture patterns indicated that moisture was an important contributing factor in the production of precipitation by the raincells. Likewise, the *initiation* of cells appeared to be related to the surface moisture pattern. Also, there was good agreement between the surface moisture pattern and precipitation on the prior day.

Raincell initiation and rain production also favored regions of above average pre-rain θ_e values, but were less strongly related to the surface temperature field. There was some indication that at least one of the heavy raincells may have been enhanced by confluence in the wind pattern downwind of the city and the possible presence of nuclei in this region.

There was a distinct tendency for the first radar echoes, as well as the first raincells, to initiate in regions where the surface air had a high moisture content. Radar data also revealed that the raincell associated with the Belleville–Collinsville precipitation maximum which produced the largest and most intense hailstreak had ample opportunity to engulf moisture laden air as well as nuclei laden air. This was readily demonstrated by the raincell's association with the merger of a radar echo that had a genesis region in the vicinity of high surface moisture with a radar echo that developed and passed through a region which usually has high Aitken nuclei production rates.

The merger mechanism was an important contributing factor to the rainfall intensification because several raincells were either spawned or intensified in general merger regions. Furthermore, temporal curves of radar and raincell characteristics revealed a tendency for echo heights and reflectivities to increase after echo merger and for raincells to intensify and/or initiate after merger. Also, the heaviest and most intense hailstreak occurred a few minutes after merger in the vicinity of the city and in an area of high surface moisture content.

Frontal Rainfall, 1730–2400

Macroscale hourly precipitation patterns for the hour ending at 2000 revealed that although the main core of the rainfall was N of the MMX circle, there was an extension of high values into the circle. After the general system passed through the circle, an isolated rainfall maximum remained. The total storm rainfall for the frontal case also revealed an extension of high rainfall into the MMX circle, although the major frontal rainfall occurred N of it.

The total storm rainfall on the network during the frontal case revealed a broad band of precipitation covering the NW part of the circle. Within the general band of precipitation, there were a series of maxima in surface precipitation lying roughly on a line extending from the Missouri River N of St. Charles through W Alton and into the extended network. These highs had maximum point values ranging from 1.07 to 3.23 inches. Hail did not fall during the frontal precipitation period.

A comparison of raincells with surface temperature and moisture patterns indicated that cells also developed preferentially in warm, moist areas during the frontal portion of this case. A comparison of raincells with CN measurements from the aircraft data indicated that Aitken nuclei concentrations were high in the general region of frontal raincells. Further, the raincells were located downwind of the city with respect to the 500 m airflow. Thus, the general area in which the frontal raincells were located was one where high surface values of temperature and moisture were present as well as high counts of CN.

Cell initiation appeared to be associated with the wetter and warmer regions of the MMX circle. Somewhat surprisingly, the areas of heavy squall-line precipitation were in the drier portion of the prefrontal moisture pattern. However, the maxima in frontal precipitation were generally downwind of the squall-line precipitation maxima.

Aircraft Observations

Aircraft operations were limited to the frontal portion of this case because below-minimum conditions for take-off existed earlier. Once airborne, the plane flew counter-clockwise around the city, released tracer over the rain chemistry network, and returned to the airport.

Aitken nuclei measurements showed that the city plume was being carried generally toward the N and NW and that air approaching the city from the S and SE was relatively low in nuclei concentrations. No evidence was found relating θ_e at flight altitude with areas of high θ_e at the surface.

Air and Rain Chemistry

The rain chemistry data available for analysis are preliminary – they include soluble but not insoluble materials. However, since tracer Li is expected to be entirely soluble, the tracer results should be essentially complete.

This was a poor tracer case. The release was made in an area of weak diffuse updrafts. While winds at flight level suggest that the tracer should have been carried toward the nearest raincell, the evidence for deposition of tracer Li by the cell is weak.

Deposition of soluble non-tracer elements strongly suggests that the city area is the primary source of Zn, while sources of Na, Mg, K, and Ca are more generally distributed. Ratios of soluble elements to K, an index of soil-derived aerosols, offer additional evidence that city air was incorporated into cell 1 (the isolated pre-squall-line storm E of the city).

Source coefficients computed from elemental concentrations in air were unable to provide significant help in distinguishing 'city air' from 'rural air' in this case.

Discussion

Weather conditions before the rain on 13 August were quite typical and conducive for summer mid-continent convective storms, but were lacking a few of the components required for very severe storms. There was ample surface heating and moisture, combined with a very unstable thermodynamic structure. However, there was little advection of warm temperatures at low altitudes or cold temperatures higher up and only moderate vertical wind shear.

The day's rainfall occurred in two parts. The afternoon squall line produced an E–W band of heavy rain across the city, and the evening front produced an even heavier NE–SW band of rain NW of the city.

Did the city play any role in causing the squall line, oriented essentially N–S, to deposit its heaviest rain on an E–W axis across the city? Similarly, did the city contribute in any way to the localization of heavy rain during the frontal passage?

In the case of the squall line, cell rainfall and initiations were strongly influenced by the surface moisture pattern, which in turn was strongly influenced by the distribution of rain the day before. If the previous day's rainfall distribution could be linked to the city, then the squall-line rainfall could be also.

However, there appears to be a more direct link to the city for the squall-line portion of this case. The low clouds and relatively cool temperatures in the N part of the MMX circle at 1400 have already been pointed out. Furthermore, it has been shown that the maximum surface temperature gradient at 1400 probably marks the S boundary of this region and that the maximum squall-line rainfall occurred along this boundary.

This situation is very similar to those treated by Purdom and Gurka (1974) and Weiss and Purdom (1974) where thunderstorms have been observed to occur at the boundary between cloudy and clear areas. Purdom and Gurka state:

> When the major factor controlling afternoon thunderstorm formation is solar heating, early morning cloud cover plays a dominant role in controlling where afternoon thunderstorms will first form. In the early cloud free areas, the sun's energy will freely heat the ground and air. The early morning cloud covered areas, however, are kept several degrees cooler due to the clouds' higher albedo as well as the evaporation of water droplets as the cloud cover dissipates. The situation which develops due to this differential heating is analogous to the land-sea breeze effect. The air in the early morning cloudy region, being more dense, sinks and spreads out, lifting the warmer and more unstable air at its perimeter. Thus, the first thunderstorms to form are along the early morning cloud cover boundary. In addition, the subsidence and slower heating rate in the early morning cloudy areas help keep that region free from convection for most of the day.

The situation described by Purdom and Gurka appears to fit the initial stages of the present case. The observed confluence line in the surface wind field at 1300 and 1400 was the manifestation of the 'land-sea breeze' mentioned by Purdom and Gurka. The first echo and raincell to form (cell 1) developed near the maximum temperature gradient and the confluence line *in advance of the approaching squall line.* This cell appears to have benefited from the great instability at ARC at 1330, but it is not clear whether that instability was in any way related to the region of low clouds.

The role of the cool cloudy region during the squall line was again that of a barrier of dense air which, when intersected by the cool outflow from the squall line, formed a preferred location for convection. This situation is very similar to the 'intersecting arcs' described by Purdom (1974) as observed in satellite data.

The foregoing is a description of the physical processes leading to the band of heavy rain across the city from the squall line. But what was the city's role? Did these events occur over the city just by chance?

The evidence is against a chance occurrence because the low clouds over the city were probably not a chance occurrence. Although there was widespread early morning fog throughout the E half of the United States, the low clouds over the N portion of the MMX circle at 1300 and 1400 appear to be a local phenomenon. As shown in table K–3, the stations in the N portion of the St. Louis area (ALT, STL, and PMQ) showed a consistent pattern of limited visibilities and low clouds relative to stations in the S portion of the local area and in the surrounding area.

The cause of this phenomenon is speculative at this point, but the positions of the moisture source from the rains of 12 August and the industrial regions combined with E or SE low-level flow

Table K-3. Cloud Cover and Visibility Conditions in and near St. Louis

Station	Height of lowest broken or overcast layer (ft) 1300	1400	Visibility (mi) and obstructions* 1300	1400
Surrounding area				
Quincy	1,800	2,200	5 H	6 H
Columbia	25,000	3,500	15	15
Kirksville	2,400	2,000	15 R--	12
Burlington	2,000	1,600	1½ GF	1½ GF
Peoria	25,000	25,000	12	12
Springfield, IL	2,500	2,000	4 H	5 H
Decatur	2,200	10,000	9	9
Champaign	20,000	none	10	10
Cape Girardeau	3,000	8,000	15	15
Vichy	8,000	(thunderstorm)	7	(thunderstorm)
Mount Vernon	2,000	missing	7	missing
St. Louis local area				
STL	1,800	2,000	2½ HK	2½ HK
ALT	1,000	800	1½ FK	1½ FK
PMQ	1,300	1,400	3 F	3 H
SUS	2,500	1,500	5 H	5 H
BLV	1,500	2,000	6 H	6 H

*Obstruction code: H=haze; R--=very light rain; GF=ground fog; K=smoke; F=fog

would suggest a pollution-augmented foggy condition. It is well established that excess cloud condensation nuclei, such as are known to be produced in the St. Louis area (Braham, 1974), contribute to colloidal stability of clouds.

Thus, for the squall-line portion of this case, the distribution of heavy rain can be explained by a chain of events leading back to a local condition (the low-cloud region) caused, probably, by a combination of local pollution and moisture sources. Evaporation of the rain of 12 August contributed some of the moisture to this particular case, but the river and lowland areas in addition to industrial sources could provide moisture. Orientation of the heavy rain in other cases like this would evidently depend on the particular juxtaposition of moisture and nuclei sources and on the low-level wind direction and the orientation of any squall lines that may be involved.

The influence of low morning clouds on the distribution of precipitation has been observed before, but this is the first time that an urban area has been identified as a cause of the low clouds.

The mechanism shown to have occurred in the squall-line portion of this case is very likely not the only one by which the city can influence the distribution of rainfall. This case suggests, however, that even small changes in meteorological conditions by cities (e.g., enhancement of fog or haze) can provide a 'trigger' that eventually leads, perhaps only after a whole chain of subsequent physical processes, to redistribution or enhancement of precipitation.

It seems clear also that urban effects on precipitation do not always cause the excess rain 'downwind'. The band of heavy rain extended all across the city. Thus, the downwind excess should be regarded as a climatological average condition only.

Within the squall line, the merger mechanism was an important contributing factor to rainfall intensification. Several raincells were either spawned or intensified in general merger regions, and temporal data indicated that there was a tendency for echo heights and reflectivities to increase after echo merger and for an intensification and/or initiation of raincells and hailstreaks after merger. Furthermore, the location of merger cells in relation to confluence of airflow patterns and their exposure to urban CN, heat, and moisture provide evidence for additional links between rainfall intensification and properties of the urban area.

For the frontal portion of the case, evidence for a city influence on the rainfall appears in the location of the heaviest rain in a warm, moist area of the city's pollution plume. However, no more specific mechanism to explain the frontal rainfall distribution is suggested at this time.

Finally, aircraft nuclei measurements have proven useful in identifying urban air, and ratios of soluble elements in precipitation provided useful supplemental information concerning input of urban air to particular storm cells.

REFERENCES

Auer, A. H., and R. A. Dirks. 1974. *Contributions to an urban meteorological study: METROMEX.* Bulletin American Meteorological Society, v. 55(2):106-110.

Braham, R. R. 1974. *Cloud physics of urban weather modification--a preliminary report.* Bulletin American Meteorological Society, v. 55(2):100-106.

Changnon, S. A., Jr. 1970. *Hailstreaks.* Journal of Atmospheric Sciences, v. 27(1):109-125.

Changnon, S. A., Jr., and F. A. Huff. 1973. *Enhancement of severe weather by the St. Louis urban-industrial complex.* 8th Conference on Severe Local Storms, Denver, Colorado; AMS, Boston, 8 pp.

Friedlander, S. K. 1973. *Chemical element balances and identification of air pollution sources.* Environmental Science and Technology, v. 1(3):235-240.

Galway, J. G. 1956. *The lifted index as a predictor of latent instability.* Bulletin American Meteorological Society, v. 37:528-529.

Gatz, D. F. 1974. *St. Louis air pollution: estimates of aerosol source coefficients and elemental emission rates.* Preprints, Symposium on Atmospheric Diffusion and Air Pollution, September 9-13, 1974, Santa Barbara, California; AMS, Boston, pp. 109-114.

Huff, F. A., and S. A. Changnon, Jr. 1972. *Climatological assessment of urban effects on precipitation at St. Louis.* Journal of Applied Meteorology, v. 11(5):823-842.

Miller, M. S., S. K. Friedlander, and G. M. Hidy. 1972. *A chemical element balance for the Pasadena aerosol.* Journal Colloid Interface Science, v. 39(1):165-176.

Purdom, J. F. W. 1974. *Satellite imagery applied to the mesoscale surface analysis and forecast.* Preprints, 5th Conference on Weather Analysis and Forecasting, March 4-7, 1974, St. Louis, Missouri; AMS, Boston, pp. 63-68.

Purdom, J. F. W., and J. J. Gurka. 1974. *The effect of early morning cloud cover on afternoon thunderstorm development.* Preprints, 5th Conference on Weather Analysis and Forecasting, March 4-7, 1974, St. Louis, Missouri; AMS, Boston, pp. 58-60.

Weiss, C. E., and J. F. W. Purdom. 1974. *The effect of early-morning cloudiness on squall line activity.* Monthly Weather Review, v. 102(5):400-402.

Wuerch, D. 1970. *A comparison of observed and calculated urban mixing depths.* U.S. Department of Commerce, Environmental Science Services Administration, Weather Bureau, Central Region, Kansas City, Missouri, ESSA Technical Memorandum WBTM CR 36.

L. SUMMARY AND RECOMMENDATIONS

Summary

The primary goal of the case investigations was to better define the urban-related mechanisms that cause the summer rainfall in and E of St. Louis and Alton–Wood River to be greater than that in surrounding areas. The nine case days, one on 11 August 1972 and the others on 14, 23, 25 July and 7, 9, 10, 12, 13 August 1973, were selected to provide a variety of summer storm situations. The extensive climatic-oriented studies of the first three years of METROMEX data (Huff, 1973; Huff, 1974) definitely established the reality of the urban-related rain and severe weather anomalies. The general placement of the anomalies and comparisons between urban-area and rural-area precipitation elements in these climatic studies led to attempts to identify the urban mechanisms affecting the rain processes.

The results of these nine case investigations more clearly point to several urban-related conditions that likely contribute to some of the observed precipitation alterations. Physically, these alterations were recognized to produce the following events in the climatically defined (Huff and Changnon, 1972) 'target':

1) Urban-area initiated and thus increased the number of precipitation echoes and subsequent raincells (all cases except 23 July and 7 August)
2) Same as event 1, plus the subsequent merger of cells with each other or with cells of a later organized system (all cases except 23 July and 7 and 9 August)
3) Intensification of rain from existing cells passing over the urban area or in its heat, moisture, and/or aerosol plume occurred (all cases except 9, 11, and 12 August)

These findings on the urban mechanisms leading to rain initiation and intensification are also enumerated in table L–1. They do not specify the causative role of various urban factors. However, the three observed conditions identified above are documented as being 'urban-related' because of careful study of their time and placement of occurrence. One example of this circumstantial evidence is afforded by the case of 13 August. The only cells that initiated ahead of the squall line (and in a circular area of 120-mi diameter) were those that developed and remained over St. Louis.

Another example of urban effects discerned by careful study of urban–rural differences was found on 10 and 12 August. Isolated cells developed in the urban area and in rural areas at the same time, but the urban cells grew in a preferential manner over the urban area, lasted longer, and became much more intense.

Other examples of how the urban processes were active and as specifically revealed by the case analyses are the situations on 14 and 25 July and 10 and 11 August. In these instances the 'feeder cells' that merged and sustained a meso-rain system (usually stationary and beyond or E of the urban areas) were forming solely and repeatedly over the urban areas. The only cell of consequence of the 13 that occurred on 7 August grew over the Alton area and in the convergence zone related to the St. Louis area. Mergers of well-developed rain entities were the result of general cell enlargements, the lack of motion of one of the two cells, or their convergent motions.

The increased severe weather (hail, heavy rain rates, and intense thunderstorms) observed in and downcity of the urban areas in seven of the case days was frequently related to the mergers of the apparent urban-related cells. The merger-related increases of severe weather occurred in six of the seven cases (14 and 25 July, and 10, 11, 12, 13 August). The severe weather (high rainfall rates over the urban area) on 23 July did not appear to be a result of merger of urban-induced echoes or raincells, but rather of a rain release process from ingestion of low θ_e air from St. Louis. The frequencies of case days with urban-related heavy point rains, hail, or thunder appear in table L–1, items 3–5.

Table L-1. Summary of Findings Expressed as Number of Cases Applying to Each Situation

	Situation	*Yes*	*No*	*Data unavailable or not analyzed*
1	Initiation of rain was urban-related	7	2	0
2	Urban effects increased rain intensity	8	1	0
3	Two-year recurrence rains occurred in possible urban-effect cells	7	2	0
4	More hail occurred in possible urban-effect cells	5	2	2
5	More thunder activity occurred in possible urban-effect cells	6	2	1
6	Project forecast of rain conditions was correct	6	3	0
7	Rain-conducive synoptic conditions existed	9	0	0
8	Cells developed over urban area	7	2	0
9	Urban cells preceded rural cells in time	4	5	0
10	Cells developed in NW bottomlands	4	5	0
11	Mergers of cells (at least one urban-related) led to enhanced rain and severe weather downcity	7	2	0
12	Mergers of isolated urban-area cells occurred	6	3	0
13	Mergers of isolated urban-area cells with organized line cells occurred	2	7	0
14	Outflow from urban storms enhanced new cells	4	3	2
15	Tracer results showed between-cell exchange	5	0	4
16	Urban-related confluence zone related to cell initiation	4	3	2
17	Clouds/raincells first developed in relatively warm and/or moist surface areas	9	0	0
18	Clouds/rain intensified in relatively warm and/or moist surface areas	4	5	0
19	Surface temperature or moisture anomalies were explained	3	6	0
20	CN plumes were defined downcity	6	0	3
21	Heat plumes were defined downcity	3	0	6
22	Urban aerosols were at cloud-base level	7	0	2
23	CN in urban updrafts were greater than those in clear air	6	0	3
24	CN in urban updrafts were greater than those in rural updrafts	3	0	6

More specific identification of the urban agents and the exact processes whereby the convective precipitation entities were initiated and/or intensified over the cities or in their urban plumes was difficult. Direct in-cloud measurements (other than by remote sensors like radar) of the large clouds suspected to be urban-related were not possible with METROMEX aircraft so that exact proof of all phases in the precipitation process could not be derived. However, inspection and integration of the key case results (table L-1) offers insights as to the various urban mechanisms and how they interacted with the cloud and rain processes. Certain other findings that pertained to only one of the cases are not listed in the table but will be discussed later.

One of the important findings relates to the synoptic weather conditions. In all nine cases the rain situation conducive to urban effects was one in which mesoscale and/or macroscale conditions were favorable for precipitation to develop. The urban factors acted only to make rain start sooner, to rain oftener in a given area, and/or to intensify existing rains. Thus, the urban influences create slightly more favorable and geographically preferential conditions for rain over or in the immediate urban locale.

Forecasting at 0900 of rain development in the next 12 hours was correct in six of the nine cases (table L–1, item 6). Failures were due to unsuspected development (or sustainment) of conditions conducive to rains (14 July and 11 August) or an inability to discern where the activity would occur (25 July). Importantly, post-storm synoptic analysis revealed that if real-time synoptic-scale surface data for objective analyses and hourly sounding data were available, update forecasting would have perceived these events 3 hours before they began. However, standard analysis techniques and the data available through 0800 were not adequate to foresee one-third of the precipitation conditions that developed 6 to 9 hours later.

Raincells developed directly over one or both of the urban areas in seven of the nine cases (table L–1, item 8), but in only four cases did they precede the cells in the surrounding rural areas. In four of the nine cases, cells developed in the NW river bottomlands, another area shown in the climatic studies to be an important rain-generation area.

Items 11 through 15 in table L–1 summarize key findings about dynamic cell interaction. Mergers of cells, in which at least one of a pair was urban related, led directly to increased rain and severe weather downcity in seven of the nine cases. As shown in the table, most of these cases were based on mergers of two or more *isolated urban cells,* but in two cases the isolated urban-generated cells merged with cells in an advancing organized line of non-urban origin.

The analyses in seven of the cases were sufficient to reveal whether the cold outflow from the mature urban-generated storms affected new cells. In four cases it *enhanced new urban cells* (10, 11, 12, 13 August), but in one case it also helped to dissipate existing cells (10 August). There were tracer (Li) releases on five of the nine days, and in every case the Li deposition patterns, when temporally related to the release path and the associated rains, revealed an exchange, often rapid, of Li between adjacent convective cells. These cells were 5 to 15 mi away from the nearest tracer release point and into the updraft of a different cell. This suggests that urban aerosols taken into cells over the city could be exchanged between (and thus potentially affect) cells relatively far away from the urban area.

A major discovery about how the urban area affects rain initiation and intensification was seen from the results for 14 July and 7, 9, 13 August. In each of these four cases (table L–1, item 16) an urban-produced confluence zone, generally just 'downwind' of the city, was the preferred area for cell initiation, and in all cases except 7 August, the cells merged and intensified as they moved to the E. Airflow data did not exist for two cases (25 July and 11 August), and in the three other cases, no urban confluence zone was found (23 July and 10, 12 August. However, on 12 August an old mesoscale system produced a confluence zone across the city and the most intense cells developed in that zone.

The second major finding on actual urban effects was that precipitation cell development in every case (table L–1, item 17) also occurred preferentially in surface warm and/or moist areas having dimensions of 100 to 1000 mi^2. These surface anomalies existed in the city and the NW bottomlands from morning to rain time on most days, but appeared in a variety of other locales in rural areas near Alton–Wood River with no apparent between-case persistence (a hot spot on one case day would be a cool spot on another). In four of the nine cases, raincells also intensified in these areas of surface anomalies. These results are *major proof that surface heating and moisture*

anomalies extend upward to affect convective precipitation development. Convection is greater in these areas, initiation and frequency of clouds of the day and subsequent growth of clouds become greater there. Certainly, this deeper convection, when it exists over the city, transports urban aerosols to the cloud bases so that it is difficult to separate the thermodynamic effects from the microphysical effects.

The importance of these warm-moist surface anomalies in explaining the local rain increase in turn demands explanation of why these anomalies occur. Why was the city hot and dry on 7 August but hot and moist on 11 August; or why was the Granite City–Wood River area hot and moist on 10 August, but cool and moist on 7 August? As noted in item 19 of table L–1, the reasons for the surface anomalies (that tend to develop in the early morning and persist until the afternoon or evening rain starts) could be adequately explained in only 3 of the 9 cases. Explanations found included mesoscale synoptic factors that controlled nocturnal and morning cloud distributions (11 and 13 August); areal distributions of antecedent heavy rainfall (12 and 13 August); and local fog and low-level pollutant layers (13 August). The general inability to explain these anomalies is a critical problem for METROMEX to address.

Aircraft flights were sufficient on six of the nine days to define possible urban aerosol (CN) or heat plumes aloft (generally measured midway between the surface and cloud-base level) and from 5 to 20 mi downwind of the city. As shown in table L–1, CN plumes were found in all six cases where flights allowed their measurement and in all three cases where the aircraft temperature data analysis was performed, there was a definable urban heat bubble or plume aloft. Clearly, these results indicate that urban-related heat, moisture, and aerosols are transported well above the surface layers.

This is confirmed by the fact that in the seven cases (table L–1) with aircraft flights at cloud-base levels, urban-produced aerosols, as defined by their concentrations in time and space, were found at cloud-base levels over and downwind of the city. As shown in items 23 and 24 of table L–1, the CN values in the updrafts of clouds in or near the urban area were much higher than CN values in non-cloud air at the same levels in all six cases where such aircraft measurements were made. More importantly, in the three cases when the aircraft made measurements of updrafts in both rural and urban clouds (25 July and 10, 11 August), the urban updrafts had much higher CN values. Clearly, urban aerosols were being ingested into the convective showers in and around St. Louis and Alton–Wood River. In two of these three cases with comparative updraft data, the urban cloud updrafts also had twice as many ice nuclei as did rural updrafts (10 and11 August). Under these circumstances, the potential for altering cloud microphysical processes appears well established.

Certain very informative findings were derived from only one or two case days and deserve mention. The observation for 13 August that the low nocturnal and morning surface winds from the S caused the pollution and fog to be pushed into the upper (N) half of theAmerican Bottoms may explain why that low elevation area has, on the average, relatively low summer temperatures (Huff, 1974).

Efforts to discern whether the urban effects led to decreased rainfall in the 23 July and 9 August cases specificially chosen to test this possibility indicated little or no effect for decreases. When the St. Louis air was relatively dry and warm (23 July and 7 August), no preferential urban area cell initiation was found. However, the dry urban air on 23 July appeared to be associated with increased rain over the northern part of St. Louis and just E of there. This low θ_e air may have ended storm growth and resulted in the 'dumping' of large quantities of water stored aloft, as Auer and Dirks (1974) have hypothesized. However, this condition was not observed in any of the other eight case days, and the W–E decrease in rainfall on 9 August was due to the normal dissipation of a system W of St. Louis. In two cases (10 and 12 August) there appeared to be good

examples of the dissipation of urban-origin storms when they moved away from the urban source air. Little or no urban effects on rain entities appeared in two nocturnal frontal shower cases (23 July and 13 August).

Analyzed cases (11 August and 23 July) where two tracers (Li and In) were released suggest that their scavenging was quite different. The natural background of Li was so high that it made the interpretation of Li tracer analyses difficult and questionable.

Cumulus clouds over the city had bases 1000 ft higher than those of rural clouds on two days of measurements (25 July and 11 August). Mergers of echoes occurred generally first in the 4000- to 10,000-ft level.

In summary, the nine case studies revealed that all previously suspected (Changnon et al., 1971) urban factors (added heating, mechanical effects on airflow, altered moisture, and increases in aerosols for cloud and precipitation nuclei) have a role in altering the precipitation, largely on a spatial scale. Surface heating and moisture anomalies extend upward and affect rain initiation placement and frequencies and in some cases even the rainfall intensity. Urban aerosols also mix upward and appear in large quantities at cloud-base levels. Urban-induced confluence zones are preferential rain initiation and intensification zones. These confluence zones are also areas of increased urban aerosol concentrations. At this time, the case studies do not reveal the magnitude of each urban effect. However, they do suggest that on some days added heating is the critical factor and on other days the urban-produced confluence zone is more critical. Aerosols appear to be available for effects on all days, but their role cannot be specified from the case results. Obviously, urban aerosols are being ingested into urban area storms and in turn are being exchanged by in-cloud processes with other adjacent but more distinct cells (Semonin, 1972). Whether the aerosols were CCN or ice nuclei active in altering cloud processes so as to increase rainfall could not be distinguished in the case studies.

Once these combinations of effects initiated precipitation entities over or near the urban area, two conditions were noted. The entities often acted to produce more nearby cells through feeder cell growth and/or by their cold downdrafts that eventually initiated new clouds and cells. In either instance, the greater frequency of cells being generated in or E of the urban area led to mergers of cells with subsequent dynamically related increases in rain, hail, and electrical activity.

Two important discoveries concerned the 'domino' effect produced by the urban area on two time scales. The first is the above-stated daily condition whereby initiation of raincells over the urban area in turn begets more urban cells. Another domino effect was revealed by the five case studies in the 7-day period of August 1973 (7, 9, 10, 12, 13 August). A several day sequence of synoptic weather conditions conducive to rainfall on each day would tend to reinforce the urban rain effects. Antecedent rainfall (moisture) effects tend to lead to repeated (day after day) development and intensification of rain in the same locales (12 and 13 August), depending on where urban-related rains developed on the first day(s) of the sequence (7, 9, 10 August). This multi-day domino effect was also noted in an 8-day rain sequence in July 1974, and this theory would explain how the urban increase would be relatively greater in above-normal rain periods (months or seasons), as noted in earlier climatic studies (Huff and Changnon, 1972).

Recommendations

Other goals of these case studies were 1) to discern missing or inadequate measurements of conditions that were critical to the future field efforts of METROMEX and other subsequent similar projects, and 2) to direct or re-focus the METROMEX research.

Recommendations Concerning the Field Effort. Certain re-orientation of the field program has already been accomplished in the 1974 and 1975 summer field operations, partially as a result of the findings from these case studies. The critical importance of the surface temperature and moisture anomalies led to the installation of several additional hygrothermograph stations so as to better define the anomalies. Low-level wind measurements (pibal) and special soundings at three sites were maintained in 1974 and 1975 partially because of the value of these data to 1) define the critical rain-producing weather conditions, and 2) delineate any urban-related confluence zone. The obvious value and need for additional cloud data demonstrated in the case investigations led to installation of added cloud cameras in 1975 and an intensive study of the Synchronous Meteorological Satellite data. The need for better and more frequent measurements of airflow motions into storms, other than those by aircraft, led to a strong recommendation for inclusion of dual doppler radar measurements in the 1975 efforts (ultimately supported by NSF). Aircraft operations, where possible, have been altered to gather urban plume and cloud information, and the problems with the Li tracer noted in the case studies led to its abandonment in 1975.

The case day analyses pointed to the extreme value of two types of atmospheric data that aircraft should seek on rain days. One recommendation is to profile the urban plume (temperature, moisture, and aerosols) in the pre-rain atmosphere to confirm its existence and 3-dimensional shape. A second is to measure updraft conditions (speed, dimensions, CN or preferably CCN, and ice nuclei) below both urban and rural clouds. Obviously, in-cloud aircraft measurement of these factors and LWC would also be of great value in proving which clouds were truly urban affected and how these effects altered in-cloud processes.

The importance of the urban-produced convergence and confluence zones for cloud and rain production leads to a major recommendation for more frequent (at least for several hours) and areally wider pre-rain sequential airflow measurements. Better measurements with pibals (or comparable devices) and aircraft of the urban-induced thermal and mechanical turbulence would allow more specific delineation of the urban cause of such convergence zones, as well as their existence.

Routine 1-hour and 2-hour soundings of the pre-rain atmosphere at five or more locales in the METROMEX circle are strongly encouraged. These would help define the urban affected air mass, allow careful meso-analysis of the rain-producing weather conditions, and if used with a communication network, would allow real-time update forecasting. Update forecasting for daytime field operations relating to rain in the 1200 to 2100 period is recommended, and objective analysis techniques should be employed. The decision-making routine of a single in-depth analysis and forecast in mid-morning followed only by radar surveillance was found to be an inadequate approach 33% of the time.

Two other major operationally related recommendations are 1) to operate a good 10-cm weather radar with standby provisions on a 24-hour continuous basis, and 2) to collect all possible cloud, fog, and visibility data. The failure to collect radar data because of power outages (no standby provisions), no nocturnal efforts, and poor decisions about when to operate the radars is lamentable. Furthermore, the value of 3-dimensional echo data in defining cell characteristics, including merging, calls for constant routine 3-dimensional scanning using non-attenuated 10-cm radar. The 3-cm RHI radars used in METROMEX are of limited value in quantitative investigations of the major convective storms involved in the urban-related rain anomaly.

The value of good cloud data, as exhibited by the 11 August case, points to the need for more data, in space and time, on all clouds. The effect of cloudiness on the unequal heating of the surface in pre-rain conditions and the inception of the clouds involved in the rain production both need to be measured to better understand the local effects on precipitation. These measurements

need to involve more surface observations, more aircraft observations, more surface cloud cameras, and satellite data.

Recommendations Concerning Research. Where possible, complete tracer budgets and chemistry analyses need to be performed for the case days. Such analyses could not be pursued in most of these case investigations because the data on the tracers and related pollutants were not yet completely analyzed in the laboratory. Although the analyses were incomplete, the case day tracer results also suggest that the surface sampling network may be too small to capture much of the rain-scavenged portion of the tracer material, especially since between-cell lateral exchange was prevalent and such multi-cell conditions are the rule rather than the exception.

Of some research interest would be to evaluate the rain rate distribution method offered as a means to delineate updraft areas (23 July). This could be done with existing data from other cases in which updrafts were measured.

A major research recommendation is to learn how the oft-appearing, spurious surface moist and warm spots develop, either on rain days or on non-rain days. They usually seemed 1) to develop early in the morning and persist until rains began, and 2) to affect cloud and/or storm (rain) initiation, and in some cases, affect the intensity of the rain. Local cloud cover (11 August) and morning fog and haze (13 August) apparently affected these patterns. Antecedent rainfall (12 and 13 August) also played a role in some cases. Clearly, in summer the city is usually hot and dry, or hot and moist, and the NW bottomlands (25 July, and 9, 11 August) and the hills (7 August) also appear to have an effect on the local temperature and moisture patterns. Thus, better information as to how these anomalies develop is needed. Data on visibility, radiation, and thickness of pollution layers at many more locales would help.

The value of the objective weather analysis technique, as displayed in the 12 August case, strongly suggests its use in future synoptic analyses of case events. It can perceive, in a uniform analytical manner, important weather conditions that may go undetected in standard analyses.

A final research recommendation is to perform more case investigations. The results from these nine cases were so useful in achieving the overall METROMEX goals that added case-day research should provide new important information as well as verify the findings from these cases. Hypotheses as to how added rain is produced by urban factors need development and testing against this type of in-depth investigation. The effect of low θ_e air from the city needs to be separated, if possible, from the effect of the simultaneous microphysical alterations by urban aerosols. The case investigation of 23 July pointed to this θ_e–aerosol condition as an explanation of the rain anomaly, but the other eight cases suggested that thermodynamic and mechanical factors plus aerosol increases led to raincell initiation followed by merging of cells so as to produce the rain anomaly. These case studies clearly reveal that the events that led to added rainfall varied considerably according to the local conditions and the synoptic weather conditions.

REFERENCES

Auer, A. H., and R. A. Dirks. 1974. *Contributions to an urban meteorological study: METROMEX.* Bulletin American Meteorological Society, v. 55(2):106-110.

Changnon, S. A., F. A. Huff, and R. G. Semonin. 1971. *METROMEX: An investigation of inadvertent weather modification.* Bulletin American Meteorological Society, v. 52, 958-967.

Huff, F. A., Editor. 1973. *Summary report of Metromex studies, 1971–1972.* Illinois State Water Survey Report of Investigation 74, 169 pp.

Huff, F. A., Editor. 1974. *Interim report for METROMEX studies: 1971–1973.* Illinois State Water Survey, Research Report, 181 pp.

Huff, F. A., and S. A. Changnon. 1972. *Climatological assessment of urban effects on precipitation at St. Louis.* Journal of Applied Meteorology, v. 11(5):823-842.

Semonin, R. G. 1972. *Tracer chemical experiments in midwest convective clouds.* Reprints Third Conference on Weather Modification, AMS, Boston, pp. 83-87.